PREDICTION OF SEISMIC DESIGN RESPONSE SPECTRA USING GROUND CHARACTERISTICS

by

S. R. Malushte and M. P. Singh
Department of Engineering Science & Mechanics
Virginia Polytechnic Institue & State University
Blacksburg, Virginia 24061

September 1987

BIBLIOGRAPHIC DATA SHEET	1. Report No. VPI-E-87-31	2.	3. Recipient's Accession No. PB88 232590

4. Title and Subtitle	5. Report Date
Prediction of Seismic Design Response Spectra Using Ground Characteristics	September 1987
	6.

7. Author(s)	8. Performing Organization Rept No.
S. R. Malushte and M. P. Singh	

9. Performing Organization Name and Address	10. Project/Task/Work Unit No.
Department of Engineering Science & Mechanics Virginia Polytechnic Institute & State University Blacksburg, VA 24061	
	11. Contract/Grant No. CEE-8214070 CEE-8412830

12. Sponsoring Organization Name and Address	13. Type of Report & Period Covered
National Science Foundation Washington, D.C. 20550	Technical
	14.

15. Supplementary Notes

16. Abstract

For seismic design of structures, earthquake input is usually defined in terms of pseudo acceleration respons spectra. However, recent research has identified the need of defining the design input in terms of the relativ velocity and relative acceleration response spectra as well. Furthermore, for the equivalent linear analysis c hysterically behaving structures, one also needs to define the response spectra of a massless oscillator. Base on the analysis of available earthquake records, this study defines the above mentioned response spectra as th seismic design input for various site conditions.

The available earthquake records are classified into five groups according to their site stiffness and epicentr distance as the grouping parameters. For the groups thus defined, normalized response spectra are obtained fc single-degree-of-freedom and massless oscillators for horizontal and vertical ground motions. The motio parameters of average frequency and significant duration are obtained for each group and their effect on th response spectra is studied. Correlation analyses between various ground motion characteristics such as pea displacement, velocity, acceleration and root mean square acceleration are also carried out for each group.

Smoothed design spectra for relative and pseudo velocities and relative acceleration responses of single degre of freedom oscillators and the velocity and acceleration responses of massless oscillators are proposed for eac group. Methods to predict relative velocity and relative acceleration spectra directly from the pseudo velocit spectra are presented. It is shown that the relative spectra can be reliably estimated from the pseudo spectra The site dependent design spectra are defined for a wide range of oscillator periods and damping ratios.

17. Key Words and Document Analysis

Earthquakes, Seismic Disign, Response Spectra, Site-dependent Spectra, Pseudo Velocity Spectra, Relativ Velocity Spectra, Relative Acceleration Spectra, Hysteretic Structures, Site Characteristics, Epicentral Distance Average Frequency, Significant Duration, Peak Ground Acceleration, R.M.S. Ground Acceleration

17b.   Identifiers/Open-Ended Terms

17c. COSATI Field/Group

18. Availability Statement	19. Security Class (This Report) UNCLASSIFIED	21. No. of Pages 328
Unlimited	20. Security Class (This Page) UNCLASSIFIED	22. Price

Acknowledgements

This report is based on the work done by Mr. S. R. Malushte for his M.S. thesis in Civil Engineering (Structures) under the guidance of Prof. M. P. Singh.

Preceding page blank

Table of Contents

Chapter I

Introduction

For design purposes, the ground response spectra are commonly used to define earthquake induced ground motion, especially for design purposes. A response spectrum of a ground motion represents its frequency response characteristics in terms of the maximum response of a series of oscillators of different frequency and damping values subjected to that ground motion. It is customary to represent the relative displacement response in terms of the pseudo velocity or pseudo acceleration spectra which are commonly used to characterize the ground motion. These response quantities are also directly related to the force in the oscillator spring. Housner (9), Newmark and Hall (21), Newmark, Blume and Kapur (22) have proposed the pseudo velocity and acceleration spectra as design inputs for important facilities like nuclear power plants.

Further research in the area of earthquake structural engineering (31) has, however, shown that for a more complete description of the design input, we also need to define the relative velocity spectra in addition to the pseudo velocity (or

acceleration) spectra. Furthermore, it has also been shown (33) that prescription of design input in terms of the relative acceleration and relative velocity spectra is even better than the prescription in terms of pseudo acceleration and relative velocity spectra (RSV spectra), as there are definite computational advantages in adopting these as the inputs. Also, in the spectrum analysis of nonlinear hysteretic structures by the equivalent linearization approach (34), it has been shown that we also need the spectra for the response of a massless oscillator. In this work, therefore, the design ground response spectra for the pseudo velocity, relative velocity, relative acceleration and the velocity and acceleration response of a massless oscillator have been developed.

The need for grouping response spectra on the basis of the earthquake characteristics and site conditions has been widely acknowledged ever since Newmark-Hall (21) and Newmark-Blume-Kapur (22) presented smoothed response spectra for design purposes. A few researchers have also presented spectra corresponding to different seismic and geological conditions (1, 8, 27, 39). However, there is still a need for a comprehensive study in this regard, especially for the development of relative velocity and relative acceleration response spectra. The physical properties to be considered for a grouping strategy should be quite explicit so that a group can be easily identified from a simple description of the site and the earthquake to be expected. This is desirable because it will enable a reasonably accurate prediction of the response for a given set of physical characteristics of the site and the expected earthquake.

The main interest of this study is, therefore, to define the design response spectra for the relative velocity and relative acceleration responses for different site conditions. It is noted that the spectra for the pseudo velocity or acceleration

responses are rather widely available and used. However, in this study, these pseudo spectra have also been defined for different site conditions.

The physical properties of the design earthquake are the magnitude (such as Richter magnitude), peak displacement, velocity and acceleration, etc. The physical properties of the site are the stiffness of the ground and the estimated epicentral distance from the potentially closest seismic source. Also, the orientation of record (viz., horizontal or vertical components) is an important characteristic as the excitation behavior is observed to be direction-dependent. Many seismologists have attempted to empirically describe the inter-relationships between these and other such properties using techniques like linear or exponential (logarithmically linear) regression analysis (6, 9, 28, 35, 36, 38). Researchers have also studied (3, 4, 5, 25, 37) the implicit properties of seismic records such as the significant duration (an estimate of the strong motion duration), root mean square (r.m.s.) levels of ground excitation, average frequency, etc. These implicit properties are dependent on the physical properties of the site and the corresponding earthquake. It is, therefore, necessary to study this dependence here.

The earthquake data used in this study were obtained from the collection of real earthquake records compiled at the Earthquake Engineering Research Laboratory, California Institute of Technology (11, 12, 13, 14) and were grouped using the parameters of site stiffness, epicentral distance and the orientation of the ground motion (viz., horizontal or vertical). Magnitude of earthquakes was not used as a parameter in this study due to the fact that the earthquakes available for this study vary within a relatively small range of magnitude (5.3 to 7.7). Based on the observations of Trifunac and Brady (37), this is not expected to cause a great variability in the duration which is deemed to be an important factor affecting the magnitudes of response peaks (35). Also, the effect of the earthquake magnitude is

commonly incorporated in a design by choosing an appropriate level of intensity expressed in terms of peak ground motion parameters. Due to its large variability in the available data, epicentral distance was, however, considered to be an important parameter for defining the groups.

The average frequency, significant duration and r.m.s. acceleration have been calculated for each record used in this study. These are important parameters, since they are reliable indicators of the damaging potential of a given record. Regression studies have also been carried out to investigate the correlation between the peak displacement, velocity, acceleration and r.m.s. acceleration of records belonging to each group.

In this study, the spectra presented are normalized for a peak acceleration of 0.50 G. For the purpose of normalization, Newmark, et al. (22) suggest using the displacement, velocity and acceleration peaks for different regions in the frequency domain. Recently, Pauschke (26) has reported a comparison between the results of normalization using peak and r.m.s. acceleration. In this present study, the spectra have also been obtained for a normalized r.m.s. level of ground acceleration. This was done to see if the two normalization schemes yield any different results (in a qualitative sense). Also, a correlation study between peak and r.m.s. acceleration was done for each group.

Chapter 2 discusses the grouping strategy based on explicit parameters, along with the methods of estimating implicit parameters. It also gives details about the seismic input used in this study. Chapter 3 describes the computational algorithms used to obtain the desired response quantities. Information about the oscillator frequencies and damping ratios used to obtain the response spectra as well as the normalization schemes used in this study is given in Chapter 3. Chapter 4 discusses the generated spectra and the proposed design response spectra. It also gives the

results of the correlation studies between the peak ground acceleration, velocity and displacement, and between the peak and root mean square acceleration for each group of ground motions. The statistical values of the important implicit parameters for each group have also been presented. Also, in Chapter 4, the proposed design spectra are compared with the design spectra given by Newmark, Blume and Kapur (22), and the Applied Technology Council (1). Methods to estimate the relative velocity and acceleration spectra from the pseudo velocity spectra (PSV spectra) are also presented in Chapter 4. Conclusions are presented in Chapter 5.

Chapter II

Grouping of Ground Motion Records

2.1 Introduction

For the purpose of design, it is desirable to have different sets of response spectra, each computed to suit a given set of physical conditions or parameters that are easily identifiable with the local site conditions as well as the seismological characteristics of the nearby topography. The obvious parameters of interest in deciding about the design ground motion are : 1) ground stiffness such as soft, medium stiff or hard, 2) epicentral distance, and 3) magnitude of earthquake. For these conditions, it is necessary to define the three components of the design earthquake.

A satisfactory scheme for grouping should be such that the variance of the response within each group is as small as possible. To check the appropriateness of the classification adopted in this study, the mean, standard deviation (s.d. or sd) and the coefficient of variation (c.o.v.) of the response spectrum values are computed

for each group. As noted earlier, the implicit parameters depend on the set of physical characteristics associated with a given group. The effect of these parameters on the response spectra corresponding to different groups has also been studied.

2.2 Seismic Input

The ground motion of 18 earthquakes which occurred in the western U.S. from 1933 to 1971, recorded at several places, has been considered in this study. This provided a total of 232 records (162 horizontal and 70 vertical components) recorded at 82 site locations. The ground motion data was obtained from tapes supplied by the Earthquake Engineering Research Laboratory (EERL), California Institute of Technology. All the relevant data about the epicentral locations, recording station locations, digitization intervals, peak readings and the actual time-histories of ground displacement, velocity and acceleration, etc. were read from the Vol. II tape provided by the EERL (see reference 12). Also, data about response spectra involving oscillator periods, damping ratios, relative displacement, relative velocity, absolute acceleration and pseudo velocity were read from Vol. IV tape of the EERL (14). In addition, some more response spectrum values were calculated as discussed later.

Not all the records stored on Vol. II were used in this study. The earthquake records considered in this study are :

1. with a larger than 0.02 G peak peak in the acceleration time-history,

2. only the main shocks, and not the after shocks,

3. recorded on ground or basements of buildings so that they were free from soil-structure interaction effects as much as possible,

4. from earthquakes of magnitudes larger than 5.0.

This screening process led to a final selection of 232 ground motion records, consisting of 162 horizontal and 70 vertical components, recorded at 82 sites. The earthquakes corresponding to these records lie in the magnitude range of 5.3 to 7.7. The epicentral distances (from the recording station to the epicenter of the earthquake) vary from 7 km to 185 km for the ensemble of records considered for this study. The acceleration time histories in Vol. II have been recorded after performing base-line correction. The periods of digitization for ground acceleration, velocity and displacement records are .02 sec, .04 sec and .10 sec, respectively.

Table 1 lists the 18 earthquakes that were used in this study. The information includes the epicenter locations, dates of occurrence and the magnitudes of the earthquakes. Table 2 tabulates the names of the recording stations with their locations and the associated epicentral distances corresponding to the 82 selected site locations. Tables 3-11 tabulates the Cal Tech record numbers along with the site locations, directions of recorded components, peak readings of ground displacement, velocity and acceleration for the 232 records recorded from the 82 locations mentioned in Table 2.

It may be mentioned here that the epicenter and recording station locations are given in terms of latitudes and longitudes, which are essentially the same as the spherical coordinates. This location information was used to calculate the rectangular coordinates of these locations assuming a constant radius of earth equal

to 3960 miles. Finally, the epicentral distances (along the earth's surface) were computed by knowing the straight line distance between these points and the earth's radius. A small computer program was written to compute the results based on this approach.

2.3 Grouping Based on Physical Characteristics

The parameters considered for classification are ground stiffness at the site (soft, medium stiff or hard), epicentral distance and magnitude of the earthquake. Of these, the magnitude parameter was considered to be the least significant, because most earthquakes used in this study belong to low to moderate level of magnitude range (from 5.3 to 7.7) and, as pointed out by Trifunac and Brady (37), for each magnitude unit, the duration increases by about 2.0 seconds for acceleration records. This means that the maximum difference that can be attributed to the range of magnitude would be about 5.0 seconds only. This variability in the magnitude is not likely to affect the shape of the design spectra. In contrast, significant duration is greatly influenced by soil stiffness and the epicentral distance. Since strong motion duration is one of the most important factors from the viewpoint of maximum oscillator response (Trifunac, 35), it was practical to consider only the parameters which can affect the significant duration more strongly than others.

The available records were grouped mainly into three groups corresponding to three soil stiffness types. The three soil categories are loosely identified as soft (alluvial), medium stiff (sand or stiff clay) and hard (rock). This site classification is rather simplistic, but with the amount of information available, it is considered as the

best choice. In fact, this method of ground classification has been extensively used in the past (Trifunac, Brady, Seed, Idriss, Dorby, et al.). Seed and others (28) have also outlined the following description of various site conditions similar to the ones used in this study:

1. Rock Sites - Shale-like or sounder rock characteristics corresponding to shear wave velocities larger than 2500 ft/sec.

2. Stiff Soil Conditions - 150ft or less thick layers of stiff clay, sand or gravel overlaying on rock.

3. Deep Cohesionless Soil Conditions - 250ft or more thick cohesionless soils overlaying on the rock.

In this study, soft, medium stiff and hard soil conditions were labelled as 0, 1 and 2, respectively, which is the same notation as the one used by Trifunac and Brady (38). This data was available for all the 82 locations considered in this study.

The epicentral distance was the other parameter used to classify the groups further. As observed by Trifunac and Brady, the duration increases by about 1.0 to 1.5 seconds for every 10 km of epicentral distance. As such, this parameter is considered to be important in the classification scheme. In this study, the available records were further subdivided into the the records with the epicentral distances smaller and larger than 60 km. In the categories of medium and hard soils, no further sub-divisions were considered for large epicentral distance criterion, since the number of such records available under these distinctions is very small. In all, the selected 232 ground motion records were subdivided into nine groups, the organizations of which are described in Tables 3-11. The comparison of the relative

influence of these parameters on the duration of strong motion is discussed in Chapter 3.

2.4 Implicit Characteristics of Ground Motion

The three implicit parameters studied in this work are significant duration, average frequency and r.m.s. acceleration. Of these, it may be noted that the significant duration is a quantity subject to different interpretations. Housner, Seed, Idriss, Dorby, Trifunac and Brady (4, 5, 10, 37) are among many researchers who have proposed ideas on this concept. The following paragraphs discuss the methods proposed to estimate the above parameters.

2.4.1 Significant Duration

It is a well known fact that the earthquake records have three distinct phases in the time domain : the build-up phase, the strong-motion phase and the decay phase. Most of the energy dissipation occurs during the strong-motion phase. The maximum values of the acceleration, velocity, displacement and the response of an oscillator subjected to the input almost invariably occur during this time interval. This leads to the concept of a significant duration which may be looked upon as the part of the record in which most of the energy input occurs. Arias (2) presented the following formula as a measure of the energy content in an earthquake record :

$$I_A = \frac{\pi}{2g} \int_0^T a^2(t)dt \tag{2.1}$$

where I_A = Arias' measure of intensity, T = actual duration of record and $a(t)$ = ground acceleration at time t. Husid (15) proposed the idea of a normalized variable, $h(t)$, to describe the evolution of the shaking level of the record as :

$$h(t) = \frac{I_A(t)}{I_A(T)} = \frac{\int_0^t a^2(\tau)d\tau}{\int_0^T a^2(\tau)d\tau} \quad ; \quad 0 \leq t \leq T \tag{2.2}$$

Obviously, $h(0) = 0$ and $h(T) = 1.0$. The plot of h(t) versus time is called as the Husid plot (13). The power, P, due to the ground motion can be expressed as

$$P(t) = \frac{1}{\Delta} \int_t^{t+\Delta} a^2(\tau)d\tau \tag{2.3}$$

where Δ is a small time period during which $P(t)$, the rate of energy input is being calculated. This power, P, can be considered as the average value of $a^2(t)$ during the interval $(t, t + \Delta)$.

Several definitions of significant duration have been proposed based on the Husid plot. Husid initially defined significant duration as the time required for h(t) to reach a level of 0.95 (95%). Trifunac and Brady defined it as the time interval in which h(t) increases from 5% to 95%. This corresponds to the time interval during which 90% of the energy is input. This interpretation of significant duration is used in this study.

Figs. 1, 2 and 3 show the Husid plots drawn for soft, medium, and hard ground conditions, respectively, for three sample records considered in this study. Note that on the X-coordinate is chosen as the normalized time (being the ratio of the elapsed time to the total time of the record). This way, it is easier to compare the three plots, as the variability of the actual duration of the record does not enter the comparison. If we consider 'R' as the ratio of the significant duration to the actual duration, then as shown in the plots, it is observed that the value of R is the smallest for hard soil conditions and is larger for soft and medium stiff ground conditions. This is due to the fact that a stiff (rock) medium transmits the energy waves at a faster rate and the bulk of the total energy is dissipated in a rather short time interval. However, for soft mediums, the waves travel slower and there is much larger scattering of them in such relatively less homogeneous media. Thus, for soft soils, the strong motion phase is later followed by a period of moderate shaking during which a considerable amount of energy is transmitted. Thus, there is a sizeable content of long period motion in these seismic records (5). The Husid plots corresponding to the ground motion records from soft soils show a steadily rising curve followed by a drop in the slope in the curve and again followed by a rising curve before it flattens. On the contrary, the Husid plot for a rock medium rises steadily with a large slope before it reaches a plateau in its decay phase. All these features are illustrated in Figs. 1 to 3. Dorby, Idriss and Ng have reported similar behavior in reference 5.

Based on the definition given earlier, significant durations were computed for the 232 records used in this study. The influence of significant duration is obvious - for the same level of normalization, a record with a large significant duration would possess more energy than the one with a smaller significant duration. Further, the one with the larger significant duration is likely to cause larger response. The same observation is generally true for the duration ratio, R. For a given level of

normalization, the records with large duration ratios have a higher content of long periods and energy compared to the ones with smaller duration ratios.

2.4.2 Root Mean Square (r.m.s.) Acceleration

The following formula is used to compute the r.m.s. acceleration :

$$\bar{a} = \sqrt{\frac{1}{T} \int_0^T a^2(t)dt} \tag{2.4}$$

A recorded acceleration time-history is defined at discrete time steps of 0.02 seconds. To calculate $\bar{a}$ for such a time history, it is customary to assume that the ground motion varies linearly during a recorded time-interval. Thus the integrand function $a^2(t)$ is a discontinuous function over a series of digitization intervals. If the number of data points is 'N', then the number of such intervals would be (N-1). Thus, we can write the following equation for r.m.s. acceleration :

$$\bar{a} = \sqrt{\frac{1}{T} \sum_{i=1}^{N-1} \int_{t_i}^{t_{i+1}} a^2(t)dt} ; \quad t_i \leq t \leq t_{i+1} \tag{2.5}$$

During any i^{th} interval, one can express the integrand as follows :

$$a^2(\tau) = \left[a_i + \frac{a_{i+1} - a_i}{h_i} \tau \right]^2 ; \quad 0 \leq \tau \leq h_i \tag{2.6}$$

where h_i denotes the (constant) value of digitization time. Knowing this, we arrive at the following result :

$$\int_{t_i}^{t_{i+1}} a^2(t)dt = \frac{h_i}{3}\left(a_i^2 + a_i a_{i+1} + a_{i+1}^2\right) \qquad (2.7)$$

For $h_i = h$, a constant, the total number of digitization points, N, is equal to T/h. Substituting this and Eq. (2.7) into Eq. (2.5), we get

$$\bar{a} = \sqrt{\frac{1}{3N}\sum_{i=1}^{N-1}\left(a_i^2 + a_i a_{i+1} + a_{i+1}^2\right)} \qquad (2.8)$$

Equation (2.8) gives the value of the r.m.s. acceleration. These values were computed for all the records. The Vol. II of the Cal Tech tapes also gives the r.m.s. accelerations. The values calculated from equation (2.8) were in close agreement with the ones recorded on the tape.

In this study, r.m.s. acceleration is also used as a normalizing parameter. It is of interest to note that for the same level of peak acceleration, the records with large r.m.s. acceleration are likely to have more damage potential. A regression study between peak and r.m.s. acceleration would identify the groups which could cause more damage than the others.

2.4.3 Average Frequency Characteristics

The response of an elastic oscillator is greatly affected by the frequency characteristics of the seismic input. For example, if a high frequency oscillator is subjected to a ground motion which is dominated by similar high frequency content, then it is almost certain that a large resonance-like response will result. As may be

expected, this characteristic of a ground motion record depends on the stiffness of the medium through which it gets filtered.

A detailed frequency analysis of the time histories would require Fourier Spectrum Analysis using techniques like Discrete Fourier Transform (DFT). However, a simple measure of the average frequency of a time history can be obtained from the rate of the upward zero-level crossings, v_0^+ (20). The quantity, v_0^+ should be obtained by averaging across the ensemble and not along the time axis unless the process under consideration is an ergodic one. In this study however, the temporal average of the upcrossing rate is used to estimate the average frequency of a record.

These average frequencies were computed for the significant duration interval of all the records. The motivation to consider only the span of significant duration is that the response maxima almost invariably occur during this time interval and as such, only the frequency constitution of this interval is important from the view point of oscillator response. The average frequencies of the records analysed here were observed to be in the low range for soft sites, in the medium range for medium stiff sites and in the high range for hard sites.

The numerical results obtained for the implicit parameters are presented in Chapter 4.

Chapter III

Computation and Normalization of Response

Spectra

3.1 Introduction

The response spectrum curve of a ground motion is the plot of the maximum response versus frequency of an oscillator of constant damping ratio subjected to the ground motion. To calculate the maximum response of an oscillator, the time history analysis using Newmark's β- method or exact solutions for linear and bilinear hysteretic systems (16 and 19) can be used. Based on the statistical analysis of the spectrum curves of several time histories, the smoothed response spectra are defined for a range of oscillator frequencies and damping ratios for design purposes.

It may be noted that on Vol. IV of the EERL tapes (14), a set of response spectra values are available for relative displacement, relative velocity, pseudo acceleration

and absolute acceleration. But it does not contain information about relative acceleration response. Here, the relative acceleration spectra (RSA spectra) as well as spectra for a massless oscillator, useful in analysis of hysteretic structures, are also obtained for the recorded ground motions considered in this study. The details of the time history analysis method used in this study are discussed in this chapter.

3.2 Selection of Frequencies & Damping Ratios

As observed by Newmark, et al. (22), it is important to select closely spaced frequency values especially in the high frequency regions. Not doing so can considerably affect the shape of response spectrum. For this study, ninety-two oscillator periods ranging from .03 sec to 10 sec (frequencies from 33 cps to 0.1 cps) were used. These periods are listed in Table 12. The selected frequencies are close enough to produce a good spectrum for the whole range. Five values of damping ratio were used in this study. Again, these are the same as the ones on Vol. IV of the EERL tapes. The values selected are deemed to be representative of the viscous damping properties exhibited by most structural systems. The values of selected damping ratios are 0, 0.02, 0.05, 0.10 and 0.20, respectively.

3.3 Computation of Response

Many time-history analysis schemes are available to compute the response in the time domain. They mainly fall under two categories - exact and approximate solutions. Exact solutions are available for linear and a few types of materially nonlinear systems (16, 19). Approximate solution schemes are applicable to both linear and nonlinear systems. In the computations performed in this study, the exact solution algorithms were used to obtain the response.

3.3.1 Response of S.D.O.F. Oscillator

Consider the following differential equation governing the behavior of a single degree of freedom (s.d.o.f.) oscillator :

$$m\ddot{x} + c\dot{x} + kx = F(t) \tag{3.1}$$

where m = mass of the oscillator, c = viscous damping coefficient of the system and k = stiffness of the system. After dividing through by m and denoting ω_o = natural frequency of the oscillator and β_o = the damping ratio (referred to as the critical damping coefficient), we can rewrite equation (3.1) as follows :

$$\ddot{x} + 2\beta_o\omega_o\dot{x} + \omega_o^2 x = \frac{F(t)}{m} \tag{3.2}$$

where $\omega_o = \sqrt{k/m}$ and $\beta_o = c/c_{cr} = c/(2\omega_o m)$. The exact solution to equation (3.2) can be expressed using the convolution integral. The following equation describes the exact response :

$$x(t) = e^{-\beta_o \omega_o t}\left\{x_o \cos \omega_d t + \frac{v_o + \beta_o \omega_o x_o}{\omega_d} \sin \omega_d t\right\} \tag{3.3}$$

$$+ \int_0^t \frac{e^{-\beta_o \omega_o(t-\tau)}}{\omega_d} \sin \omega_d(t - \tau)\, \frac{F(\tau)}{m}\, d\tau$$

where $\omega_d = \omega_o\sqrt{1 - \beta_o^2} \wedge x_o$ and v_o are the displacement and the velocity at time $t = 0$ (initial conditions).

For the case of response due to base excitation, we can rewrite equation (3.2) as follows :

$$\ddot{x} + 2\beta_o \omega_o \dot{x} + \omega_o^2 x = -a(t) \tag{3.4}$$

where $a(t)$ = ground acceleration at time t.

The exact step-wise time history solution for the response of a linear elastic oscillator subjected to a time history of ground acceleration was first presented by Nigam and Jennings (23, 24). Their results can be expressed in a matrix form as follows :

$$\left\{\begin{array}{c} x_{i+1} \\ v_{i+1} \end{array}\right\} = \left[\begin{array}{cc} A_{11} & A_{12} \\ A_{21} & A_{22} \end{array}\right] \left\{\begin{array}{c} x_i \\ v_i \end{array}\right\} + \left[\begin{array}{cc} B_{11} & B_{12} \\ B_{21} & B_{22} \end{array}\right] \left\{\begin{array}{c} a_i \\ a_{i+1} \end{array}\right\} \tag{3.5}$$

where the entries of the coefficient matrices have been given by Nigam and Jennings in reference 23. Note that in the above equation, the subscripts i and $i + 1$ indicate

the values of the quantities (appearing in the equation) at times t_i and t_{i+1}, respectively.

The relative acceleration response can be obtained simply from the equation of motion. Substituting the known responses x_{i+1} and $\dot{x}_{i+1}$ in equation (3.4) and rearranging the terms, we can write

$$\ddot{x}_{i+1} = -2\beta_o\omega_o v_{i+1} - \omega_o^2 x_{i+1} - a_{i+1} \tag{3.6}$$

A computer program was written to implement the above scheme and the relative acceleration response was computed for all the oscillator periods considered in this study, since this data was not available in the Vol. IV tape of the EERL.

3.3.2 Response of Massless Oscillator

Consider now the following differential equation :

$$\dot{v} + \frac{1}{p} v = a(t) \tag{3.7}$$

where $\dot{v}$ is the acceleration and v is the velocity response. This equation has been referred to as the equation of a massless oscillator, since there is no mass involved with that equation. The parameter, p has the dimensions of time, and therefore, it is considered as the period of the massless oscillator. The ground excitation input is denoted by $a(t)$.

We again assume that the ground acceleration varies linearly between any two consecutive time steps. Thus, solving the governing differential equation of motion,

we get the following expression for the velocity response of the massless oscillator subjected to a ground acceleration time history :

$$v_{i+1} = e^{-h_i/p} v_i + p\left\{ \left(1 - e^{-h_i/p}\right)\left(1 + \frac{p}{h_i}\right) - 1 \right\} a_i \tag{3.8}$$

$$+ p\left\{ 1 - \frac{p\left(1 - e^{-h_i/p}\right)}{h_i} \right\} a_{i+1}$$

where h_i is the size of the ith time step. Knowing v_{i+1}, the velocity of the massless oscillator at time t_{i+1}, we can then write the expression for the acceleration at that time as :

$$\dot{v}_{i+1} = a_{i+1} - \frac{v_{i+1}}{p} \tag{3.9}$$

A computer program was also written to obtain the response of the massless oscillator in the period range of 0.03 seconds to 10.0 seconds.

3.4 Normalization of Response Spectra

One needs to have some kind of uniform normalization scheme for comparison of response spectra of different earthquake records, since, each record is unique as far as its explicit and implicit characteristics are concerned. It is customary to use peak acceleration as a normalization parameter as it is the most conspicuous characteristic of any ground motion record. Most response spectra are presented using this normalization scheme (21, 22, etc.). However, this is not the only way to

normalize responses. Pauschke (26) has attempted to use r.m.s. acceleration as a normalizing parameter. Among other approaches, peak velocity and peak displacement have been tried, too. Newmark, et al. (22) report that normalizations employing different peak ground responses over different frequency regions of the response spectra have also been made. It is suggested that the best results could perhaps be obtained by normalizing with respect to peak acceleration for developing spectra in the high frequency range, peak velocity for intermediate frequency range and peak displacement for low frequency range.

Based on the survey of the available literature and on the preliminary exploration done in this study, it appears that normalization is not a clear-cut task. As far as using a peak of the ground motion is concerned, the results are bound to be different depending upon which peak is used unless the various peaks of the expected ground motion are very well correlated. It was found in this study that the peaks of ground motion are well correlated only in the case of ground motions recorded in hard soil mediums. This is to be expected, since a hard medium practically behaves like an elastic oscillator. For other soil stiffness conditions, it is found that there is no strong correlation between the peaks of ground motion. This implies that the design spectra will depend on the choice of the normalization peak used in the cases of soft and medium stiff soil stiffnesses.

As mentioned earlier, r.m.s. value of ground motion is an attractive choice, but it is not an explicit but a derived characteristic of ground motion. Here, too, as observed in this study, a good correlation between peak and r.m.s. magnitudes of motion would mean that the results of either approach would be in close agreement. Since the groups are formed on the basis of similar physical characteristics, the r.m.s. and the peak values of the ground motion are expected to be well correlated. Herein, both these normalization procedures are used.

3.4.1 Normalization Using Peak Acceleration

The peak acceleration has traditionally been the most commonly used normalizing parameter. It is common to associate the severity of an earthquake record mainly with the peak ground acceleration. Generally, it is assumed that a record with high peak acceleration would cause larger response than the one with a lower peak acceleration value. However, this may not be true, since it does not take into account the role of other motion parameters.

In this scheme, first, a certain level of peak acceleration is chosen for the purpose of normalization. Then the response spectrum values of each record are multiplied by the ratio of normalized peak acceleration to the peak acceleration of that record. The underlying assumption which allows the computation of normalized response in this manner is that the oscillator behaves linearly. Finally, the averages of all the normalized responses (for any particular response quantity under consideration) are computed to obtain the mean normalized spectrum of that response quantity.

The argument that is often made against using the peak acceleration as a normalizing parameter is that this parameter is rather inadequate to describe to describe the intensity of a seismic record. For instance, an isolated peak preceded and followed by lower amplitude ripples in the ground-motion time-history is not likely to cause a large response. Also, it does not contain any information about the duration of the record. The peak acceleration may be a valid normalizing parameter only if the different records belonging to the ensemble are similar in nature as far as the other features are concerned. For example, a time-history of horizontal ground motion recorded on rock may not be comparable to the one of vertical ground motion

recorded on clay, since their peak, r.m.s., frequency and duration characteristics may be completely different, which will render the normalization scheme pointless.

In this study, most of the work was done using the peak normalization scheme. This was considered to be reasonable since the records used in this study have been grouped into ensembles of time-histories possessing similar physical characteristics. The normalization level of peak acceleration was chosen as 0.50G. Smoothed design spectra are then obtained for this level. It may be noted that in case of designing for any other peak level, the appropriate spectra can be obtained by simply multiplying the design spectrum by the ratio of design peak level to the normalization peak level.

3.4.2 Normalization Using R.M.S. Acceleration

The r.m.s. acceleration describes the input characteristics somewhat better than peak acceleration. This is due to the fact that a higher value of r.m.s. acceleration is a definite indicator of a greater power content. Also, it incorporates information about the duration characteristics. As mentioned earlier, the same may not be true if we use peak acceleration to characterize the input. Hence, one can be more confident in assuming that a larger level of r.m.s. acceleration causes a larger response. This makes r.m.s. acceleration seem like an attractive normalizing parameter. But it is not a popular choice, since r.m.s. acceleration is not an explicit property of a time-history like peak acceleration. The r.m.s. values have to be computed whereas the peaks are conspicuous enough to be simply picked out. Nevertheless, some researchers have tried to use r.m.s. acceleration to normalize the spectra. Pauschke (26) has compared spectra normalized by the r.m.s. and the peak accelerations. Our

own observations show that the shape of spectra thus obtained is similar to the traditional spectra obtained using the peaks of ground motion.

For implementation of this normalization strategy, a certain level of r.m.s. acceleration is chosen. Then, just as in the case of peak normalization, the individual responses are normalized to this level of acceleration using the concept of linearity of response. Finally, the means are computed to obtain the response spectra.

In this study, a few spectra obtained with the r.m.s. and the peak acceleration normalization process are compared. As mentioned in chapter 2, the best spectra are the ones which possess a relatively low variance of response over the range of the spectra. If r.m.s. normalization yields such low variance spectra then it would qualify as a better way of specifying response spectra. Linear regression analysis was carried out between peaks and corresponding r.m.s. accelerations for the records of each group to see the correlation of these parameters for that group. It may be noted that a good correlation (approximately straight line relationship) between these parameters would indicate that peak acceleration is as good a normalizing parameter as the r.m.s. acceleration. The results of all these studies are discussed in the next chapter.

Chapter IV

Numerical Results

4.1 Introduction

In this chapter, the numerical results obtained for various ground motion parameters, their statistical correlation, and the computed response spectra are presented. Correlation of the peak acceleration with the r.m.s. acceleration was considered to be important, since a good correlation between these two signifies that the results of response normalization are then independent of the choice of either of these parameters. Also, in a good grouping strategy, it would be expected that these two be well correlated. Finally, smoothed design spectra for single degree of freedom (s.d.o.f.) and massless oscillators are presented. Methods to estimate relative velocity and relative acceleration spectra from pseudo velocity spectra are also presented. The numerical results showing the applicability of these methods are also given.

4.2 Regression of Various Ground Motion Characteristics

It is of interest to examine the correlation between the various peak ground motion parameters like peak displacement, peak velocity and peak acceleration. Such correlation studies can be used to ascertain the validity of the concept of a standard earthquake as originally proposed by Newmark and Hall (21). In this study, a pair-wise correlation analysis was carried between peak values of displacement and velocity, velocity and acceleration, acceleration and displacement. The results are presented in Table 13. It is seen that in most cases, displacement and velocity are well correlated, but the other pairs of peak are not generally so, except in the case of group 5 belonging to the hard ground category, in which case they are rather well correlated. Because of the weak correlation pattern between the three peak ground motion parameters, the idea of defining a standard earthquake is considered to be inappropriate.

The results of the correlation of the peak with the r.m.s. acceleration are also given in Table 13. A good correlation between these two parameters is noted. The correlation is especially very good for group 5. Figs. 4 to 12 show the scattergrams and the lines of linear regression of r.m.s. acceleration on the peak acceleration for various groups considered in this study. On the line of best fit, the value of r.m.s. acceleration corresponding to a peak value of 0.50 G is also indicated. This particular r.m.s. value is utilized in response normalization later.

4.3 Peak Factor, Frequency & Duration Statistics

Peak factor is the ratio of the peak to the r.m.s. value of a given random process. In this study, the peak factor of ground acceleration was studied. The records with low peak factor will have a higher intensity (on Arias' scale) and r.m.s. value for a given level of peak acceleration. Such records are also likely to be more damaging than the ones with higher peak factors. The results of the study are presented in Table 14. The table shows the mean value and the standard deviation of the peak factor for each group. It is seen that the mean peak factor is generally lower for the groups belonging to the soft ground category. It is also observed that the peak factor is higher for the vertical motions than for the horizontal motions. Also, the peak factor is generally lower for the groups with larger epicentral distances. It can be seen that the groups for medium and hard ground have lower coefficient of variation compared to the groups in the soft ground category. This is probably due to the fact that the stiffer ground media closely behave like an elastic medium and hence display more consistent ground motion characteristics than the soft media.

The averages of the upcrossing rates, indicating the average frequency of the motion, are also shown in Table 14 for various groups. As seen from these results, the upcrossing rate is low for the soft ground conditions. For the medium and hard ground categories, the rate is observed to be higher for the vertical records, thus indicating the presence of higher frequencies in the vertical motion. Furthermore, the groups with smaller epicentral distance have a higher upcrossing rate when compared with the groups with larger epicentral distance.

Table 14 also gives the results for the duration ratios for the various groups. The duration ratio is defined as the ratio of significant duration to the actual duration. It

is obvious that the groups with high duration ratios are more potent than the ones with low duration ratios, especially for the response of low frequency oscillators, since the maximum response for these oscillators occurs toward the end of the strong motion phase. From Table 14, it can be seen that groups 1, 2, 3 and 4 in the soft and medium hard ground categories have higher duration ratios compared to group 5 in the hard ground category. Also, for a given ground stiffness, it can be seen that higher epicentral distance causes an increase in the duration ratio,and also the duration ratio is slightly larger for the vertical records than for the horizontal records belonging to the same group.

Also listed in Table 14 are the average values of ratios of the maximum jerk to the maximum ground acceleration and maximum ground velocity to the maximum ground displacement. These values are needed when one wants to predict the relative velocity spectra from the pseudo velocity spectra. The relevance of these parameters will be discussed later in this chapter.

4.4 Computed Spectra

Many response spectrum quantities have been considered in this study. The ones of particular interest are the relative velocity, pseudo velocity (or pseudo acceleration) and relative acceleration responses.

Figs. 13 to 21 show the mean relative velocity spectra corresponding to the nine cases of the five groups considered in this study. It can be seen that the shapes of each of these spectra are distinct when compared to each other. This is due to the fact that these shapes reflect the specific frequency and duration related

characteristics of the groups they represent. Figs. 22 to 30 show the plots for the pseudo velocity. Here, it is observed that the shapes of these spectra are similar to the relative velocity spectra. However, the major difference is that the pseudo velocity spectra are larger in magnitude in the high frequency (low period) range. These observations are consistent with the known characteristics of relative velocity and pseudo velocity spectra.

Figs. 31 to 39 show the plots for the mean relative acceleration spectra and Figs. 40 to 48 show the plots for the mean absolute acceleration spectra. It is seen that their shapes are also influenced by frequency and duration characteristics. However, it may be noted that here, the influence of duration parameter is not as apparent here as it was in the case of relative and pseudo velocity. The shifting of the frequency region in which response is maximum can be seen very clearly in these plots as one goes from one group to another. It is also noted that the absolute and relative acceleration spectra are almost the mirror images of each other. Figs. 49 to 84 show the same plots as in Figs. 13 to 48, but now drawn for the mean-plus-one-standard-deviation response quantities. It is noted that the same observations made earlier about the mean level response spectra are also true for the mean-plus-one-standard-deviation spectra.

Figs. 85 to 96 show plots of c.o.v. spectra for relative velocity, pseudo velocity, relative acceleration and absolute acceleration responses, respectively. It can be seen that for the relative and pseudo velocity and the relative acceleration spectra, the coefficient of variation generally increases with increasing oscillator period. Also, smaller values of damping ratio produce slightly larger c.o.v. spectra. Like in the case of the response spectra, the c.o.v. spectra for absolute acceleration shown in Figs. 94 through 96 are also the mirror images of the corresponding c.o.v. spectra for

relative acceleration, which is not surprising, since their actual spectra exhibit similar characteristic.

Figs. 97 to 99 show some sample plots of the ratio of the maximum relative velocity to the maximum pseudo velocity plotted against period. It is seen that the two spectra are approximately equal over the intermediate frequency range between 2.5 cps to about 0.3 cps. However, they are different outside of this frequency range. The difference over the higher frequency range has a special significance for the design and analysis of most civil engineering structures, since most low-rise structures lie in this frequency range. Taking the relative velocity spectrum equal to the pseudo velocity spectrum in the response calculation could thus give rise to inaccurate response values (30, 32). Figs. 100 to 102 show some sample plots of the ratio of the relative to the pseudo acceleration response spectrum values. In this case, however, there is no frequency range over which the two spectra can be considered equal.

Figs. 103 to 108 compare the horizontal and vertical spectra within a group and similar spectra in different groups. In Figs. 103 and 104, the horizontal and vertical response spectra belonging to to the same group are compared. This is done to highlight the effect of ground motion component on the response of an s.d.o.f. oscillator. Vertical ground motion records have, in general, a higher frequency content. As such, they cause larger response in the high frequency domain. Figs. 105 and 106 show the effect of ground stiffness on the response. As expected, the stiffer the ground the larger the oscillator response in the high frequency range. Figs. 107 and 108 show the effect of the epicentral distance on the oscillator response. As expected, the larger epicentral distances increase the response in the low frequency region. Thus it is seen that the grouping parameters do indeed affect the shape and

the magnitude of the response spectra; this validates the use of these parameters for grouping purposes.

In Figs. 102 to 108, the normalization of the different response spectra was done with respect to the peak ground acceleration. In Figs. 109 to 114, we show similar comparison between spectra now normalized with respect to the r.m.s. value of the ground acceleration. It is noted that the observations made for peak normalized response also apply to this case.

Figs. 115 to 132 are presented to compare the mean and the c.o.v. response spectra obtained with peak and r.m.s. normalization for some sample groups. The peak normalized spectra are for a maximum ground acceleration of 0.50 G, whereas, the r.m.s. normalized spectra are for the r.m.s. values calculated from regression equations given in Table 13, corresponding to the peak level of 0.50 G. It is observed that the spectra corresponding to the peak normalization are always higher than the ones corresponding to the r.m.s. normalization approach for all groups. For stiffer groups, the the two spectra are very close to each other. This is due to the very good correlation between the peak and the r.m.s. ground acceleration for these groups. This correlation was discussed earlier and is shown in Table 13. Comparison of the c.o.v. spectra shows that the r.m.s. approach gives higher c.o.v. values in the high frequency region and slightly lower values in the low frequency region. In fact, for very high frequencies, the c.o.v. values for the pseudo velocity and absolute acceleration should approach zero for the peak normalization scheme. For the r.m.s. normalization scheme, the c.o.v. values for these response quantities in the high frequency range reflects the variability of the r.m.s. values of the ground acceleration (corresponding to the fixed peak value), and not the variability of the response quantities themselves.

Figs. 133 to 138 compare the spectra of some sample groups with the corresponding spectra of the ungrouped ensemble of 162 horizontal and 70 vertical records. The comparison of the response spectra in Figs. 133, 135, and 137 shows the differences which occur due to the considerations of the differences in the frequency and duration characteristics of the input. Such separation of characteristics is lost in the case of the spectra obtained for the complete ensemble. This justifies the use of physical characteristics for grouping purposes. Figs. 134, 136 and 138 show that there is no significant difference in the magnitudes of the coefiicient of variation spectra corresponding to the grouped and ungrouped ensembles.

4.5 Proposed Smoothed Spectra for S.D.O.F. Oscillators

One of the primary objectives of this study was to define the design response spectra for various site characteristics. In this section, we define the mean and mean-plus-one-standard deviation design spectra for the pseudo velocity, relative velocity and relative acceleration quantities.

Generally, the design spectra are formed of straight line segments (on a log-log plot) that envelope the actual response spectra for a selected ensemble of ground motion time histories. In construction of design spectra, various zones of frequency that exhibit different response characteristics are identified by stipulating the corner frequencies (or the corner periods). Such a procedure was used by Newmark and Hall (21) and Newmark, Blume and Kapur (22) to define design response spectra for the design of nuclear reactor facilities. In their study, however, they lumped all

available ground motion records, without any grouping or site characteristics consideration. Since now we have a rather large ensemble of earthquake motions available to us, we can include the site classification in the construction of design response spectra.

To do this, it was first necessary to identify the corner periods (or corner frequencies) for each group of ground motions. These corner periods were selected by trial and error to give the best possible fit between the prescribed and the calculated ground response spectra. Their values for different groups of the ground motions are given in Tables 15 to 23.

To construct the design spectra for a set of damping ratios, it is necessary to know the amplification values at the corner periods. Herein, equations are provided to obtain the design ground response spectrum values for relative velocity, pseudo velocity and relative acceleration response, for a peak ground acceleration of 0.50 G at each corner period. For damping ratios between 0.02 and 0.20, these equations are of the following form :

$$Q = a \, \log(\beta) + b; \quad 0.02 \leq \beta \leq 0.20 \tag{4.1}$$

The coefficients a and b for different groups, at various periods, are given in Tables 15 to 23. These coefficients were obtained by regression analysis with some adjustments to provide the best possible fit between the prescribed and the calculated ground response spectra. These coefficients are provided both for mean and (mean + sd) spectrum values.

For the damping ratios less than 0.02, it is proposed to use the following linear relationship :

$$Q = Q(0) - \frac{\beta}{0.02} \, (Q(0.) - Q(0.02)) \tag{4.2}$$

where $Q(x)$ indicates the response spectrum value at damping ratio $\beta = x$. The Q values for $\beta = 0.0$ are provided in the tables. These values are slightly higher than the actual computed spectrum values for $\beta = 0$.

As mentioned earlier, the design values provided in Tables 15 to 23 correspond to a peak ground acceleration of 0.50 G. To obtain the design spectrum for any other level of peak ground acceleration, these coefficients need to be multiplied by the ratio = (prescribed peak acceleration in G-units / 0.50 G). In other words, the coefficients need to be multiplied by twice the prescribed (design) ground acceleration in G-units.

Figs. 139 to 147 show the comparison of the computed spectra with the smoothed spectra obtained using the coefficients proposed in Tables 5-13. It is seen that smoothed spectra compare well with the computed spectra. Figs. 148 to 156 show the proposed mean relative velocity (RSV) spectra for various groups. Each plot shows the curves corresponding to five damping ratios that were considered in this study. Figs. 157 to 165 show the same response quantity smoothed at (mean + sd) level. In the same way Figs. 166 to 183 show the proposed pseudo velocity spectra for mean and (mean + sd) levels. Figs. 184 to 201 present the smoothed response spectra for relative acceleration. It may be noted that the acceleration is expressed in 'G' units.

4.6 Comparison of the Proposed Spectra with the N-B-K & ATC Spectra

It is of interest to compare the pseudo acceleration (PSA) spectra proposed here with the spectra proposed by Newmark, Blume and Kapur referred to as the NBK spectra, and by the Applied Technology Council (1) referred to as the ATC spectra. The ATC spectra are prescribed for different site conditions whereas the NBK spectra are not. Figs. 202 to 205 compare the proposed mean-plus-one-standard-deviation spectra for various site stiffnesses with the NBK spectra, for the horizontal and vertical records, respectively. These spectra are drawn for a maximum ground acceleration of 0.40 G. Figs. 202 and 203 show that the NBK spectrum for horizontal motion underestimates the response in the middle frequency range (periods between 0.10 to 0.40 seconds). It is probably because the NBK spectrum does not usually represent an envelop of the ensemble spectra. On the other hand, the design spectra proposed herein are intended to closely envelop the ensemble spectra as much as possible. Also the NBK spectrum in Figs. 202 and 203 seems to disregard the presence of response peaks which have been observed for the medium stiff sites by Seed, et al as well. The NBK spectrum, however, provides higher values of response when compared with the spectrum for hard sites (group 5) in the low frequency region. Figs. 204 and 205 show that the NBK spectrum for vertical motion gives significantly higher design response values than the spectra of the groups selected in this study, especially so in the medium frequency range. Thus, it appears that the amplification of the vertical ground motion implied by the NBK spectra is overly conservative.

Although not explicitly stated, it appears that the ATC spectra represent the mean of the ensemble spectra, and therefore, here they are compared with the mean proposed spectra. Also, it should be noted that the ATC spectra are normalized for an "effective peak acceleration" (EPA) of 0.40 G. The proposed spectra are shown here for comparing them with the ATC spectra have also been calculated for a peak acceleration of 0.40 G. Figs. 206 and 207 show the comparisons between the proposed spectra for groups 1 and 2 and the corresponding ATC spectra for soft site conditions (site type S1) for horizontal and vertical excitations, respectively. Group 1 is for epicentral distances less than 60 km and group 2 is for epicentral distances greater than 60 km. The figures show that that compared to the proposed mean spectra, the ATC spectrum is generally higher, except around a period of 0.25 seconds. The same observation is seen to be true in Figs. 208 to 211; which have been drawn to show a similar comparison between the ATC spectra and the corresponding proposed spectra for medium stiff and hard site conditions (site types S2 and S1, respectively). This is probably because of the fact that the average of the computed spectra showed some peak spectrum values in the neighborhood of this period. These higher values have been accommodated in the proposed design spectra. Similar peak values were also shown in the results by Seed, et al (27).

4.7 Prediction of Relative Velocity from Pseudo Velocity

In the current earthquake designs, the pseudo velocity spectra are commonly prescribed. Usually this satisfies most design needs. However, as mentioned earlier, Singh, et al (30, 31, 32, 33) have demonstrated the need for the relative

velocity spectra in seismic response analysis of structures. The two types of velocity spectra are nearly equal to each other only in the medium frequency range. In the very low and very high frequency ranges, however, they differ from each other.

Due to a rather wide availability of the pseudo velocity spectra, it is of interest to see if the relative velocity spectra can be obtained from the pseudo velocity spectra. Gupta and Jaw (7) have reported an approach for this purpose. Their method utilizes the following two parameters related to the frequency characteristics of the input ground motion :

$$\omega_h = \frac{\text{Maximum Jerk}}{\text{Maximum Ground Acceleration}} \qquad (4.3a)$$

$$\omega_l = \frac{\text{Maximum Ground Velocity}}{\text{Maximum Ground Displacement}} \qquad (4.3b)$$

where the jerk is the time rate of change of the acceleration.

In this study, it was found that better estimation of the relative spectra can be obtained by suitably modifying the values of ω_h and ω_l. A technique was proposad in this study in which two frequency related related parameters, $\overline{\omega}_h$ and $\overline{\omega}_l$, are used to estimate the PSV spectrum. The technique proposed herein is appropriate for the case when the characteristics of the ground motion and the site corresponding to the available PSV spectrum are known. The following are the relationships proposed in this study :

$$RSV \simeq \frac{\overline{\omega}_h}{\omega_o} (PSV); \quad T \leq T_l \qquad (4.4a)$$

$$RSV \simeq [\,\overline{\omega}_h - \frac{(T - T_l)}{(T_3 - T_l)} (\overline{\omega}_h - \omega_3)] \frac{(PSV)}{\omega_o}; \quad T_l \leq T \leq T_3 \qquad (4.4b)$$

$$RSV \simeq (PSV); \quad T_3 \le T \le T_h \tag{4.4c}$$

$$RSV \simeq \frac{\overline{\omega}_l}{\omega_o} (PSV); \quad T \ge T_h \tag{4.4d}$$

where RSV and PSV are the relative and pseudo velocity spectrum values at oscillator period, T, and $\overline{\omega}_h$ and $\overline{\omega}_l$ are the frequency parameters, which have been obtained for each group of records and are given in Tables 15-23. As mentioned earlier, these are related to the maximum jerk, acceleration, velocity and displacement values of the records. T and ω_o are, respectively, the period and natural frequency for the oscillator at which the relative velocity spectrum value is being calculated. T_3 is the third corner period corresponding to the group of ground motion under consideration (see Tables 2 to 10) and $T_l = \frac{2\pi}{\omega_h}$, $T_h = \frac{2\pi}{\omega_l}$, and $\omega_3 = \frac{2\pi}{T_3}$.

Figs. 212-214 compare a sample of computed relative velocity spectra with the predicted spectrum calculated using (i) equations (4.4) and (ii) the method proposed of Gupta and Jaw. The compariosons have been shown for some sample groups of ground motions considered in this study. It is seen that the method proposed in this study gives a good estimate in all frequency regions unlike the Gupta-Jaw method which overestimates the RSV spectrum in the low frequency end of the spectrum. In Figs. 215-217, RSV spectra for some individual spectra have been predicted using the proposed (group-based) method and the (self-based) method similar to Gupta and Jaw. Here, it is observed that the two methods produce noticeably different results in high and low frequency regions of the spectrum. Again, the results of the proposed method are seen to be better agreement with the computed RSV spectra.

4.8 Prediction of Relative Acceleration from Other Known Spectra

As mentioned earlier, the need for relative acceleration as a design input has also been reported by Singh, et al. (31, 33), but such spectra are rarely available. Singh and Mehta (33) have proposed the following equation to estimate the relative acceleration response spectrum values :

$$(RSA)^2 = (\ddot{x}_{g_{max}})^2 - (PSA)^2 + 2\omega_o^2(1 - 2\beta_o^2)(RSV)^2 \tag{4.6}$$

In this study, the above equation was used to estimate the mean relative acceleration spectra knowing the mean pseudo acceleration and relative velocity spectra. Sample results were obtained for each group considered in this study. Figs. 218 to 220 show some representative plots obtained using the above-mentioned approach. It is seen that the comparison between the computed and predicted spectra is very good, except for a very small band of frequency in the high frequency region. However, even here the prediction error is not significant.

In order to test the suitability of this approach for individual earthquake records, the computed and the predicted RSA spectra were compared for three sample earthquake records. The results of this comparison are shown in Figs. 221 to 223. It may be noted that the spectra shown there are normalized for a peak acceleration of 0.50 G. As in the case of group spectra, it is observed here that the proposed prediction method works very well, although it performs slightly better for the spectra corresponding to the groups than for the individual records.

4.9 Computed & Smoothed Spectra for Massless Oscillators

As mentioned earlier, a need has recently been felt for the response characteristics of massless (half-degree-of-freedom) oscillators. One needs to know these response characteristics in order to be able to predict the response of hysteretic oscillators using equivalent linearization approach (34). With this goal in mind, herein in this study, the response of massless oscillators to the earthquake groups considered in this study was examined. The results of this work are presented in this section.

Figs. 224 to 232 show the mean and (mean + sd) velocity response of massless oscillators. The same figures also show the proposed smoothed response spectra. It is seen that the spectra are quite well defined in that they are almost linear and increasing with the oscillator period. The smoothed response spectra have been proposed by considering four corner periods (three frequency regions). At each corner period the value of design response is stipulated simply by increasing the actual response value by a suitable safety margin. Table 24 provides the response values to be used at these corner periods. As seen in Figs. 224 to 232, the proposed spectra well approximate the actual spectra. Fig. 233 shows the coefficient of variation (c.o.v.) spectra for relative velocity response of some sample groups. It is seen that the c.o.v. values increase monotonically with increasing oscillator period.

Figs. 234 to 242 show the spectra for acceleration response of a massless oscillator. It is seen that the acceleration values reach an asymptote at large period values. At low periods (high frequencies), the acceleration values increase in a parabolic-like manner. The same figures show the proposed smoothed response

spectra. For the low period range, the following parabolic equation is proposed to estimate the response in that range :

$$Q = A [\log(p)]^2 + B \log(p) + C \qquad (4.7)$$

where 'Q' is the estimated acceleration value at oscillator period 'p'. The constants A, B and C for the best fit are given in Table 25.

In Figs. 234 to 242, it can be seen that the proposed spectra are in good agreement with the actual spectra, with a slight underestimation ($< 5\%$) in the low period range. Fig. 243 shows c.o.v. spectra of the acceleration response for a few sample groups. It is observed that the magnitude of the c.o.v. spectra for acceleration is much smaller than for the velocity response. Also, it is seen that the c.o.v. spectra for acceleration decrease monotonically with increasing period until oscillator periods of about 1.0 to 2.0 seconds. However, for periods higher than that, there is a slight increase in the c.o.v. values.

Chapter V

Conclusions

This study examines the need and appropriateness of grouping the earthquake ground motions according to geological characteristics of the site to obtain the site dependent spectra. The parameters considered are the site stiffness and epicentral distance. The study shows that the spectra corresponding to different site conditions are indeed distinct in their shapes. It has also been shown that the different criteria considered in this study do indeed affect the shapes of response spectra in a way that is predictable.

In the past, the concept of a standard earthquake has been used in defining design motion. The results of correlation studies between different ground motion parameters, however, show that it is not reasonable to propose a standard earthquake, since the peak values of the ground displacement, velocity and acceleration are not well correlated except in the case of the hard ground category. The correlation study between the peak and the r.m.s. acceleration of the ground motion within each group showed that the two are generally well correlated. This

implies that the response spectrum prediction based on either the peak or r.m.s. acceleration parameters would be in reasonably good agreement. To verify this, the spectra obtained with the peak and r.m.s. normalizaton schemes have been compared. It was observed that the two give results that are in reasonably good agreement, particularly for the groups corresponding to medium stiff and hard sites. The spectra obtained by using the r.m.s. normalization slightly smaller magnitude than the ones obtained by the peak normalization.

In practice, the N-B-K (22) and the ATC (1) spectra, which provide smoothed response spectra only for the pseudo velocity response, are commonly used. Lately, however, the need for defining the input in terms of the relative velocity and acceleration spectra has also been identified. Thus, in this work, relative velocity and relative acceleration spectra along with the pseudo acceleration spectra have been proposed for various groups of earthquake ground motions. Also, a method has been presented to predict the relative velocity spectra directly from the pseudo velocity spectra of each group. The results show that the proposed method of prediction works very well except (sometimes) in the very low period region, which is usually not of design interest.

Prediction of relative acceleration spectra is also considered important in the light of the mode acceleration approach proposed by Singh (31, 33) for the analysis of high frequency structures. It is hard to predict relative acceleration spectra directly from the pseudo velocity spectra. However, if the relative velocity spectra are also known, then relative acceleration spectra can be accurately predicted using the approach proposed by Singh and Mehta (33). The numerical results show that this method works very well for all the groups considered in this study. Since, the relative velocity spectra can be predicted from the pseudo velocity spectra, one can also develop the relative acceleration spectra directly from the pseudo velocity spectra.

The proposed pseudo velocity or acceleration spectra have also been compared with the commonly used N-B-K (22) and ATC (1) spectra. This comparison shows that the N-B-K spectra overestimate the response for medium and high frequencies. Comparison between the ATC and the corresponding proposed smoothed spectra revealed that the ATC spectra provide higher values in the medium frequency range. Yet, they generally compare well with the spectra proposed in this study. It is noted that the effect of the epicentral distance parameter seen in the proposed spectra is absent in the spectra proposed by ATC.

In addition to the pseudo velocity spectra and the relative velocity and acceleration spectra for single degree of freedom oscillators, the spectra for the response of a massless oscillator, with one half degree of freedom, have also been defined for different groups of earthquake ground motions. These spectra are utilized as input in the response analysis of nonlinear hysteretic structures using the equivalent linearization method (34). It is observed that the response spectra corresponding to the relative velocity and the relative acceleration of the massless oscillator are generally very smooth and well behaved. Here, smoothed design spectra have also been proposed for these response quantities.

References

1. Applied Technology Council, 'Tentative Provisions for the Development of Seismic Regulations for Buildings', ATC Publication ATC 3-06, Published by the U. S. Government Printing Office, Washington, D. C., June 1978.

2. Arias, A., 'A Measure of Earthquake Intensity, in Seismic Design for Nuclear Power Plants', Ed. R. J. Hansen, Massachusetts Institute of Technology Press, Cambridge, MA, 1970.

3. Arnold, P., Vanmarcke, E. H. and Gazetas, G., 'Frequency Content of Ground Motions During the 1971 San Fernando Earthquake', Research Report Publication No. R76-3, Department of Civil Engineering, Massachusetts Institute of Technology, Cambridge, MA, 1976.

4. Bolt, B. A., 'Duration of Strong Ground Motion', 6-D, Paper No. 292, Proceedings of the 5th World Conference on Earthquake Engineering, Rome, Italy, 1973.

5. Dorby, R., Idriss, I. M., Chang, C.-Y. and Ng, E., 'Influence of Magnitude, Site Conditions and Distance on Significant Duration of Earthquakes', Proceedings of the 6th World conference on Earthquake Engineering, New Delhi, India, 1977.

6. Dorby, R., Idriss, I. M. and Ng, E., 'Duration Characteristics of Horizontal Components of Strong-Motion Earthquake Records', Earthquake Engineering Research Laboratory, California Institute of Technology, 1978.

7. Gupta, A. K. and Jaw, J. W., 'Response Spectrum Method for Nonclassically Damped Systems', Civil Engineering Research Report, Department of Civil Engineering, North Carolina State University at Raleigh, NC, April 1985.

8. Hall, W. J., Nau, J. M. and Zahrah, T. H., 'Scaling of Response Spectra and Energy Dissipation in SDOF Systems', Proceedings of the 8th World Conference on Earthquake Engineering, Vol. IV, pp. 7-14, San Francisco, CA, July 1984.

9. Housner, G. W., ' Intensity of Ground Motion During Strong Earthquakes' Earthquake Engineering Research Laboratory, California Institute of Technology, Pasadena, CA, 1952.

10. Housner, G. W., 'Measures of Severity of Earthquake Ground Shaking', Proceedings of the United States National Conference on Earthquake Engineering, Ann Arbor, MI, 1975.

11. Hudson, D. E., Brady, A. G. and Trifunac, M. D., 'Strong-Motion Earthquake Accelerograms, Digitized and Plotted Data - Vol. I', Earthquake Engineering Research Laboratory, California Institute of Technology, Pasadena, CA, 1969.

12. Hudson, D. E., Brady, A. G., Trifunac, M. D. and Vijayaraghavan, A., 'Strong-Motion Earthquake Accelerograms, Corrected Accelerograms and Integrated Ground Velocity and Displacement Curves - Vol. II' Earthquake Engineering Research Laboratory, California Institute of Technology, Pasadena, CA, 1971.

13. Hudson, D. E., Trifunac, M. D. and Brady, A. G., 'Strong-Motion Earthquake Accelerograms, Response Spectra - Vol. III', Earthquake Engineering Research Laboratory, California Institute of Technology, Pasadena, CA, 1972.

14. Hudson, D. E., Trifunac, M. D., Udwadia, F. E., Brady, A. G. and Vijayaraghavan, A., 'Strong-Motion Earthquake Accelerograms, Fourier Spectra - Vol. IV', Earthquake Engineering Research Laboratory, California Institute of Technology, Pasadena, CA, 1972.

15. Husid, R., 'Gravity Effects on the Earthquake Response of Yielding Structures', Earthquake Engineering Research Laboratory, California Institute of Technology, Pasadena, CA, 1967.

16. Malushte, S. R., 'Seismic Design Response of Simple Nonlinear Hysteretic Structures', M. S. Thesis, Department of Engineering Science & Mechanics, Virginia Tech, Blacksburg, VA, Sept. 1984.

17. McCown, B. E. and Singh, M. P., 'Seismic Design Response of Nonclassically Damped Structures: A Mode Acceleration Approach', Technical Report Submitted to the National Science Foundation Under Grant No. CEE-8214070, June 1984.

18. Mohraz, B., 'A study of Earthquake Response Spectra for Different Geological Conditions', Bulletin of the Seismological Society of America, Vol. 66, pp. 915-935, 1976.

19. Nau, J. M., 'Computation of Inelastic Response Spectra', Journal of the Engineering Mechanics Division, ASCE, Vol. 109, No. 1, Feb. 1983.

20. Newland, D. E., 'An Introduction to Random Vibrations and Spectral Analysis', Longman Group Ltd., London, Chapter 8 of Fourth Impression, 1981.

21. Newmark, N. M. and Hall, W. J., 'Procedures and Criteria for Earthquake-Resistant Design', Building Practices for Disaster Mitigation, Building Science Series 46, NBS, pp. 209-237, 1973.

22. Newmark, N. M., Blume, J. A. and Kapur, K. K., 'Seismic Design Spectra for Nuclear Power Plants', Journal of the Power Division, ASCE, Vol. 99, Nov. 1973.

23. Nigam, N. C. and Jennings, P. C., 'Digital Calculation of Response Spectra from Strong-Motion Earthquake Records', Earthquake Engineering Research Laboratory, California Institute of Technology, Pasadena, CA, June 1968.

24. Nigam, N. C. and Jennings, P. C., 'Calculation of Response Spectra from Strong-Motion Earthquake Records', Bulletin of the Seismological Society of America, Vol. 59, No. 2, April 1969.

25. Ohi, K. and Tanaka, H., 'Frequency-Domain Analysis of Energy Input Made by Earthquakes', Proceedings of the 8th World Conference on Earthquake Engineering, Vol. IV, pp. 67-74, San Francisco, CA, July 1984.

26. Pauschke, J. M. and Krishnamurty, S., 'Peak Vs. Root Mean Square (RMS) Acceleration as a Response Parameter', Proceedings of the 8th World Conference on Earthquake Engineering, Vol. IV, pp. 45-52, San Francisco, CA, July 1984.

27. Seed, H. B., Ugas, C. and Lysmer, J., 'Site Dependent Spectra for Earthquake-Resistant Design', Report No. EERC 74-12, College of Engineering, University of California, Berkeley, CA, 1974.

28. Seed, H. B., Murarka, R., Lysmer, J. and Idriss, I. M., 'Relationships of Maximum Acceleration, Maximum Velocity, Distance from Source and Local Site Conditions for Moderately Strong Earthquakes', Report No. EERC 75-17, College of Engineering, University of California, Berkeley, CA, 1975.

29. Singh, M. P., 'Seismic Design Input for Secondary Systems', Journal of the Structural Division, ASCE, Vol. 106, No. ST2, Proc. Paper 15207, February 1980, pp. 505-517.

30. Singh, M. P., 'Seismic Response Combination of High Frequency Modes', Proceedings of the 7th European Conference on Earthquake Engineering, Athens, Greece, Sept. 1982.

31. Singh, M. P., 'Extended Applications of Relative Acceleration and Velocity as Seismic Design Inputs', Proceedings of the 8th World Conference on Earthquake Engineering, Vol. IV, pp. 29-36, San Francisco, CA, July 1984.

32. Singh, M. P. and Chu, S. L., 'Stochastic Considerations in Seismic Analysis of Structures', Earthquake Engineering and Structural Dynamics, Vol. 4, pp. 295-307, 1976.

33. Singh, M. P. and Mehta, K. B., 'Seismic Design Response by an Alternative SRSS Rule', Earthquake Engineering and Structural Dynamics, Vol. II, pp. 771-783, 1983.

34. Singh, M. P., Maldonado, G. O., Heller, R. A. and Faravelli, L., 'Modal Analysis of Nonlinear Hysteretic Structures for Seismic Motions', Proceedings of IUTAM Symposium on Nonlinear Stochastic Dynamic Engineering Systems, Innsbruck, June 21-26, 1987.

35. Trifunac, M. D., 'Ground Motion - Dependence of Peaks on Earthquake Magnitude, Epicentral Distance and Recording Site Conditions', Earthquake Engineering Research Laboratory, California Institute of Technology, 1975.

36. Trifunac, M. D. and Brady, A. G., 'On the Correlation of Seismic Intensity Scales with the Peaks of Recorded Strong Ground Motion', Bulletin of the Seismological Society of America, Vol. 65, No. 1, pp. 139-162, Feb. 1975.

37. Trifunac, M. D. and Brady, A. G., 'A study on the Duration of Strong Earthquake Ground Motion', Bulletin of the Seismological Society of America, Vol. 65, No. 3, pp. 581-626, June 1975.

38. Trifunac, M. D. and Brady, A. G., 'Correlations of Peak Accelerations, Velocity and Displacement with Earthquake Magnitude, Distance and Site Conditions', International Journal of Earthquake Engineering and Structural Dynamics, 1975.

39. Zhou, X., Wang, G. and Su, J., 'Seismic Design Response Spectra Considering Intensity, Epicentral Distance and Site Condition', Proceedings of the 8th World Conference on Earthquake Engineering, Vol. IV, pp. 15-22, San Francisco, CA, July 1984.

TABLE 1

List of the Earthquakes Selected for the Study

No.	Earthquake Area	Time Time Zone	Mo. Day Year	Long. (W) 0 ' "	Lat. (N) 0 ' "	Mag.
01	Imperial Valley, Cal	2037 PST	May 18, 1940	115 27 00	32 44 00	6.7
02	Northwest California	2011 PST	Oct 07, 1951	124 48 00	40 17 00	5.8
03	Kern County, Cal	0453 PDT	Jul 21, 1952	119 02 00	35 00 00	7.7
04	San Hose, Cal	1801 PST	Sep 04, 1955	121 47 00	37 22 00	5.8
05	El Alamo, Baja, Cal	0633 PST	Feb 09, 1956	115 55 00	31 45 00	6.8
06	San Francisco, Cal	1144 PST	Mar 22, 1957	122 29 00	37 40 00	5.3
07	Hollister, Cal	2323 PST	Apr 08, 1961	121 18 00	36 40 00	5.7
08	Borrego Mountain, Cal	1830 PST	Apr 08, 1968	116 08 00	33 09 00	6.4
09	Southern California	0110 PST	Oct 02, 1933	118 08 00	33 47 00	5.4
10	Lower California	0552 PST	Dec 30, 1934	115 30 00	32 12 00	6.5
11	First Northwest Cal	2210 PST	Sep 11, 1938	124 48 00	40 18 00	5.5
12	Second Northwest Cal	0145 PST	Feb 09, 1941	125 24 00	40 54 00	6.4
13	Western Washington	1156 PST	Apr 13, 1949	122 42 00	47 06 00	7.1
14	Northern California	0441 PDT	Sep 22, 1952	124 25 00	40 12 00	5.5
15	Wheeler Ridge, Cal	1534 PST	Jan 12, 1954	119 01 00	35 00 00	5.9
16	Puget Sound, Wash	0729 PST	Apr 29, 1965	122 18 00	47 24 00	6.5
17	Parkfield, Cal	2026 PST	Jun 26, 1966	120 54 00	35 54 00	5.6
18	San Fernando, Cal	0600 PST	Feb 09, 1971	118 23 42	34 24 00	6.4

TABLE 2

Selected Recording Locations and Relevant Data

No.	Recording Station	Long. (W) 0 ' "	Lat. (N) 0 ' "	Site Type	Year of Record	Epicentral Distance (in km)
001	El Centro Site Imperial Valley Irrigation Dist.	115 32 55	32 47 43	Soft	May 1940	11.56
002	Ferndale City Hall	124 15 00	40 34 00	Medium	Oct 1951	56.47
003	Cal Tech Athenaeum, Pasadena, California	118 07 17	34 08 20	Soft	Jul 1952	127.62
004	Taft Lincoln School Tunnel	119 27 00	35 09 00	Soft	Jul 1952	41.61
005	Santa Barbara Court House	119 42 05	34 25 28	Soft	Jul 1952	88.86
006	Hollywood Storage Basement	118 20 00	34 05 00	Soft	Jul 1952	120.96
007	Hollywood Storage P.E. Lot	118 20 00	34 05 00	Soft	Jul 1952	120.96
008	San Hose Bank of America Basement	121 53 00	37 20 00	Soft	Sep 1955	9.63
009	El Centro Site Imperial Valley Irrigation Dist.	115 32 55	32 47 43	Soft	Feb 1956	121.82
010	San Francisco Southern Pacific Building Basement	122 24 00	37 48 00	Soft	Mar 1957	16.61
011	San Francisco Alexander Building Basement	122 24 00	37 47 00	Medium	Mar 1957	14.97
012	San Francisco Golden Gate Park	122 28 42	37 46 12	Medium	Mar 1957	11.55
013	San Francisco State Building Basement	122 25 00	37 47 00	Medium	Mar 1957	14.30
014	Oakland City Hall Basment	122 16 00	37 48 00	Medium	Mar 1957	24.25
015	Hollister City Hall	121 24 00	36 51 00	Soft	Apr 1961	22.35
016	El Centro Site Imperial Valley Irrigation Dist.	115 32 55	32 47 43	Soft	Apr 1968	67.62
017	Ferndale City Hall	124 15 00	40 34 00	Medium	Sep 1938	55.44
018	Ferndale City Hall	124 15 00	40 34 00	Medium	Feb 1941	104.22
019	Seattle, Wash. Dist. Engr. Office at Army Base	122 20 31	47 33 34	Soft	Apr 1949	58.04
020	Olympia, Wash. Highway Test Laboratory	122 54 00	47 02 00	Soft	Apr 1949	16.94
021	Ferndale City Hall	124 15 00	40 34 00	Medium	Sep 1952	14.22
022	Taft Lincoln School Tunnel	119 27 00	35 09 00	Soft	Jan 1954	43.01
023	Olympia, Wash. Highway Test Laboratory	122 54 00	47 02 00	Soft	Apr 1965	61.23
024	Cholame-Shandon California Array No. 02	120 17 13	35 43 35	Soft	Jun 1966	58.82
025	Cholame-Shandon California Array No. 05	120 19 42	35 42 00	Soft	Jun 1966	56.40
026	Cholame-Shandon California Array No. 08	120 54 00	35 40 18	Soft	Jun 1966	25.51
027	Cholame-Shandon California Array No. 12	120 24 12	35 38 12	Soft	Jun 1966	53.77
028	Pacoima Dam, California	118 23 48	34 20 06	Hard	Feb 1971	7.26
029	250 E First Street Basement, Los Angeles, Cal	118 14 26	34 03 01	Soft	Feb 1971	41.64
030	445 Figueroa Street, Sub-Basement, Los Angeles, Cal	118 15 24	34 03 12	Soft	Feb 1971	40.82
031	Castaic Old Ridge Route, California	118 39 24	34 33 18	Medium	Feb 1971	29.55

TABLE 2 (contd.)

No.	Recording Station	Long. (W) 0 ' "	Lat. (N) 0 ' "	Site Type	Year of Record	Epicentral Distance (in km)
032	Hollywood Storage Basement	118 20 00	34 05 00	Soft	Feb 1971	35.85
033	Hollywood Storage P.E. Lot	118 20 00	34 05 00	Soft	Feb 1971	35.85
034	1901 Ave of The Stars Sub- Basement, Los Angeles, Cal	118 24 58	34 03 14	Soft	Feb 1971	38.70
035	3710 Wilshire Boulevard, Basement, Los Angeles, Cal	118 18 24	34 03 42	Medium	Feb 1971	38.69
036	7080 Hollywood Boulevard, Basement, Los Angeles, Cal	118 20 37	34 06 05	Soft	Feb 1971	33.71
037	Wheeler Ridge, California	118 59 05	35 01 05	Soft	Feb 1971	87.65
038	4680 Wilshire Boulevard, Basement, Los Angeles, Cal	118 19 51	34 03 41	Medium	Feb 1971	38.31
039	Water and Power Building Basement, Los Angeles, Cal	118 15 00	34 03 00	Medium	Feb 1971	41.38
040	Santa Felicia Dam - Outlet Works, California	118 45 02	34 27 41	Medium	Feb 1971	33.32
041	3407 Sixth Street Basement Los Angeles, Cal	118 17 43	34 03 45	Soft	Feb 1971	38.84
042	Engineering Building Santa Ana, Orange County, Cal	117 52 00	33 45 00	Soft	Feb 1971	87.61
043	808 South Olive St, Street Level, Los Angeles, Cal	118 15 03	34 02 07	Soft	Feb 1971	42.91
044	2011 Zonal Avenue, Basement, Los Angeles, Cal	118 12 16	34 03 36	Medium	Feb 1971	41.92
045	120 N Robertson Blvd, Sub- Basement, Los Angeles, Cal	118 22 58	34 04 32	Soft	Feb 1971	36.26
046	646 South Olive Avenue, Basement, Los Angeles, Cal	118 15 14	34 02 50	Soft	Feb 1971	41.55
047	Edison Company, Colton, California	117 18 45	34 03 34	Soft	Feb 1971	107.11
048	Pumping Plant, Pearblossom California	117 55 18	34 30 30	Soft	Feb 1971	45.39
049	OSO Pumping Plant, Gorman, California	118 43 03	34 48 05	Medium	Feb 1971	45.39
050	UCLA Reactor Laboratory, Los Angeles, Cal	118 27 00	34 04 00	Soft	Feb 1971	53.67
051	Cal Tech Seismological Lab Pasadena, California	118 10 15	34 08 55	Hard	Feb 1971	34.97
052	Cal Tech Athenaeum, Pasadena, California	118 07 17	34 08 20	Soft	Feb 1971	38.68
053	Cal Tech Millikan Library, Pasadena, California	118 07 30	34 08 12	Soft	Feb 1971	38.65
054	Jet Propulsion Lab, Base- ment, Pasadena, California	118 10 25	34 12 01	Medium	Feb 1971	30.35
055	611 W Sixth Floor Basement Los Angeles, Cal	118 15 16	34 02 57	Soft	Feb 1971	41.33
056	Palmdale Fire Station, Store Room, Palmdale, Cal	118 06 45	34 34 40	Soft	Feb 1971	32.85
057	15250 Ventura Boulevard, Basement, Los Angeles, Cal	118 27 50	34 09 14	Soft	Feb 1971	28.18
058	8639 Lincoln Ave, Basement Los Angeles, Cal	118 25 07	33 57 36	Soft	Feb 1971	49.19
059	900 South Fremont Ave, Basement, Alhambra, Cal	118 08 56	34 05 06	Soft	Feb 1971	41.97
060	2600 Nutwood Ave, Basement Fullerton, Cal	117 52 53	33 52 39	Soft	Feb 1971	75.34

TABLE 2 (contd.)

No.	Recording Station	Long. (W) 0 ' "	Lat. (N) 0 ' "	Site Type	Year of Record	Epicentral Distance (in km)
061	435 N. Oakhurst Ave, Basement, Beverly Hills, Cal	118 23 26	34 04 40	Soft	Feb 1971	35.99
062	1800 Century Pk East, Bsmt (P-3), Los Angeles, Cal	118 24 52	34 03 46	Soft	Feb 1971	37.70
063	15910 Ventura Boulevard, Basement, Los Angeles, Cal	118 28 48	34 09 36	Soft	Feb 1971	27.77
064	Lake Hughes, Array Station No. 01, California	118 26 24	34 40 30	Hard	Feb 1971	30.98
065	Lake Hughes, Array Station No. 04, California	118 28 48	34 38 30	Hard	Feb 1971	27.94
066	Lake Hughes, Array Station No. 09, California	118 33 42	34 36 30	Hard	Feb 1971	27.79
067	Lake Hughes, Array Station No. 12, California	118 33 36	34 34 18	Medium	Feb 1971	24.37
068	15107 Vanowen Street, Basement, Los Angeles, Cal	118 07 42	34 11 42	Soft	Feb 1971	33.73
069	616 South Normandie Ave, Basement, Los Angeles, Cal	118 17 56	34 03 45	Medium	Feb 1971	38.77
070	3838 Lankershim Boulevard, Basement, Los Angeles, Cal	118 21 39	34 08 15	Medium	Feb 1971	29.51
071	1150 South Hill St., Sub-Basement, Los Angeles, Cal	118 15 34	34 02 40	Soft	Feb 1971	41.69
072	Tehachapi Pumping Plant, CWR Site, Grapevine, Cal	118 49 36	34 56 30	Medium	Feb 1971	72.26
073	4000 West Chapman Ave, Basement, Orange, Cal	117 53 33	33 46 51	Soft	Feb 1971	83.42
074	6074 Park Drive, Ground Level, Wrighthood, Cal	117 37 58	34 21 40	Medium	Feb 1971	70.55
075	Carbon Canyon Dam, Cal	117 50 26	33 54 52	Medium	Feb 1971	74.73
076	Whittier Narrows Dam, Cal	118 03 10	34 01 12	Soft	Feb 1971	53.02
077	San Antonio Dam, Upland, California	117 40 47	34 09 26	Soft	Feb 1971	71.51
078	2516 Via Tejon-Cal, Ground Level, Palos Verdes Estate	118 23 13	33 48 02	Medium	Feb 1971	66.96
079	2500 Wilshire Boulevard, Basement, Los Angeles, Cal	118 16 47	34 03 35	Medium	Feb 1971	39.51
080	San Juan Capistrano, Cal	117 40 14	33 29 22	Soft	Feb 1971	121.95
081	Long Beach State College, Gr Level, Long Beach, Cal	118 06 45	33 46 35	Soft	Feb 1971	74.45
082	Anza Post Office, Storage Room, Anza, California	116 40 25	33 33 20	Soft	Feb 1971	185.39

TABLE 3

Data for the Horizontal Records of Group No. 1

Group Characteristics : Soft Sites, Epicentral Distance < 60 km

No.	Cal Tech Id No.	Corresponding Station No. in Table #2	Component Direction	Max. Disp. (inches)	Max. Vel. (ft/sec)	Max. Acc. (G-Units)
01	A001(001)	01	S00E	4.278	1.0974	0.348
02	A001(002)	01	S90W	7.788	1.2113	0.214
03	A004(010)	04	N21E	2.636	0.5157	0.156
04	A004(011)	04	S69E	3.603	0.5812	0.179
05	A010(028)	08	N31W	1.104	0.3558	0.102
06	A010(029)	08	N59E	0.659	0.1456	0.108
07	A013(037)	10	N45E	0.433	0.0949	0.047
08	A013(038)	10	N45W	0.550	0.1626	0.046
09	A018(052)	15	S01W	1.117	0.2548	0.065
10	A018(053)	15	N89W	1.512	0.5622	0.179
11	B028(082)	21	S02W	0.948	0.2698	0.068
12	B028(083)	21	N88W	1.052	0.2605	0.067
13	B029(085)	22	N04W	3.378	0.7021	0.165
14	B029(086)	22	N86E	4.085	0.5607	0.280
15	B031(091)	24	N21E	0.656	0.1945	0.065
16	B031(092)	24	S69E	0.418	0.1208	0.068
17	B032(094)	25	S04E	1.076	0.2643	0.137
18	B032(095)	25	S86W	1.514	0.4282	0.198
19	B033(097)	26	N65E	10.415	2.5619	0.489
20	B034(100)	27	N05W	2.089	0.7602	0.355
21	B034(101)	27	N85E	2.801	0.8346	0.434
22	B035(103)	28	N50E	1.742	0.3557	0.237
23	B035(104)	28	N40W	1.548	0.3858	0.275
24	B036(106)	29	N50E	1.611	0.2303	0.053
25	B036(107)	29	N40W	2.239	0.2633	0.064
26	C051(151)	31	N36E	3.631	0.5626	0.100
27	C051(152)	31	N54W	4.585	0.7188	0.125
28	C054(160)	32	N52W	4.658	0.5701	0.150
29	C054(161)	32	S38W	4.634	0.5679	0.119
30	D057(169)	34	S00W	3.398	0.5566	0.106
31	D057(170)	34	N90E	5.172	0.6379	0.151
32	D058(172)	35	S00W	3.170	0.5415	0.171
33	D058(173)	35	N90E	5.797	0.6935	0.211
34	D059(175)	36	N46W	2.955	0.3165	0.136
35	D059(176)	36	S44W	4.816	0.5493	0.150
36	D068(202)	38	N00E	3.201	0.4127	0.083
37	D068(203)	38	N90E	2.822	0.4378	0.100
38	E083(247)	43	S00W	3.562	0.6035	0.161

Data for the Horizontal Records of Group No. 1 (contd.)

Group Characteristics : Soft Sites, Epicentral Distance < 60 km

No.	Cal Tech Id No.	Corresponding Station No. in Table #2	Component Direction	Max. Disp. (inches)	Max. Vel. (ft/sec)	Max. Acc. (G-Units)
39	E083(248)	43	N90E	4.083	0.5445	0.165
40	F089(265)	45	S53E	5.721	0.6830	0.134
41	F089(266)	45	S37W	4.586	0.6803	0.142
42	F095(283)	47	S88E	4.177	0.5527	0.098
43	F095(284)	47	S02W	4.779	0.5857	0.086
44	F098(292)	48	S53E	5.189	0.7144	0.241
45	F098(293)	48	S37W	5.301	0.6056	0.196
46	F103(307)	50	N00E	0.995	0.1454	0.093
47	F103(308)	50	N90W	0.943	0.1785	0.123
48	F105(313)	52	S00W	1.594	0.2732	0.085
49	F105(314)	52	N90E	1.948	0.2781	0.079
50	G107(319)	54	N00E	1.164	0.2613	0.095
51	G107(320)	54	N90E	2.900	0.4679	0.109
52	G108(322)	55	N00E	1.071	0.3230	0.202
53	G108(323)	55	N90E	2.716	0.5396	0.185
54	G112(334)	57	N38E	4.321	0.5577	0.104
55	G112(335)	57	N52W	3.640	0.5148	0.080
56	G114(340)	58	S60E	1.511	0.4650	0.113
57	G114(341)	58	S30W	1.088	0.3067	0.139
58	H115(343)	59	N11E	5.298	0.9268	0.225
59	H115(344)	59	N79W	4.065	0.7696	0.149
60	H118(352)	60	S45E	3.478	0.3888	0.034
61	H118(353)	60	S45W	3.079	0.2974	0.033
62	H121(361)	61	S90W	3.418	0.5659	0.122
63	H121(362)	61	S00W	1.733	0.3479	0.114
64	I128(379)	63	N00E	2.857	0.4346	0.062
65	I128(380)	63	S90W	3.188	0.4923	0.093
66	I134(397)	64	N54E	4.480	0.5472	0.100
67	I134(398)	64	S36E	2.451	0.3516	0.084
68	I137(406)	65	S81E	2.797	0.5280	0.143
69	I137(407)	65	S09W	3.328	0.7304	0.131
70	J145(427)	70	S00W	6.926	1.0381	0.116
71	J145(428)	70	S90W	6.019	0.9441	0.105
72	M176(487)	73	N37E	5.425	0.6859	0.085
73	M176(488)	73	S53E	5.398	0.5842	0.118
74	M186(517)	78	S37E	1.945	0.2873	0.098
75	M186(518)	78	S53W	1.976	0.3194	0.099

TABLE 4

Data for the Vertical Records of Group No. 1

Group Characteristics : Soft Sites, Epicentral Distance < 60 km

No.	Cal Tech Id No.	Corresponding Station No. in Table #2	Component Direction	Max. Disp. (inches)	Max. Vel. (ft/sec)	Max. Acc. (G-Units)
01	A001(003)	01	VERT	2.188	0.3555	0.210
02	A004(012)	04	VERT	1.982	0.2190	0.105
03	A010(030)	08	VERT	0.469	0.0402	0.045
04	A013(039)	10	VERT	0.346	0.0482	0.027
05	A018(054)	15	VERT	0.851	0.1539	0.050
06	B028(084)	21	VERT	0.906	0.0784	0.022
07	B029(087)	22	VERT	1.587	0.2306	0.092
08	B031(093)	23	VERT	1.142	0.0772	0.036
09	B032(096)	24	VERT	0.661	0.0984	0.061
10	B033(099)	25	VERT	1.707	0.4635	0.206
11	B034(102)	26	VERT	1.355	0.2389	0.119
12	B035(105)	27	VERT	0.817	0.1482	0.079
13	B036(108)	29	VERT	1.016	0.1633	0.045
14	C051(153)	31	VERT	2.288	0.2568	0.049
15	C054(162)	32	VERT	2.011	0.3497	0.053
16	D057(171)	34	VERT	1.501	0.1972	0.051
17	D058(174)	35	VERT	1.183	0.1681	0.089
18	D059(177)	36	VERT	0.968	0.1577	0.068
19	D068(204)	38	VERT	1.642	0.1836	0.058
20	E083(249)	43	VERT	1.752	0.2885	0.057
21	F089(267)	45	VERT	2.370	0.3275	0.077
22	F095(285)	47	VERT	1.540	0.2033	0.027
23	F098(294)	48	VERT	2.083	0.3162	0.071
24	F103(309)	50	VERT	0.666	0.0770	0.048
25	F105(315)	52	VERT	1.141	0.1473	0.068
26	G107(321)	54	VERT	1.048	0.2179	0.095
27	G108(324)	55	VERT	0.931	0.2942	0.093
28	G112(336)	57	VERT	2.065	0.3281	0.054
29	G114(342)	58	VERT	0.948	0.2545	0.088
30	H115(345)	59	VERT	1.699	0.3078	0.096
31	H118(354)	60	VERT	1.546	0.2260	0.042
32	H121(363)	61	VERT	1.344	0.2675	0.081
33	I128(381)	63	VERT	0.906	0.1899	0.037
34	I134(399)	64	VERT	0.981	0.1894	0.064
35	I137(408)	65	VERT	1.045	0.2619	0.102
36	J145(429)	70	VERT	2.755	0.5945	0.108
37	M176(489)	73	VERT	1.703	0.2917	0.042
38	M186(519)	78	VERT	0.925	0.1194	0.060

TABLE 5

Data for the Horizontal Records of Group No. 2

Group Characteristics : Soft Sites, Epicentral Distance > 60 km

No.	Cal Tech Id No.	Corresponding Station No. in Table #2	Component Direction	Max. Disp. (inches)	Max. Vel. (ft/sec)	Max. Acc. (G-Units)
01	A003(007)	03	S00E	1.059	0.2045	0.047
02	A003(008)	03	S90E	1.133	0.2976	0.053
03	A005(013)	05	N42E	1.829	0.3861	0.090
04	A005(014)	05	S48E	2.267	0.6325	0.131
05	A006(016)	06	S00W	2.013	0.2009	0.055
06	A006(017)	06	N90E	2.318	0.3077	0.044
07	A007(019)	07	S00W	1.789	0.2157	0.059
08	A007(020)	07	N90E	2.537	0.2924	0.042
09	A011(031)	09	S00W	0.964	0.1302	0.033
10	A011(032)	09	S90W	1.612	0.2284	0.051
11	A019(055)	16	S00W	4.820	0.8469	0.130
12	A019(056)	16	S90W	4.326	0.4819	0.057
13	D071(211)	39	S00W	0.556	0.0614	0.027
14	D071(212)	39	N90E	0.821	0.0820	0.026
15	F087(259)	44	S04E	1.405	0.1643	0.027
16	F087(260)	44	S86W	2.238	0.2620	0.029
17	F101(301)	48	S00W	0.426	0.0858	0.038
18	F101(302)	48	N90E	0.505	0.0724	0.031
19	H124(370)	62	S90W	0.840	0.1451	0.036
20	H124(371)	62	S00W	1.069	0.1904	0.035
21	M180(499)	75	S00W	1.397	0.1875	0.024
22	M180(500)	75	S90W	2.579	0.2775	0.030
23	M187(520)	79	N15E	0.279	0.1010	0.057
24	M187(521)	79	N75W	0.308	0.1205	0.077
25	N195(544)	82	N33E	0.940	0.1167	0.042
26	N195(545)	82	N57W	0.964	0.1522	0.032
27	N196(547)	83	N76W	3.138	0.3115	0.036
28	N196(548)	83	S14W	2.652	0.3036	0.032
29	N197(550)	84	N45E	0.465	0.0719	0.026

TABLE 6

Data for the Vertical Records of Group No. 2

Group Characteristics : Soft Sites, Epicentral Distance > 60 km

No.	Cal Tech Id No.	Corresponding Station No. in Table #2	Component Direction	Max. Disp. (inches)	Max. Vel. (ft/sec)	Max. Acc. (G-Units)
01	A003(009)	03	VERT	1.194	0.1487	0.030
02	A005(015)	05	VERT	0.847	0.1643	0.044
03	A006(018)	06	VERT	0.855	0.1371	0.023
04	A007(021)	07	VERT	1.341	0.0996	0.021
05	A019(057)	16	VERT	1.523	0.1131	0.030
06	F101(303)	48	VERT	0.533	0.0499	0.020
07	M187(522)	79	VERT	0.311	0.0512	0.029
08	N195(546)	82	VERT	0.622	0.1124	0.021
09	N196(549)	83	VERT	1.481	0.1601	0.026

TABLE 7

GROUND MOTION DATA FOR THE RECORDS USED IN THE STUDY

Data for the Horizontal Records of Group No. 3

Group Characteristics : Medium Stiff Sites, Epicentral Distance < 60 km

No.	Cal Tech Id No.	Corresponding Station No. in Table #2	Component Direction	Max. Disp. (inches)	Max. Vel. (ft/sec)	Max. Acc. (G-Units)
01	A002(004)	02	S44W	0.938	0.1577	0.104
02	A002(005)	02	N46W	1.078	0.2424	0.112
03	A014(040)	11	N09W	0.514	0.0944	0.043
04	A014(041)	11	N81E	0.393	0.0697	0.465
05	A015(043)	12	N10E	0.887	0.1613	0.083
06	A015(044)	12	S80E	0.325	0.1512	0.105
07	A016(046)	13	S09E	0.448	0.1657	0.085
08	A016(047)	13	S81W	0.360	0.1325	0.056
09	A017(049)	14	N26E	0.591	0.0641	0.040
10	A017(050)	14	S64E	0.443	0.0391	0.024
11	B026(076)	19	N45E	1.532	0.2166	0.144
12	B026(077)	19	S45E	0.653	0.2225	0.089
13	B030(088)	23	N44E	0.805	0.2280	0.054
14	B030(089)	23	S46E	0.732	0.1557	0.076
15	C056(166)	33	N21E	1.664	0.5630	0.315
16	C056(167)	33	N69W	3.735	0.9126	0.271
17	D065(193)	37	S00W	4.067	0.5929	0.150
18	D065(194)	37	S90W	5.068	0.7244	0.159
19	D072(214)	40	N75W	5.788	0.6843	0.084
20	D072(215)	40	N15E	4.643	0.7065	0.117
21	D078(232)	41	N50W	5.400	0.7674	0.129
22	D078(233)	41	S40W	3.498	0.5291	0.172
23	D081(241)	42	S08E	2.763	0.3241	0.217
24	D081(242)	42	S82W	1.809	0.2048	0.202
25	F092(274)	46	S62E	4.060	0.4531	0.065
26	F092(275)	46	S28W	2.486	0.3804	0.081
27	F104(310)	51	N00E	0.812	0.2790	0.087
28	F104(311)	51	N90W	0.927	0.2007	0.105
29	G110(328)	56	S82E	1.951	0.4570	0.212
30	G110(329)	56	S08W	1.139	0.3017	0.142
31	J144(424)	69	N21E	0.698	0.4839	0.353
32	J144(425)	69	N69W	3.487	0.4188	0.283
33	J148(436)	71	N00E	2.880	0.5302	0.110
34	J148(437)	71	S90W	4.386	0.5734	0.114
35	L166(457)	72	N00E	1.913	0.4071	0.167
36	L166(458)	72	S90W	2.143	0.4919	0.150
37	N192(535)	81	N29E	3.041	0.4870	0.099
38	N192(536)	81	N61W	3.097	0.6419	0.101

TABLE 8

Data for the Vertical Records of Group No. 3

Group Characteristics : Medium Stiff Sites, Epicentral Distance < 60 km

No.	Cal Tech Id No.	Corresponding Station No. in Table #2	Component Direction	Max. Disp. (inches)	Max. Vel. (ft/sec)	Max. Acc. (G-Units)
01	A002(006)	02	VERT	0.637	0.0724	0.027
02	A014(042)	11	VERT	0.173	0.0439	0.031
03	A015(045)	12	VERT	0.268	0.0398	0.038
04	A016(048)	13	VERT	0.253	0.0766	0.044
05	B026(078)	19	VERT	0.239	0.0471	0.032
06	B030(090)	23	VERT	0.600	0.0993	0.030
07	C056(168)	33	VERT	1.380	0.2116	0.156
08	D065(195)	37	VERT	1.919	0.2984	0.075
09	D072(216)	40	VERT	1.244	0.2261	0.066
10	D078(234)	41	VERT	2.548	0.3367	0.069
11	D081(243)	42	VERT	1.114	0.1510	0.065
12	F092(276)	46	VERT	1.494	0.2328	0.050
13	F104(312)	51	VERT	0.484	0.1259	0.036
14	G110(330)	56	VERT	1.032	0.1940	0.129
15	J144(426)	69	VERT	1.286	0.1358	0.107
16	J148(438)	71	VERT	1.342	0.2184	0.053
17	L166(459)	72	VERT	0.947	0.1640	0.071
18	N192(537)	81	VERT	1.307	0.2513	0.043

TABLE 9

Data for the Horizontal Records of Group No. 4

Group Characteristics : Medium Stiff Sites, Epicentral Distance > 60 km

No.	Cal Tech Id No.	Corresponding Station No. in Table #2	Component Direction	Max. Disp. (inches)	Max. Vel. (ft/sec)	Max. Acc. (G-Units)
01	B027(079)	20	N45E	0.784	0.1153	0.062
02	B027(080)	20	S45E	0.847	0.1128	0.039
03	M179(496)	74	S00W	0.292	0.0376	0.021
04	M179(497)	74	N90E	0.360	0.0931	0.048
05	M183(508)	76	N65W	0.482	0.1257	0.043
06	M183(509)	76	N25E	0.343	0.0851	0.057
07	M185(514)	77	S50E	0.673	0.1137	0.069
08	M185(515)	77	S40W	0.814	0.1461	0.069
09	N191(532)	80	N65E	1.020	0.1361	0.025
10	N191(533)	80	S25E	1.324	0.1634	0.041

TABLE 10

Data for the Horizontal Records of Group No. 5

Group Characteristics : Hard Sites, Epicentral Distance < 60 km

No.	Cal Tech Id No.	Corresponding Station No. in Table #2	Component Direction	Max. Disp. (inches)	Max. Vel. (ft/sec)	Max. Acc. (G-Units)
01	C041(121)	30	S16E	14.828	3.7150	1.170
02	C041(122)	30	S74W	4.259	1.8944	1.075
03	G106(316)	53	S00W	0.651	0.1968	0.089
04	G106(317)	53	S90W	1.955	0.3810	0.192
05	J141(415)	66	N21E	1.350	0.5890	0.148
06	J141(416)	66	S69E	1.166	0.4733	0.111
07	J142(418)	67	S69E	0.489	0.1885	0.171
08	J142(419)	67	S21W	0.686	0.2827	0.146
09	J143(421)	68	N21E	0.780	0.1573	0.122
10	J143(422)	68	N69W	0.950	0.1477	0.112

TABLE 11

Data for the Vertical Records of Group No. 5

Group Characteristics : Hard Sites, Epicentral Distance < 60 km

No.	Cal Tech Id No.	Corresponding Station No. in Table #2	Component Direction	Max. Disp. (inches)	Max. Vel. (ft/sec)	Max. Acc. (G-Units)
01	C041(123)	30	VERT	7.605	1.9129	0.709
02	G106(318)	53	VERT	0.911	0.1923	0.085
03	J141(417)	66	VERT	1.122	0.3826	0.095
04	J142(420)	67	VERT	0.632	0.2345	0.154
05	J143(423)	68	VERT	0.872	0.1000	0.073

TABLE 12

List of the Ninety Two Periods Used for the Response Spectra

0.030	0.032	0.034	0.036	0.038	0.040	0.042	0.044	0.046	0.046
0.050	0.055	0.060	0.065	0.070	0.075	0.080	0.085	0.090	0.095
0.100	0.110	0.120	0.130	0.140	0.150	0.160	0.170	0.180	0.180
0.200	0.220	0.235	0.250	0.265	0.280	0.300	0.320	0.340	0.360
0.380	0.400	0.420	0.440	0.460	0.480	0.500	0.550	0.600	0.650
0.700	0.750	0.800	0.850	0.900	0.950	1.000	1.100	1.200	1.300
1.400	1.500	1.600	1.700	1.800	1.900	2.000	2.200	2.400	2.600
2.800	3.000	3.200	3.400	3.600	3.800	4.000	4.200	4.400	4.600
4.800	5.000	5.500	6.000	6.500	7.000	7.500	8.000	8.500	9.000
9.500	10.000								

TABLE 13

Correlation Coefficients Between Various Ground Motion Parameters

Group No.	R.M.S.and Peak Acceleration	Correlation Coefficient Peak Velocity and Peak Displacement	Peak Acceleration and Peak Velocity	Peak Displacement and Peak Acceleration
1H	0.8580	0.8414	0.6819	0.3937
1V	0.9081	0.8040	0.5854	0.3461
2H	0.8214	0.8510	0.7843	0.4274
2V	0.8039	0.5788	0.4821	0.0685
3H	0.7667	0.8629	0.4828	0.2216
3V	0.7265	0.9464	0.4291	0.4567
4H	0.8234	0.8305	0.2947	-0.0236
5H	0.9983	0.9716	0.9377	0.8489
5V	0.9984	0.9932	0.9888	0.9873

TABLE 14

Statistics of the Implicit Parameters for the Groups Considered

Parameter	Statistical Quantity	Group No.								
		1H	1V	2H	2V	3H	3V	4H	5H	5V
Acceleration Peak Factor	Mean	7.83	7.64	5.75	5.66	8.99	7.99	6.19	9.75	9.99
	C.O.V.	0.28	0.26	0.24	0.19	0.33	0.34	0.24	0.15	0.21
Duration Ratio	Mean	0.37	0.43	0.57	0.62	0.37	0.44	0.59	0.25	0.26
	C.O.V.	0.41	0.36	0.26	0.21	0.54	0.51	0.29	0.38	0.41
Upcrossing Rate	Mean	4.06	4.67	3.17	3.95	4.39	5.19	4.47	5.87	7.51
	C.O.V.	0.30	0.32	0.40	0.36	0.30	0.37	0.46	0.30	0.16
f	Mean	4.88	6.44	3.67	4.92	4.65	6.15	4.90	5.55	6.64
	C.O.V.	0.30	0.37	0.36	0.27	0.25	0.30	0.33	0.33	0.18
f	Mean	0.35	0.31	0.31	0.25	0.42	0.34	0.34	0.61	0.49
	C.O.V.	0.35	0.32	0.45	0.33	0.54	0.28	0.30	0.33	0.36

TABLE 15

Design Coefficients for Horizontal Records of Group #1

Group Characteristics : Soft Sites, Epicentral Distance < 60 kms

ω_h = 43.35 rad/sec and ω_l = 1.73 rad/sec

Corner Period (sec)	Response Quantity	Q at BETA=0		Q = A LOG (BETA) + B; .02 < BETA < .20			
				A		B	
		Mean	Mean+SD	Mean	Mean+SD	Mean	Mean+SD
0.034	RSV (IN/S)	0.575	1.040	-0.0524	-0.0959	0.1947	0.2474
	PSV (IN/S)	1.380	1.777	-0.0299	-0.0569	0.9728	0.9791
	RSA (IN G)	0.245	0.470	-0.0333	-0.0590	0.0378	0.0521
0.085	RSV (IN/S)	10.743	17.616	-2.2851	-3.6083	-0.0237	-0.2968
	PSV (IN/S)	11.639	18.399	-1.9939	-3.4069	2.1453	1.3340
	RSA (IN G)	2.023	3.345	-0.4489	-0.7018	-0.0575	-0.1085
0.170	RSV (IN/S)	35.494	51.988	-9.7750	-13.9358	-0.9293	-2.0146
	PSV (IN/S)	36.565	52.771	-9.4199	-13.7288	0.7934	-1.0756
	RSA (IN G)	3.392	4.974	-0.9320	-1.3216	-0.0934	-0.1738
0.420	RSV (IN/S)	69.123	106.208	-21.9920	-32.8469	-0.7373	-4.7486
	PSV (IN/S)	70.287	107.596	-22.6856	-33.3831	-0.3249	-3.4442
	RSA (IN G)	2.716	4.137	-0.8186	-1.2234	0.1325	-0.0462
4.400	RSV (IN/S)	83.770	181.613	-28.6026	-64.0812	16.3012	12.9065
	PSV (IN/S)	79.691	178.747	-30.6494	-66.3217	6.2148	3.2202
	RSA (IN G)	0.602	0.888	-0.0310	-0.1216	0.5152	0.4804
10.000	RSV (IN/S)	32.836	49.961	-2.5892	-3.5511	28.5267	44.1305
	PSV (IN/S)	17.294	28.120	-3.6231	-5.1094	10.2021	17.8849
	RSA (IN G)	0.520	0.534	0.0002	0.0006	0.5204	0.5340

TABLE 16

Design Coefficients for Vertical Records of Group #1

Group Characteristics : Soft Sites, Epicentral Distance < 60 kms

ω_h = 45.66 rad/sec and ω_l = 1.79 rad/sec

Corner Period (sec)	Response Quantity	Q at BETA=0		Q = A LOG (BETA) + B; .02 < BETA < .20 A		B	
		Mean	Mean+SD	Mean	Mean+SD	Mean	Mean+SD
0.034	RSV (IN/S)	1.344	2.502	-0.2417	-0.4571	0.2016	0.2290
	PSV (IN/S)	2.002	3.050	-0.1661	-0.3397	0.9047	0.8745
	RSA (IN G)	0.618	1.180	-0.1132	-0.2150	0.0593	0.0718
0.120	RSV (IN/S)	31.930	48.281	-8.1160	-11.4967	-1.5661	-2.6387
	PSV (IN/S)	32.692	48.809	-7.7767	-11.2389	-0.5499	-1.7905
	RSA (IN G)	4.316	6.549	-1.1028	-1.5455	-0.1965	-0.3011
0.300	RSV (IN/S)	57.834	85.370	-17.6702	-25.6137	-2.1948	-4.5772
	PSV (IN/S)	58.308	85.929	-17.4247	-25.0777	-1.6394	-3.6384
	RSA (IN G)	3.169	4.634	-0.9244	-1.3621	0.0172	-0.1370
1.500	RSV (IN/S)	75.066	110.858	-24.5732	-36.5876	4.1433	2.9304
	PSV (IN/S)	75.458	112.719	-24.9567	-35.9411	2.6247	4.2027
	RSA (IN G)	0.921	1.235	-0.1375	-0.2332	0.4823	0.4950
3.800	RSV (IN/S)	82.029	155.060	-32.6772	-65.0770	7.9230	2.8114
	PSV (IN/S)	77.755	151.217	-32.9311	-65.9810	1.4376	-4.1917
	RSA (IN G)	0.638	0.841	-0.0649	-0.1502	0.4833	0.4652
10.000	RSV (IN/S)	29.674	44.152	-4.0844	-6.0558	22.0913	32.8004
	PSV (IN/S)	16.902	27.590	-5.0243	-8.7306	6.4045	9.0281
	RSA (IN G)	0.513	0.553	0.0006	0.0002	0.5139	0.5533

TABLE 17

Design Coefficients for Horizontal Records of Group #2

Group Characteristics : Soft Sites, Epicentral Distance > 60 kms

ω_h= 31.22 rad/sec and ω_l= 1.44 rad/sec

Corner Period (sec)	Response Quantity	Q at BETA=0 Mean	Q at BETA=0 Mean+SD	Q = A LOG (BETA) + B; .02 < BETA < .20 — A Mean	A Mean+SD	B Mean	B Mean+SD
	RSV (IN/S)	0.425	0.595	-0.0356	-0.0558	0.1426	0.2016
0.034	PSV (IN/S)	1.255	1.350	-0.0029	0.0015	0.9860	1.0062
	RSA (IN G)	0.186	0.268	-0.0220	-0.0358	0.0302	0.0487
	RSV (IN/S)	20.857	33.514	-4.8420	-7.8348	-0.4425	-1.1097
0.130	PSV (IN/S)	22.052	34.424	-4.2966	-7.3935	2.4685	0.3519
	RSA (IN G)	2.577	4.168	-0.6204	-0.9891	-0.0979	-0.1637
	RSV (IN/S)	74.727	114.459	-24.0790	-36.3230	-4.0262	-8.3143
0.300	PSV (IN/S)	76.416	115.670	-23.3329	-35.5141	-2.0791	-6.5458
	RSA (IN G)	4.057	6.235	-1.3211	-1.9862	-0.2200	-0.4548
	RSV (IN/S)	141.831	225.128	-45.3971	-71.2812	-5.1000	-12.0808
1.000	PSV (IN/S)	143.273	227.446	-46.2643	-70.5222	-6.9200	-12.0013
	RSA (IN G)	2.375	3.691	-0.6493	-1.0427	0.2025	0.0573
	RSV (IN/S)	140.492	275.786	-50.0020	-106.6407	11.0803	-1.0998
5.500	PSV (IN/S)	134.518	270.919	-53.7922	-109.2238	-4.5513	-14.1754
	RSA (IN G)	0.689	0.961	-0.0769	-0.1941	0.4762	0.4050
	RSV (IN/S)	51.325	81.463	-8.2174	-13.6794	33.5204	50.4320
10.000	PSV (IN/S)	35.998	63.318	-11.7509	-21.4166	10.7318	15.2908
	RSA (IN G)	0.521	0.534	0.0004	-0.0006	0.5222	0.5331

TABLE 18

Design Coefficients for Vertical Records of Group #2

Group Characteristics : Soft Sites, Epicentral Distance > 60 kms

ω_h = 42.85 rad/sec and ω_l = 1.75 rad/sec

Corner Period (sec)	Response Quantity	Q at BETA=0		Q = A LOG (BETA) + B; .02 < BETA < .20			
				A		B	
		Mean	Mean+SD	Mean	Mean+SD	Mean	Mean+SD
0.034	RSV (IN/S)	0.935	1.517	-0.1110	-0.1421	0.1757	0.2166
	PSV (IN/S)	1.582	2.077	-0.0460	-0.0926	0.9724	0.9703
	RSA (IN G)	0.426	0.706	-0.0614	-0.0880	0.0421	0.0448
0.090	RSV (IN/S)	21.115	37.868	-3.1465	-5.0843	-0.1952	-0.8508
	PSV (IN/S)	22.186	38.387	-2.9208	-5.0464	1.4259	-0.1316
	RSA (IN G)	3.790	6.808	-0.5842	-0.9212	-0.0742	-0.1640
0.280	RSV (IN/S)	87.972	146.650	-19.4164	-29.2271	-3.3689	-7.8729
	PSV (IN/S)	88.786	147.500	-19.0640	-29.2289	-2.1615	-6.8848
	RSA (IN G)	5.129	8.525	-1.1217	-1.6164	-0.1593	-0.3586
1.000	RSV (IN/S)	119.171	193.057	-42.8953	-74.1051	-8.5922	-21.7759
	PSV (IN/S)	118.141	191.223	-43.1350	-73.4008	-9.8642	-22.2795
	RSA (IN G)	2.024	3.239	-0.6438	-1.1939	0.1378	-0.1990
3.200	RSV (IN/S)	151.719	287.614	-44.8149	-87.4556	-0.5386	-18.8947
	PSV (IN/S)	150.174	286.096	-47.5253	-87.7579	-5.3100	-19.0622
	RSA (IN G)	0.966	1.534	-0.1744	-0.3117	0.3993	0.3113
10.000	RSV (IN/S)	44.774	57.848	-9.4481	-12.2721	26.6473	34.2256
	PSV (IN/S)	36.266	51.096	-12.9195	-18.2510	8.8152	11.2832
	RSA (IN G)	0.524	0.548	-0.0026	-0.0103	0.5191	0.5295

TABLE 19

Design Coefficients for Horizontal Records of Group #3

Group Characteristics : Medium Stiff Sites, Epicentral Distance < 60 kms

ω_h = 37.51 rad/sec and ω_L = 1.70 rad/sec

Corner Period (sec)	Response Quantity	Q at BETA=0		Q = A LOG (BETA) + B; .02 < BETA < .20			
				A		B	
		Mean	Mean+SD	Mean	Mean+SD	Mean	Mean+SD
0.034	RSV (IN/S)	0.518	0.799	-0.0694	-0.1163	0.1926	0.2403
	PSV (IN/S)	1.334	1.537	-0.0308	-0.0592	0.9675	0.9712
	RSA (IN G)	0.222	0.362	-0.0346	-0.0502	0.0501	0.0830
0.120	RSV (IN/S)	18.097	28.145	-4.8338	-7.5860	-0.1144	-0.8079
	PSV (IN/S)	18.921	28.730	-4.2232	-7.0350	2.6612	0.9362
	RSA (IN G)	2.440	3.808	-0.6771	-1.0616	-0.0615	-0.1454
0.250	RSV (IN/S)	48.235	69.960	-16.1590	-23.2619	-1.5001	-3.3772
	PSV (IN/S)	49.193	70.897	-15.7884	-23.0081	-0.4356	-2.4196
	RSA (IN G)	3.150	4.546	-1.0395	-1.4781	-0.0536	-0.1622
1.200	RSV (IN/S)	57.474	97.338	-20.0306	-35.6188	7.2526	7.0864
	PSV (IN/S)	57.052	98.511	-22.4218	-39.6102	0.5177	-1.2835
	RSA (IN G)	0.949	1.426	-0.2095	-0.4477	0.4589	0.3810
5.000	RSV (IN/S)	46.865	97.245	-15.5114	-37.6535	15.0019	18.7950
	PSV (IN/S)	41.396	90.739	-16.3538	-37.7674	6.3591	10.2202
	RSA (IN G)	0.535	0.593	-0.0098	-0.0388	0.5206	0.5164
10.000	RSV (IN/S)	24.751	40.658	-2.0416	-2.7990	21.1120	36.1694
	PSV (IN/S)	13.843	22.981	-3.8995	-5.2174	6.2059	12.7052
	RSA (IN G)	0.518	0.525	0.0000	0.0007	0.5180	0.5264

TABLE 20

Design Coefficients for Vertical Records of Group #3

Group Characteristics : Medium Stiff Sites, Epicentral Distance < 60 kms

ω_h = 49.75 rad/sec and ω_l = 1.81 rad/sec

Corner Period (sec)	Response Quantity	Q at BETA=0 Mean	Mean+SD	Q = A LOG (BETA) + B; .02 < BETA < .20 A Mean	Mean+SD	B Mean	Mean+SD
0.034	RSV (IN/S)	1.002	1.501	-0.1835	-0.3157	0.2240	0.2743
	PSV (IN/S)	1.674	2.137	-0.0750	-0.1429	0.9551	0.9337
	RSA (IN G)	0.448	0.684	-0.0876	-0.1404	0.0695	0.1050
0.090	RSV (IN/S)	12.751	19.859	-3.7156	-6.1068	-0.2157	-0.8494
	PSV (IN/S)	13.565	20.424	-3.3339	-5.6448	1.7236	0.2043
	RSA (IN G)	2.288	3.618	-0.6750	-1.0851	-0.0694	-0.1395
0.300	RSV (IN/S)	54.549	82.200	-19.0847	-29.0661	-2.1312	-5.1022
	PSV (IN/S)	55.198	83.067	-19.5369	-29.0073	-2.1758	-4.7363
	RSA (IN G)	2.995	4.490	-0.9724	-1.5185	-0.0043	-0.1968
1.200	RSV (IN/S)	61.141	105.896	-23.9097	-44.9144	0.8995	-5.8243
	PSV (IN/S)	60.852	105.725	-24.5191	-44.2859	-1.3079	-4.9924
	RSA (IN G)	1.023	1.547	-0.2642	-0.5120	0.3661	0.2378
4.000	RSV (IN/S)	56.362	107.234	-20.1288	-43.6755	11.8320	11.8822
	PSV (IN/S)	52.983	104.870	-23.1044	-48.3616	1.3841	-1.1735
	RSA (IN G)	0.563	0.653	-0.0343	-0.0685	0.4933	0.5004
10.000	RSV (IN/S)	23.165	33.448	-2.3022	-2.5308	18.4989	28.9459
	PSV (IN/S)	14.760	20.463	-4.6605	-5.6132	4.7162	7.6301
	RSA (IN G)	0.518	0.527	-0.0012	0.0006	0.5160	0.5279

TABLE 21

Design Coefficients for Horizontal Records of Group #4

Group Characteristics : Medium Stiff Sites, Epicentral Distance > 60 kms

ω_h = 41.33 rad/sec and ω_l = 1.49 rad/sec

Corner Period (sec)	Response Quantity	Q at BETA=0		Q = A LOG (BETA) + B; .02 < BETA < .20			
				A		B	
		Mean	Mean+SD	Mean	Mean+SD	Mean	Mean+SD
0.034	RSV (IN/S)	0.679	1.026	-0.0926	-0.1832	0.1892	0.2168
	PSV (IN/S)	1.398	1.691	-0.0360	-0.0840	0.9548	0.9348
	RSA (IN G)	0.303	0.468	-0.0445	-0.0750	0.0472	0.0741
0.100	RSV (IN/S)	17.170	29.390	-3.4049	-5.7527	-0.0113	-0.5106
	PSV (IN/S)	18.375	30.027	-3.2178	-5.7213	2.1095	0.3897
	RSA (IN G)	2.753	4.775	-0.5594	-0.9154	-0.0445	-0.0843
0.250	RSV (IN/S)	69.906	123.909	-19.9900	-31.6066	-3.0471	-8.4440
	PSV (IN/S)	71.018	125.199	-19.2291	-30.6555	-1.7897	-6.9339
	RSA (IN G)	4.568	8.058	-1.3415	-2.0608	-0.2009	-0.5512
1.600	RSV (IN/S)	70.946	172.045	-19.4424	-50.8765	2.2945	-12.2208
	PSV (IN/S)	70.782	173.132	-21.2449	-49.6951	-3.2639	-14.6474
	RSA (IN G)	0.943	1.869	-0.1081	-0.3491	0.4961	0.3545
5.500	RSV (IN/S)	69.288	164.074	-29.1664	-72.1828	-0.3897	-14.7147
	PSV (IN/S)	64.076	155.962	-30.0310	-73.6310	-5.8735	-22.0371
	RSA (IN G)	0.586	0.736	-0.0238	-0.0703	0.5132	0.4805
10.000	RSV (IN/S)	21.094	30.899	-1.6438	-1.9835	18.0563	27.9461
	PSV (IN/S)	12.885	20.202	-3.5751	-5.5204	5.7256	8.5479
	RSA (IN G)	0.516	0.520	0.0026	0.0028	0.5203	0.5250

TABLE 22

Design Coefficients for Horizontal Records of Group #5

Group Characteristics : Hard Sites, Epicentral Distance < 60 kms

ω_h = 41.86 rad/sec and ω_l = 2.40 rad/sec

Corner Period (sec)	Response Quantity	Q at BETA=0		Q = A LOG (BETA) + B; .02 < BETA < .20			
		Mean	Mean+SD	A Mean	Mean+SD	B Mean	Mean+SD
0.034	RSV (IN/S)	0.936	1.638	-0.1154	-0.2263	0.1857	0.2037
	PSV (IN/S)	1.630	2.236	-0.0529	-0.1519	0.9573	0.9000
	RSA (IN G)	0.420	0.762	-0.0515	-0.0979	0.0445	0.0537
0.120	RSV (IN/S)	21.960	35.935	-5.9787	-9.7962	-0.7027	-2.0696
	PSV (IN/S)	22.784	36.563	-5.4282	-9.2823	1.1284	-0.9237
	RSA (IN G)	2.947	4.843	-0.8150	-1.3553	-0.1027	-0.2773
0.250	RSV (IN/S)	44.043	63.360	-12.6584	-19.6257	-0.8835	-2.7898
	PSV (IN/S)	44.238	63.319	-12.5824	-19.5893	0.0154	-1.8703
	RSA (IN G)	2.925	4.147	-0.8356	-1.2729	0.0164	-0.1032
1.000	RSV (IN/S)	54.209	96.980	-18.5711	-32.9523	6.9330	7.4353
	PSV (IN/S)	53.900	97.068	-17.9561	-30.6764	6.2487	9.5525
	RSA (IN G)	1.089	1.712	-0.2141	-0.3979	0.5075	0.5545
3.600	RSV (IN/S)	21.949	32.366	-2.3273	-2.9677	16.7183	25.1886
	PSV (IN/S)	15.666	24.963	-4.6659	-6.2563	4.6530	7.1887
	RSA (IN G)	0.521	0.537	0.0001	0.0003	0.5279	0.5431
10.000	RSV (IN/S)	15.625	21.705	-0.7735	-0.3931	14.3287	21.2372
	PSV (IN/S)	5.848	8.811	-1.7937	-3.1398	2.3237	2.6706
	RSA (IN G)	0.517	0.522	-0.0013	-0.0023	0.5147	0.5179

TABLE 23

Design Coefficients for Vertical Records of Group #5

Group Characteristics : Hard Sites, Epicentral Distance < 60 kms

ω_h = 55.70 rad/sec and ω_l = 3.11 rad/sec

Corner Period (sec)	Response Quantity	Q at BETA=0		Q = A LOG (BETA) + B; .02 < BETA < .20			
				A		B	
		Mean	Mean+SD	Mean	Mean+SD	Mean	Mean+SD
0.034	RSV (IN/S)	1.920	3.292	-0.2574	-0.4742	0.1723	0.0718
	PSV (IN/S)	2.432	3.659	-0.2295	-0.3852	0.8599	0.8168
	RSA (IN G)	0.915	1.572	-0.1307	-0.2054	0.0271	0.0212
0.075	RSV (IN/S)	17.448	24.591	-3.9906	-6.4078	-0.8256	-1.8008
	PSV (IN/S)	17.685	24.818	-3.7993	-6.2151	-0.0698	-1.0380
	RSA (IN G)	3.759	5.303	-0.8739	-1.3882	-0.2141	-0.4103
0.200	RSV (IN/S)	47.442	68.354	-14.5750	-20.7278	-2.7258	-4.7982
	PSV (IN/S)	47.431	68.747	-13.9945	-20.4226	-1.8954	-4.3070
	RSA (IN G)	3.885	5.589	-1.1099	-1.6388	-0.0987	-0.3220
0.700	RSV (IN/S)	52.695	103.108	-19.5785	-43.1341	-0.7329	-8.4149
	PSV (IN/S)	52.499	103.623	-18.8887	-40.6276	-1.4848	-6.2629
	RSA (IN G)	1.426	2.494	-0.4757	-1.0360	0.2096	-0.1412
2.000	RSV (IN/S)	42.529	58.184	-12.3972	-17.1912	10.6002	19.4598
	PSV (IN/S)	39.779	53.092	-13.4198	-17.8216	4.9062	10.8109
	RSA (IN G)	0.625	0.749	-0.0648	-0.1246	0.5076	0.5231
10.000	RSV (IN/S)	18.169	22.559	-1.7115	-1.7208	15.1063	19.4185
	PSV (IN/S)	9.817	14.837	-2.9882	-5.4248	3.8334	4.1282
	RSA (IN G)	0.516	0.522	-0.0017	-0.0014	0.5131	0.5194

TABLE 24

Design Coefficients for Velocity (in/sec) of Massless Oscillators

| Group No. | Corner Periods | | | | | | | |
| | Period=0.034 | | Period=0.170 | | Period=1.200 | | Period=10.00 | |
	Mean	Mean+SD	Mean	Mean+SD	Mean	Mean+SD	Mean	Mean+SD
1H	5.429	6.111	13.388	17.440	23.415	34.436	26.071	38.338
1V	4.853	5.670	11.256	14.654	19.908	29.378	22.061	31.853
2H	5.786	6.428	14.994	19.438	29.085	42.284	32.267	47.122
2V	5.371	6.121	12.894	16.391	23.782	30.104	27.058	35.395
3H	5.174	5.875	11.487	14.914	18.375	28.716	20.254	31.775
3V	4.836	5.605	11.403	15.193	17.104	25.108	18.721	26.935
4H	5.180	5.595	10.357	12.403	15.078	21.109	16.527	23.698
5H	5.046	5.874	11.456	15.478	14.553	20.991	14.879	21.217
5V	4.906	5.680	10.207	14.239	14.217	19.604	16.096	22.146

TABLE 25

Design Coefficients for Acceleration (in/s*s) of Massless Oscillators

| Group No. | Response Level | Q = A LOG(P)*LOG(P) + B LOG(P) + C
.034 sec < P < .30 sec | | | Q at
PD= 1.60 | Q at
PD=10.00 |
		A	B	C		
1H	MEAN	-0.1747976	-0.1416633	2.2609433	197.2680	197.1660
1H	MEAN+SD	-0.1570425	-0.1611287	2.2747668	201.7756	198.3336
1V	MEAN	-0.1130529	-0.0772673	2.2795767	195.6360	195.0240
1V	MEAN+SD	-0.0826351	-0.0598633	2.3208126	211.3749	210.3977
2H	MEAN	-0.2270104	-0.1719505	2.2614549	197.6760	197.3700
2H	MEAN+SD	-0.2019952	-0.1867950	2.2765662	203.4323	199.1051
2V	MEAN	-0.1747279	-0.1324973	2.2580302	197.3700	197.6760
2V	MEAN+SD	-0.1341536	-0.1272092	2.2787692	201.0095	199.7239
3H	MEAN	-0.1644295	-0.1227119	2.2689405	197.2680	197.0640
3H	MEAN+SD	-0.1471777	-0.1345330	2.2788722	200.0416	198.1175
3V	MEAN	-0.1025423	-0.0480139	2.2777433	195.6360	196.7580
3V	MEAN+SD	-0.1174728	-0.1043633	2.2818425	200.3410	198.4216
4H	MEAN	-0.1787769	-0.1547439	2.2645563	198.1860	197.3700
4H	MEAN+SD	-0.1872856	-0.2062475	2.2606576	200.1877	198.4840
5H	MEAN	-0.1835970	-0.1919980	2.2427643	195.8400	196.9620
5H	MEAN+SD	-0.1227950	-0.1391435	2.2827510	197.5403	197.3867
5V	MEAN	-0.1051880	-0.0673749	2.2652436	194.9220	196.6560
5V	MEAN+SD	-0.1106504	-0.0914974	2.2764161	197.0155	197.1398
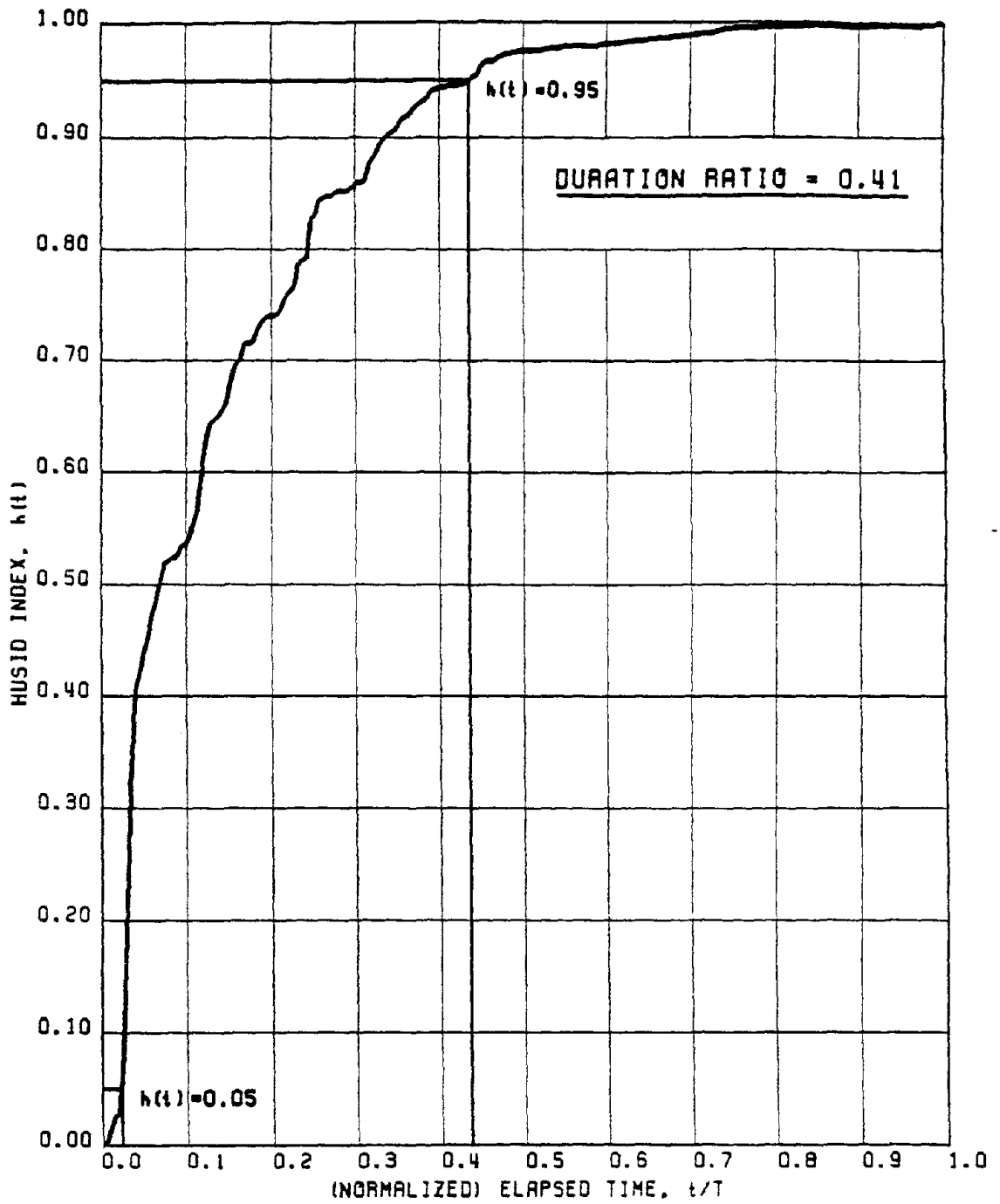
FIG. 1   HUSID PLOT FOR 1961-HOLISTER CITY HALL, N89W RECORD (SOFT SITE)
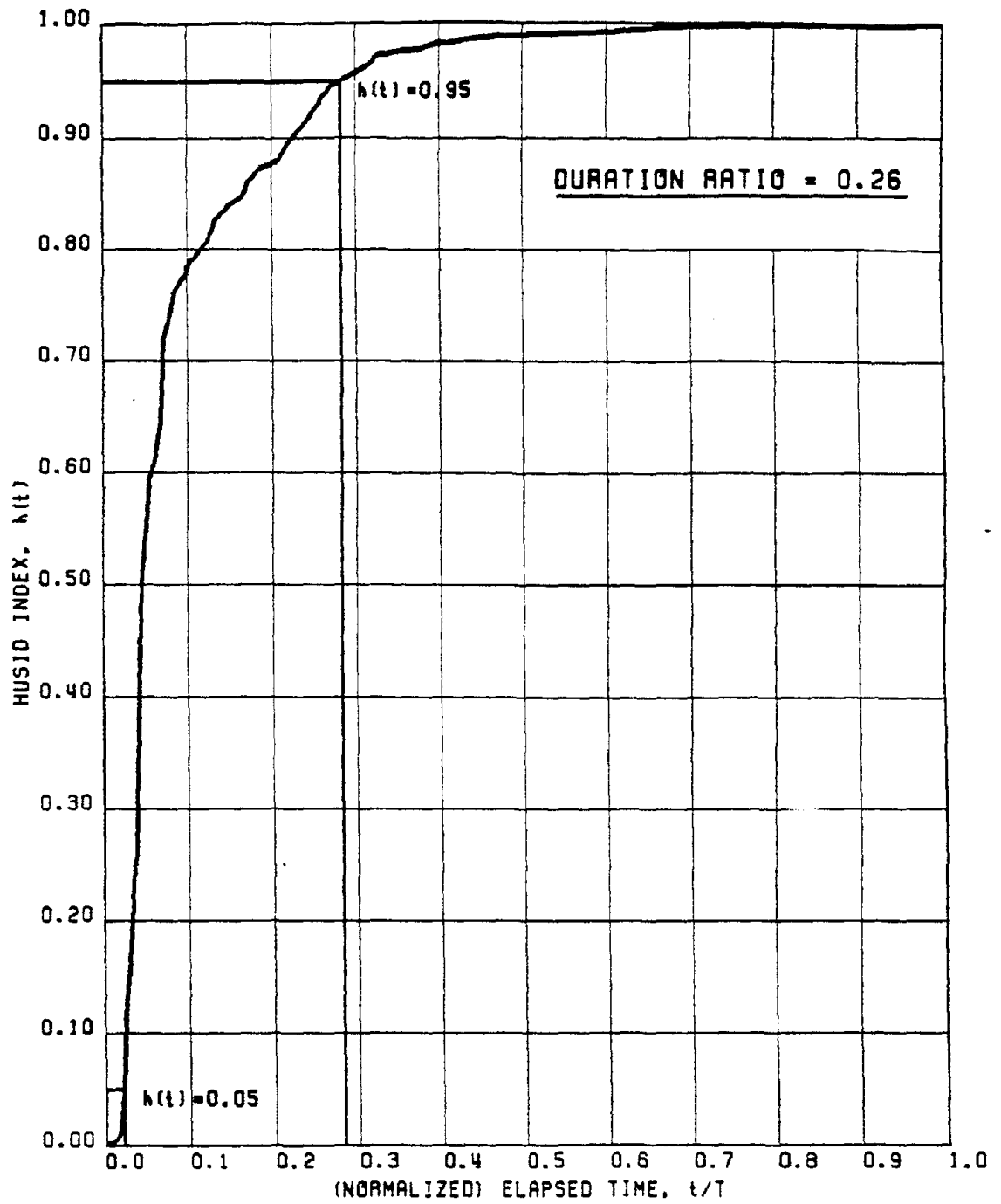
FIG. 2 HUSID PLOT FOR 1971-CASTAIC OLD RIDGE-N21E RECORD (MED. HARD SITE)
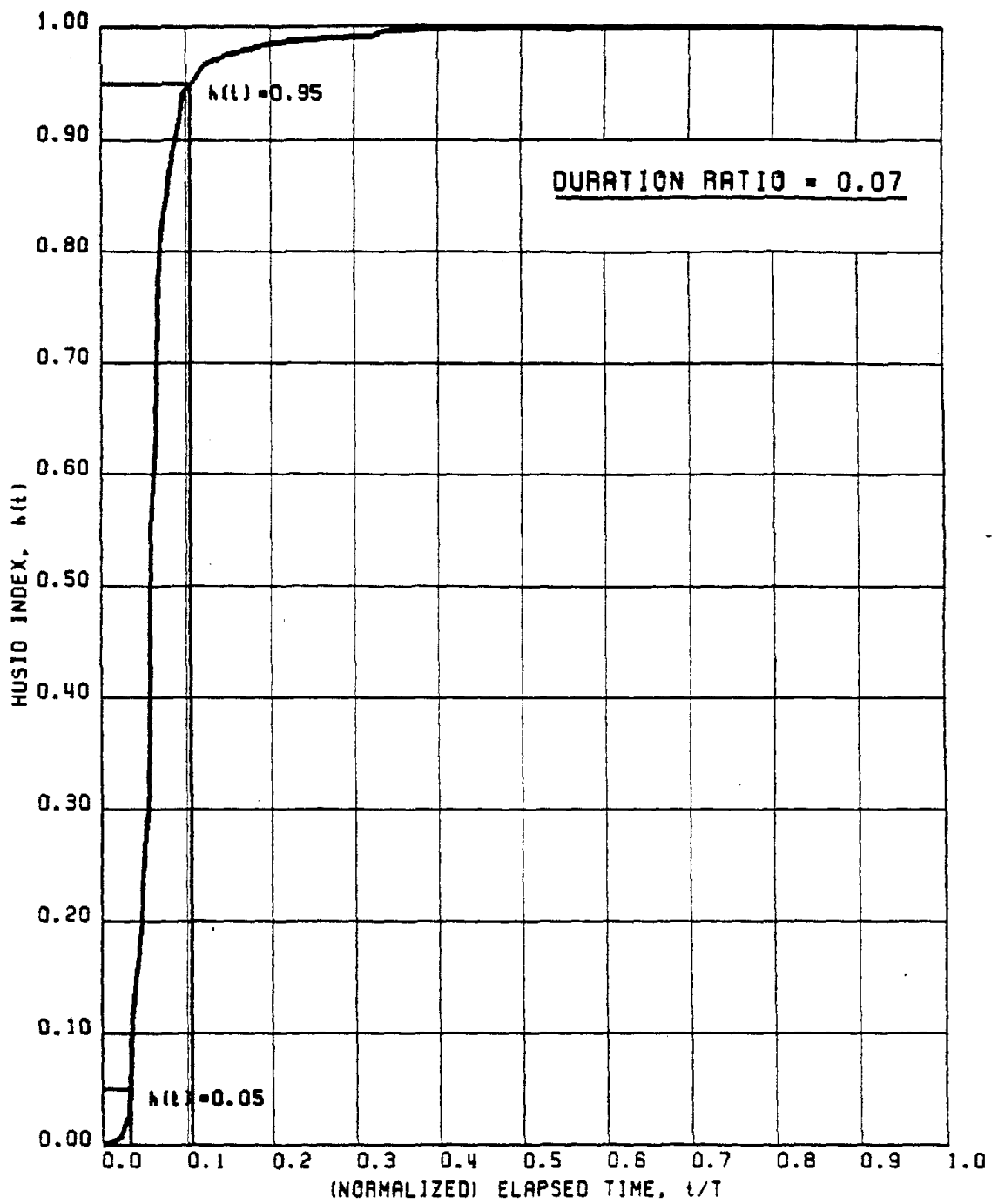
FIG. 3   HUSID PLOT FOR 1971-CAL TECH SEISMIC LAB-S90W RECORD (HARD SITE)
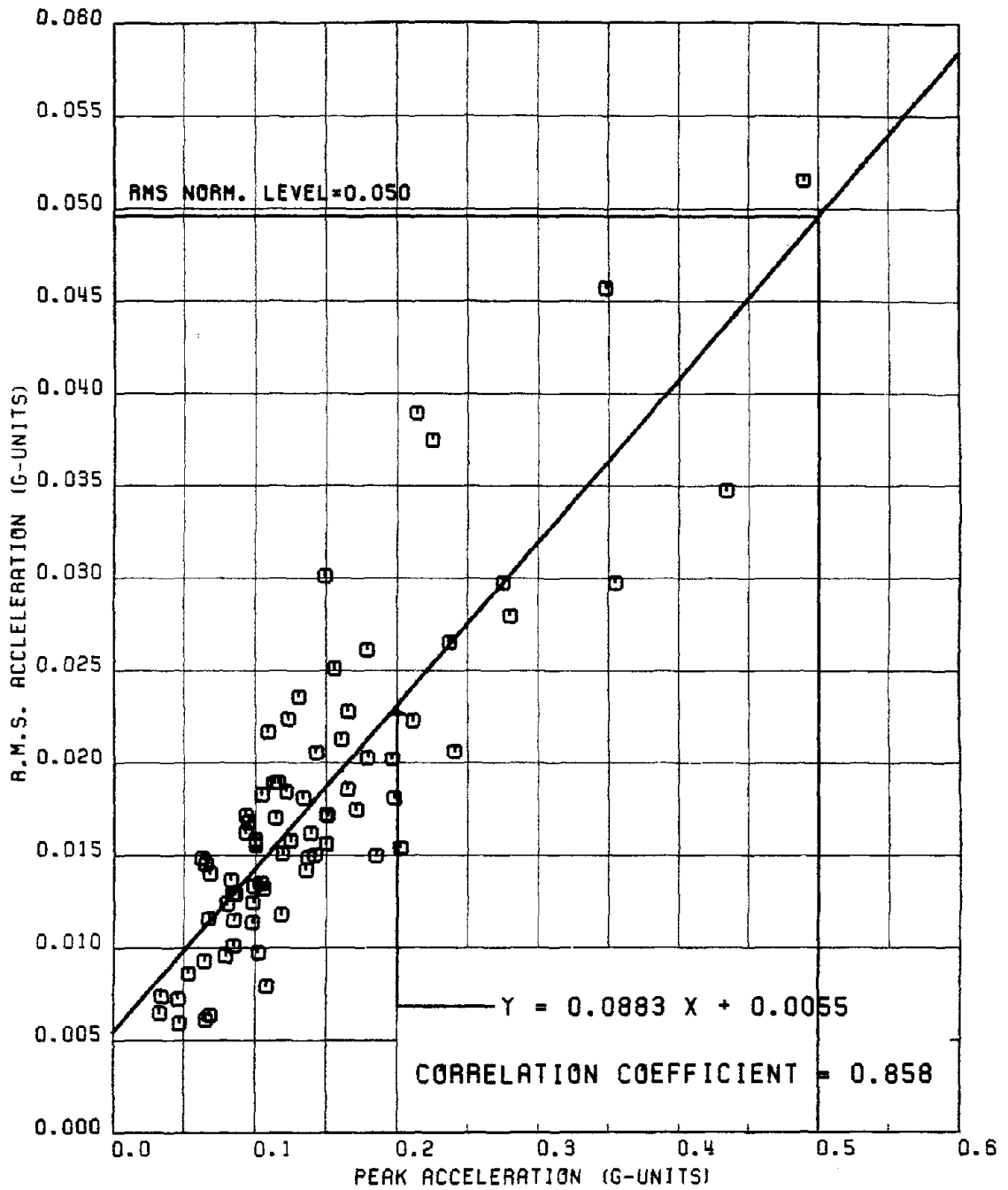
FIG. 4   REGRESSION OF R.M.S. & PEAK ACCELERATION FOR RECORDS OF GROUP #1H
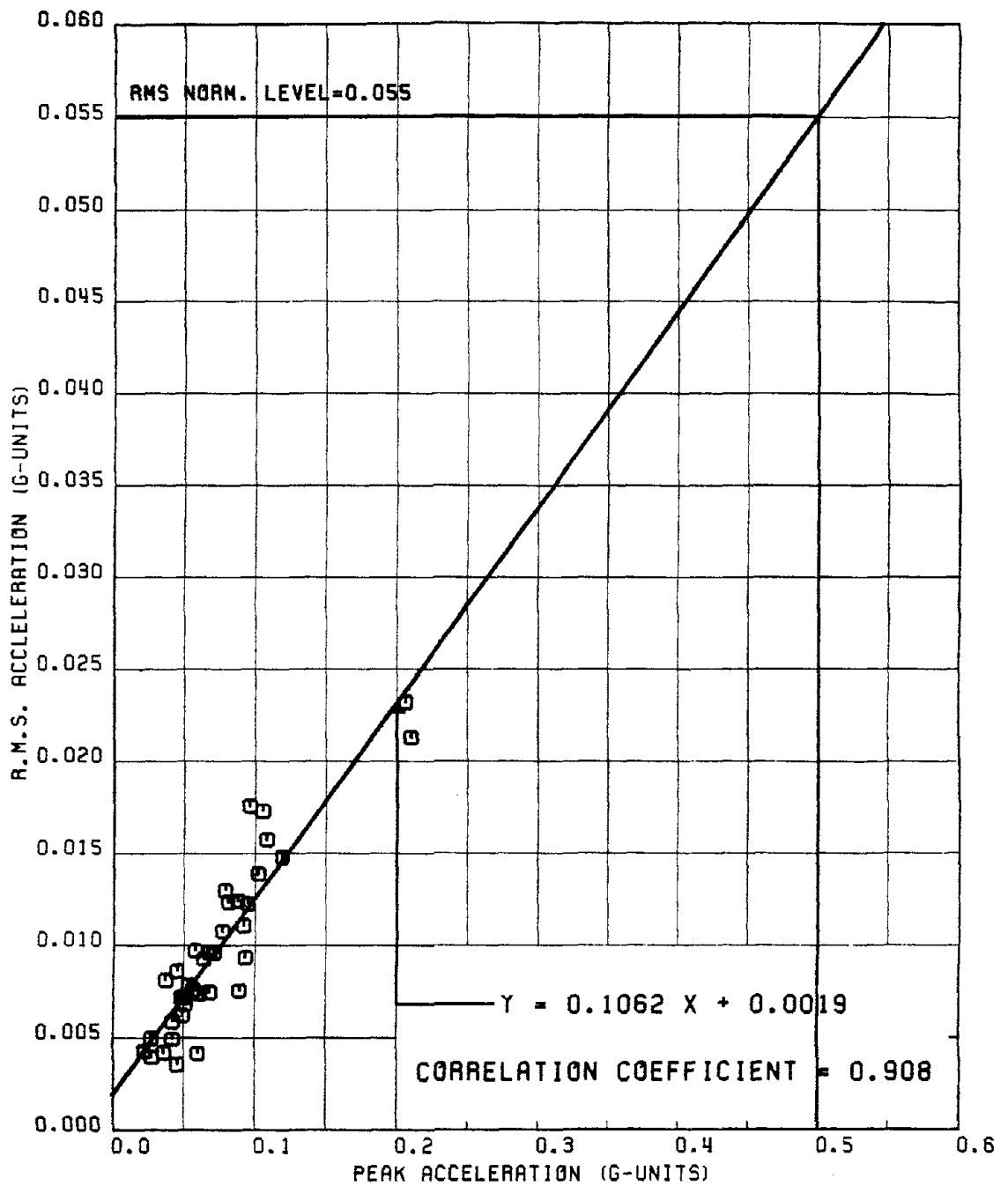
FIG. 5   REGRESSION OF R.M.S. & PEAK ACCELERATION FOR RECORDS OF GROUP ≠1V
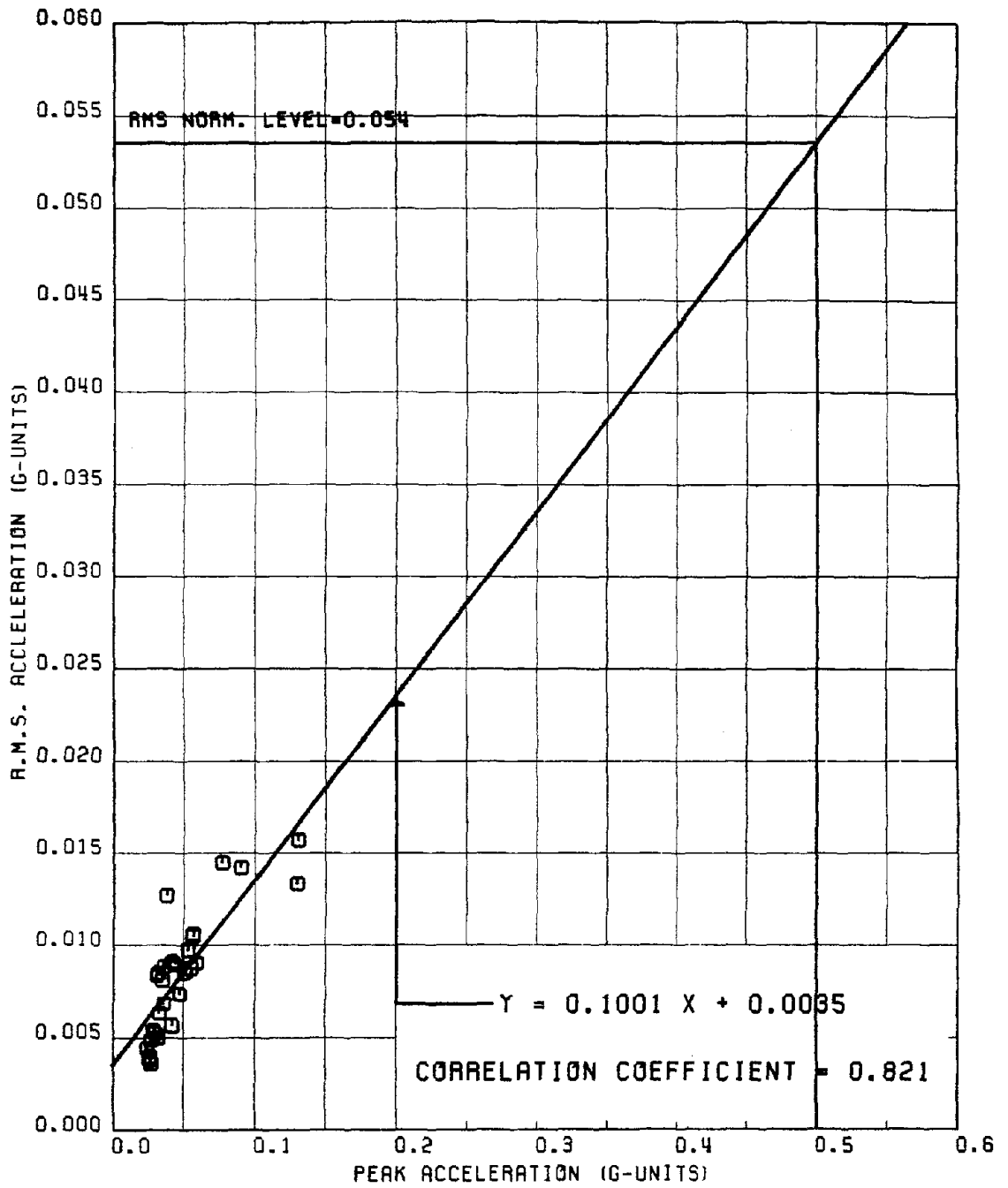
FIG. 6   REGRESSION OF R.M.S. & PEAK ACCELERATION FOR RECORDS OF GROUP #2H
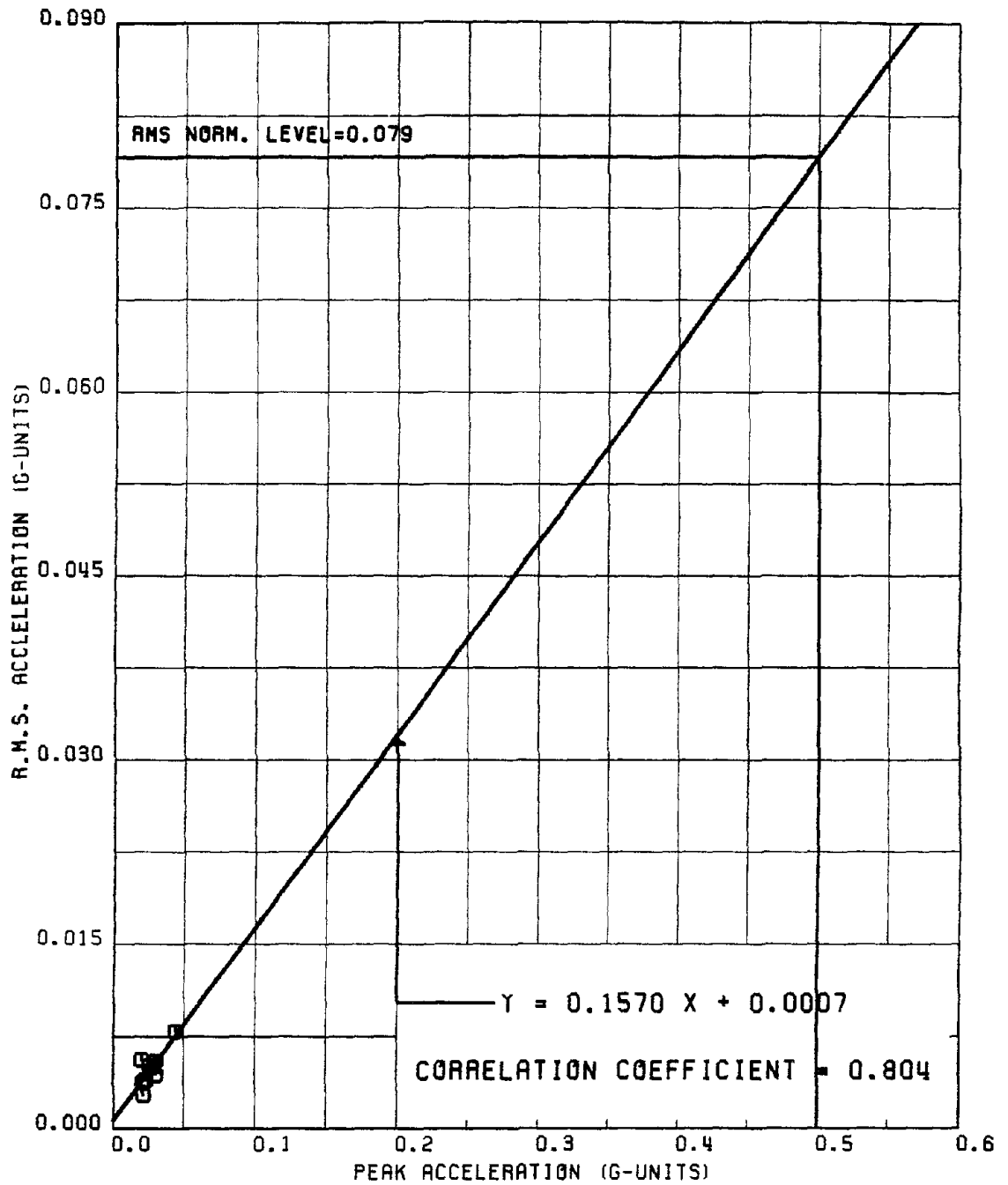
FIG. 7   REGRESSION OF R.M.S. & PEAK ACCELERATION FOR RECORDS OF GROUP #2V
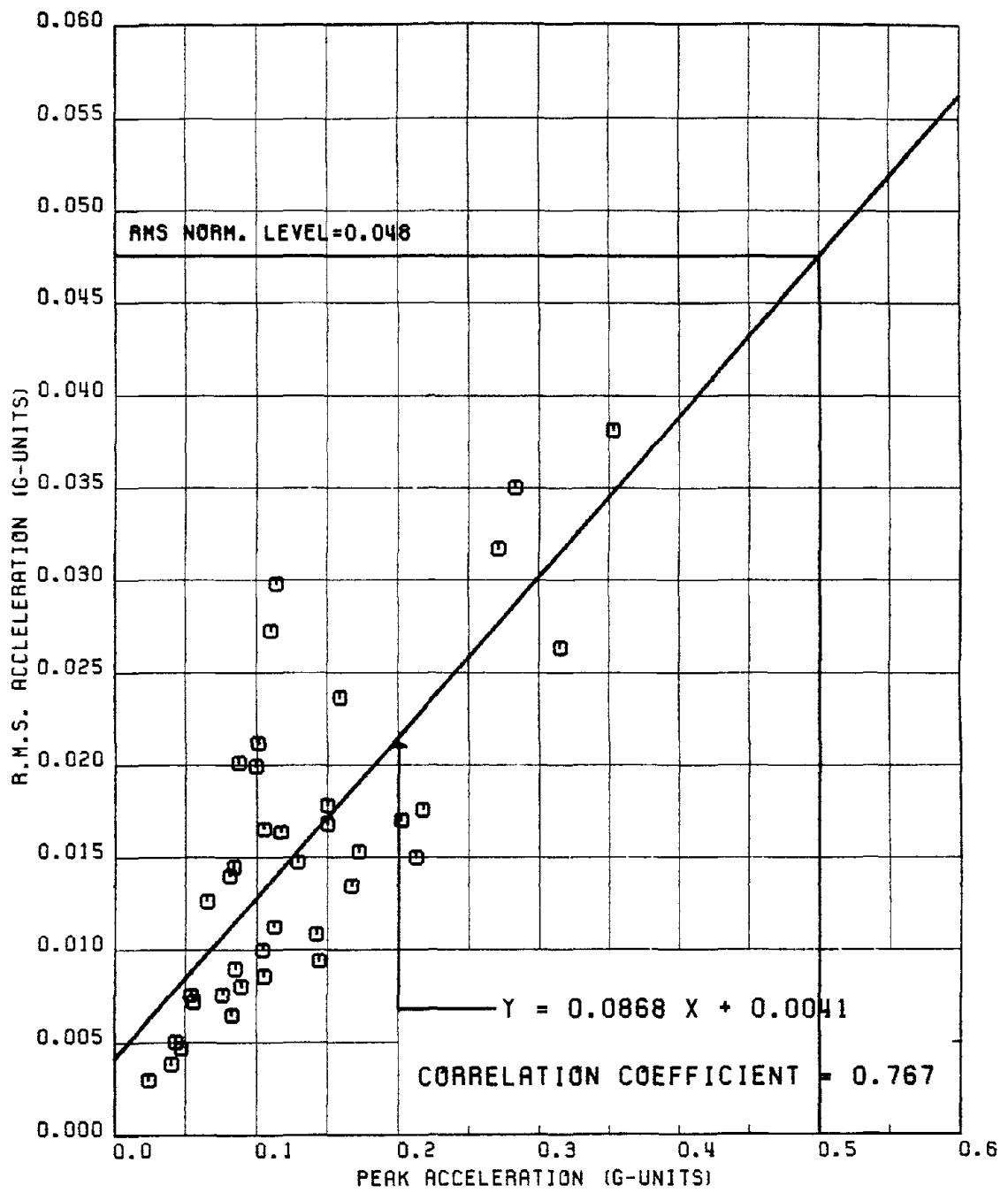
FIG. 8 REGRESSION OF R.M.S. & PEAK ACCELERATION FOR RECORDS OF GROUP #3H
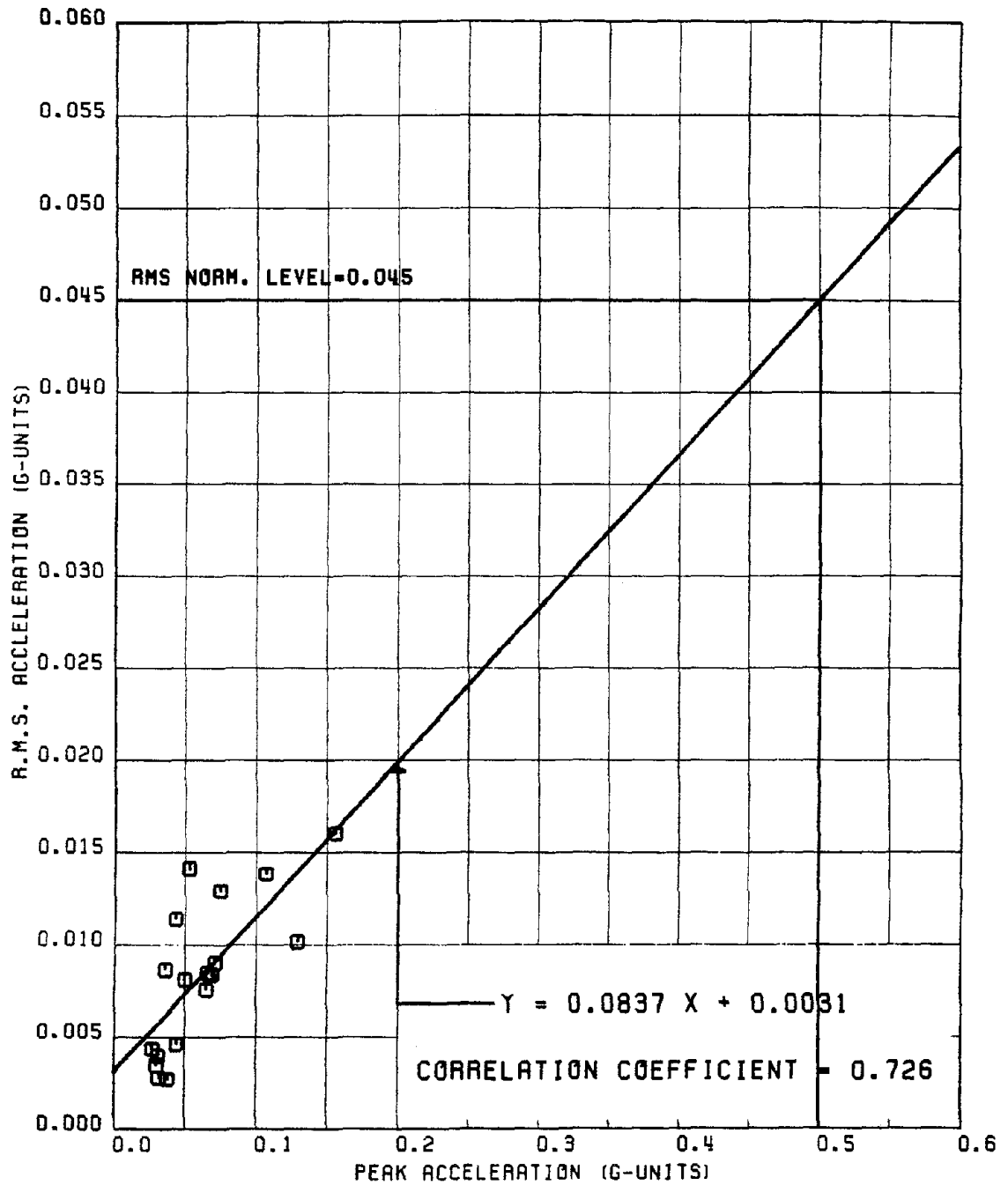
FIG. 9   REGRESSION OF R.M.S. & PEAK ACCELERATION FOR RECORDS OF GROUP #3V
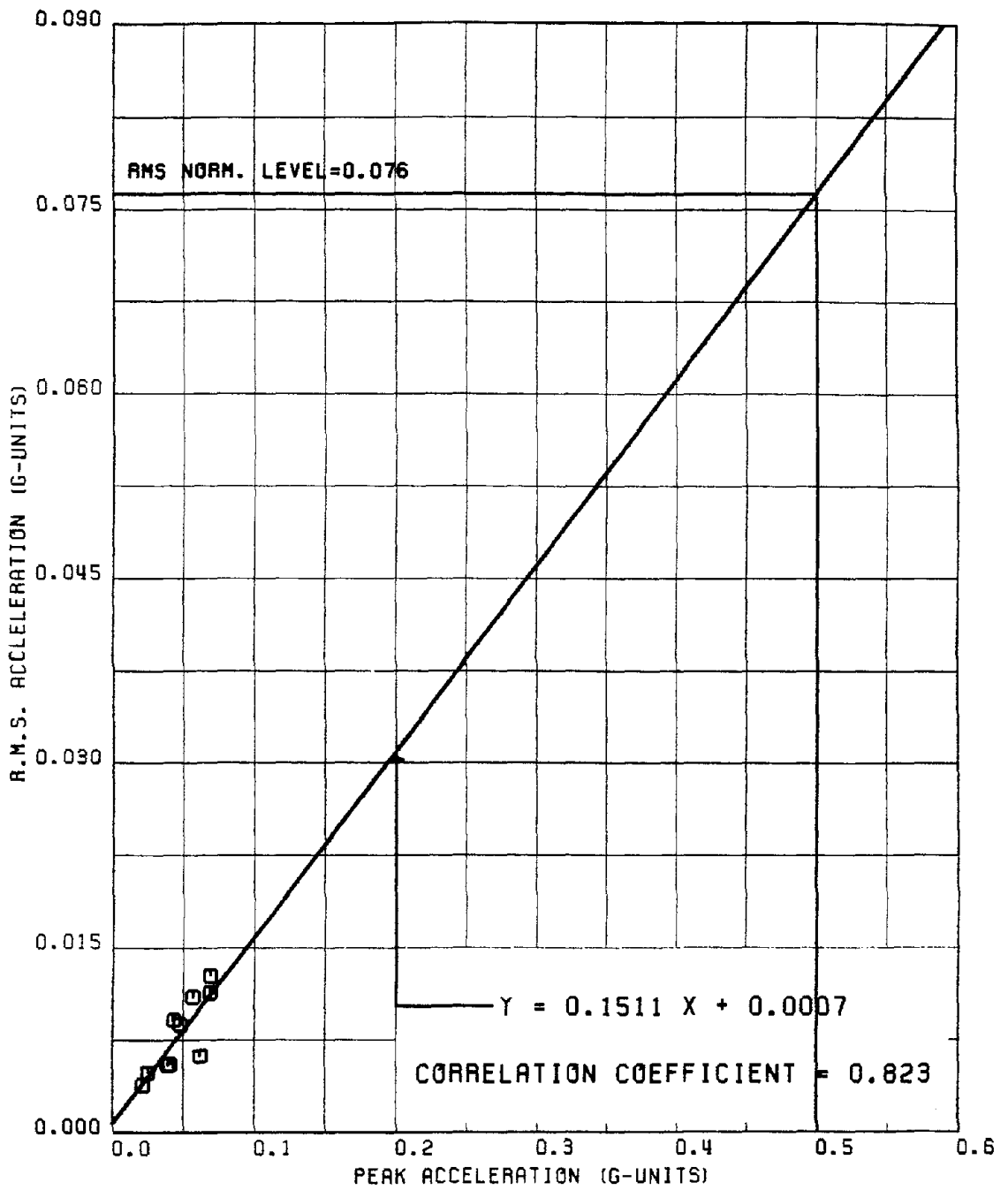
FIG. 10   REGRESSION OF R.M.S. & PEAK ACCELERATION FOR RECORDS OF GROUP #4H
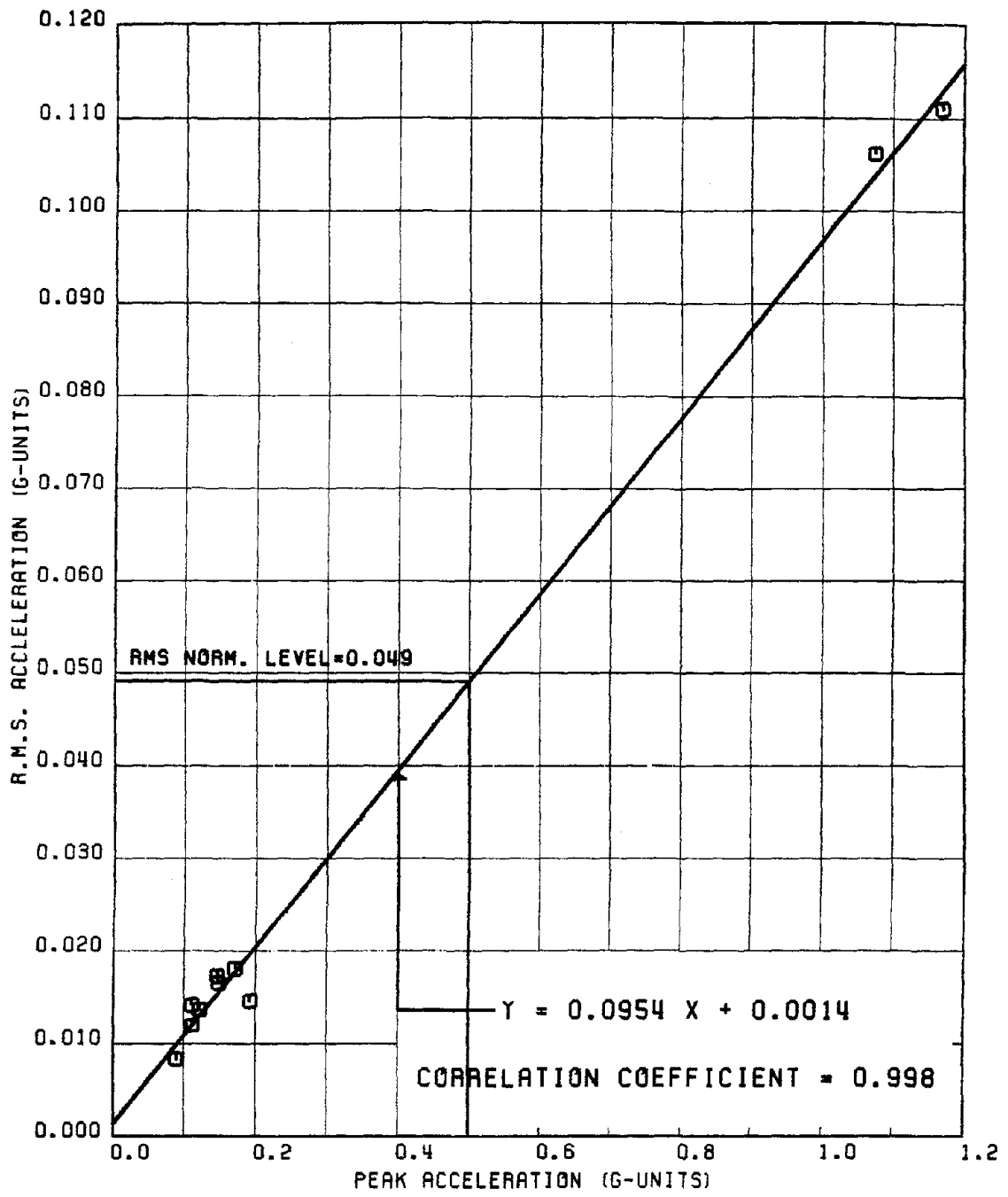
FIG. 11   REGRESSION OF R.M.S. & PEAK ACCELERATION FOR RECORDS OF GROUP ≈5H
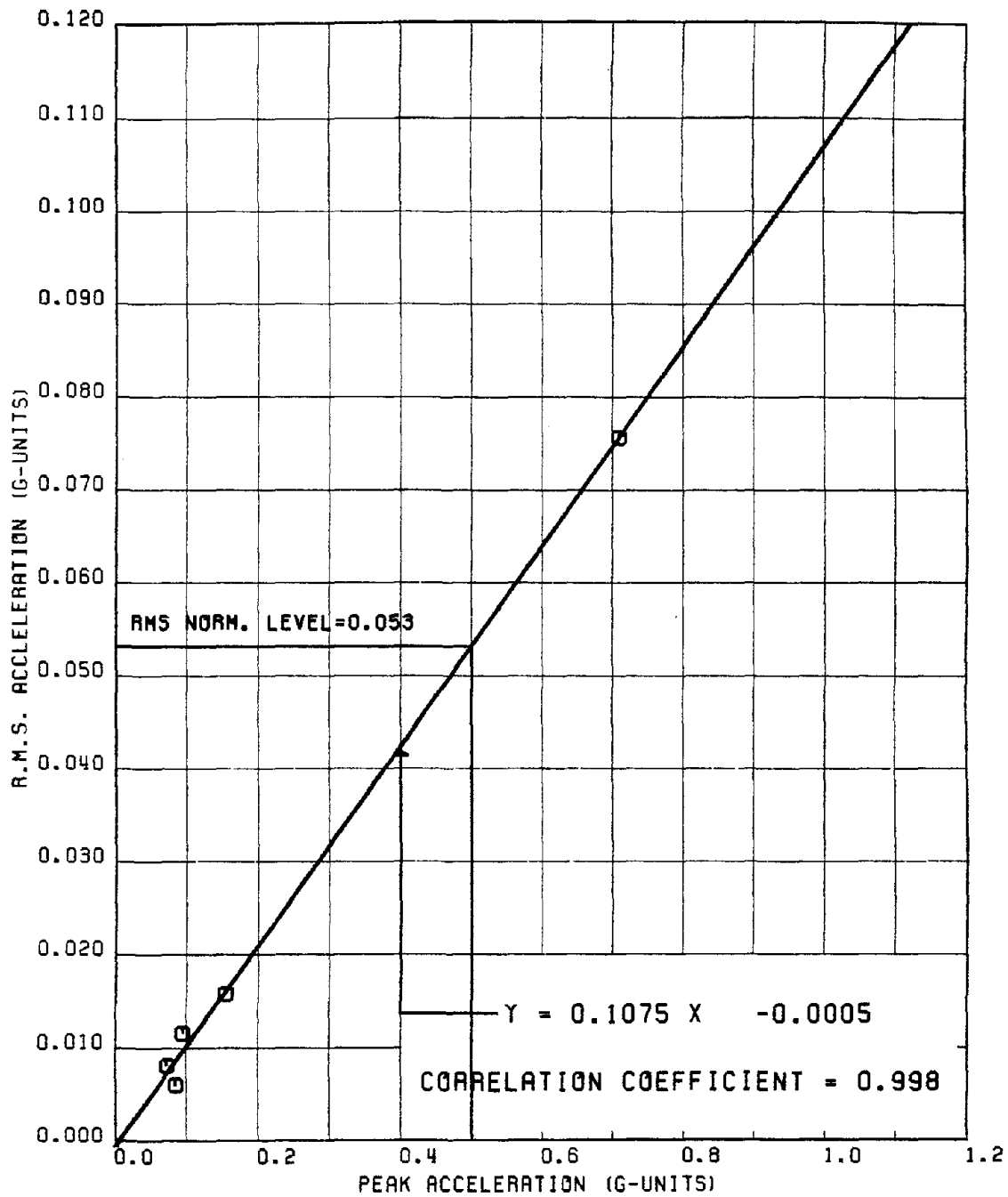
FIG. 12   REGRESSION OF R.M.S. & PEAK ACCELERATION FOR RECORDS OF GROUP #5V
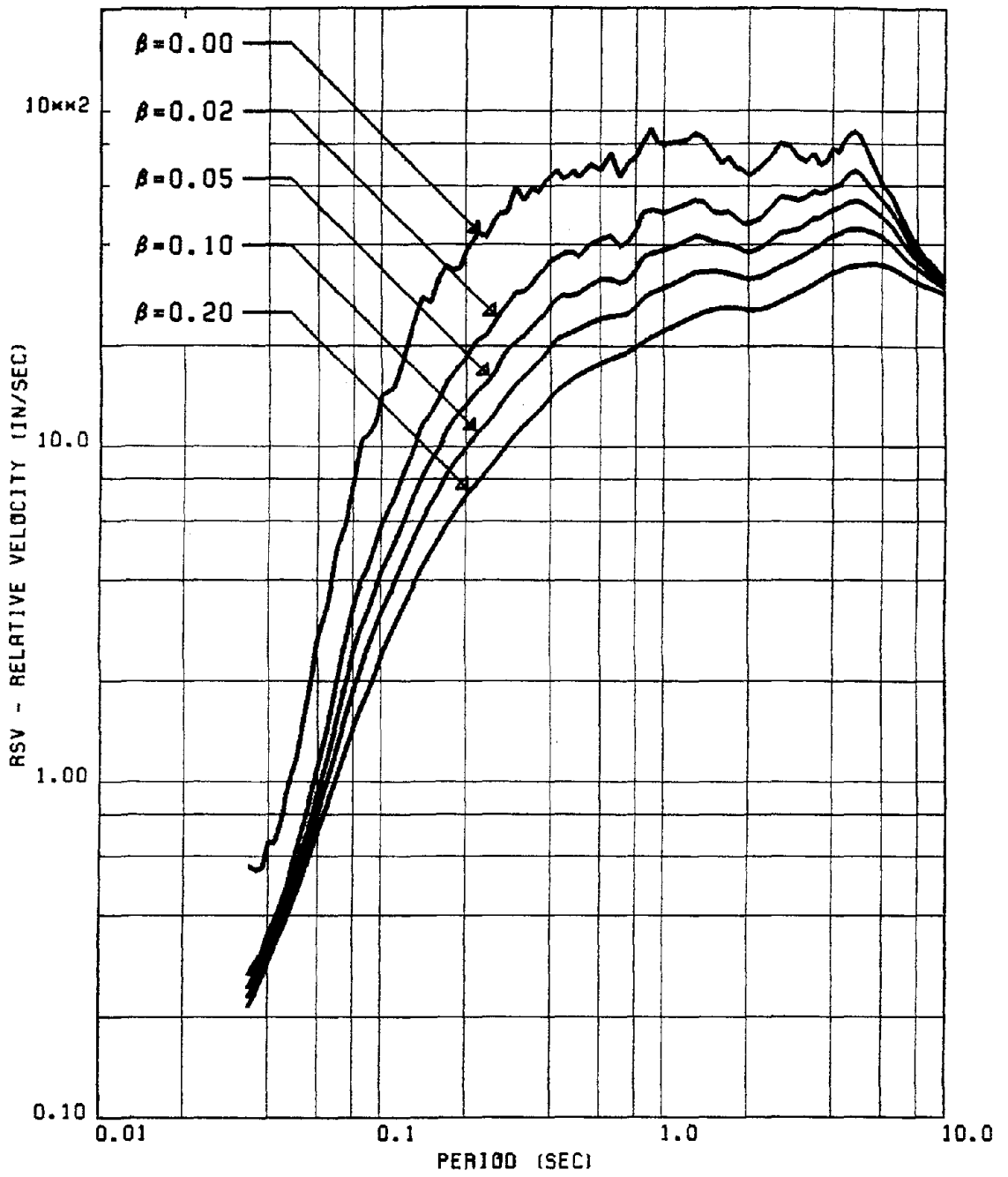
FIG. 13 MEAN RELATIVE VELOCITY SPECTRA FOR HORIZONTAL RECORDS OF GROUP *1
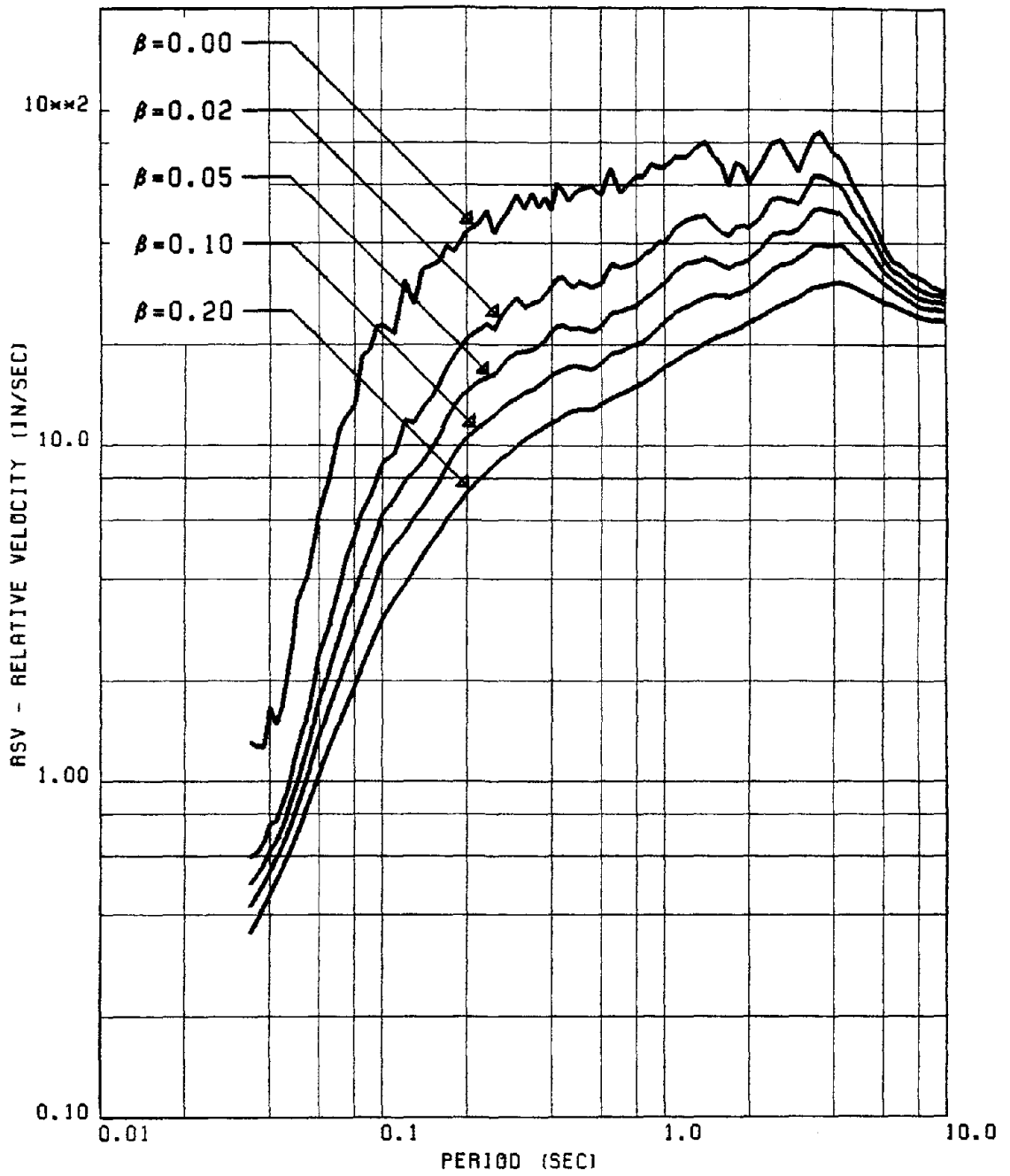
FIG. 14 MEAN RELATIVE VELOCITY SPECTRA FOR VERTICAL RECORDS OF GROUP #1
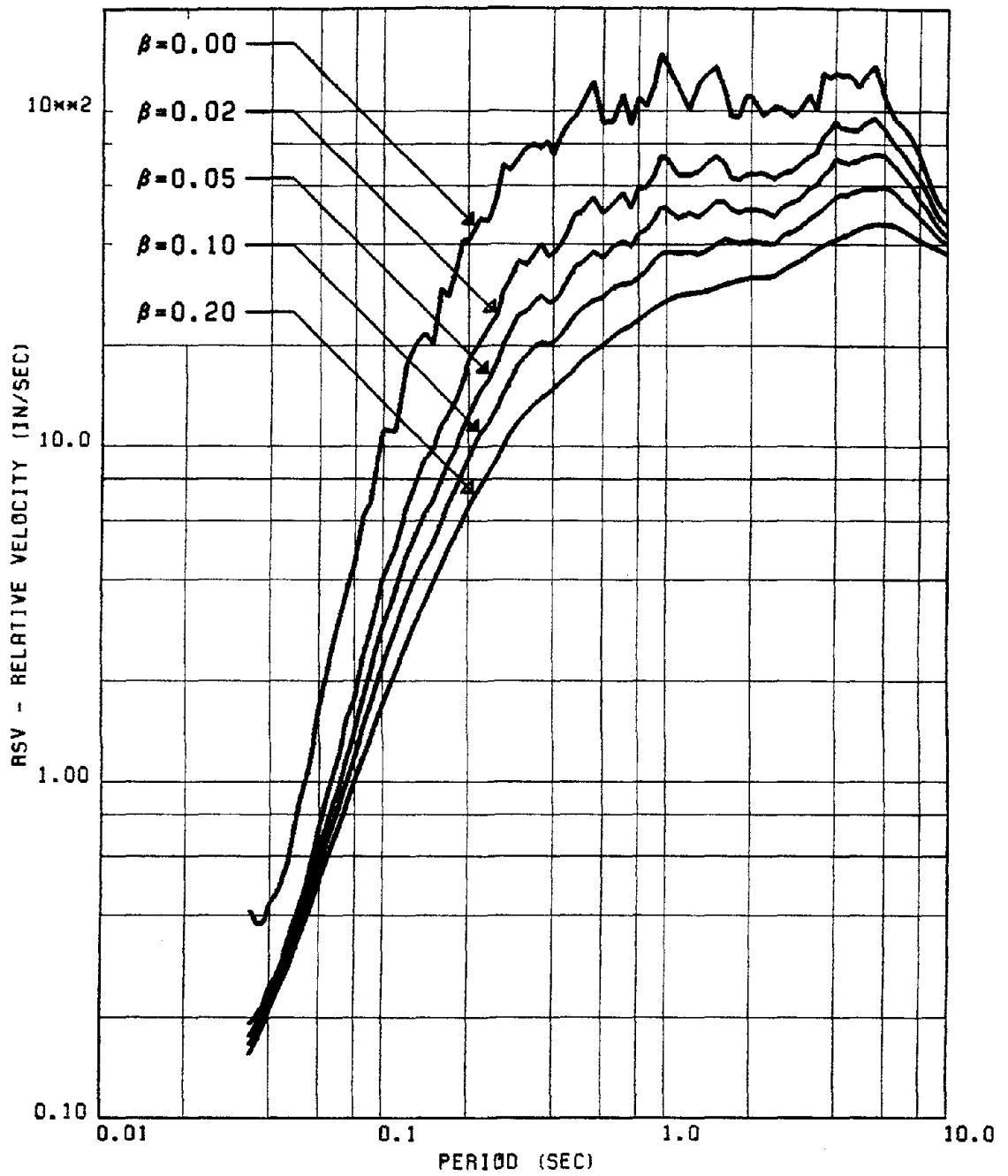
FIG. 15 MEAN RELATIVE VELOCITY SPECTRA FOR HORIZONTAL RECORDS OF GROUP #2
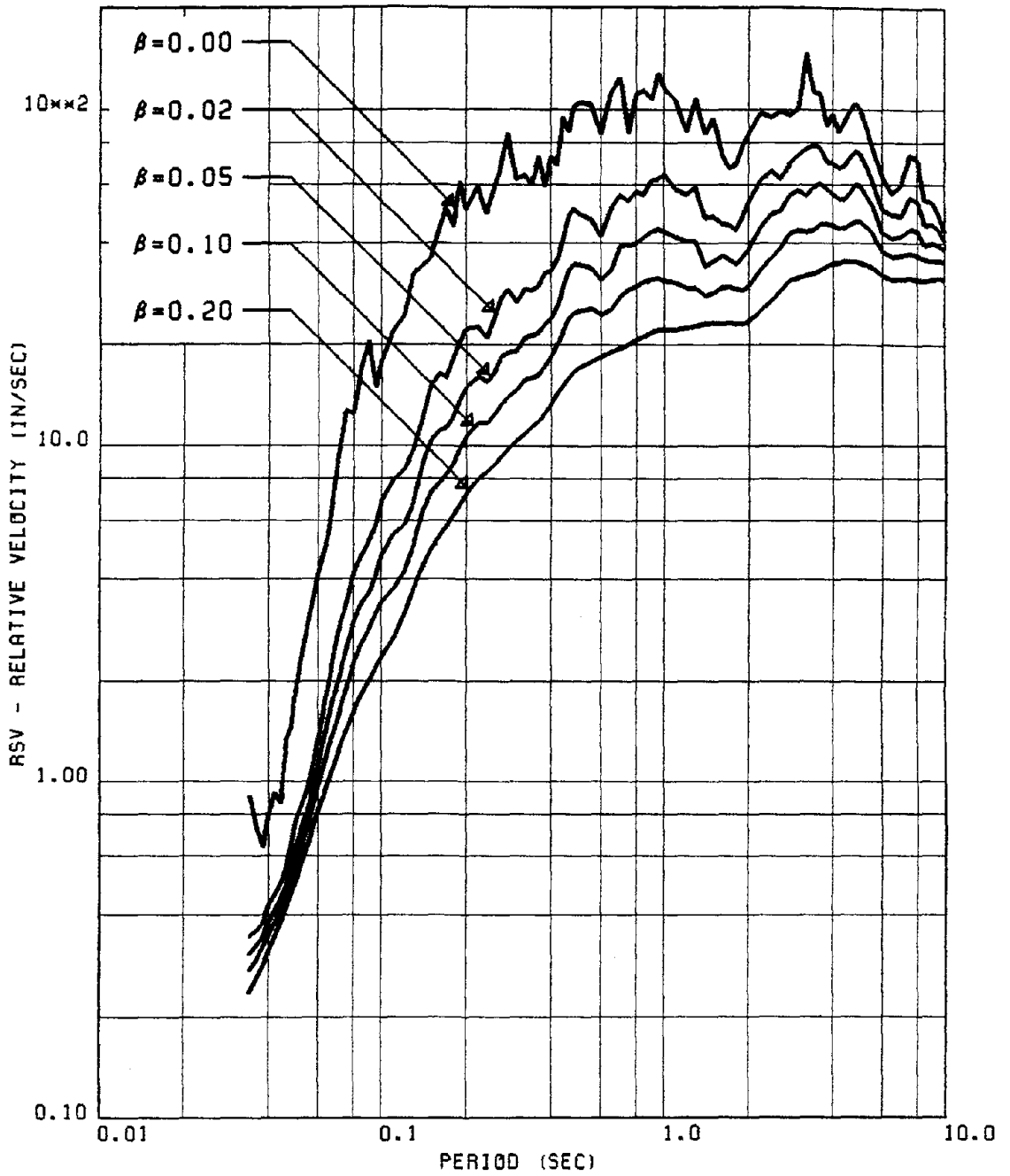
FIG. 16   MEAN RELATIVE VELOCITY SPECTRA FOR VERTICAL RECORDS OF GROUP #2
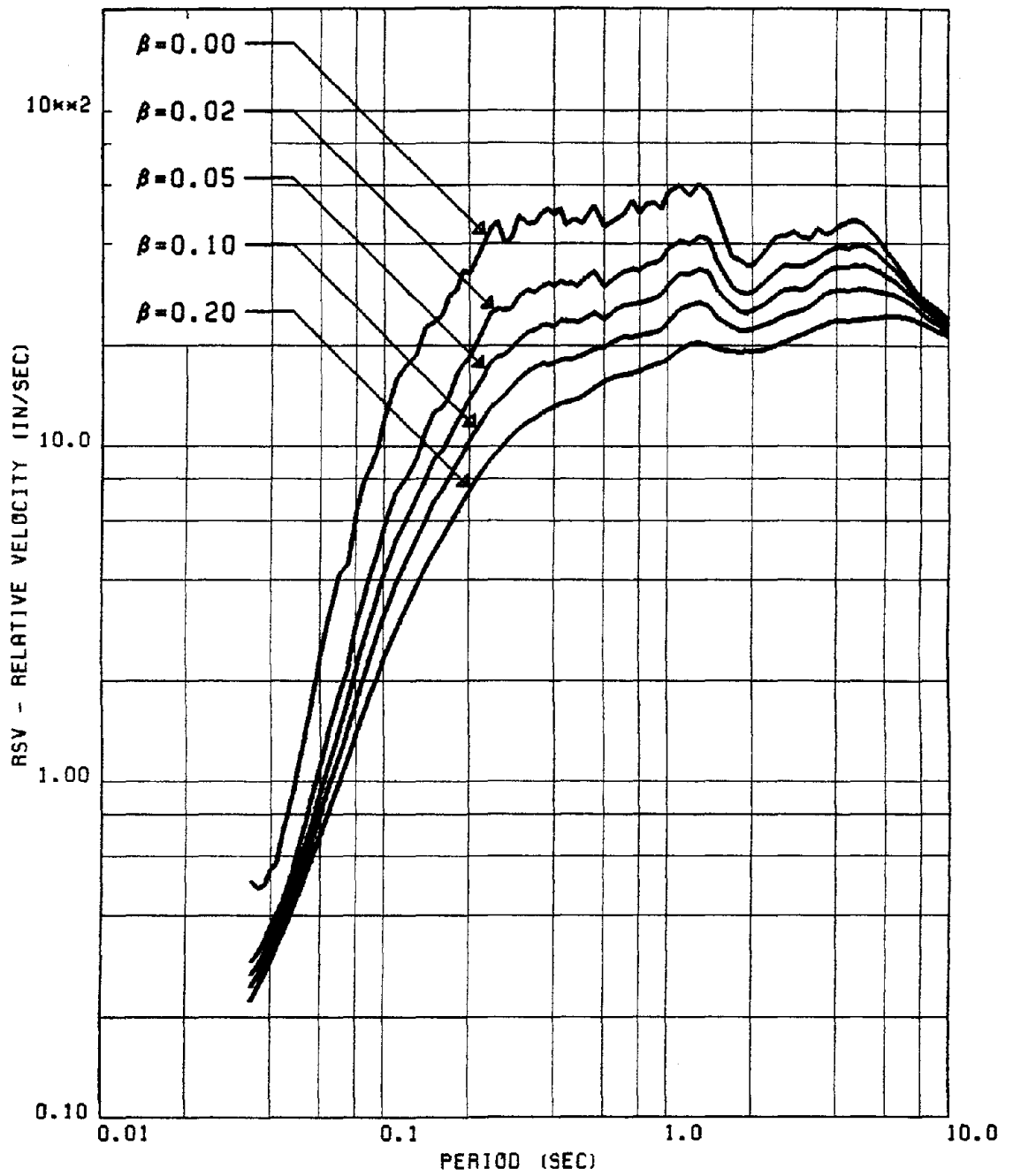
FIG. 17 MEAN RELATIVE VELOCITY SPECTRA FOR HORIZONTAL RECORDS OF GROUP *3
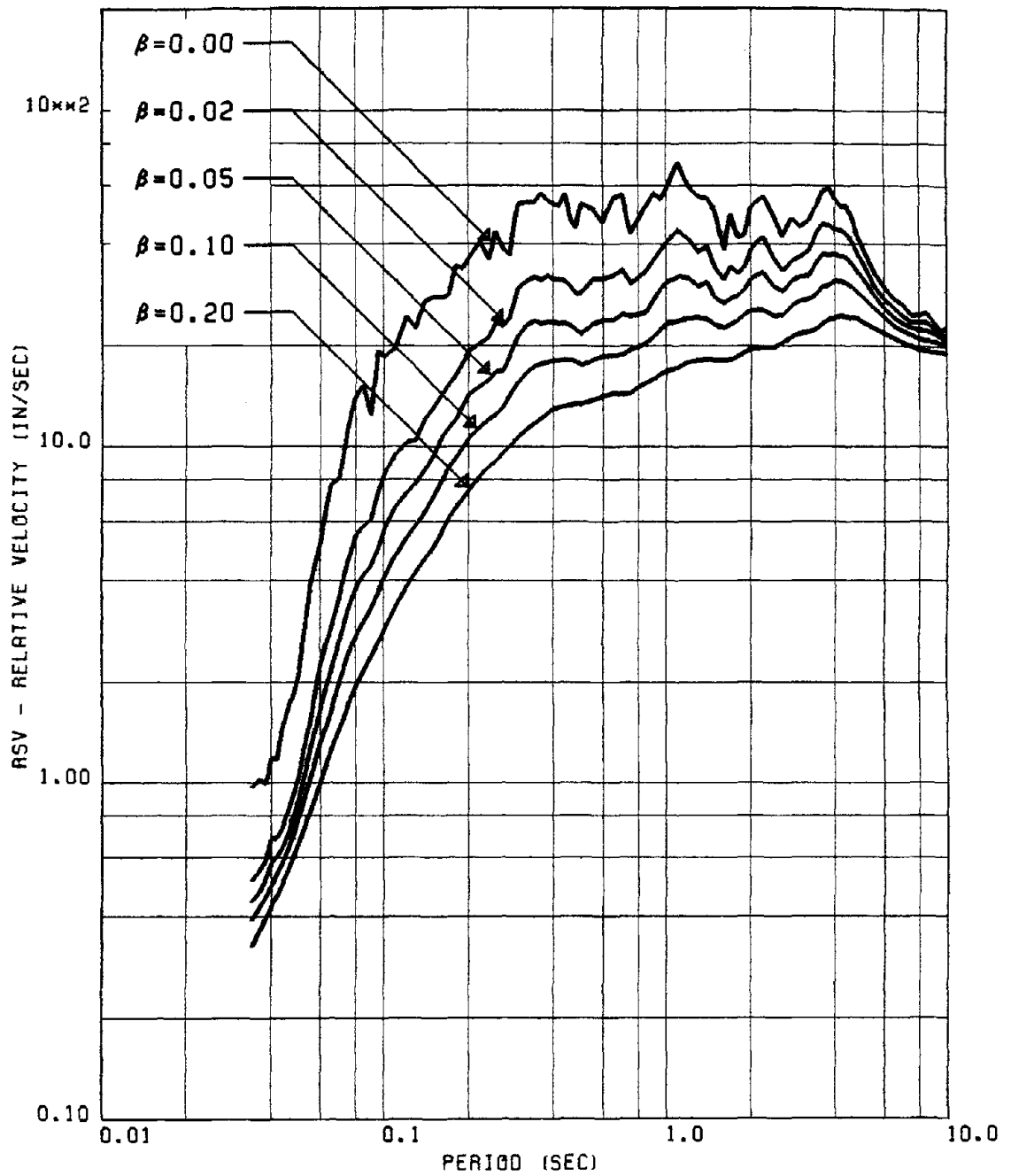
FIG. 18 MEAN RELATIVE VELOCITY SPECTRA FOR VERTICAL RECORDS OF GROUP #3
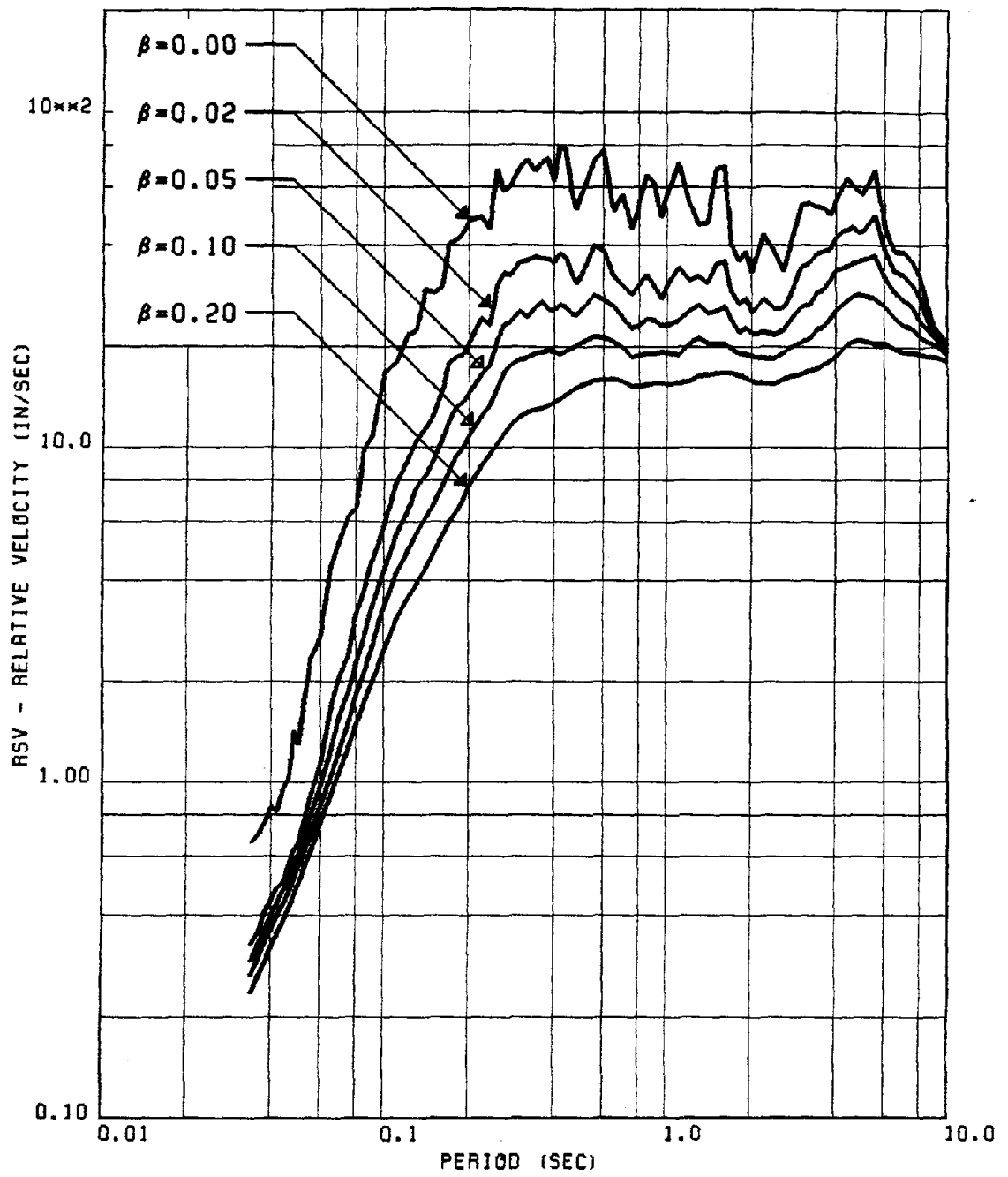
FIG. 19 MEAN RELATIVE VELOCITY SPECTRA FOR HORIZONTAL RECORDS OF GROUP #4

97
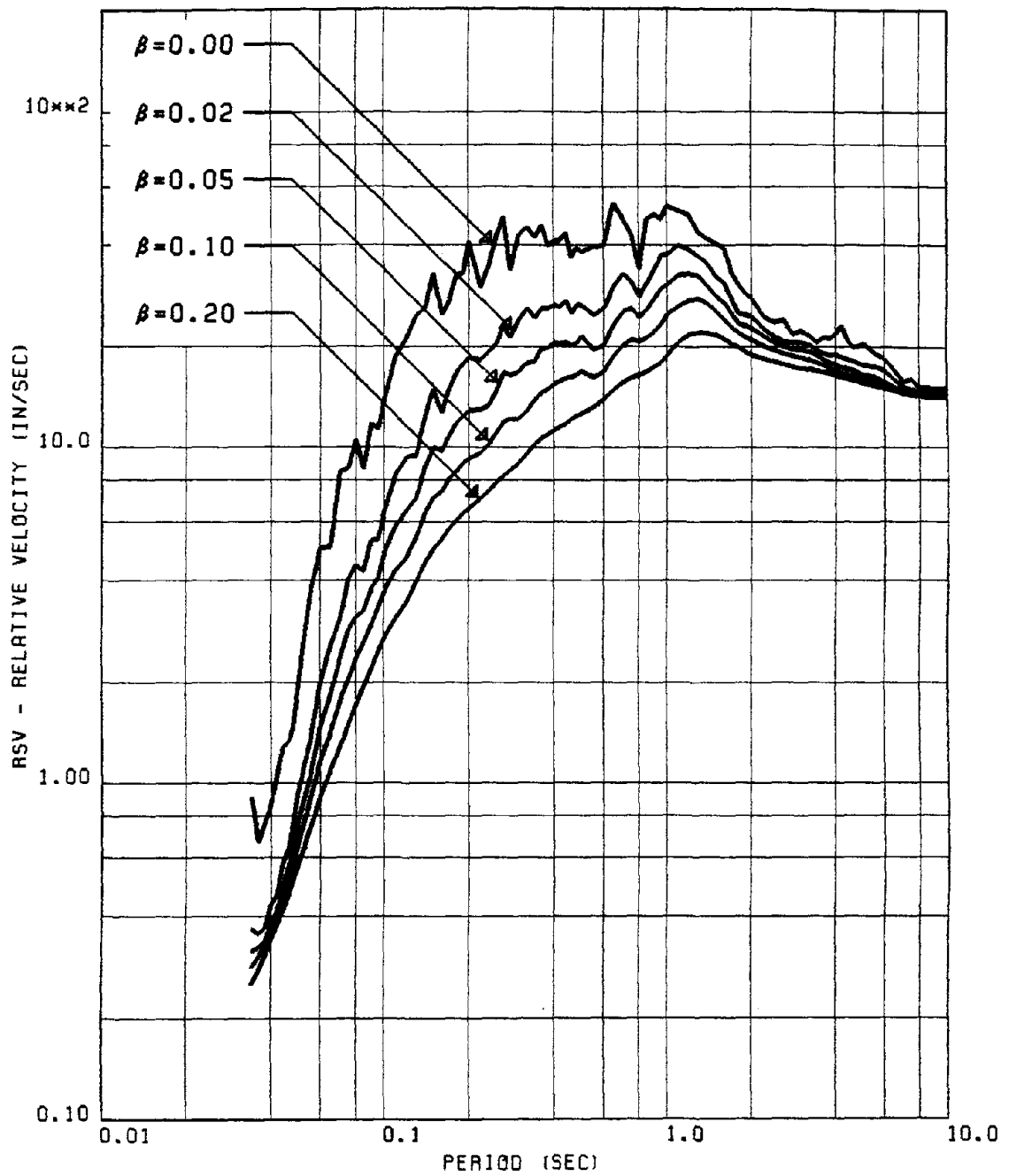
FIG. 20   MEAN RELATIVE VELOCITY SPECTRA FOR HORIZONTAL RECORDS OF GROUP #5
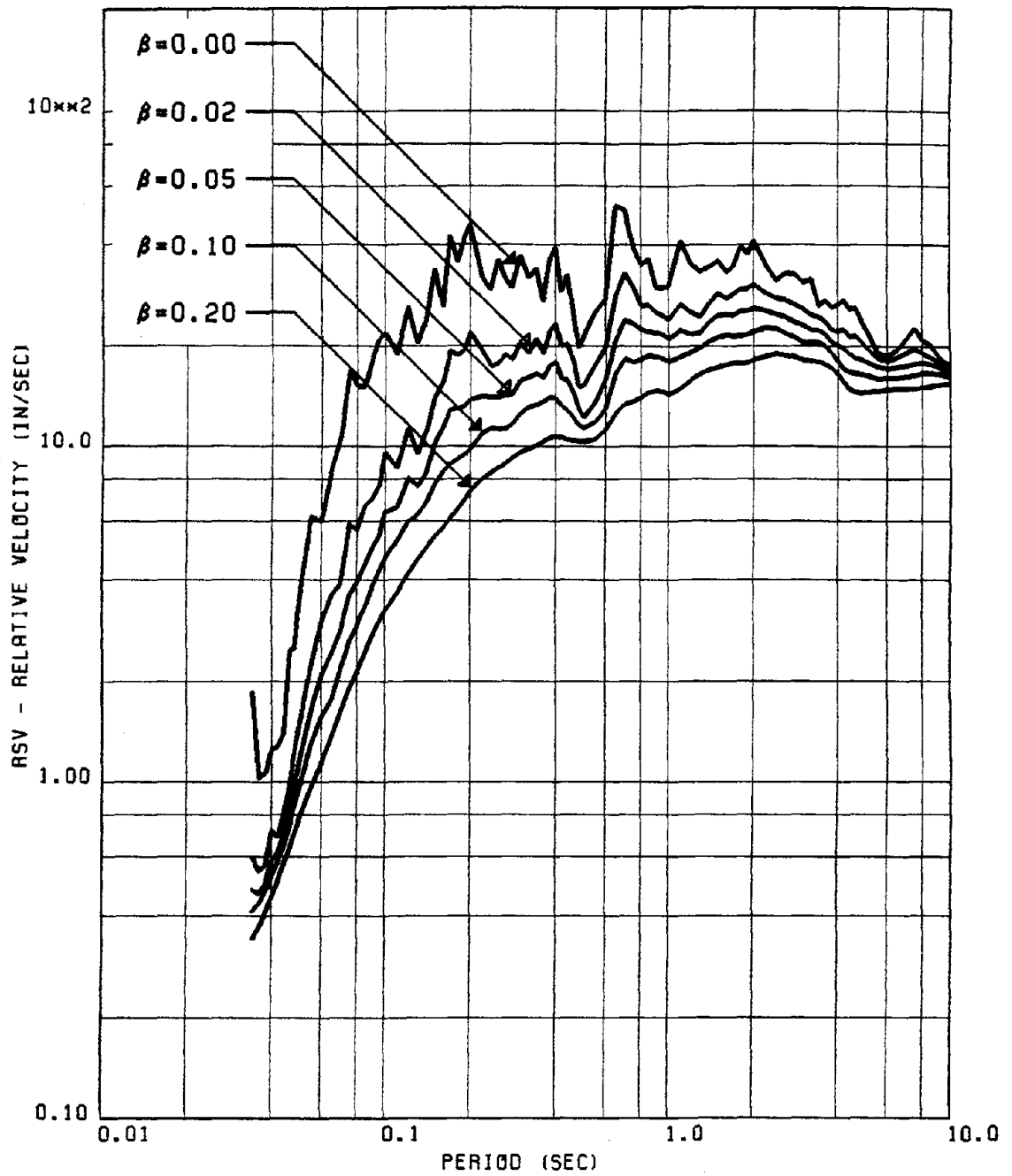
FIG. 21 MEAN RELATIVE VELOCITY SPECTRA FOR VERTICAL RECORDS OF GROUP #5
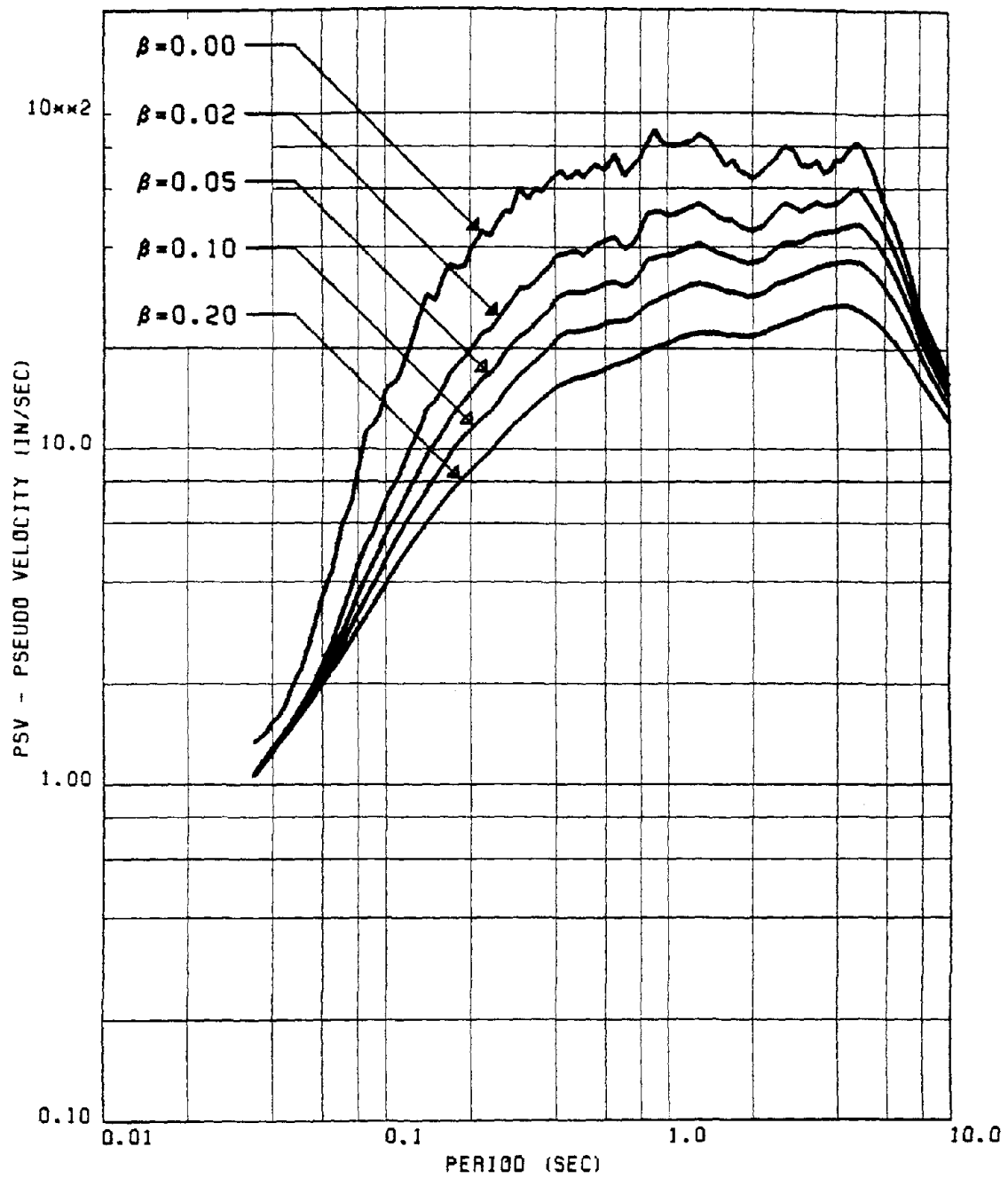
FIG. 22   MEAN PSEUDO VELOCITY SPECTRA FOR HORIZONTAL RECORDS OF GROUP #1
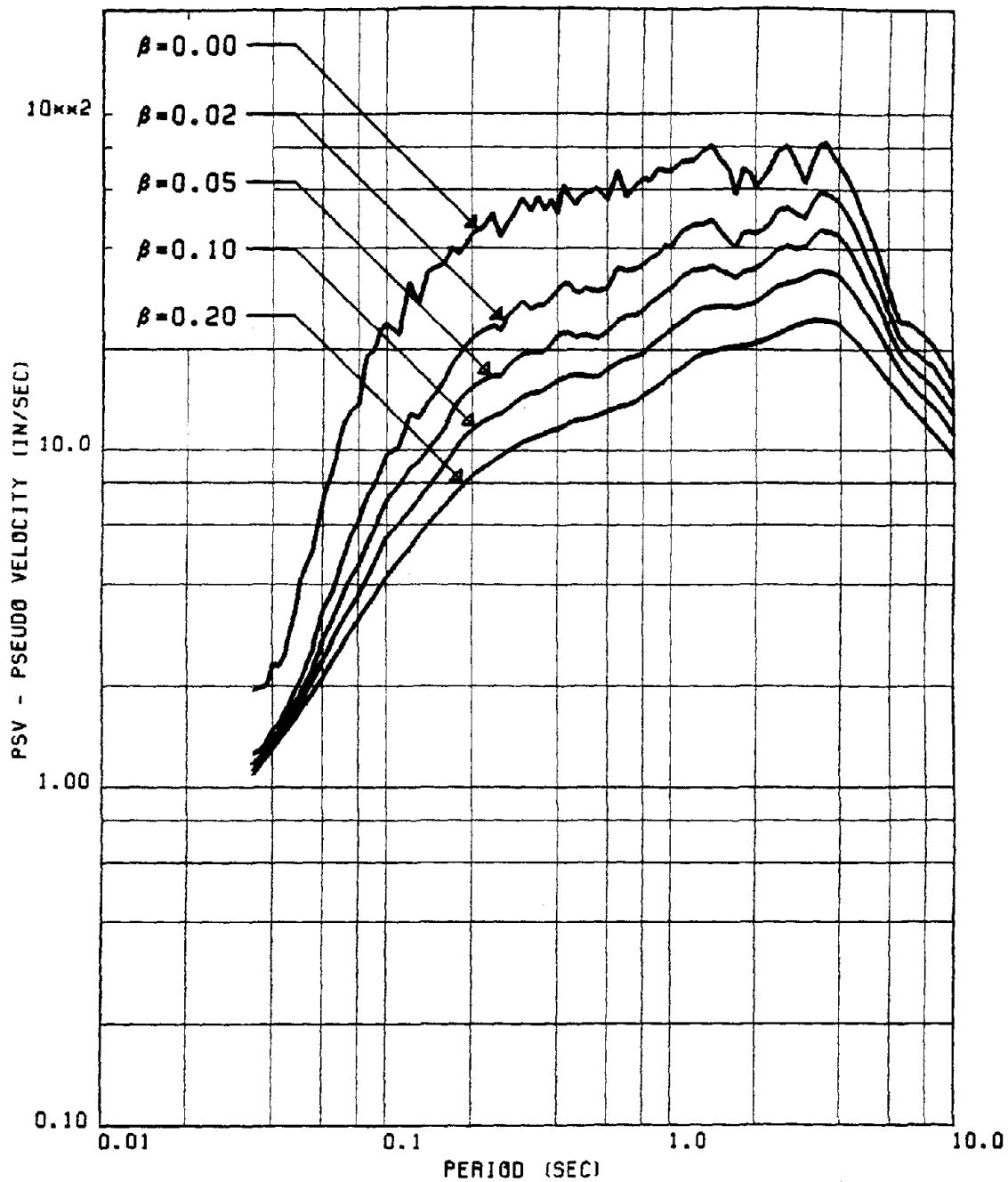
FIG. 23   MEAN PSEUDO VELOCITY SPECTRA FOR VERTICAL RECORDS OF GROUP #1

101
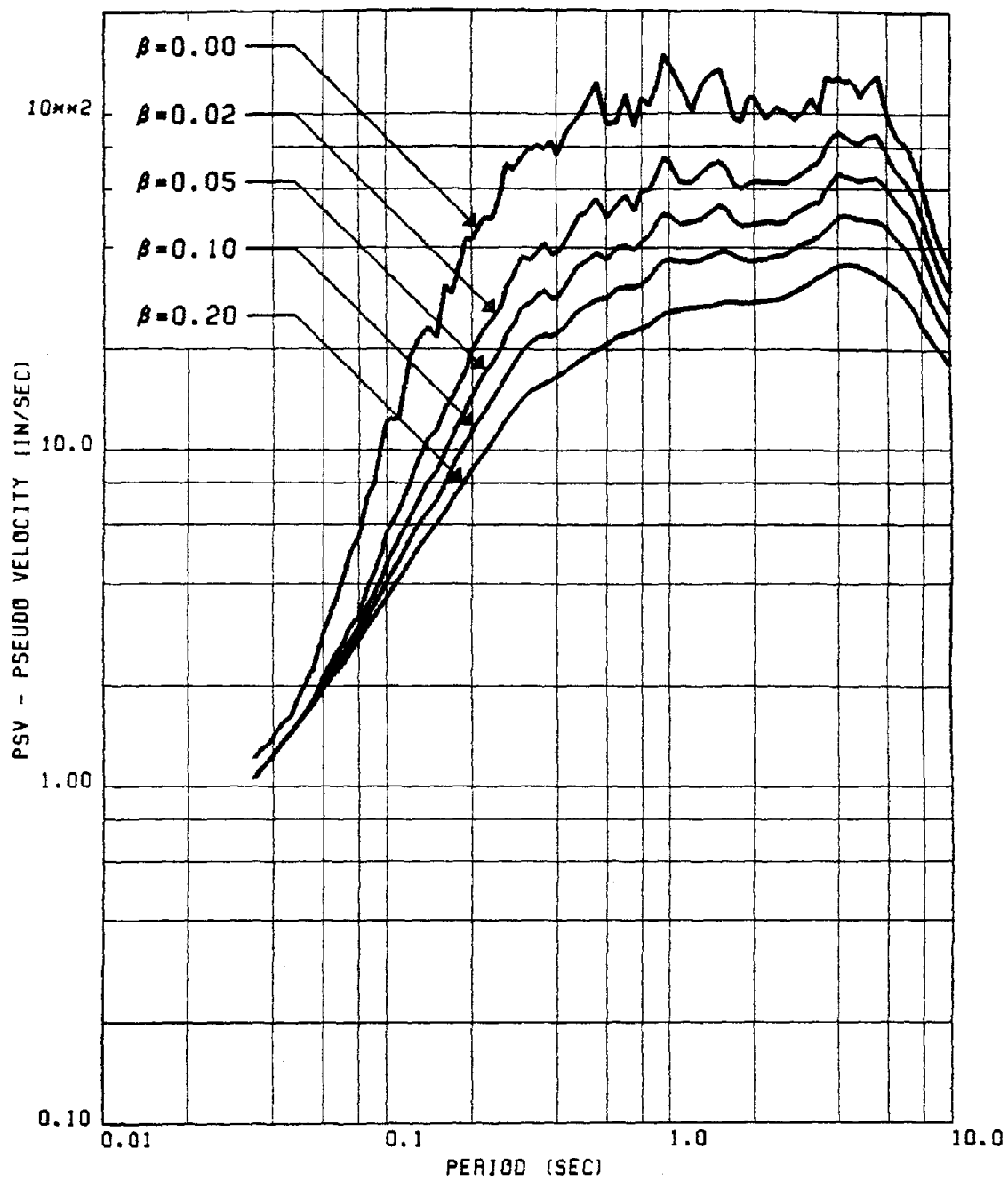
FIG. 24   MEAN PSEUDO VELOCITY SPECTRA FOR HORIZONTAL RECORDS OF GROUP #2
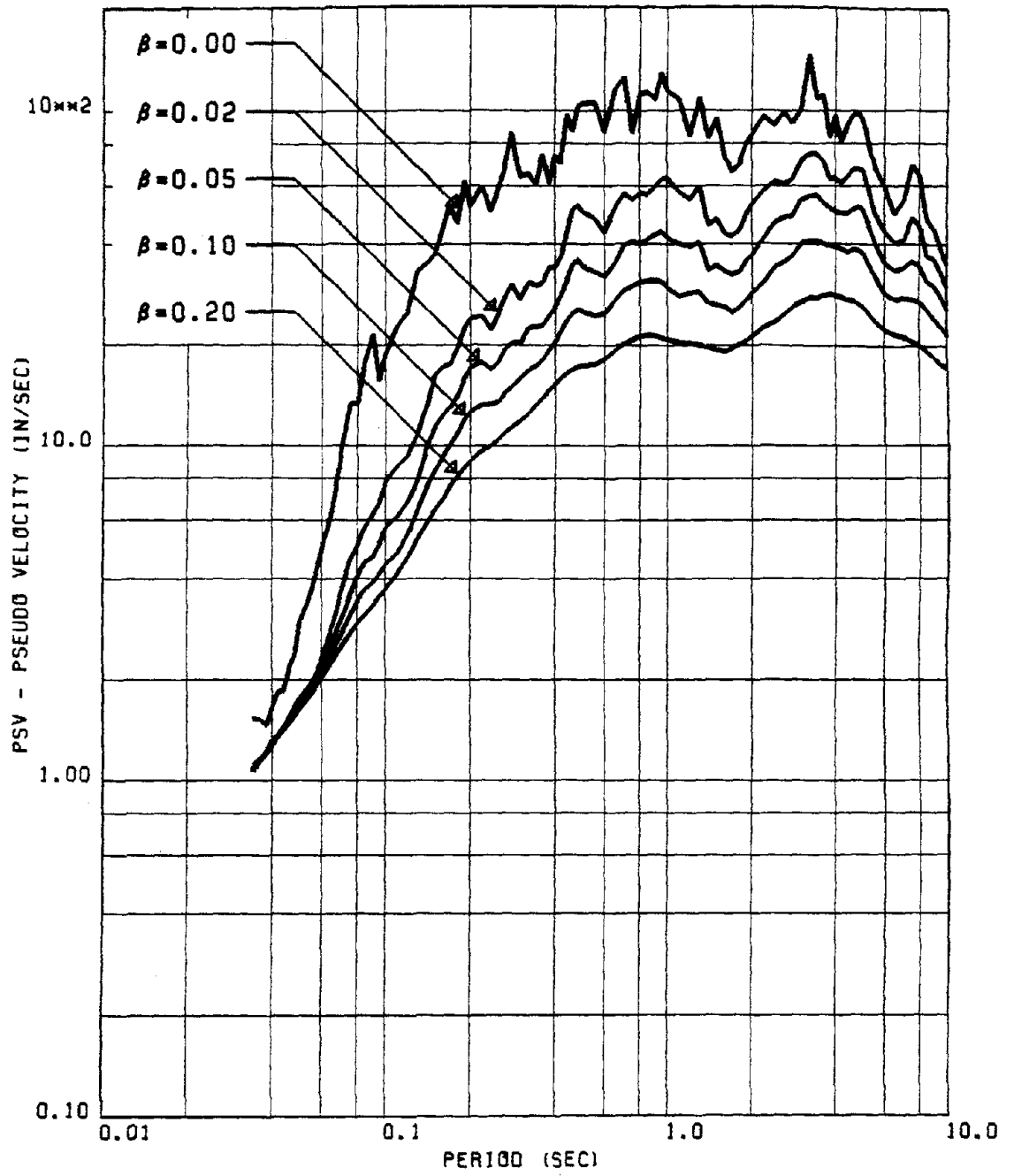
FIG. 25 MEAN PSEUDO VELOCITY SPECTRA FOR VERTICAL RECORDS OF GROUP #2
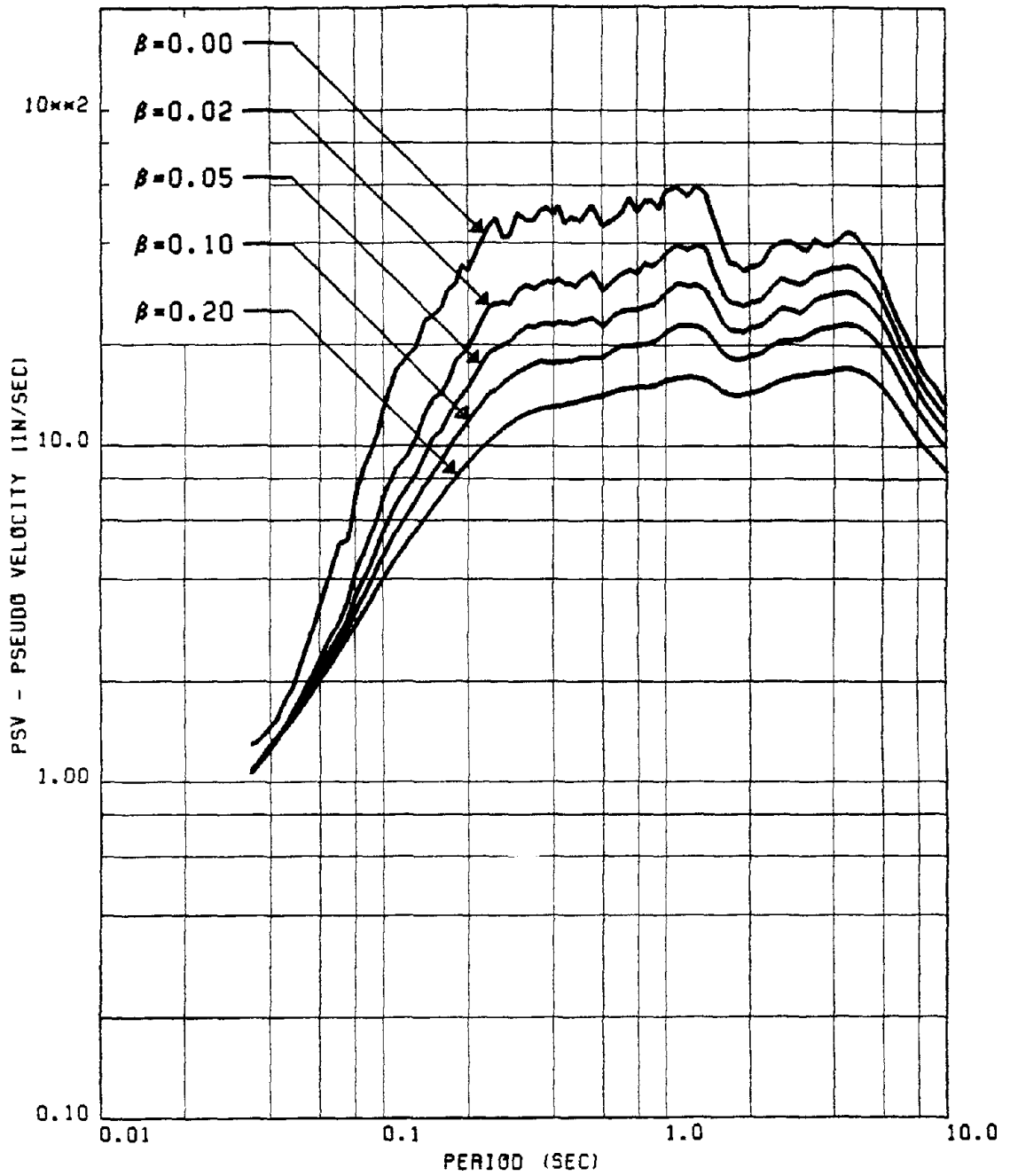
FIG. 26   MEAN PSEUDO VELOCITY SPECTRA FOR HORIZONTAL RECORDS OF GROUP #3
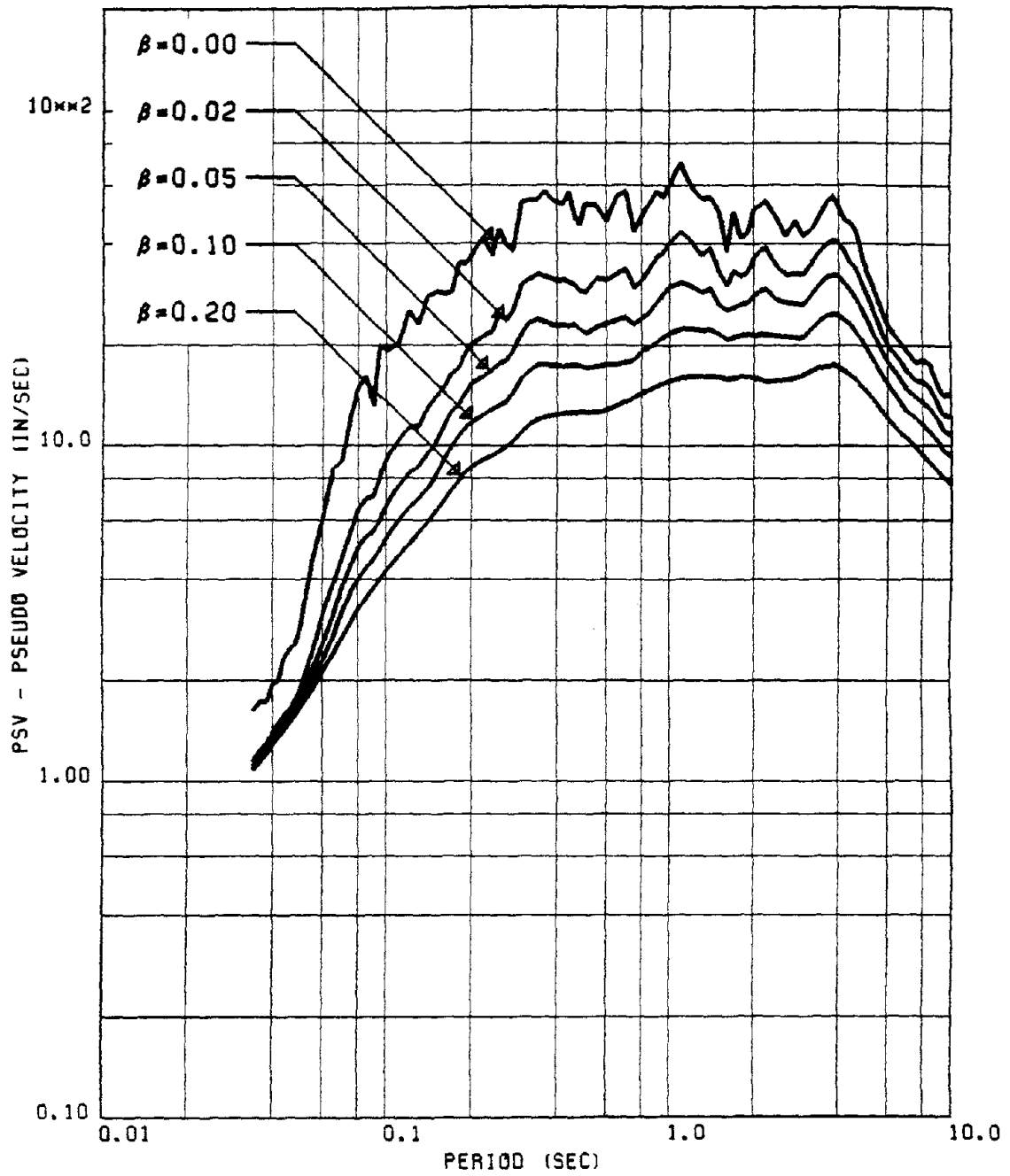
FIG. 27 MEAN PSEUDO VELOCITY SPECTRA FOR VERTICAL RECORDS OF GROUP #3
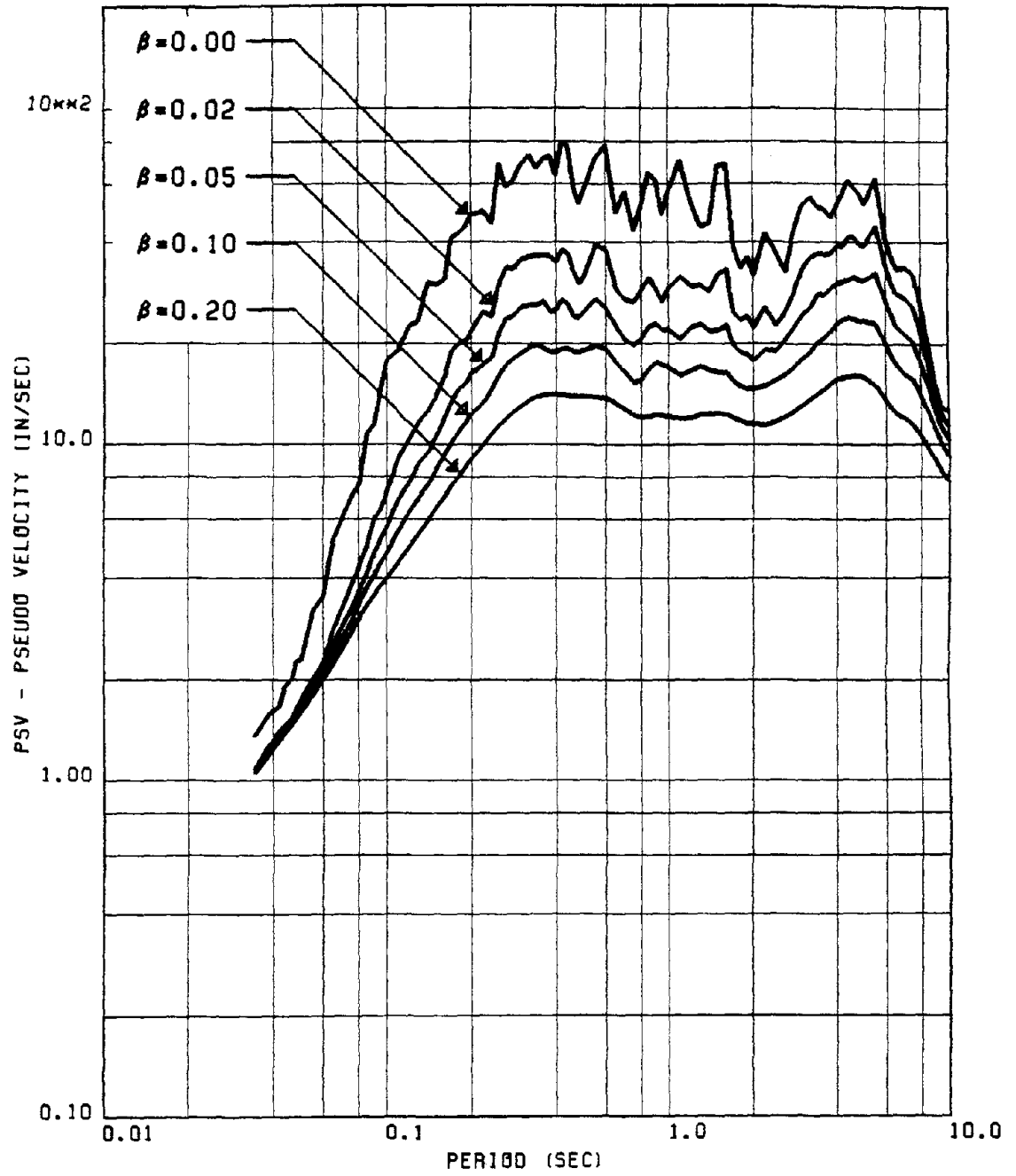
FIG. 28 MEAN PSEUDO VELOCITY SPECTRA FOR HORIZONTAL RECORDS OF GROUP #4

106
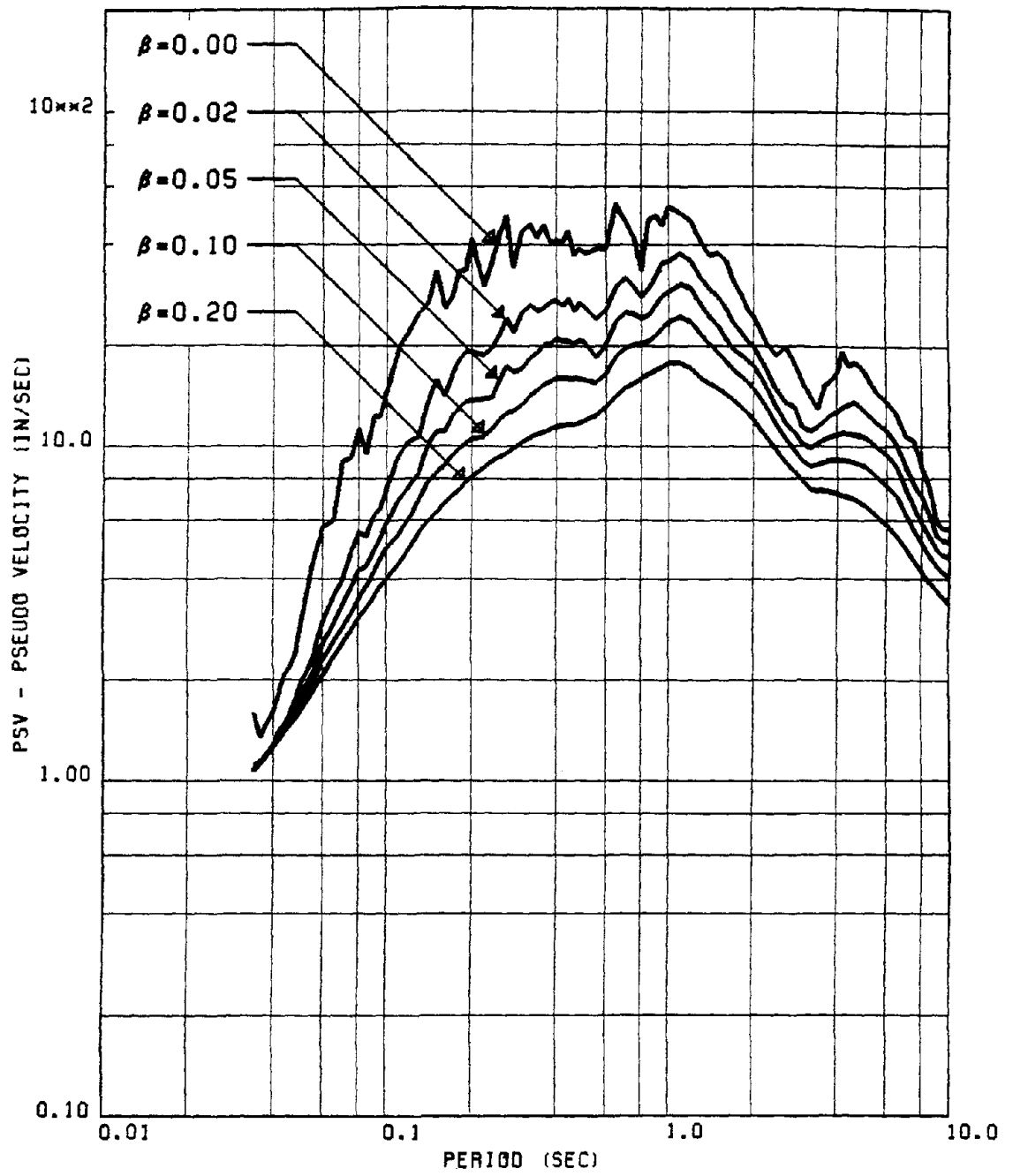
FIG. 29   MEAN PSEUDO VELOCITY SPECTRA FOR HORIZONTAL RECORDS OF GROUP #5
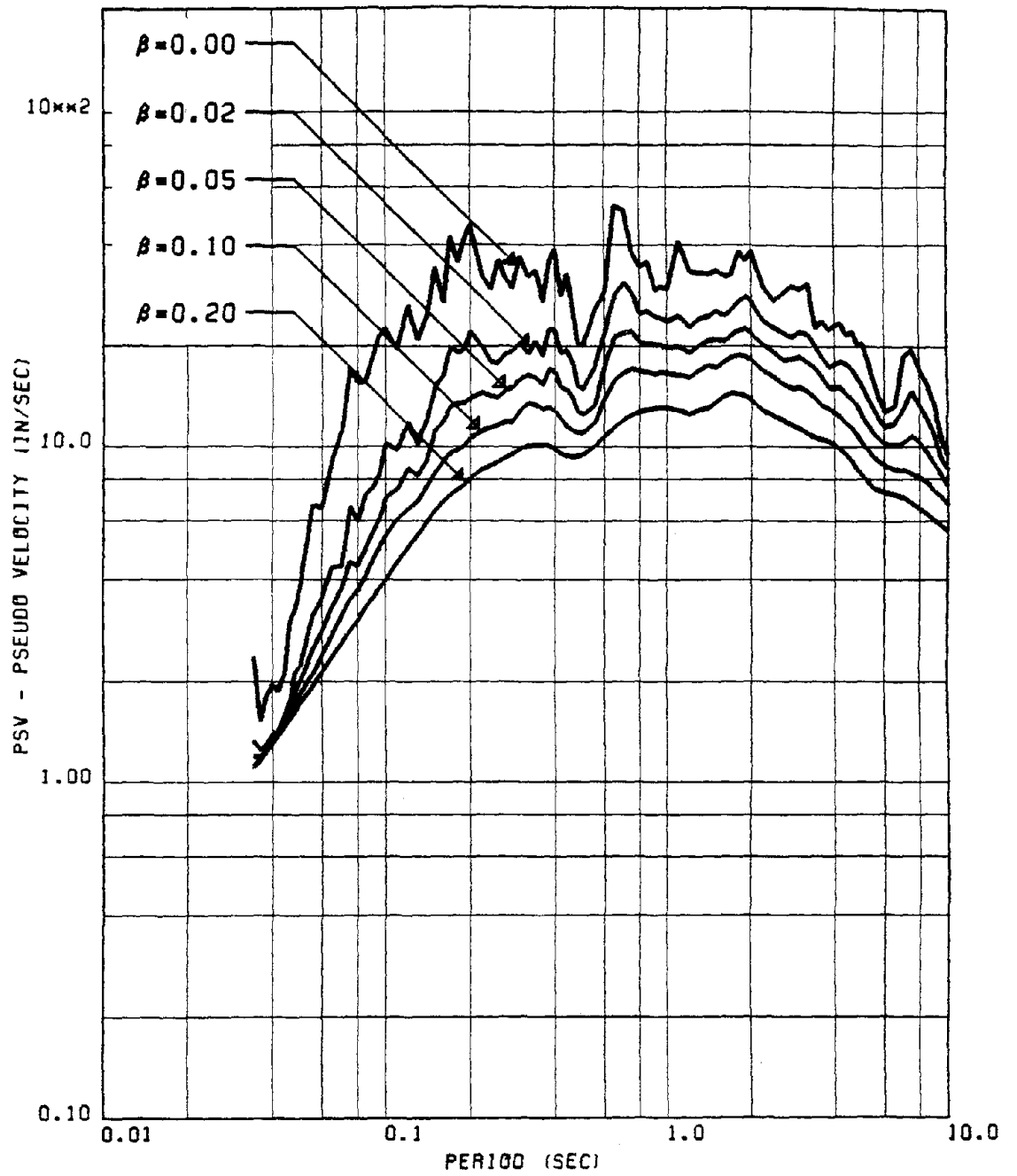
FIG. 30   MEAN PSEUDO VELOCITY SPECTRA FOR VERTICAL RECORDS OF GROUP #5
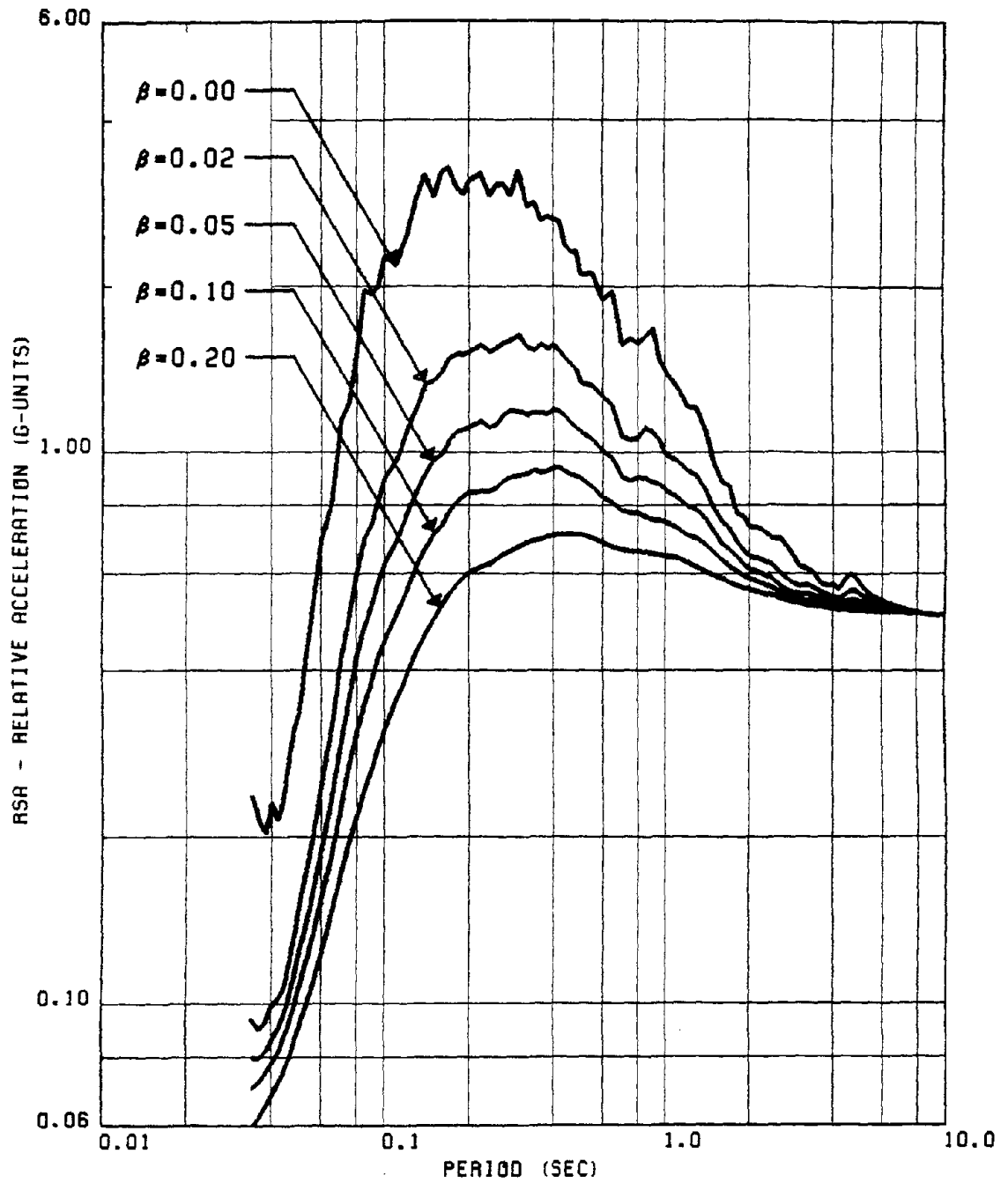
FIG. 31 MEAN REL. ACCELERATION SPECTRA FOR HORIZONTAL RECORDS OF GROUP #1
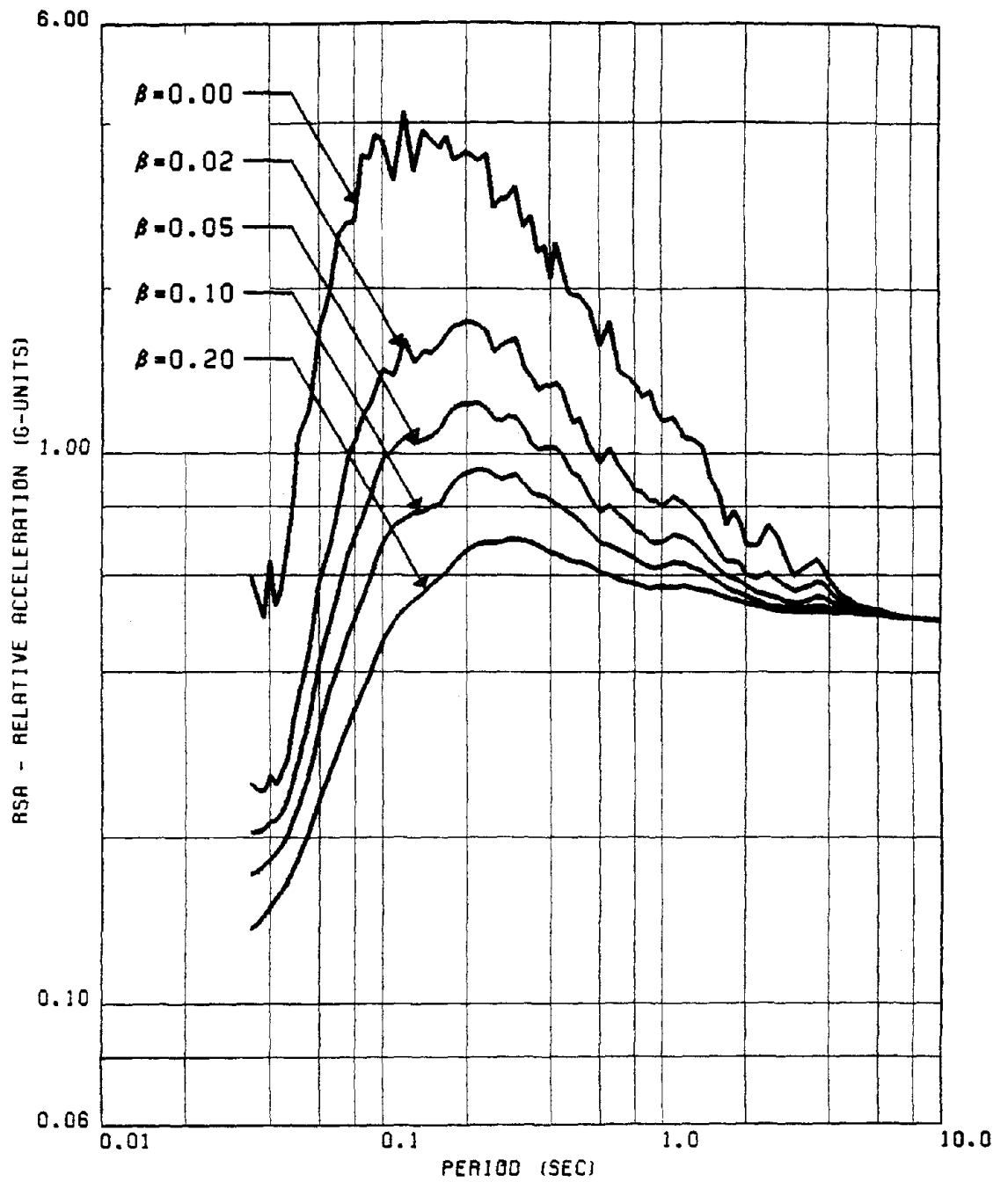
FIG. 32 MEAN REL. ACCELERATION SPECTRA FOR VERTICAL RECORDS OF GROUP #1
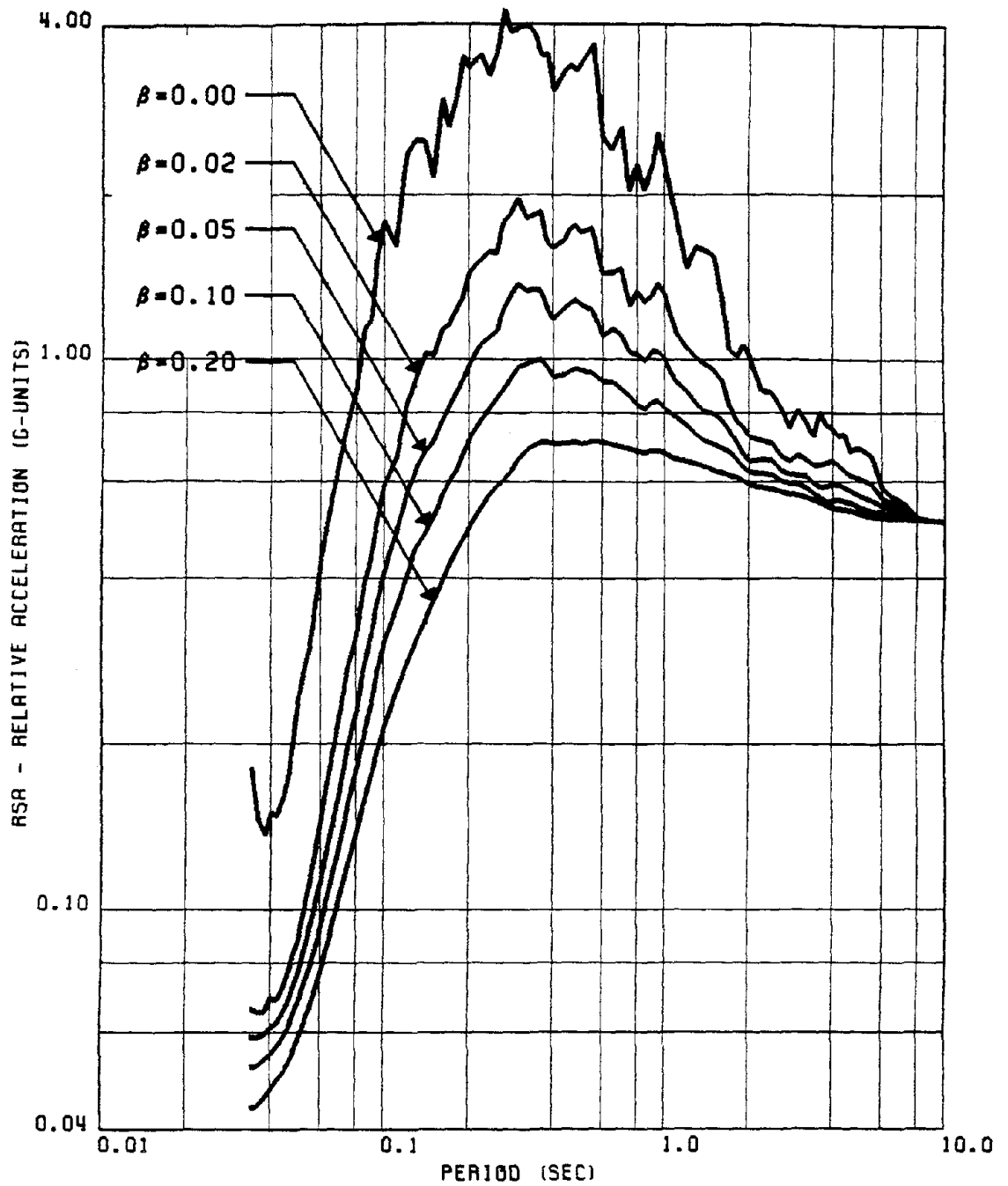
FIG. 33 MEAN REL. ACCELERATION SPECTRA FOR HORIZONTAL RECORDS OF GROUP #2

111
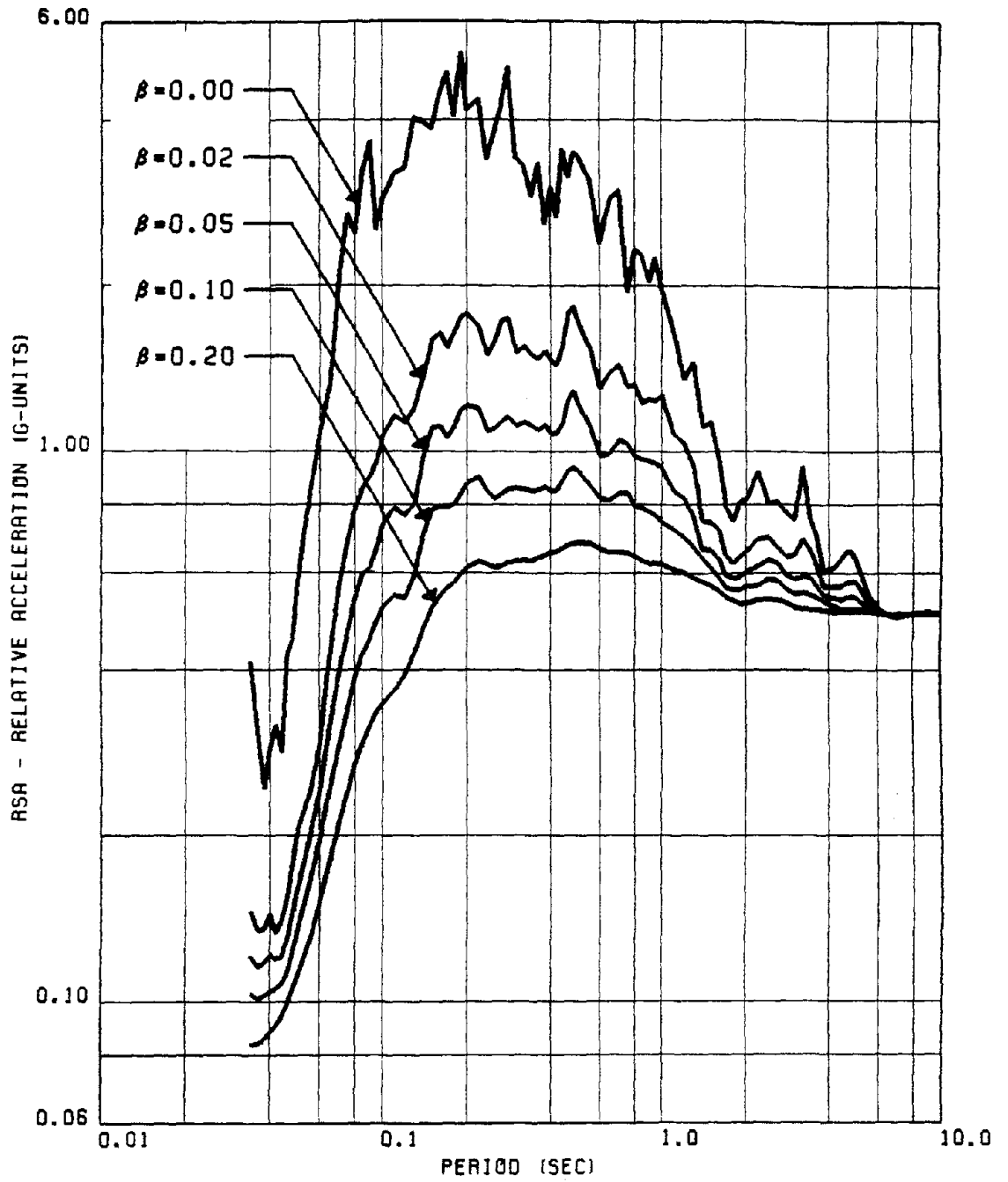
FIG. 34 MEAN REL. ACCELERATION SPECTRA FOR VERTICAL RECORDS OF GROUP #2
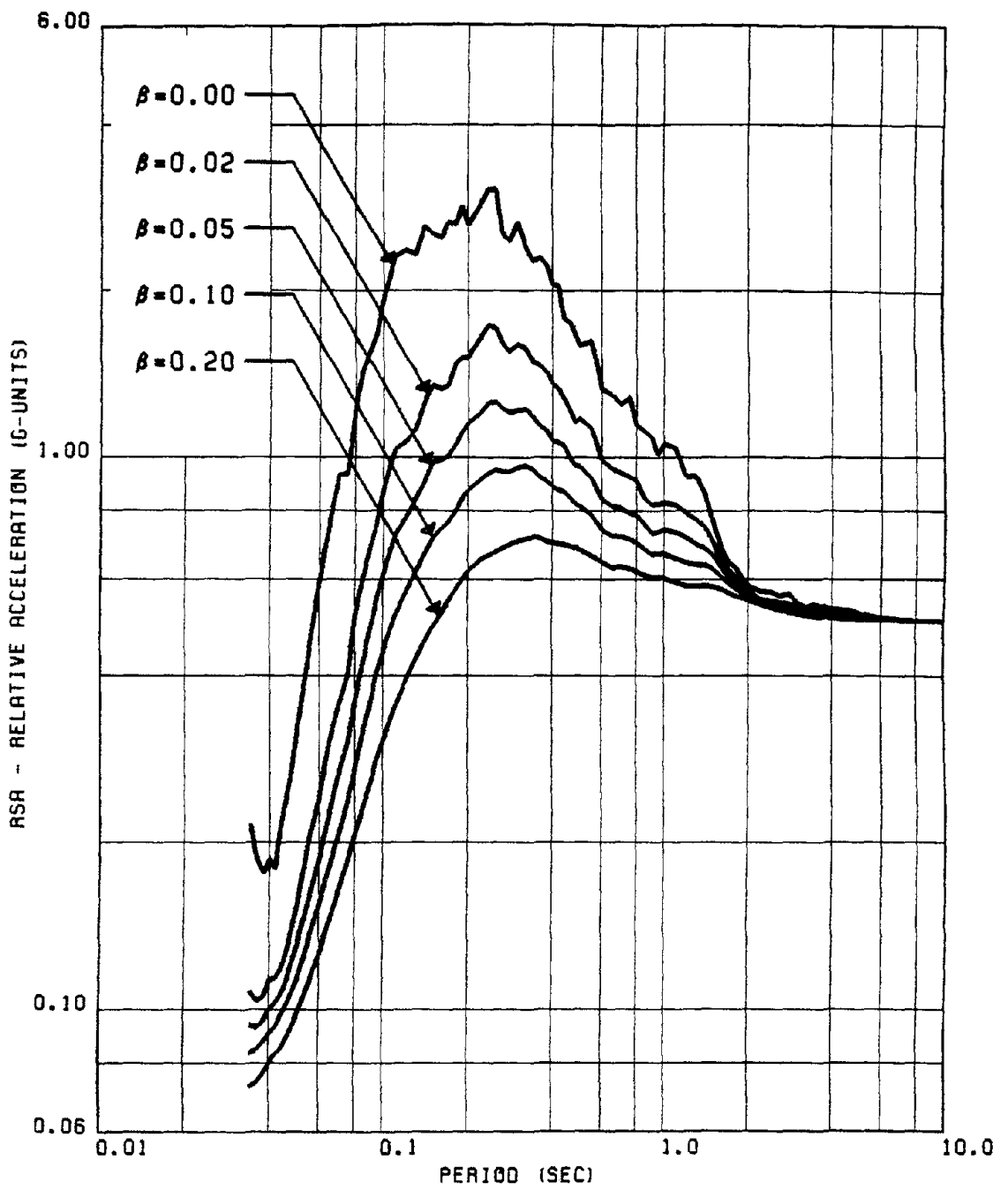
FIG. 35 MEAN REL. ACCELERATION SPECTRA FOR HORIZONTAL RECORDS OF GROUP #3
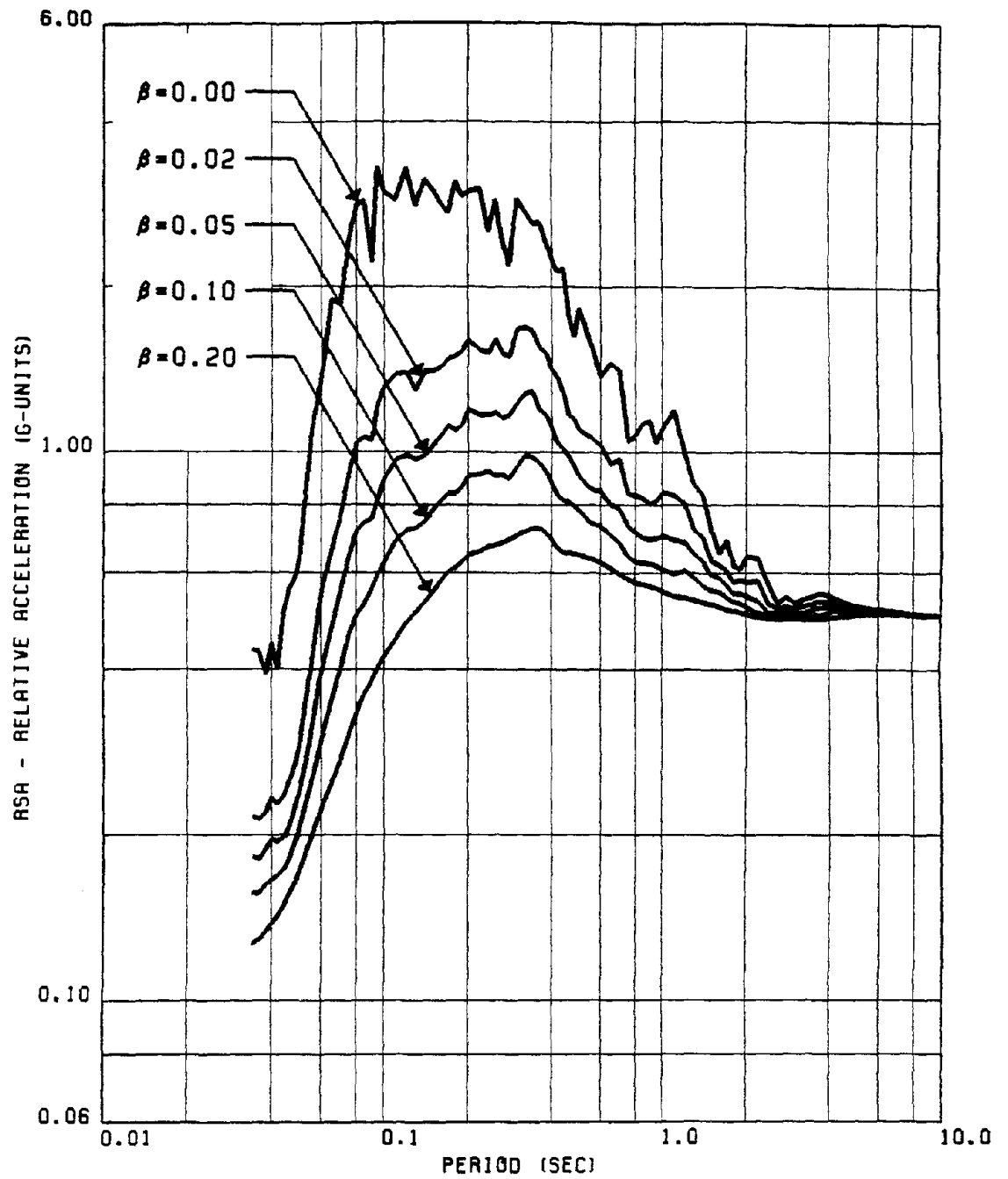
FIG. 36   MEAN REL. ACCELERATION SPECTRA FOR VERTICAL RECORDS OF GROUP #3
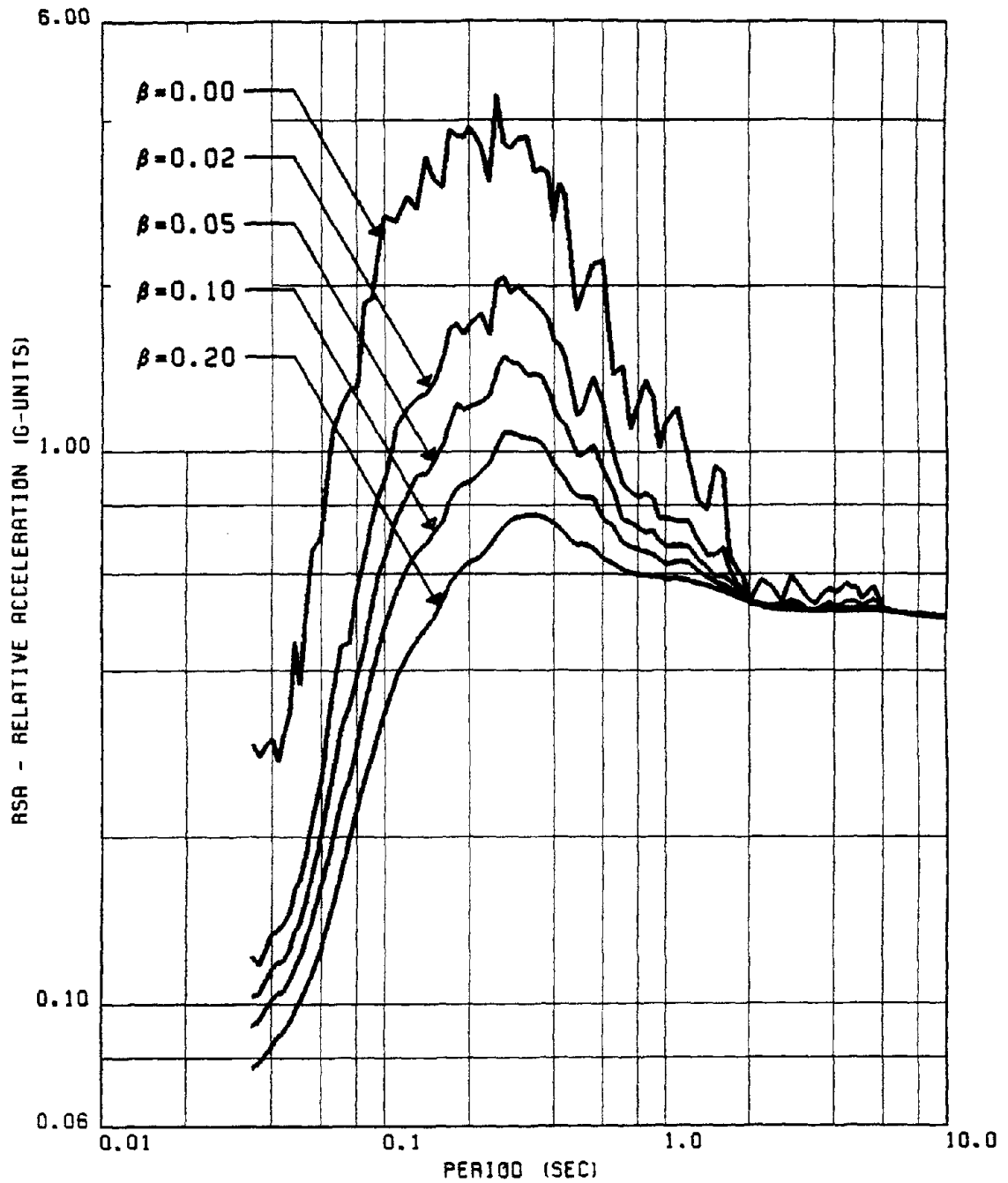
FIG. 37 MEAN REL. ACCELERATION SPECTRA FOR HORIZONTAL RECORDS OF GROUP #4
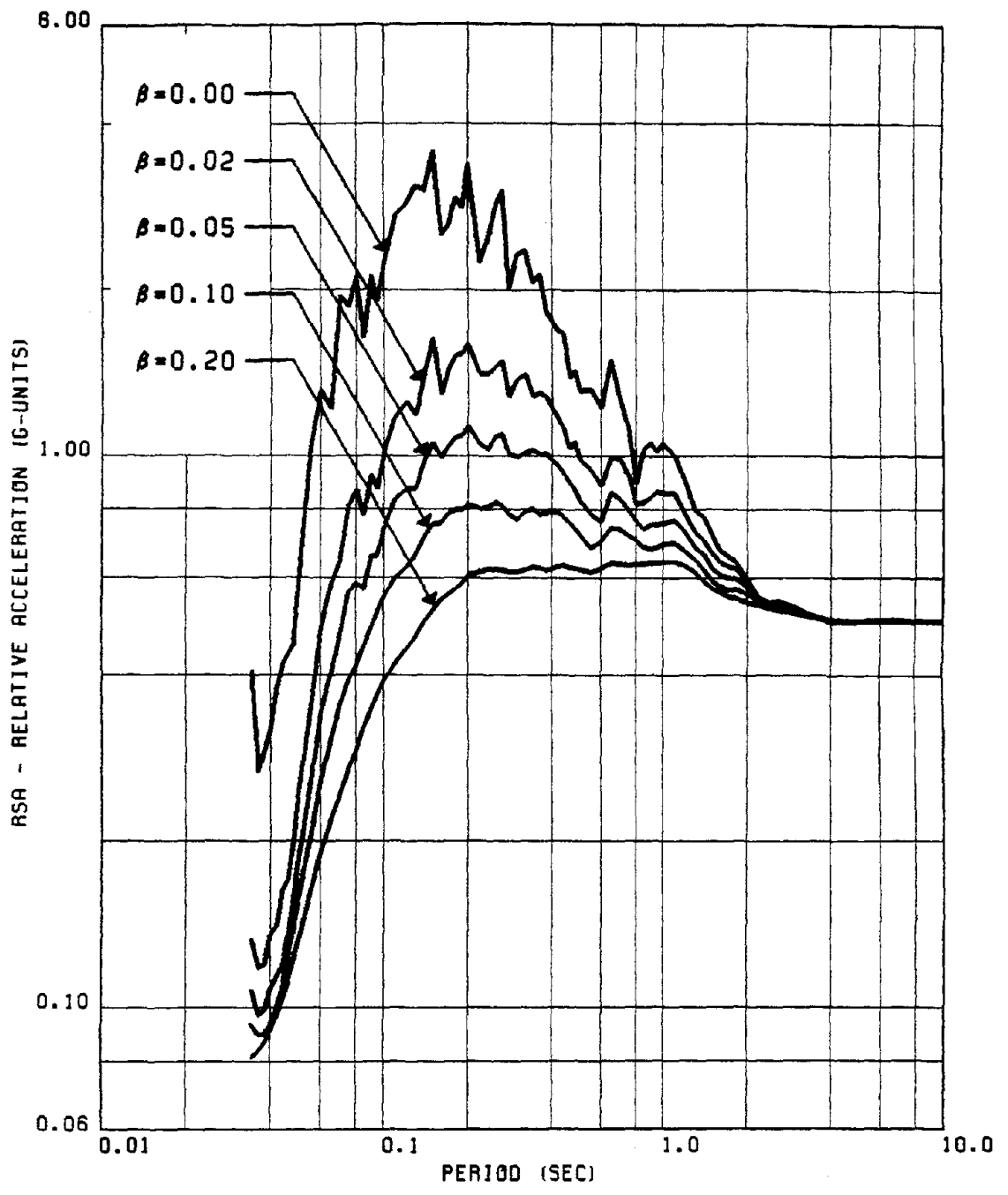
FIG. 38   MEAN REL. ACCELERATION SPECTRA FOR HORIZONTAL RECORDS OF GROUP #5
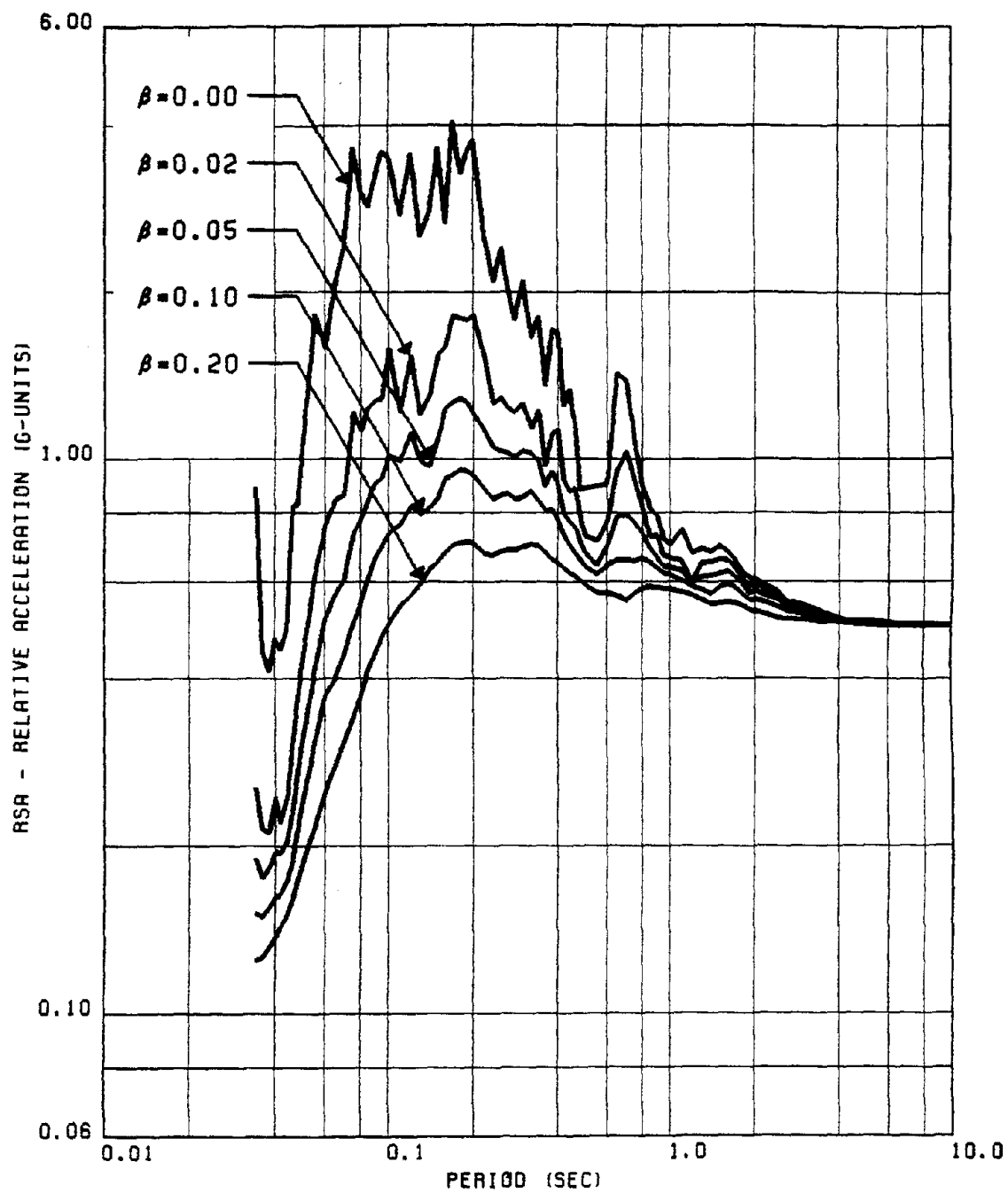
FIG. 39 MEAN REL. ACCELERATION SPECTRA FOR VERTICAL RECORDS OF GROUP *5

117
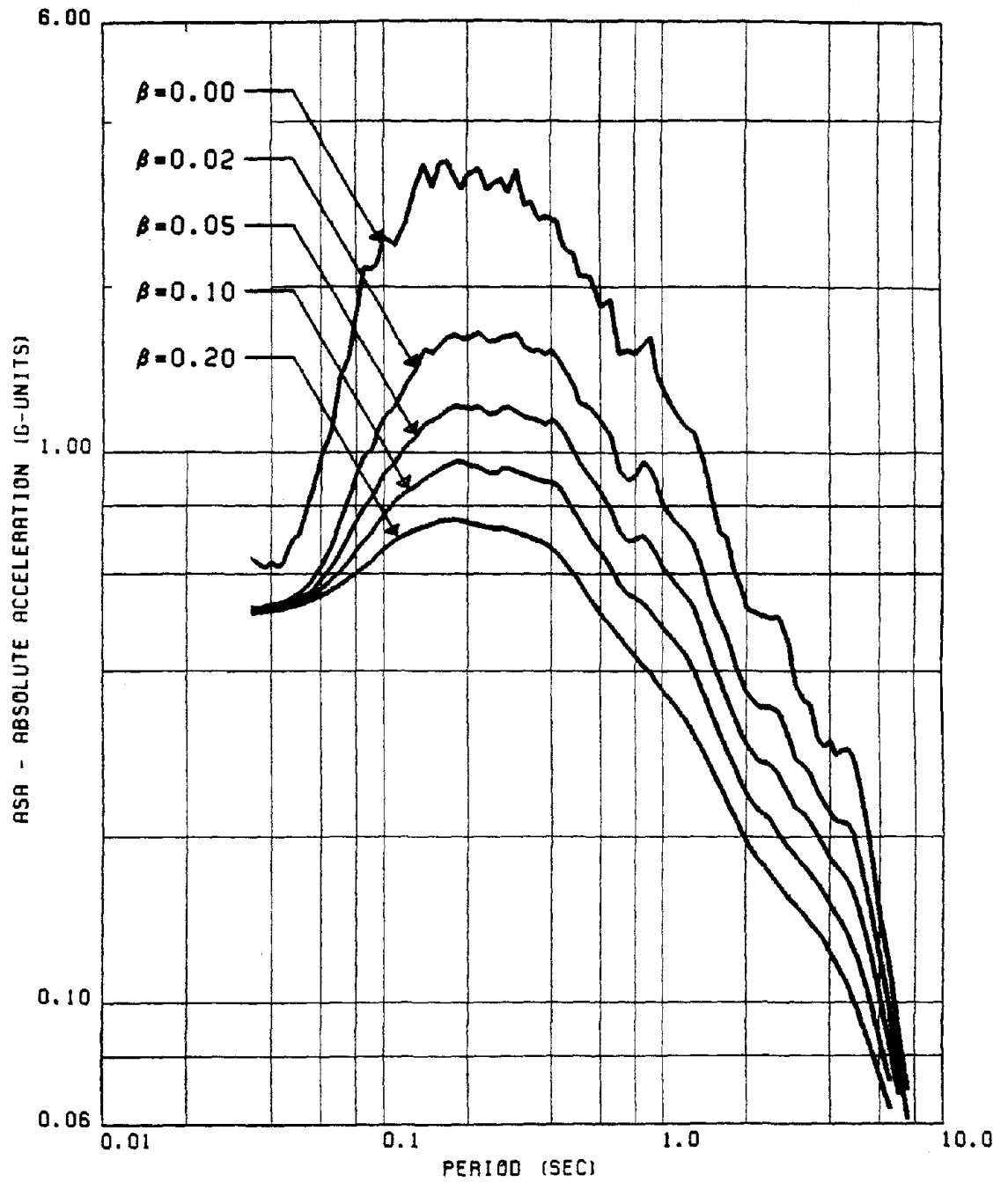
FIG. 40   MEAN ABS. ACCELERATION SPECTRA FOR HORIZONTAL RECORDS OF GROUP #1
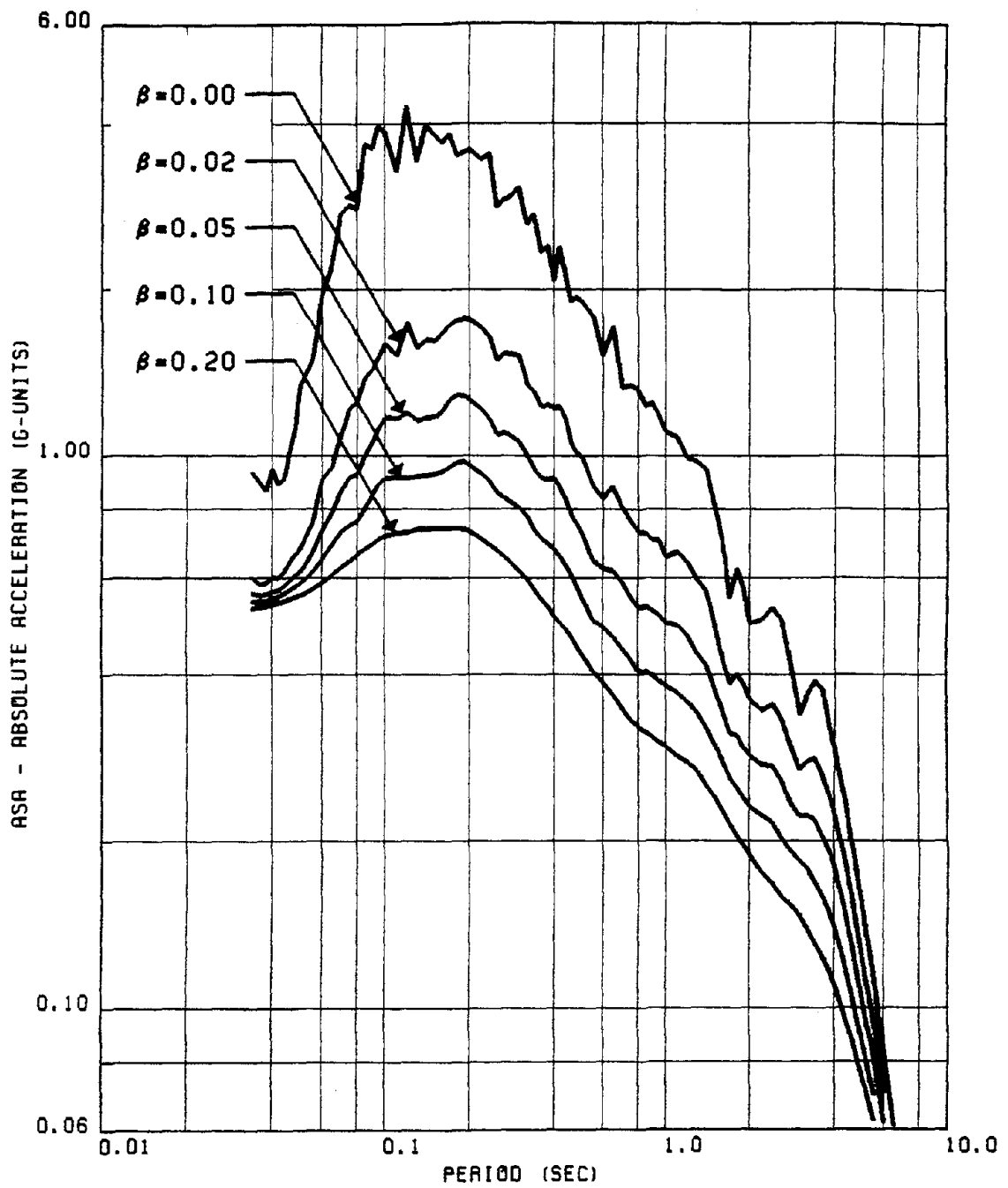
FIG. 41 MEAN ABS. ACCELERATION SPECTRA FOR VERTICAL RECORDS OF GROUP #1

119
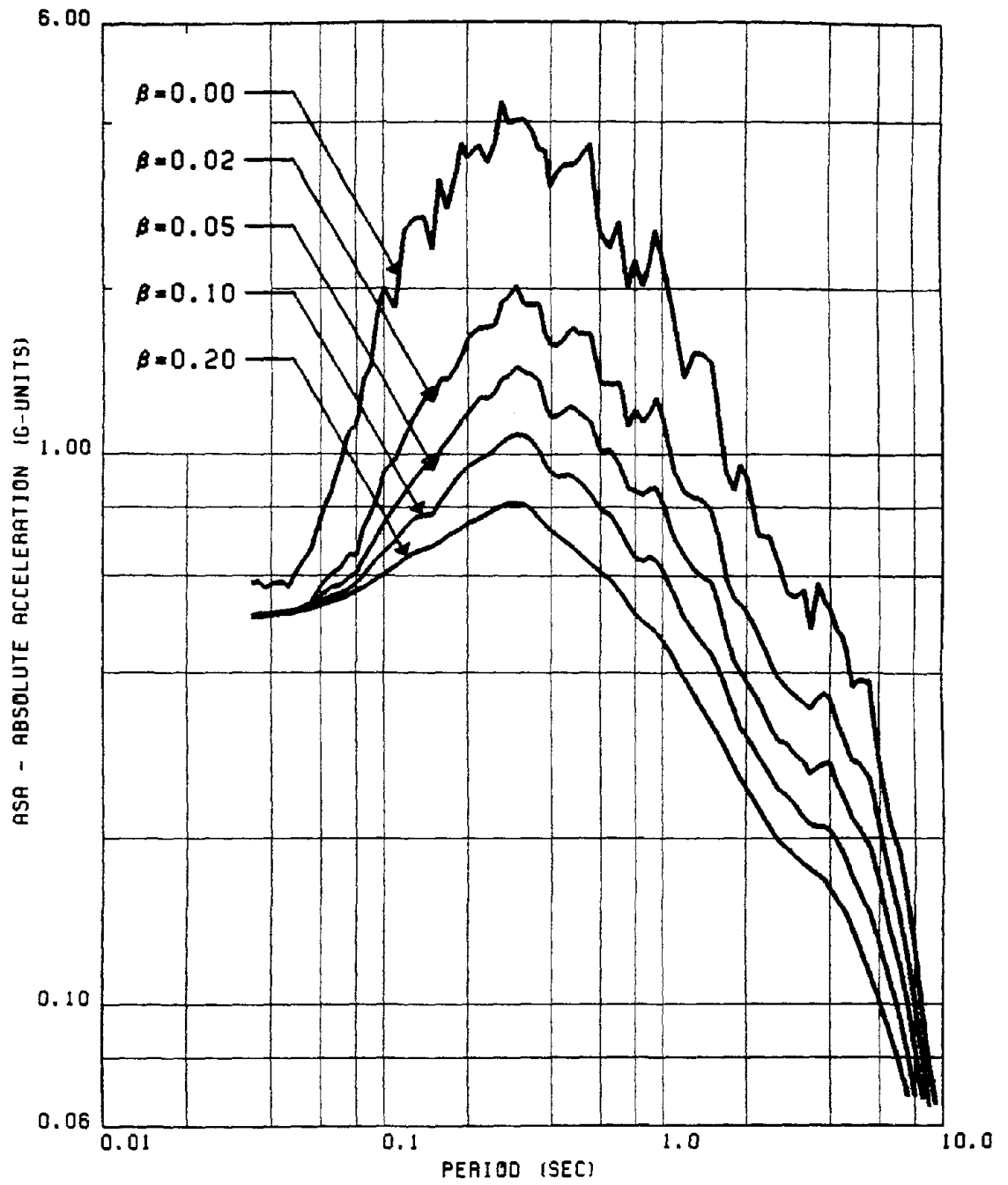
FIG. 42 MEAN ABS. ACCELERATION SPECTRA FOR HORIZONTAL RECORDS OF GROUP #2
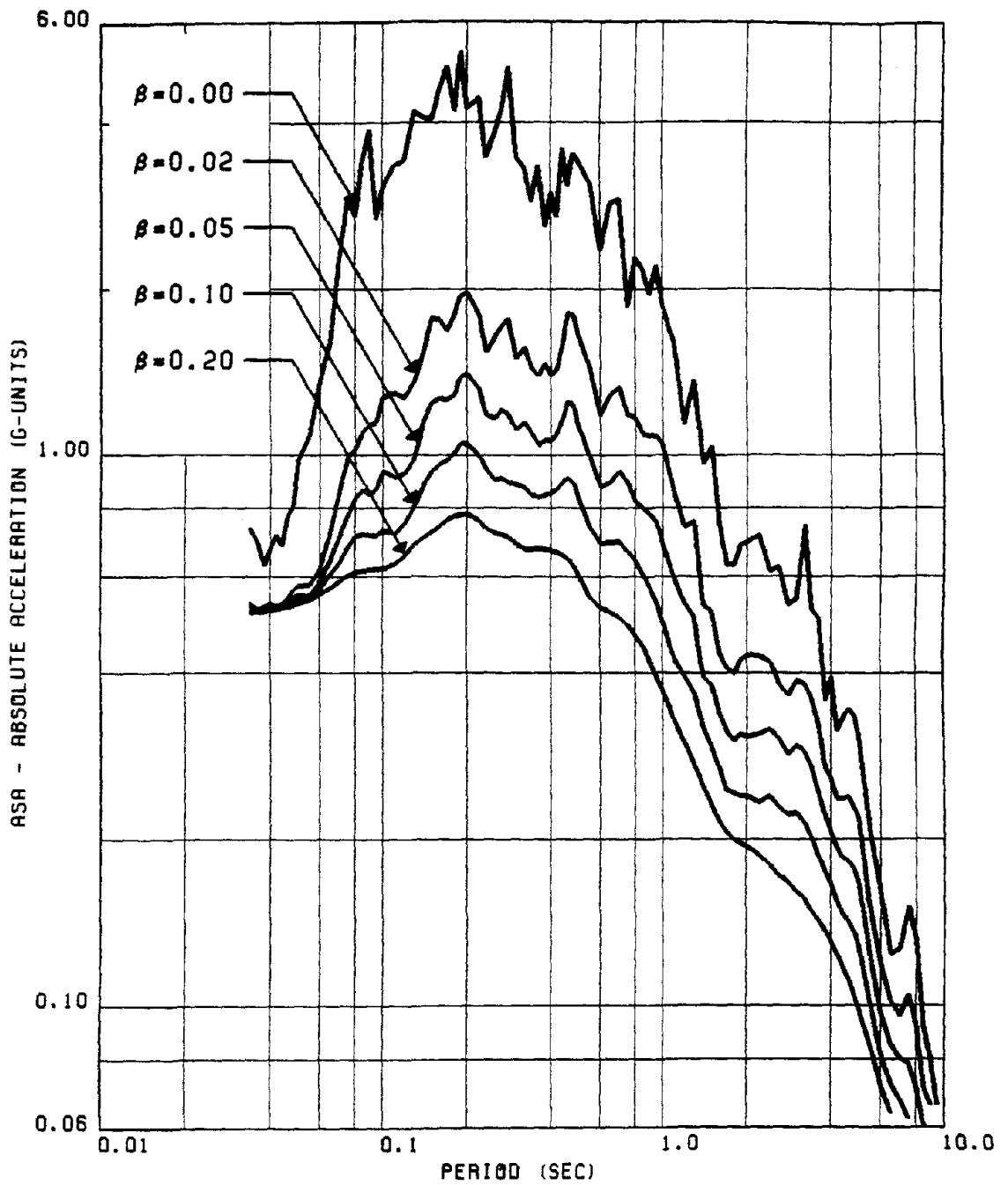
FIG. 43 MEAN ABS. ACCELERATION SPECTRA FOR VERTICAL RECORDS OF GROUP *2
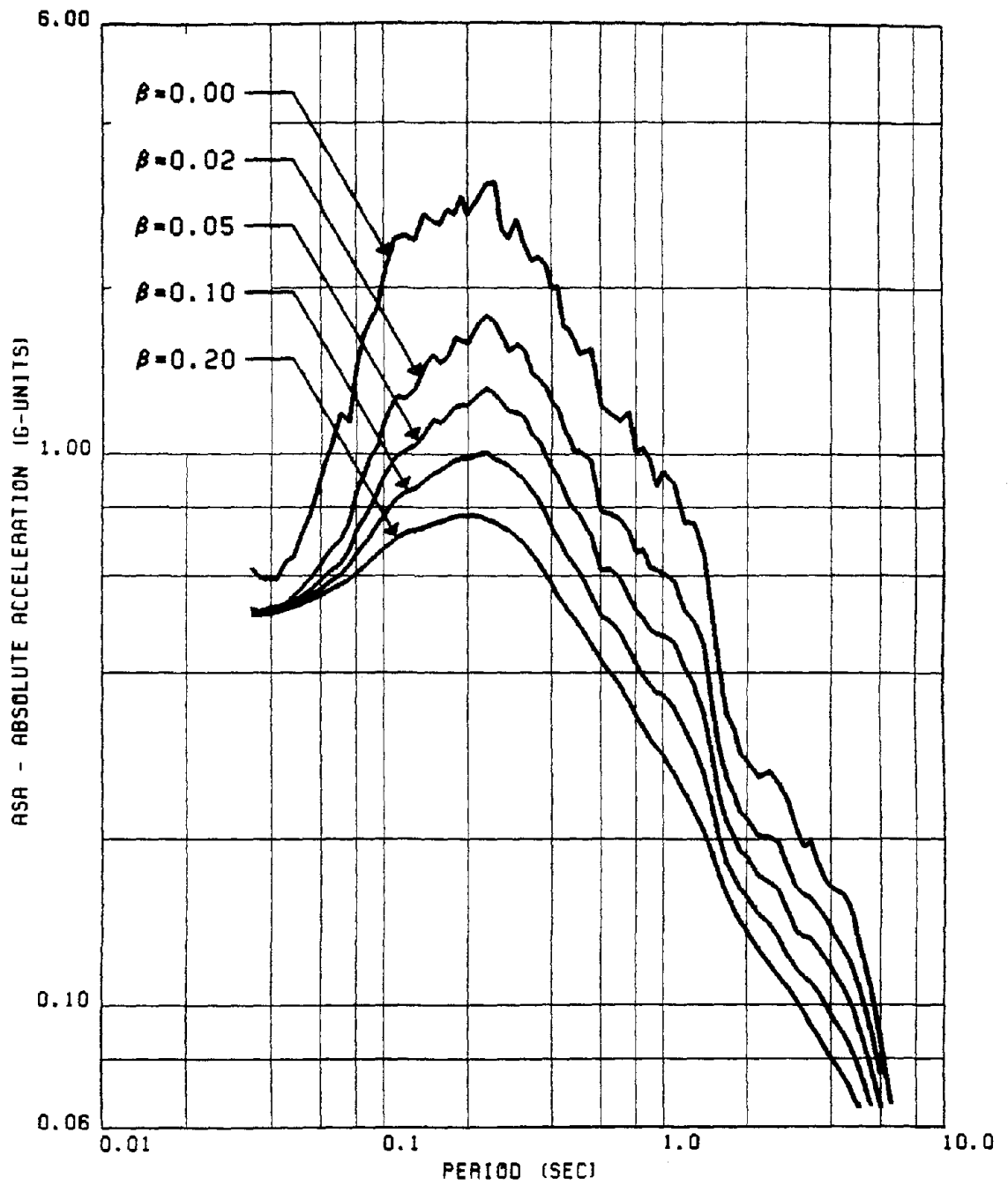
FIG. 44 MEAN ABS. ACCELERATION SPECTRA FOR HORIZONTAL RECORDS OF GROUP #3
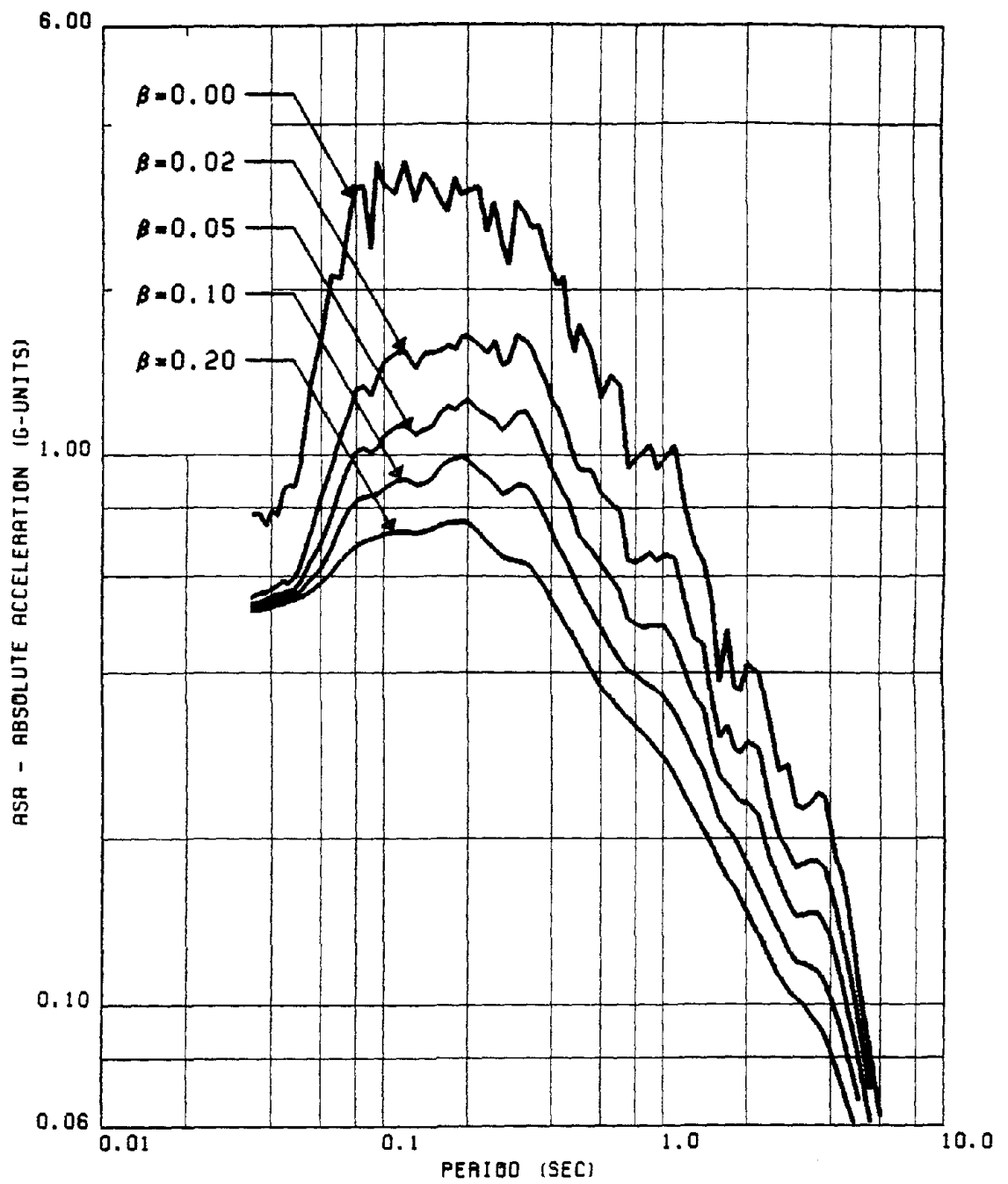
FIG. 45 MEAN ABS. ACCELERATION SPECTRA FOR VERTICAL RECORDS OF GROUP #3
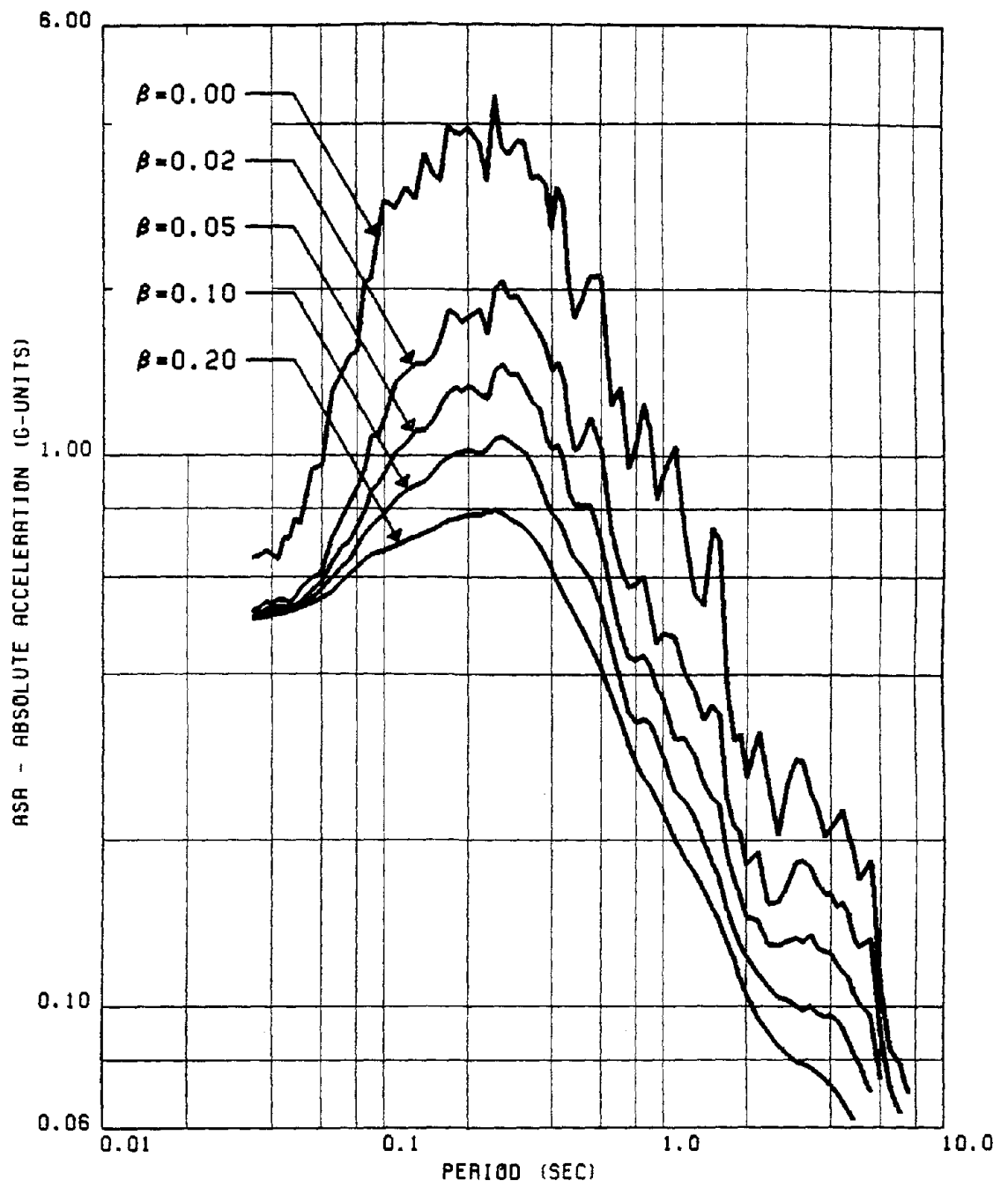
FIG. 46   MEAN ABS. ACCELERATION SPECTRA FOR HORIZONTAL RECORDS OF GROUP #4
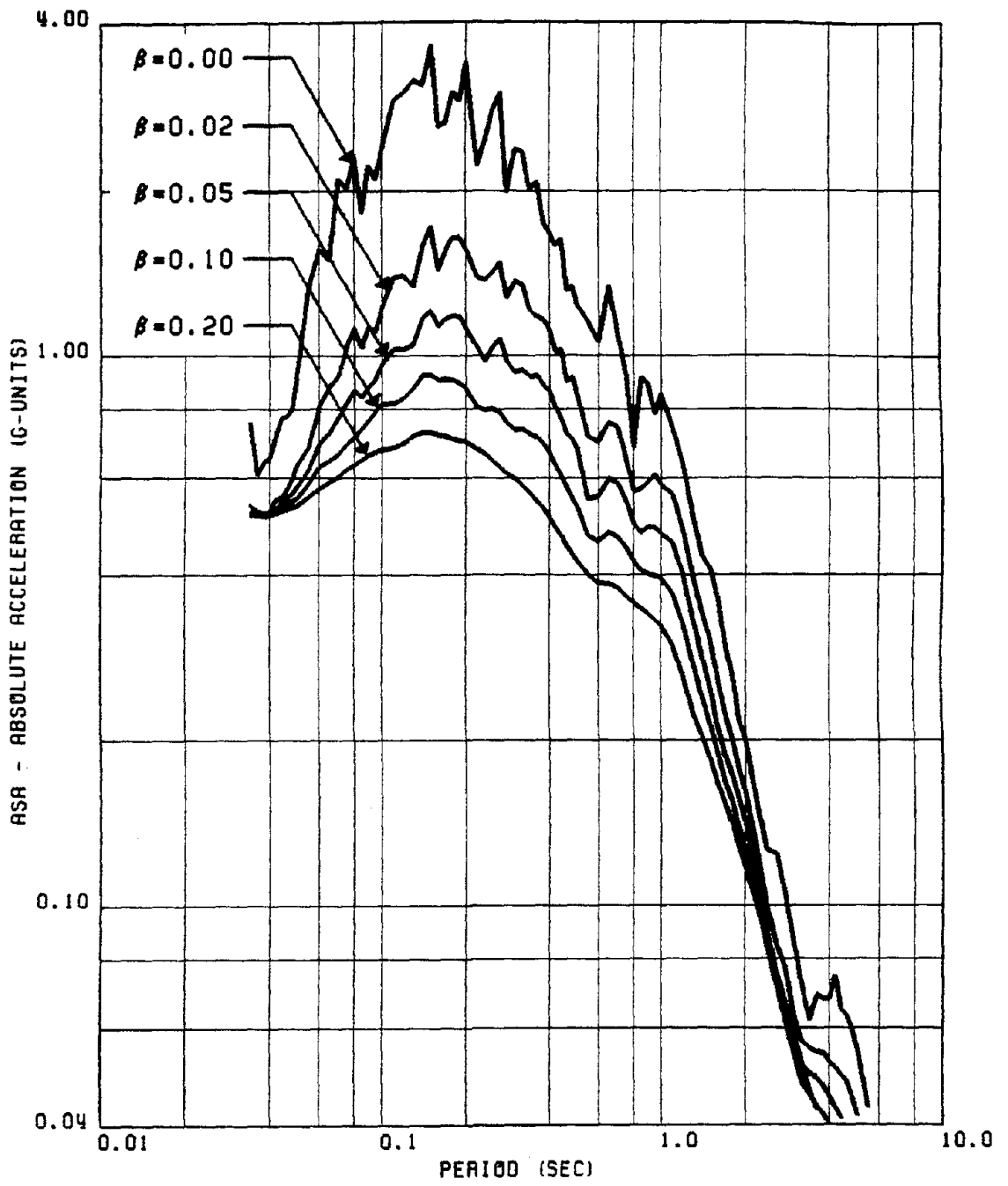
FIG. 47 MEAN ABS. ACCELERATION SPECTRA FOR HORIZONTAL RECORDS OF GROUP #5
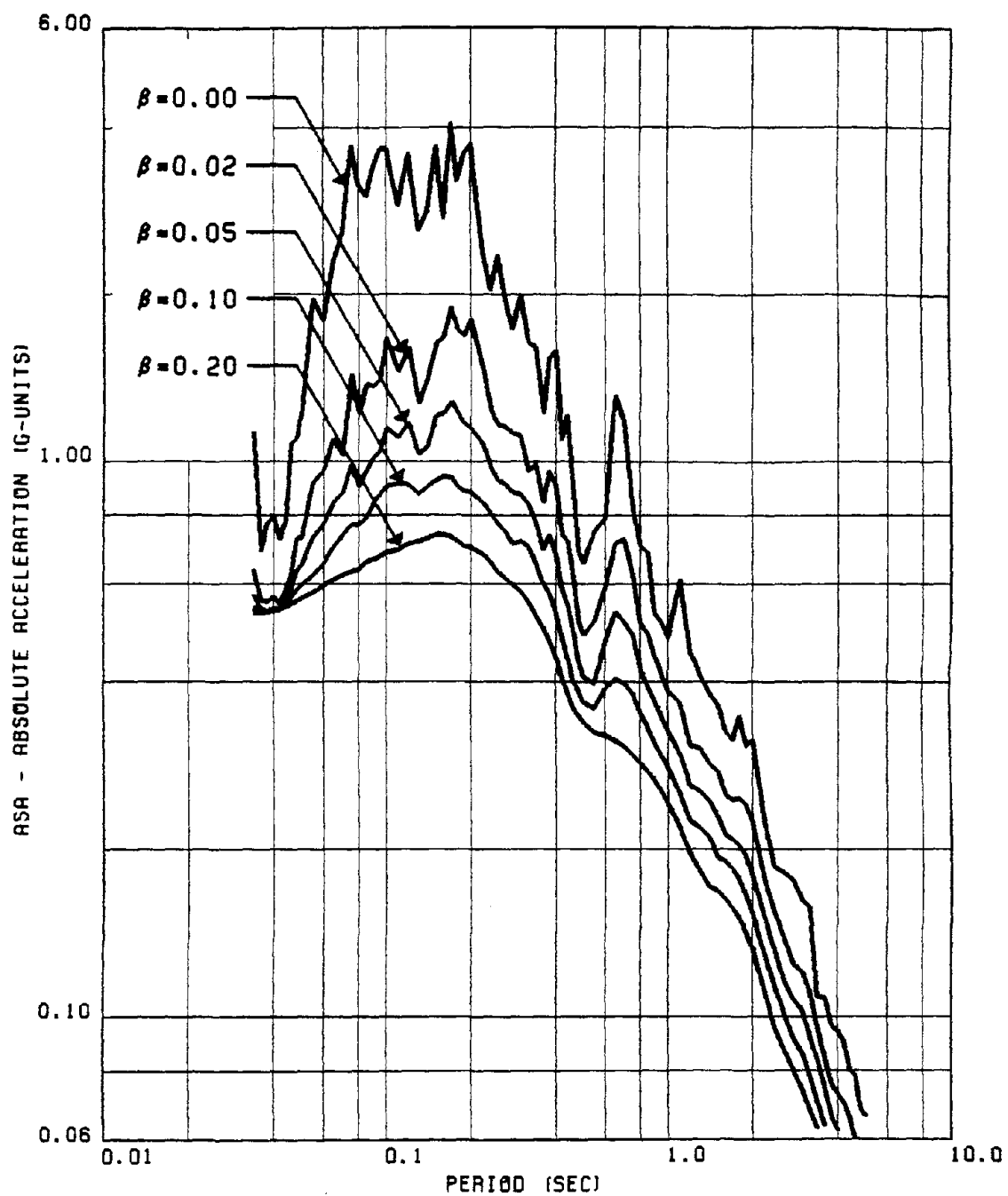
FIG. 48 MEAN ABS. ACCELERATION SPECTRA FOR VERTICAL RECORDS OF GROUP #5
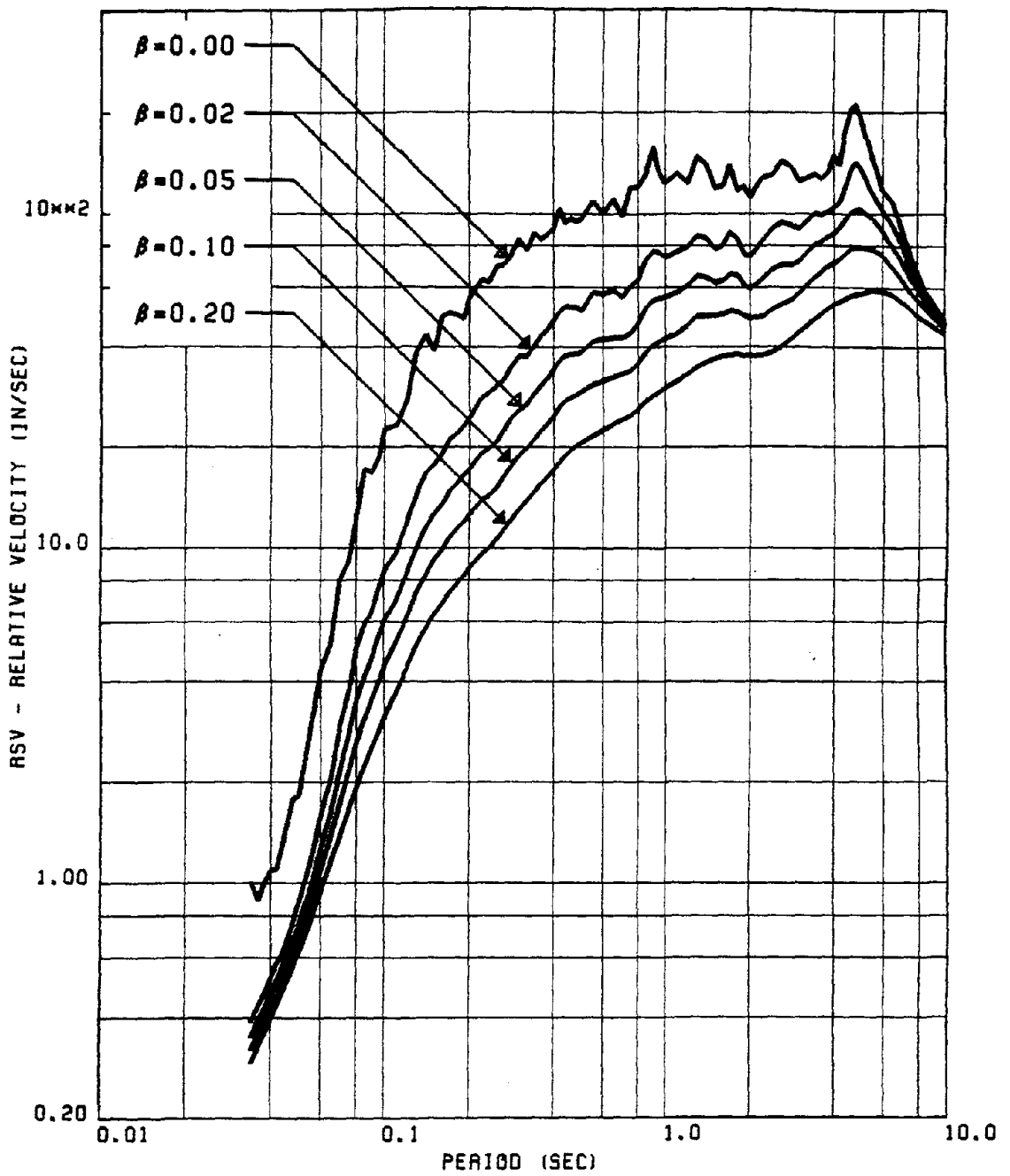
FIG. 49 (MEAN+SD) REL VELOCITY SPECTRA FOR HORIZONTAL RECORDS OF GROUP #1

127
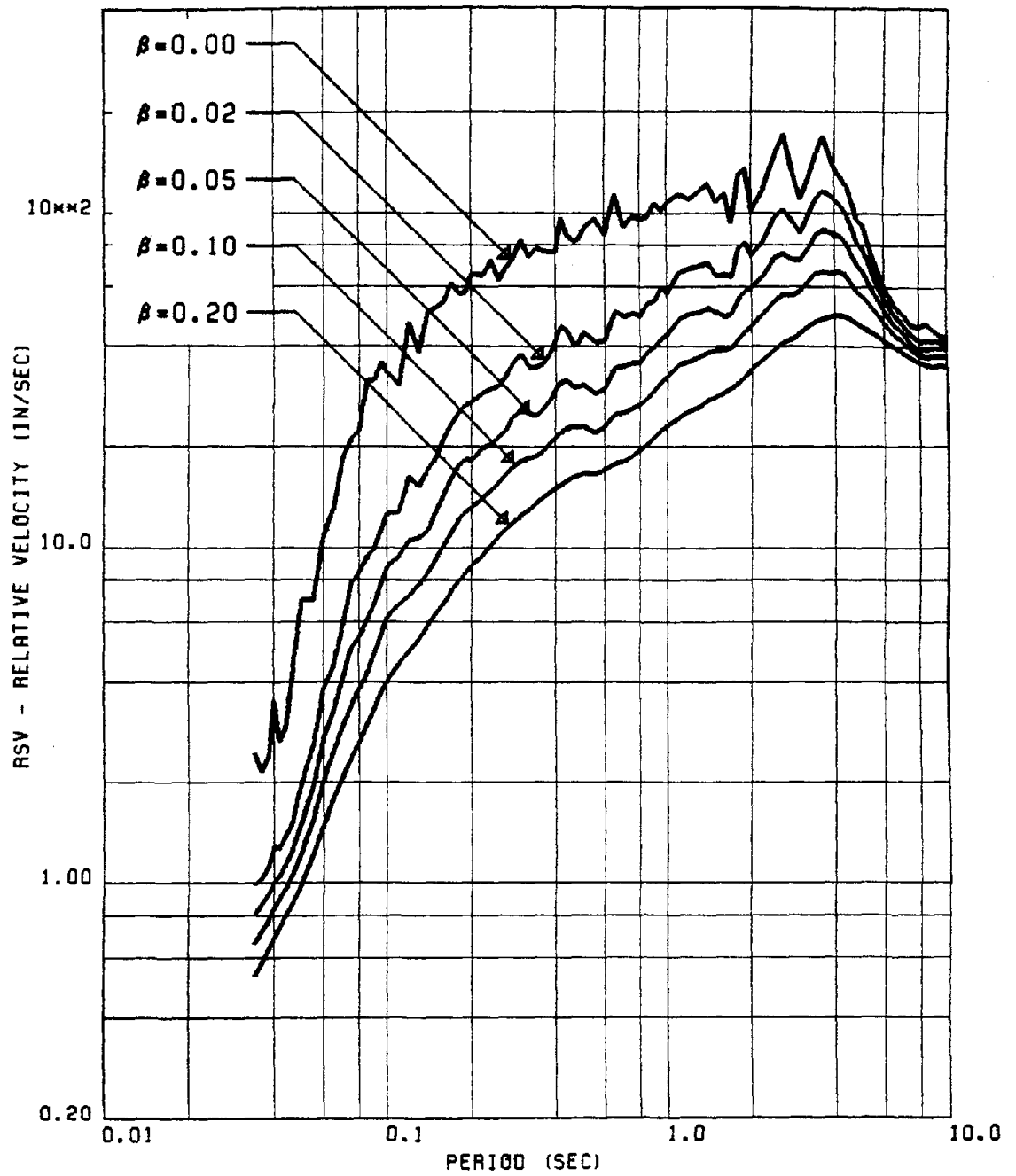
FIG. 50 (MEAN+SD) REL VELOCITY SPECTRA FOR VERTICAL RECORDS OF GROUP #1

128
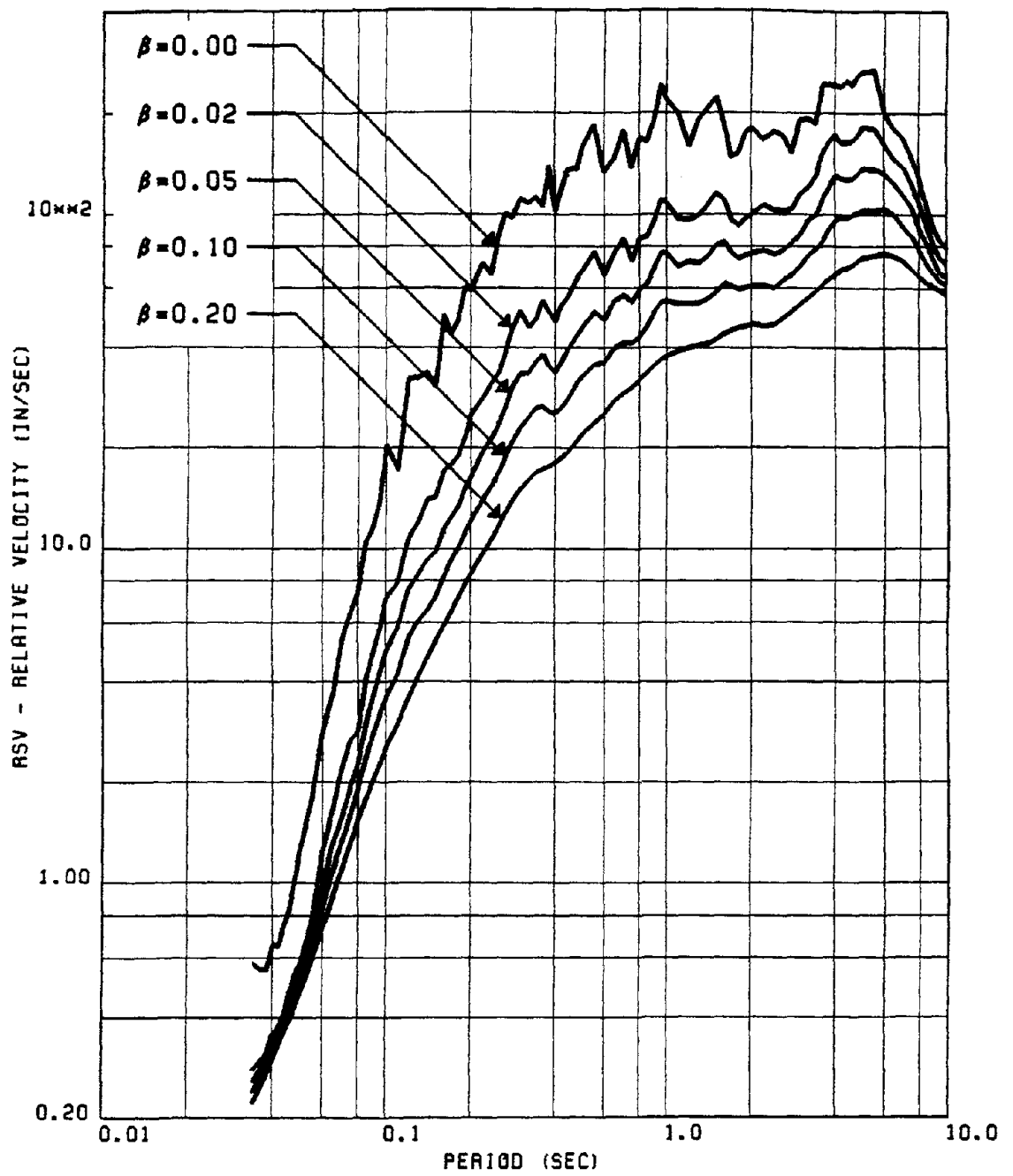
FIG. 51 (MEAN+SD) REL VELOCITY SPECTRA FOR HORIZONTAL RECORDS OF GROUP #2

129
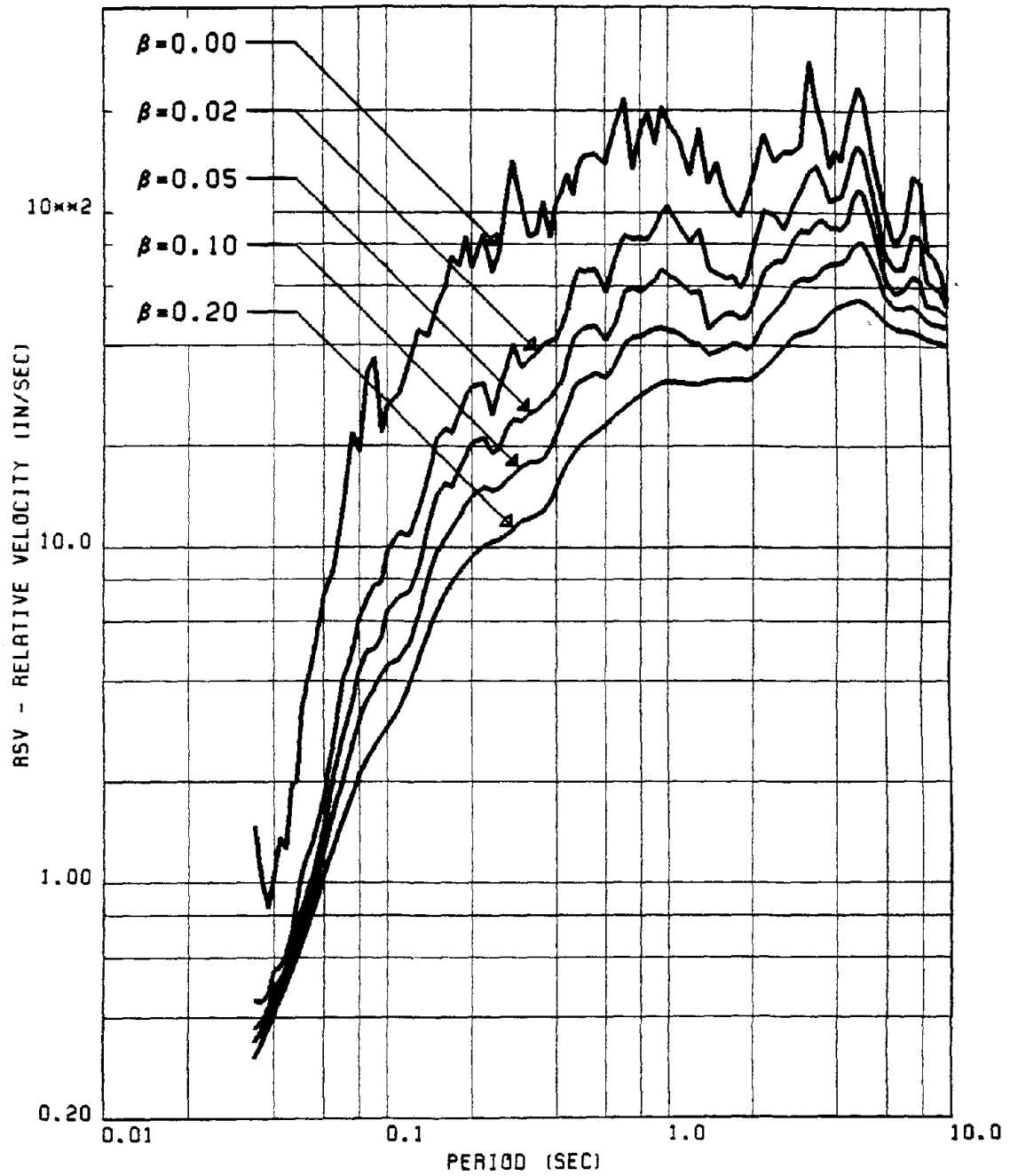
FIG. 52 (MEAN+SD) REL VELOCITY SPECTRA FOR VERTICAL RECORDS OF GROUP #2
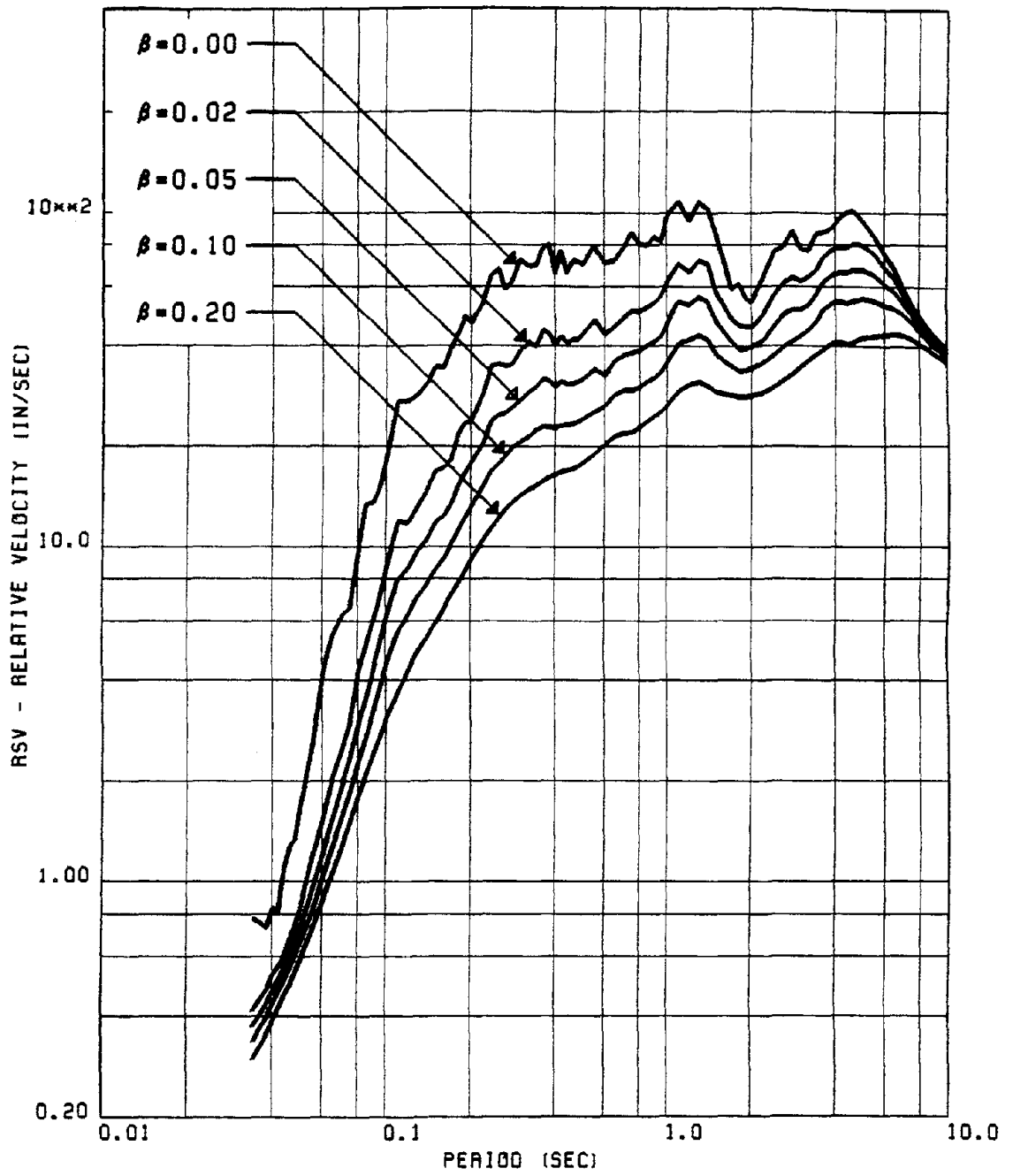
FIG. 53 (MEAN+SD) REL VELOCITY SPECTRA FOR HORIZONTAL RECORDS OF GROUP #3
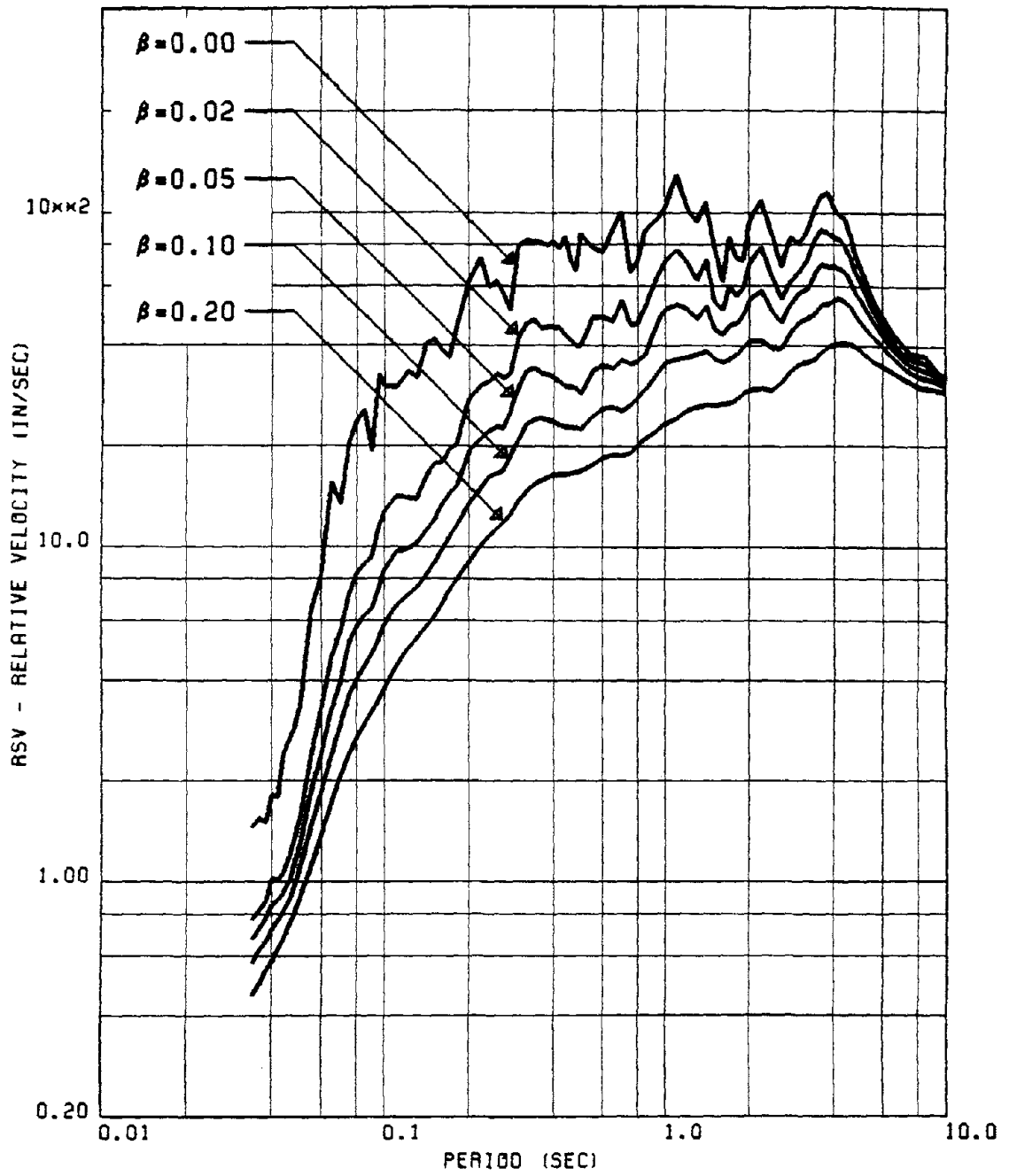
FIG. 54   (MEAN+SD) REL VELOCITY SPECTRA FOR VERTICAL RECORDS OF GROUP #3

132
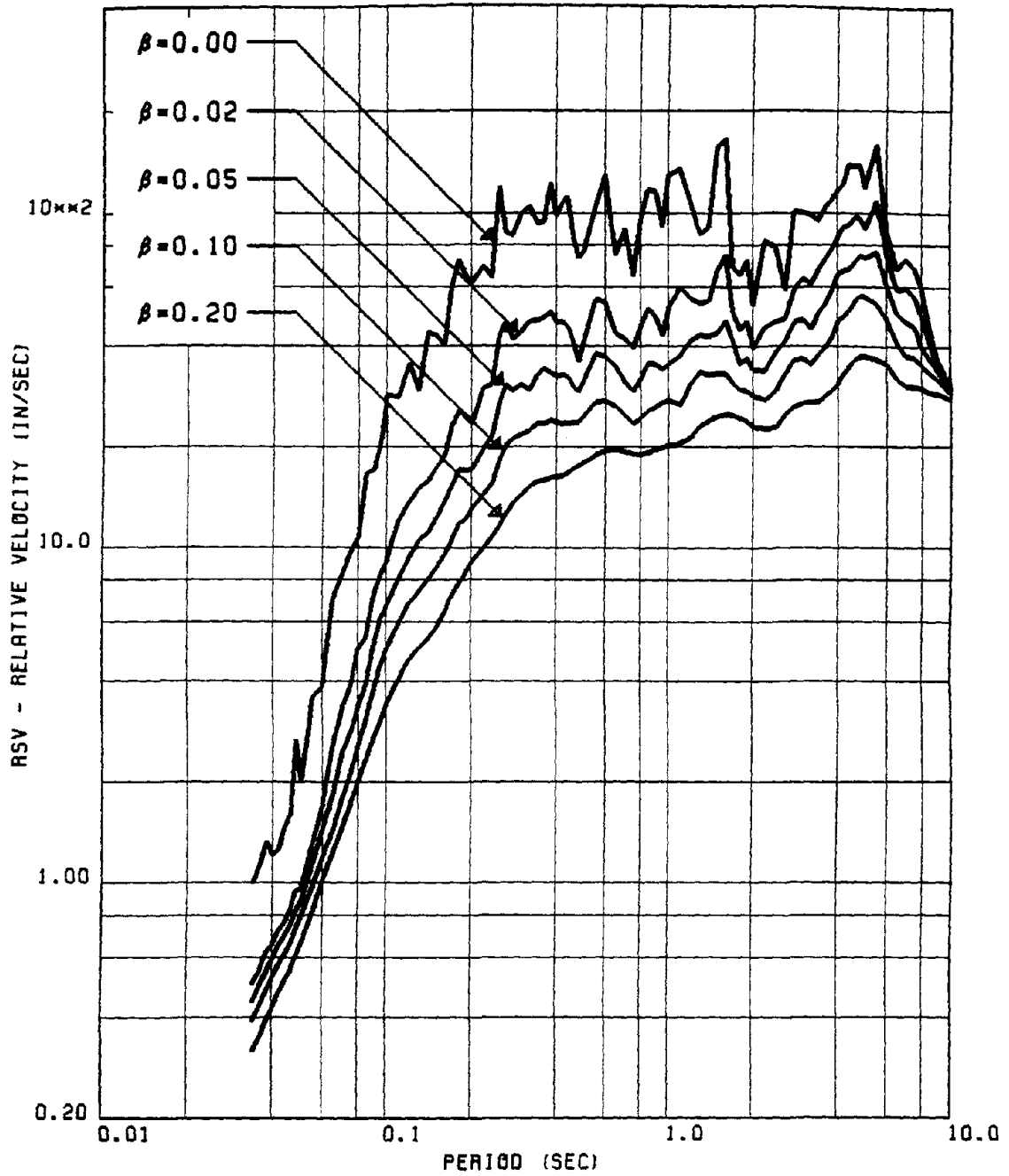
FIG. 55 (MEAN+SD) REL VELOCITY SPECTRA FOR HORIZONTAL RECORDS OF GROUP #4
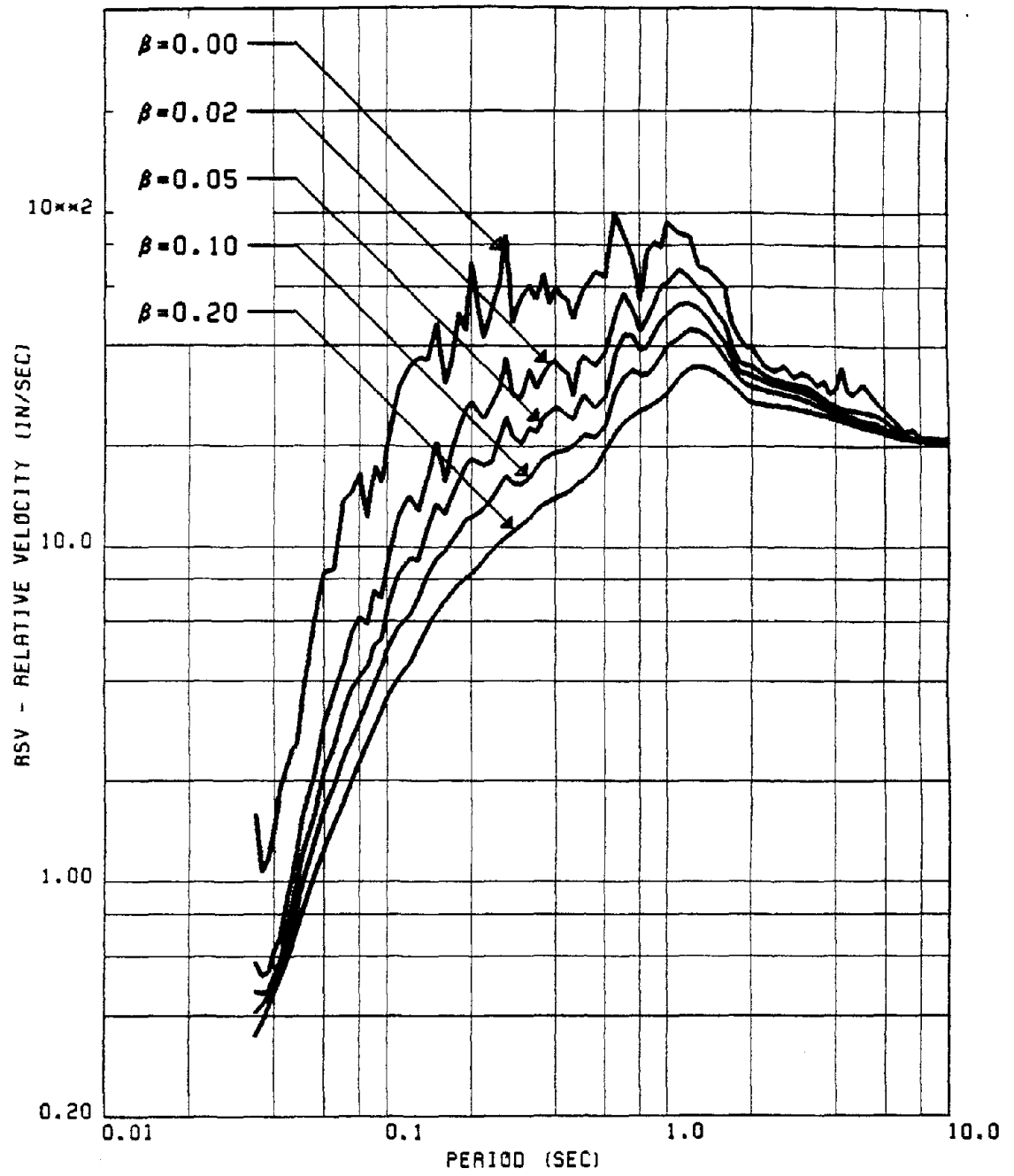
FIG. 56 (MEAN+SD) REL VELOCITY SPECTRA FOR HORIZONTAL RECORDS OF GROUP #5

134
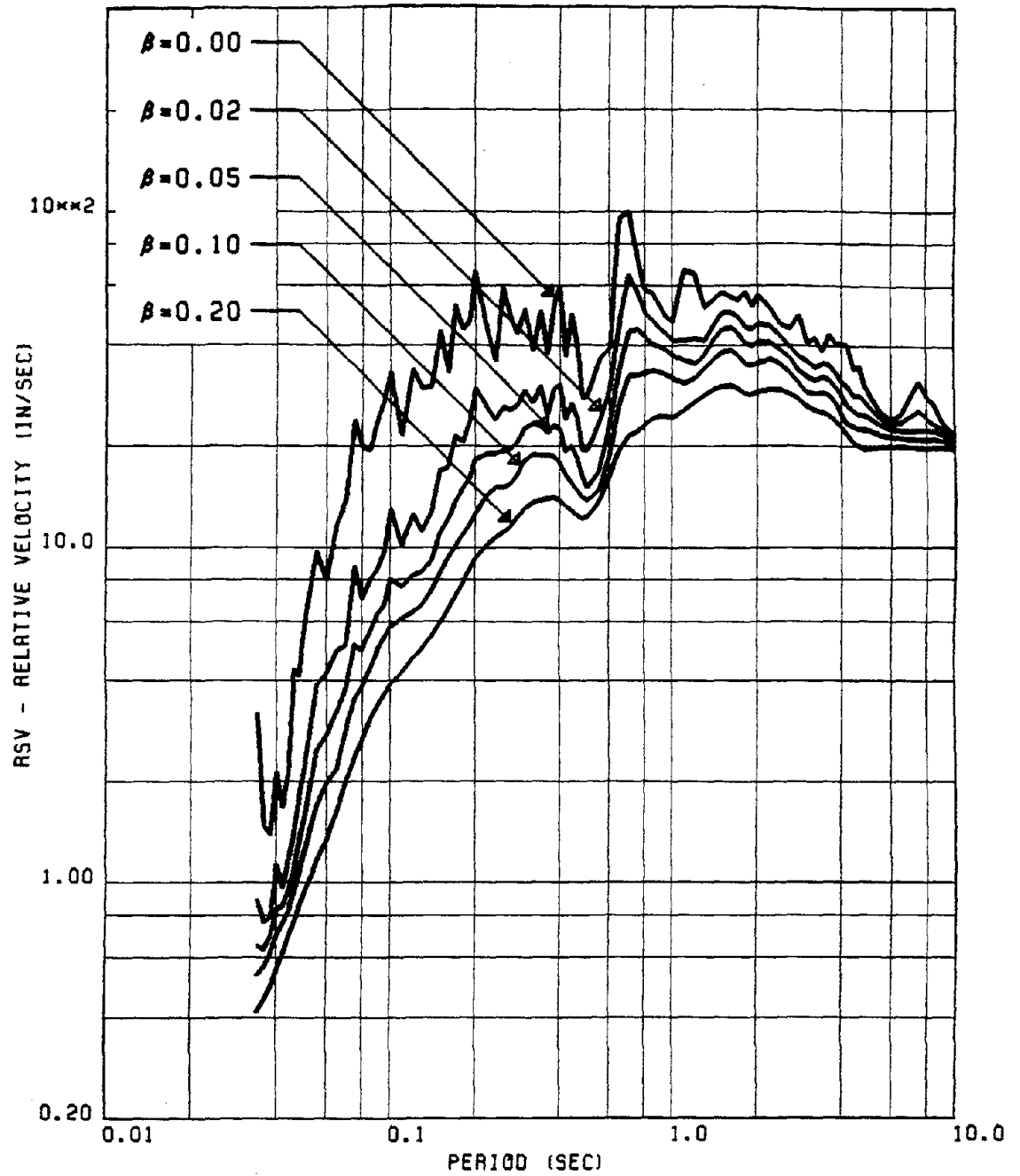
FIG. 57   (MEAN+SD) REL VELOCITY SPECTRA FOR VERTICAL RECORDS OF GROUP #5

135
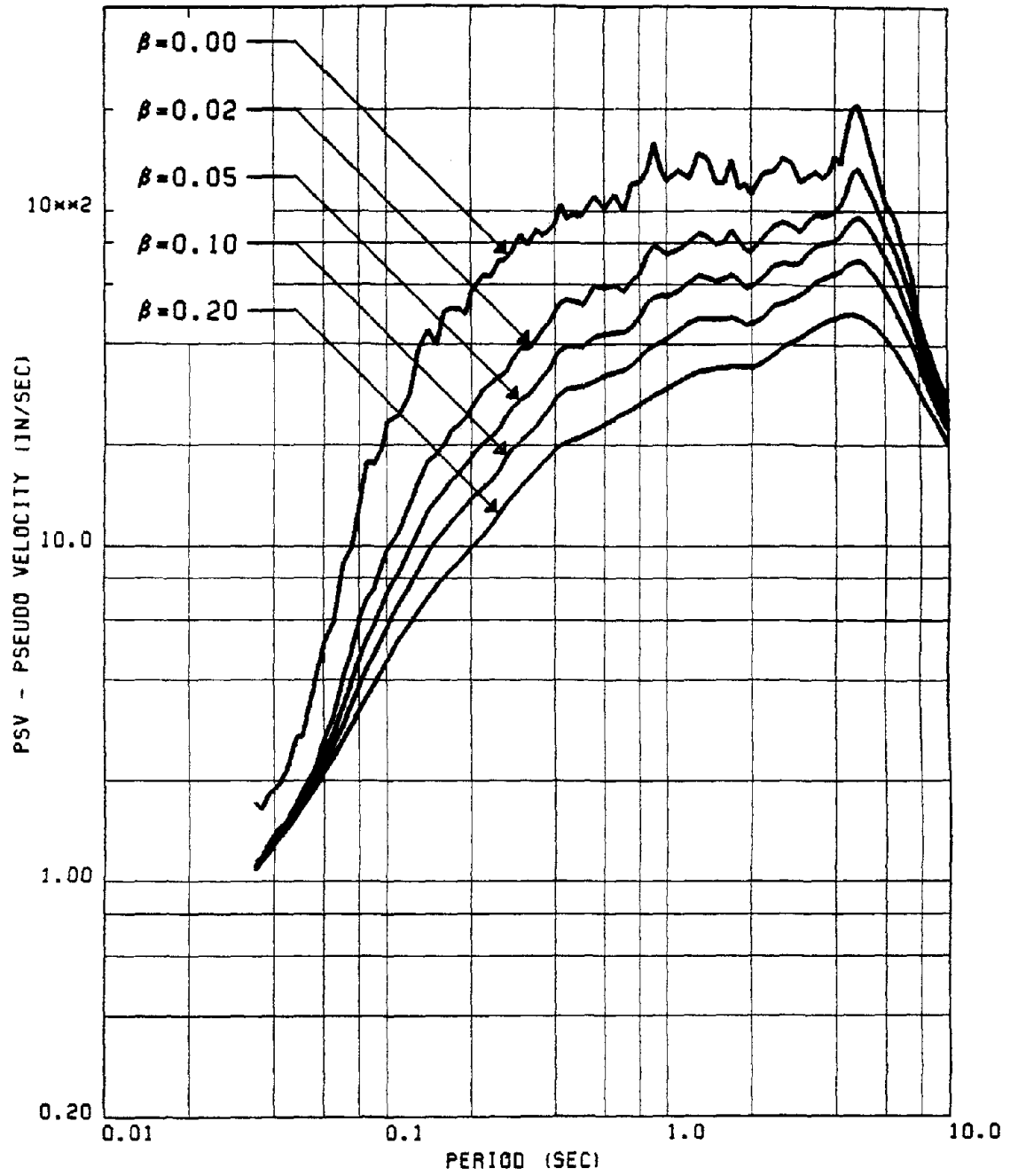
FIG. 58 (MEAN+SD) PSEUDO VEL SPECTRA FOR HORIZONTAL RECORDS OF GROUP #1

136
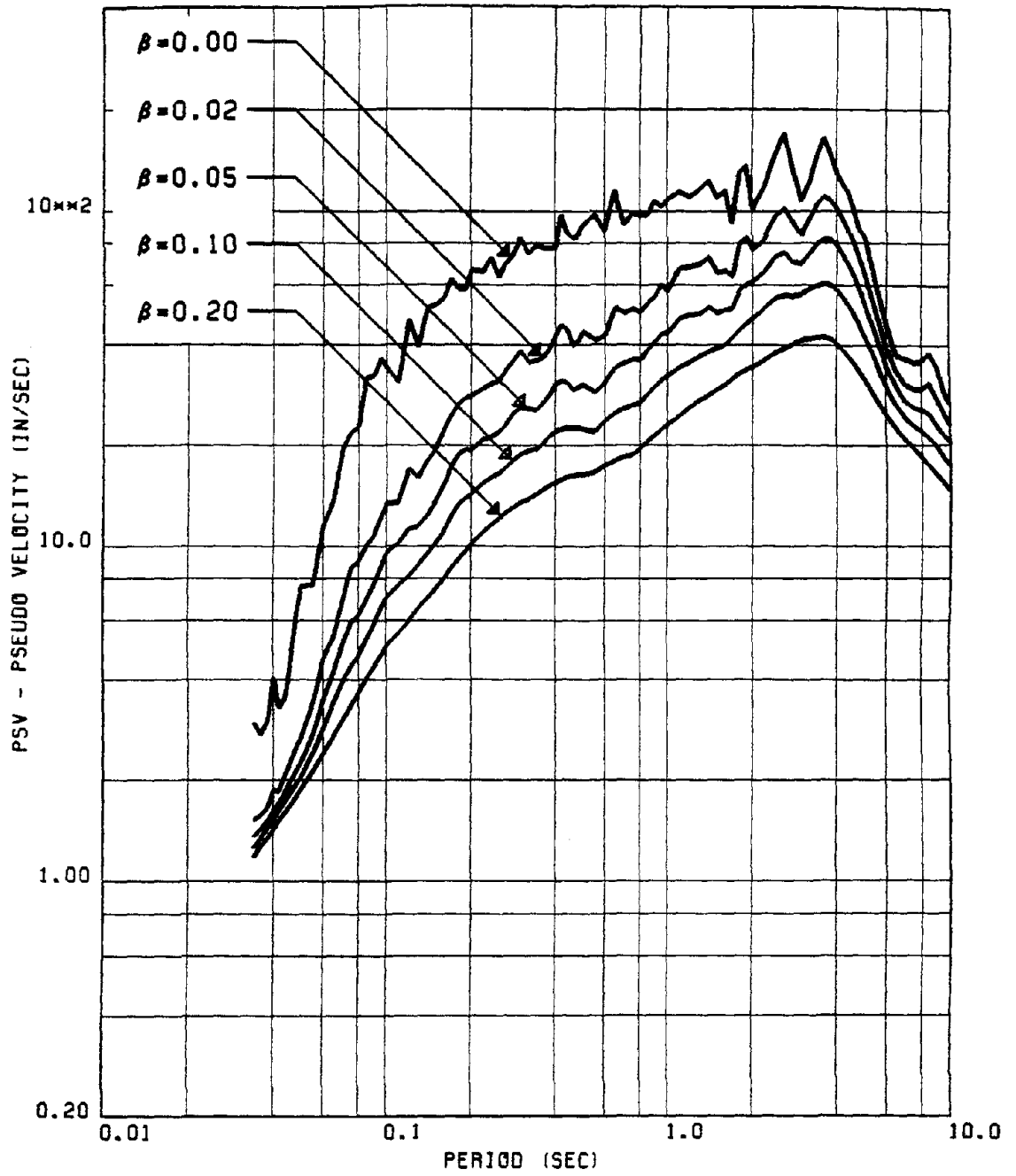
FIG. 59   (MEAN+SD) PSEUDO VEL SPECTRA FOR VERTICAL RECORDS OF GROUP #1
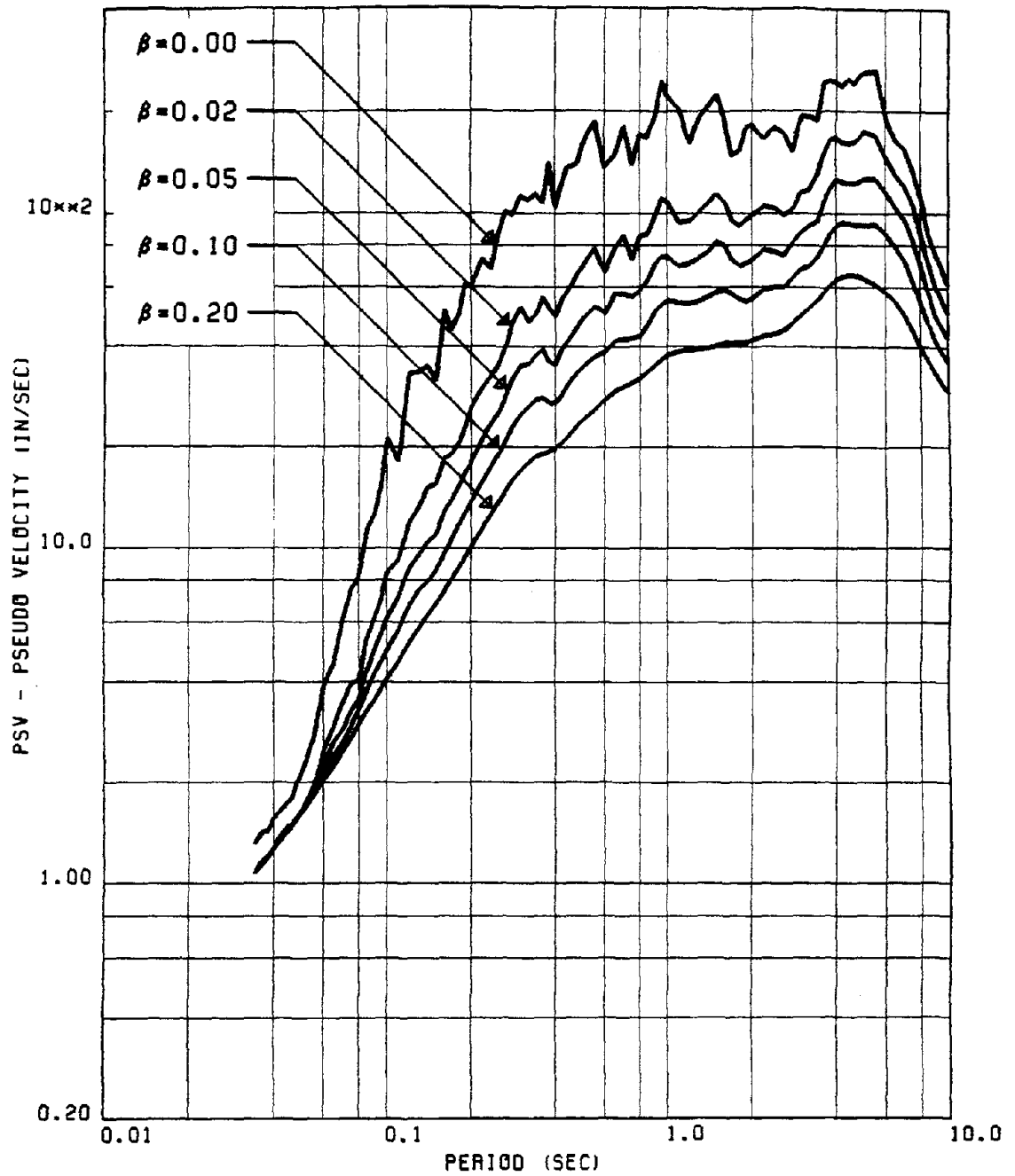
FIG. 60 (MEAN+SD) PSEUDO VEL SPECTRA FOR HORIZONTAL RECORDS OF GROUP #2

138
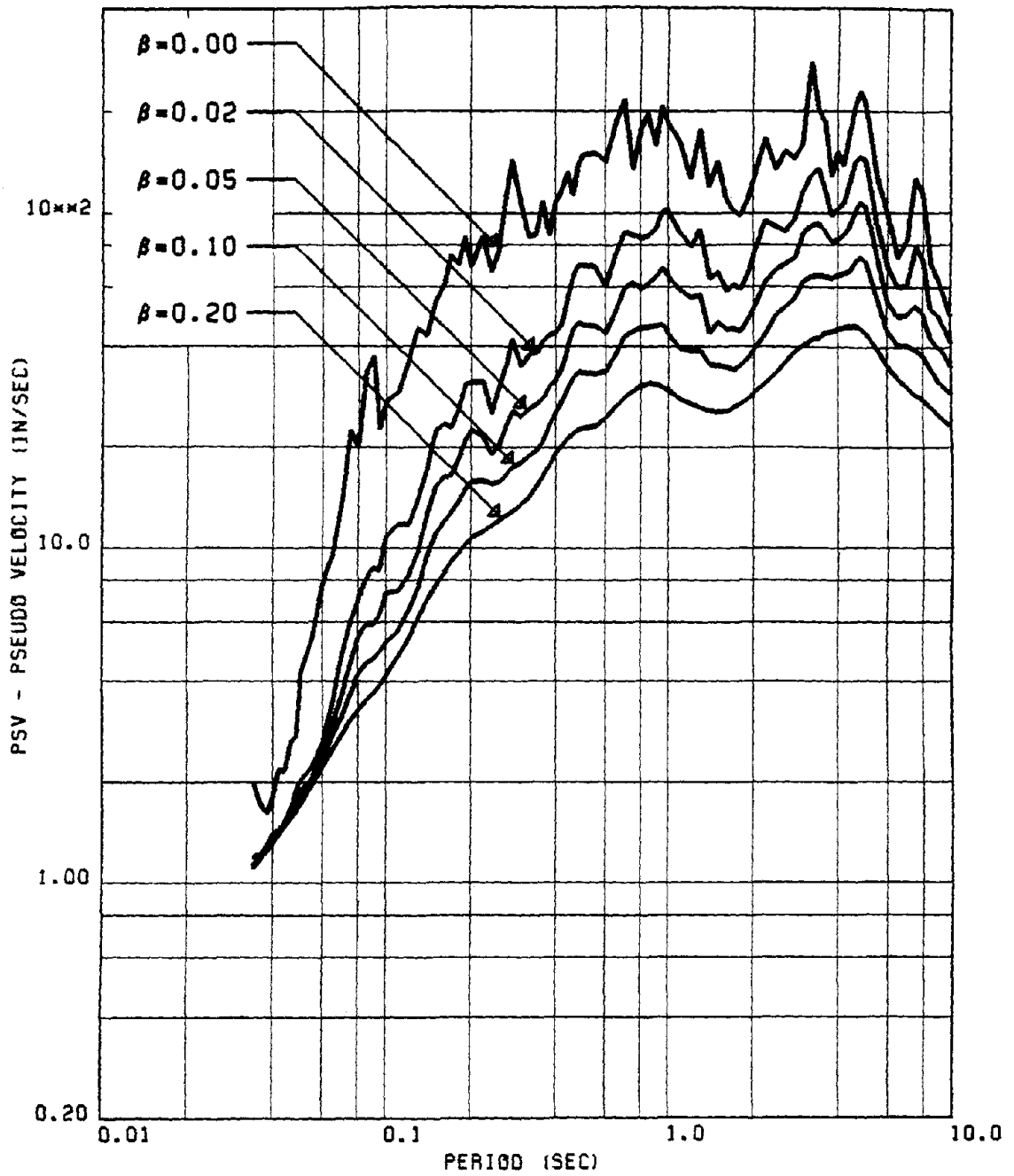
FIG. 61   (MEAN+SD) PSEUDO VEL SPECTRA FOR VERTICAL RECORDS OF GROUP #2

139
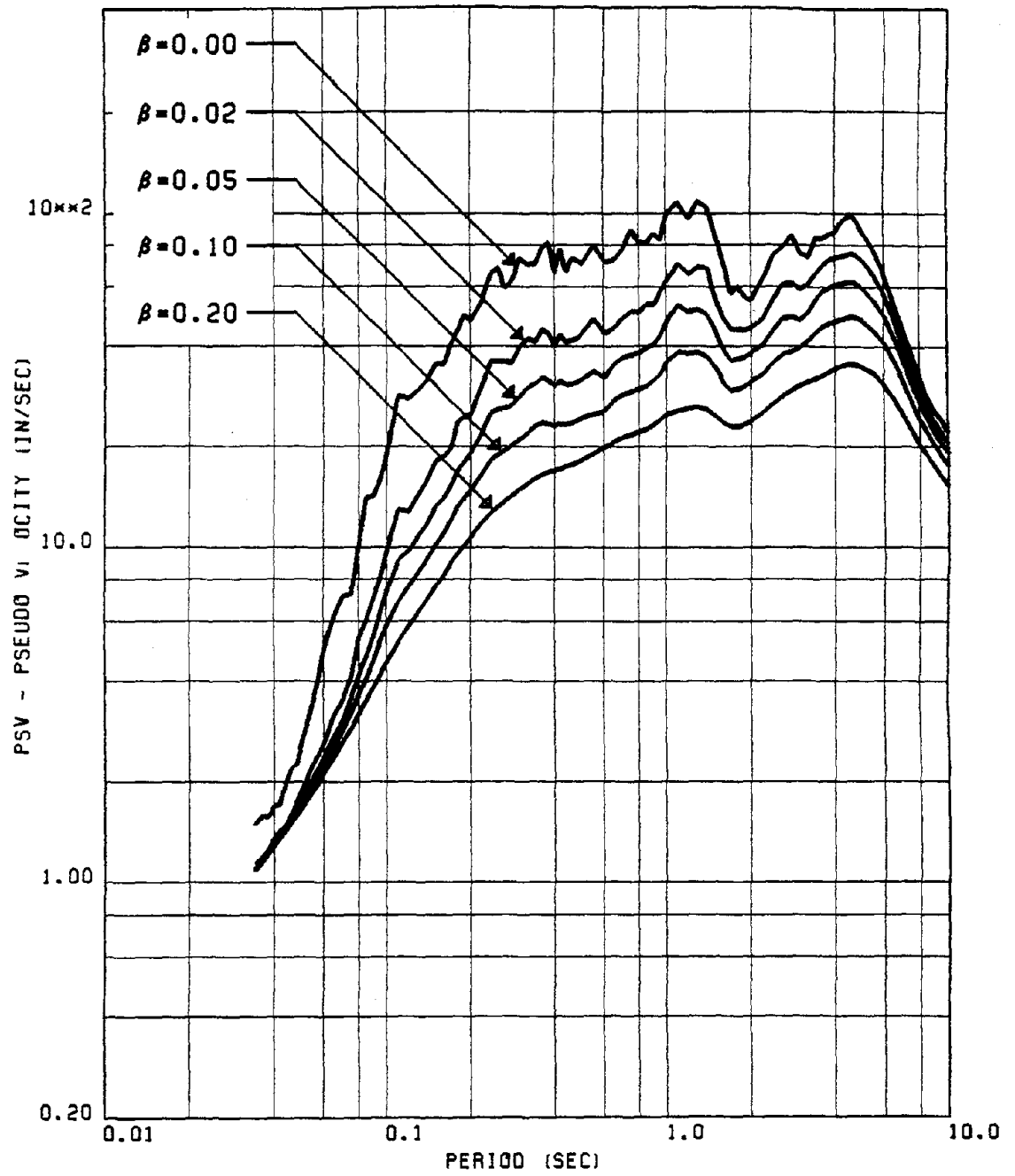
FIG. 62   (MEAN+SD) PSEUDO VEL SPECTRA FOR HORIZONTAL RECORDS OF GROUP #3

140
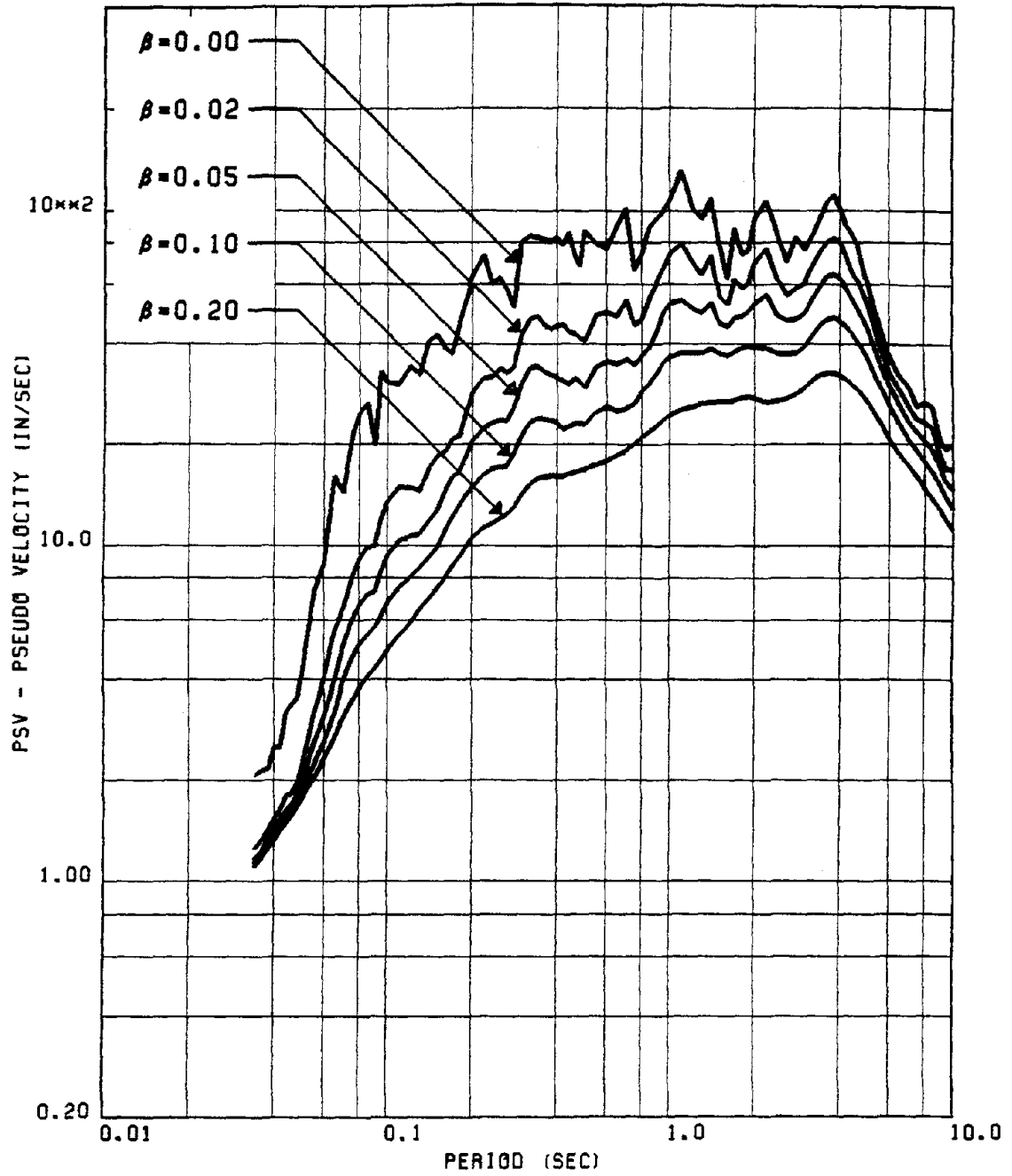
FIG. 63 (MEAN+SD) PSEUDO VEL SPECTRA FOR VERTICAL RECORDS OF GROUP #3

141
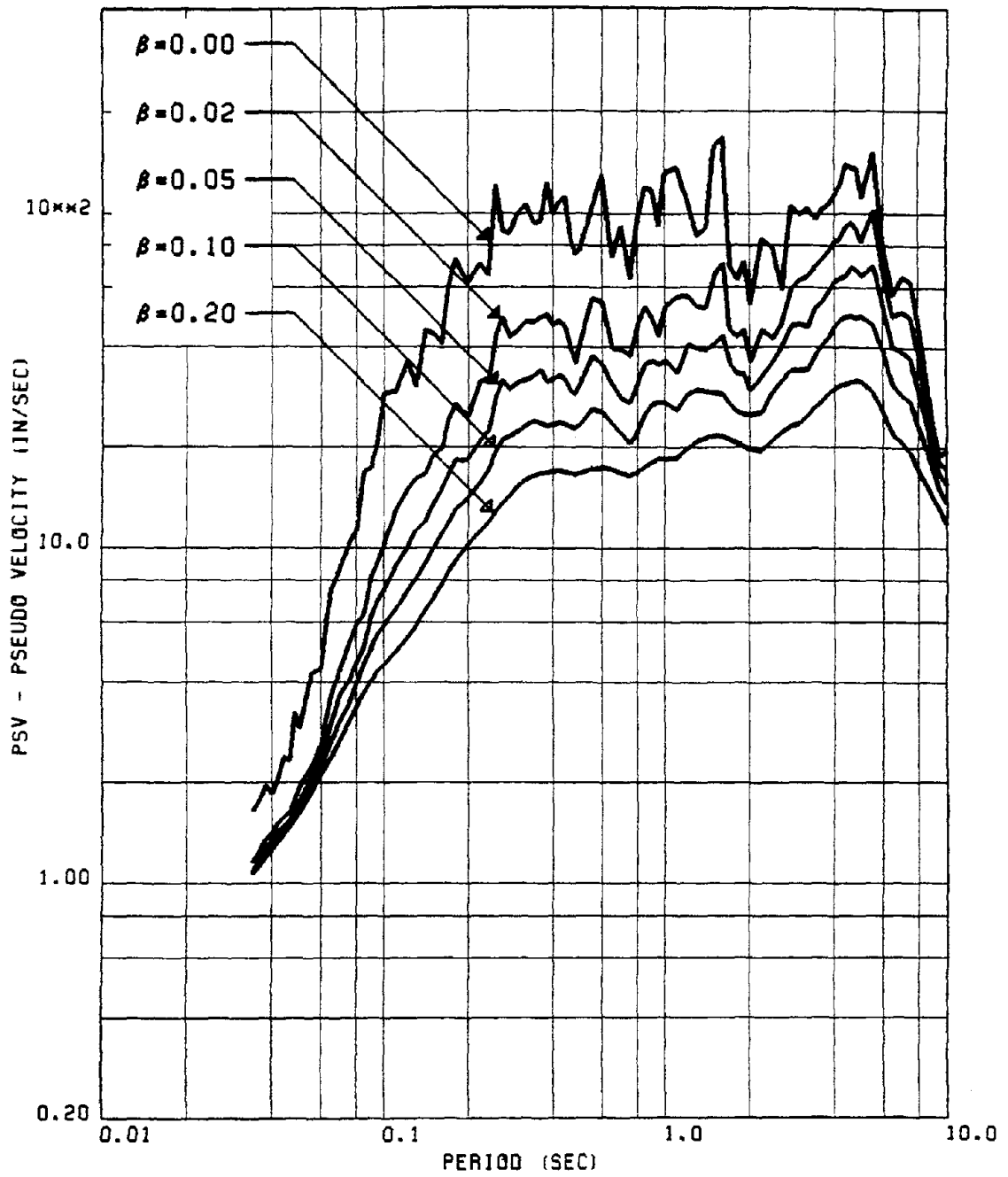
FIG. 64 (MEAN+SD) PSEUDO VEL SPECTRA FOR HORIZONTAL RECORDS OF GROUP #4
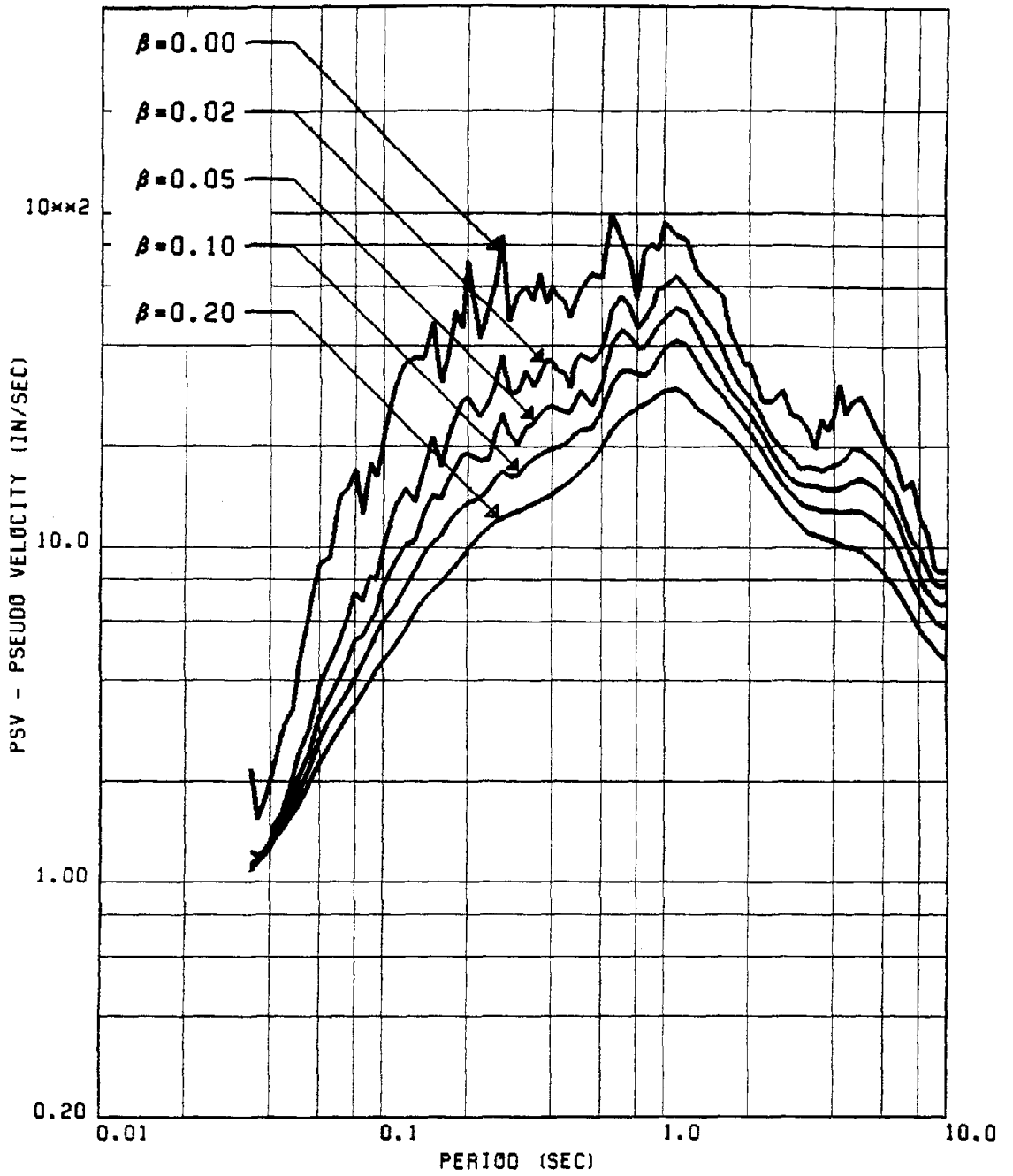
FIG. 65   (MEAN+SD) PSEUDO VEL SPECTRA FOR HORIZONTAL RECORDS OF GROUP #5
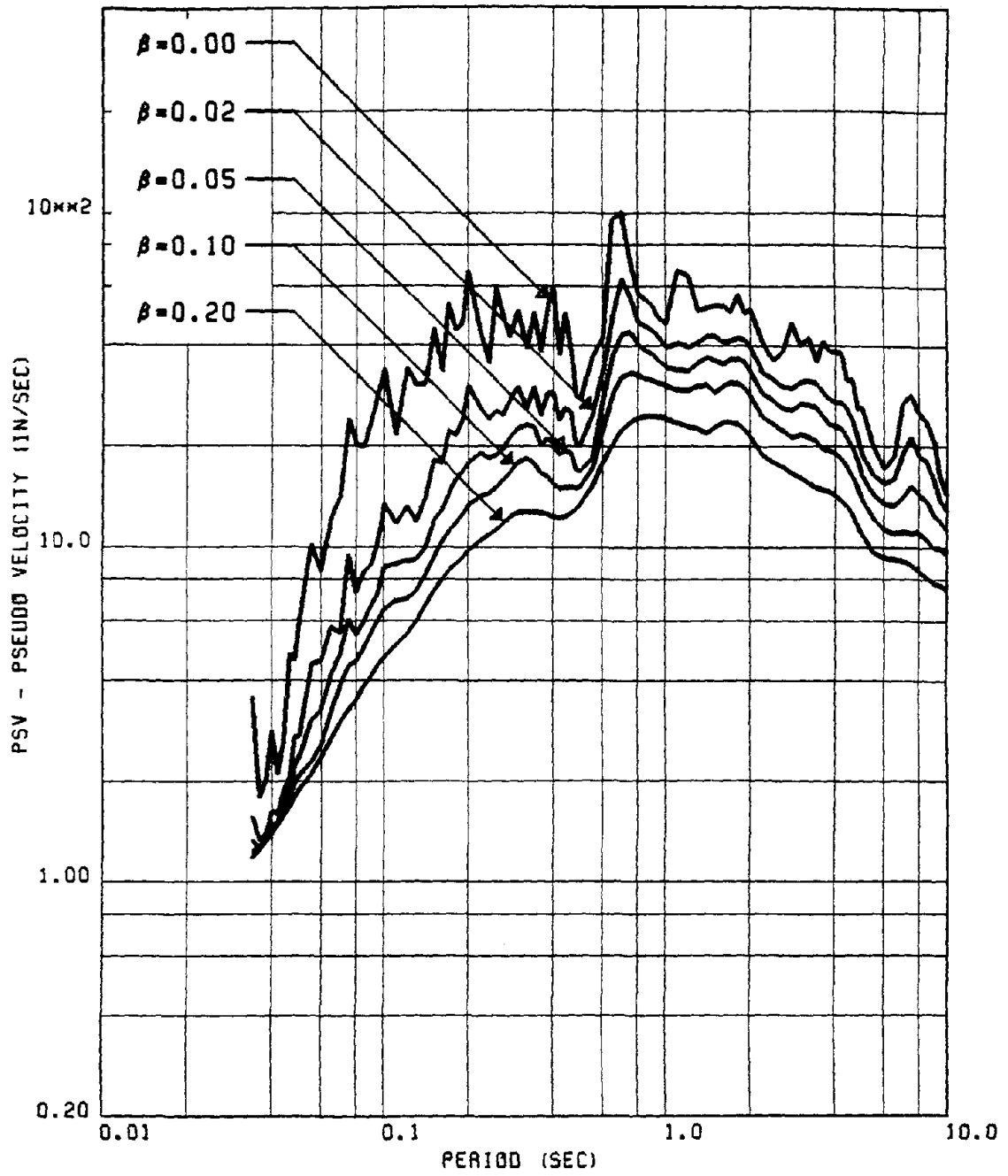
FIG. 66   (MEAN+SD) PSEUDO VEL SPECTRA FOR VERTICAL RECORDS OF GROUP #5
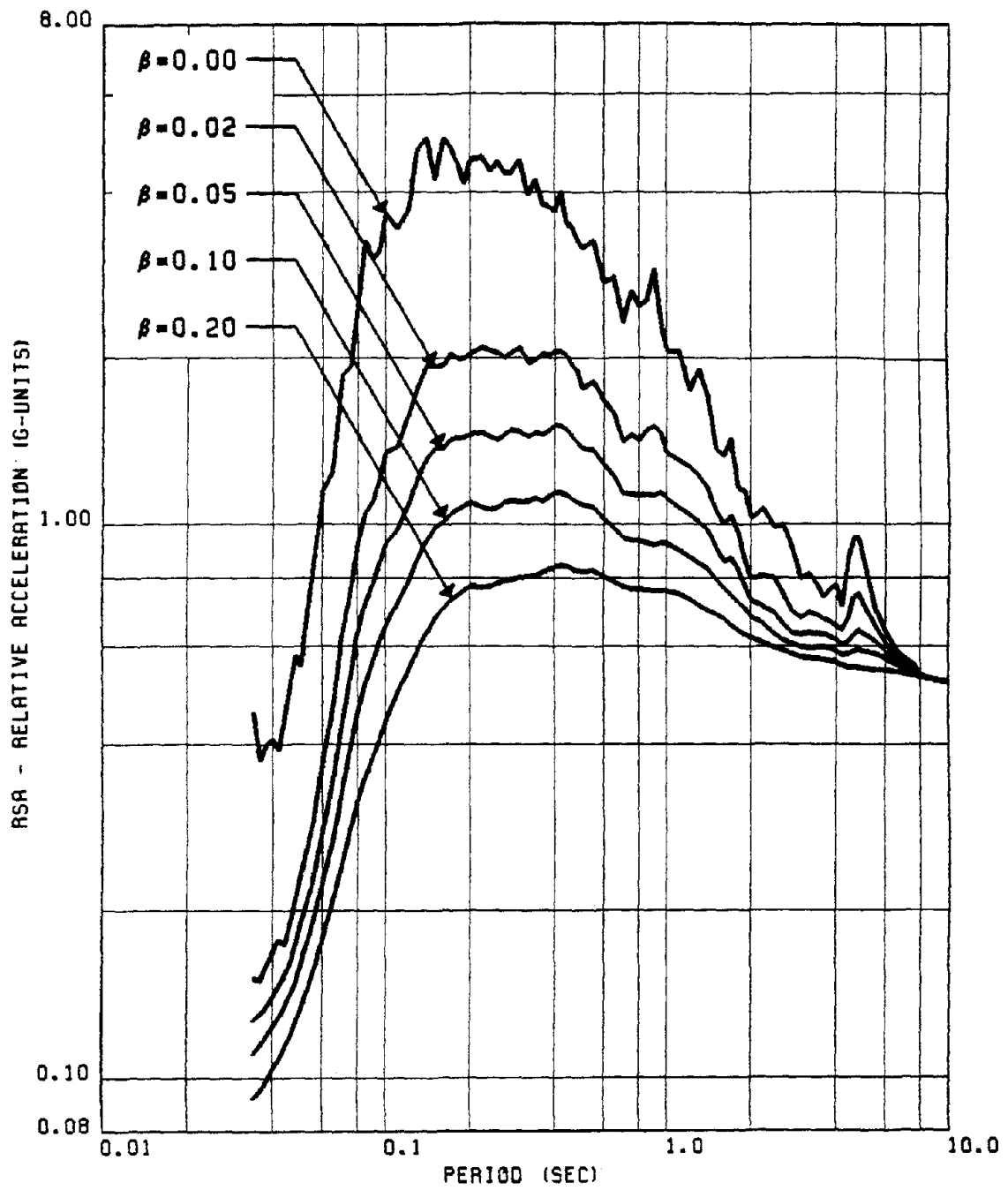
FIG. 67 (MEAN + SD) REL. ACCL. SPECTRA FOR HORIZONTAL RECORDS OF GROUP #1
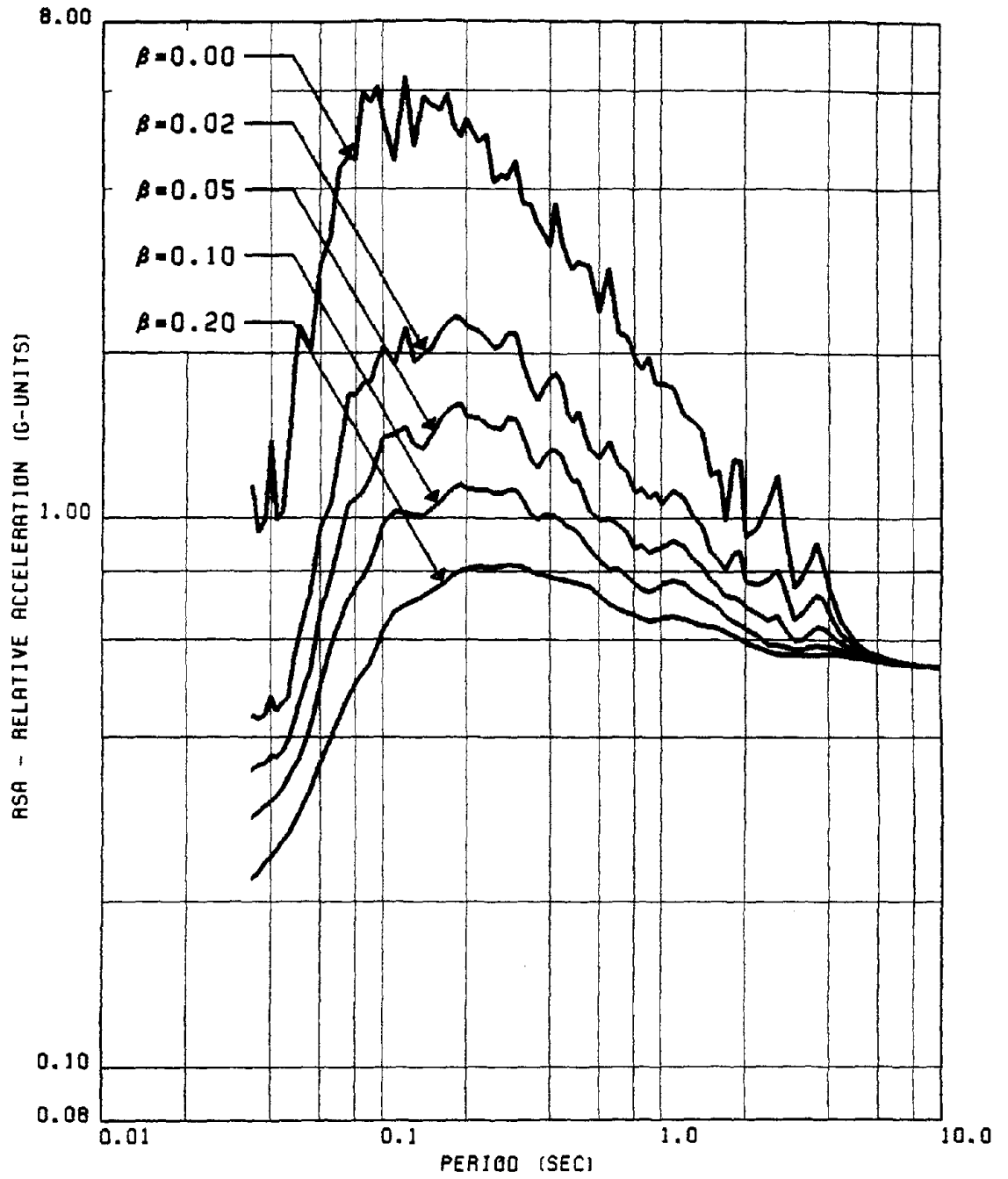
FIG. 68 (MEAN + SD) REL. ACCL. SPECTRA FOR VERTICAL RECORDS OF GROUP #1

146
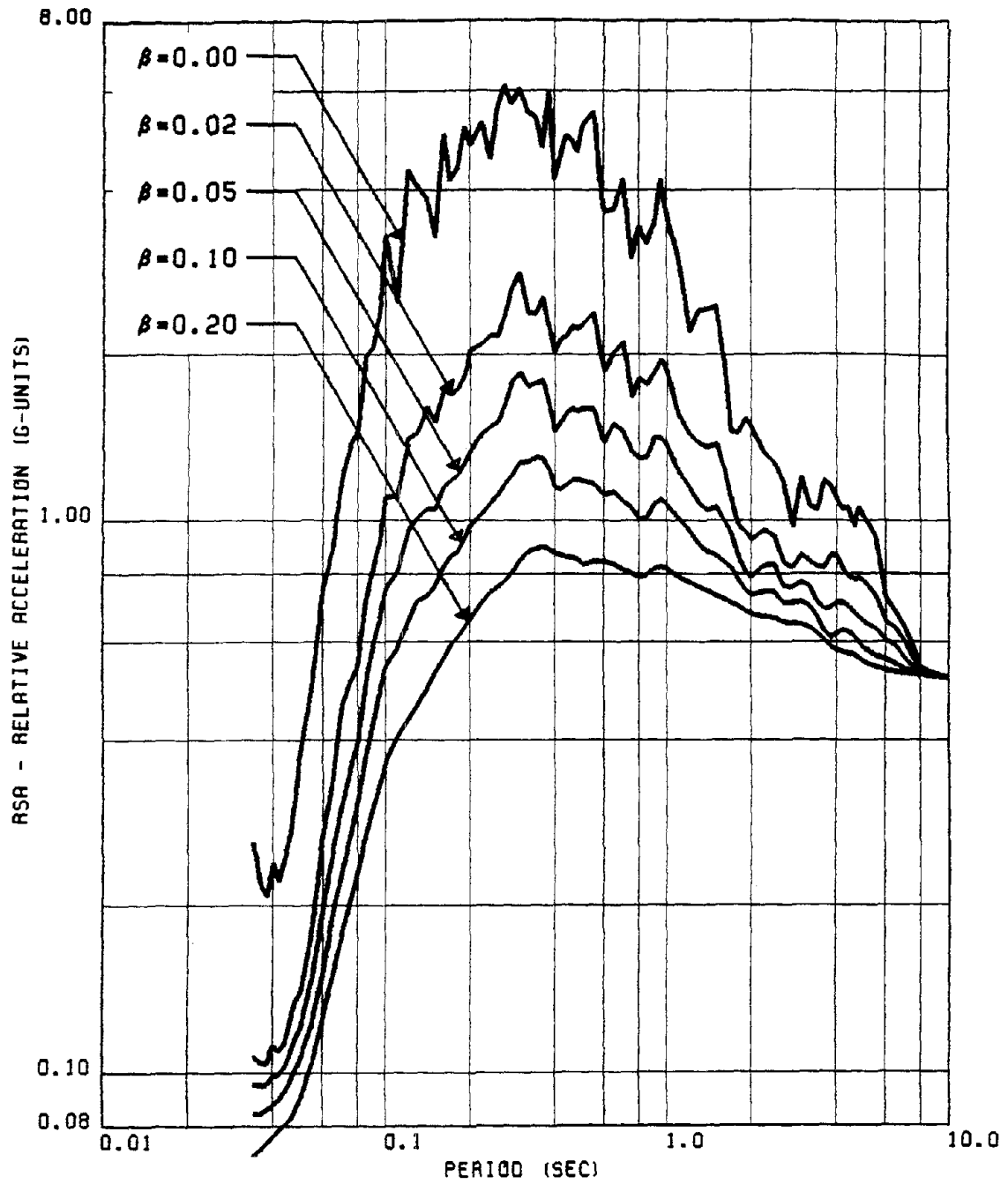
FIG. 69   (MEAN + SD) REL. ACCL. SPECTRA FOR HORIZONTAL RECORDS OF GROUP #2
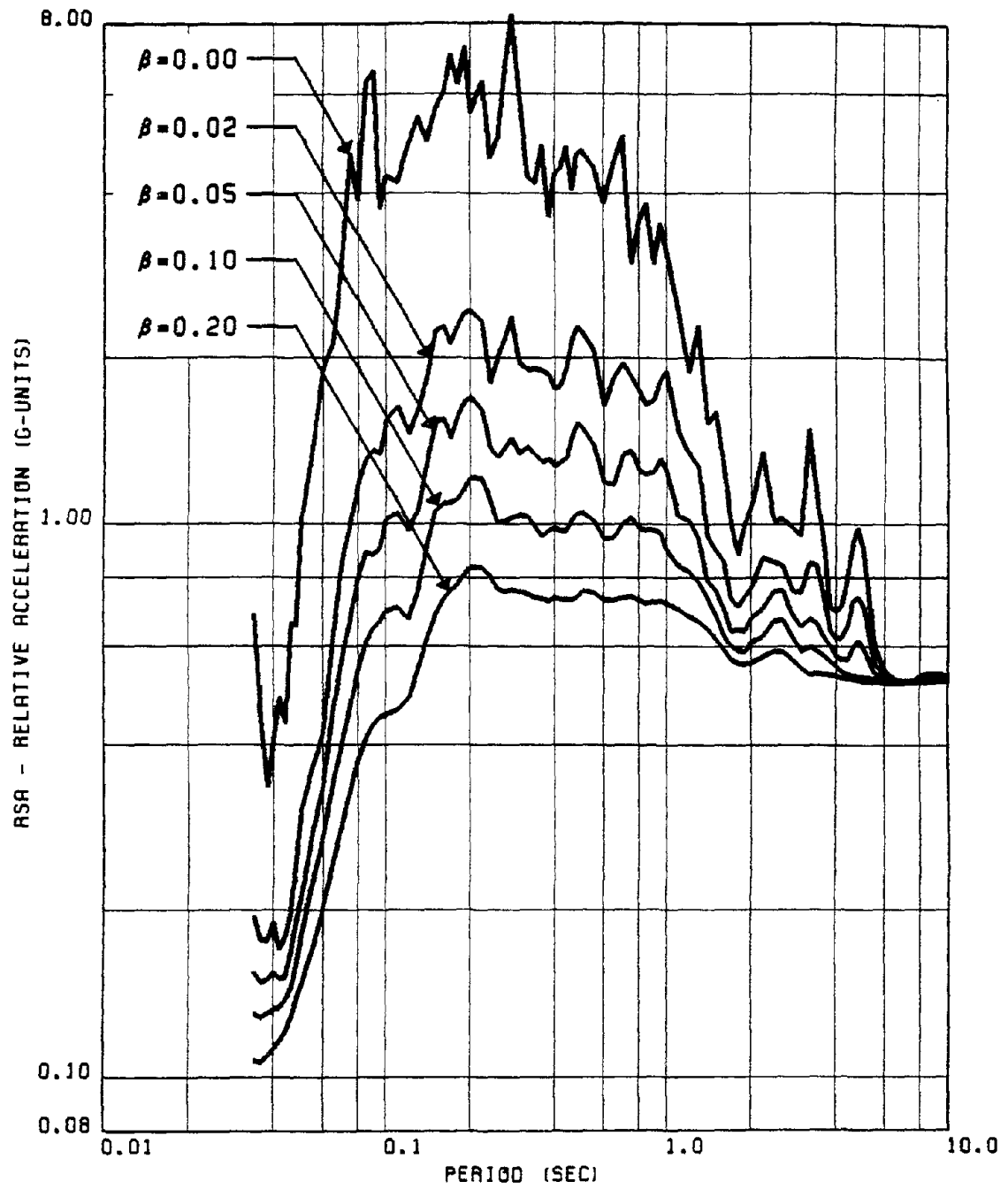
FIG. 70   (MEAN + SD) REL. ACCL. SPECTRA FOR VERTICAL RECORDS OF GROUP #2

148
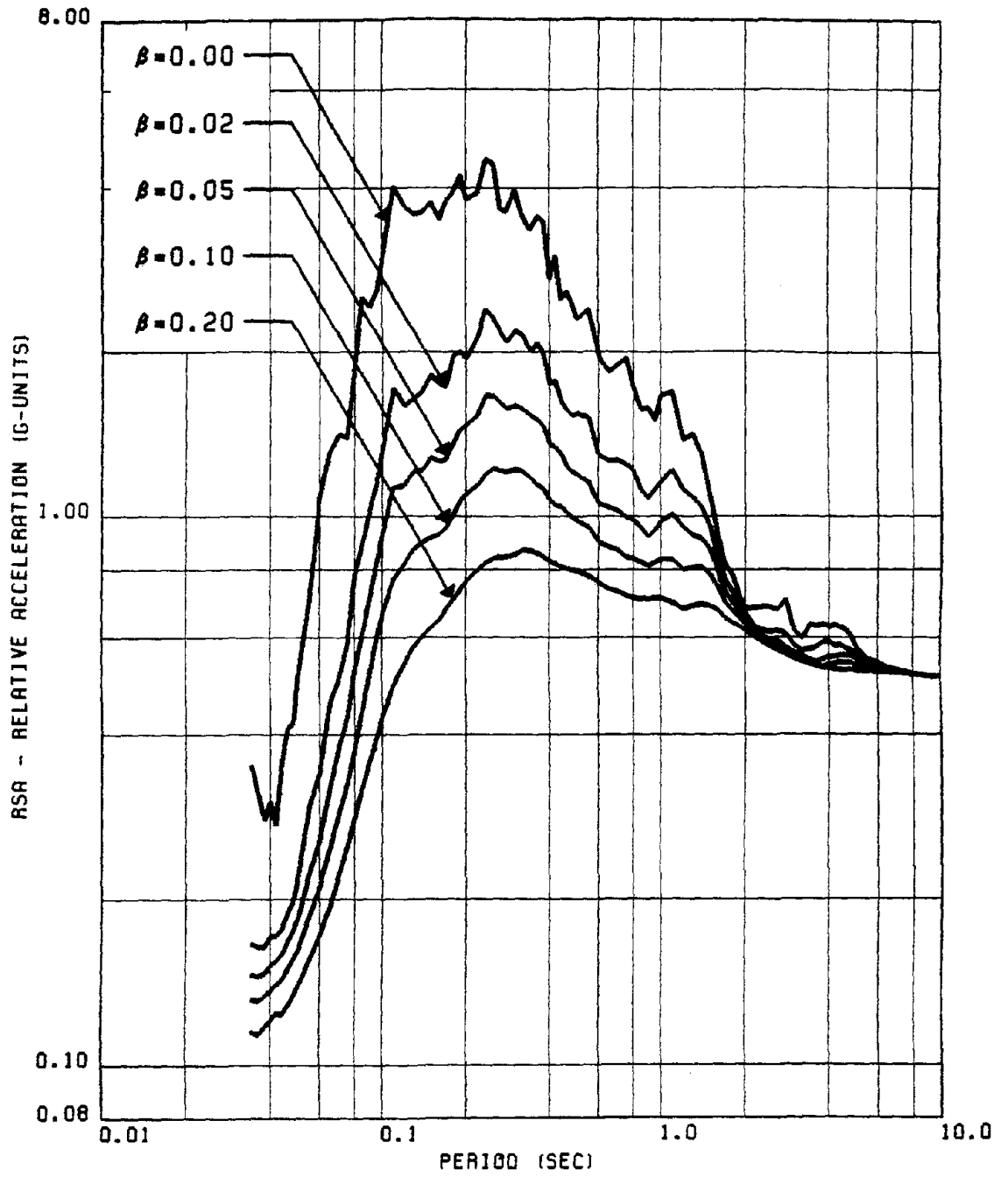
FIG. 71 (MEAN + SD) REL. ACCL. SPECTRA FOR HORIZONTAL RECORDS OF GROUP #3

149
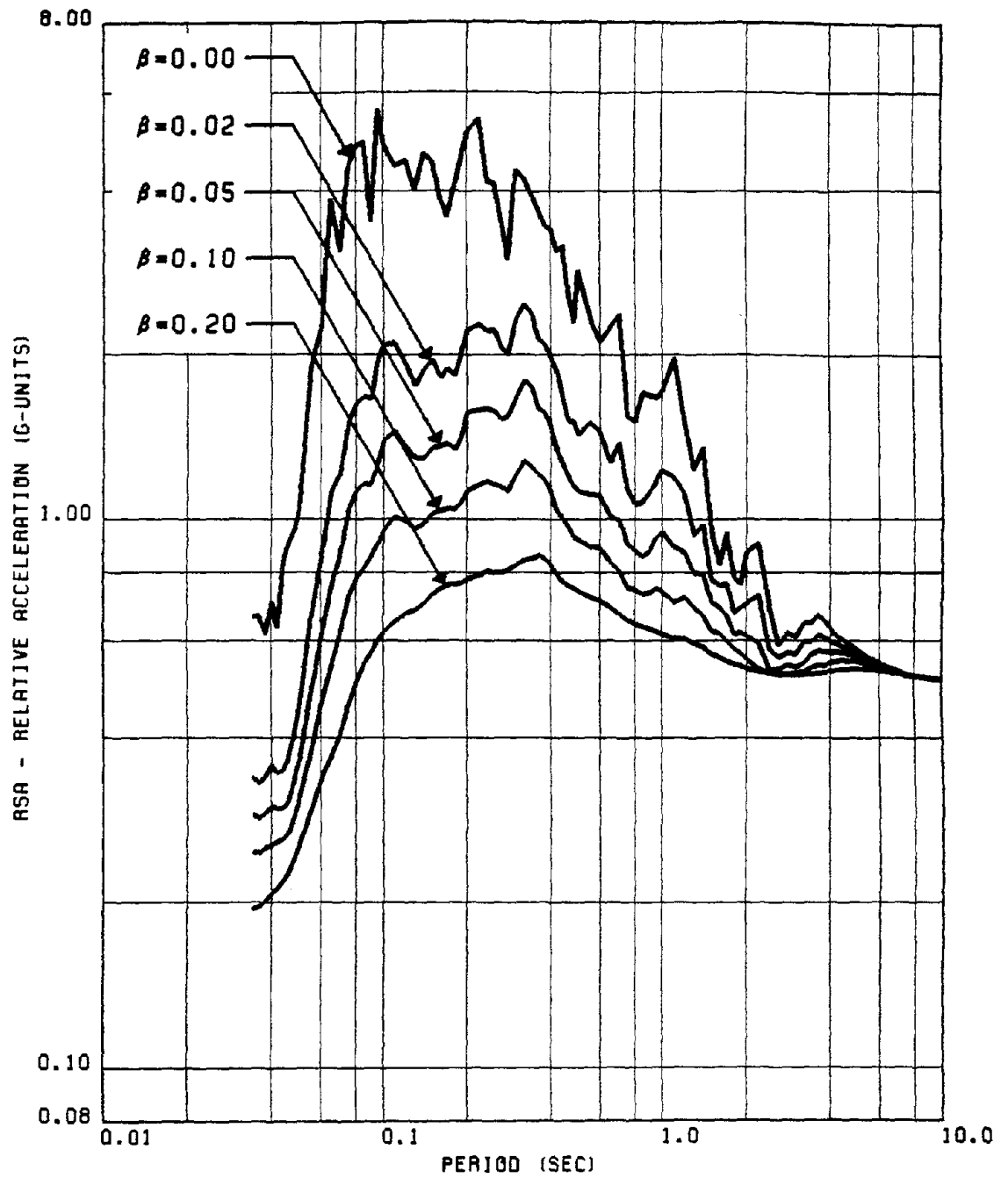
FIG. 72   (MEAN + SD) REL. ACCL. SPECTRA FOR VERTICAL RECORDS OF GROUP #3
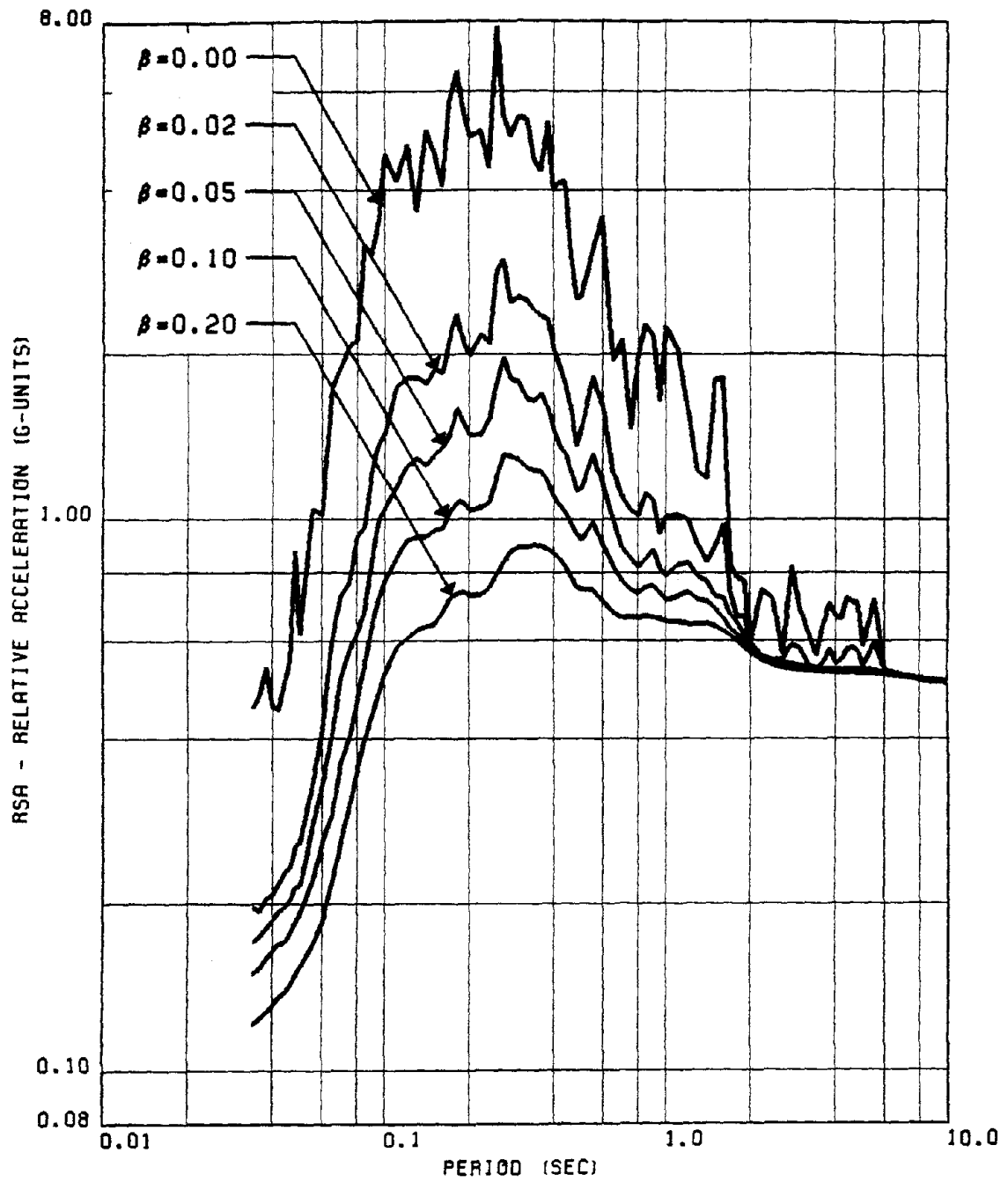
FIG. 73 (MEAN + SD) REL. ACCL. SPECTRA FOR HORIZONTAL RECORDS OF GROUP #4
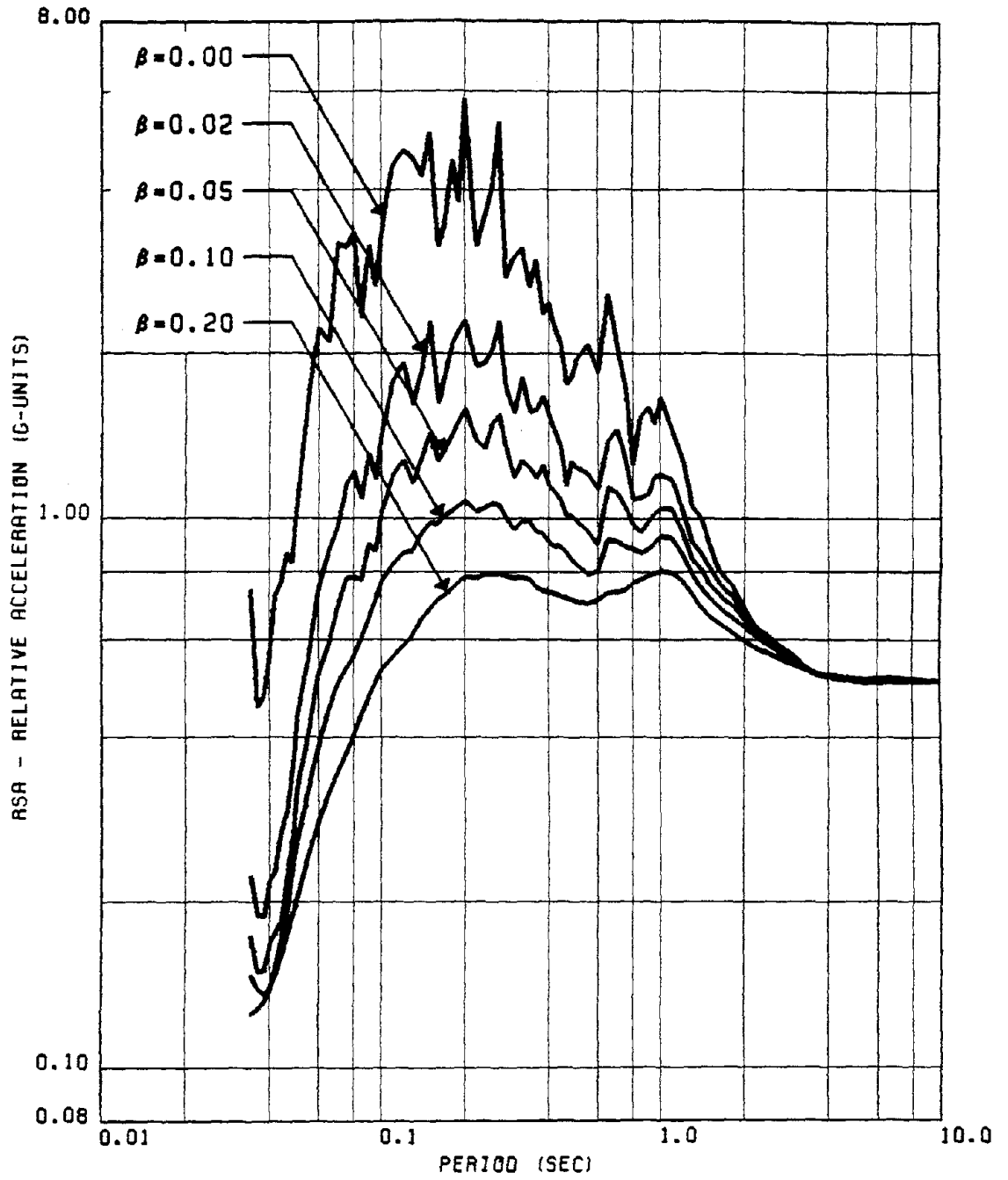
FIG. 74   (MEAN + SD) REL. ACCL. SPECTRA FOR HORIZONTAL RECORDS OF GROUP #5

152
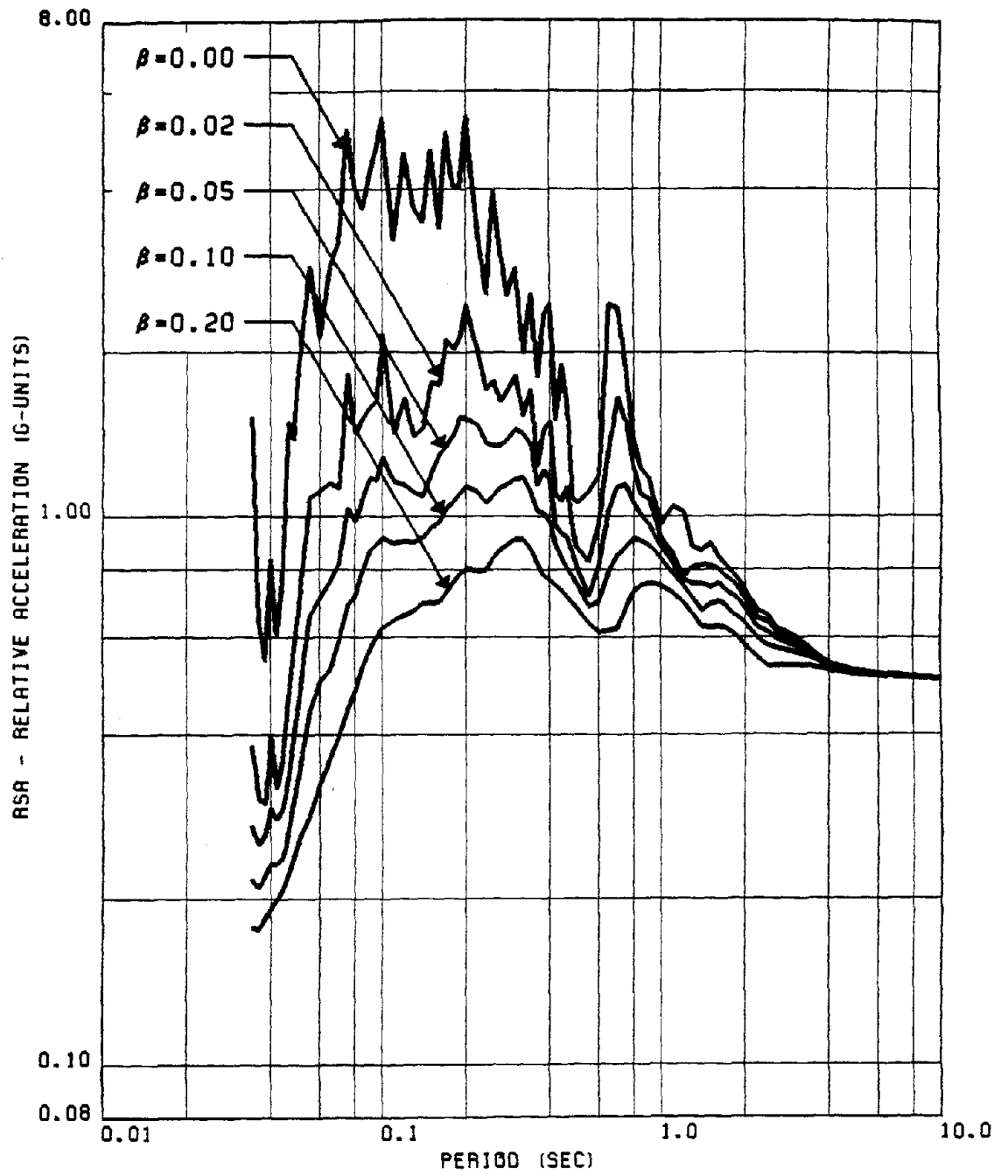
FIG. 75 (MEAN + SD) REL. ACCL. SPECTRA FOR VERTICAL RECORDS OF GROUP #5
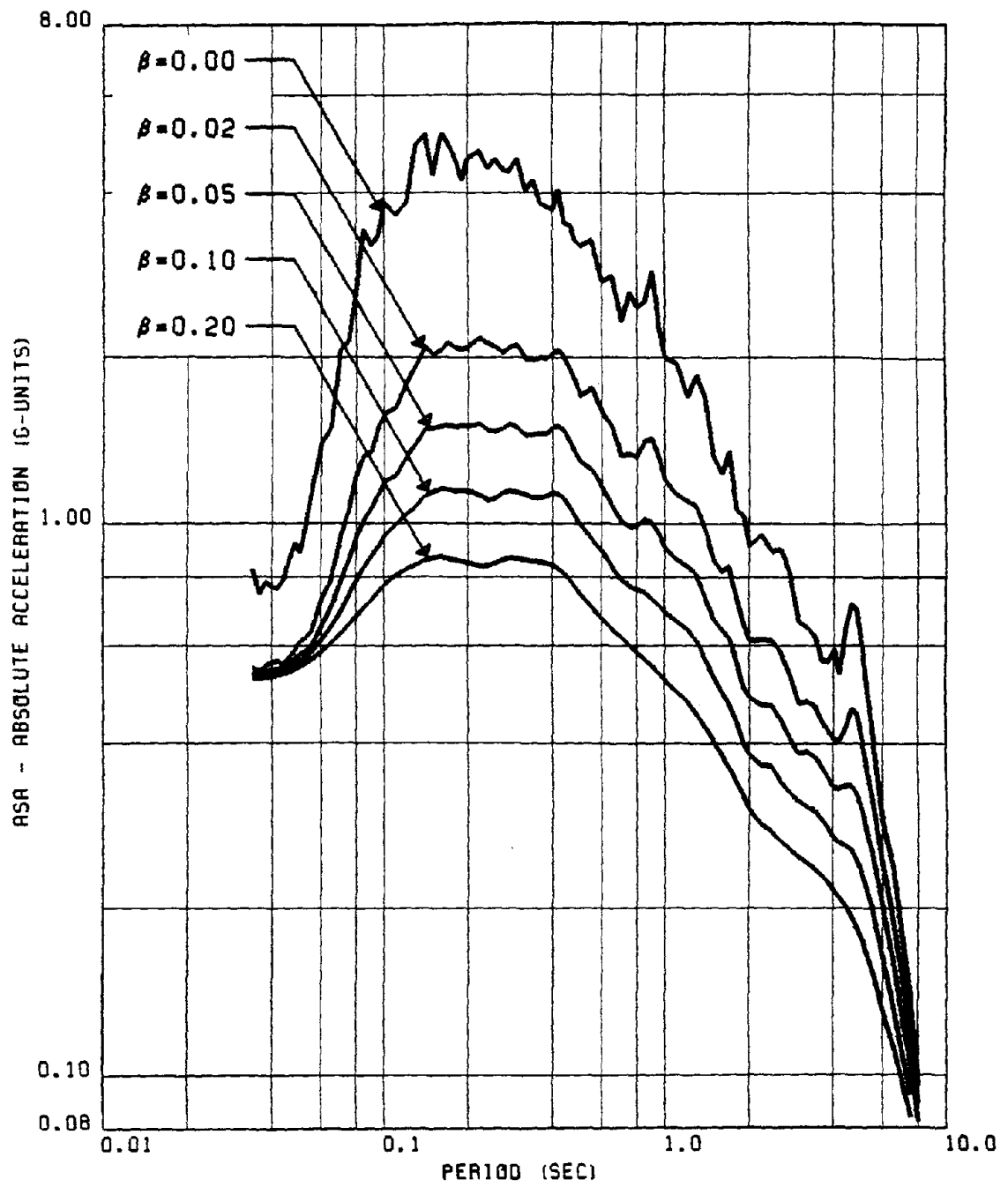
FIG. 76 (MEAN + SD) ABS. ACCL. SPECTRA FOR HORIZONTAL RECORDS OF GROUP #1
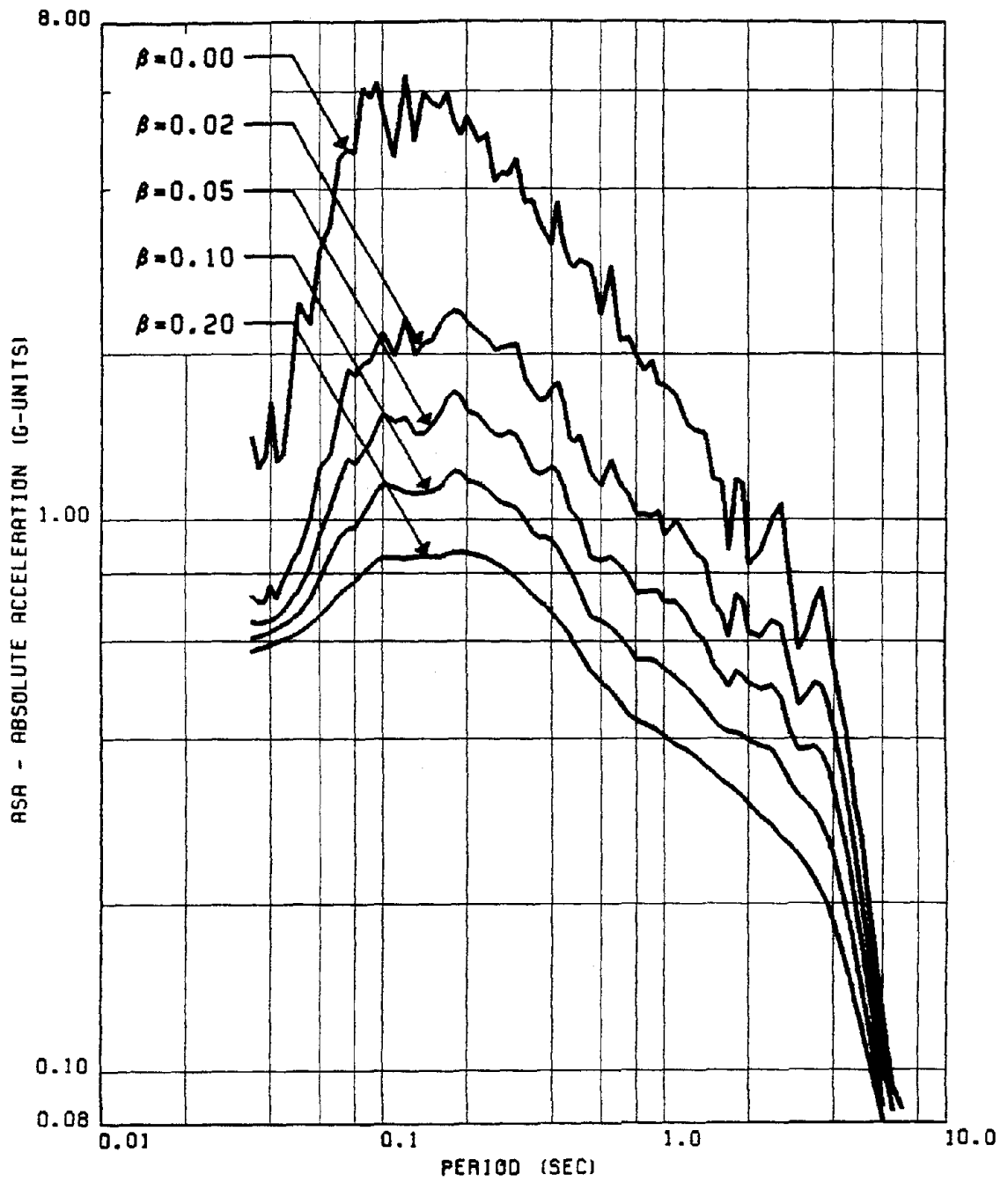
FIG. 77 (MEAN + SD) ABS. ACCL. SPECTRA FOR VERTICAL RECORDS OF GROUP #1

155
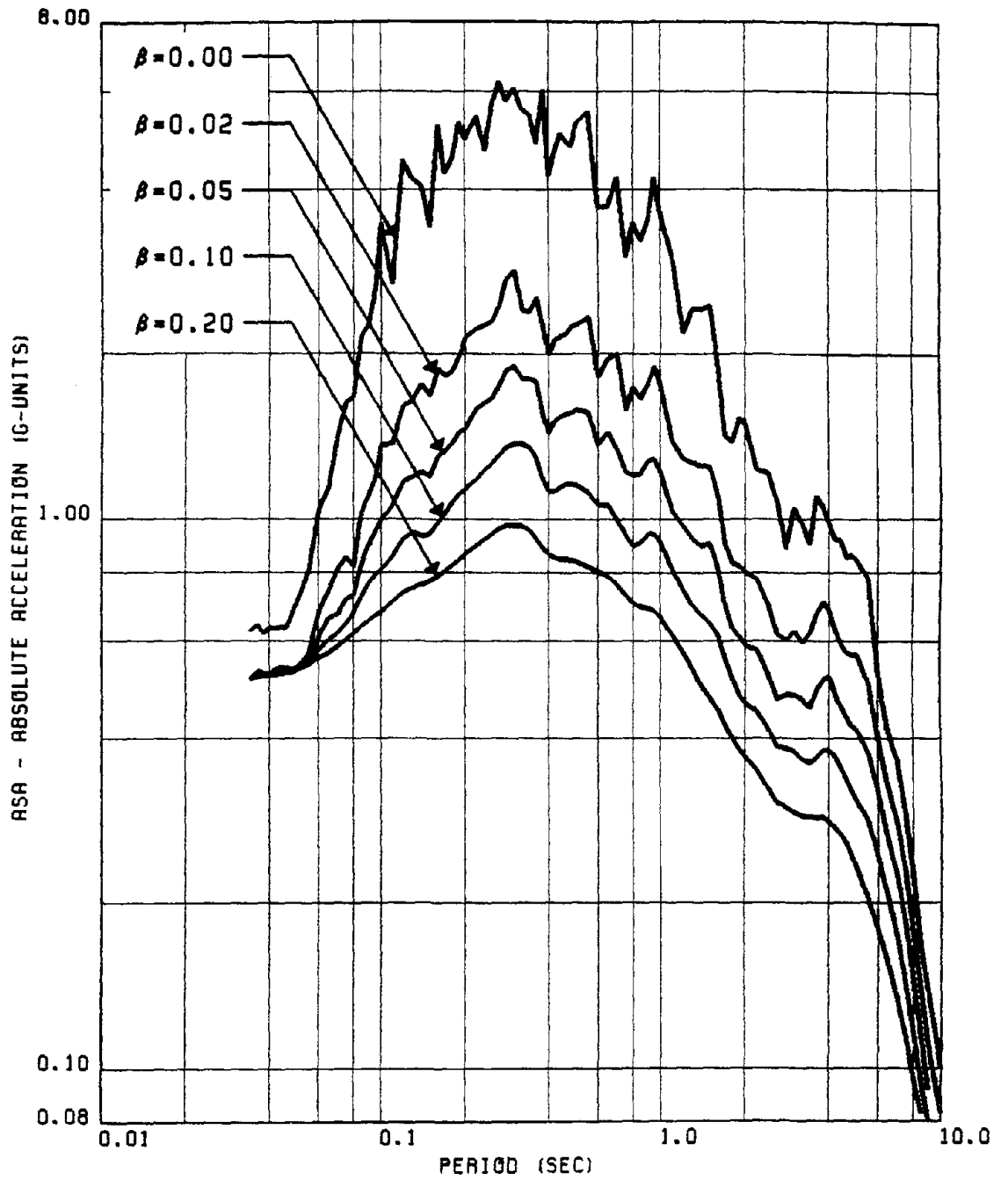
FIG. 78 (MEAN + SD) ABS. ACCL. SPECTRA FOR HORIZONTAL RECORDS OF GROUP #2

156
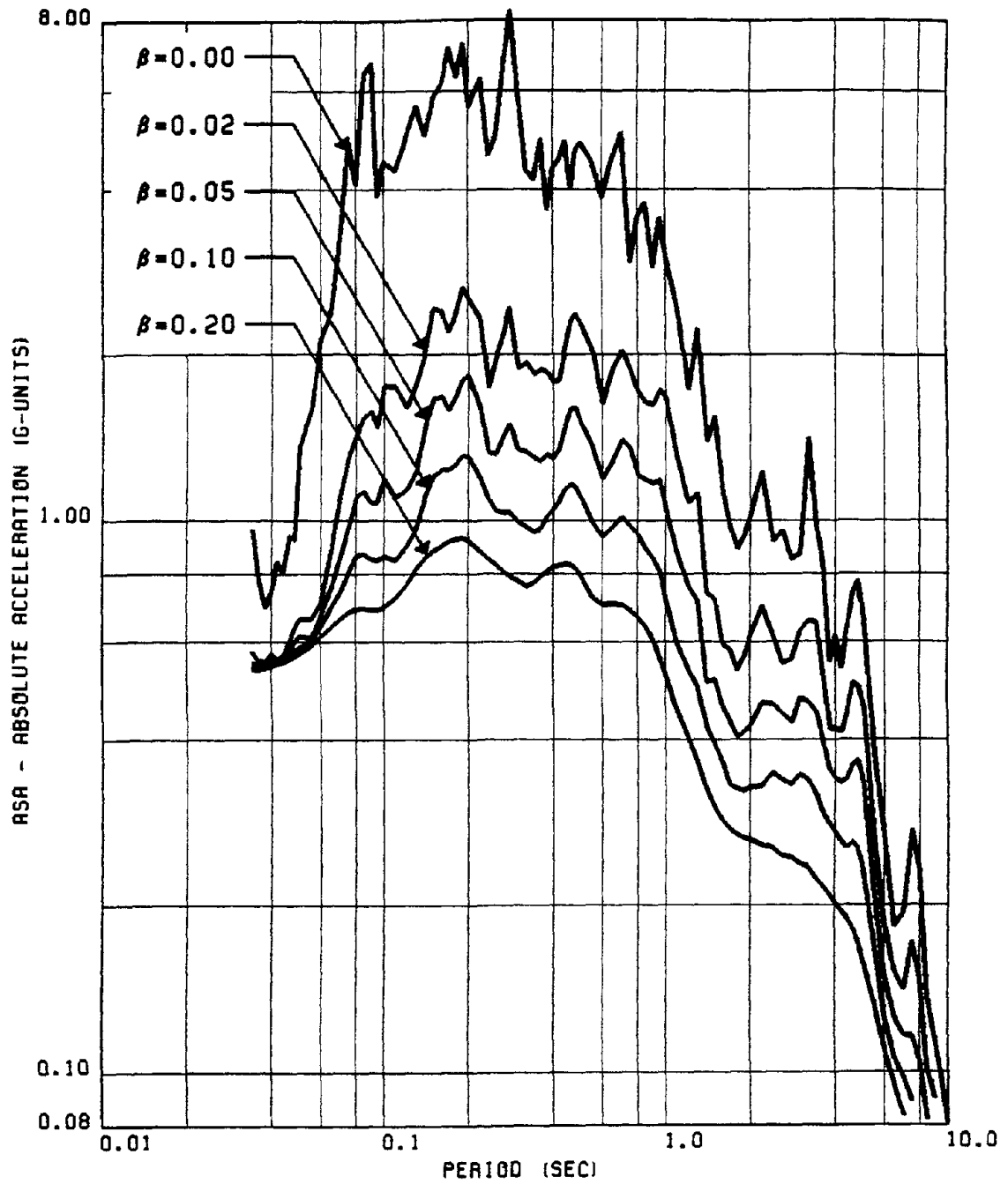
FIG. 79   (MEAN + SD) ABS. ACCL. SPECTRA FOR VERTICAL RECORDS OF GROUP *2
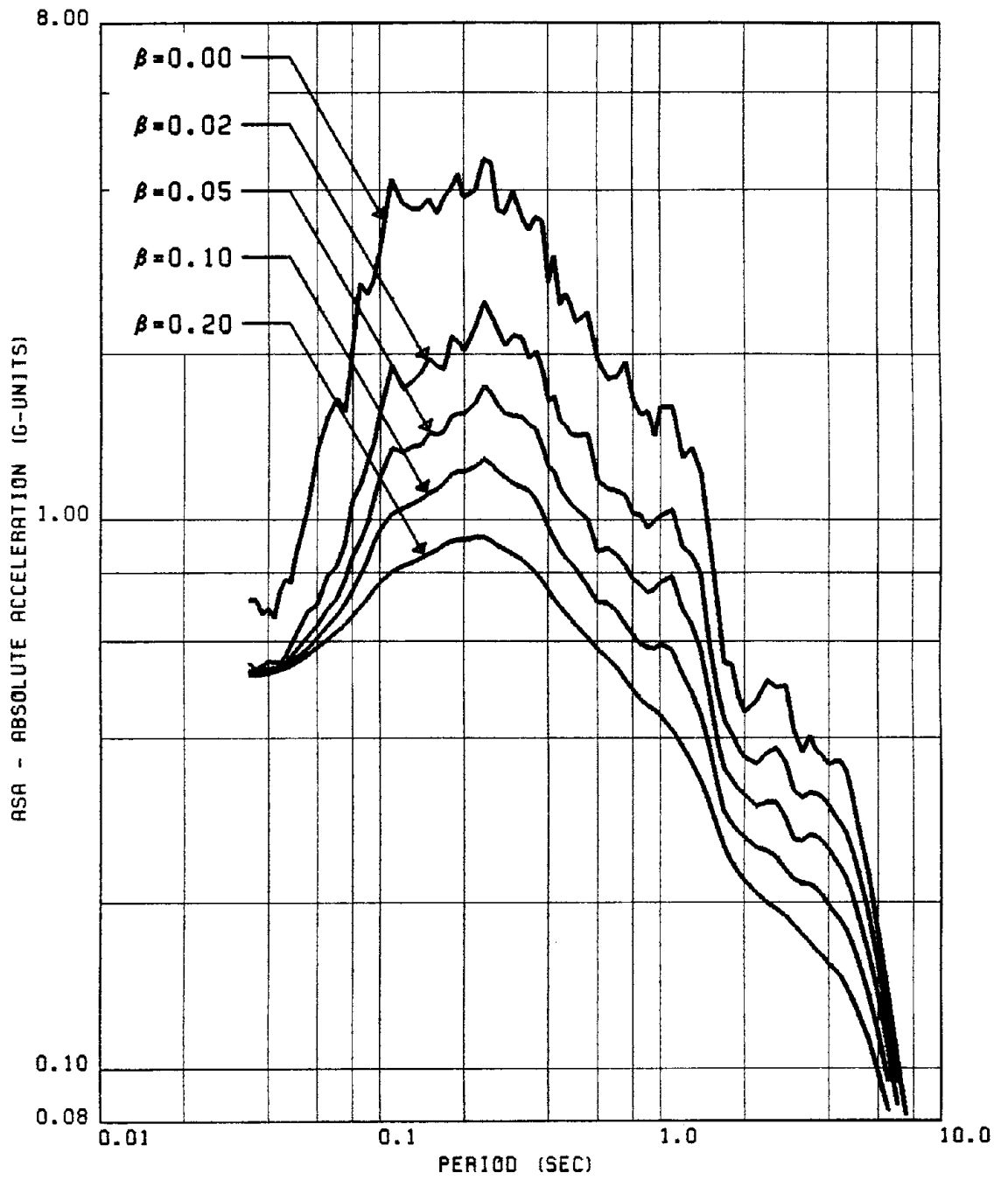
FIG. 80 (MEAN + SD) ABS. ACCL. SPECTRA FOR HORIZONTAL RECORDS OF GROUP #3
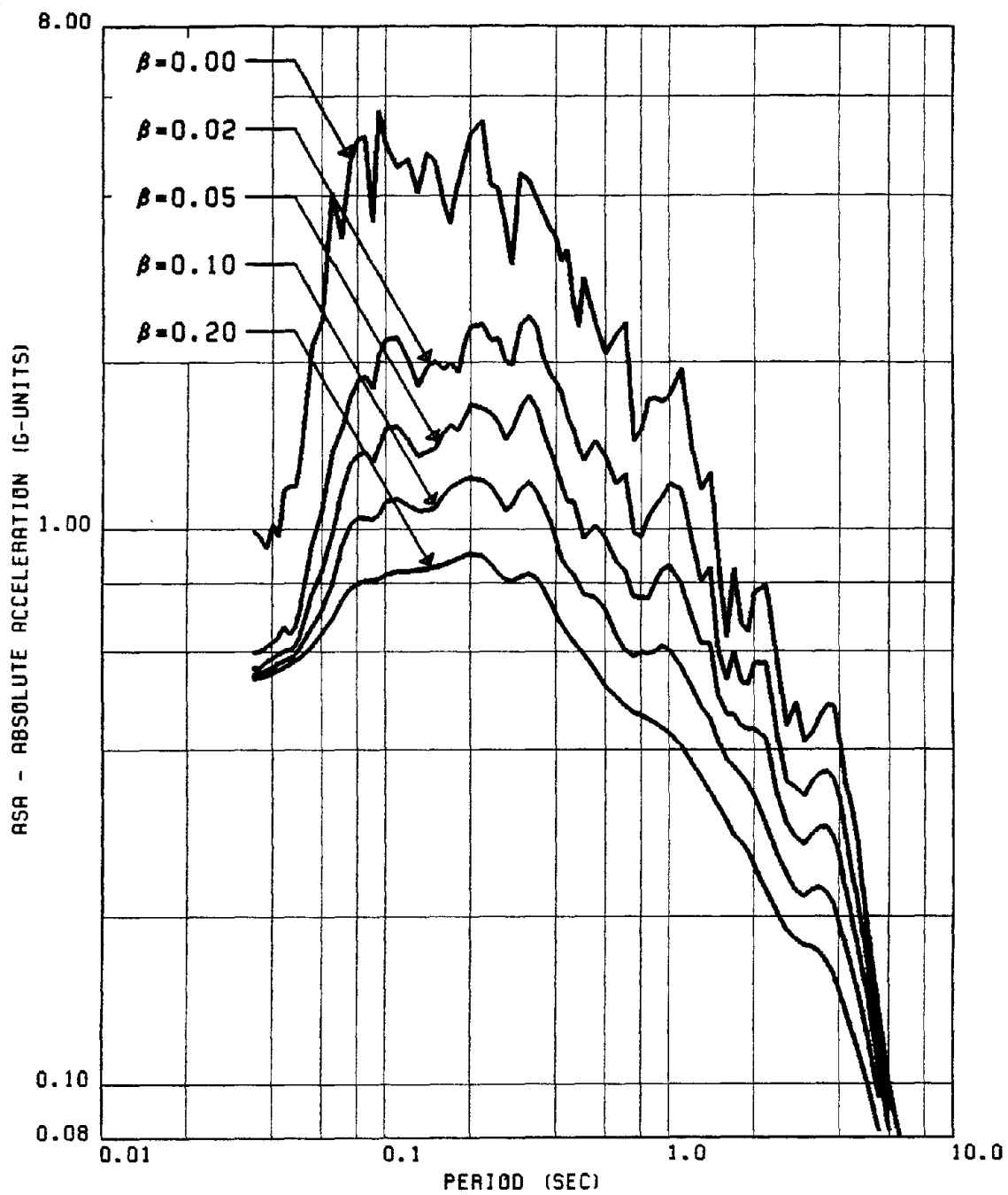
FIG. 81 (MEAN + SD) ABS. ACCL. SPECTRA FOR VERTICAL RECORDS OF GROUP #3

159
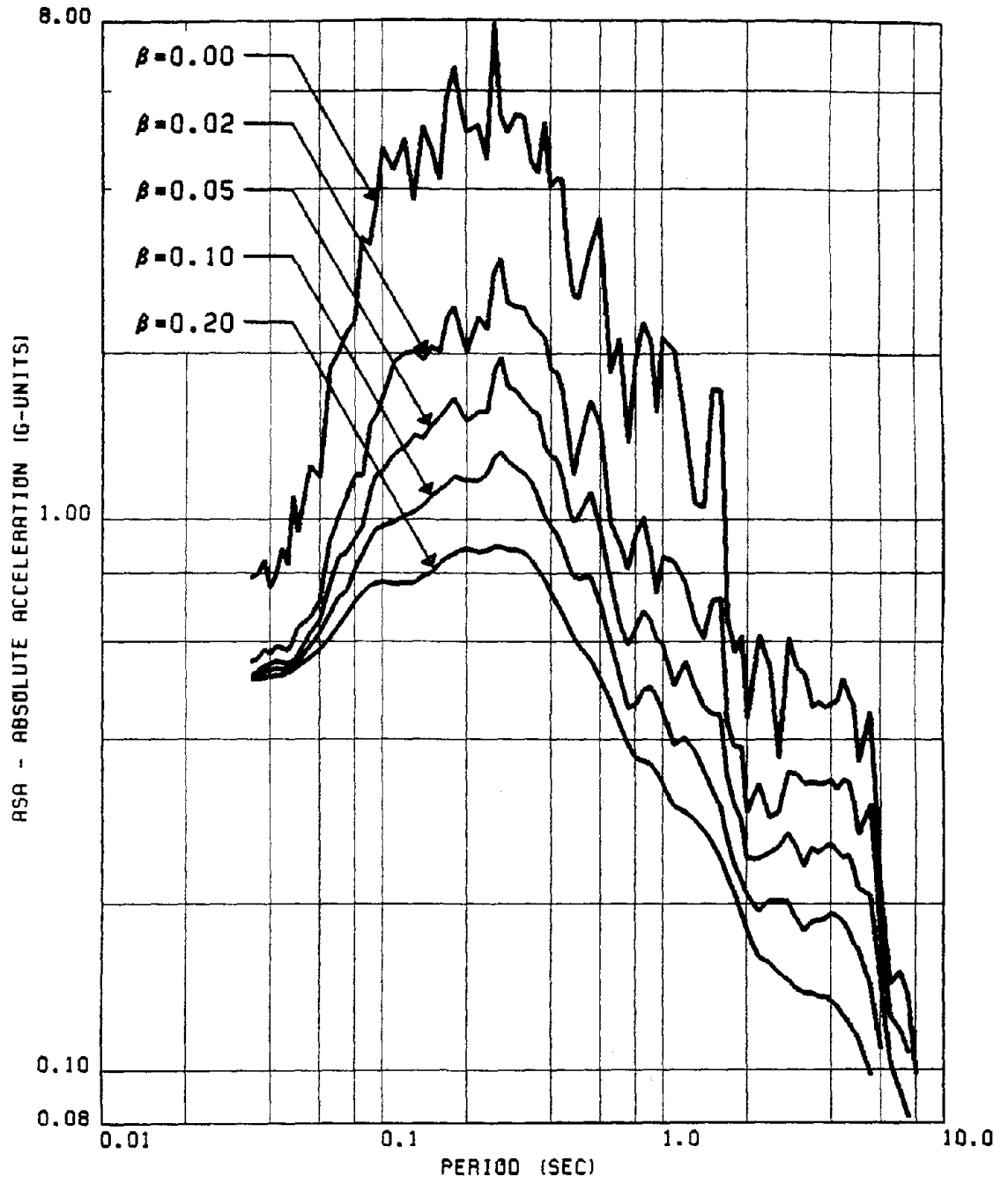
FIG. 82 (MEAN + SD) ABS. ACCL. SPECTRA FOR HORIZONTAL RECORDS OF GROUP #4

160
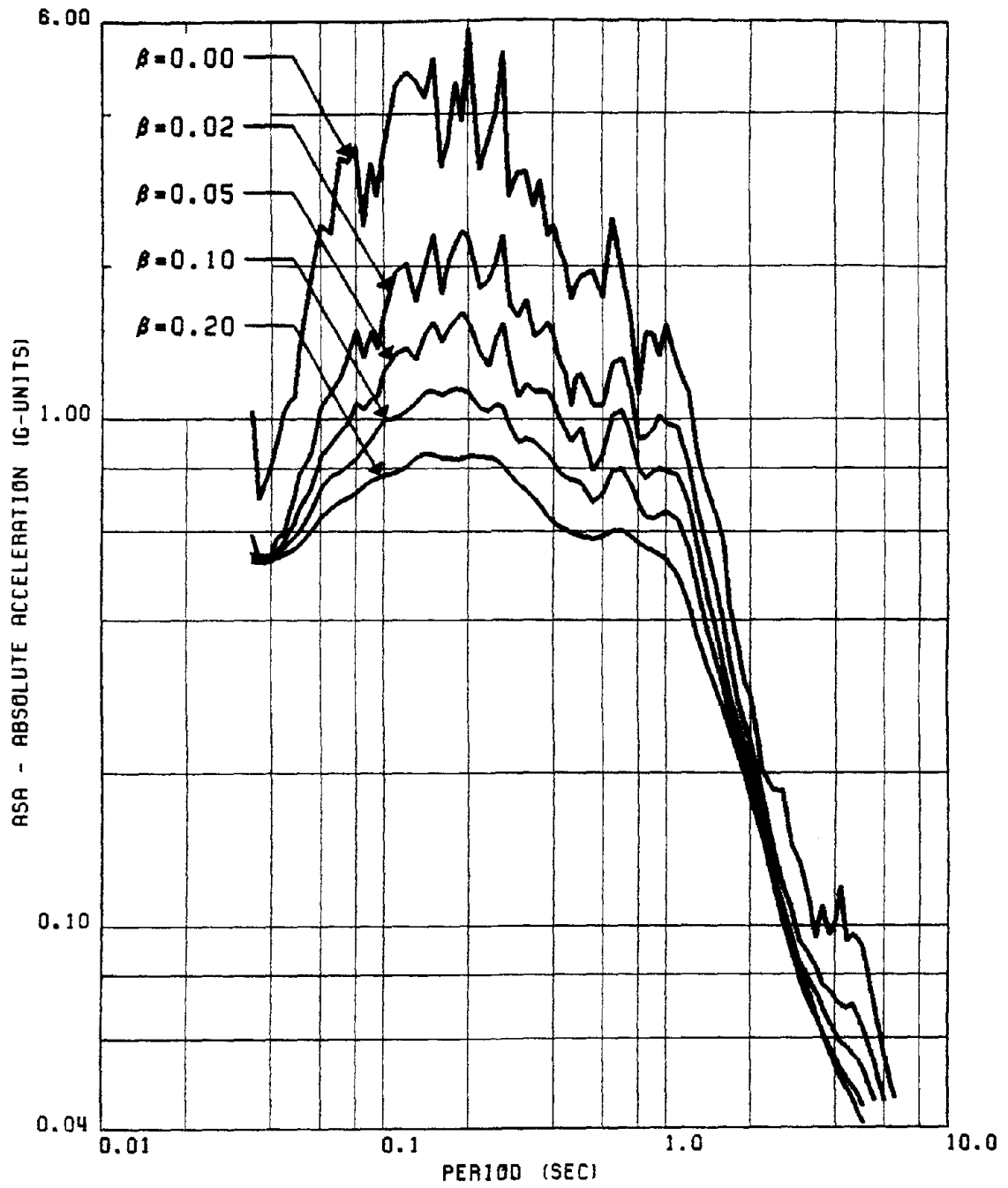
FIG. 83   (MEAN + SD) ABS. ACCL. SPECTRA FOR HORIZONTAL RECORDS OF GROUP #5
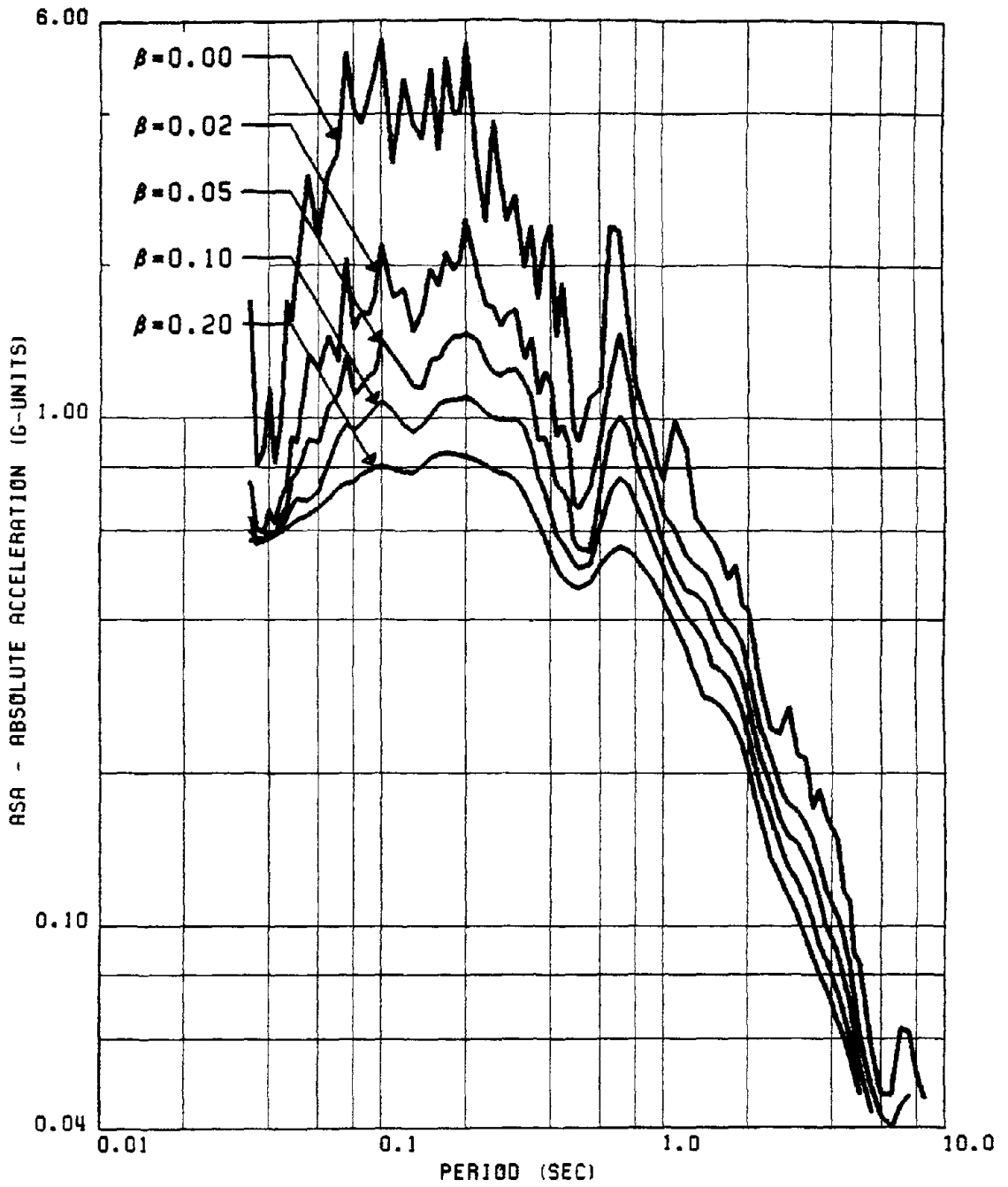
FIG. 84   (MEAN + SD) ABS. ACCL. SPECTRA FOR VERTICAL RECORDS OF GROUP #5
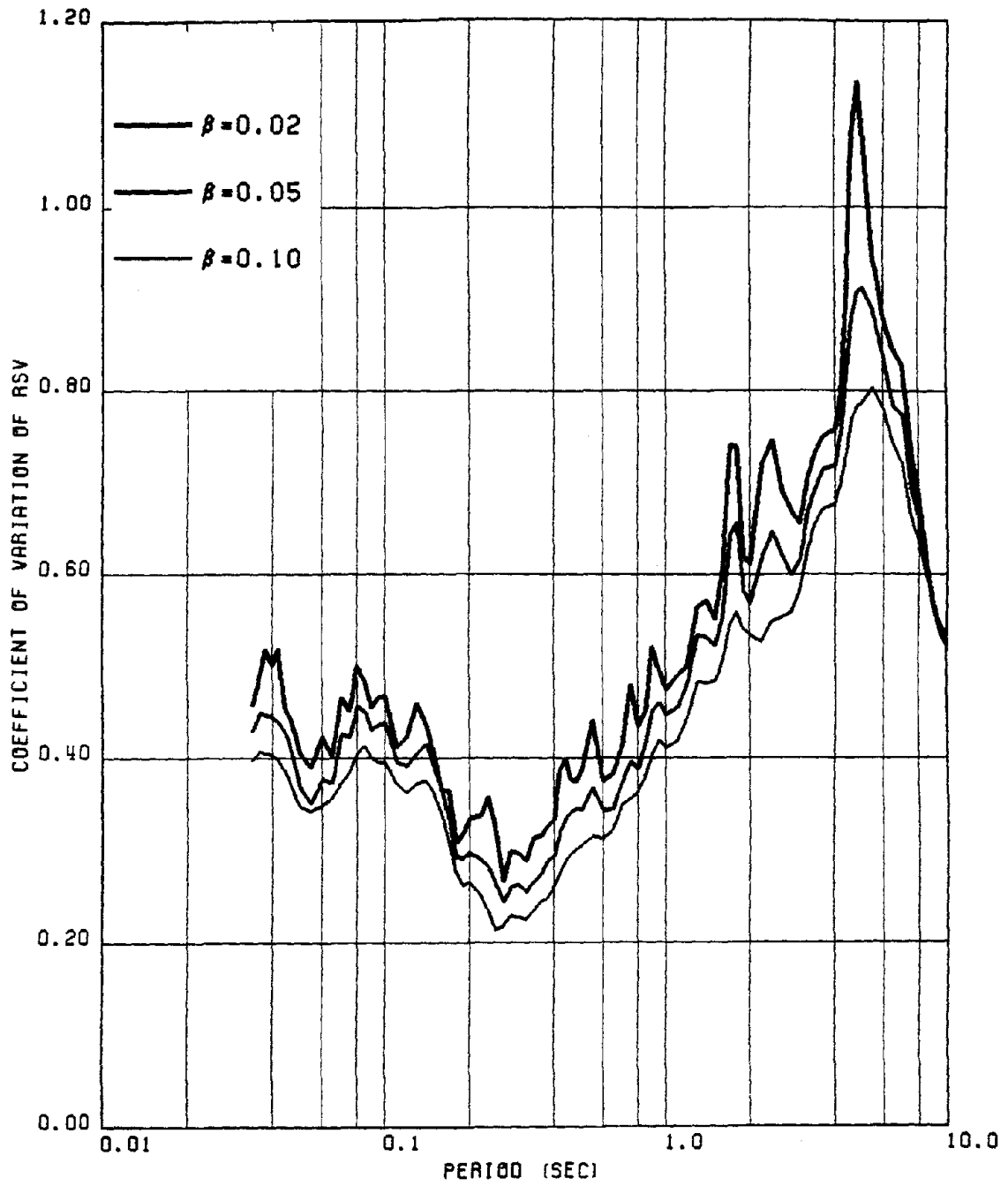
FIG. 85   COEFFICIENT OF VARIATION OF 'HORIZONTAL' RSV FOR GROUP #1
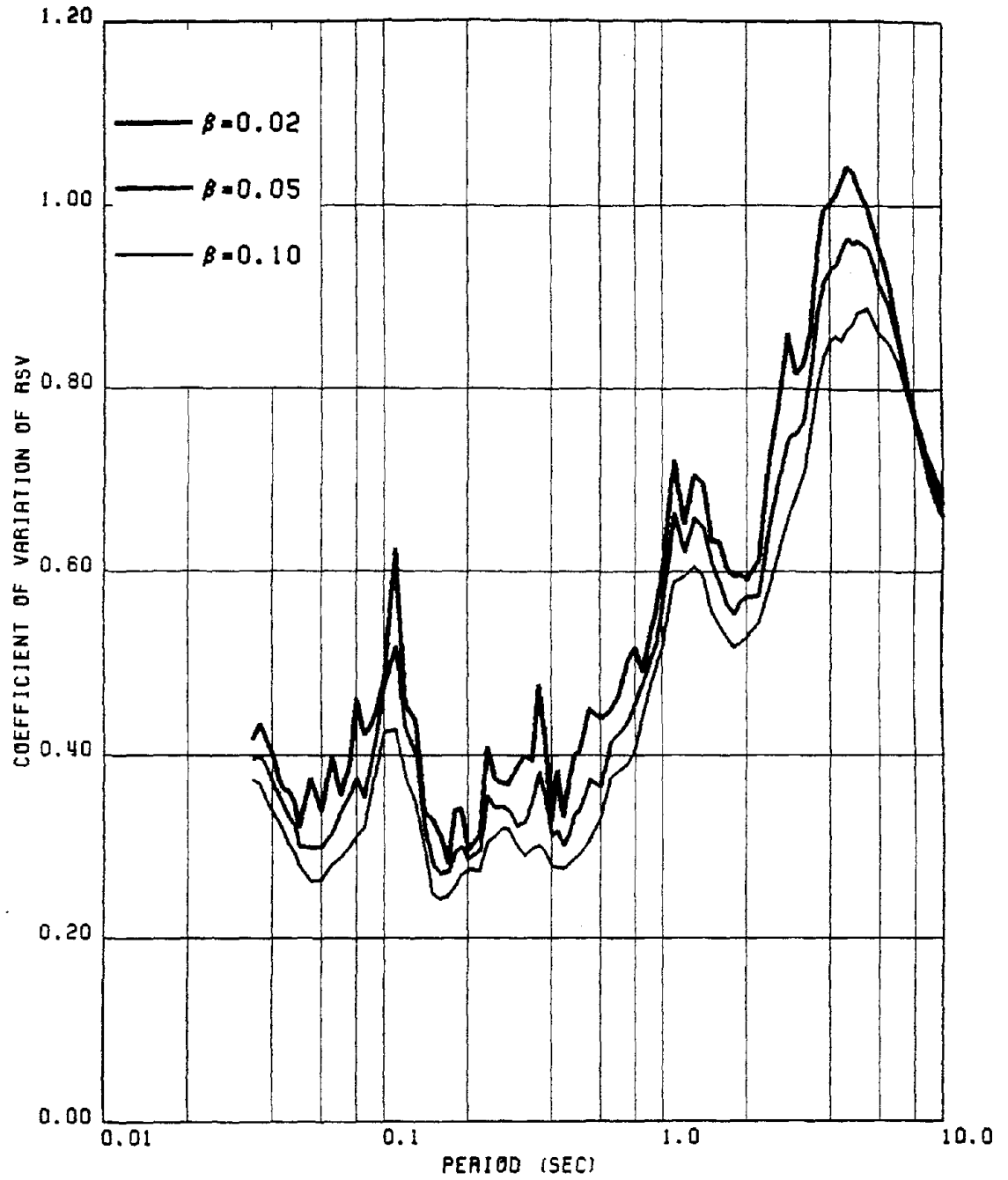
FIG. 86 COEFFICIENT OF VARIATION OF 'HORIZONTAL' RSV FOR GROUP #3
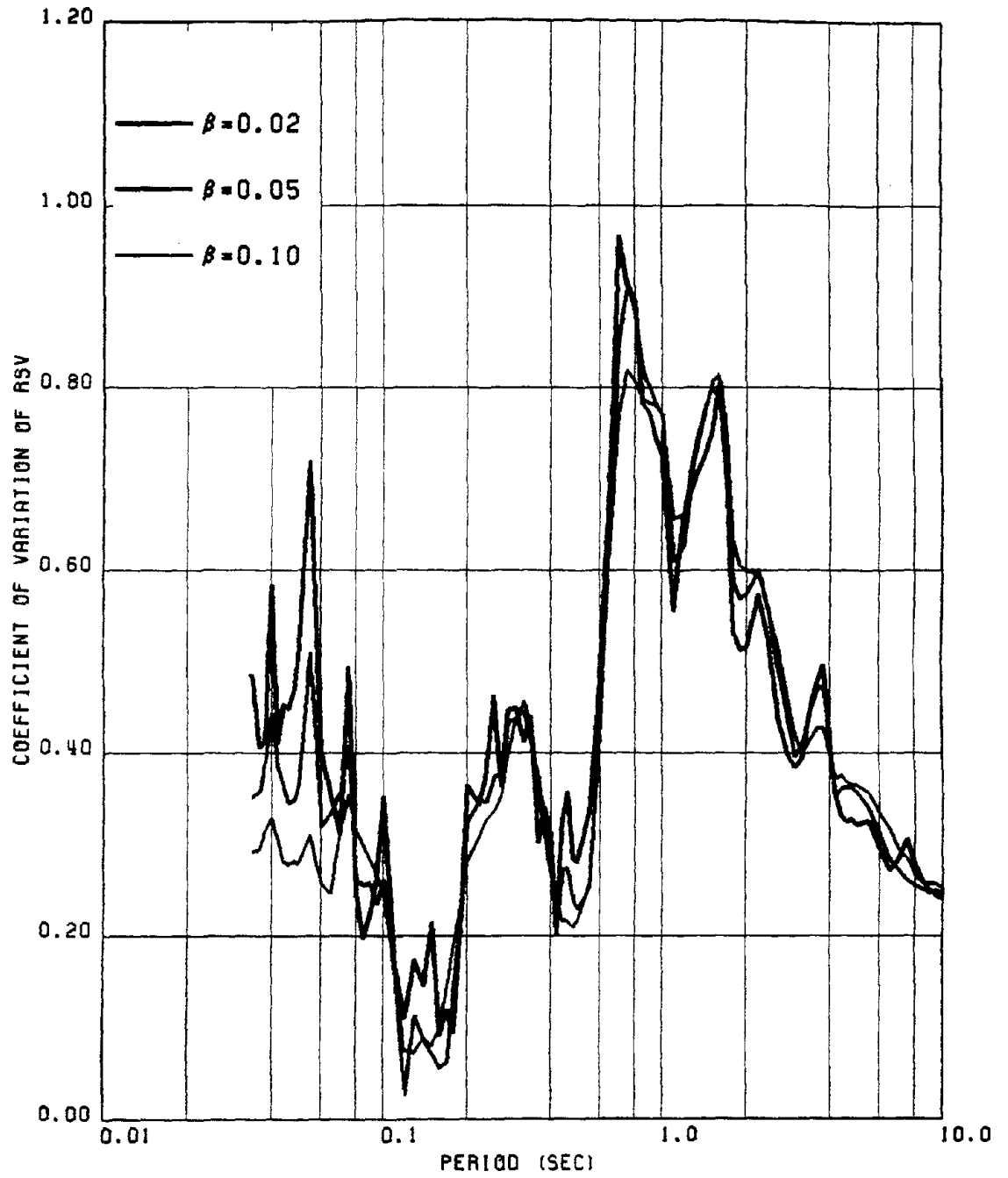
FIG. 87 COEFFICIENT OF VARIATION OF 'VERTICAL' RSV FOR GROUP #5
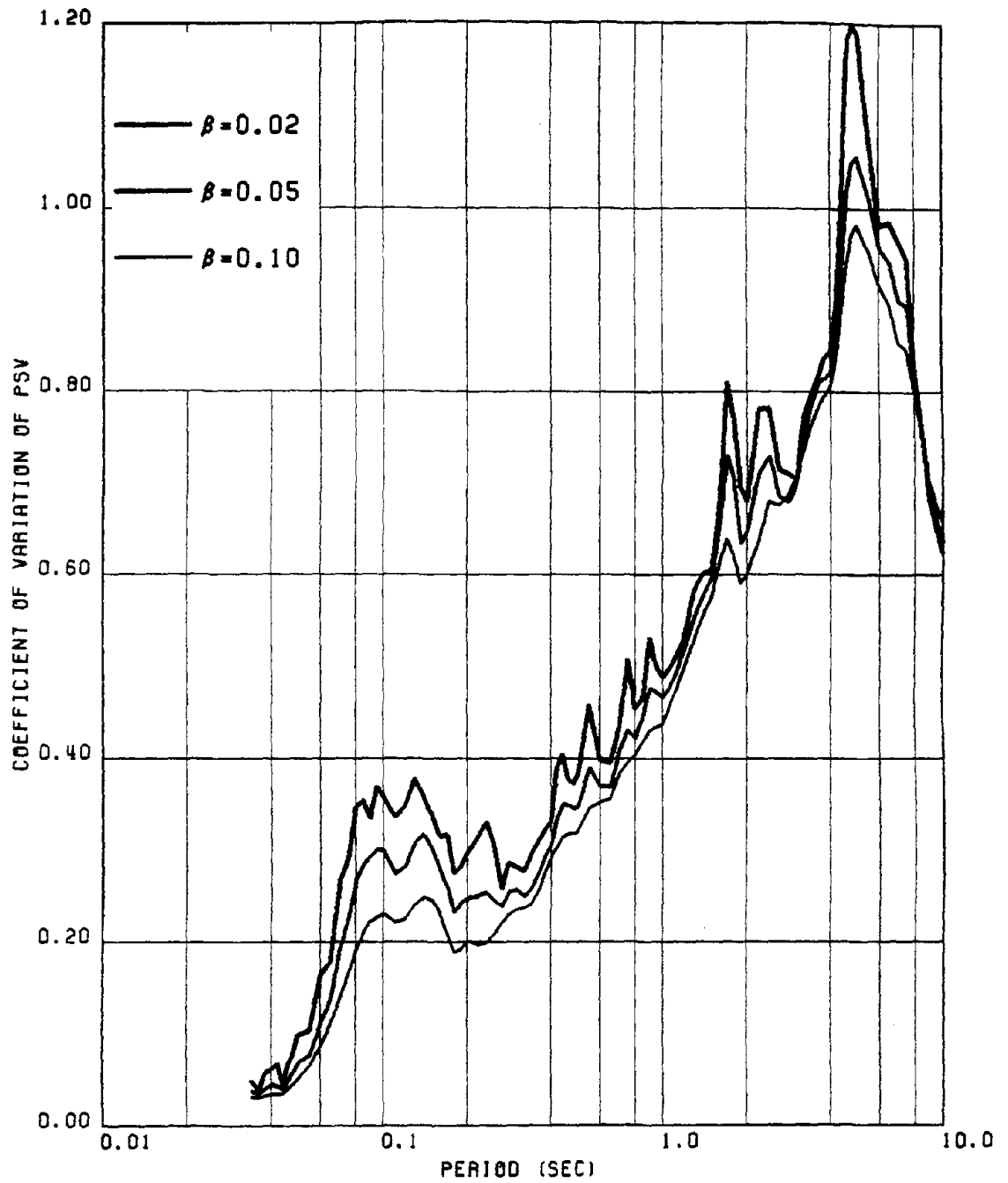
FIG. 88   COEFFICIENT OF VARIATION OF 'HORIZONTAL' PSV FOR GROUP #1
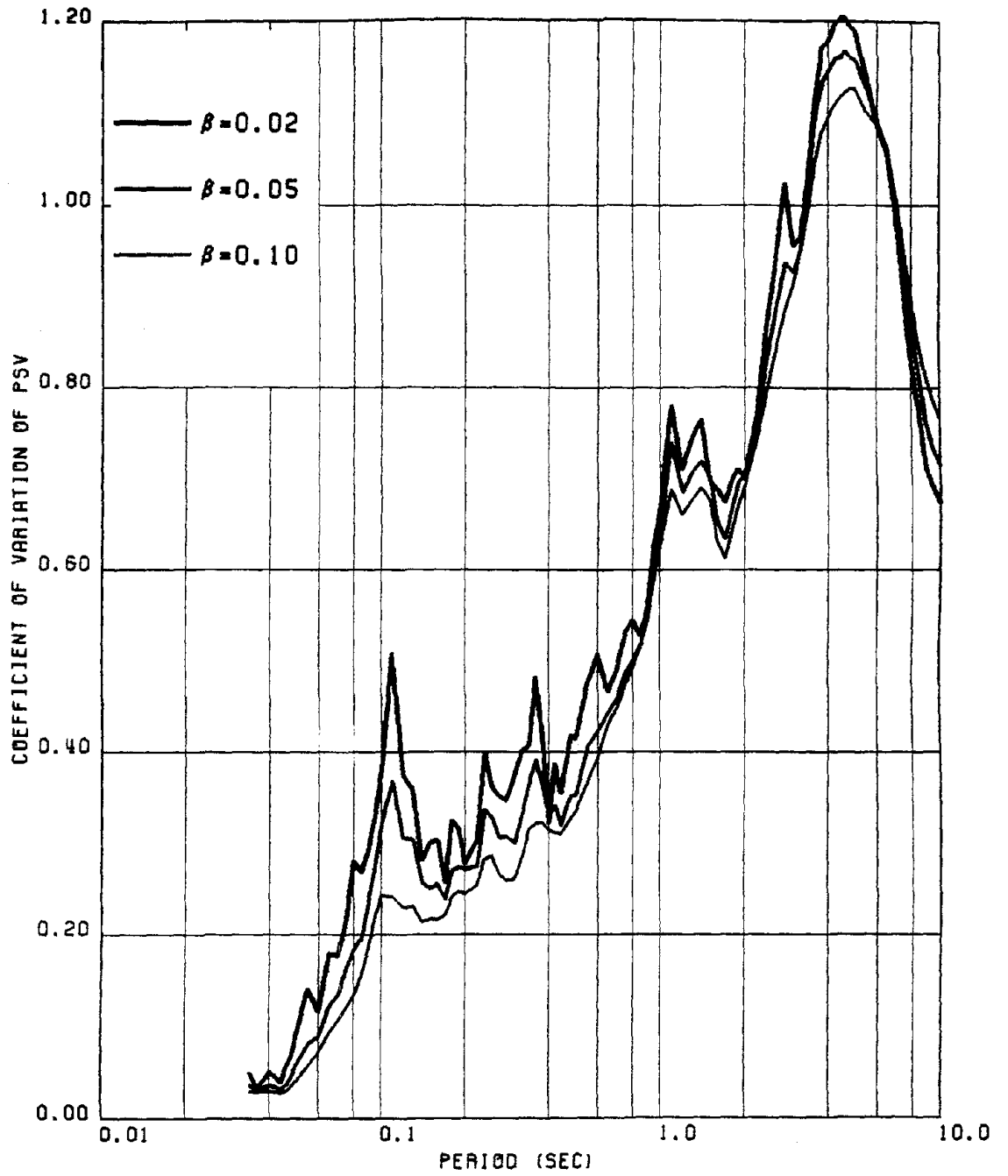
FIG. 89 COEFFICIENT OF VARIATION OF 'HORIZONTAL' PSV FOR GROUP #3
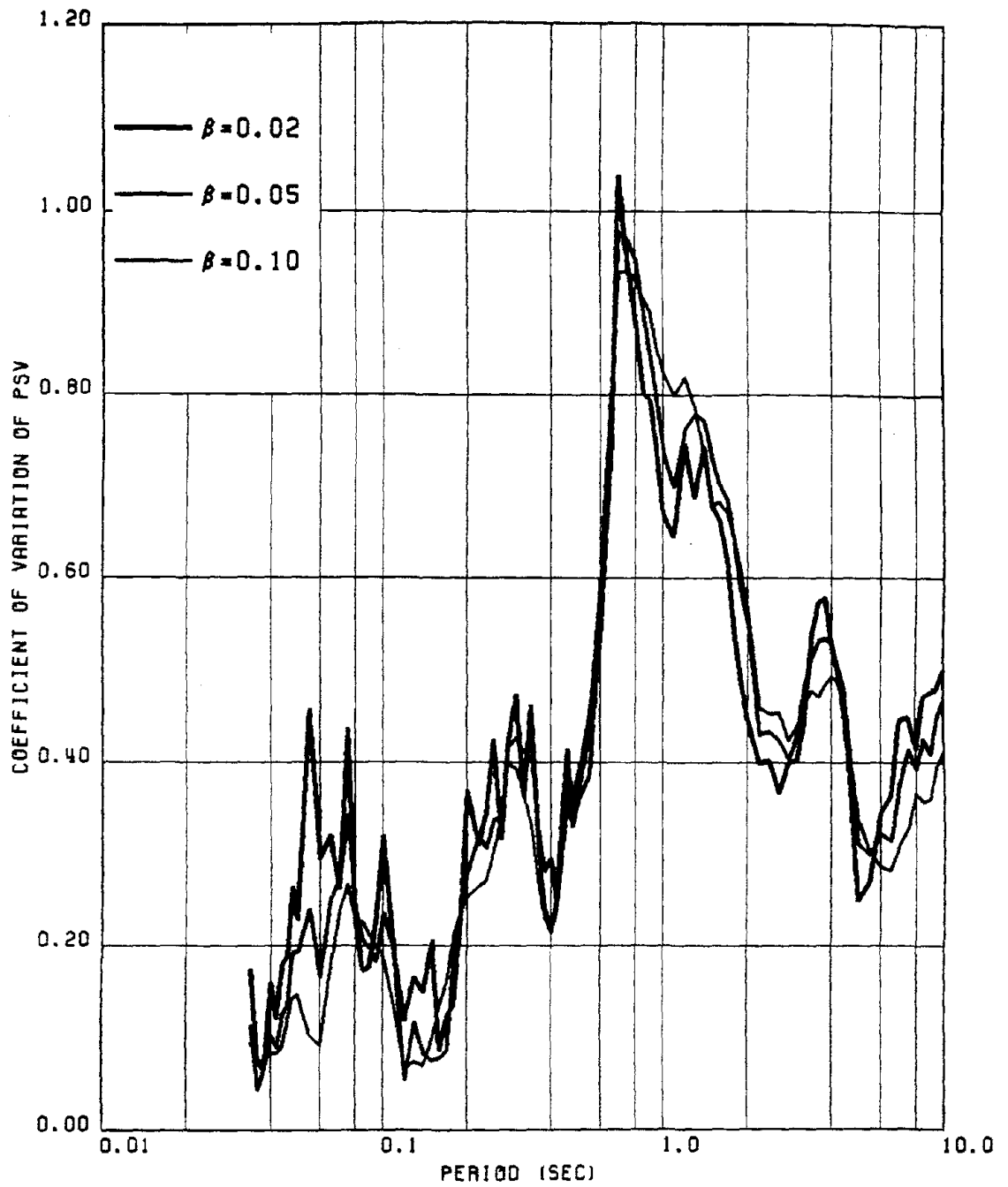
FIG. 90 COEFFICIENT OF VARIATION OF 'VERTICAL' PSV FOR GROUP #5
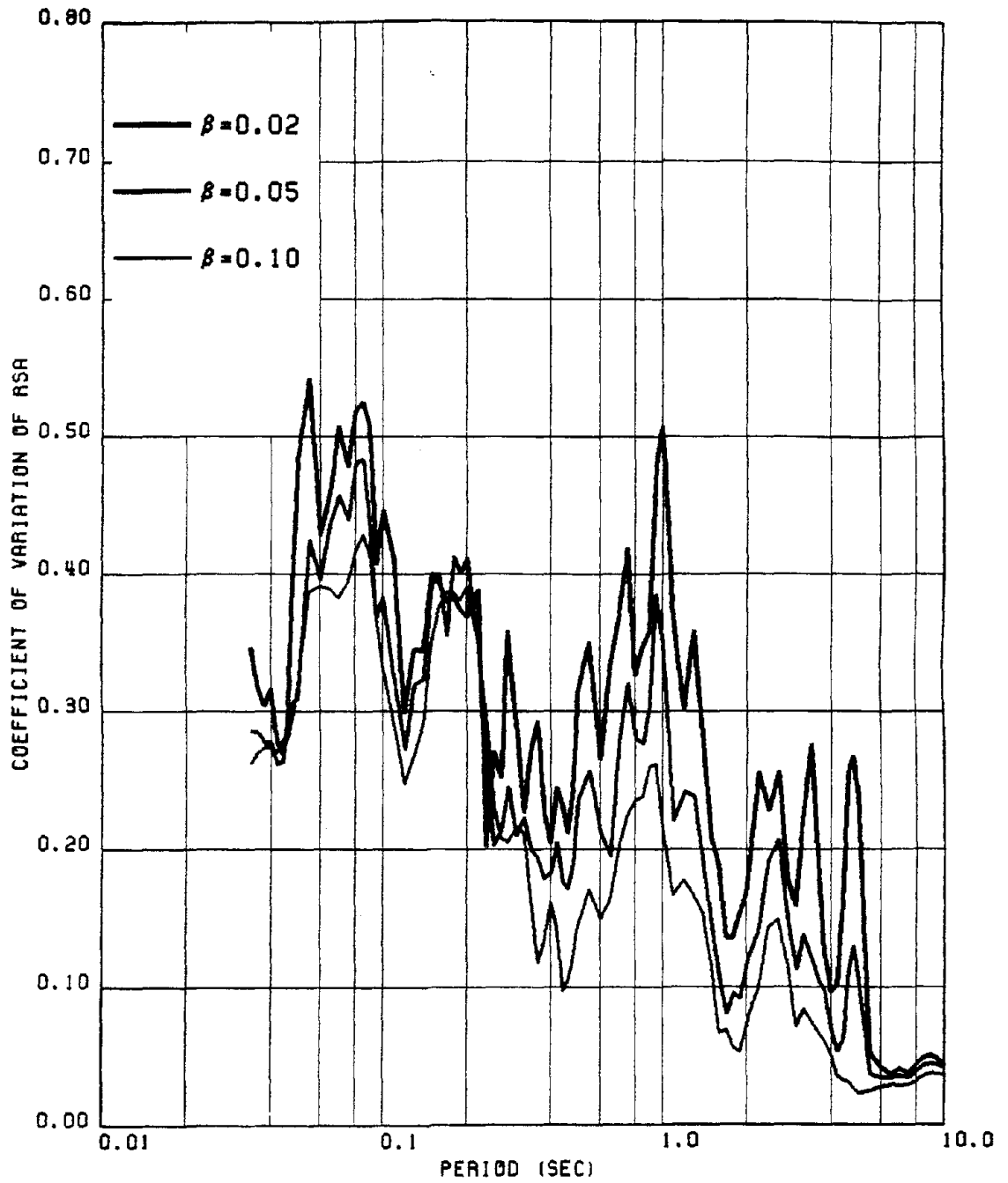
FIG. 91 COEFFICIENT OF VARIATION OF 'VERTICAL' RSA FOR GROUP #2
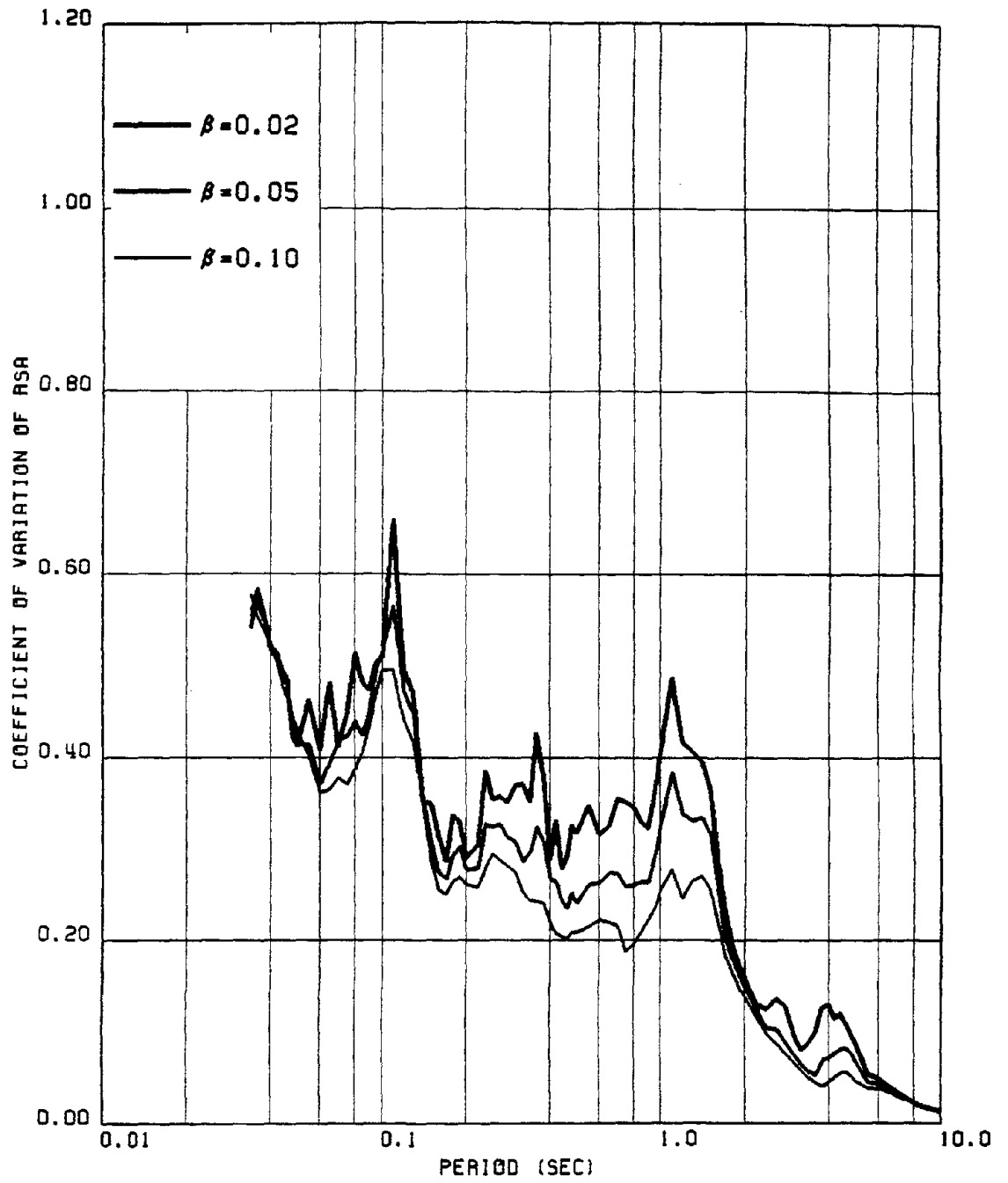
FIG. 92 COEFFICIENT OF VARIATION OF 'HORIZONTAL' RSA FOR GROUP #3
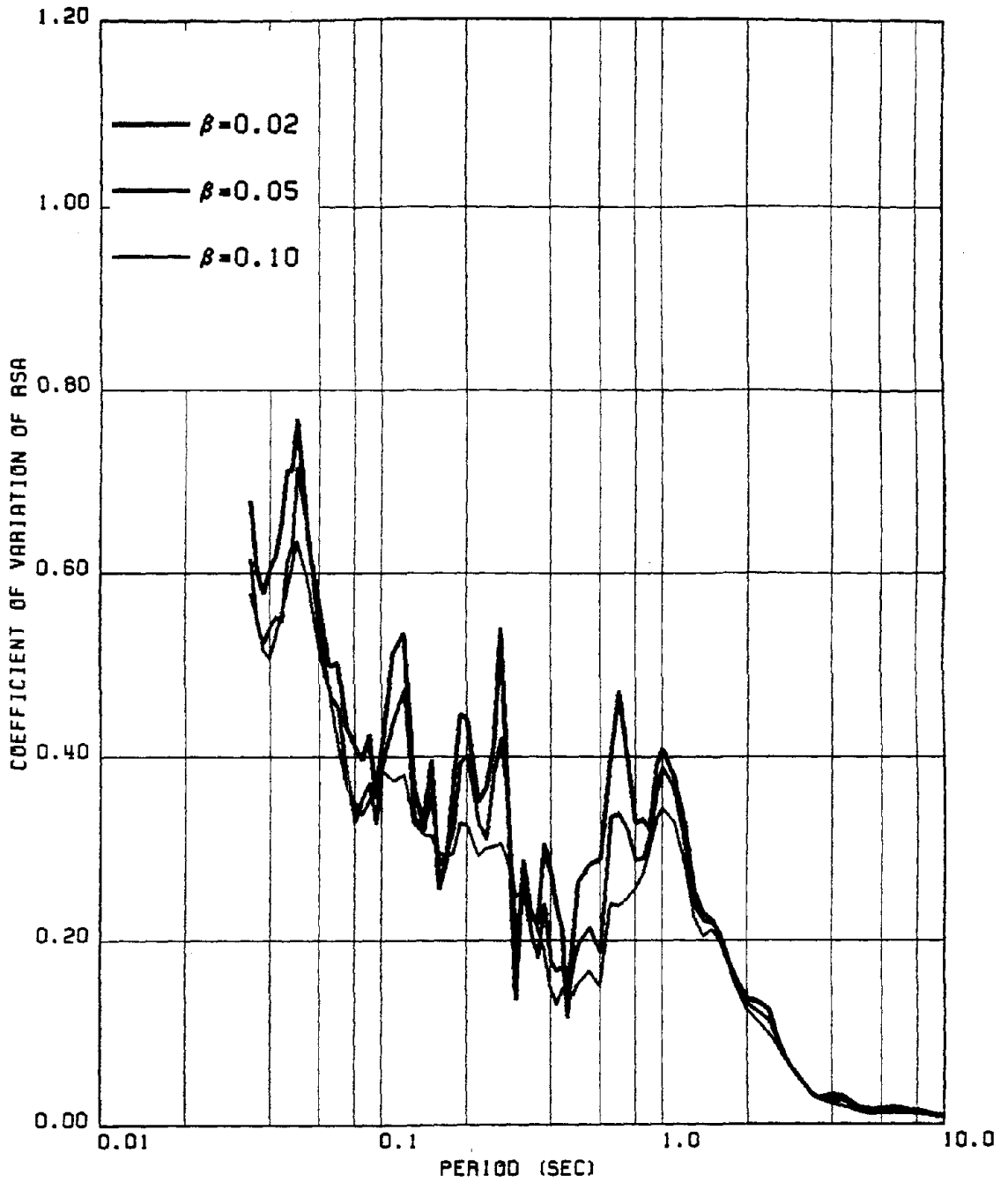
FIG. 93 COEFFICIENT OF VARIATION OF 'HORIZONTAL' RSA FOR GROUP #5

171
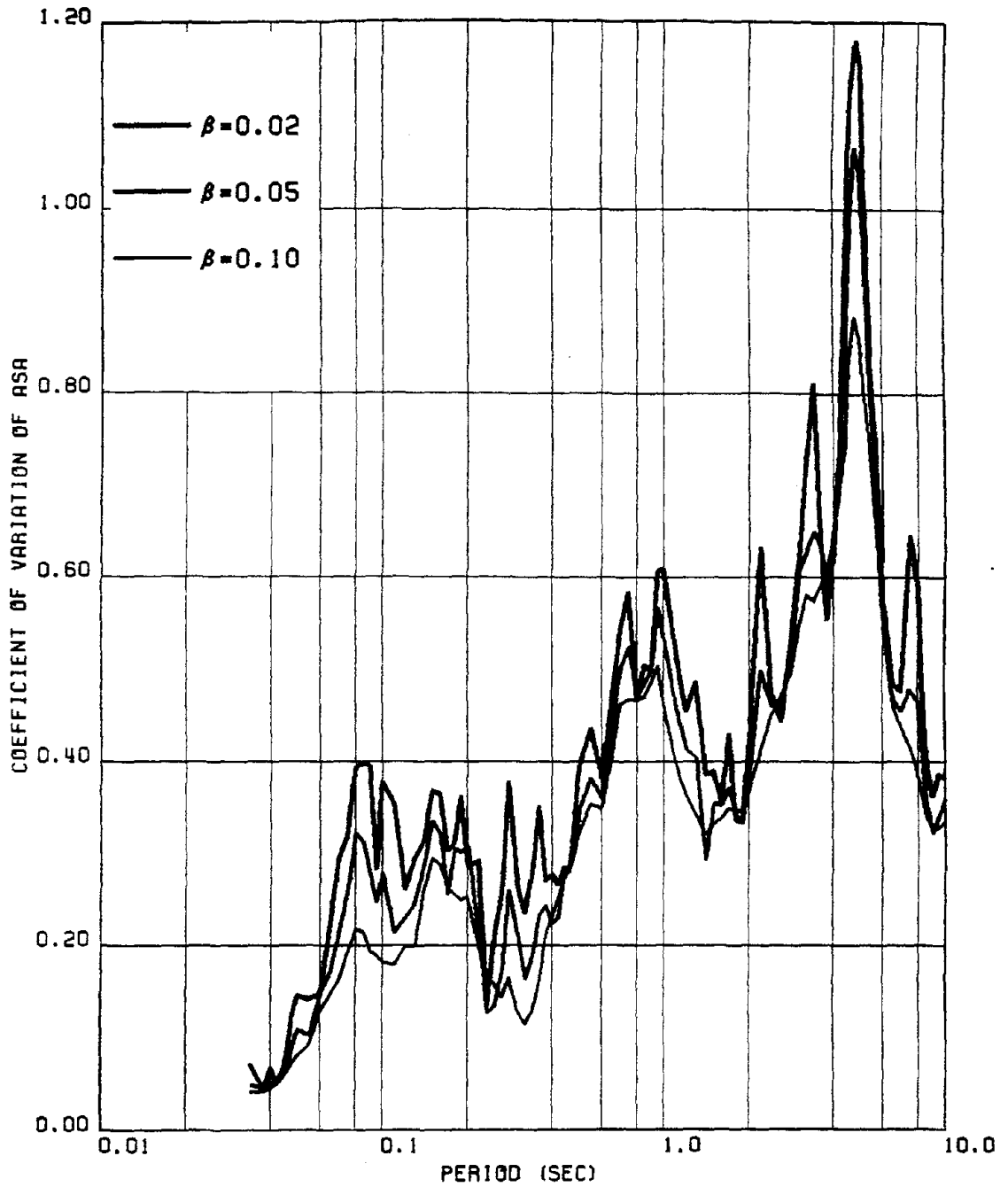
FIG. 94   COEFFICIENT OF VARIATION OF 'VERTICAL' ASA FOR GROUP #2
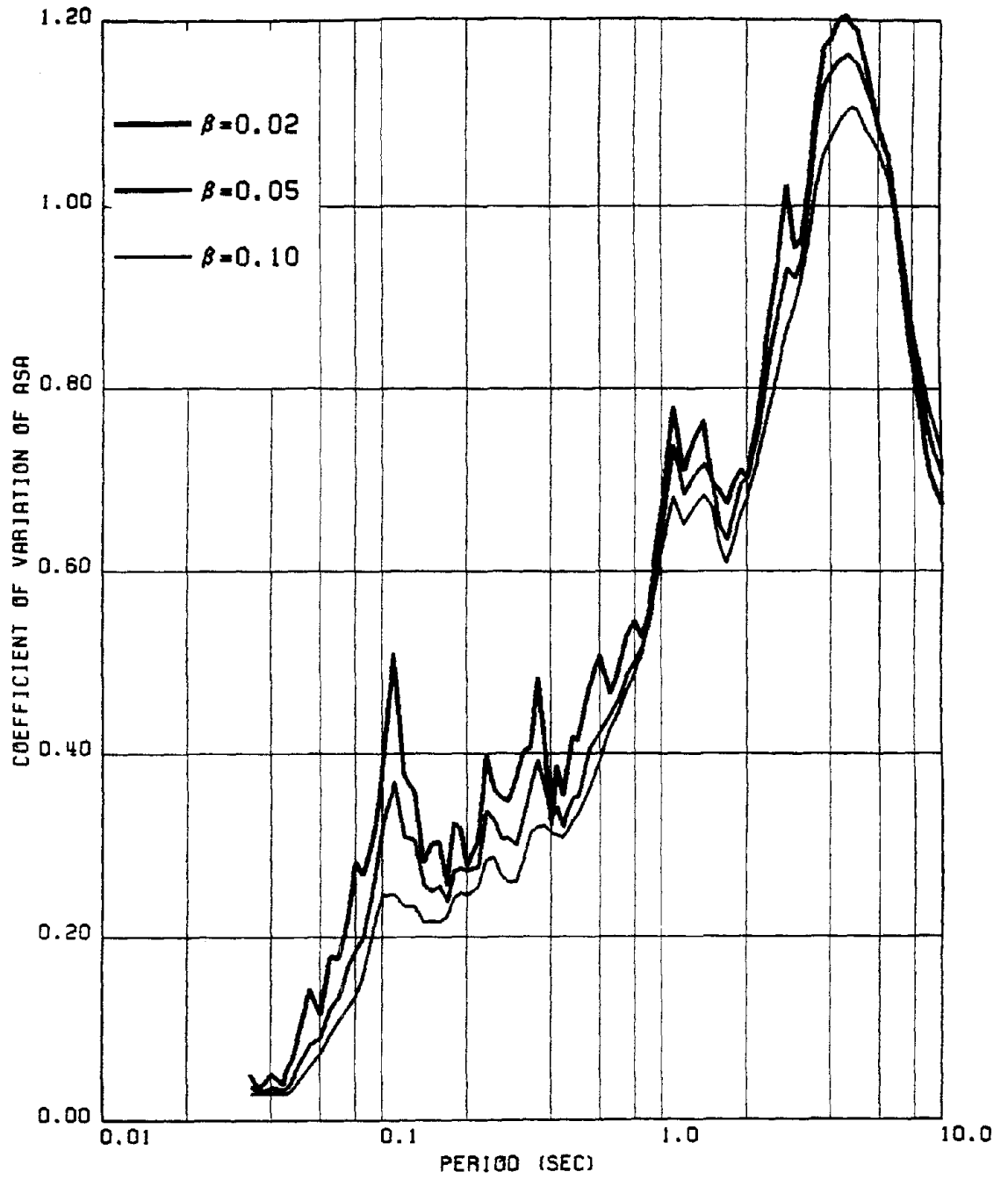
FIG. 95   COEFFICIENT OF VARIATION OF 'HORIZONTAL' ASA FOR GROUP #3
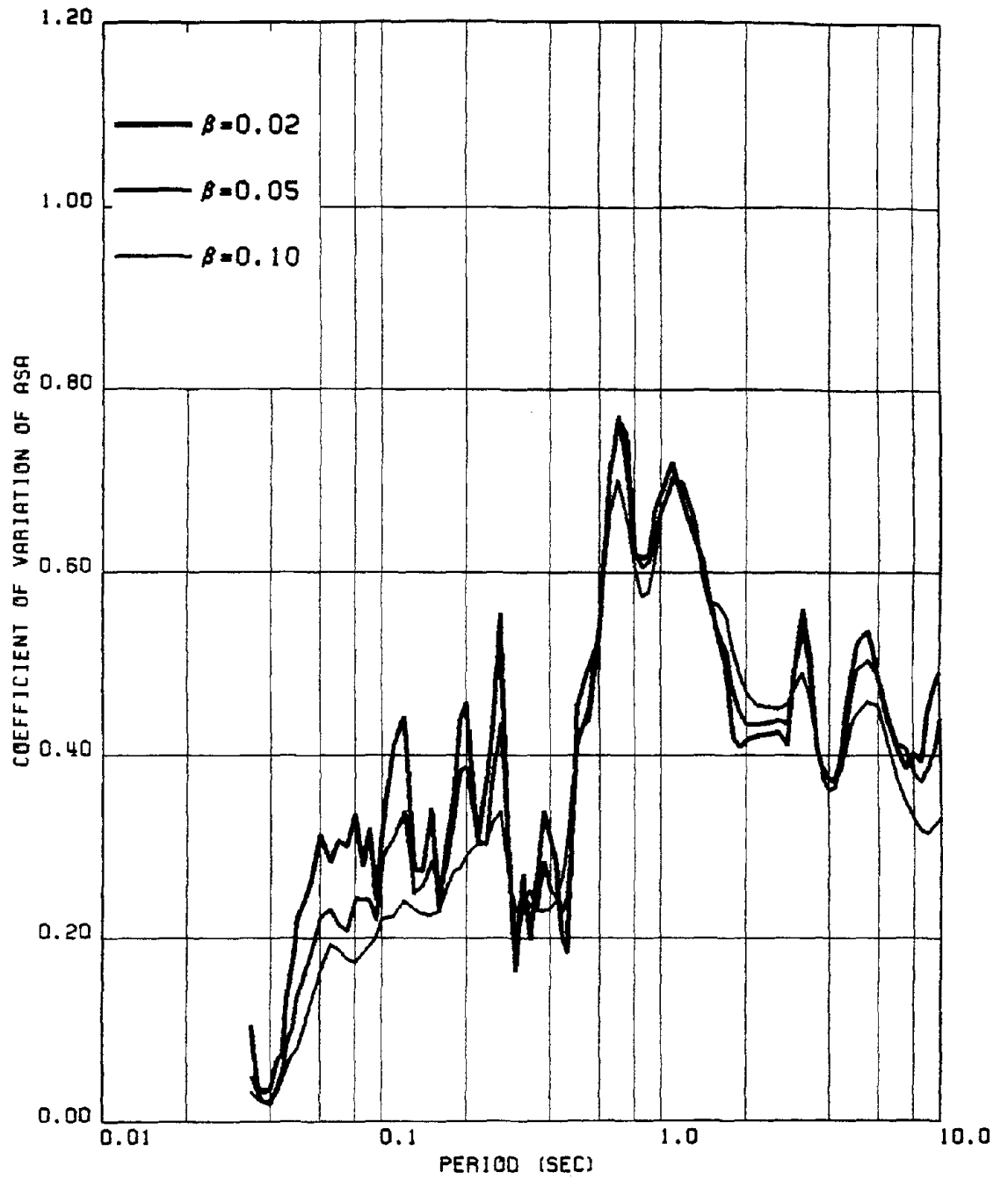
FIG. 96 COEFFICIENT OF VARIATION OF 'HORIZONTAL' ASA FOR GROUP #5
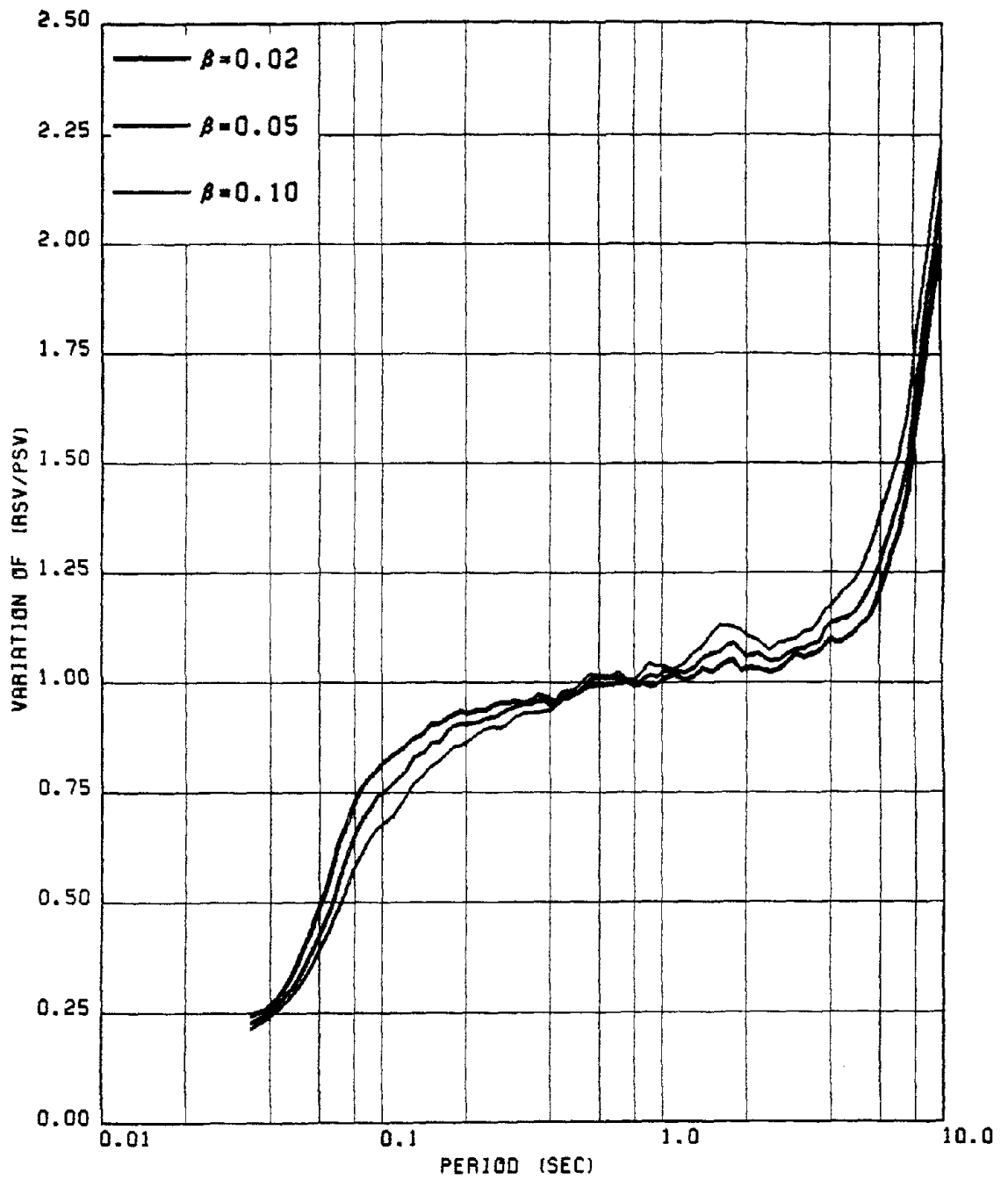
FIG. 97 VARIATION OF (RSV/PSV) FOR HORIZONTAL RECORDS OF GROUP #1
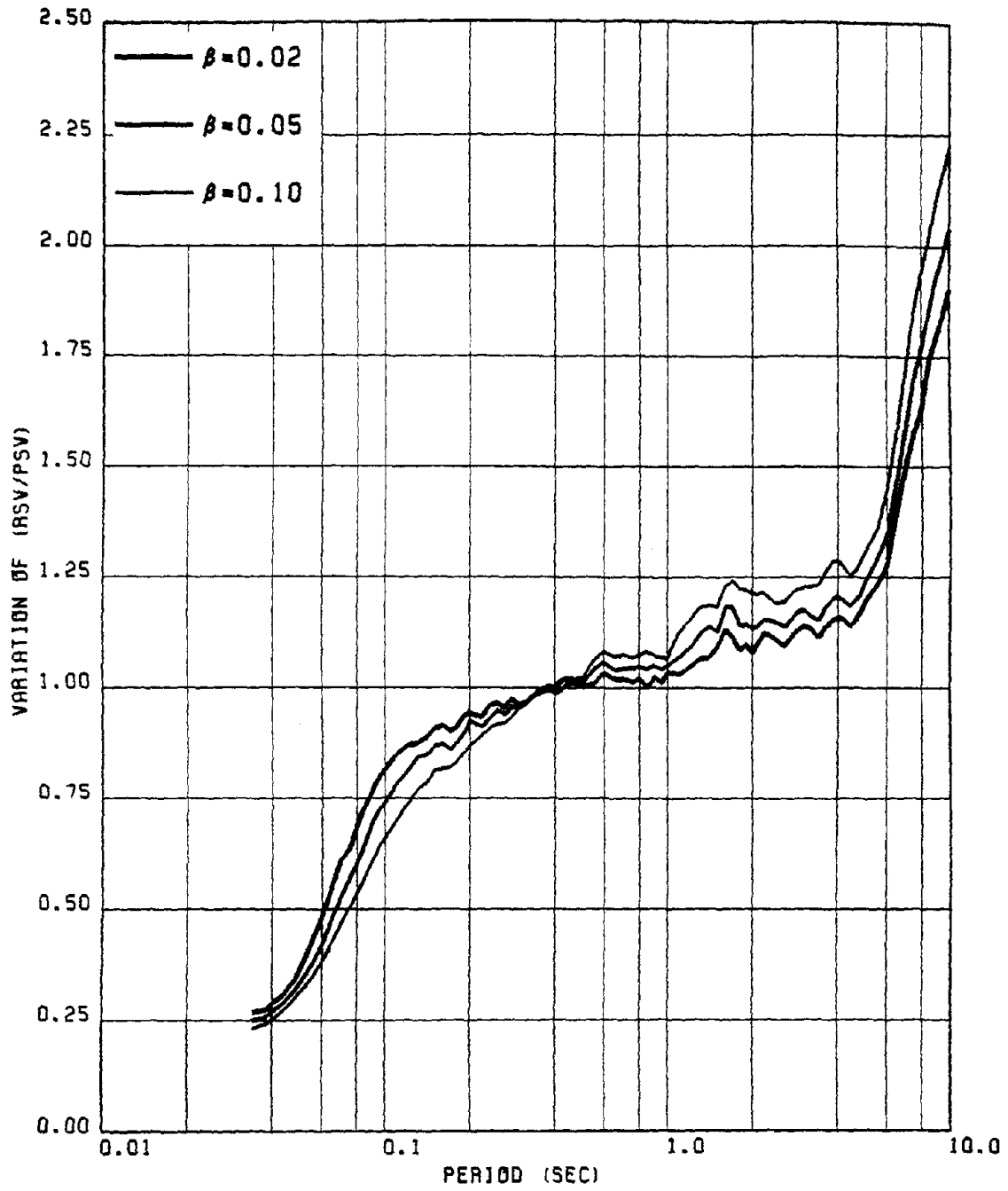
FIG. 98   VARIATION OF (RSV/PSV) FOR HORIZONTAL RECORDS OF GROUP #3
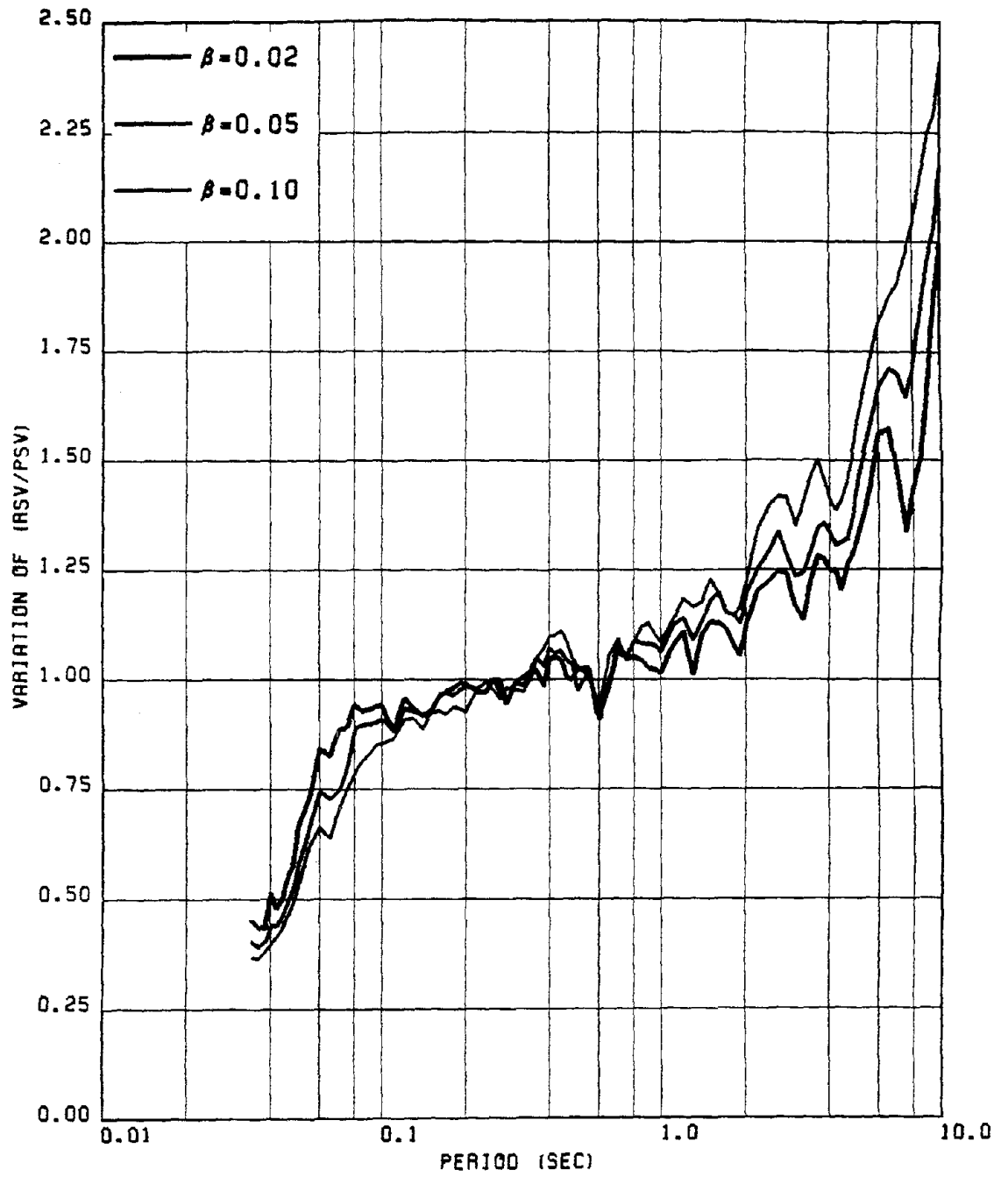
FIG. 99   VARIATION OF (RSV/PSV) FOR VERTICAL RECORDS OF GROUP #5
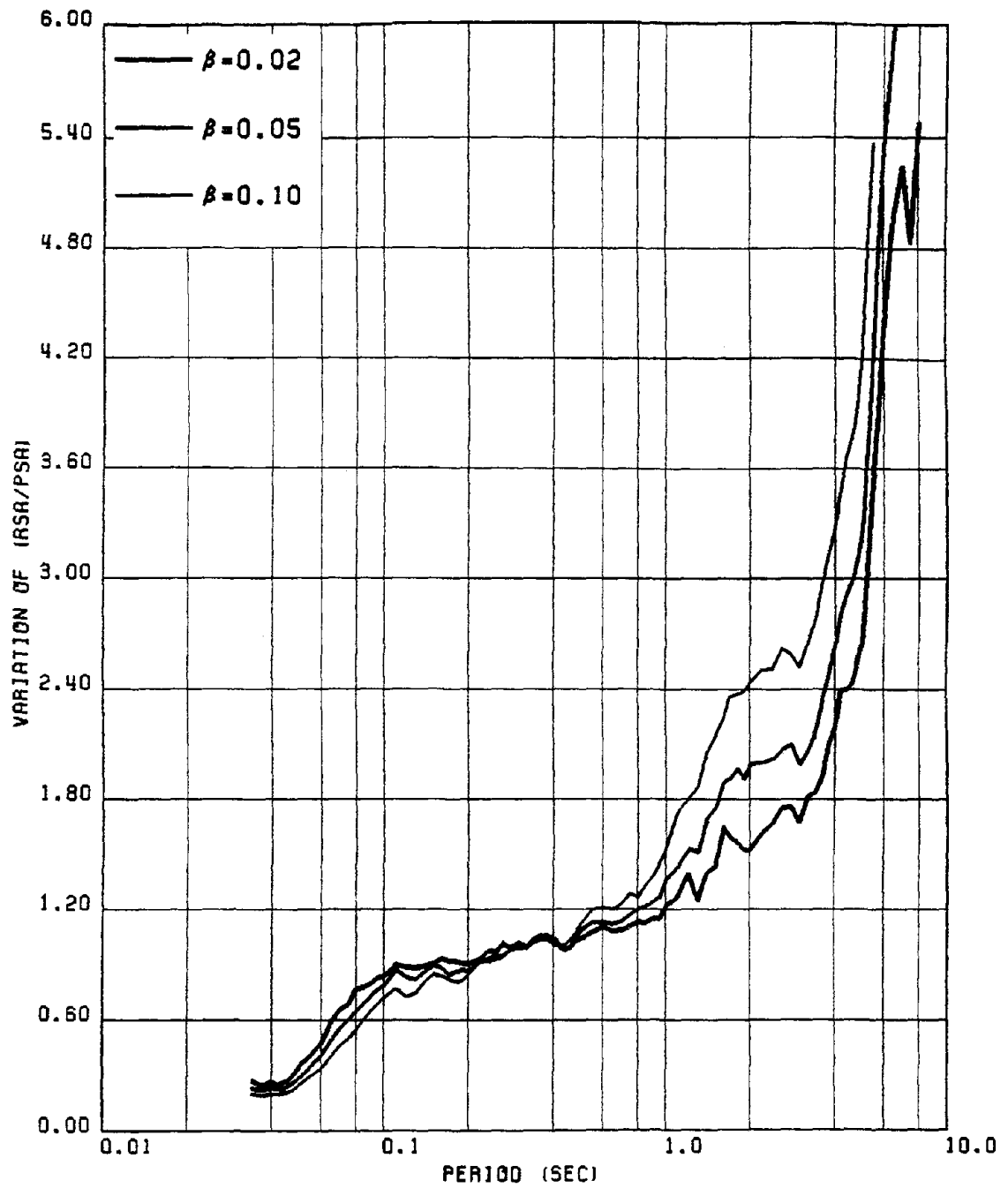
FIG. 100 VARIATION OF (RSA/PSA) FOR VERTICAL RECORDS OF GROUP #2
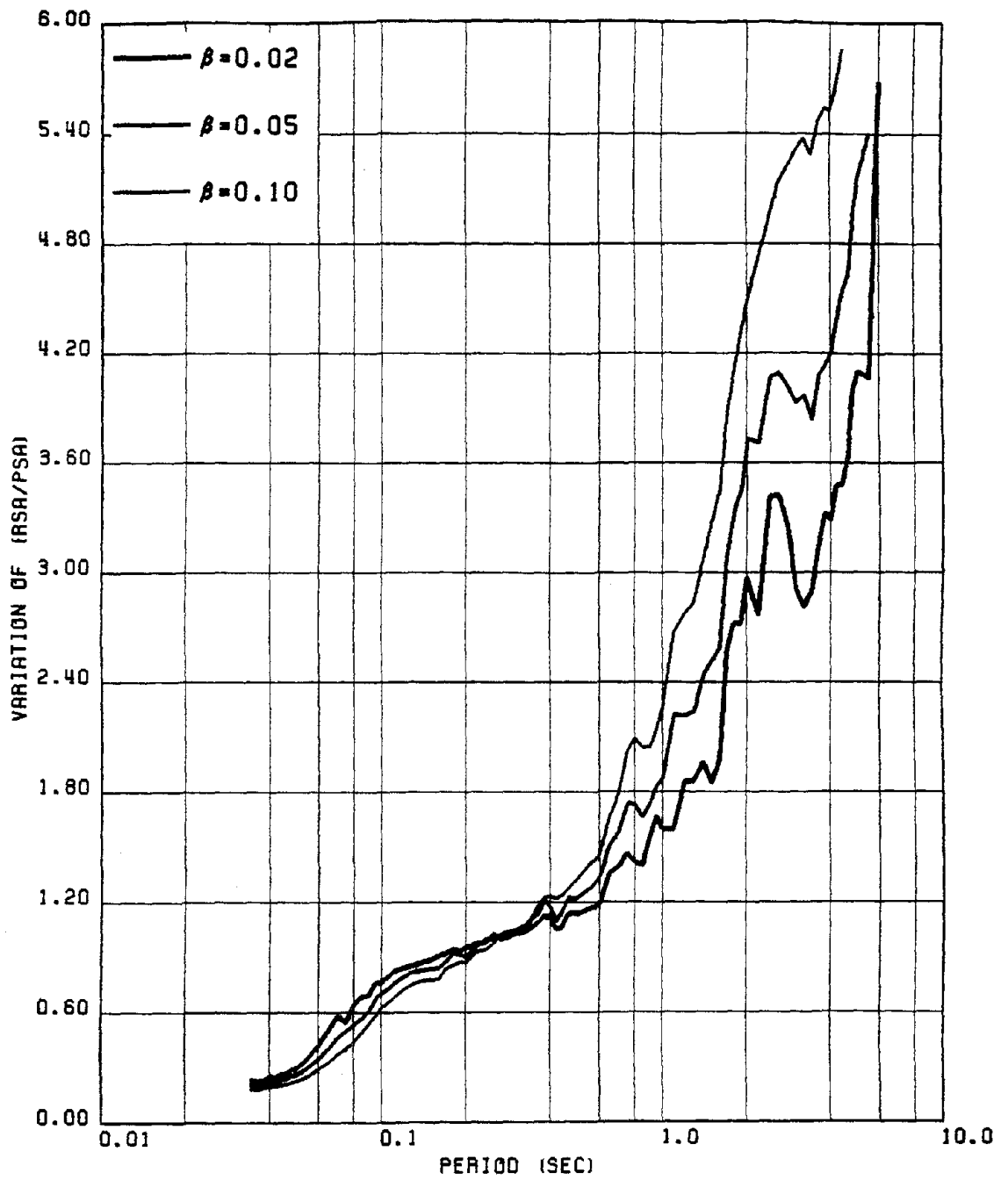
FIG. 101 VARIATION OF (RSA/PSA) FOR HORIZONTAL RECORDS OF GROUP #4
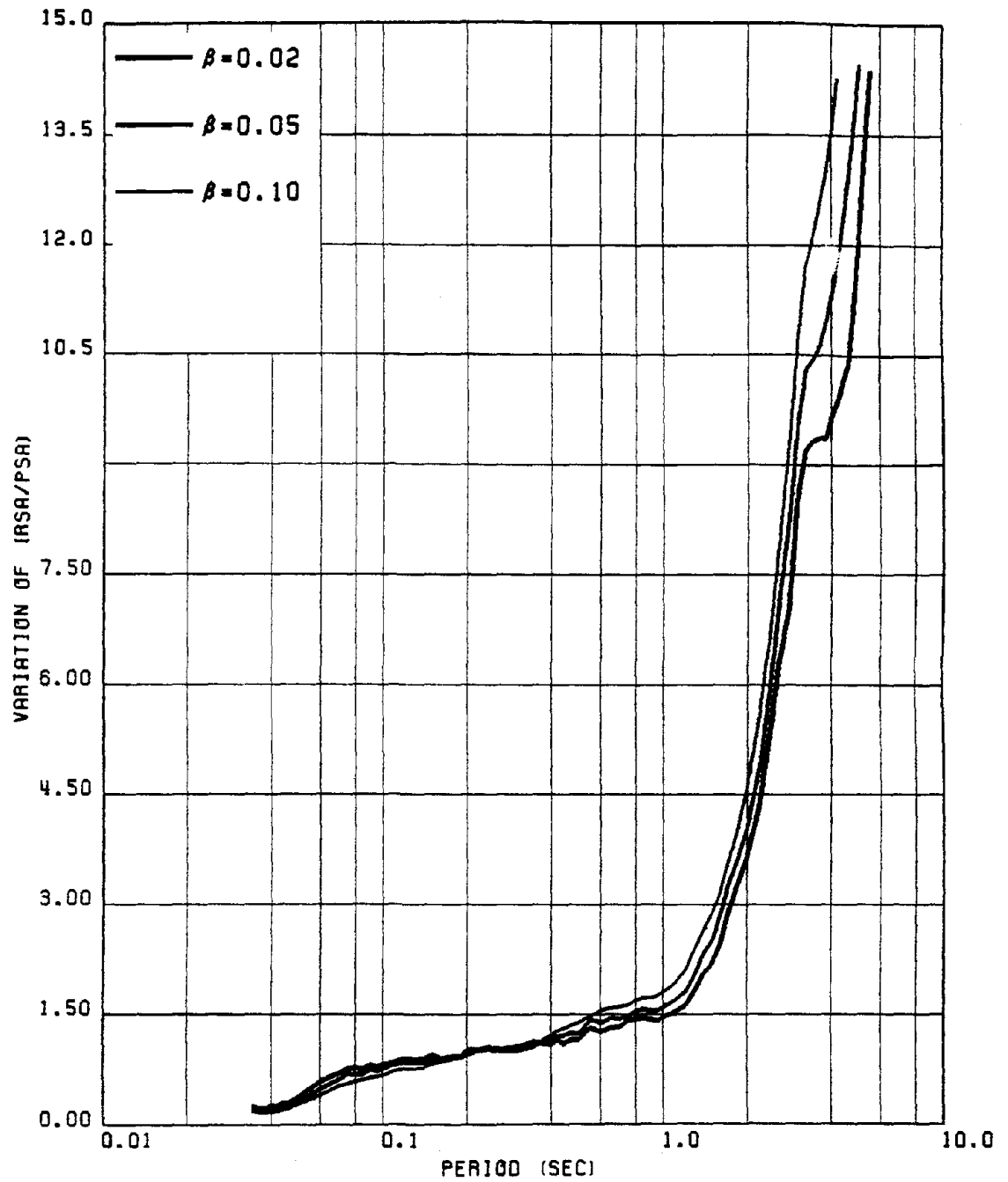
FIG. 102 VARIATION OF (RSA/PSA) FOR HORIZONTAL RECORDS OF GROUP #8
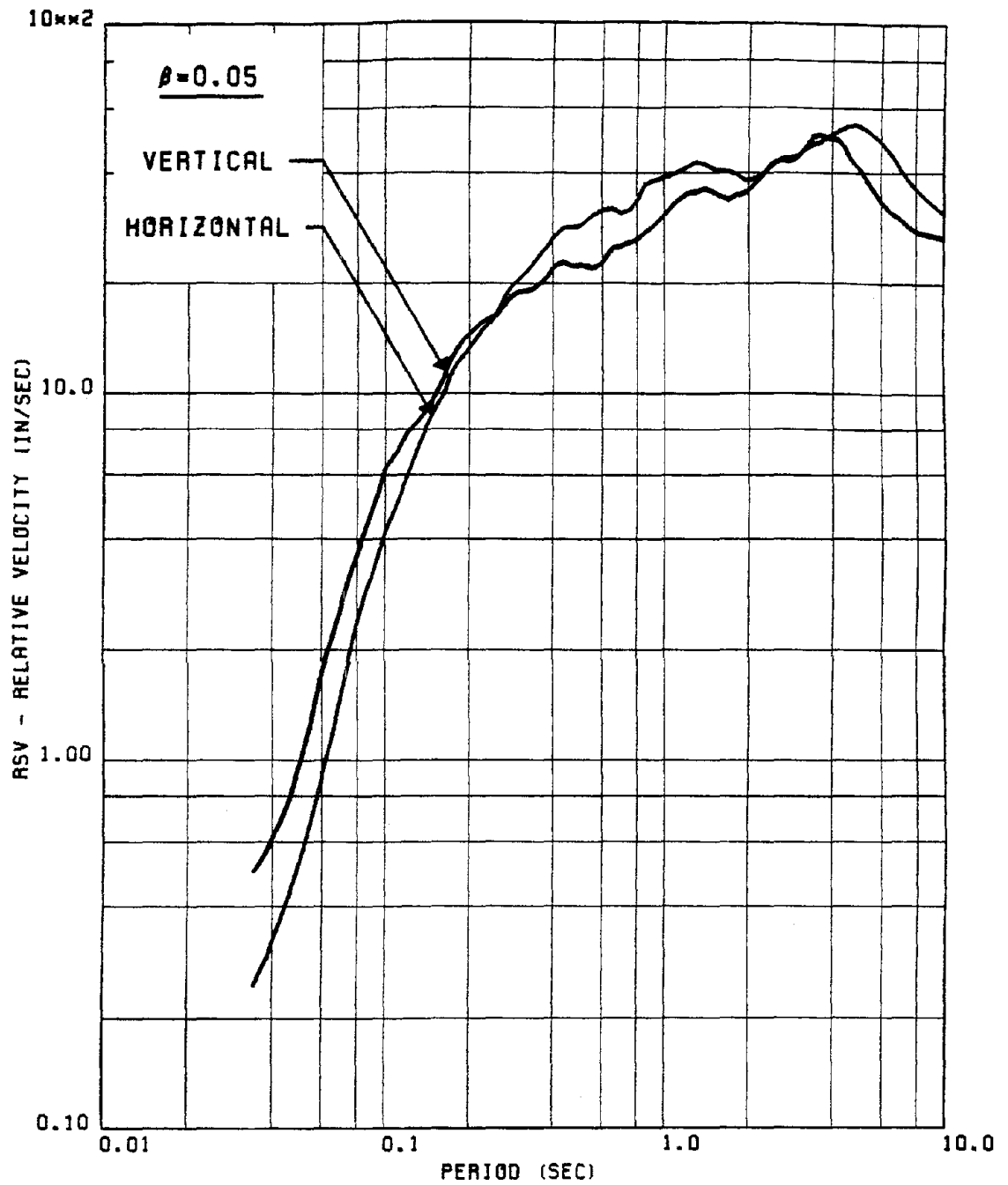
FIG. 103 COMPARISON OF PEAK NORMALIZED RSV SPECTRA CORRESPONDING TO
THE HORIZONTAL AND VERTICAL GROUND MOTION RECORDS OF GROUP #1
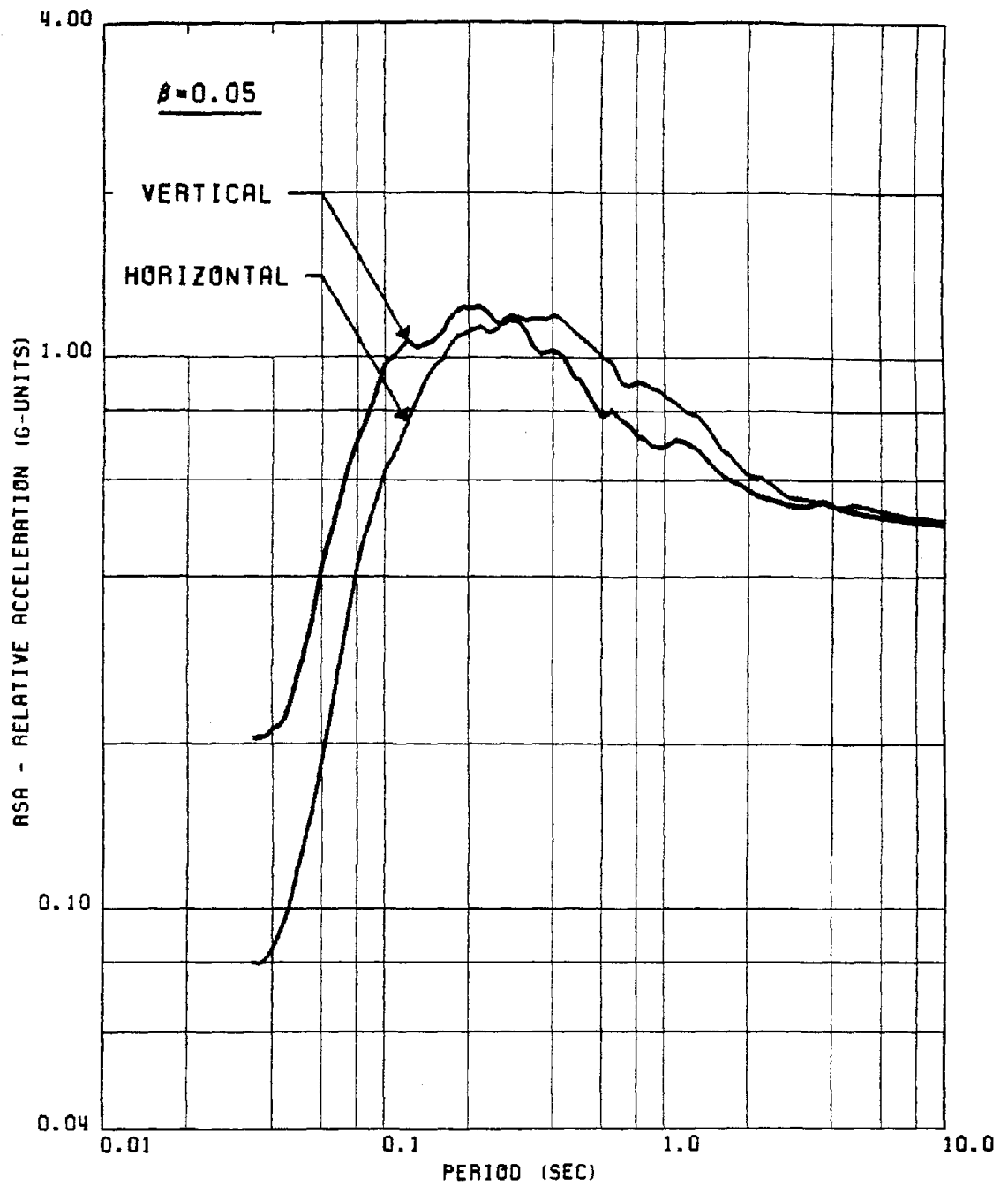
FIG. 104 COMPARISON OF PEAK NORMALIZED RSA SPECTRA CORRESPONDING TO
THE HORIZONTAL AND VERTICAL GROUND MOTION RECORDS OF GROUP #1
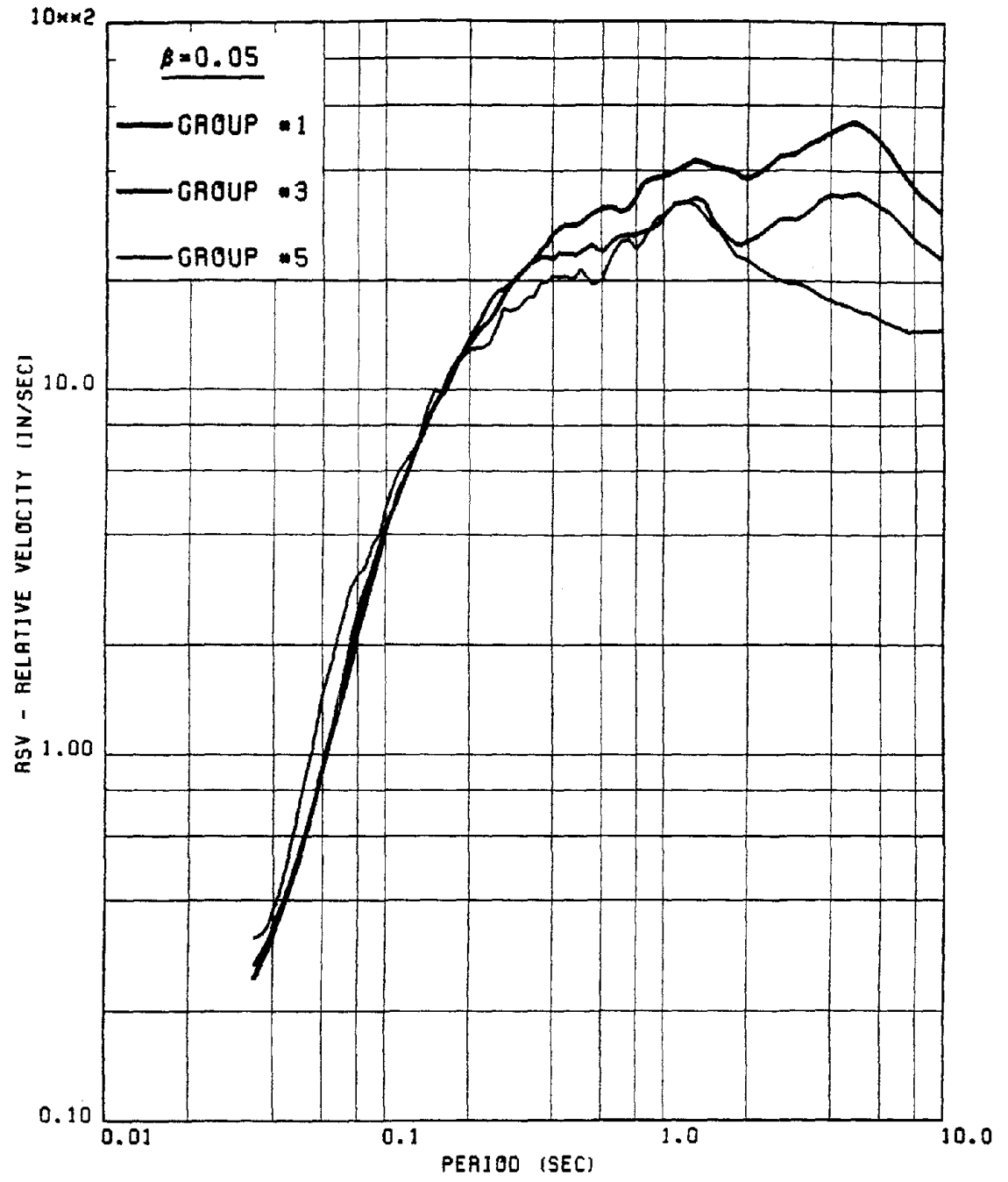
FIG. 105 COMPARISON OF PEAK NORMALIZED 'HORIZONTAL' RSV SPECTRA OF GROUPS #1, 3 & 5, TO STUDY THE EFFECT OF GROUND STIFFNESS (SOFT / MEDIUM / HARD)
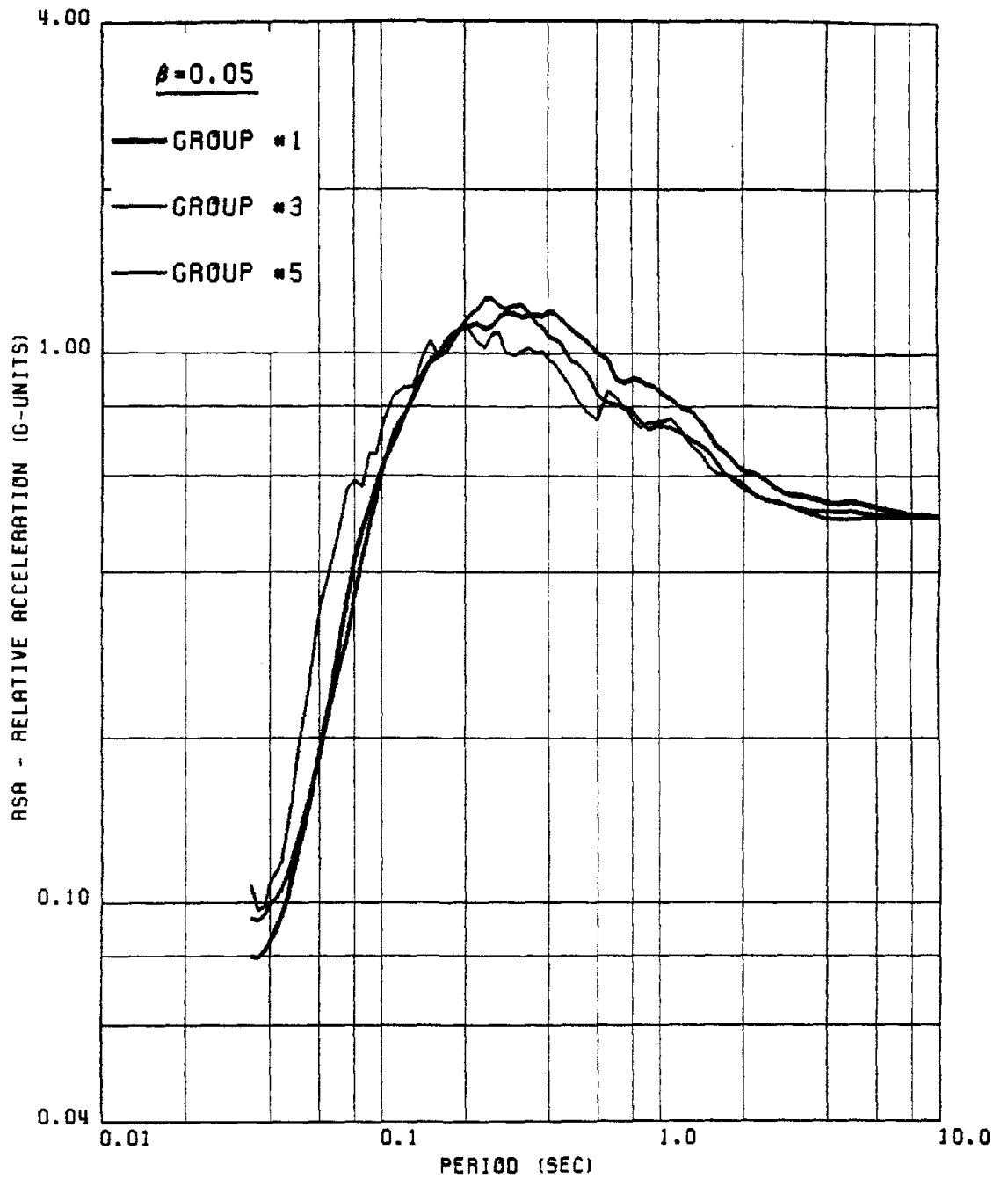
FIG. 106 COMPARISON OF PEAK NORMALIZED 'HORIZONTAL' RSA SPECTRA OF GROUPS #1, 3 & 5, TO STUDY THE EFFECT OF GROUND STIFFNESS (SOFT / MEDIUM / HARD)
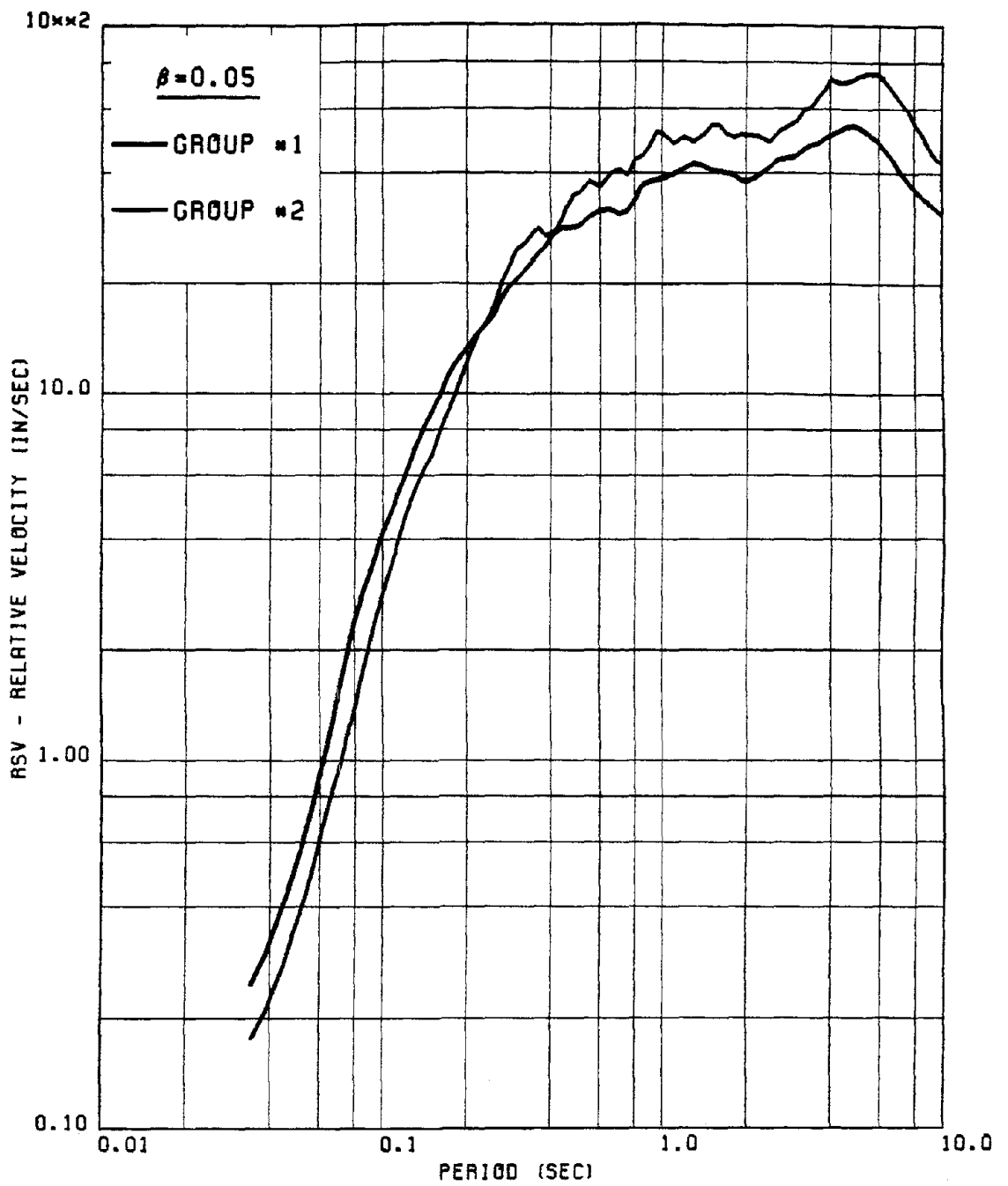
FIG. 107 COMPARISON OF PEAK NORMALIZED 'HORIZONTAL' RSV SPECTRA OF GROUPS
#1 AND 2 TO STUDY THE EFFECT OF THE EPICENTRAL DISTANCE (SMALL V/S LARGE)
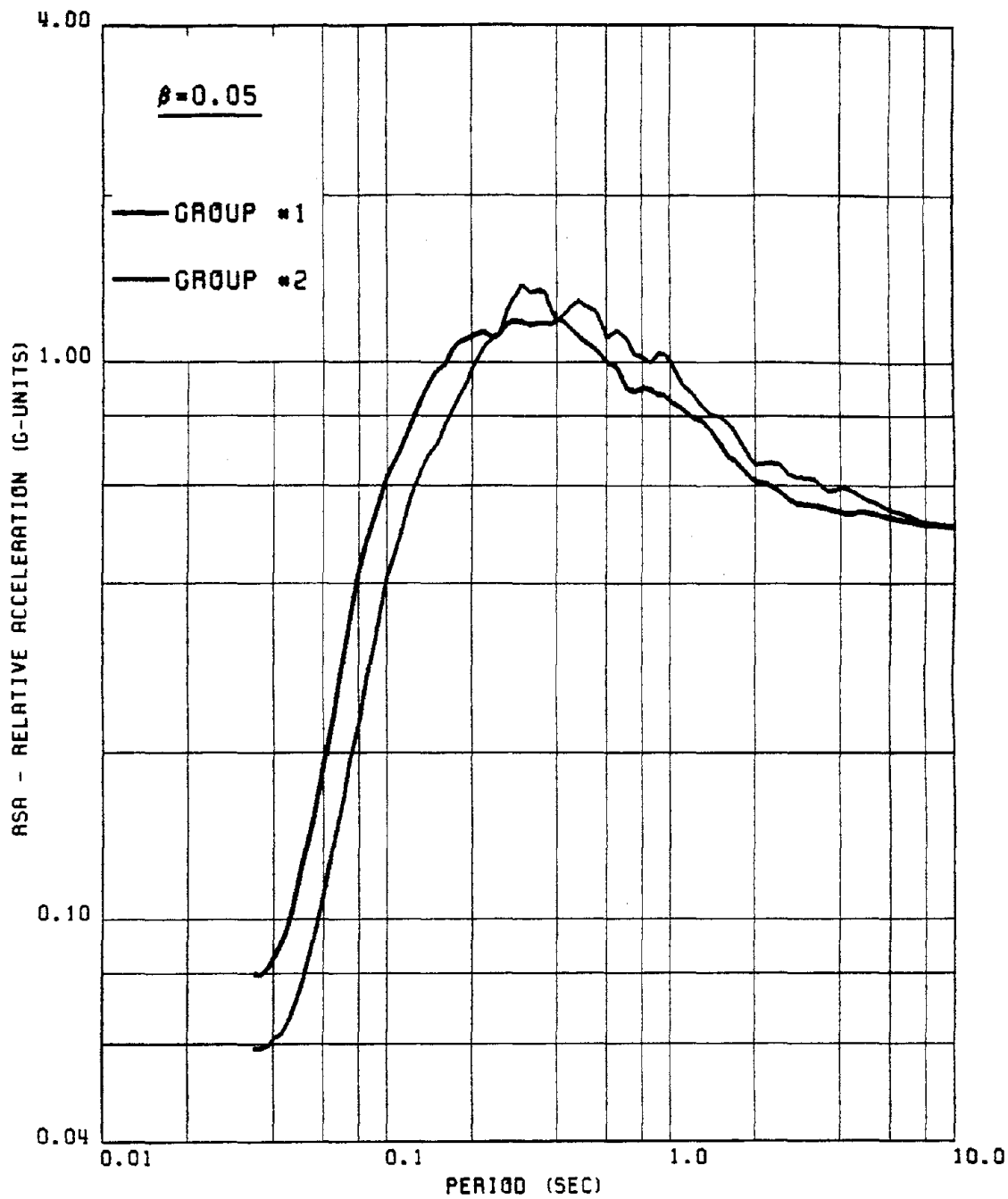
FIG. 108 COMPARISON OF PEAK NORMALIZED 'HORIZONTAL' RSA SPECTRA OF GROUPS
#1 AND 2 TO STUDY THE EFFECT OF THE EPICENTRAL DISTANCE (SMALL V/S LARGE)
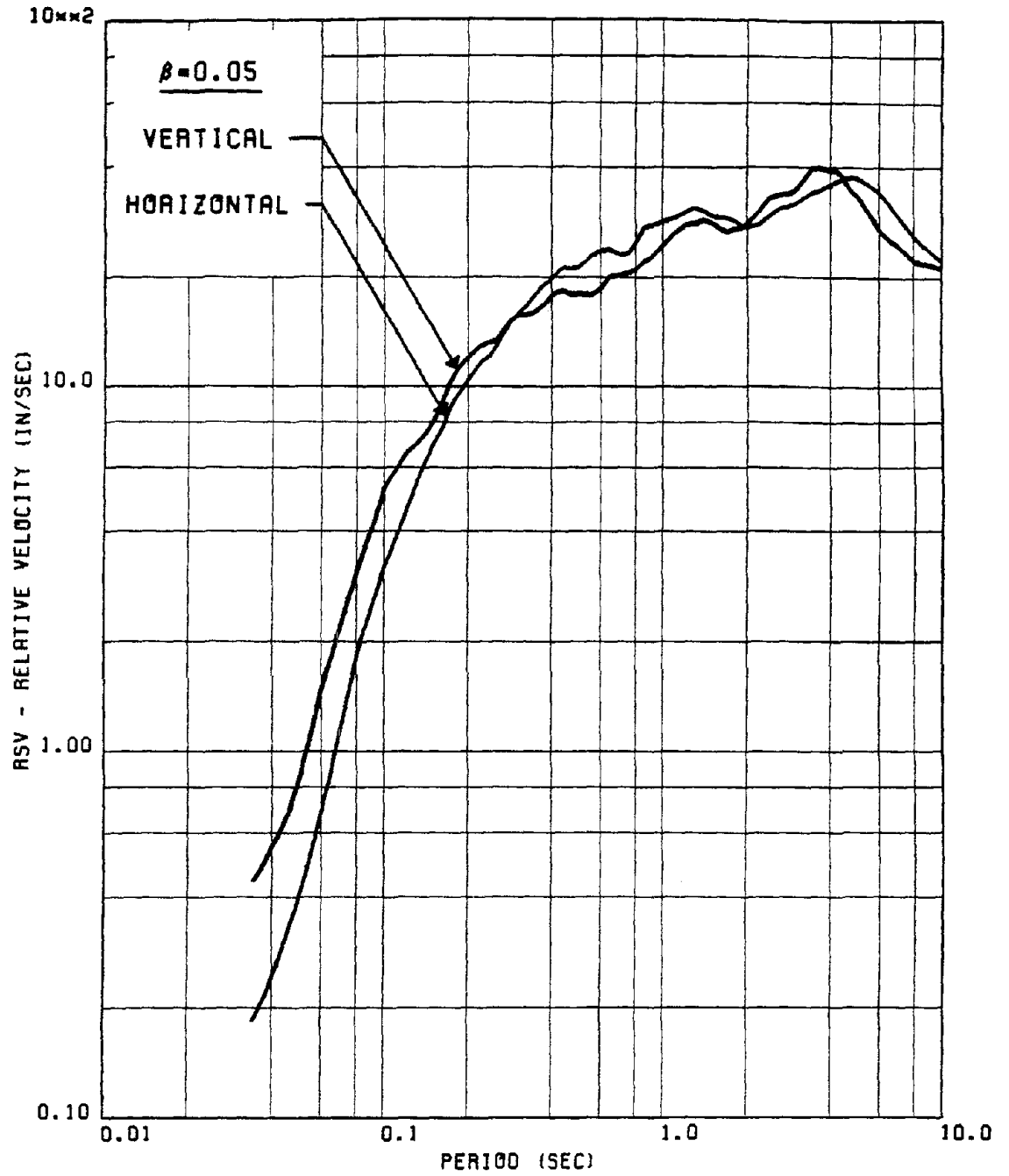
FIG. 109 COMPARISON OF R.M.S. NORMALIZED RSV SPECTRA CORRESPONDING TO
THE HORIZONTAL AND VERTICAL GROUND MOTION RECORDS OF GROUP #1
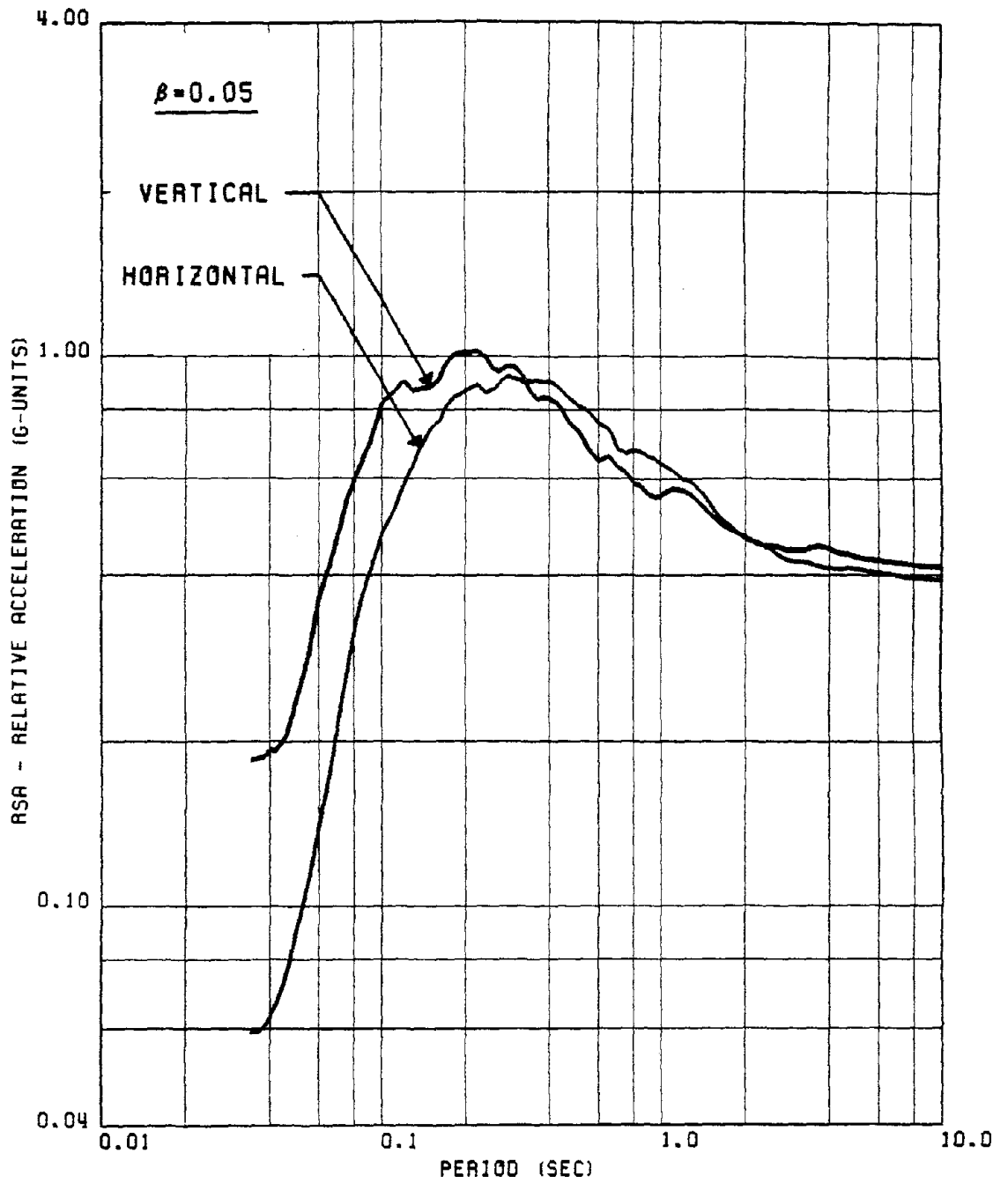
FIG. 110 COMPARISON OF R.M.S. NORMALIZED RSA SPECTRA CORRESPONDING TO
THE HORIZONTAL AND VERTICAL GROUND MOTION RECORDS OF GROUP #1
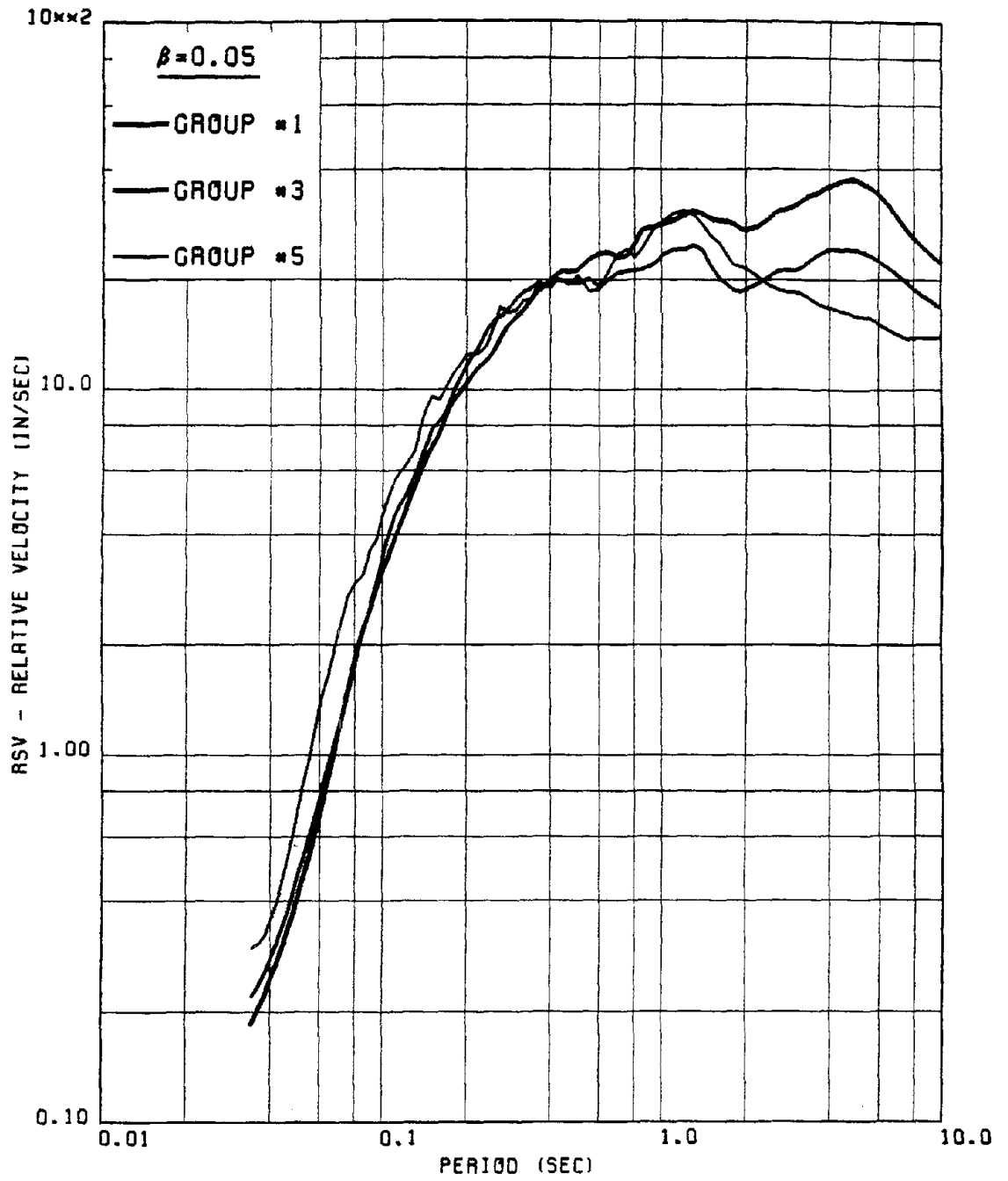
FIG. 111 COMPARISON OF R.M.S. NORMALIZED 'HORIZONTAL' RSV SPECTRA OF GROUPS #1, 3 & 5, TO STUDY THE EFFECT OF GROUND STIFFNESS (SOFT / MEDIUM / HARD)
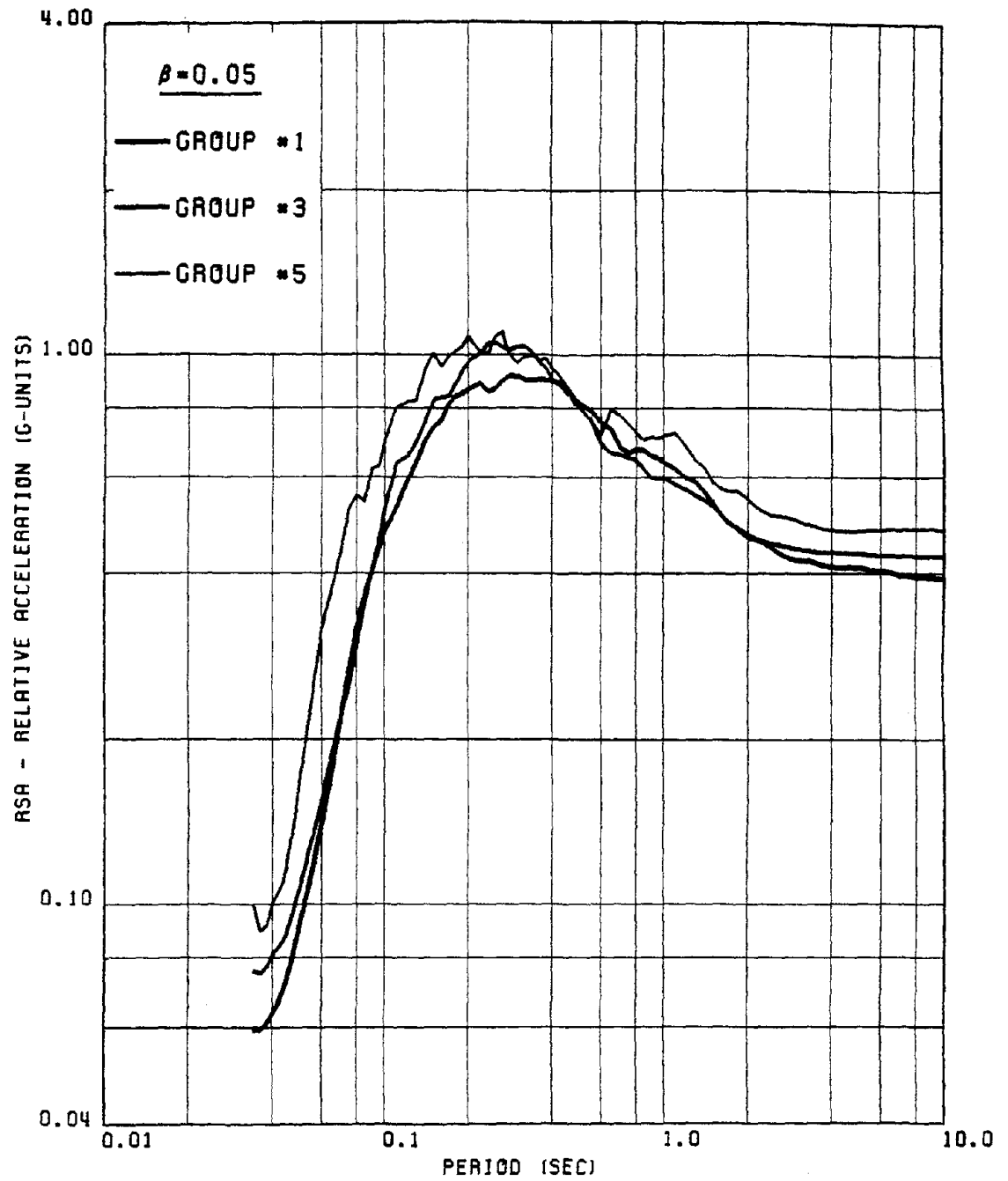
FIG. 112 COMPARISON OF R.M.S. NORMALIZED 'HORIZONTAL' RSA SPECTRA OF GROUPS #1, 3 & 5. TO STUDY THE EFFECT OF GROUND STIFFNESS (SOFT / MEDIUM / HARD)
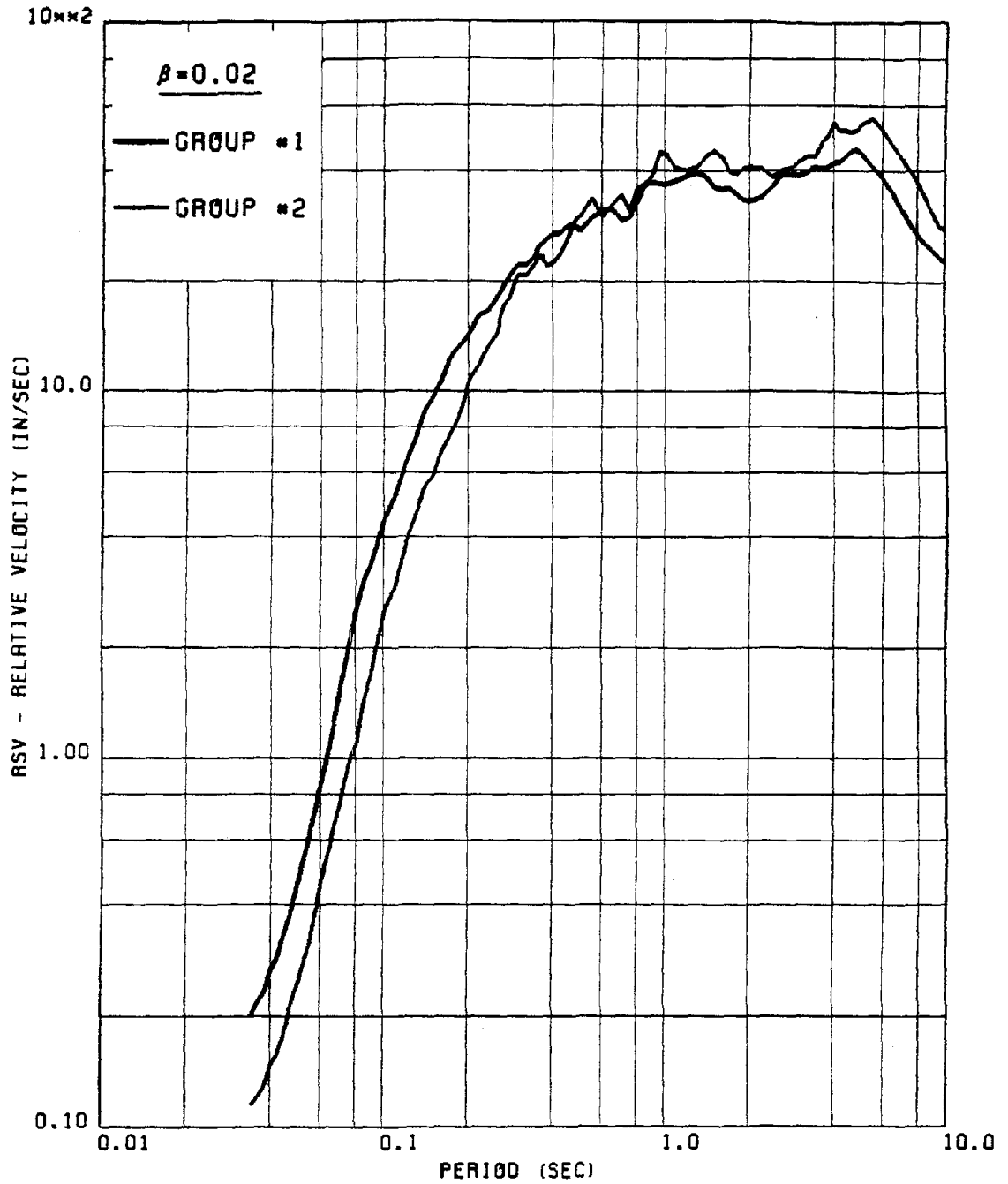
FIG. 113 COMPARISON OF R.M.S. NORMALIZED 'HORIZONTAL' RSV SPECTRA OF GROUPS #1 AND 2 TO STUDY THE EFFECT OF THE EPICENTRAL DISTANCE (SMALL V/S LARGE)
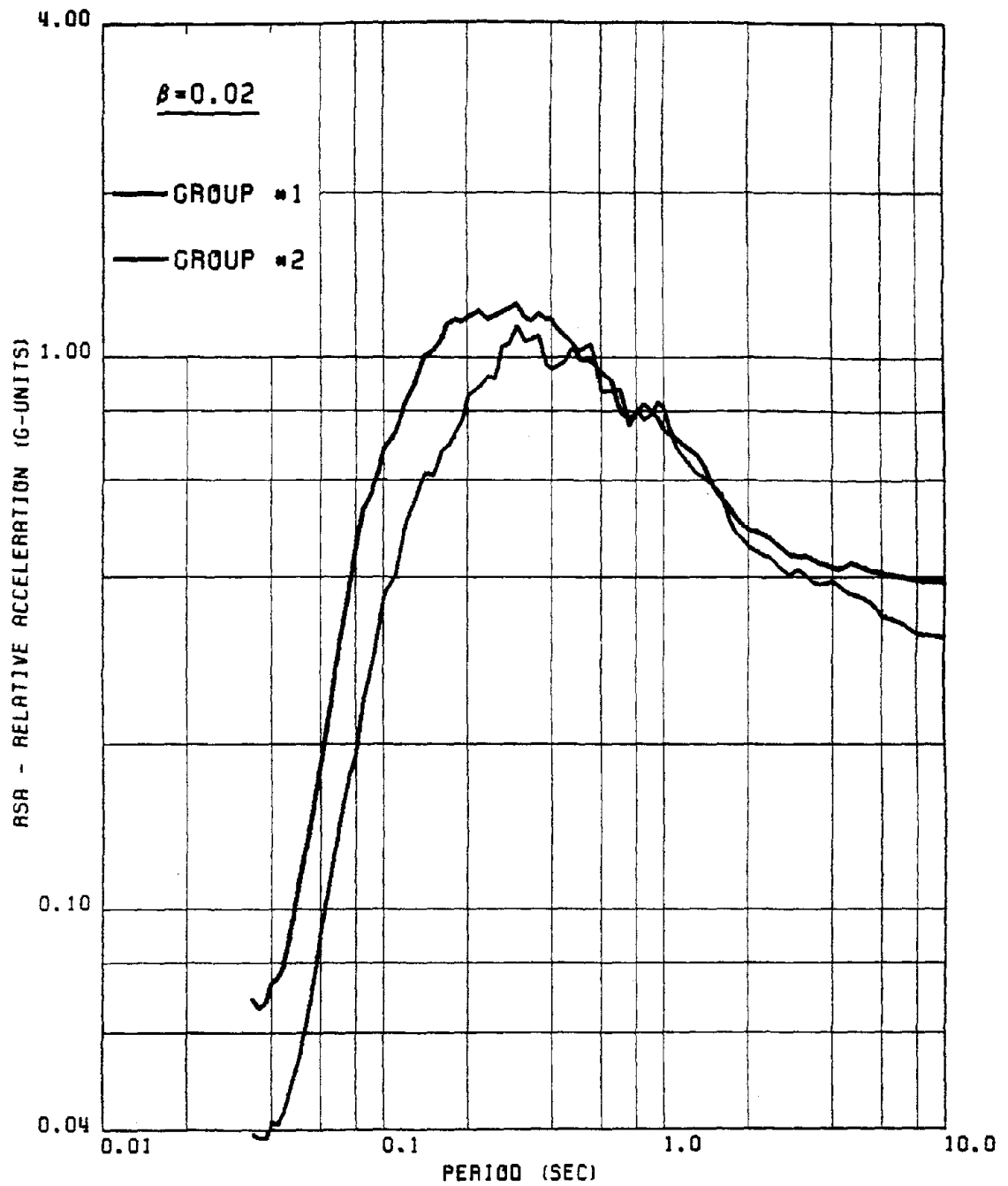
FIG. 114 COMPARISON OF R.M.S. NORMALIZED 'HORIZONTAL' RSA SPECTRA OF GROUPS
#1 AND 2 TO STUDY THE EFFECT OF THE EPICENTRAL DISTANCE (SMALL V/S LARGE)
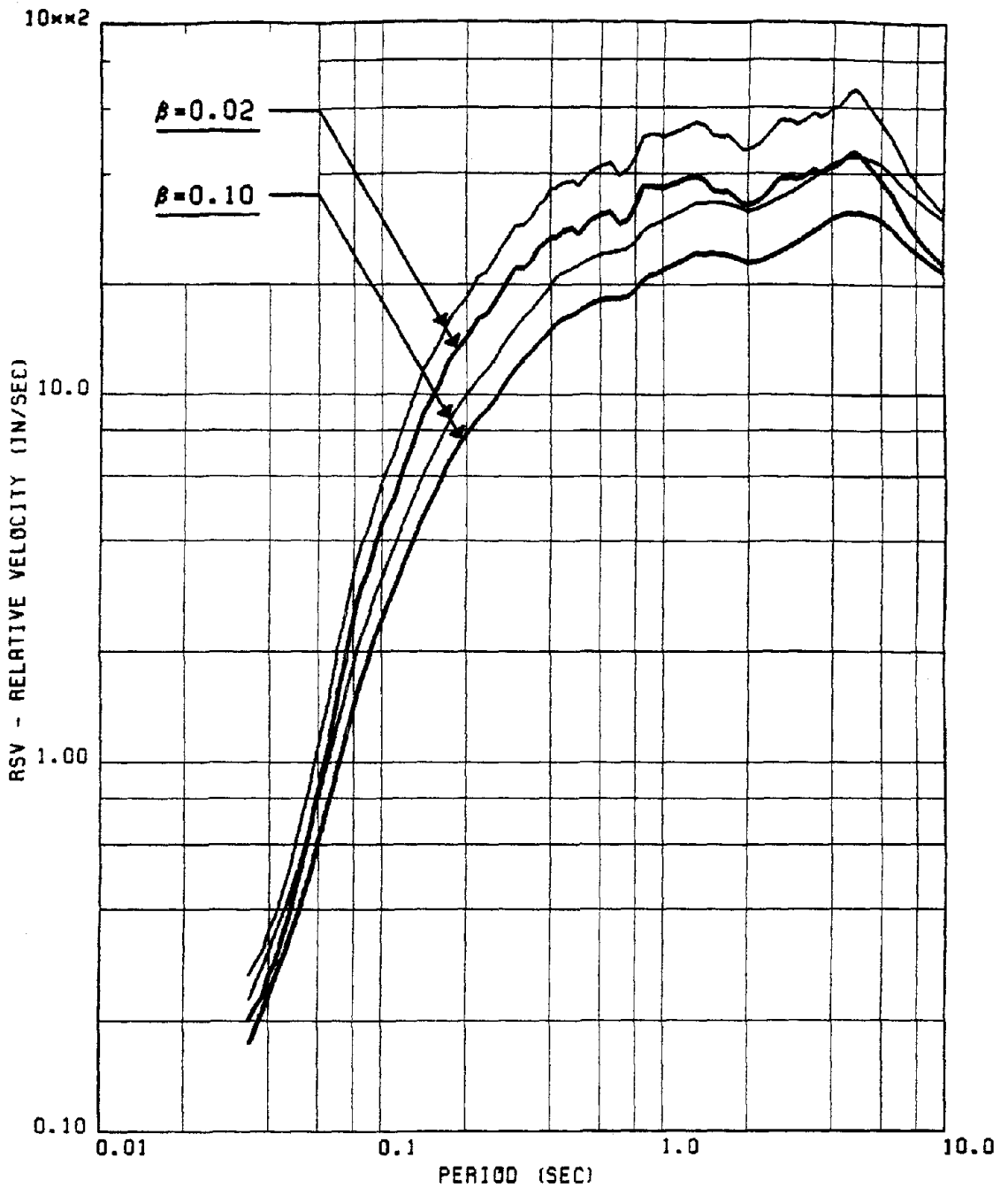
FIG. 115 COMPARISON OF THE PEAK & RMS NORMALIZED RSV SPECTRA FOR GROUP #1
NOTE : THE RMS NORMALIZED SPECTRA ARE INDICATED BY THE THICKER CURVES
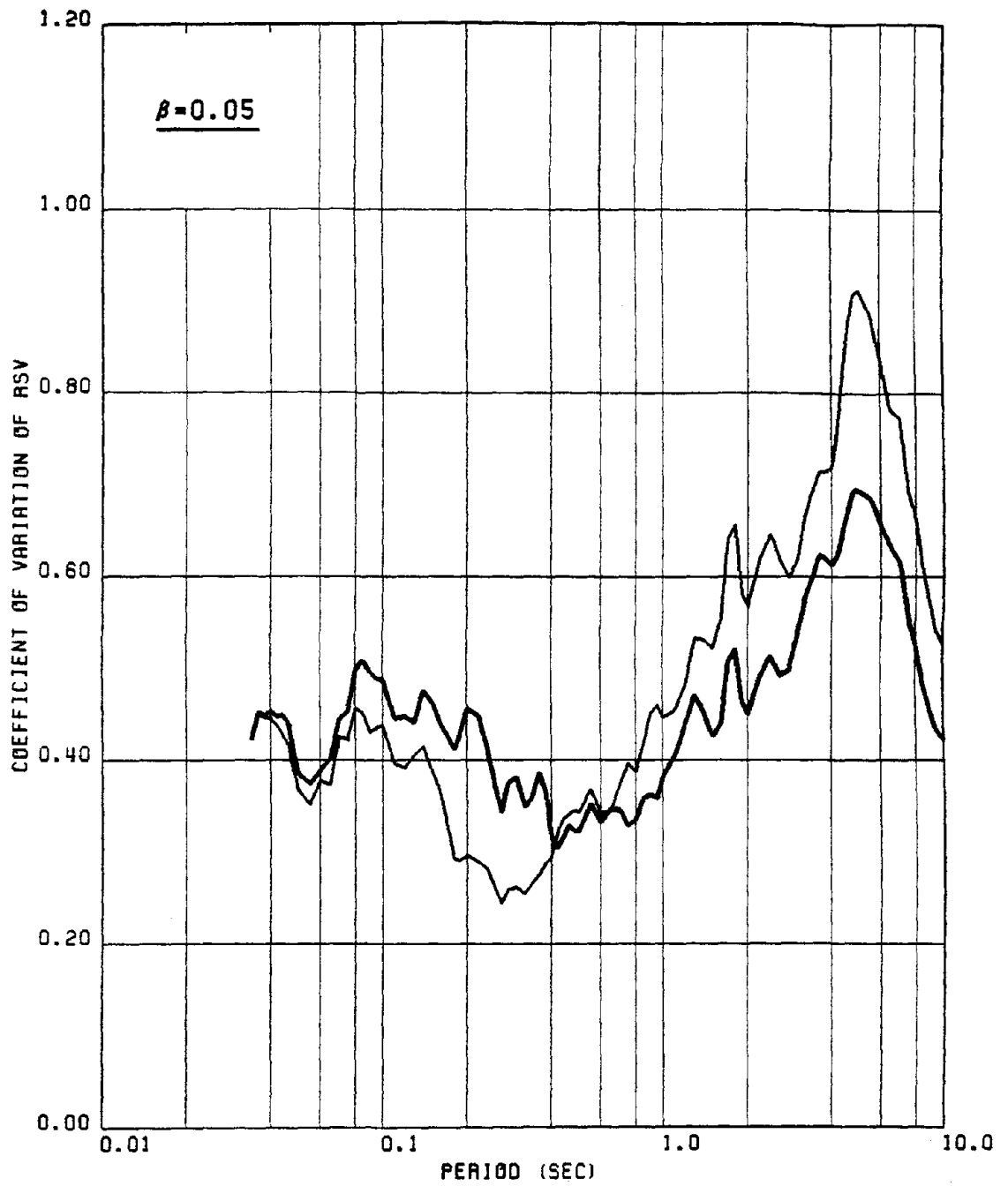
FIG. 116 COEFFICIENT OF VARIATION OF PEAK & RMS NORMALIZED RSV FOR GROUP #1
NOTE : THE RMS NORMALIZED SPECTRUM IS INDICATED BY THE THICKER CURVE
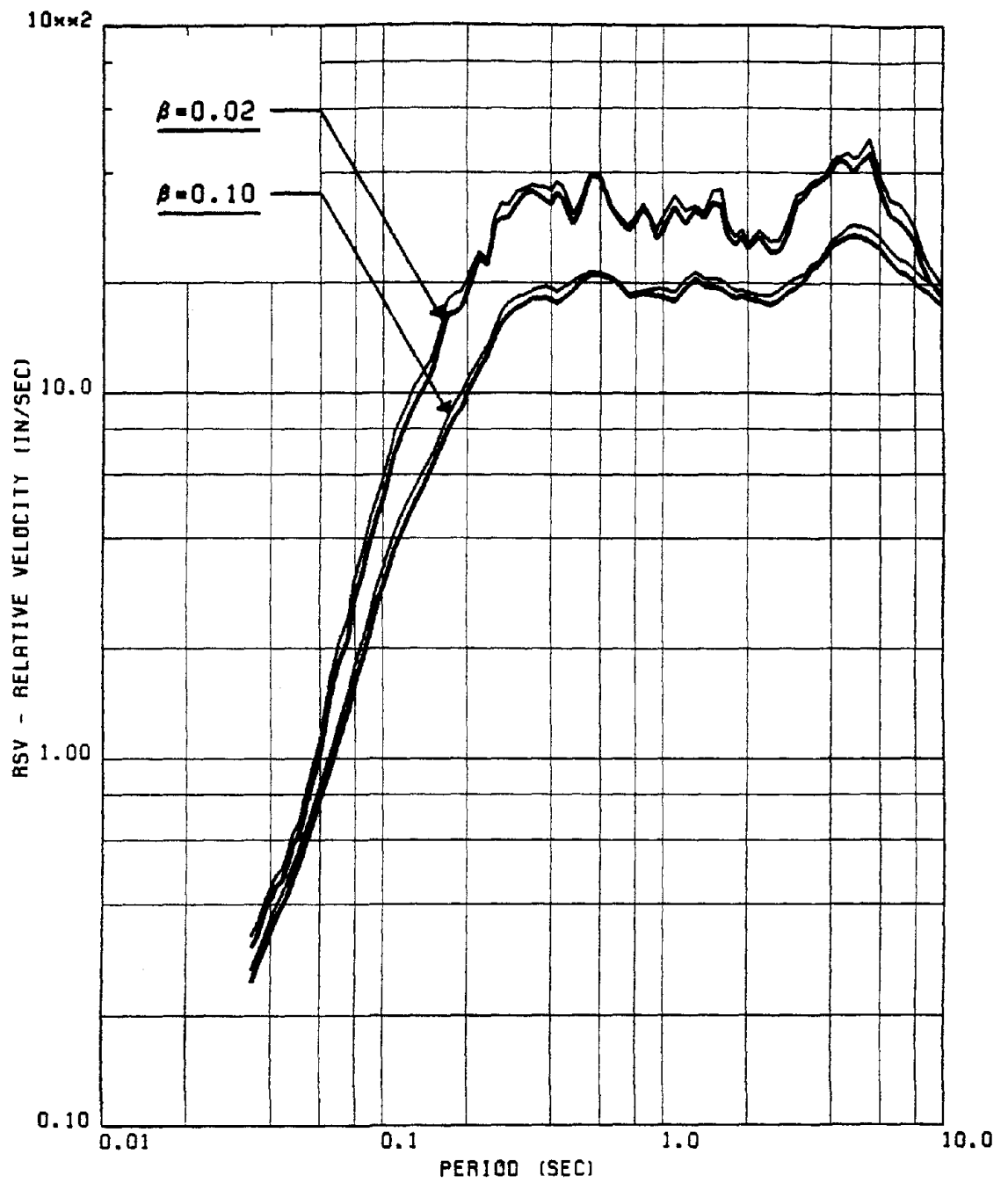
FIG. 117 COMPARISON OF THE PEAK & RMS NORMALIZED RSV SPECTRA FOR GROUP #4
NOTE : THE RMS NORMALIZED SPECTRA ARE INDICATED BY THE THICKER CURVES
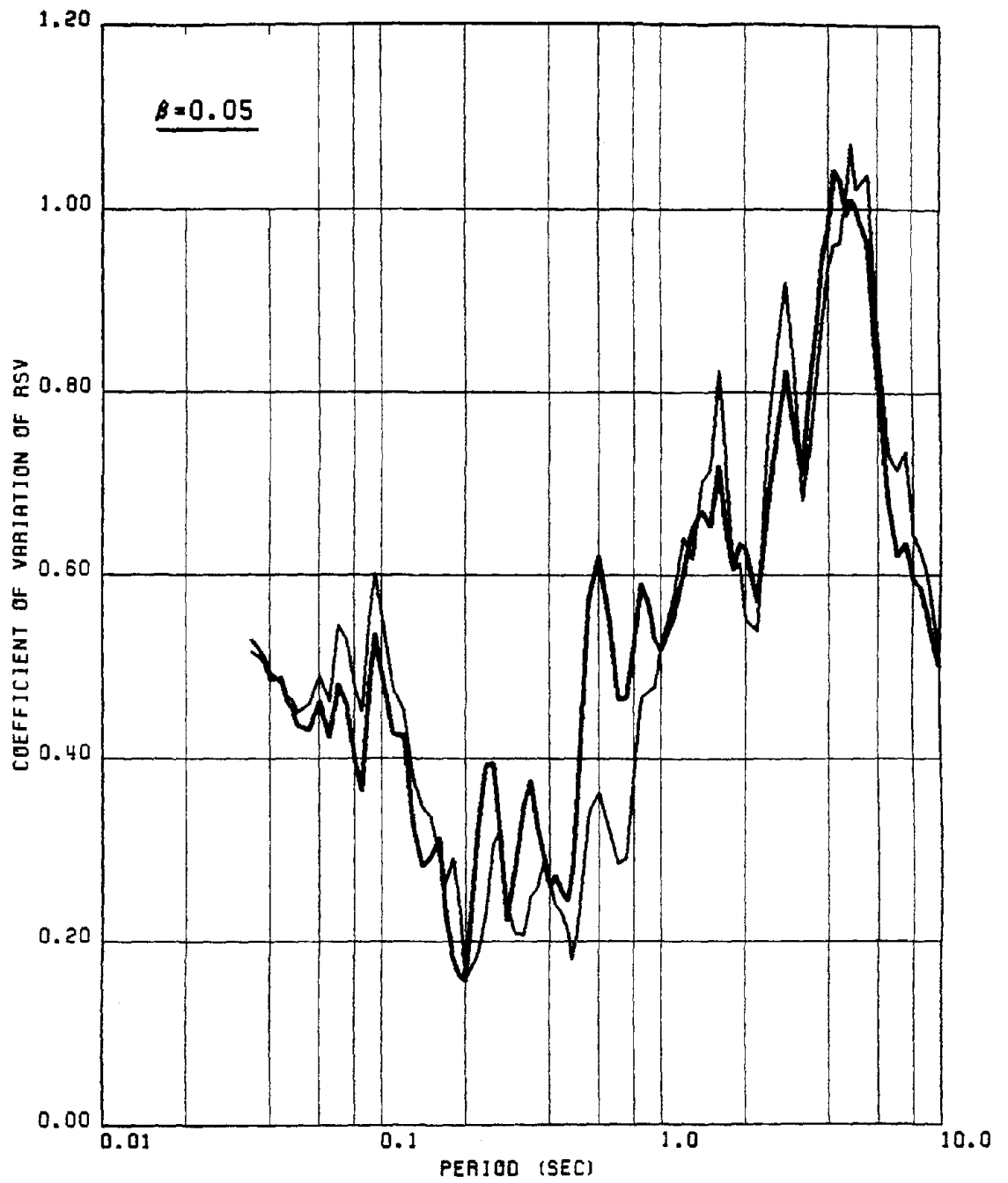
FIG. 118 COEFFICIENT OF VARIATION OF PEAK & RMS NORMALIZED RSV FOR GROUP #4
NOTE : THE RMS NORMALIZED SPECTRUM IS INDICATED BY THE THICKER CURVE
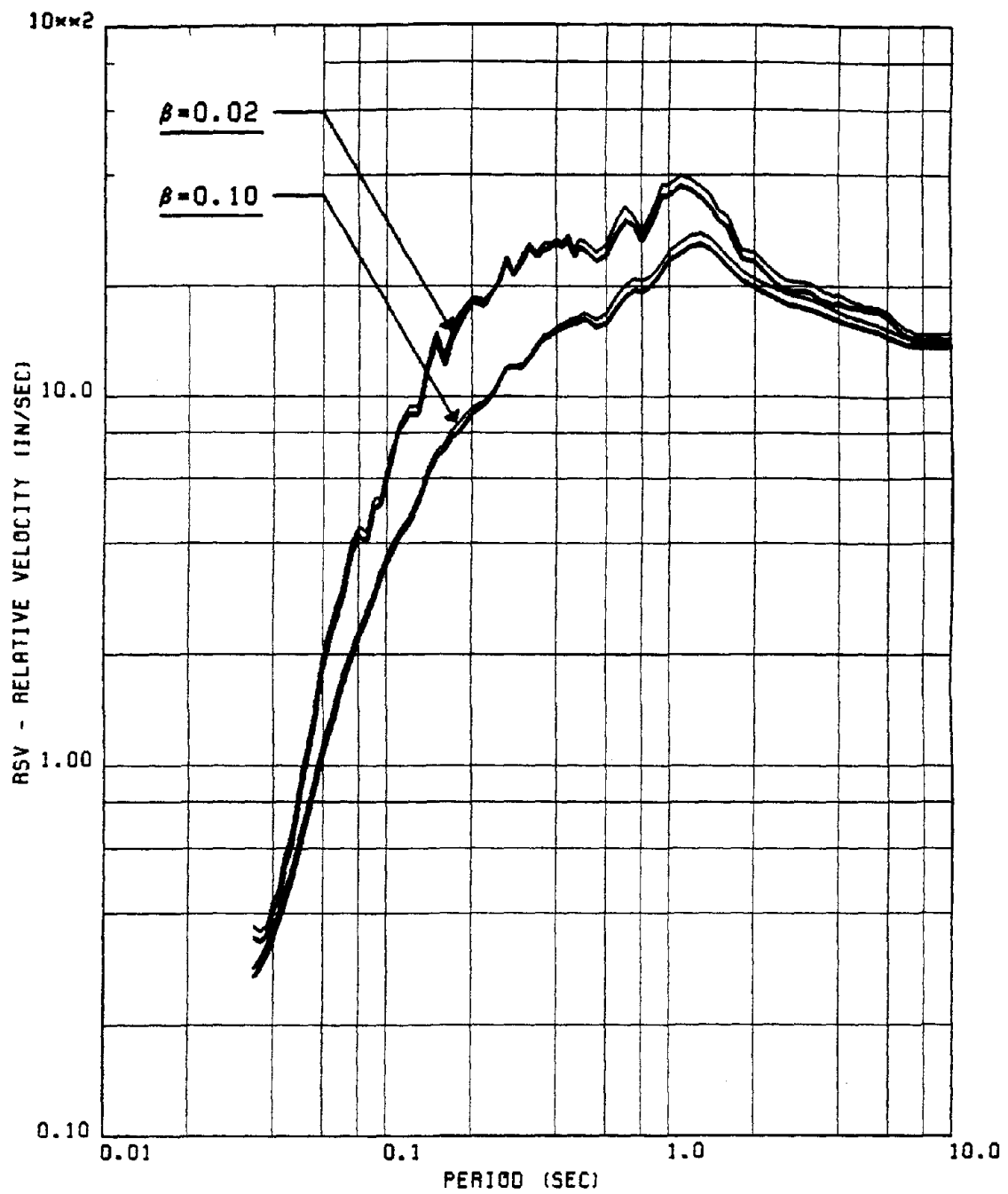
FIG. 119 COMPARISON OF THE PEAK & RMS NORMALIZED RSV SPECTRA FOR GROUP ₅5
NOTE : THE RMS NORMALIZED SPECTRA ARE INDICATED BY THE THICKER CURVES
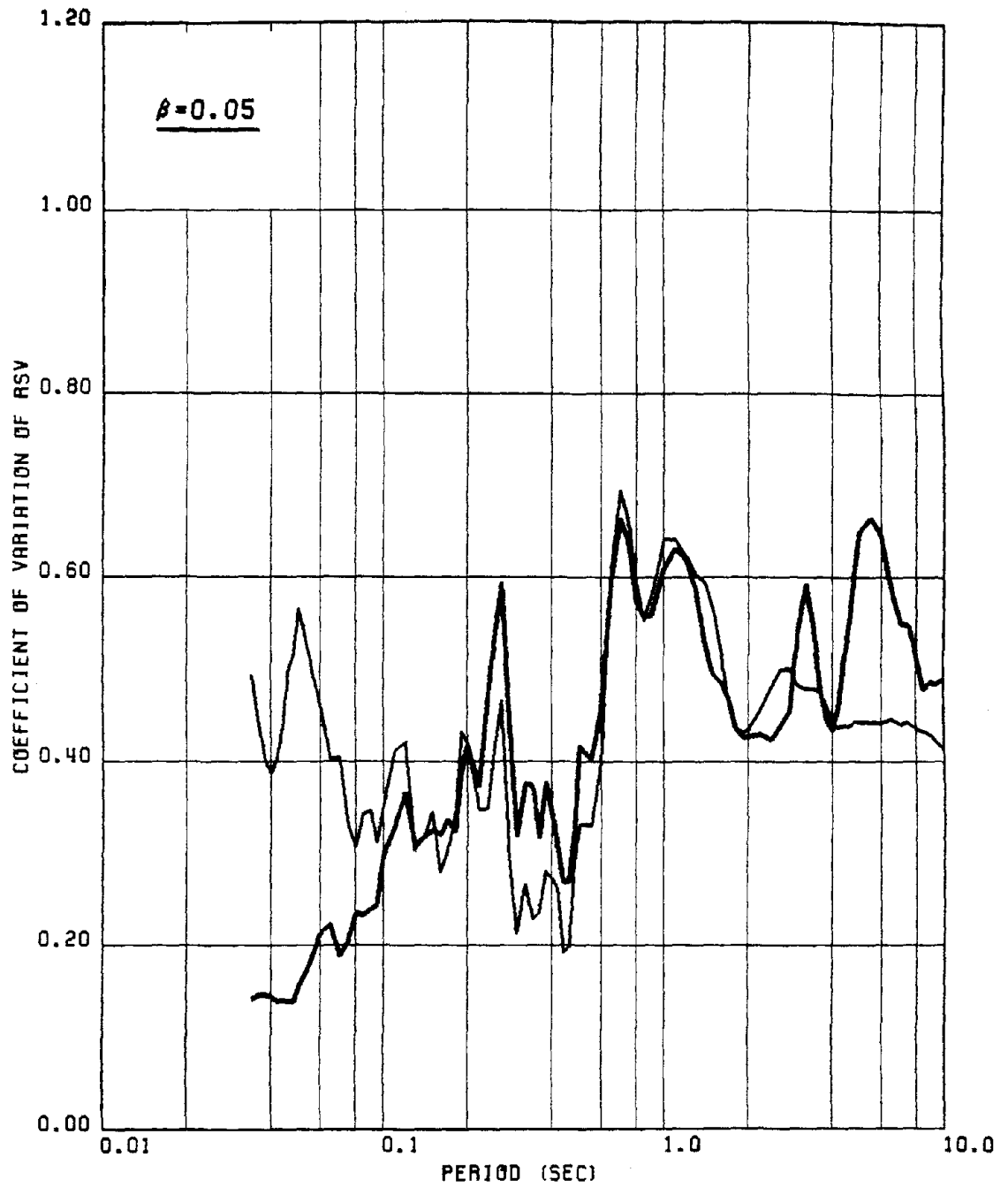
FIG. 120 COEFFICIENT OF VARIATION OF PEAK & RMS NORMALIZED RSV FOR GROUP #5
NOTE : THE RMS NORMALIZED SPECTRUM IS INDICATED BY THE THICKER CURVE

198
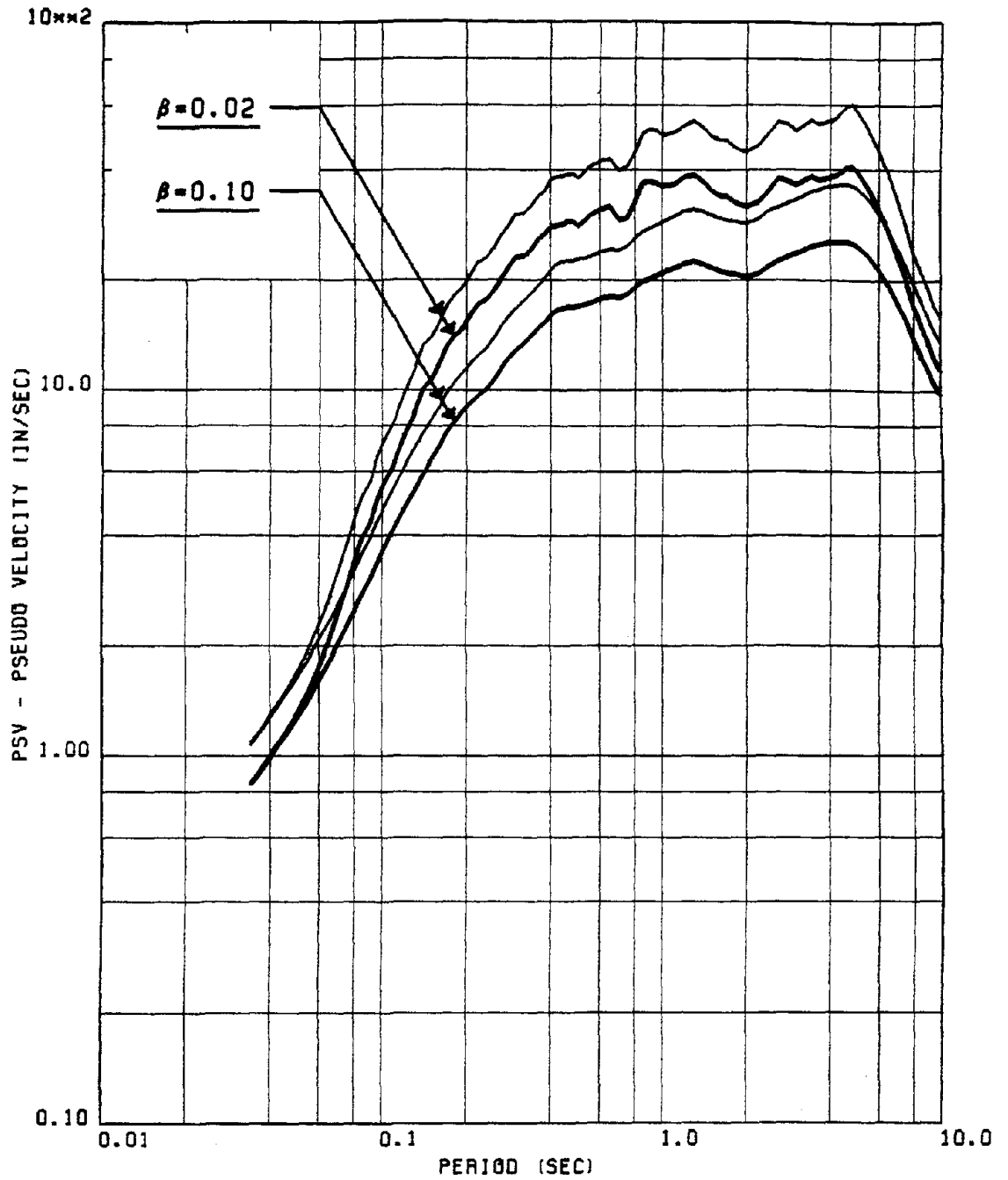
FIG. 121 COMPARISON OF THE PEAK & RMS NORMALIZED PSV SPECTRA FOR GROUP *1
NOTE : THE RMS NORMALIZED SPECTRA ARE INDICATED BY THE THICKER CURVES
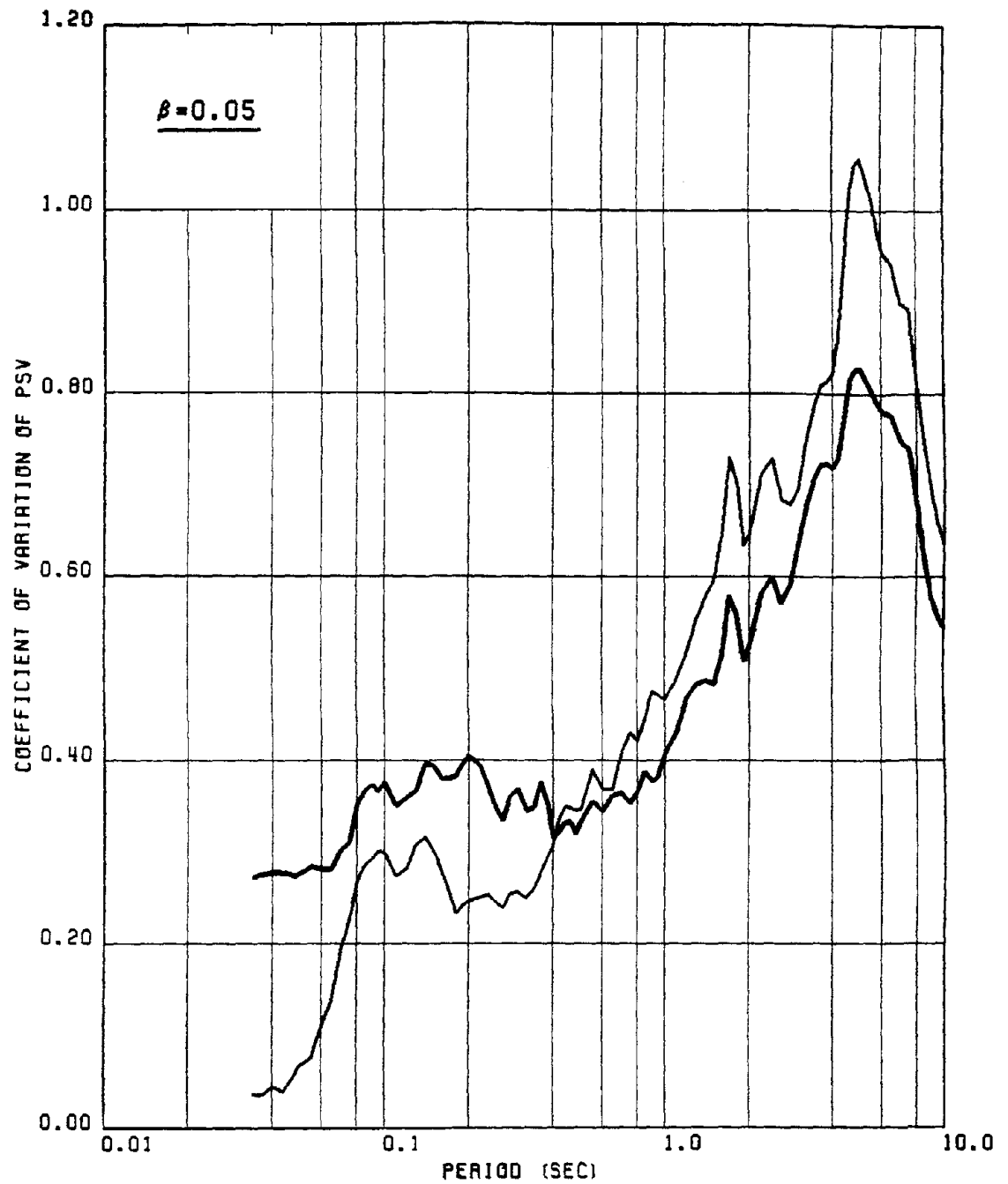
FIG. 122 COEFFICIENT OF VARIATION OF PEAK & RMS NORMALIZED PSV FOR GROUP #1
NOTE : THE RMS NORMALIZED SPECTRUM IS INDICATED BY THE THICKER CURVE
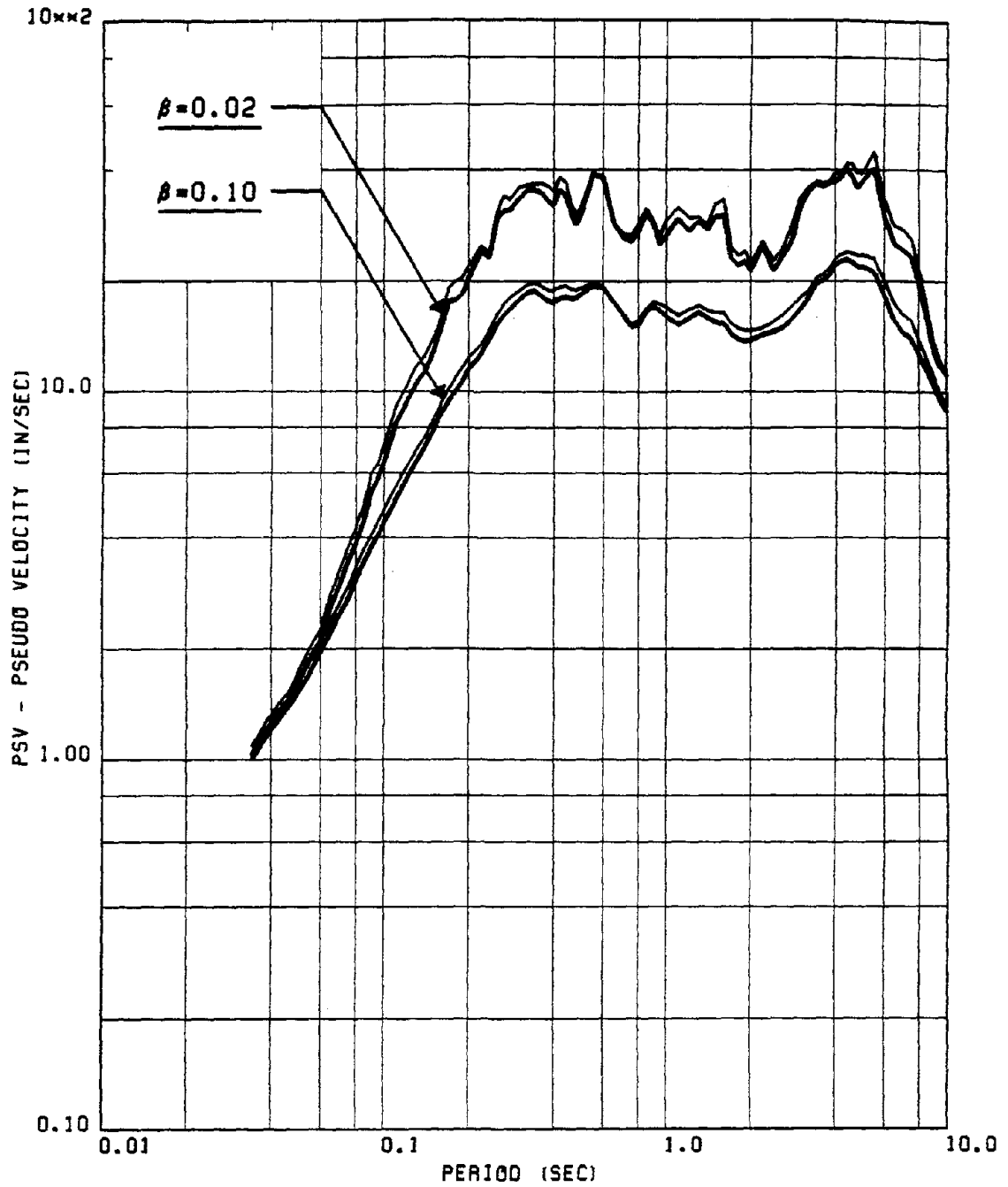
FIG. 123 COMPARISON OF THE PEAK & RMS NORMALIZED PSV SPECTRA FOR GROUP #4
NOTE : THE RMS NORMALIZED SPECTRA ARE INDICATED BY THE THICKER CURVES
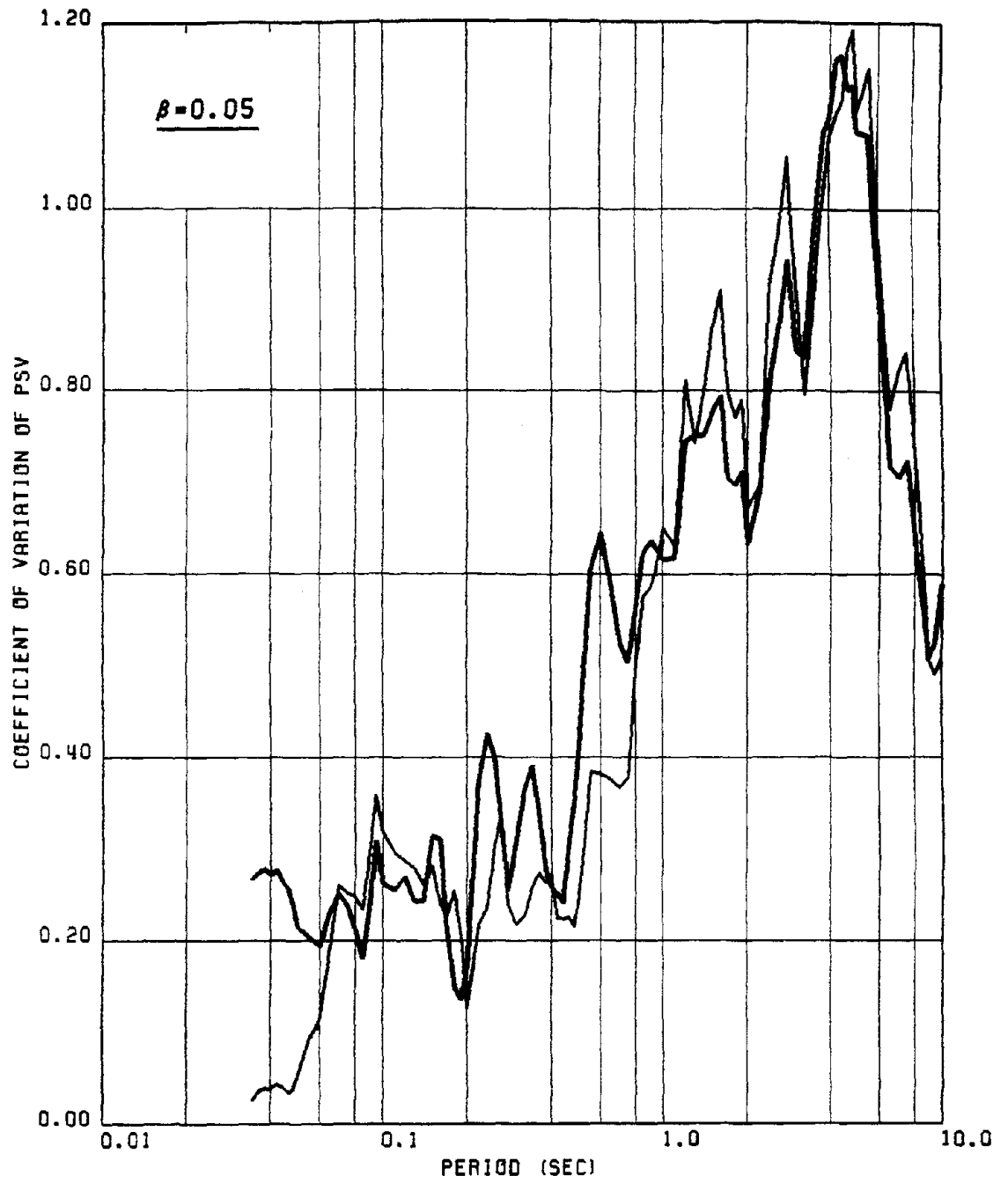
FIG. 124 COEFFICIENT OF VARIATION OF PEAK & RMS NORMALIZED PSV FOR GROUP #4
NOTE : THE RMS NORMALIZED SPECTRUM IS INDICATED BY THE THICKER CURVE
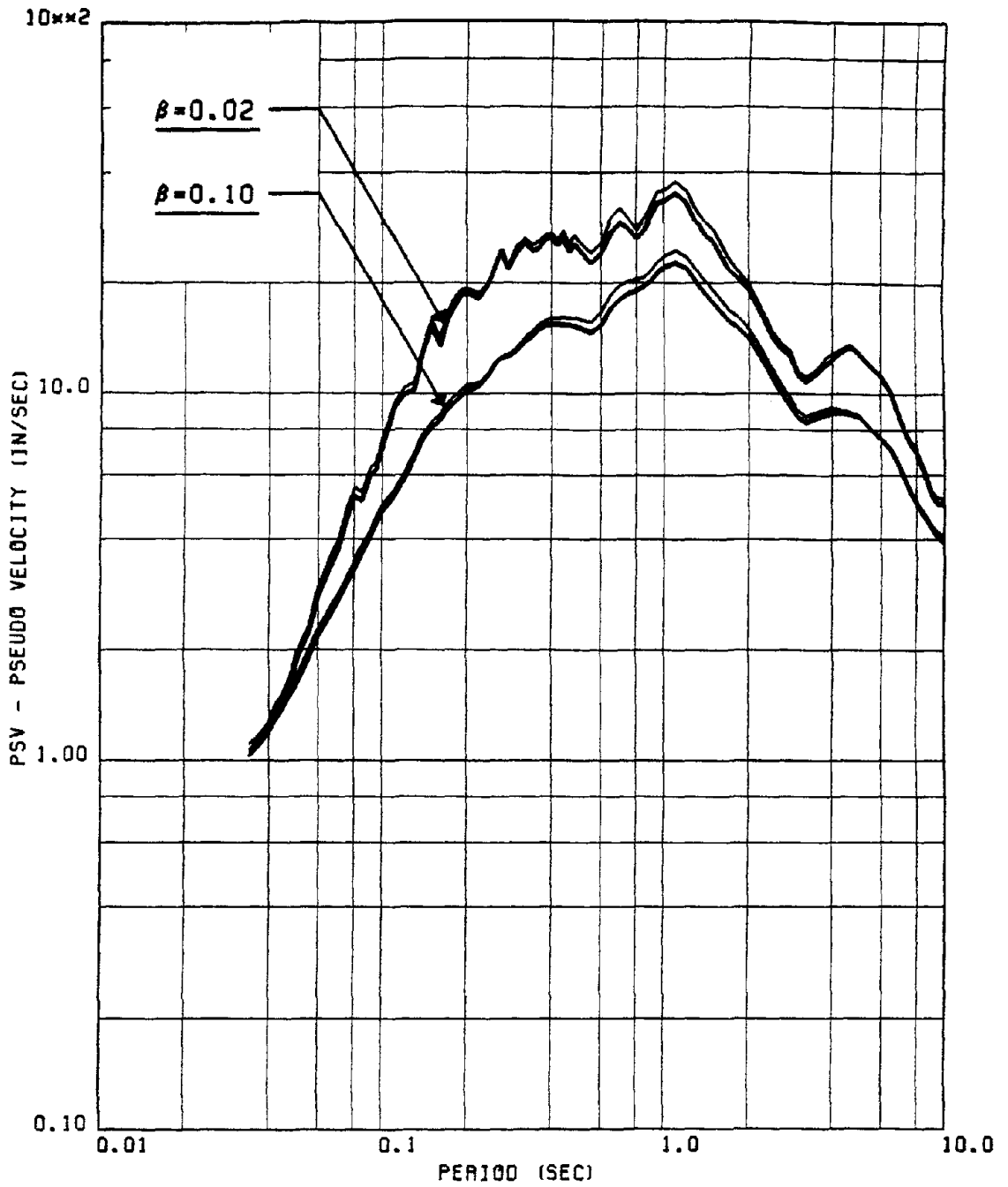
FIG. 125 COMPARISON OF THE PEAK & RMS NORMALIZED PSV SPECTRA FOR GROUP #5
NOTE : THE RMS NORMALIZED SPECTRA ARE INDICATED BY THE THICKER CURVES
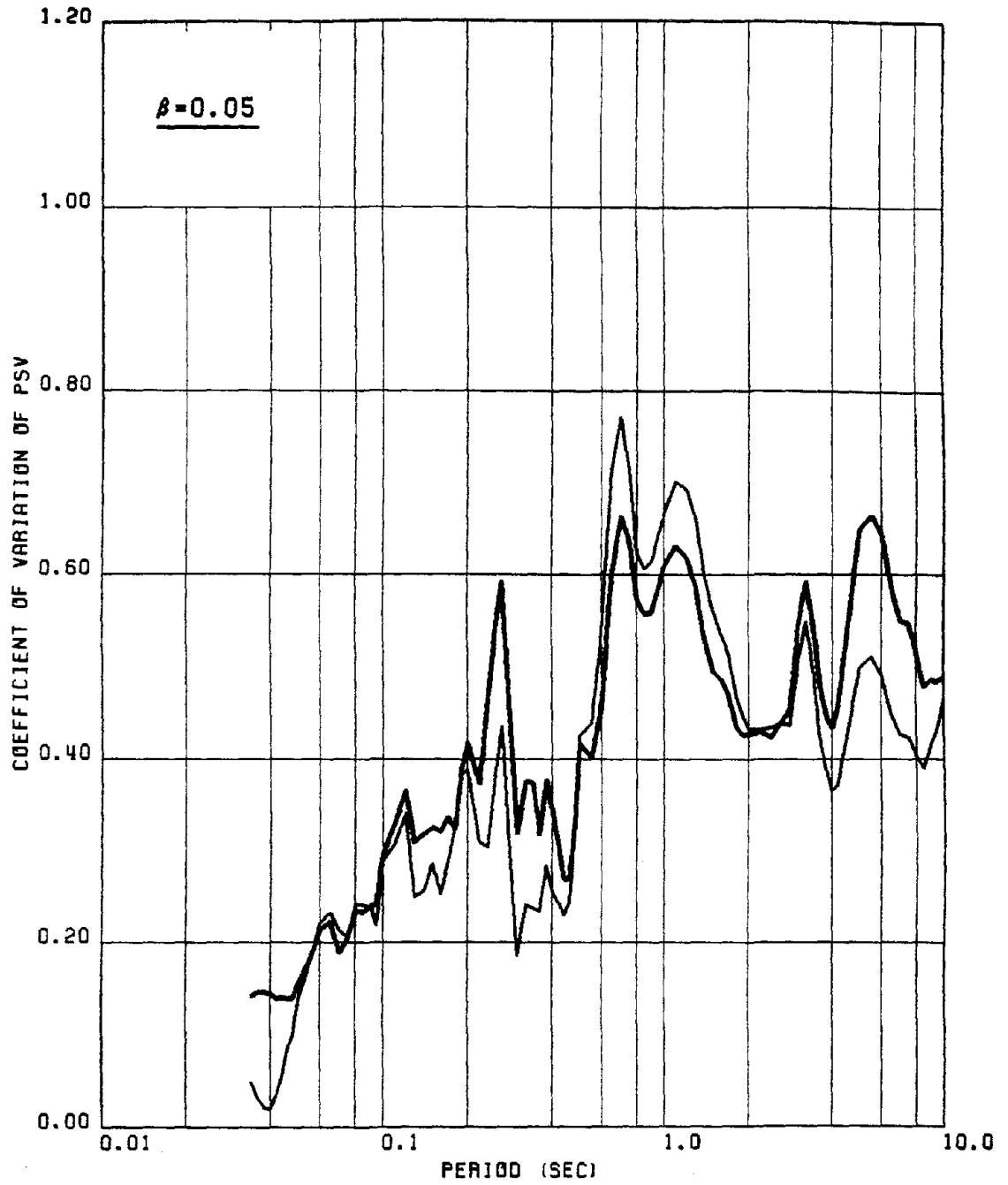
FIG. 126 COEFFICIENT OF VARIATION OF PEAK & RMS NORMALIZED PSV FOR GROUP #5
NOTE : THE RMS NORMALIZED SPECTRUM IS INDICATED BY THE THICKER CURVE
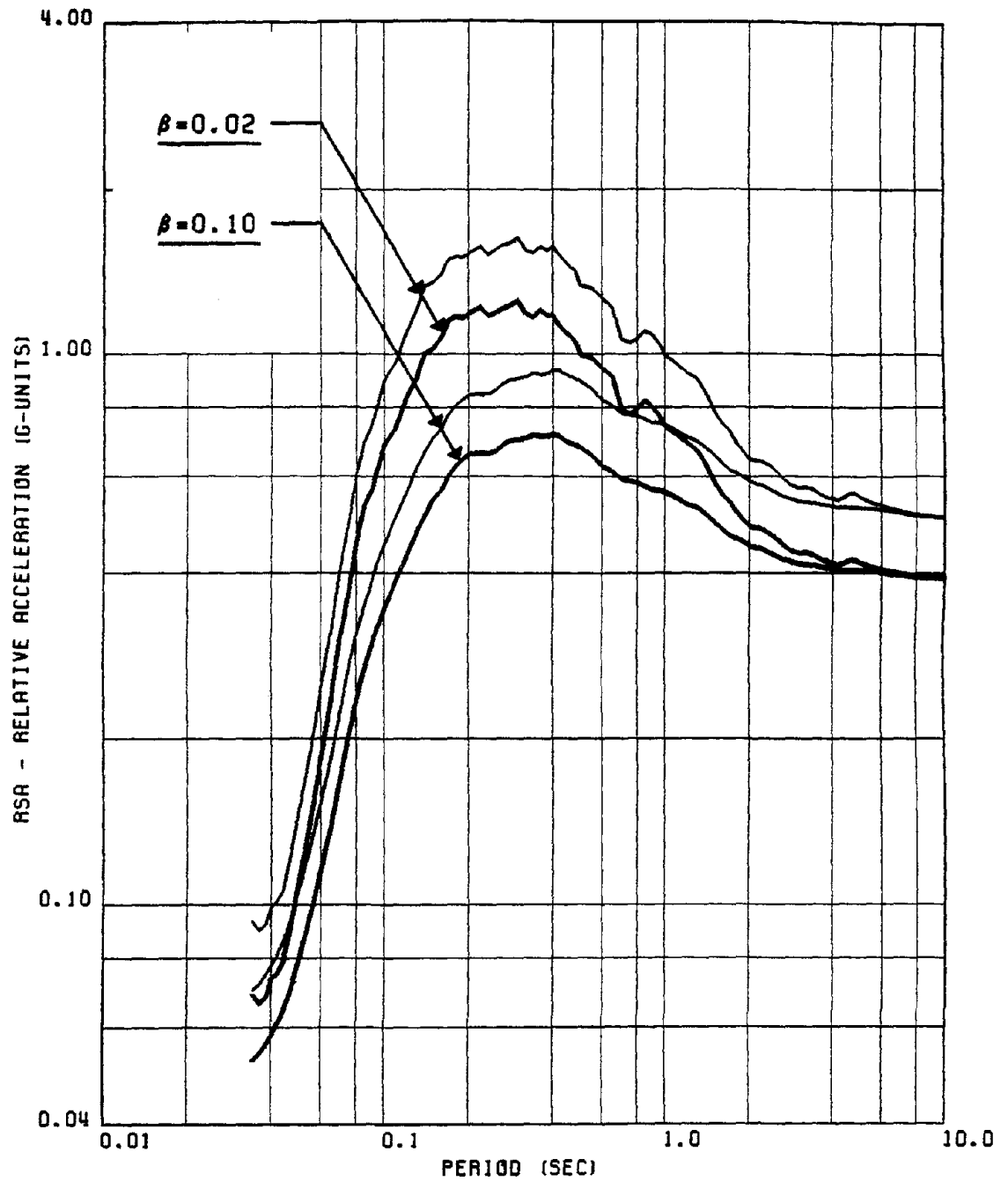
FIG. 127 COMPARISON OF THE PEAK & RMS NORMALIZED RSA SPECTRA FOR GROUP #1
NOTE : THE RMS NORMALIZED SPECTRA ARE INDICATED BY THE THICKER CURVES
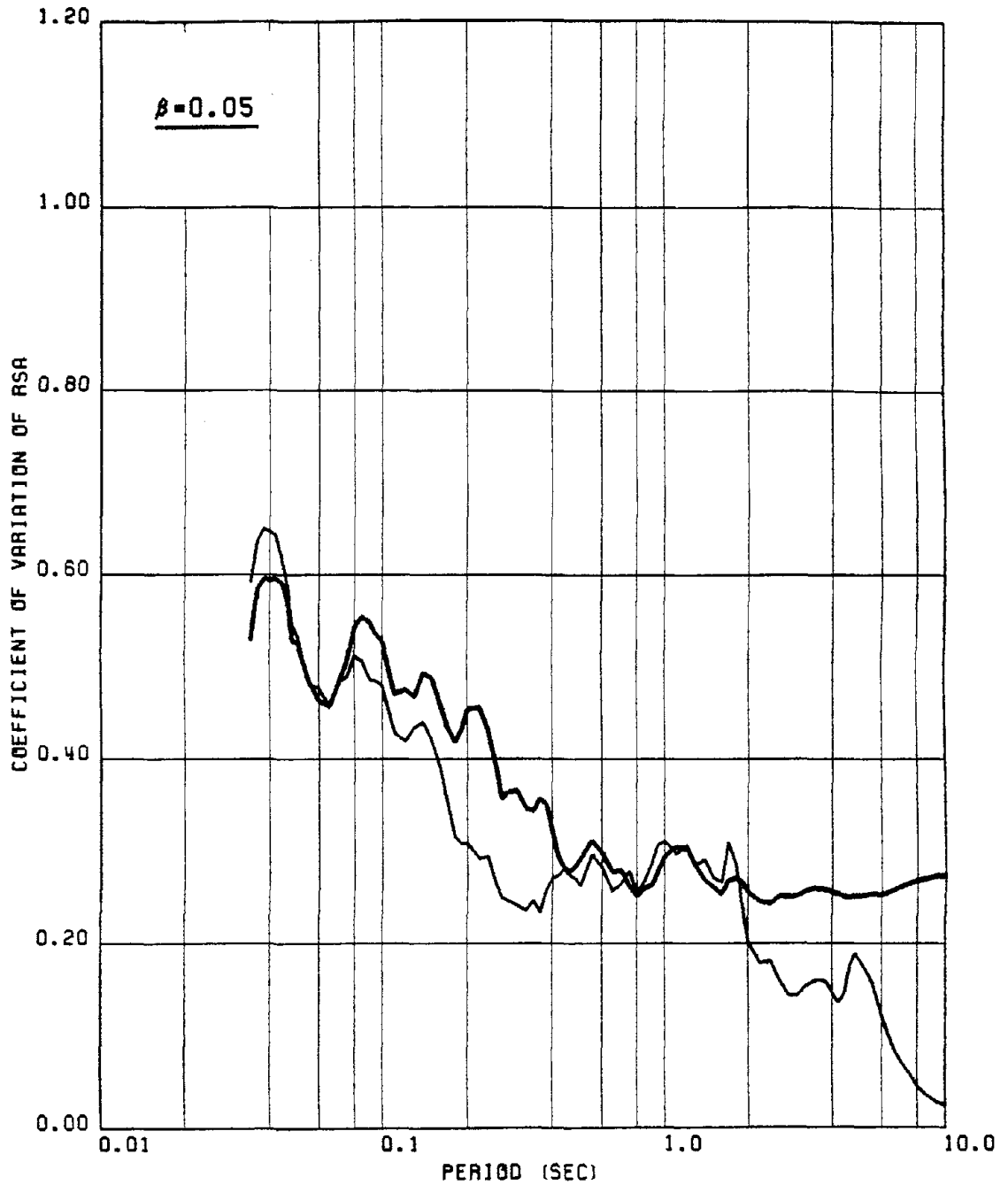
FIG. 128 COEFFICIENT OF VARIATION OF PEAK & RMS NORMALIZED RSA FOR GROUP #1
NOTE : THE RMS NORMALIZED SPECTRUM IS INDICATED BY THE THICKER CURVE
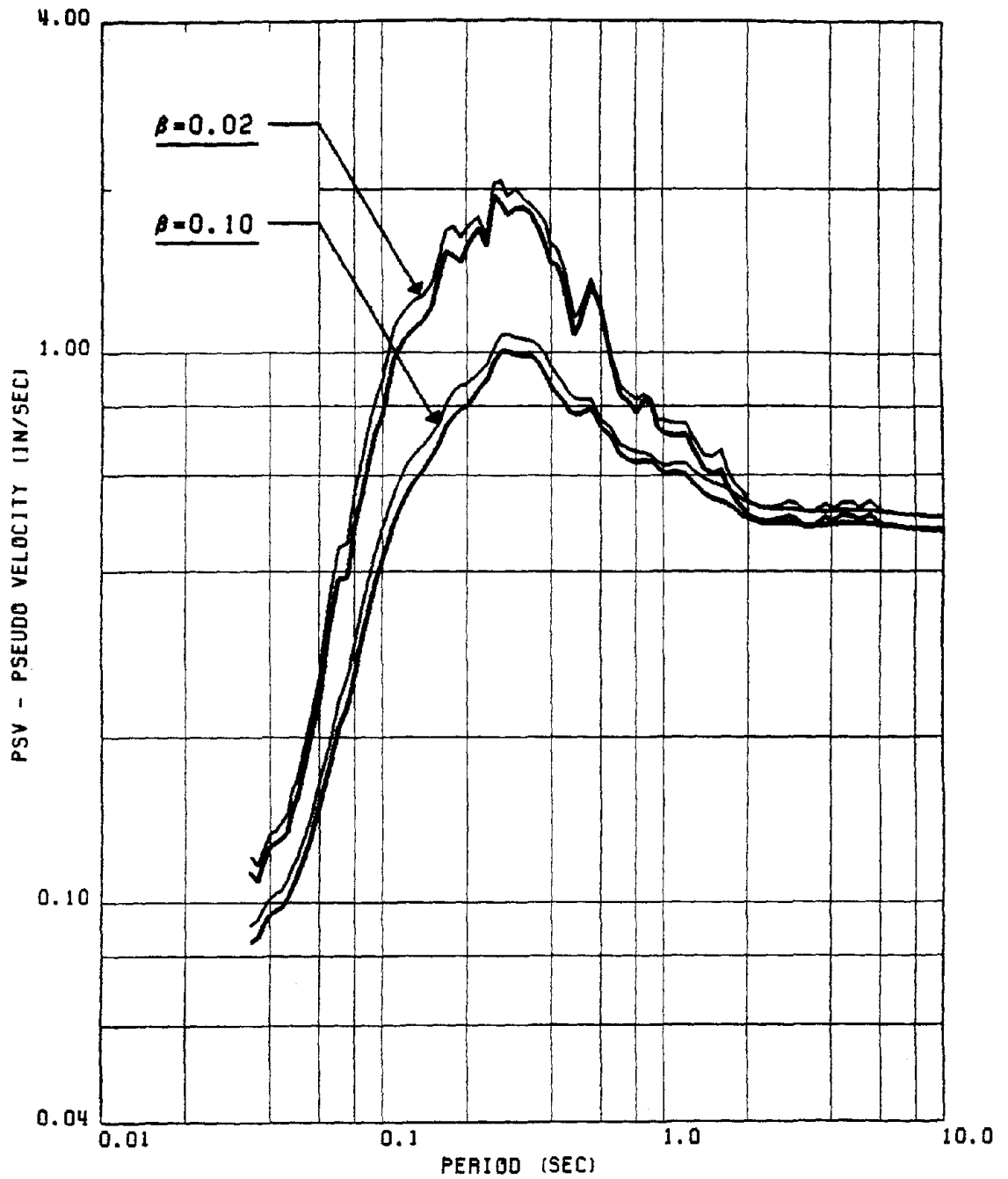
FIG. 129 COMPARISON OF THE PEAK & RMS NORMALIZED RSA SPECTRA FOR GROUP #4
NOTE : THE RMS NORMALIZED SPECTRA ARE INDICATED BY THE THICKER CURVES
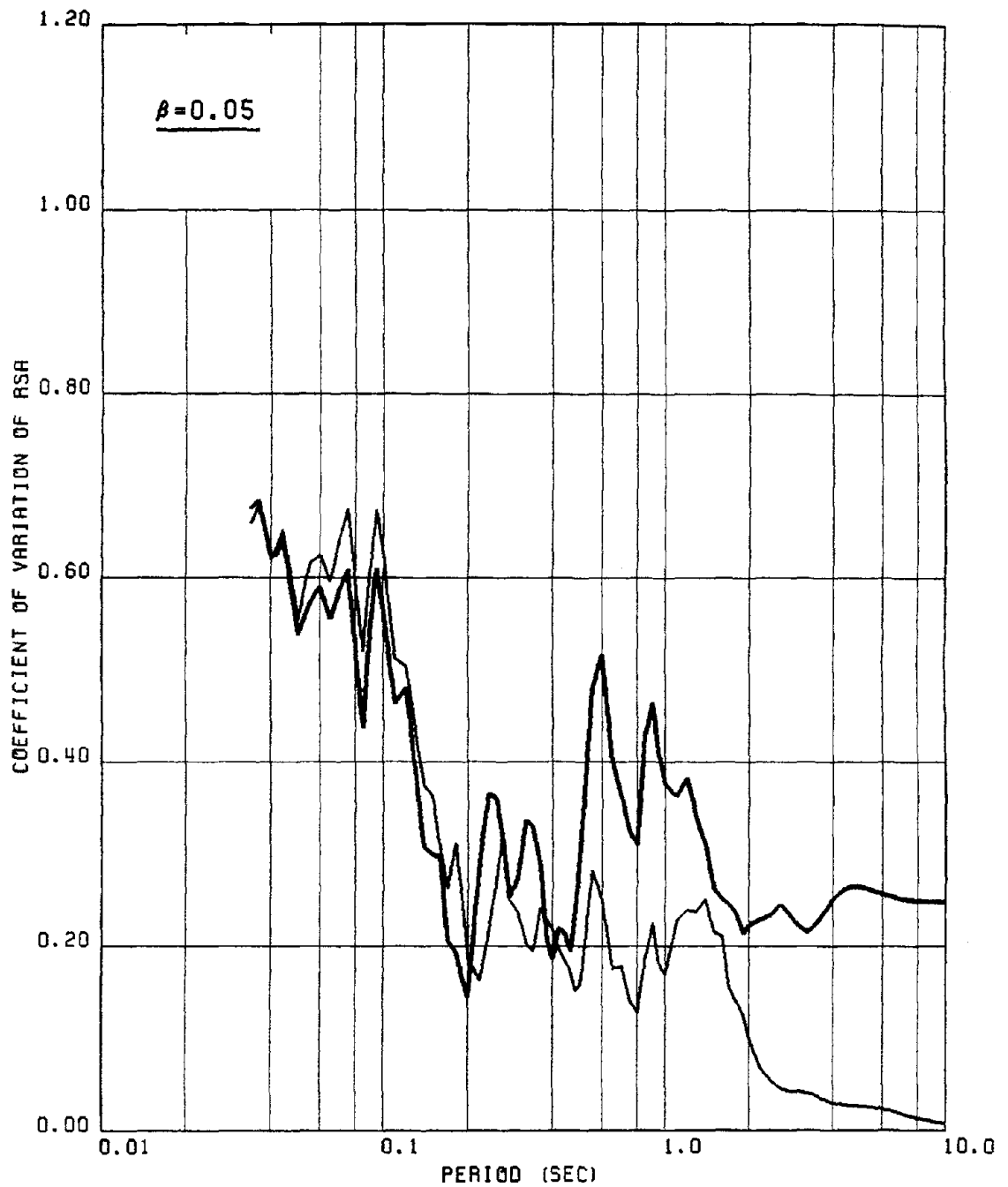
FIG. 130 COEFFICIENT OF VARIATION OF PEAK & RMS NORMALIZED RSA FOR GROUP #4
NOTE : THE RMS NORMALIZED SPECTRUM IS INDICATED BY THE THICKER CURVE
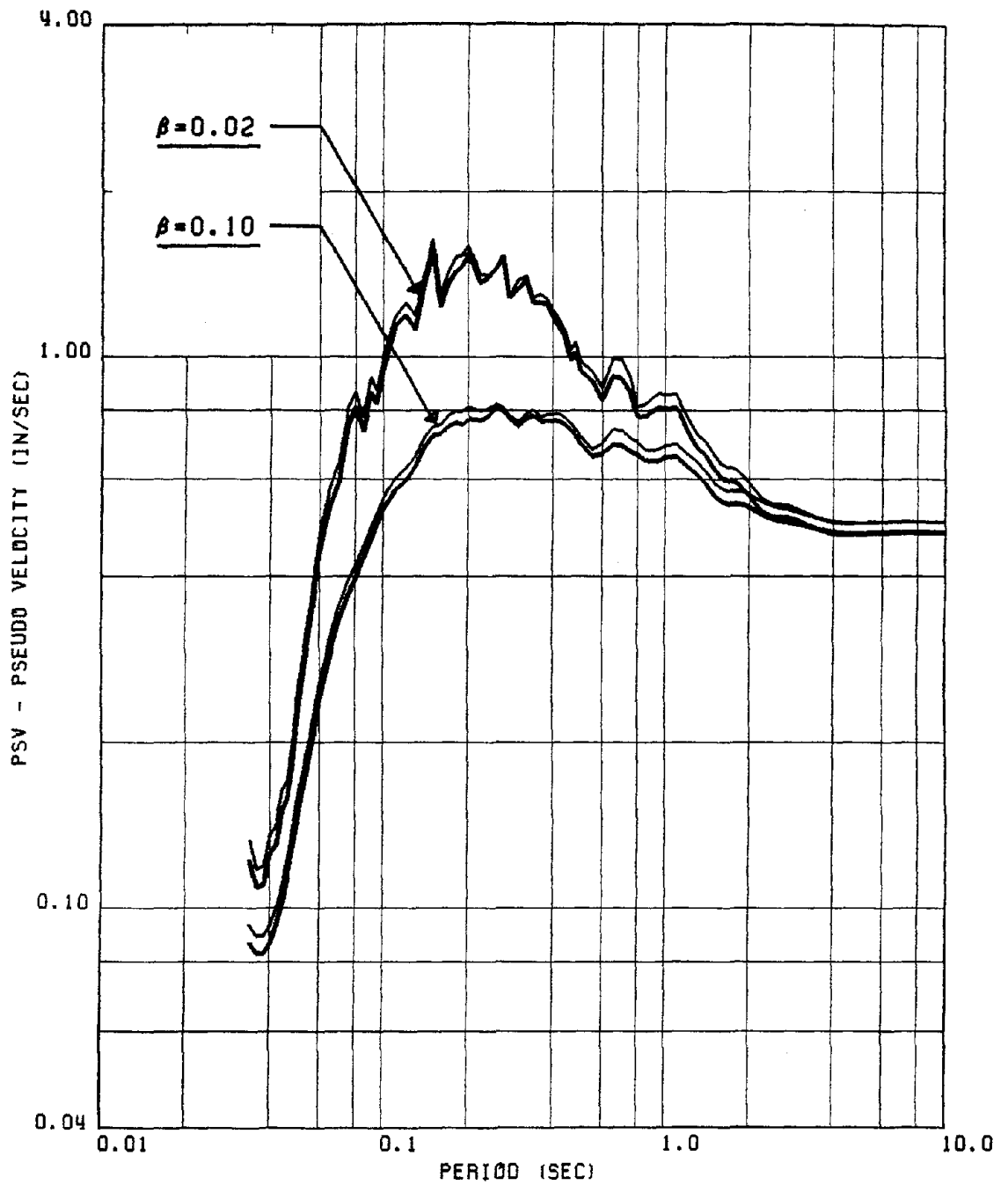
FIG. 131 COMPARISON OF THE PEAK & RMS NORMALIZED RSA SPECTRA FOR GROUP #5
NOTE : THE RMS NORMALIZED SPECTRA ARE INDICATED BY THE THICKER CURVES
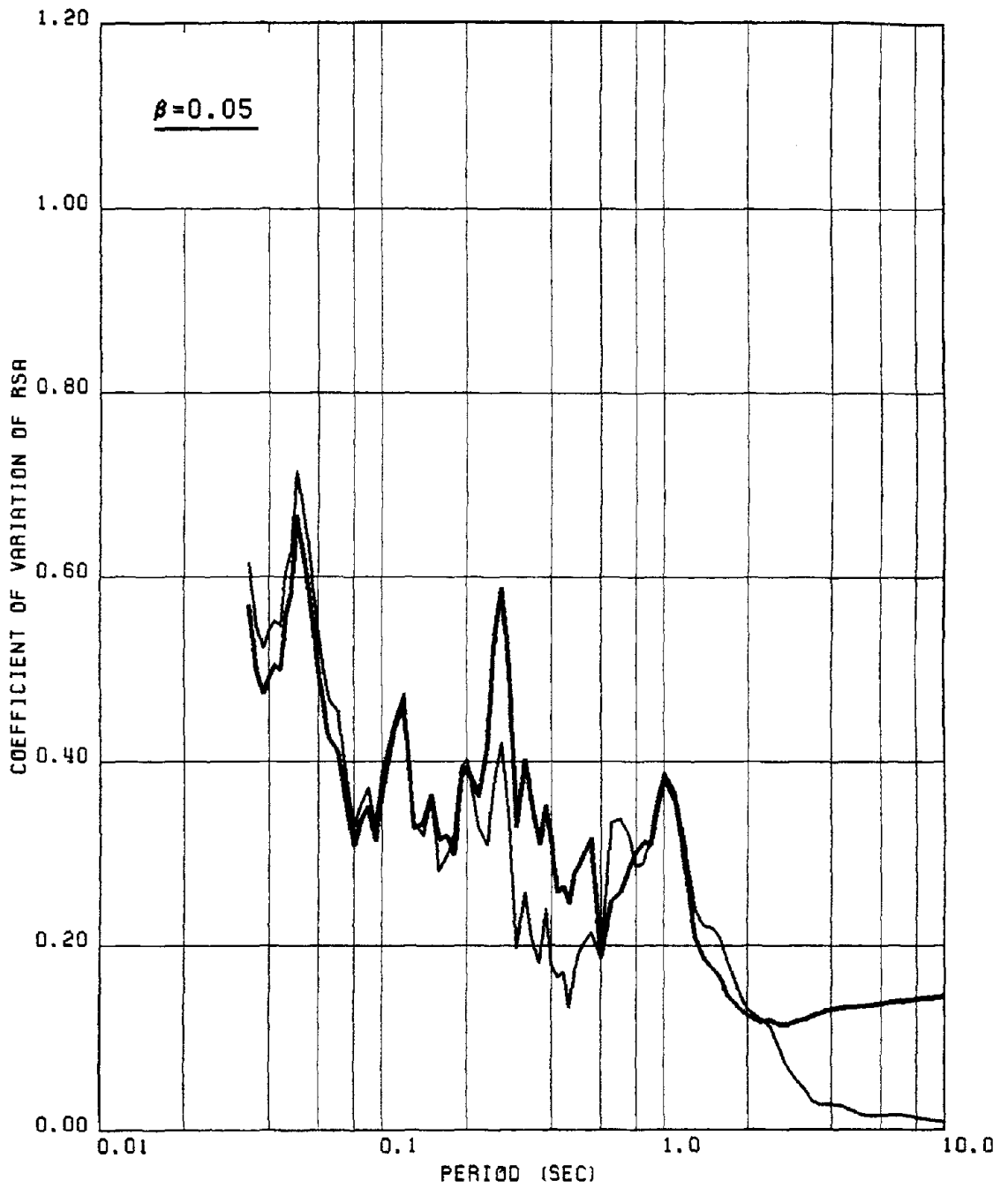
FIG. 132 COEFFICIENT OF VARIATION OF PEAK & RMS NORMALIZED RSA FOR GROUP #5
NOTE : THE RMS NORMALIZED SPECTRUM IS INDICATED BY THE THICKER CURVE
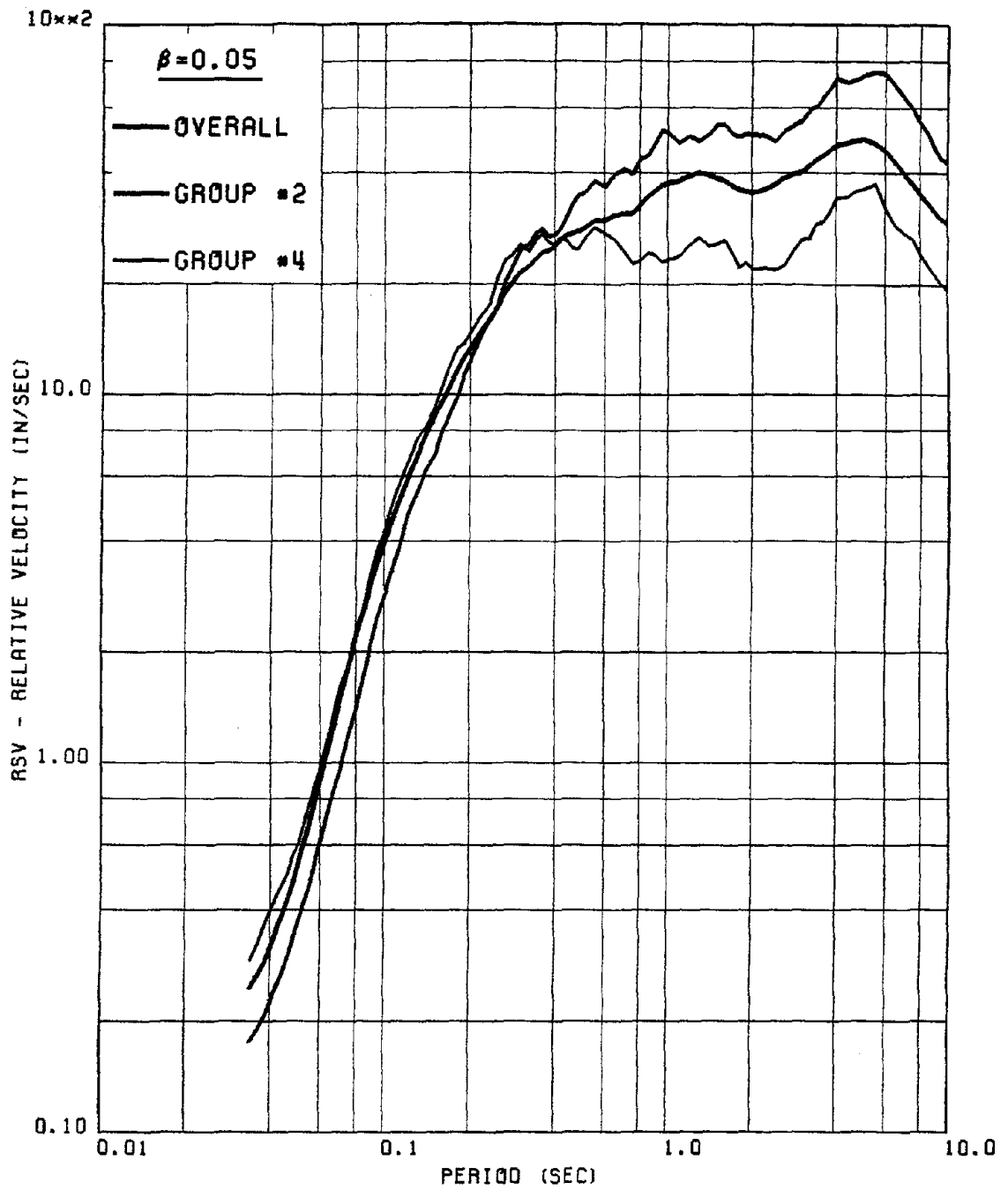
FIG. 133 COMPARISON BETWEEN THE OVERALL 'HORIZONTAL' RSV AND THE SPECTRUM
AND THE 'HORIZONTAL' RSV SPECTRA CORRESPONDING TO GROUPS #2 AND 4
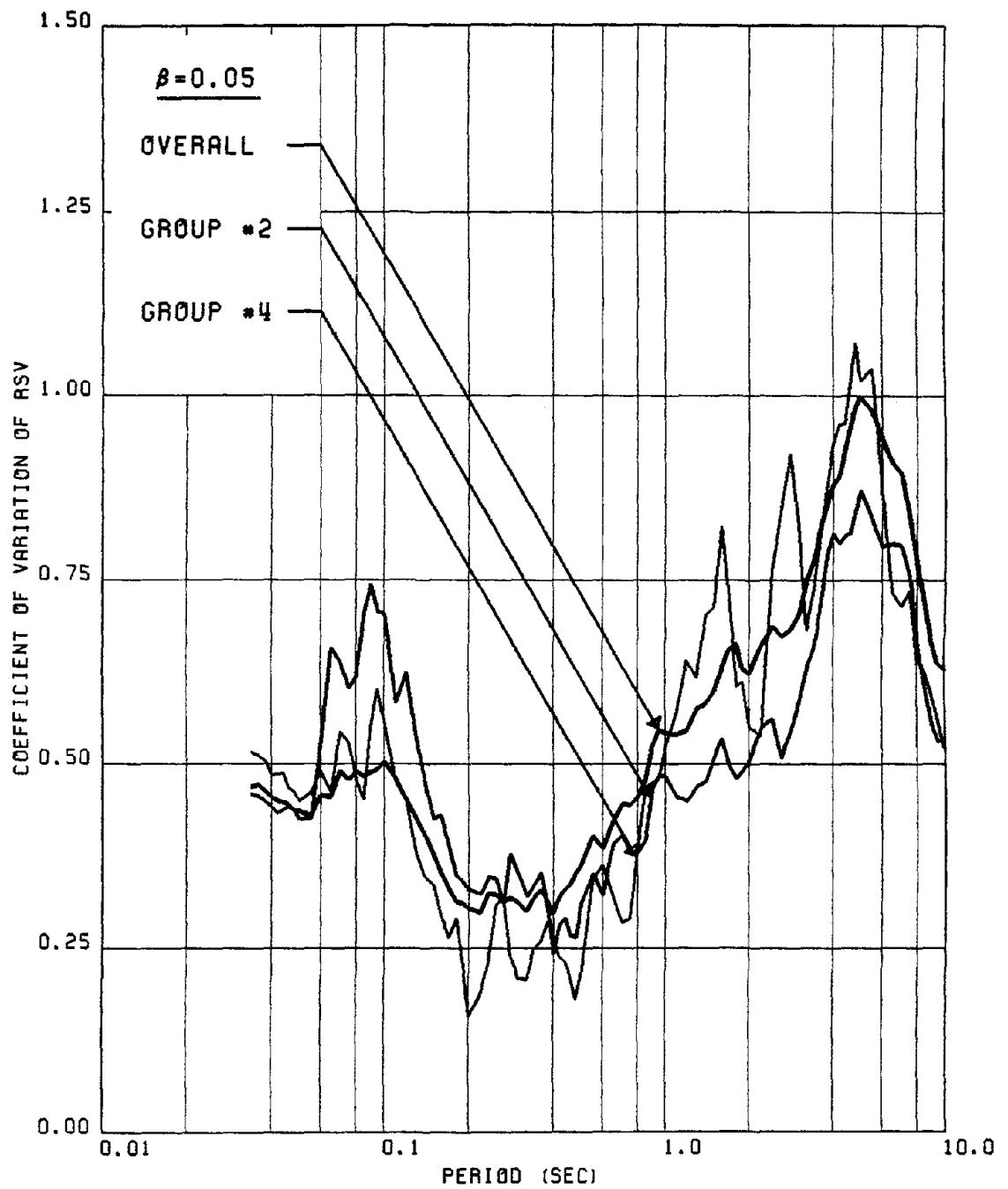
FIG. 134 COMPARISON BETWEEN THE COEFFICIENT OF VARIATION SPECTRA OF 'HORIZONTAL' RSV FOR THE OVERALL ENSEMBLE, AND FOR GROUPS #2 & 4
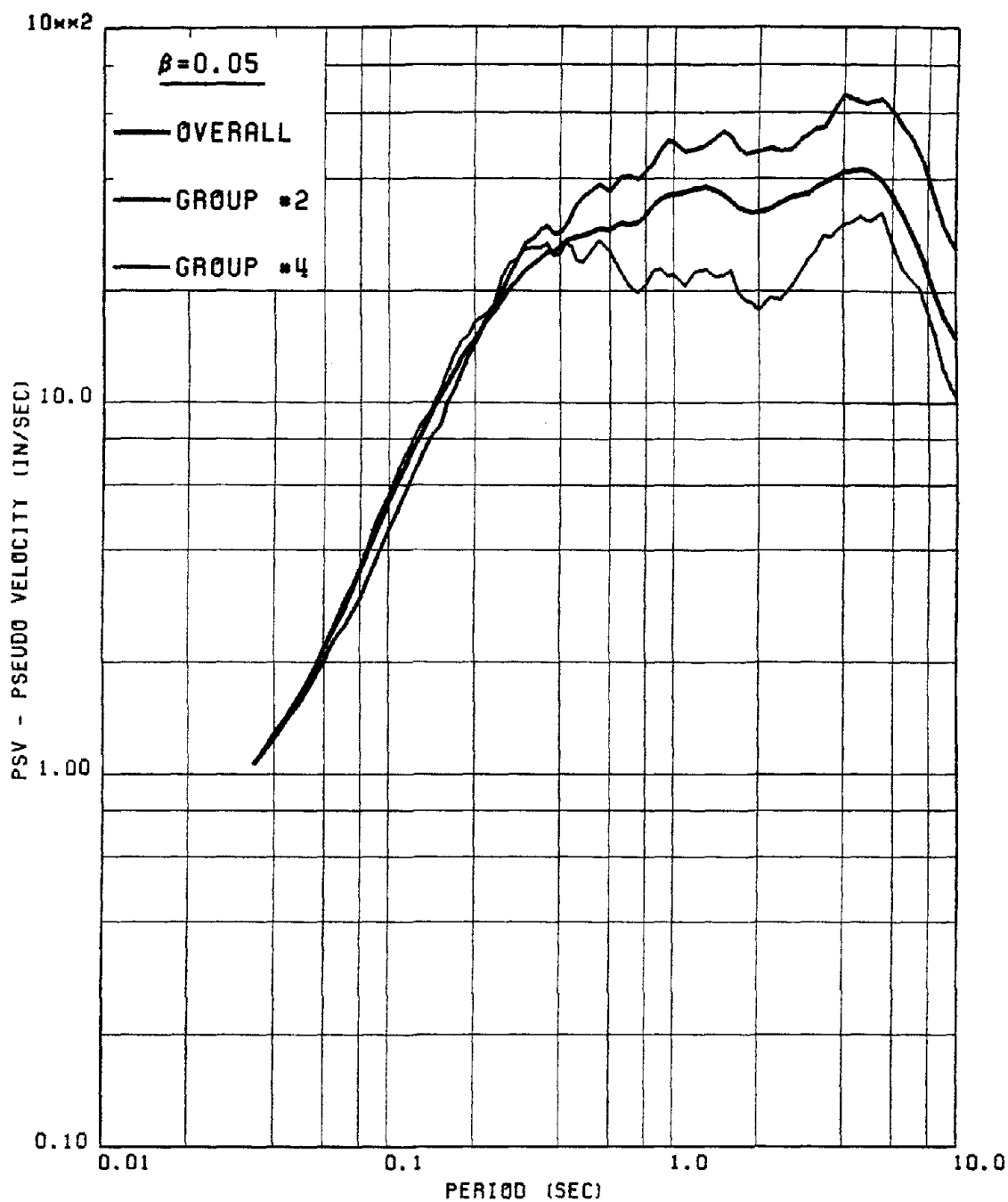
FIG. 135 COMPARISON BETWEEN THE OVERALL 'HORIZONTAL' PSV AND THE SPECTRUM
AND THE 'HORIZONTAL' PSV SPECTRA CORRESPONDING TO GROUPS #2 AND 4
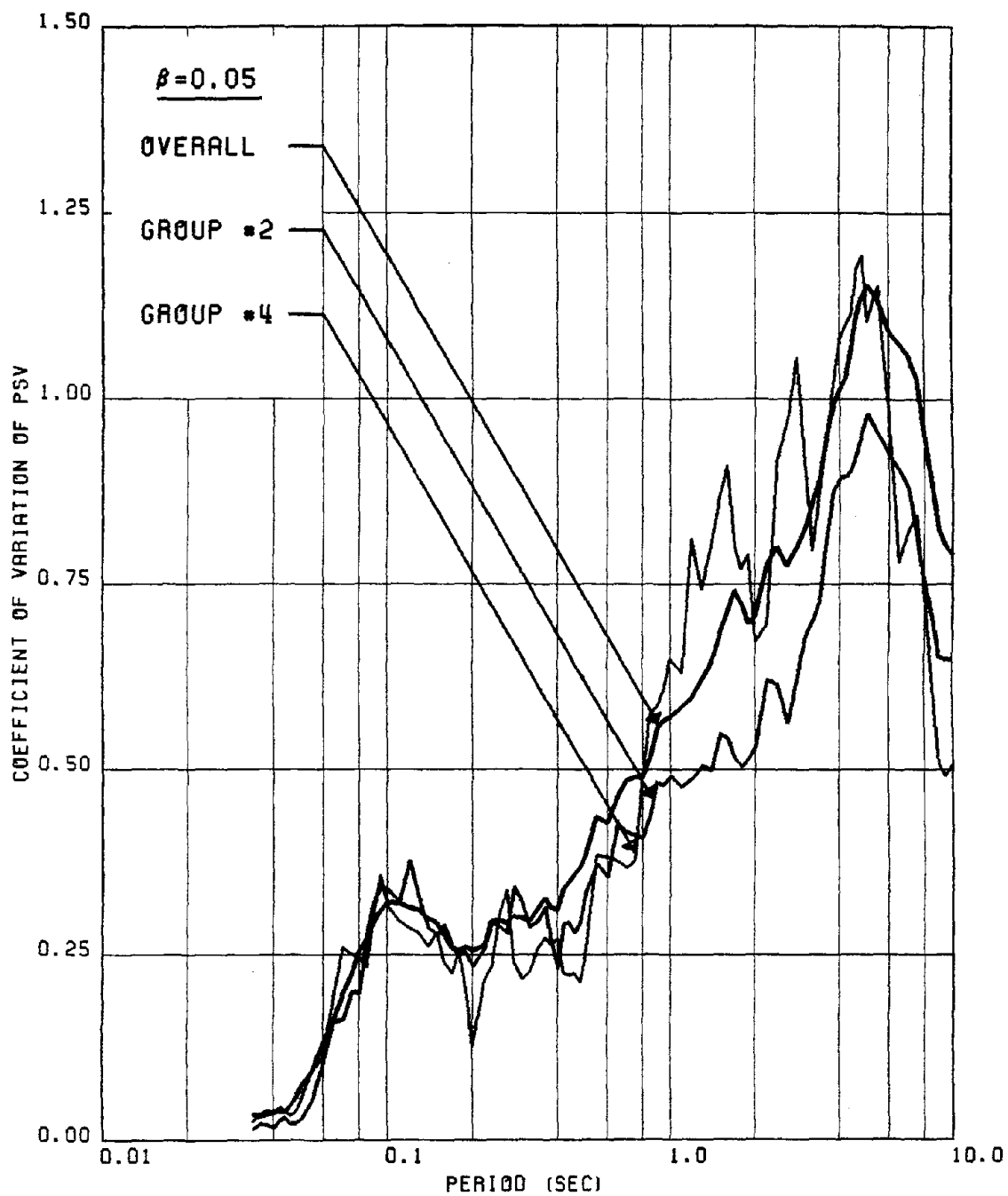
FIG. 136 COMPARISON BETWEEN THE COEFFICIENT OF VARIATION SPECTRA OF 'HORIZONTAL' PSV FOR THE OVERALL ENSEMBLE, AND FOR GROUPS #2 & 4
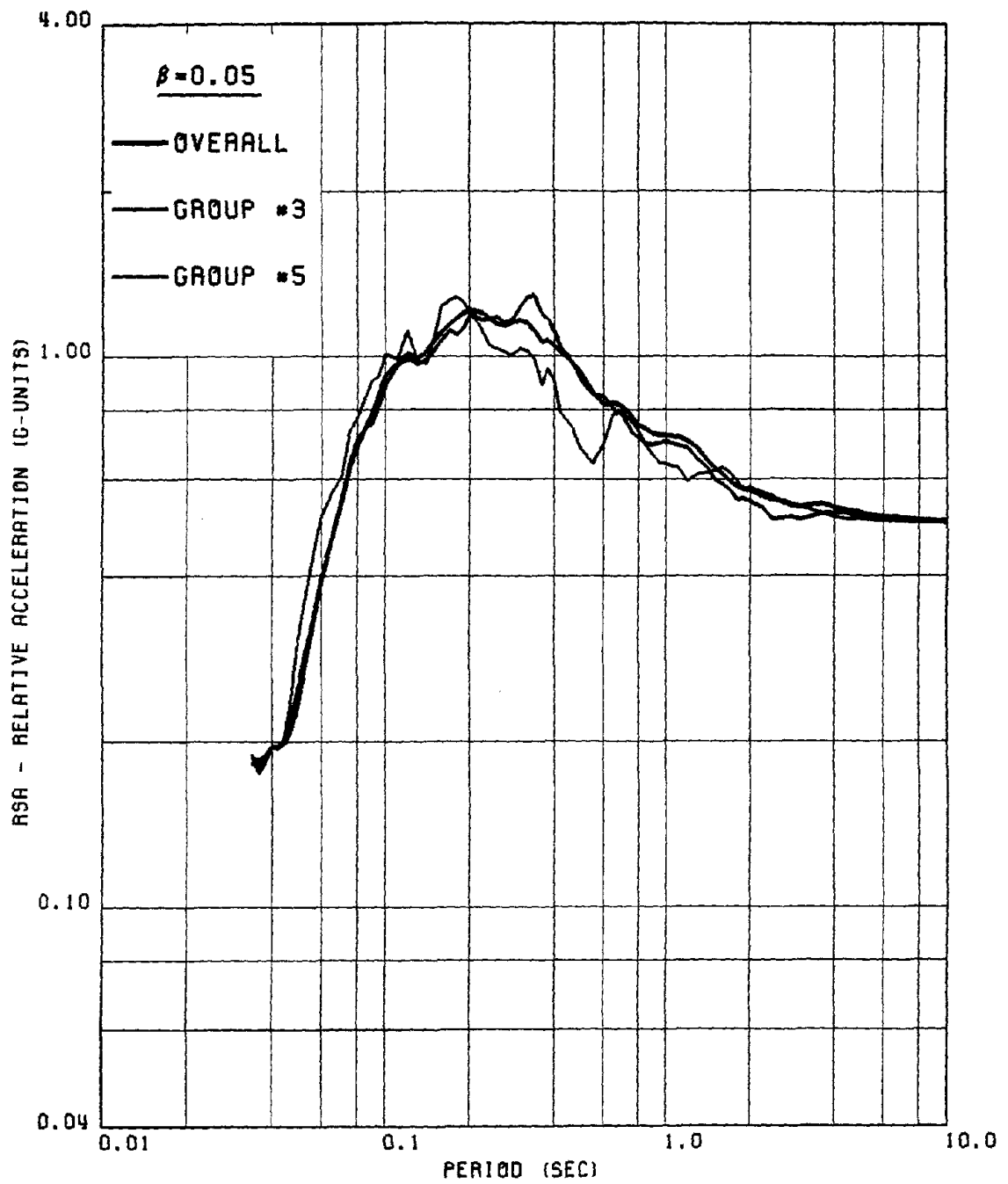
FIG. 137 COMPARISON BETWEEN THE OVERALL 'VERTICAL' RSA AND THE SPECTRUM
AND THE 'VERTICAL' RSA SPECTRA CORRESPONDING TO GROUPS #3 AND 5
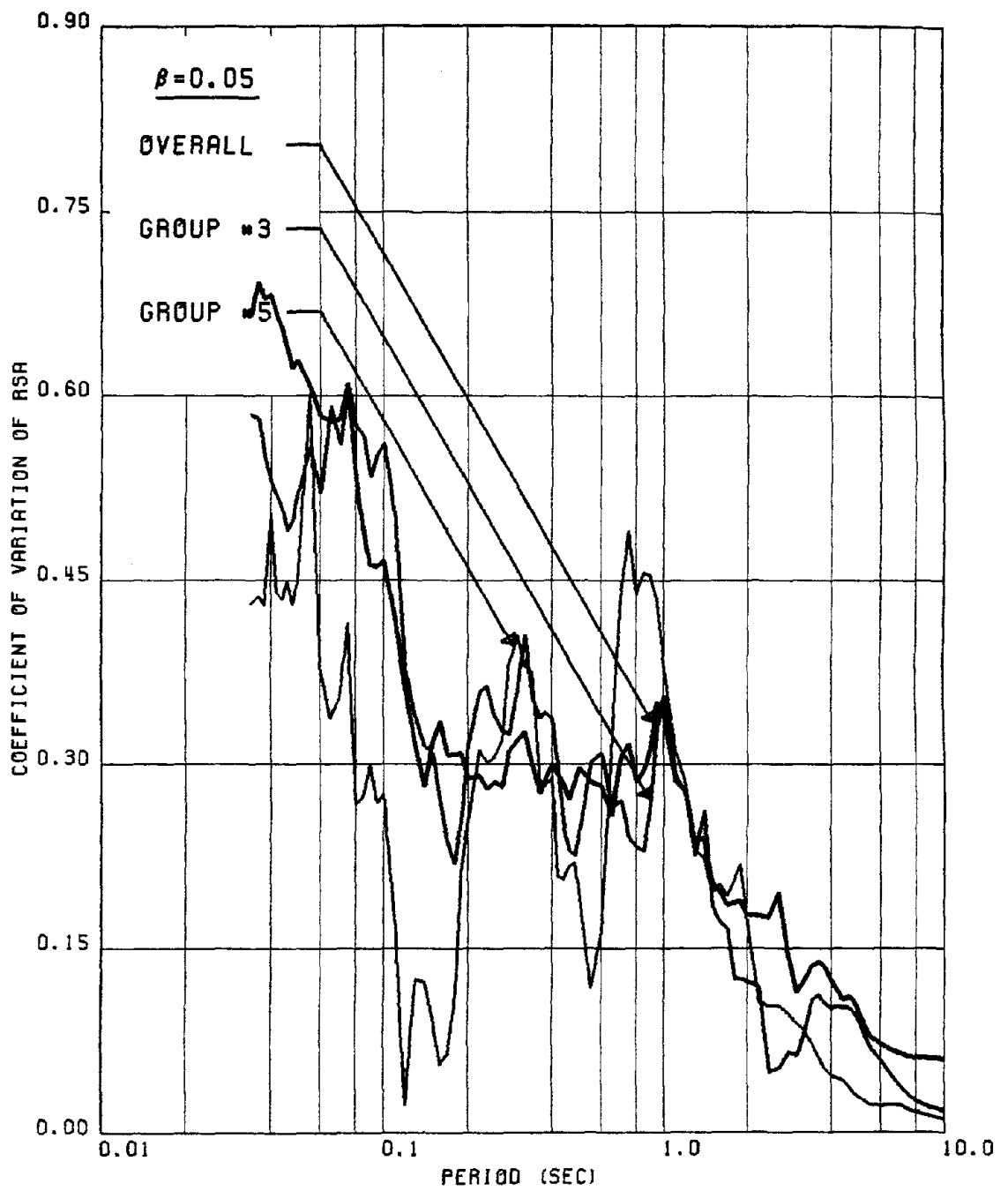
FIG. 13B COMPARISON BETWEEN THE COEFFICIENT OF VARIATION SPECTRA OF
'VERTICAL' RSA FOR THE OVERALL ENSEMBLE, AND FOR GROUPS #3 & 5
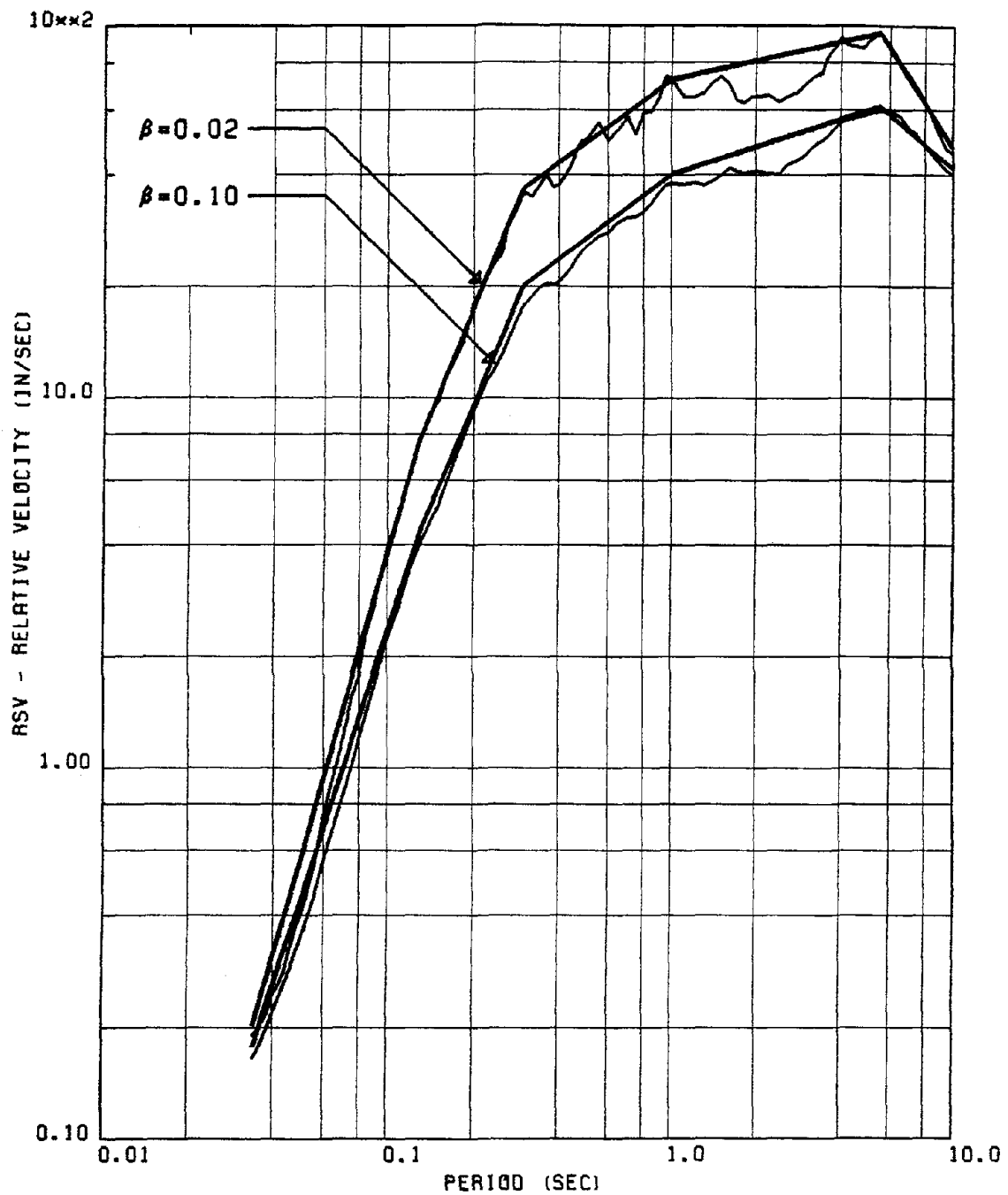
FIG. 139 COMPARISON OF THE PROPOSED AND COMPUTED RSV SPECTRA FOR GROUP #2H
NOTE : THE ABOVE COMPARISON HAS BEEN SHOWN FOR THE MEAN RESPONSE QUANTITY
NOTE : THE PROPOSED SPECTRA ARE REPRESENTED BY A SERIES OF STRAIGHT LINES
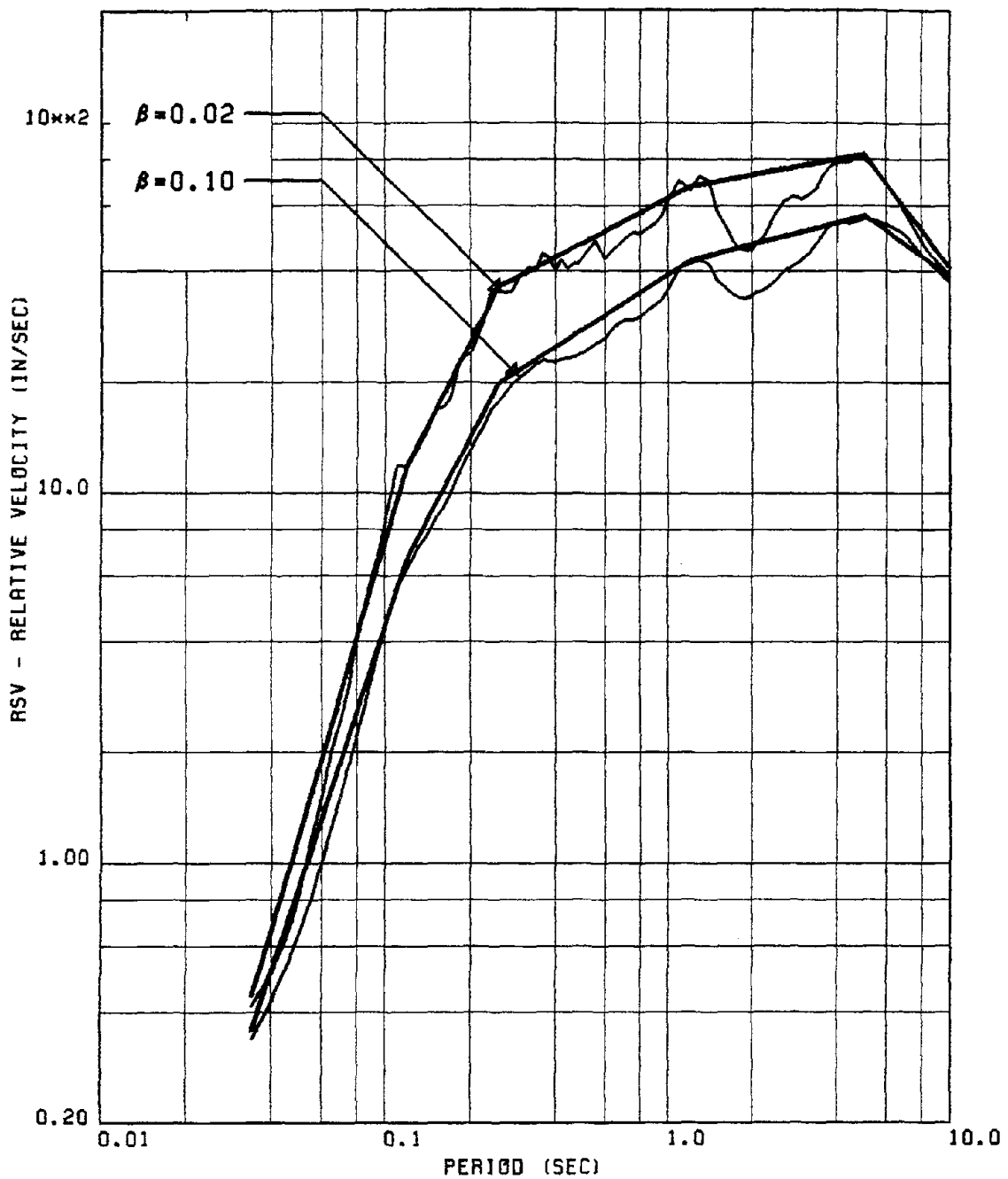
FIG. 140 COMPARISON OF THE PROPOSED AND COMPUTED RSV SPECTRA FOR GROUP *3H
NOTE : THE ABOVE COMPARISON HAS BEEN SHOWN FOR (MEAN+SD) RESPONSE QUANTITY
NOTE : THE PROPOSED SPECTRA ARE REPRESENTED BY A SERIES OF STRAIGHT LINES
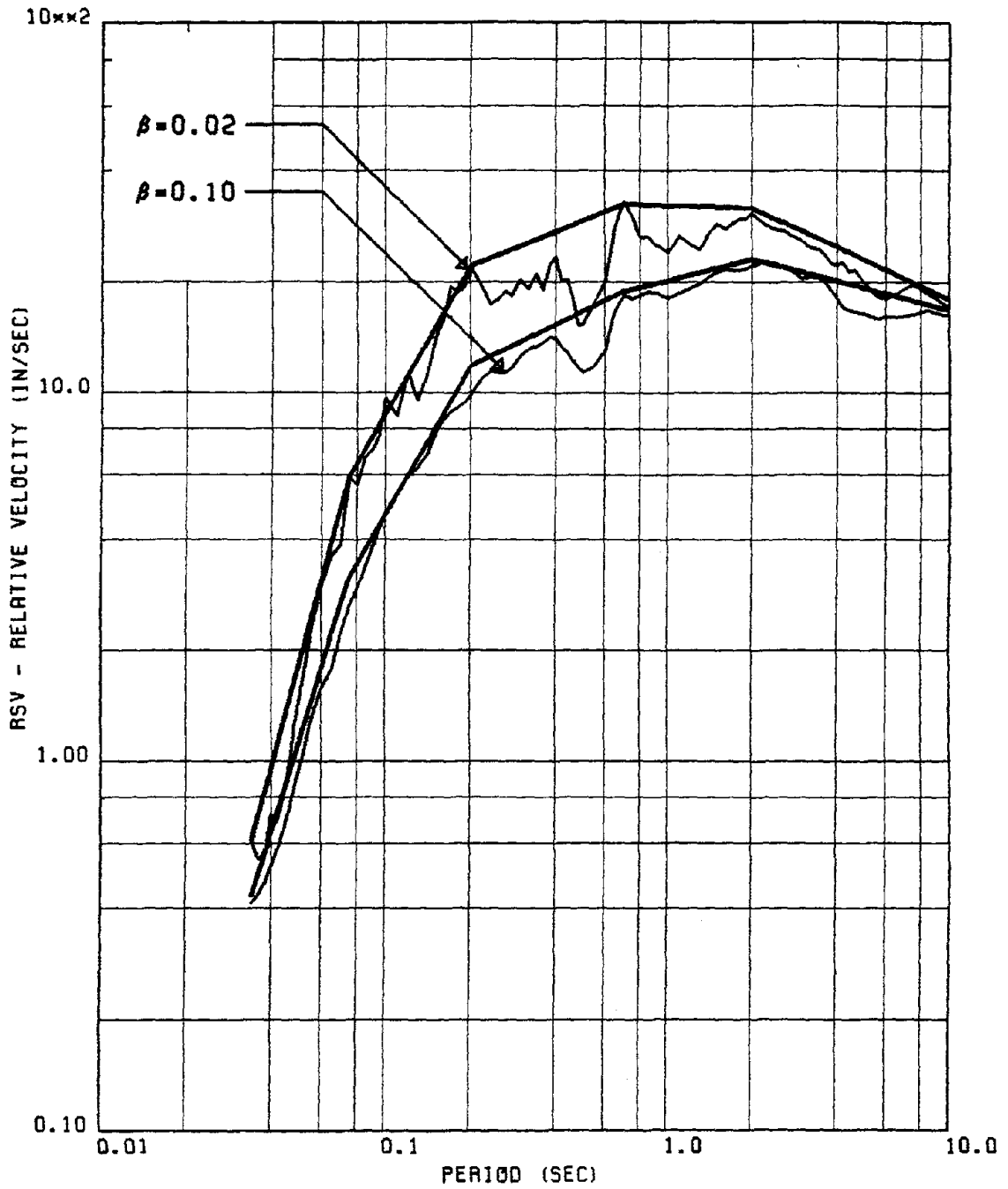
FIG. 141 COMPARISON OF THE PROPOSED AND COMPUTED RSV SPECTRA FOR GROUP #5V
NOTE : THE ABOVE COMPARISON HAS BEEN SHOWN FOR THE MEAN RESPONSE QUANTITY
NOTE : THE PROPOSED SPECTRA ARE REPRESENTED BY A SERIES OF STRAIGHT LINES
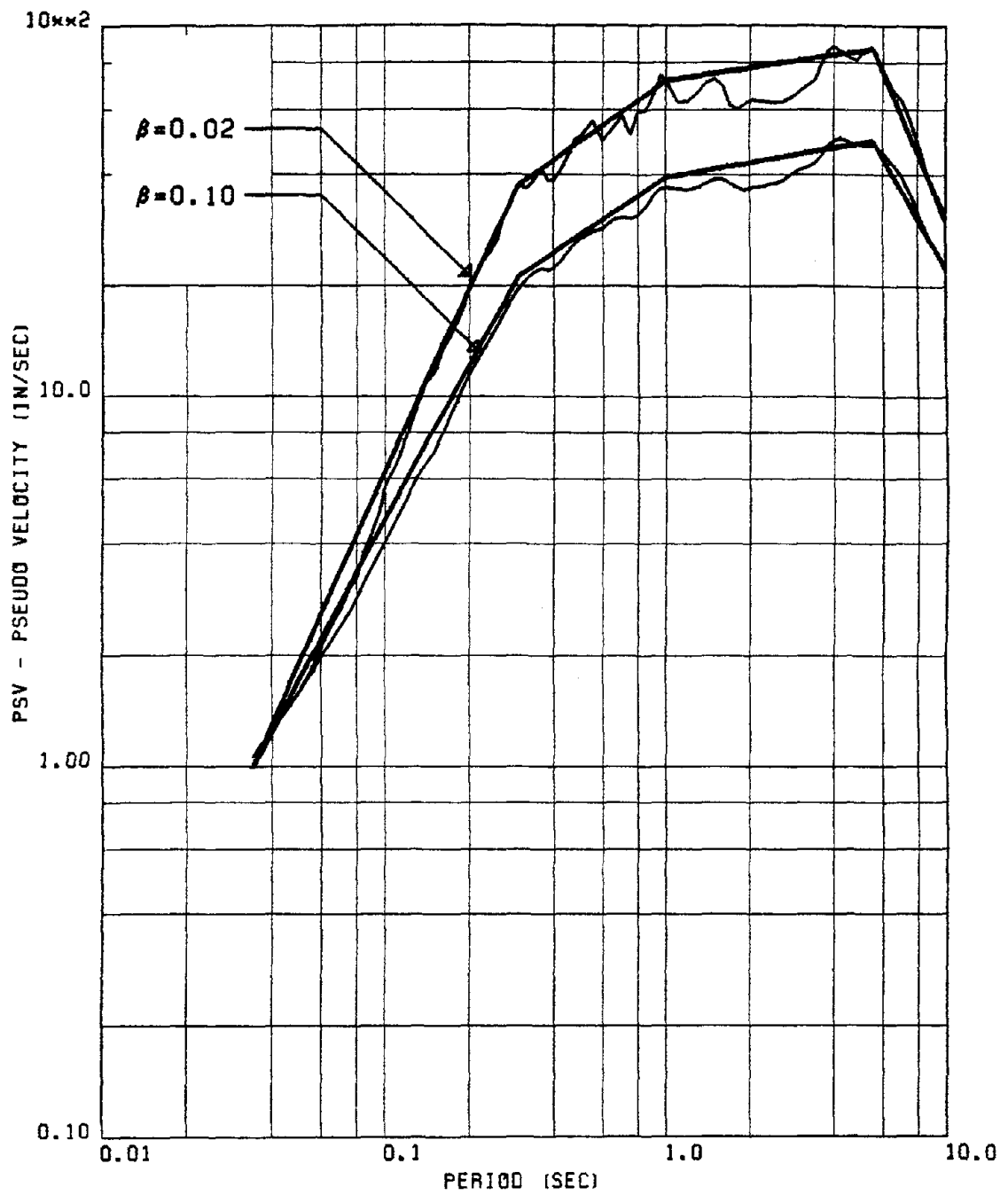
FIG. 142 COMPARISON OF THE PROPOSED AND COMPUTED PSV SPECTRA FOR GROUP #2H
NOTE : THE ABOVE COMPARISON HAS BEEN SHOWN FOR THE MEAN RESPONSE QUANTITY
NOTE : THE PROPOSED SPECTRA ARE REPRESENTED BY A SERIES OF STRAIGHT LINES
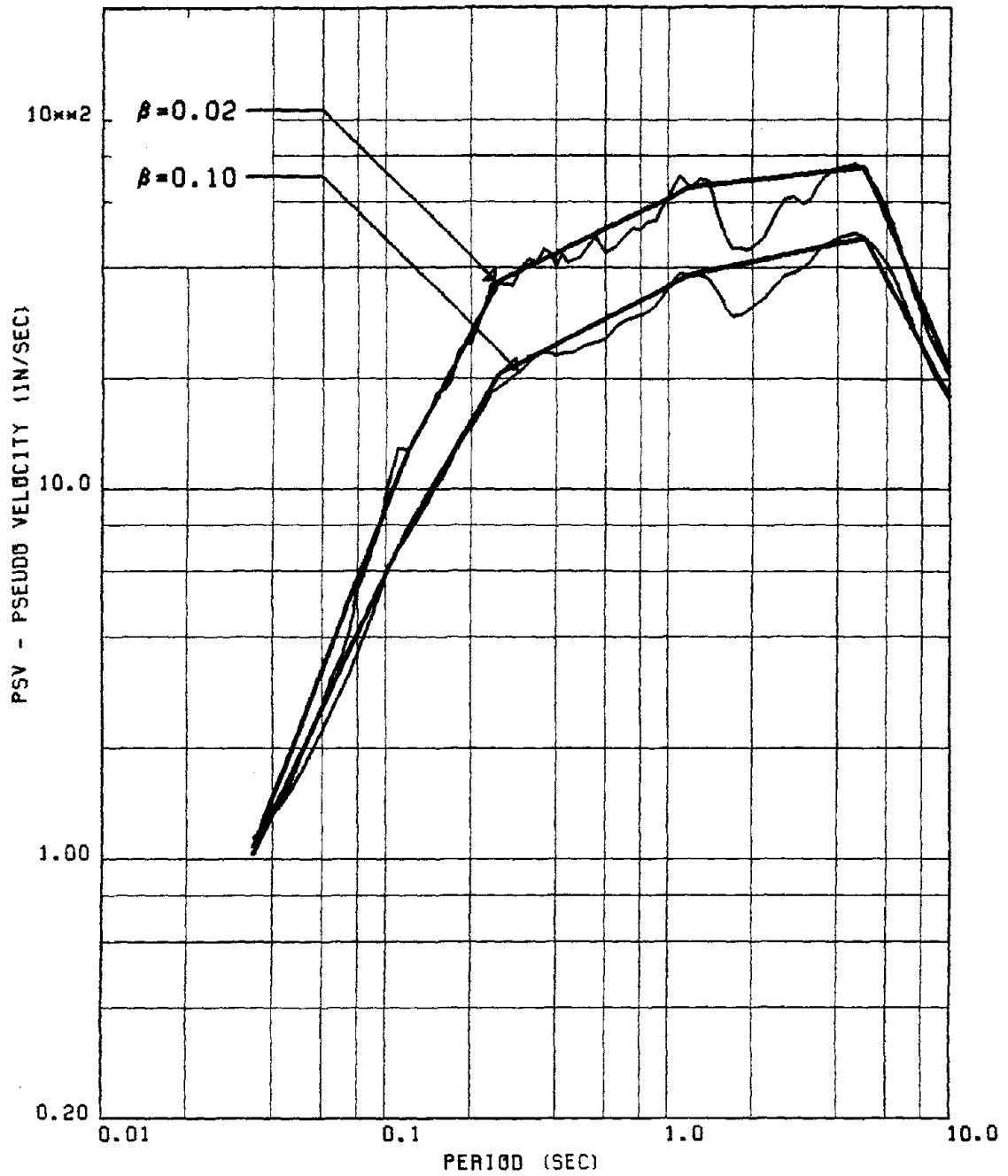
FIG. 143 COMPARISON OF THE PROPOSED AND COMPUTED PSV SPECTRA FOR GROUP *3H
NOTE : THE ABOVE COMPARISON HAS BEEN SHOWN FOR (MEAN+SD) RESPONSE QUANTITY
NOTE : THE PROPOSED SPECTRA ARE REPRESENTED BY A SERIES OF STRAIGHT LINES
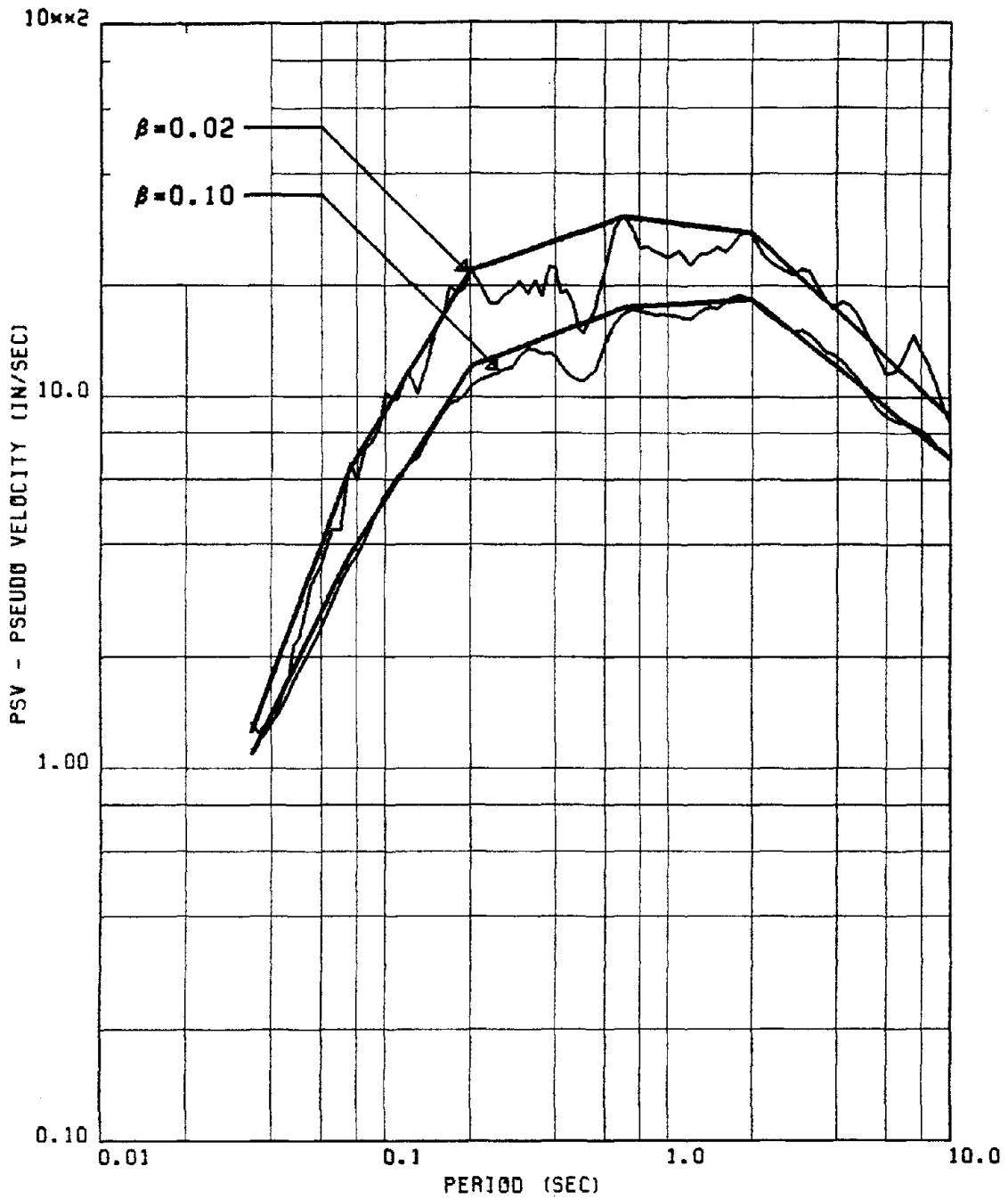
FIG. 144 COMPARISON OF THE PROPOSED AND COMPUTED PSV SPECTRA FOR GROUP *5V
NOTE : THE ABOVE COMPARISON HAS BEEN SHOWN FOR THE MEAN RESPONSE QUANTITY
NOTE : THE PROPOSED SPECTRA ARE REPRESENTED BY A SERIES OF STRAIGHT LINES
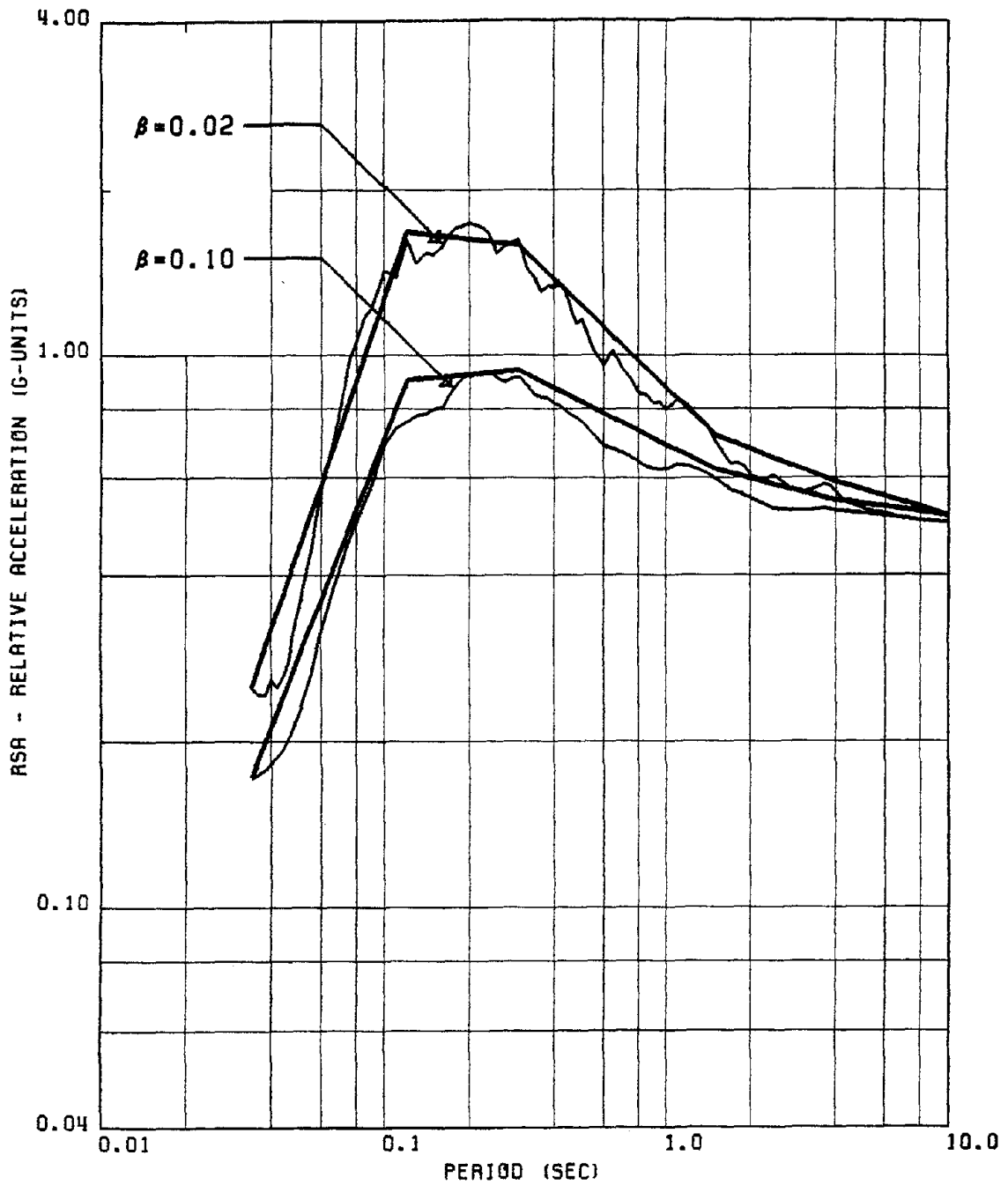
FIG. 145 COMPARISON OF THE PROPOSED AND COMPUTED RSA SPECTRA FOR GROUP *1V
NOTE : THE ABOVE COMPARISON HAS BEEN SHOWN FOR THE MEAN RESPONSE QUANTITY
NOTE : THE PROPOSED SPECTRA ARE REPRESENTED BY A SERIES OF STRAIGHT LINES
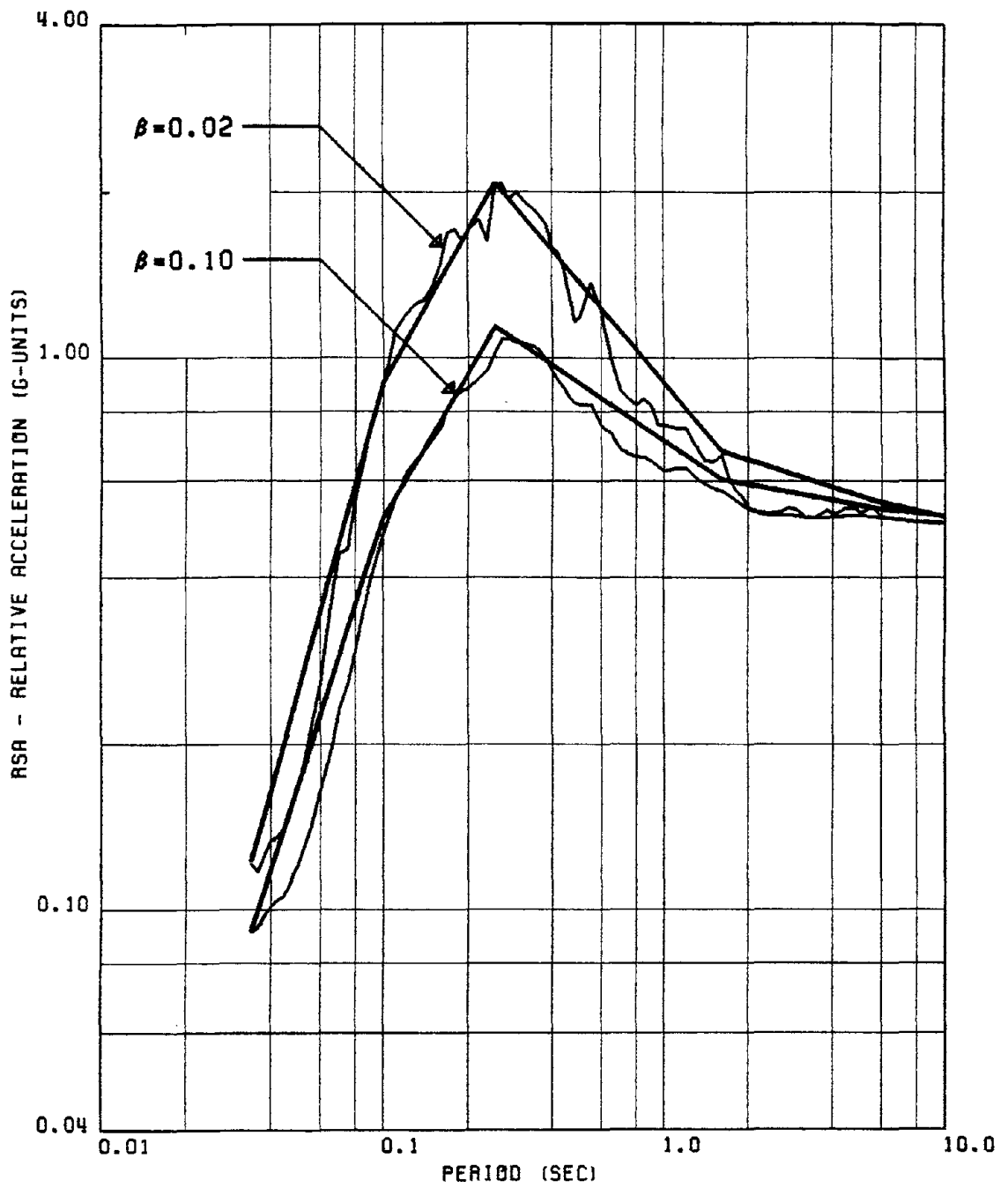
FIG. 146 COMPARISON OF THE PROPOSED AND COMPUTED RSA SPECTRA FOR GROUP #4H
NOTE : THE ABOVE COMPARISON HAS BEEN SHOWN FOR THE MEAN RESPONSE QUANTITY
NOTE : THE PROPOSED SPECTRA ARE REPRESENTED BY A SERIES OF STRAIGHT LINES
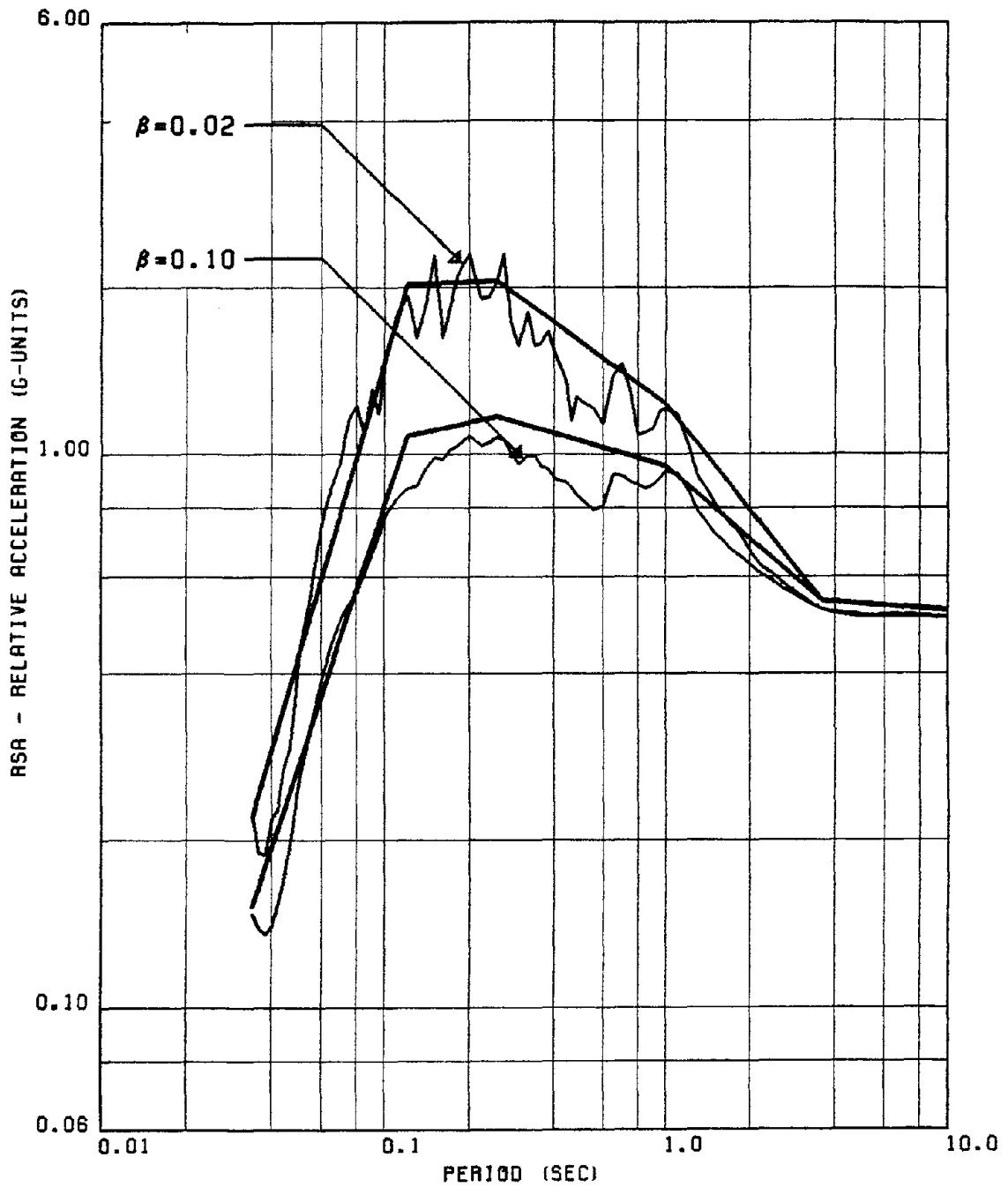
FIG. 147 COMPARISON OF THE PROPOSED AND COMPUTED RSA SPECTRA FOR GROUP #5H
NOTE : THE ABOVE COMPARISON HAS BEEN SHOWN FOR (MEAN+SD) RESPONSE QUANTITY
NOTE : THE PROPOSED SPECTRA ARE REPRESENTED BY A SERIES OF STRAIGHT LINES
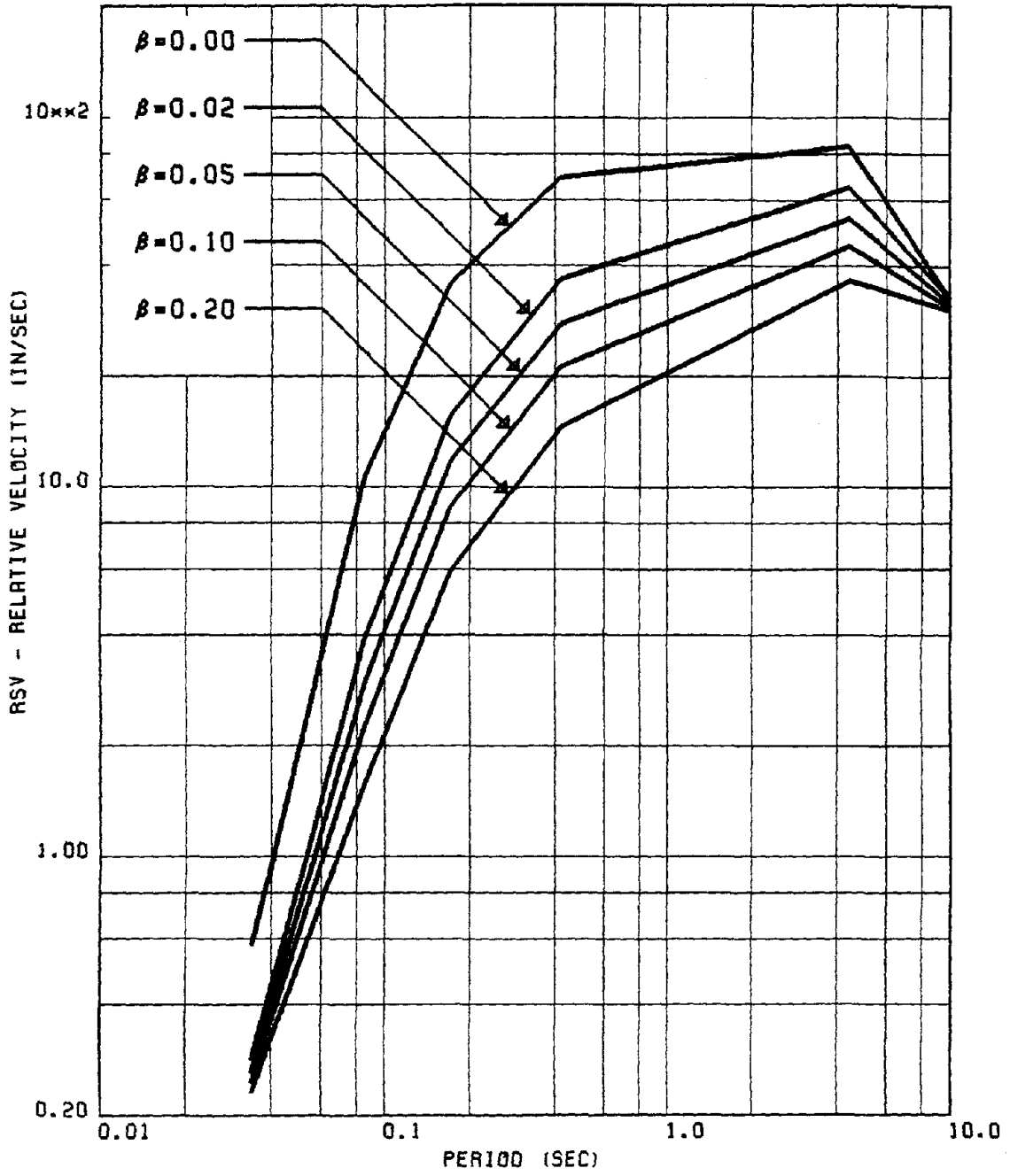
FIG. 148 PROPOSED SPECTRA FOR MEAN RSV FOR HORIZONTAL RECORDS OF GROUP #1
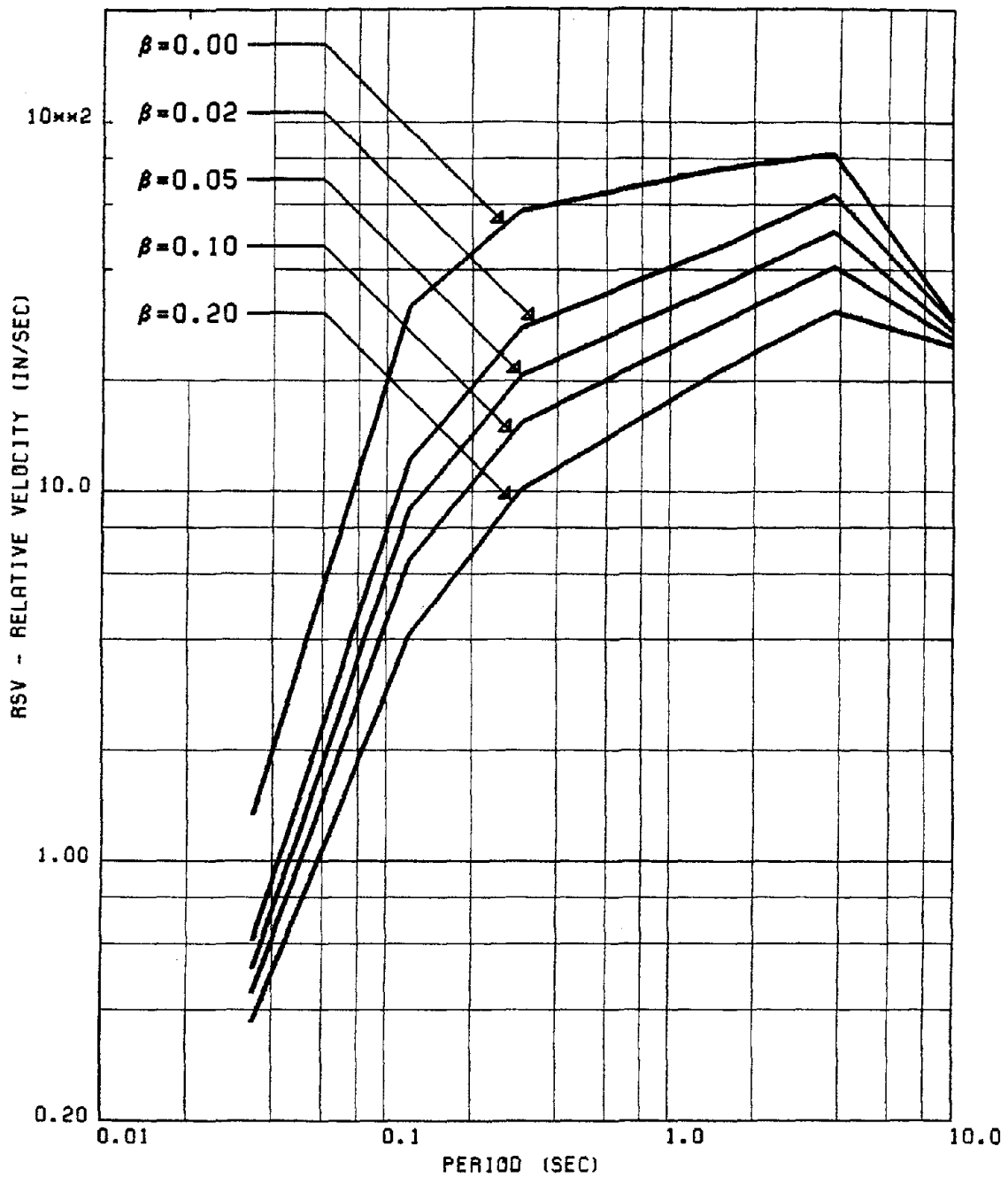
FIG. 149 PROPOSED SPECTRA FOR MEAN RSV FOR VERTICAL RECORDS OF GROUP #1
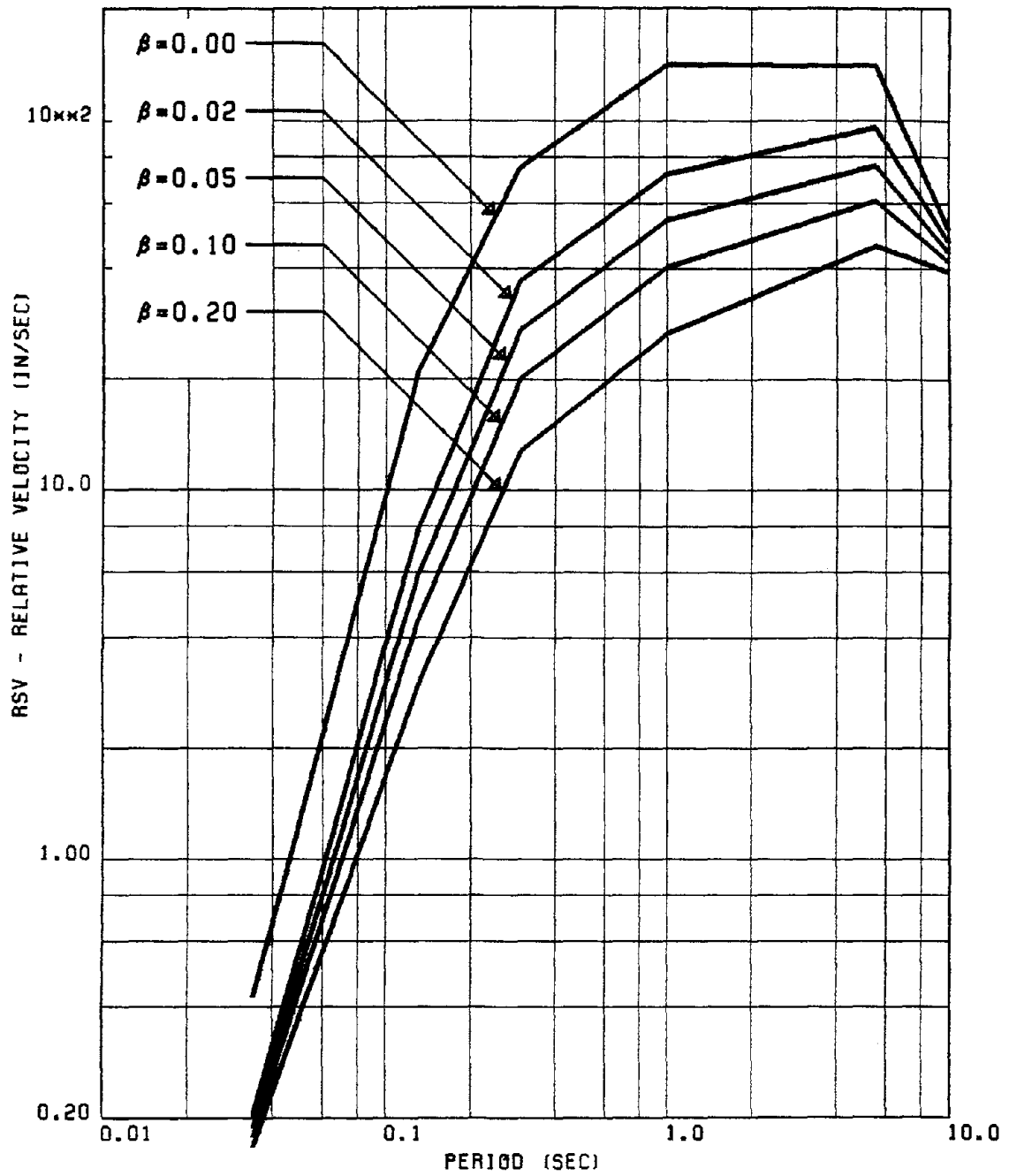
FIG. 150 PROPOSED SPECTRA FOR MEAN RSV FOR HORIZONTAL RECORDS OF GROUP #2

228
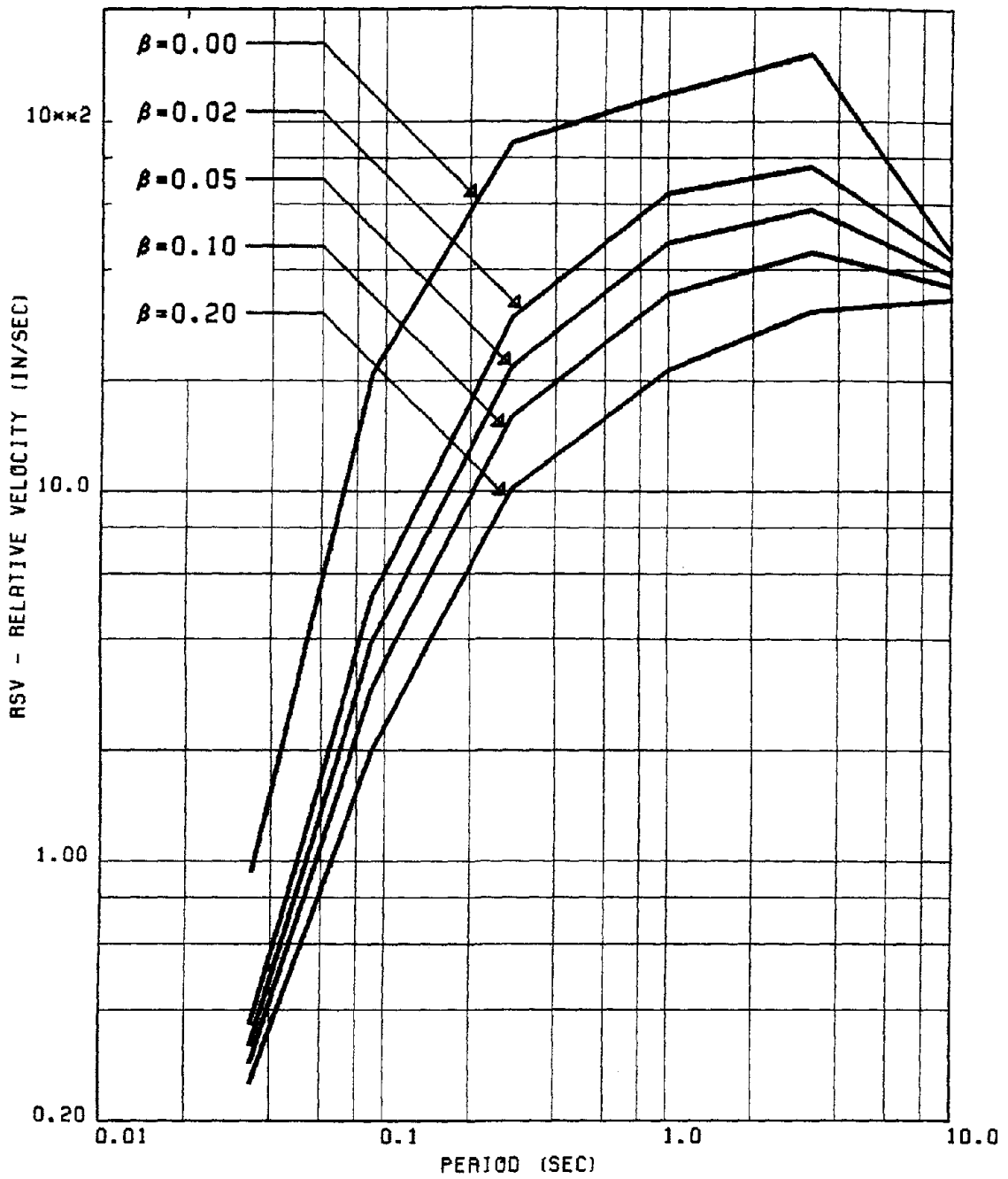
FIG. 151 PROPOSED SPECTRA FOR MEAN RSV FOR VERTICAL RECORDS OF GROUP #2
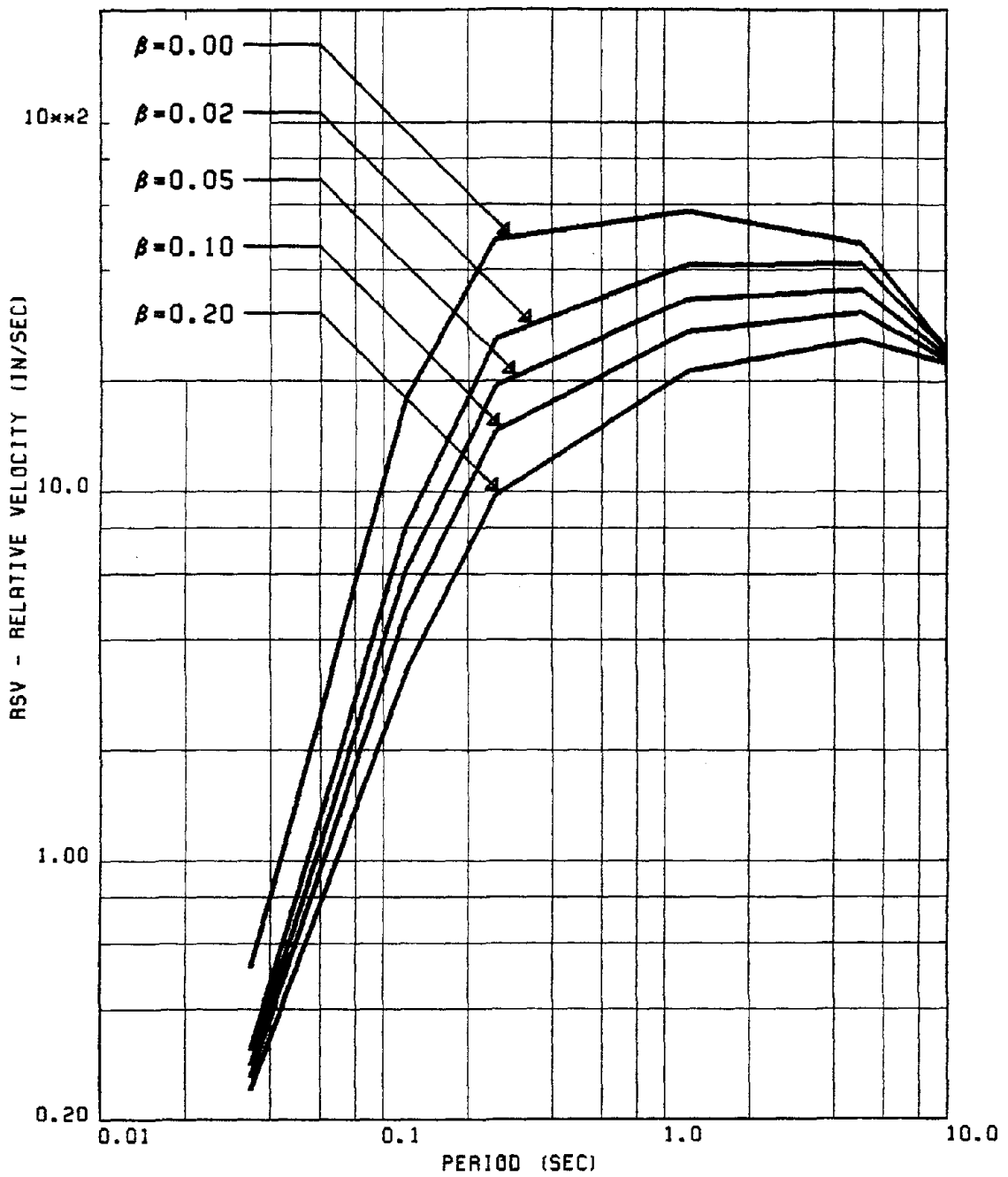
FIG. 152 PROPOSED SPECTRA FOR MEAN RSV FOR HORIZONTAL RECORDS OF GROUP #3
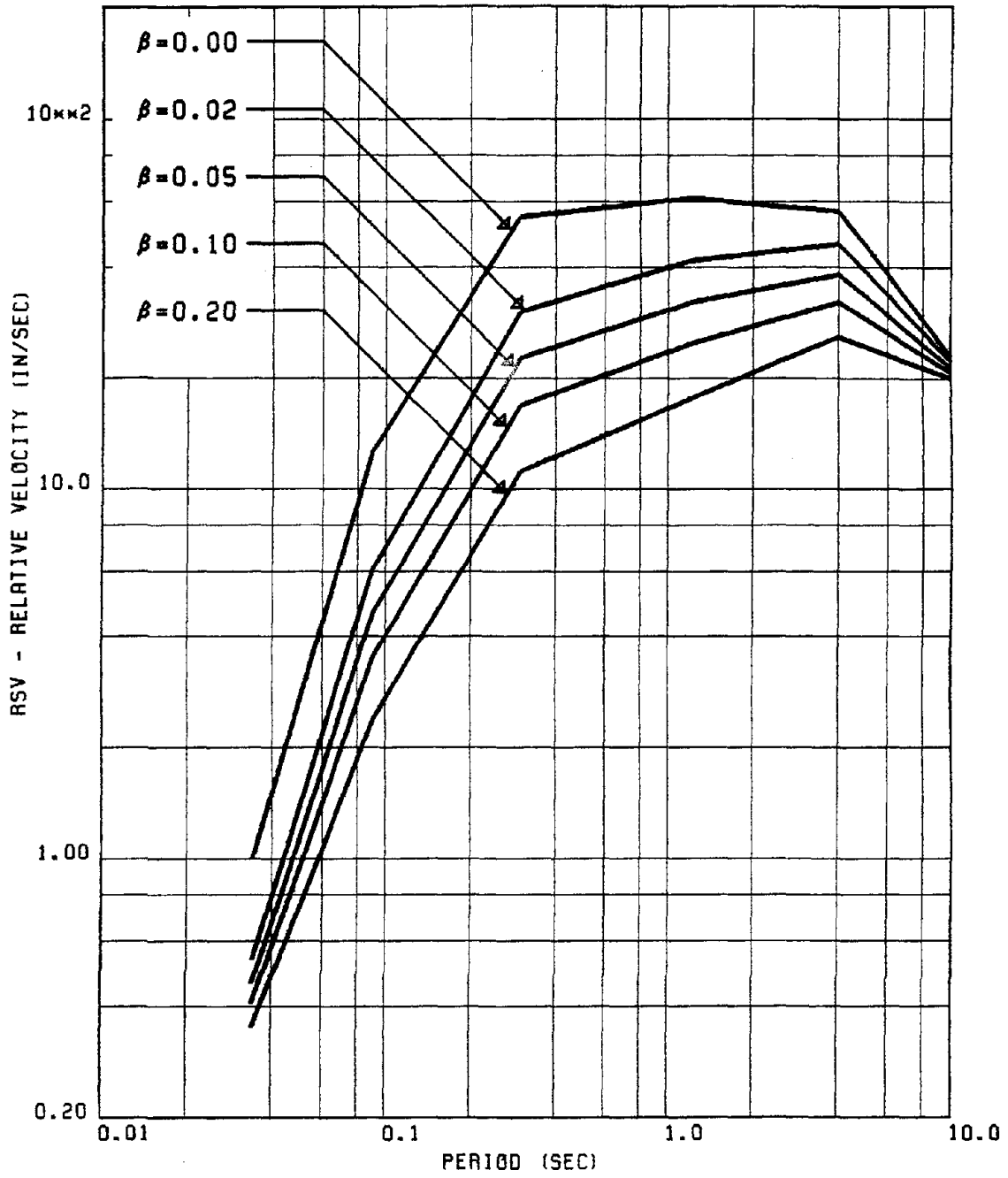
FIG. 153 PROPOSED SPECTRA FOR MEAN RSV FOR VERTICAL RECORDS OF GROUP #3
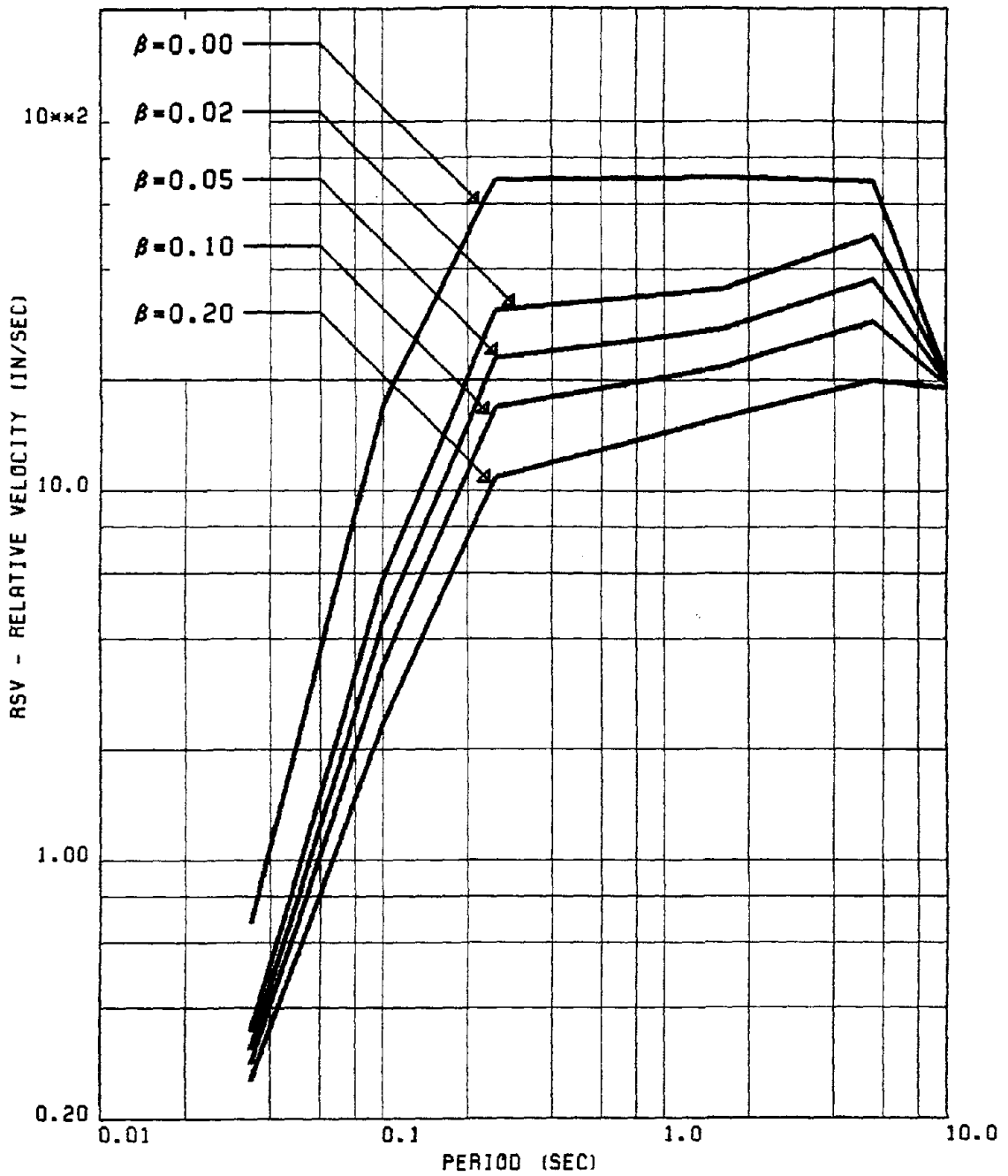
FIG. 154 PROPOSED SPECTRA FOR MEAN RSV FOR HORIZONTAL RECORDS OF GROUP #4
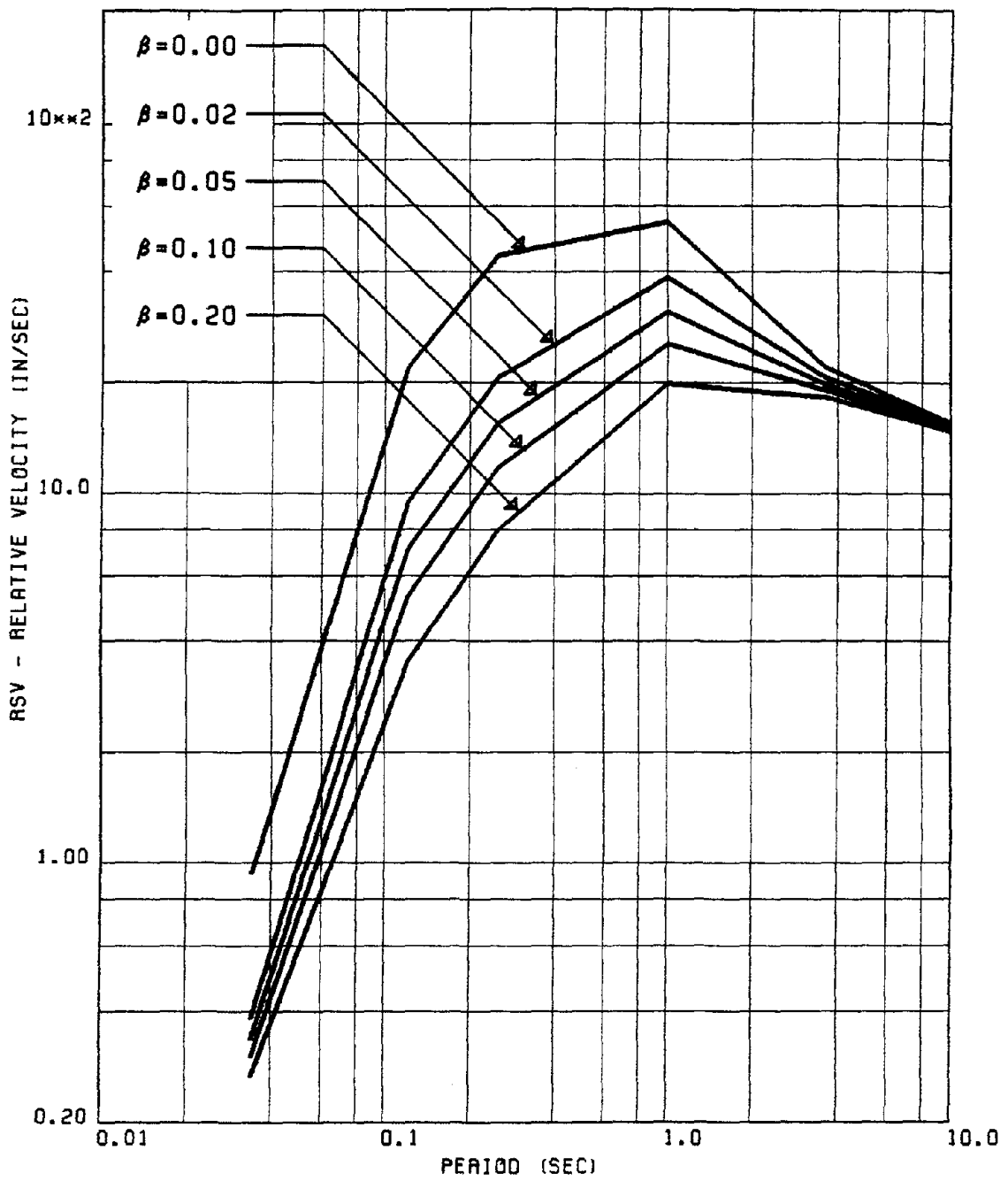
FIG. 155 PROPOSED SPECTRA FOR MEAN RSV FOR HORIZONTAL RECORDS OF GROUP #5
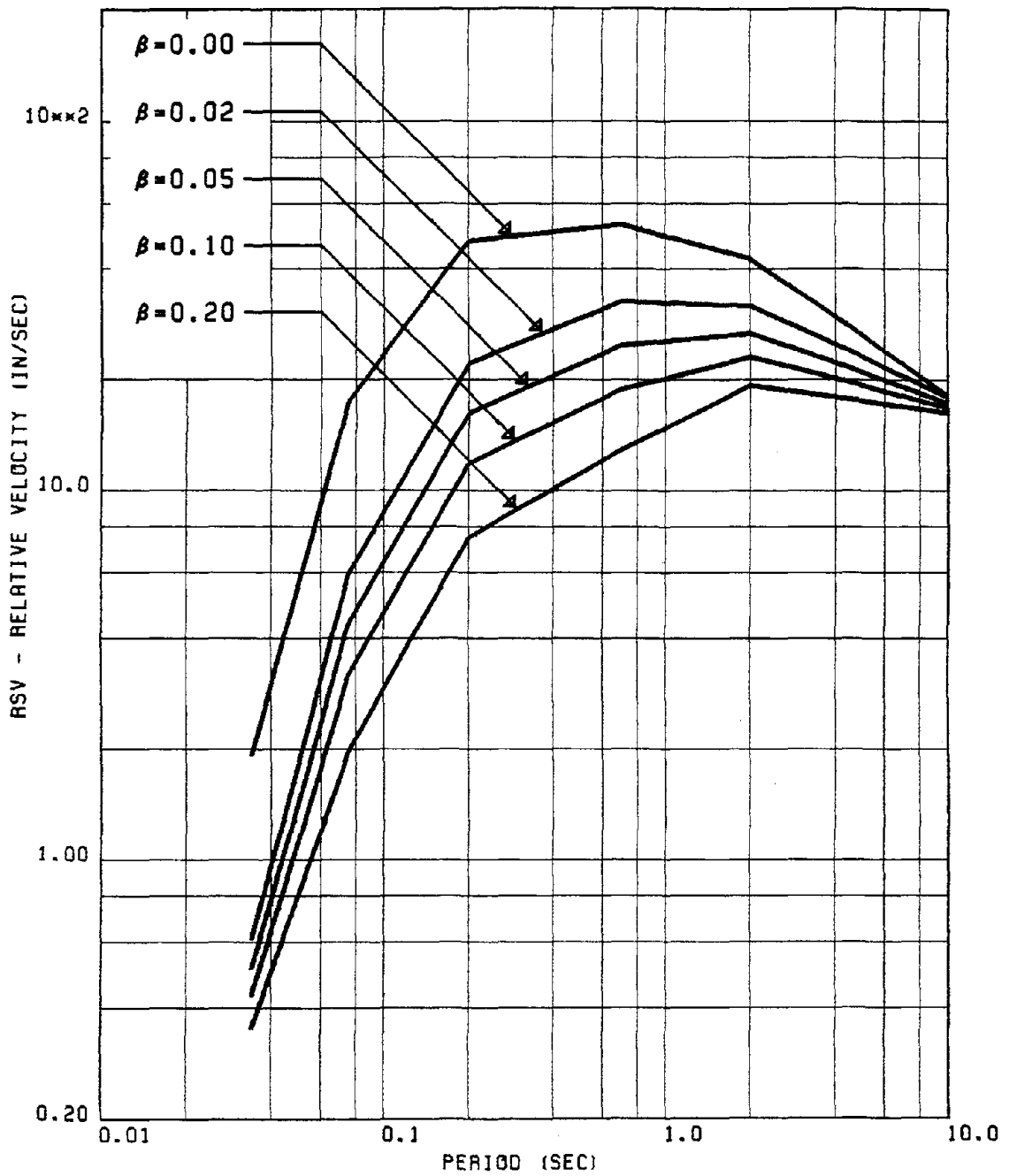
FIG. 156 PROPOSED SPECTRA FOR MEAN RSV FOR VERTICAL RECORDS OF GROUP #5
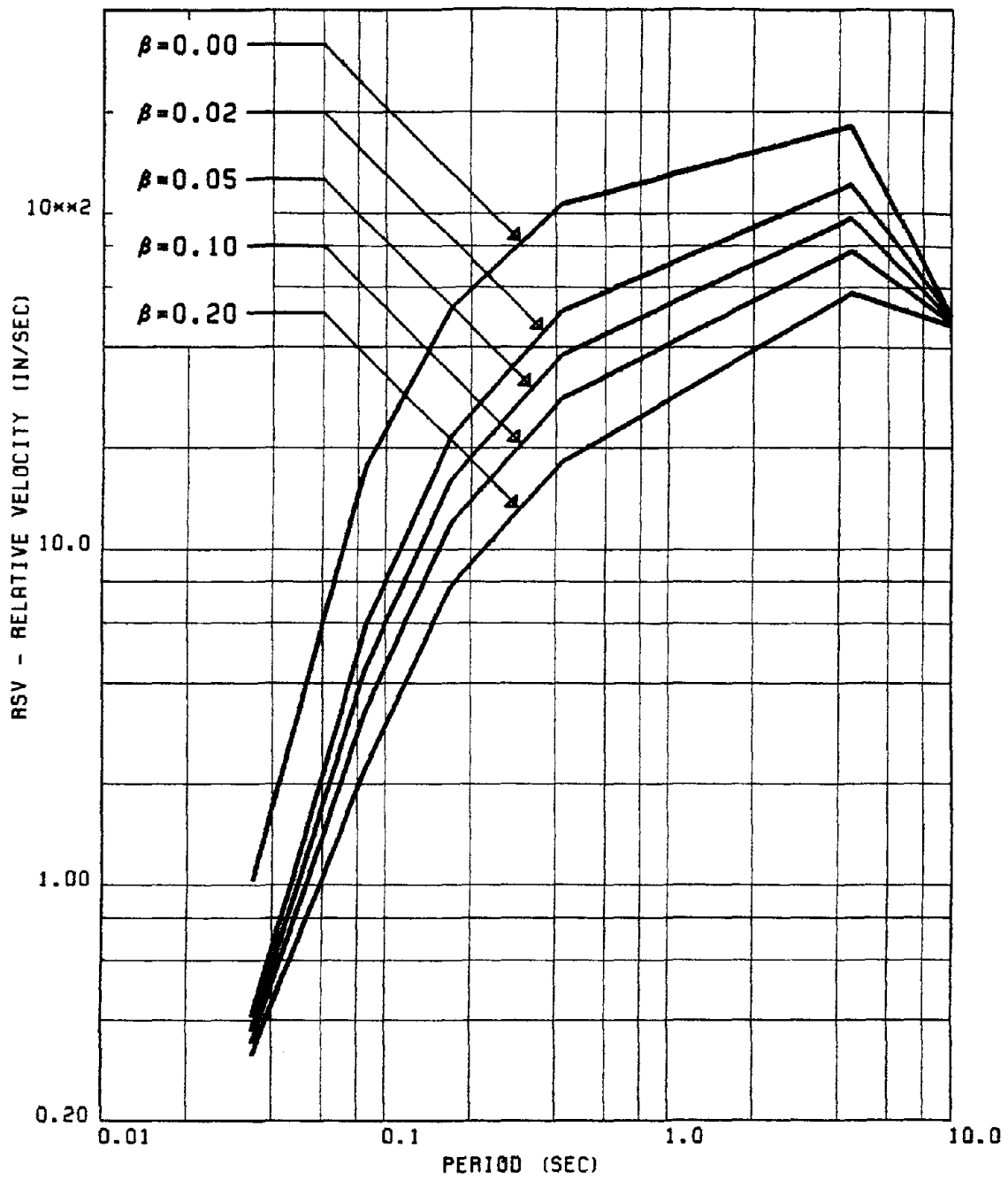
FIG. 157 PROPOSED (MEAN+SD) RSV SPECTRA FOR HORIZONTAL RECORDS OF GROUP #1
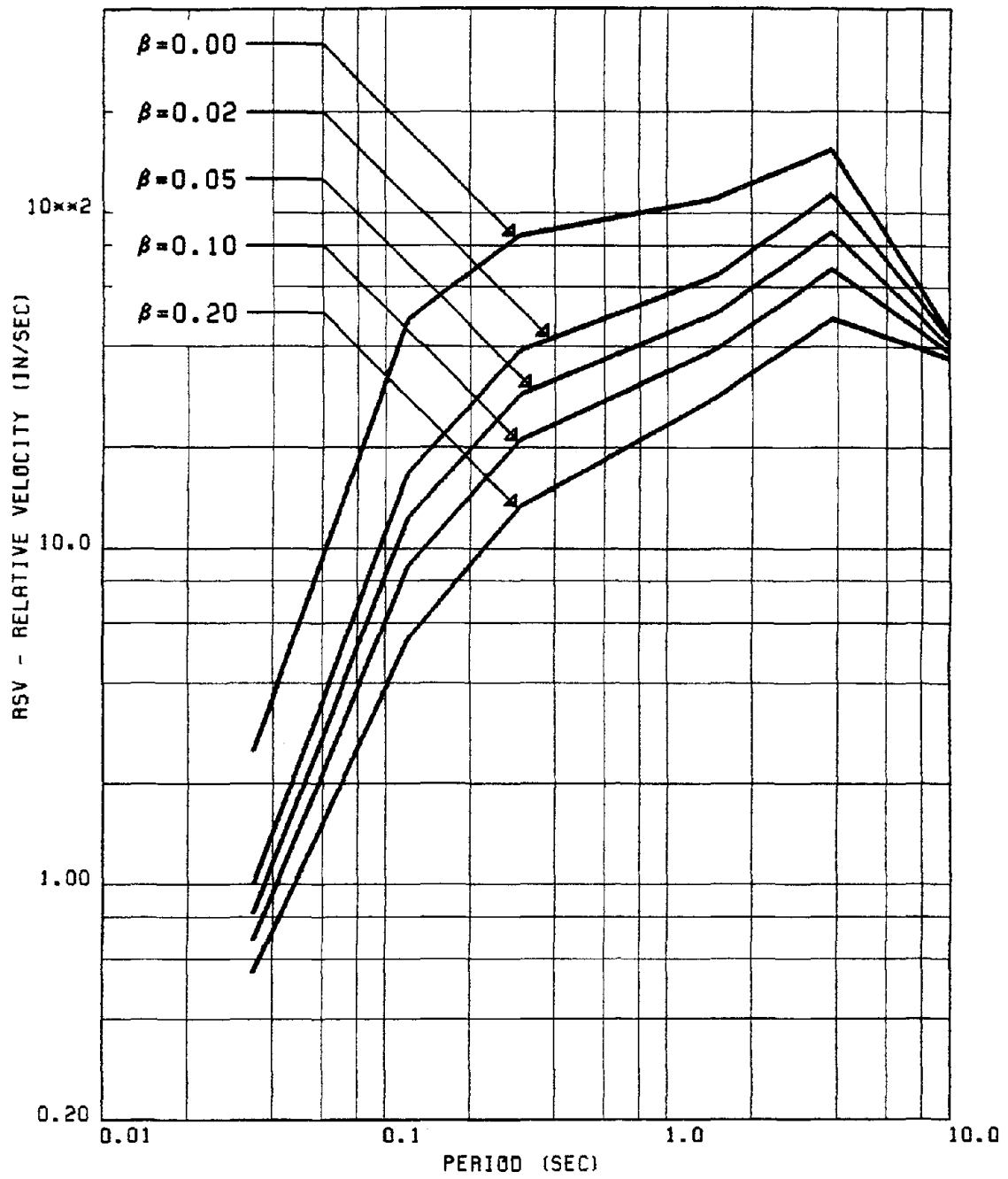
FIG. 158 PROPOSED (MEAN+SD) RSV SPECTRA FOR VERTICAL RECORDS OF GROUP #1
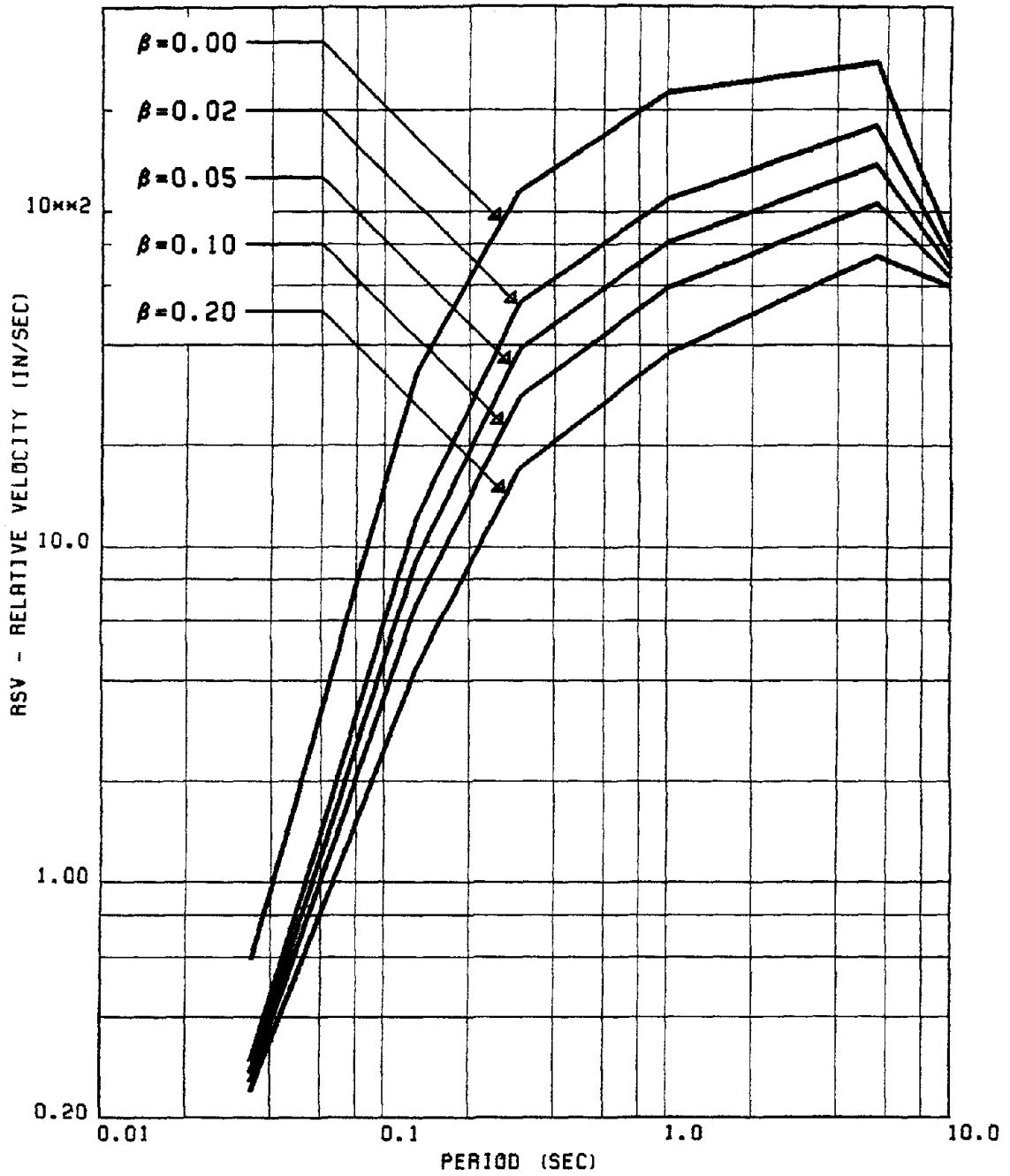
FIG. 159 PROPOSED (MEAN+SD) RSV SPECTRA FOR HORIZONTAL RECORDS OF GROUP #2
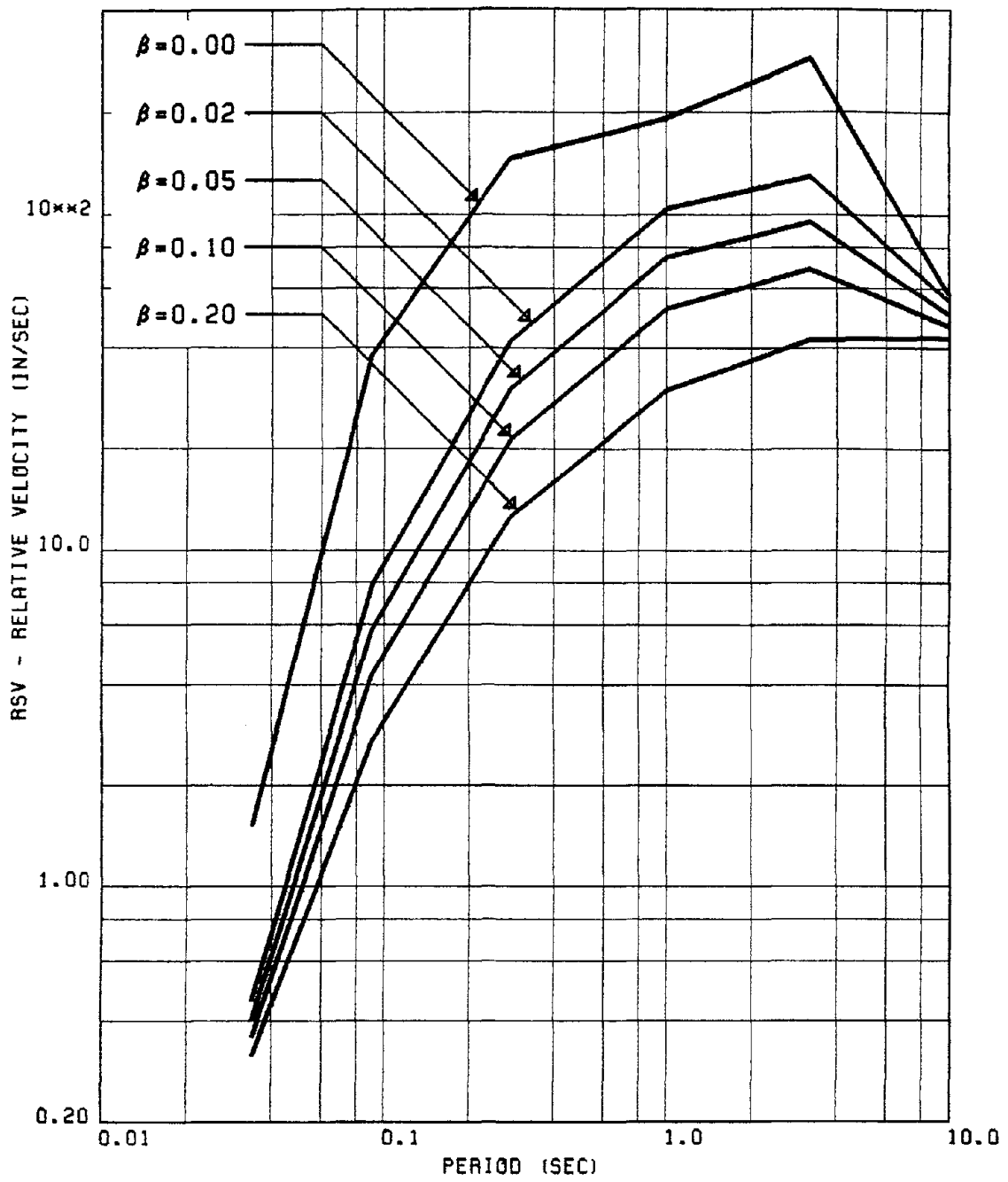
FIG. 160 PROPOSED (MEAN+SD) RSV SPECTRA FOR VERTICAL RECORDS OF GROUP #2
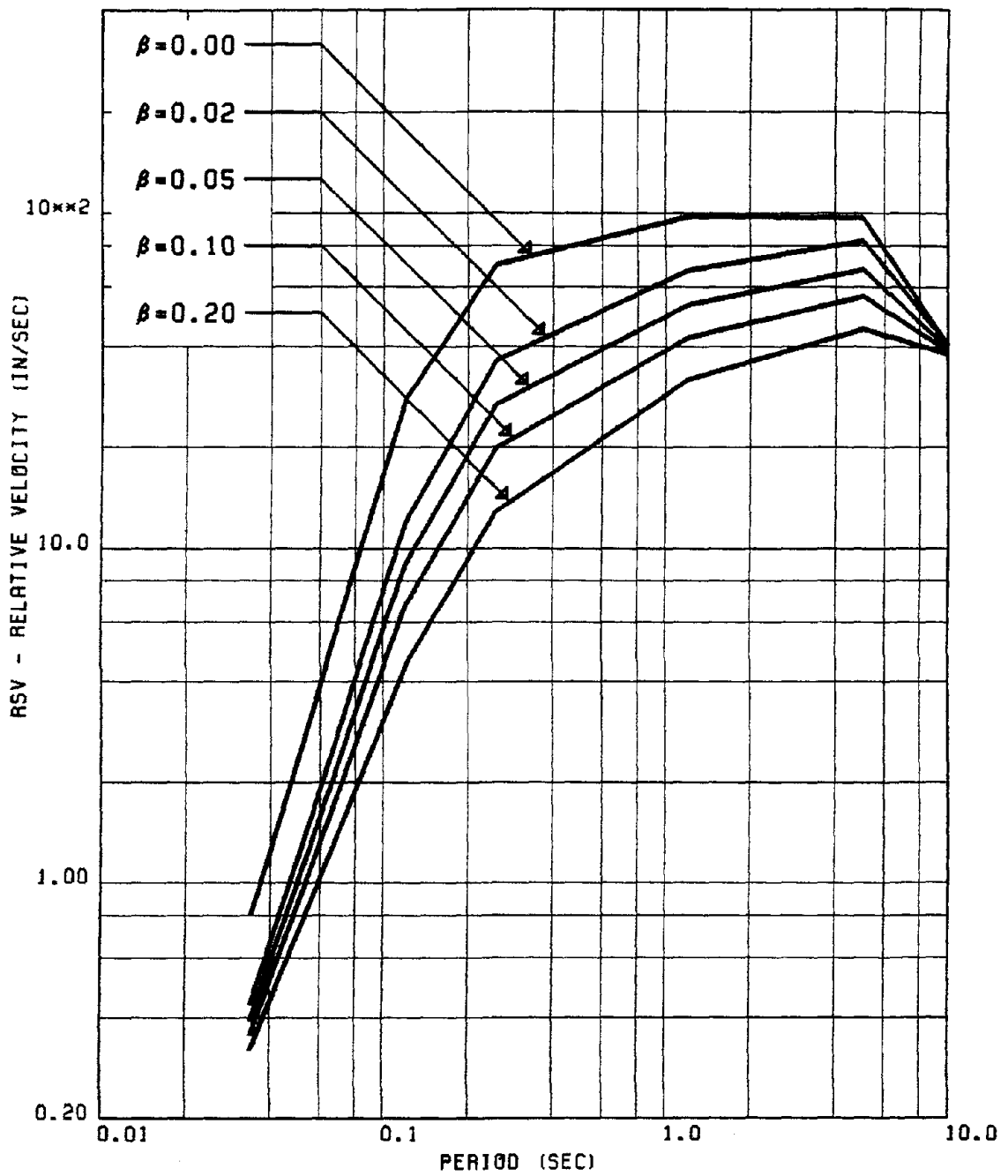
FIG. 161 PROPOSED (MEAN+SD) RSV SPECTRA FOR HORIZONTAL RECORDS OF GROUP #3
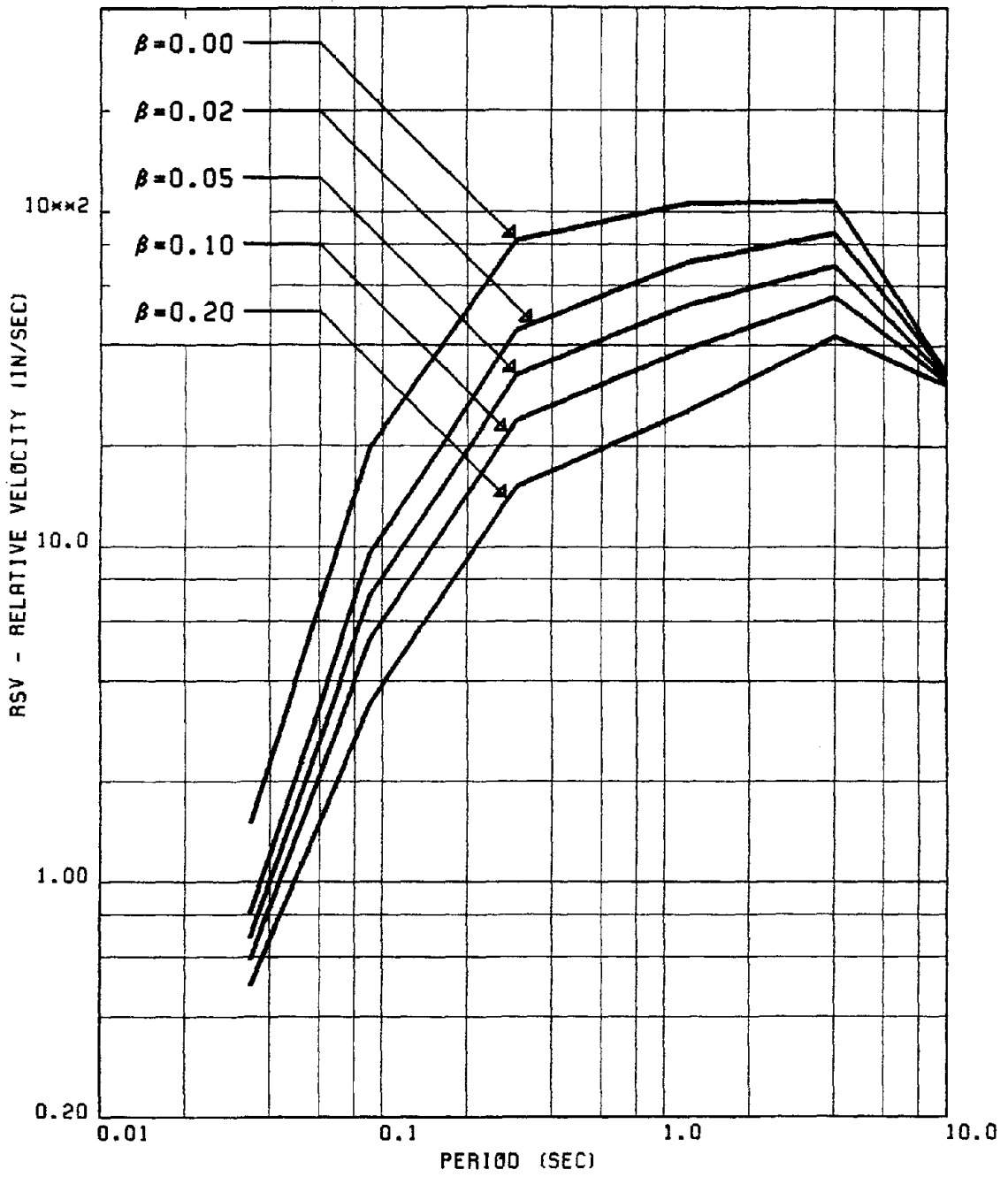
FIG. 162 PROPOSED (MEAN+SD) RSV SPECTRA FOR VERTICAL RECORDS OF GROUP #3
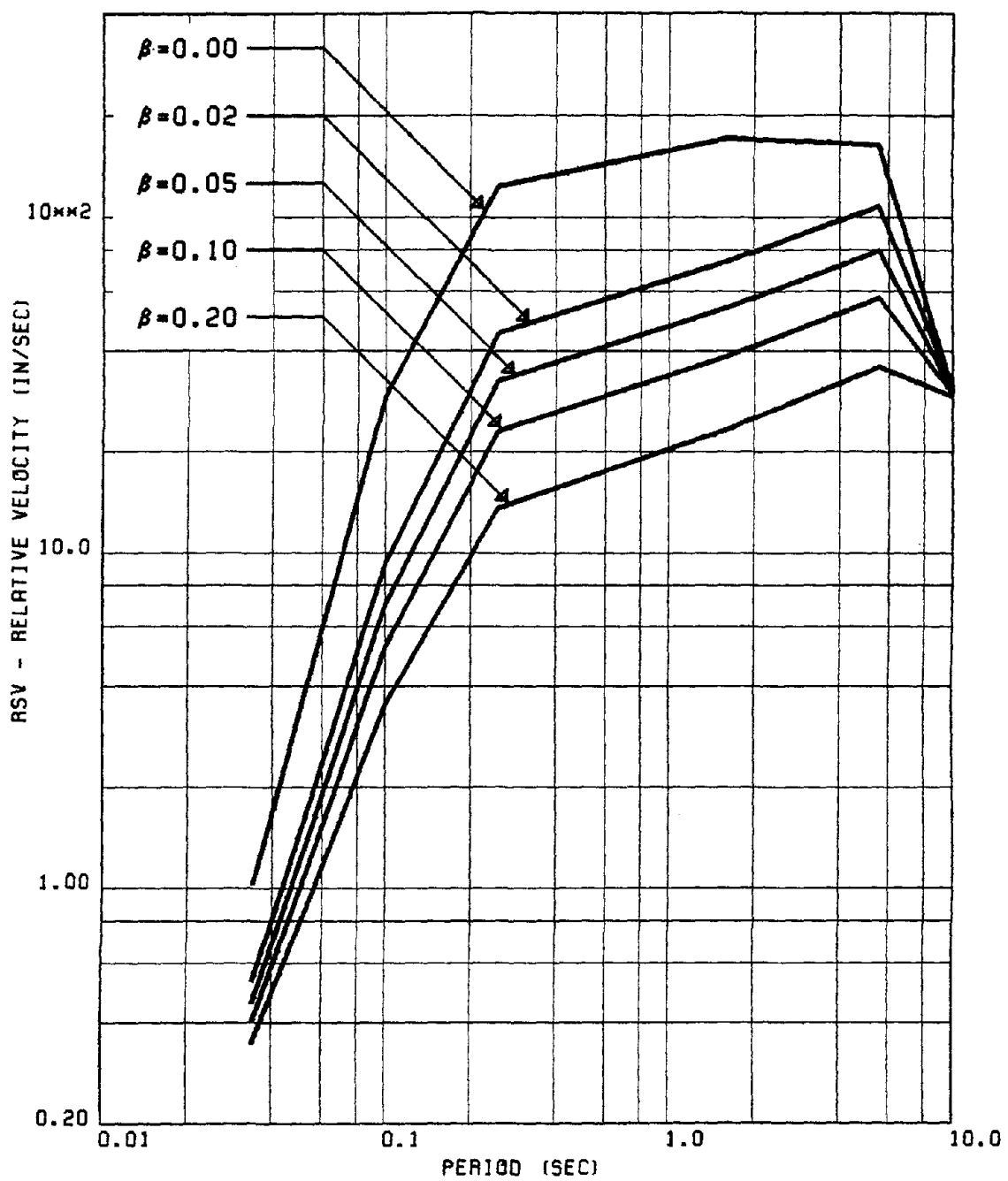
FIG. 163 PROPOSED (MEAN+SD) RSV SPECTRA FOR HORIZONTAL RECORDS OF GROUP #4
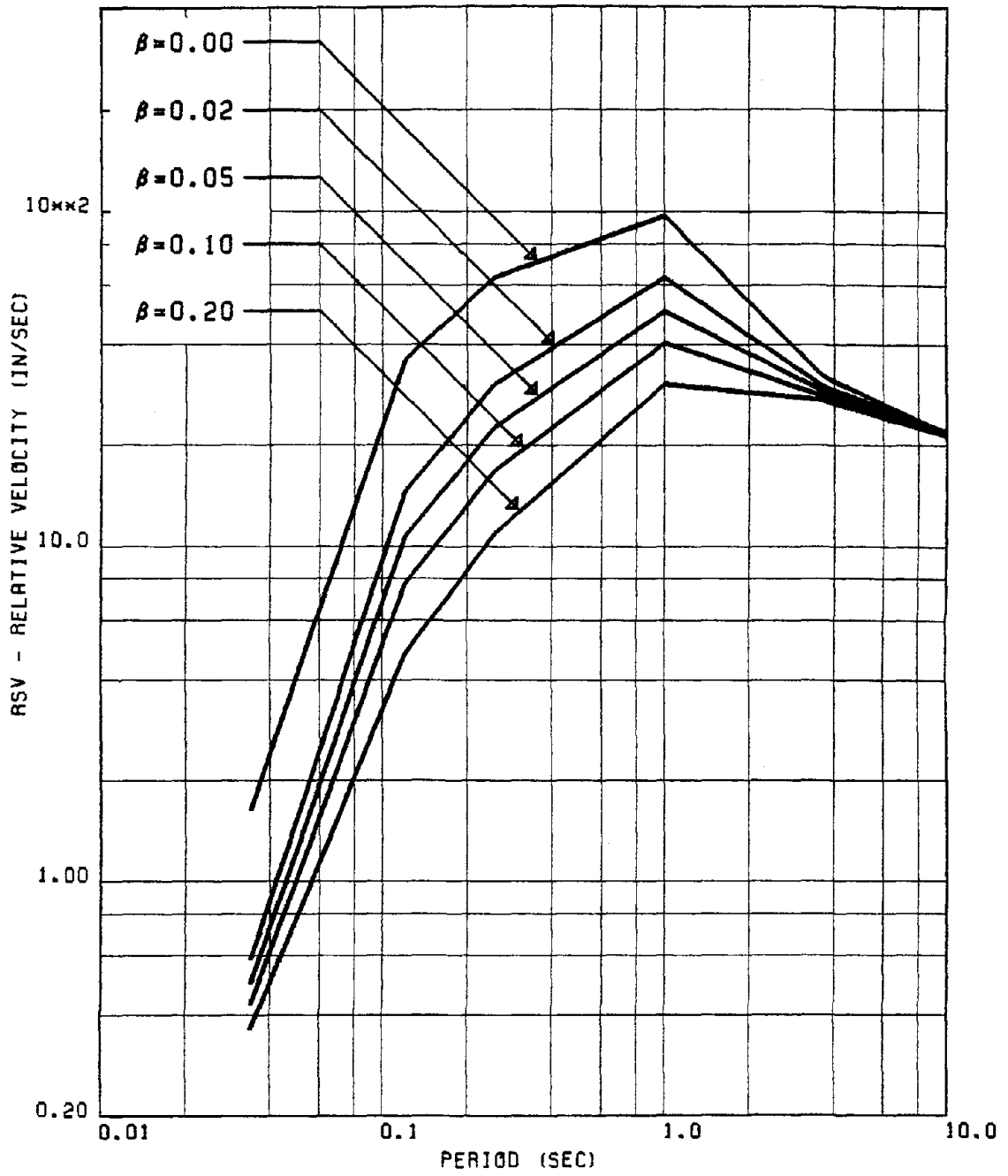
FIG. 164 PROPOSED (MEAN+SD) RSV SPECTRA FOR HORIZONTAL RECORDS OF GROUP #5
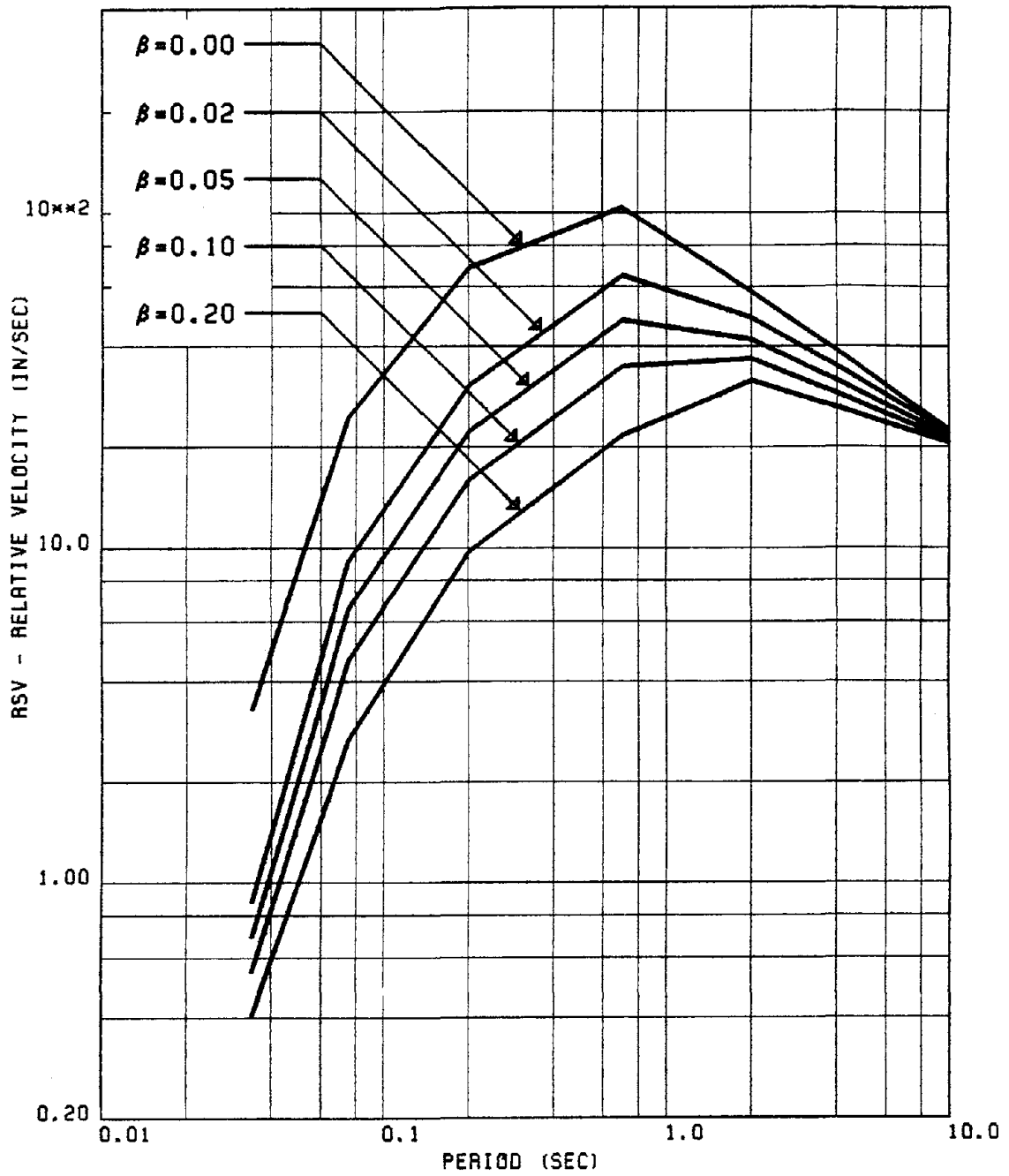
FIG. 165 PROPOSED (MEAN+SD) RSV SPECTRA FOR VERTICAL RECORDS OF GROUP *5
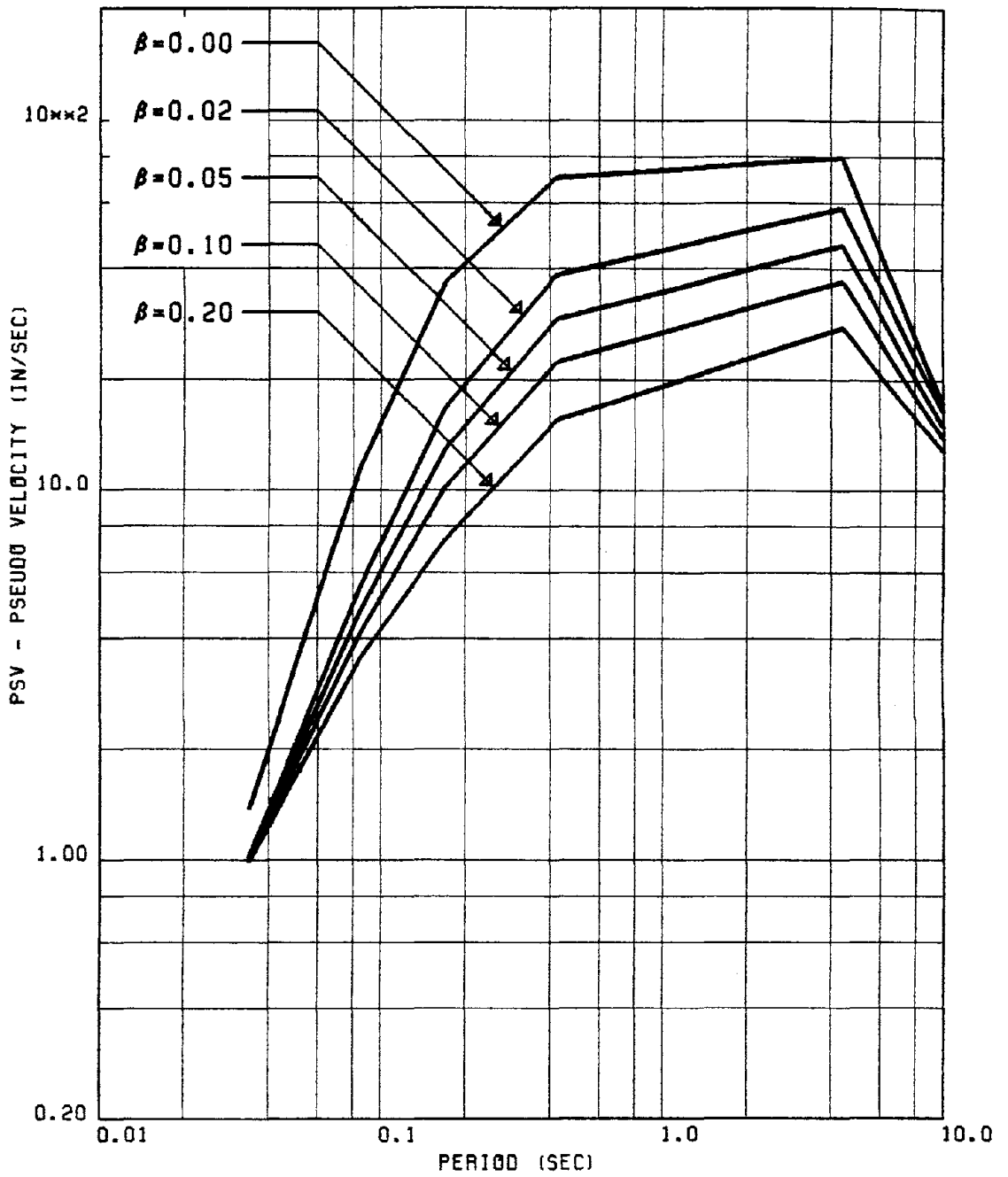
FIG. 166 PROPOSED SPECTRA FOR MEAN PSV FOR HORIZONTAL RECORDS OF GROUP #1
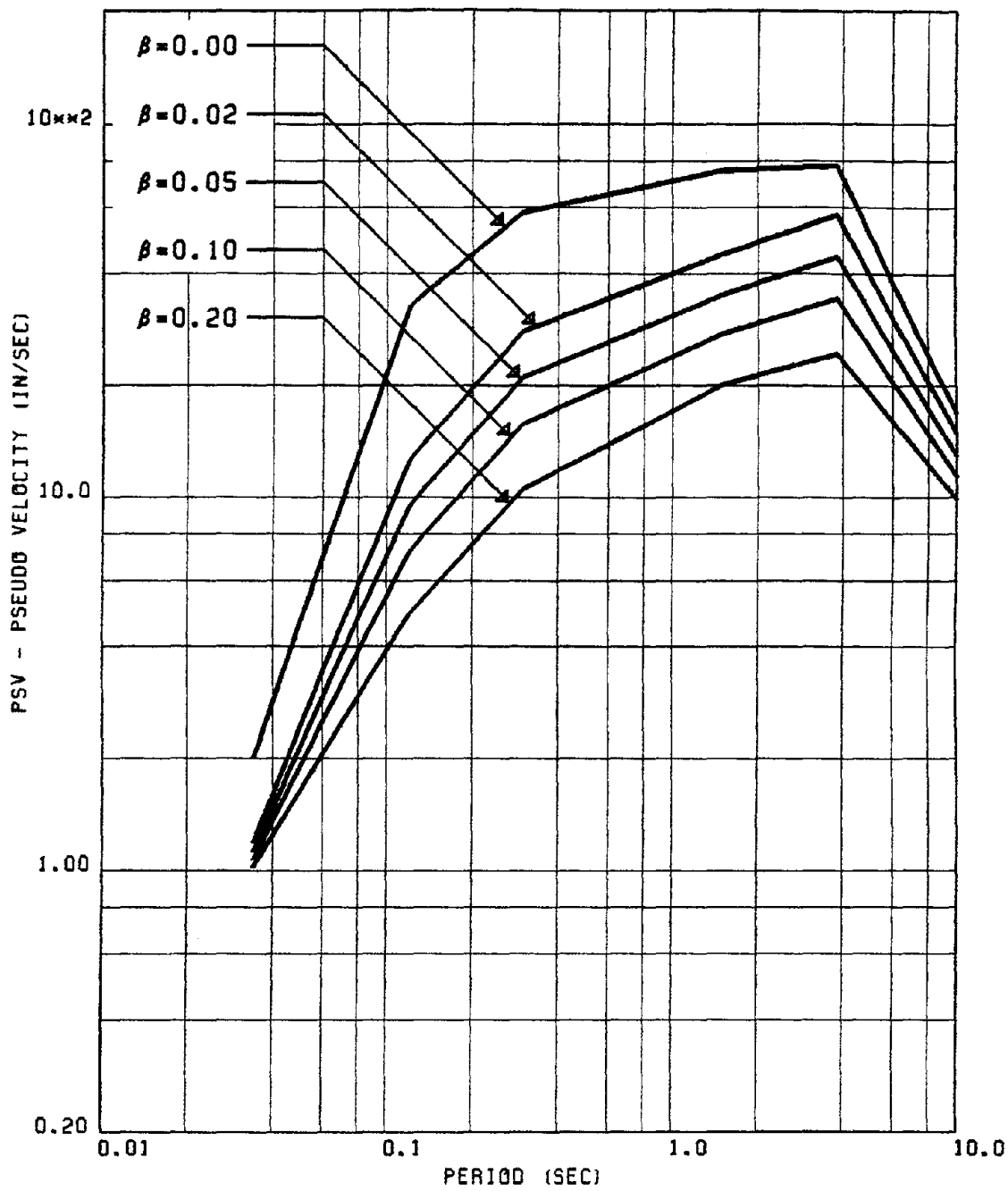
FIG. 167 PROPOSED SPECTRA FOR MEAN PSV FOR VERTICAL RECORDS OF GROUP #1

245
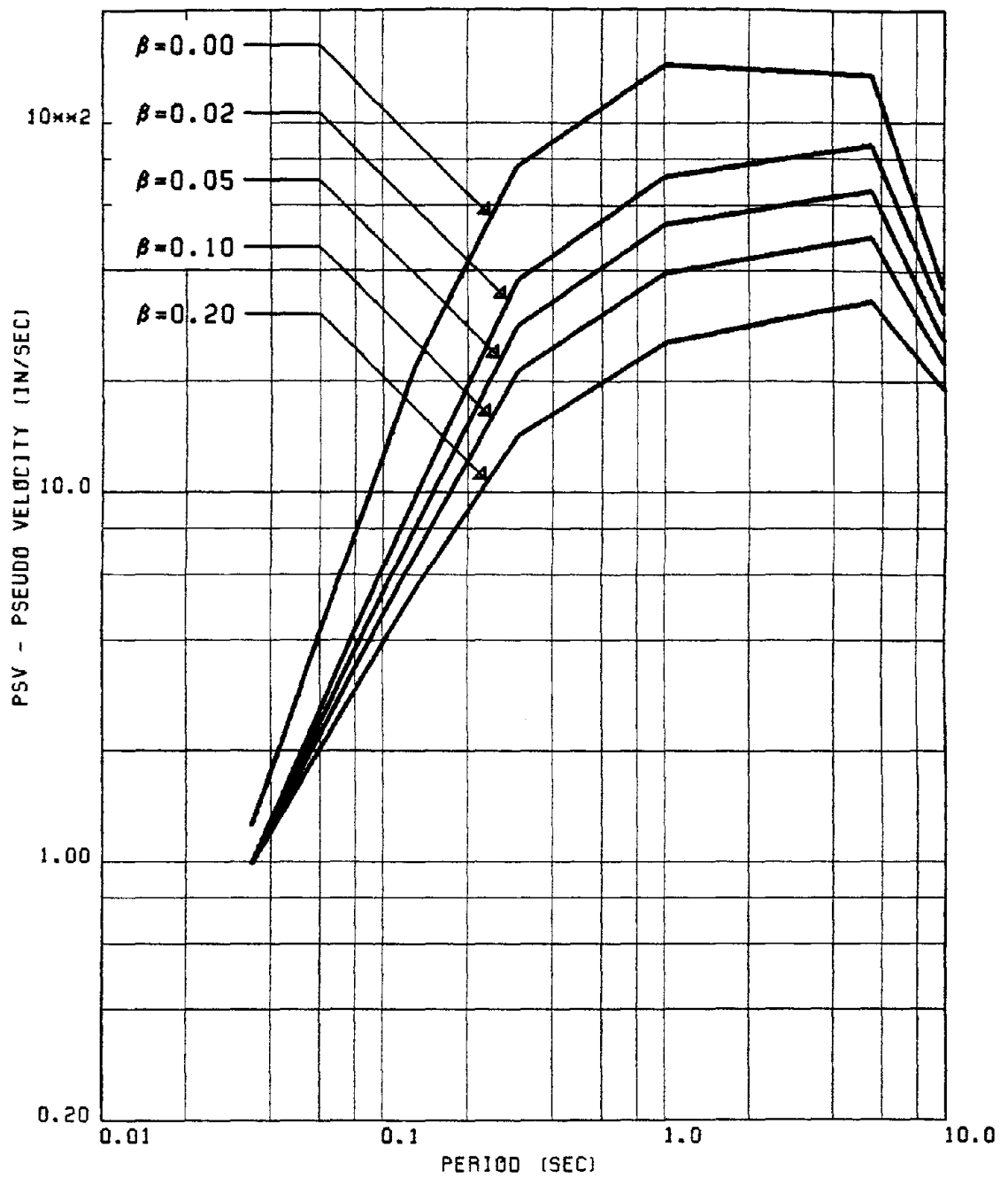
FIG. 168 PROPOSED SPECTRA FOR MEAN PSV FOR HORIZONTAL RECORDS OF GROUP #2
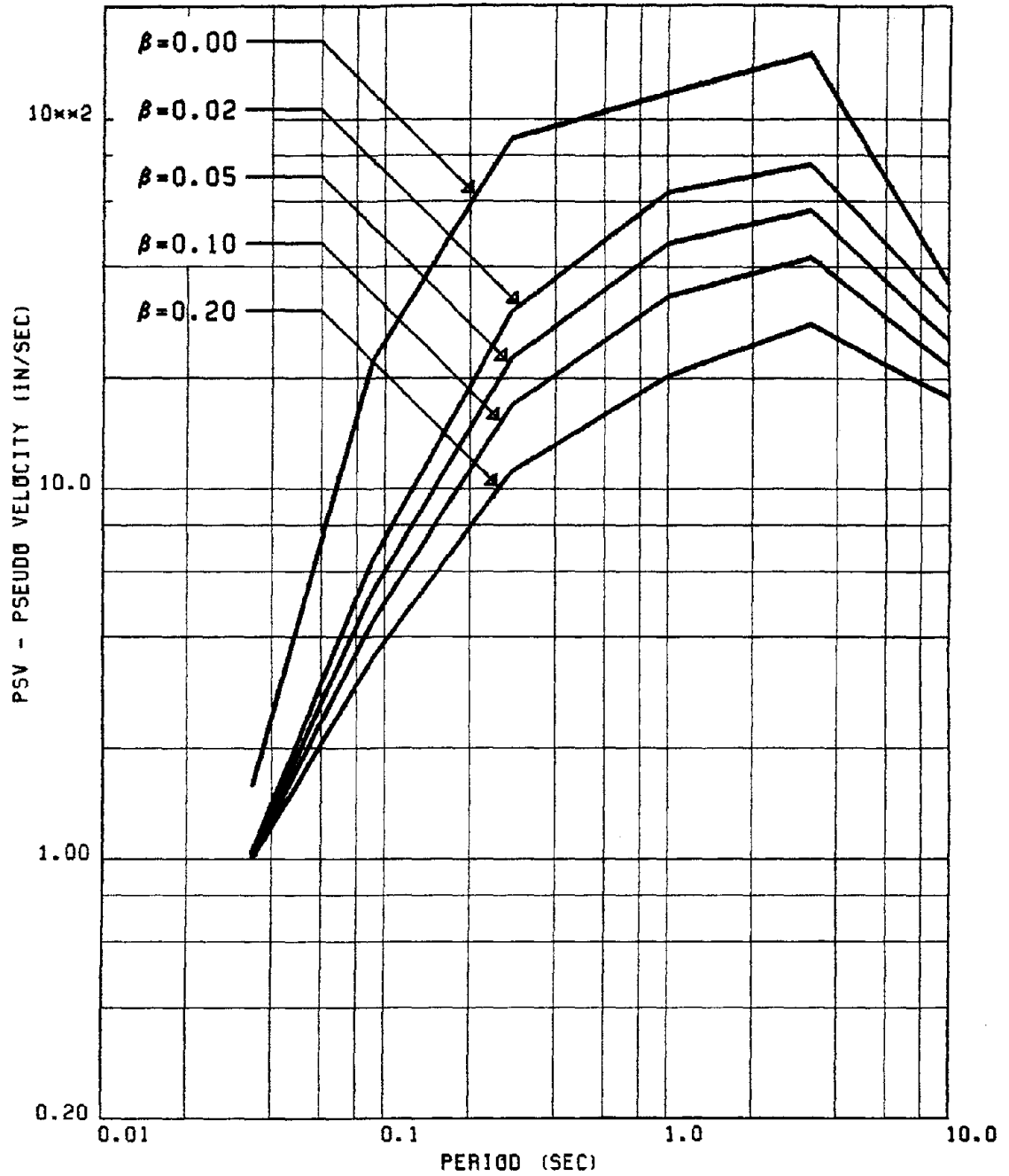
FIG. 169 PROPOSED SPECTRA FOR MEAN PSV FOR VERTICAL RECORDS OF GROUP #2
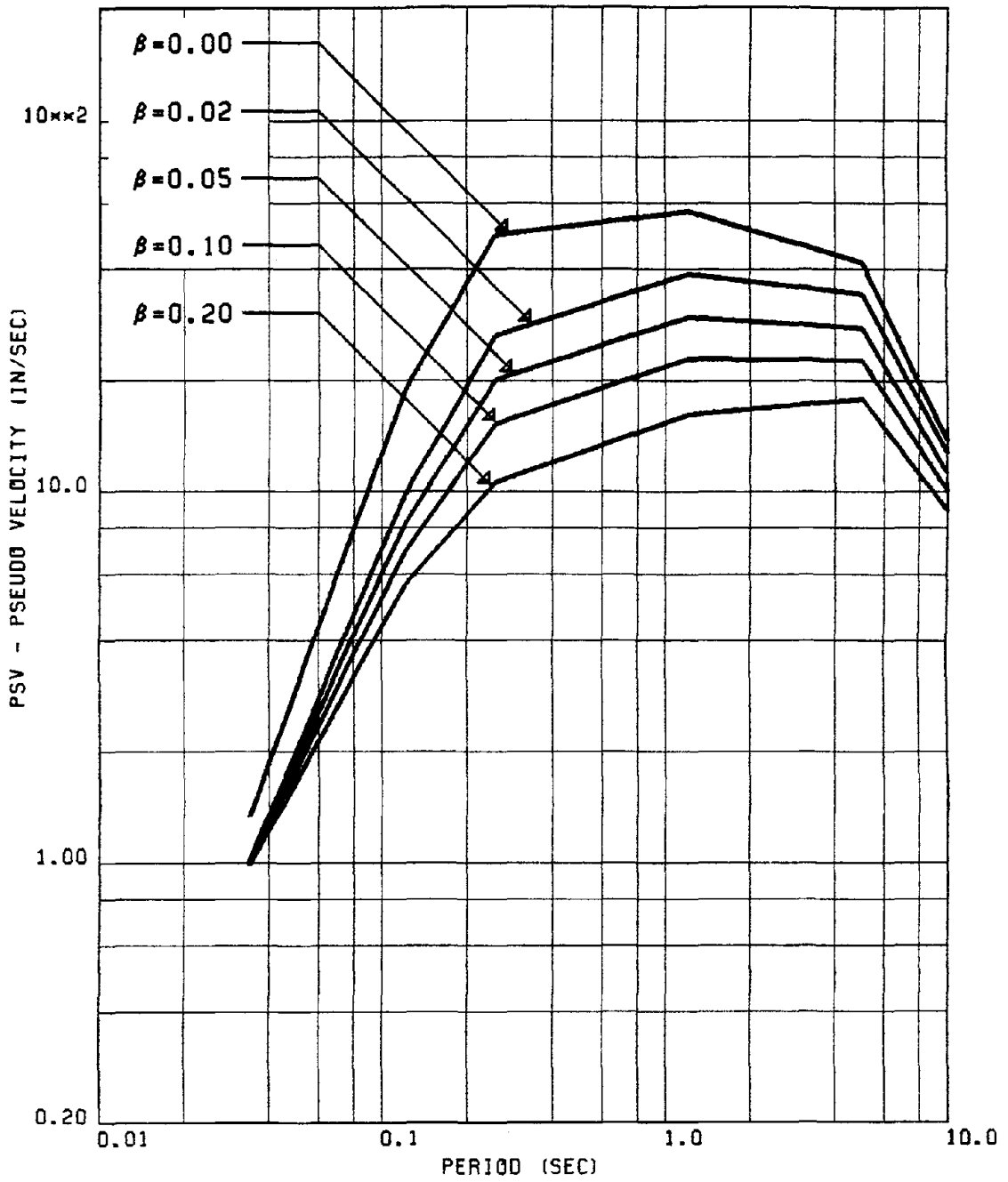
FIG. 170 PROPOSED SPECTRA FOR MEAN PSV FOR HORIZONTAL RECORDS OF GROUP #3
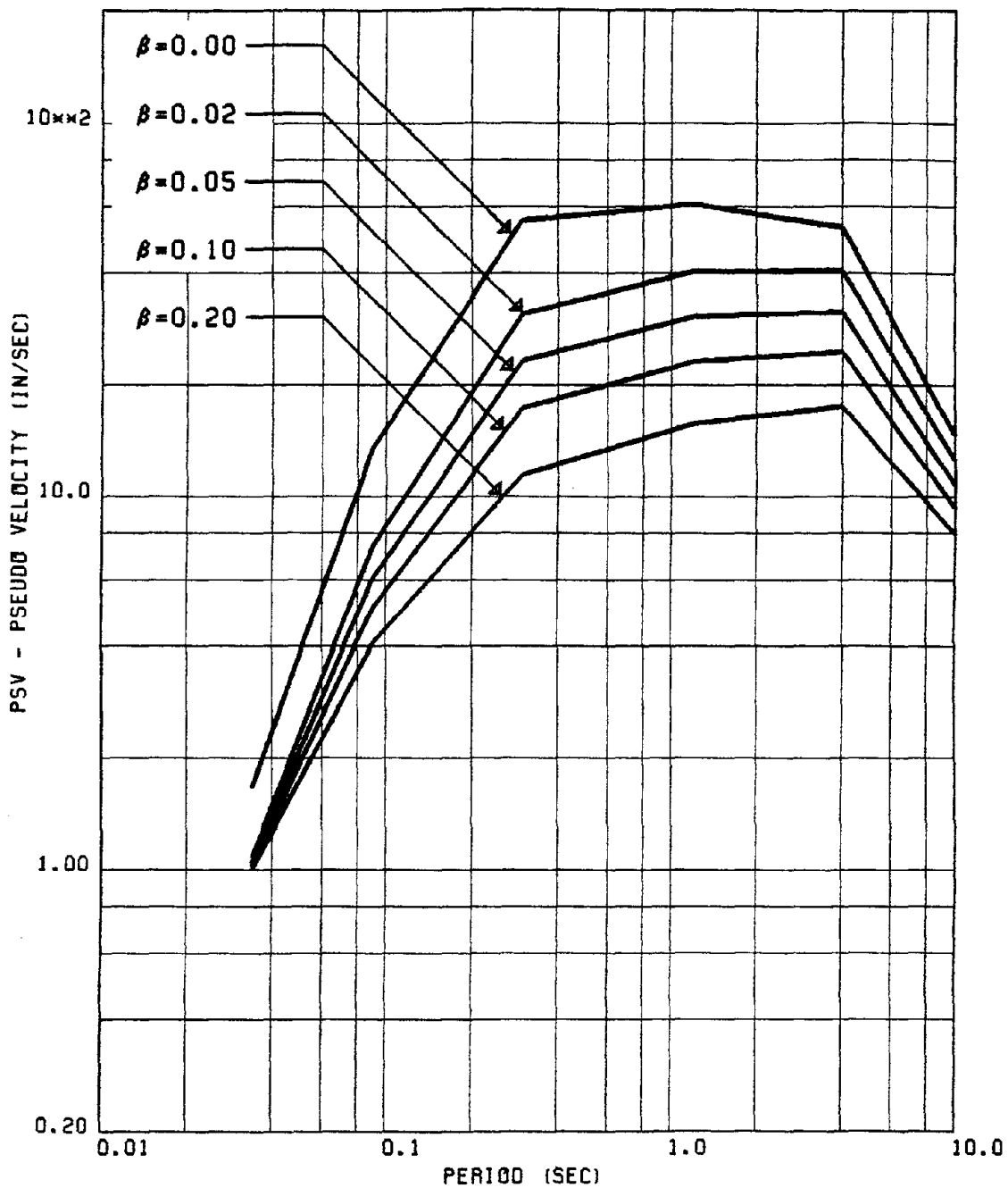
FIG. 171 PROPOSED SPECTRA FOR MEAN PSV FOR VERTICAL RECORDS OF GROUP #3
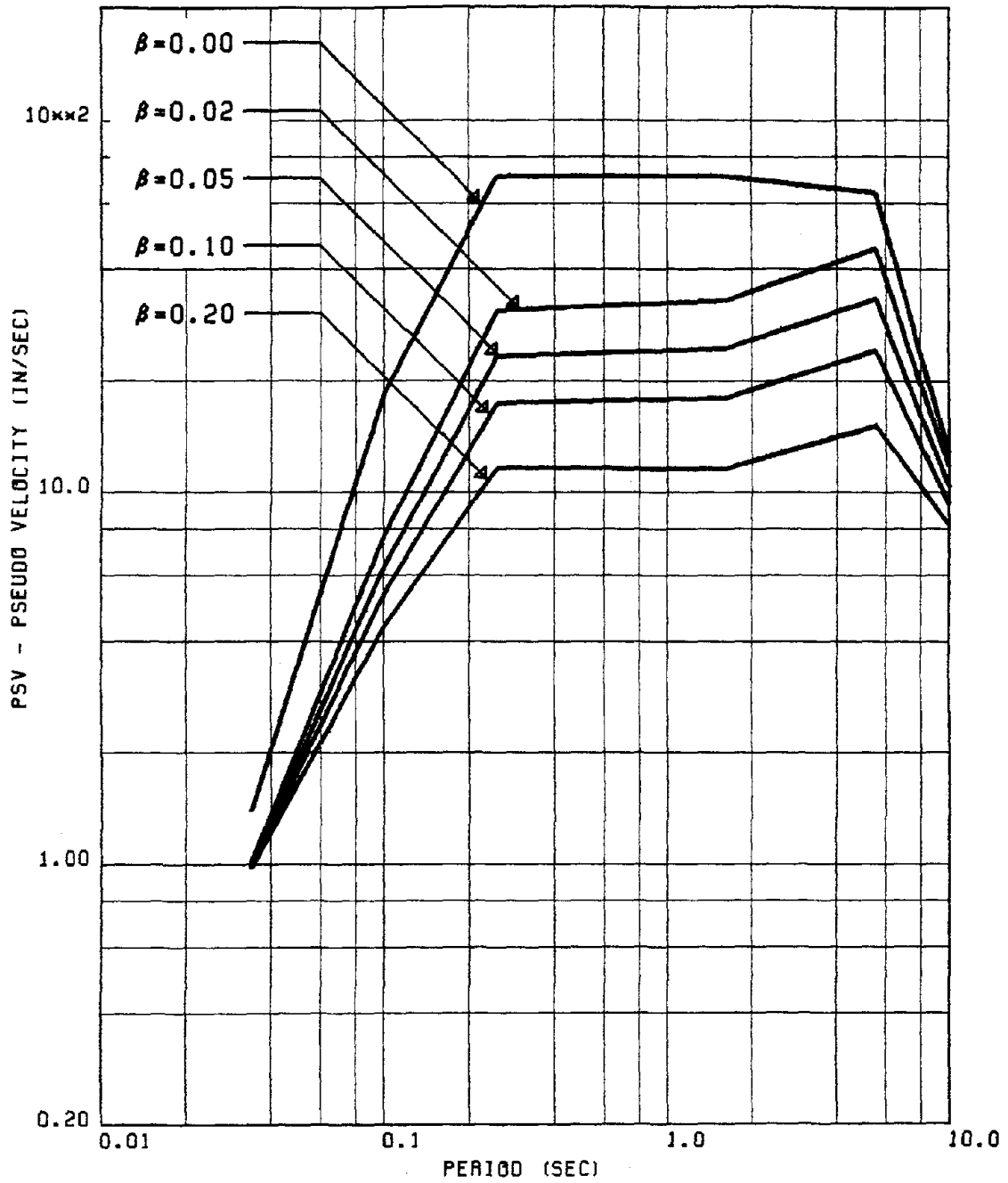
FIG. 172 PROPOSED SPECTRA FOR MEAN PSV FOR HORIZONTAL RECORDS OF GROUP #4
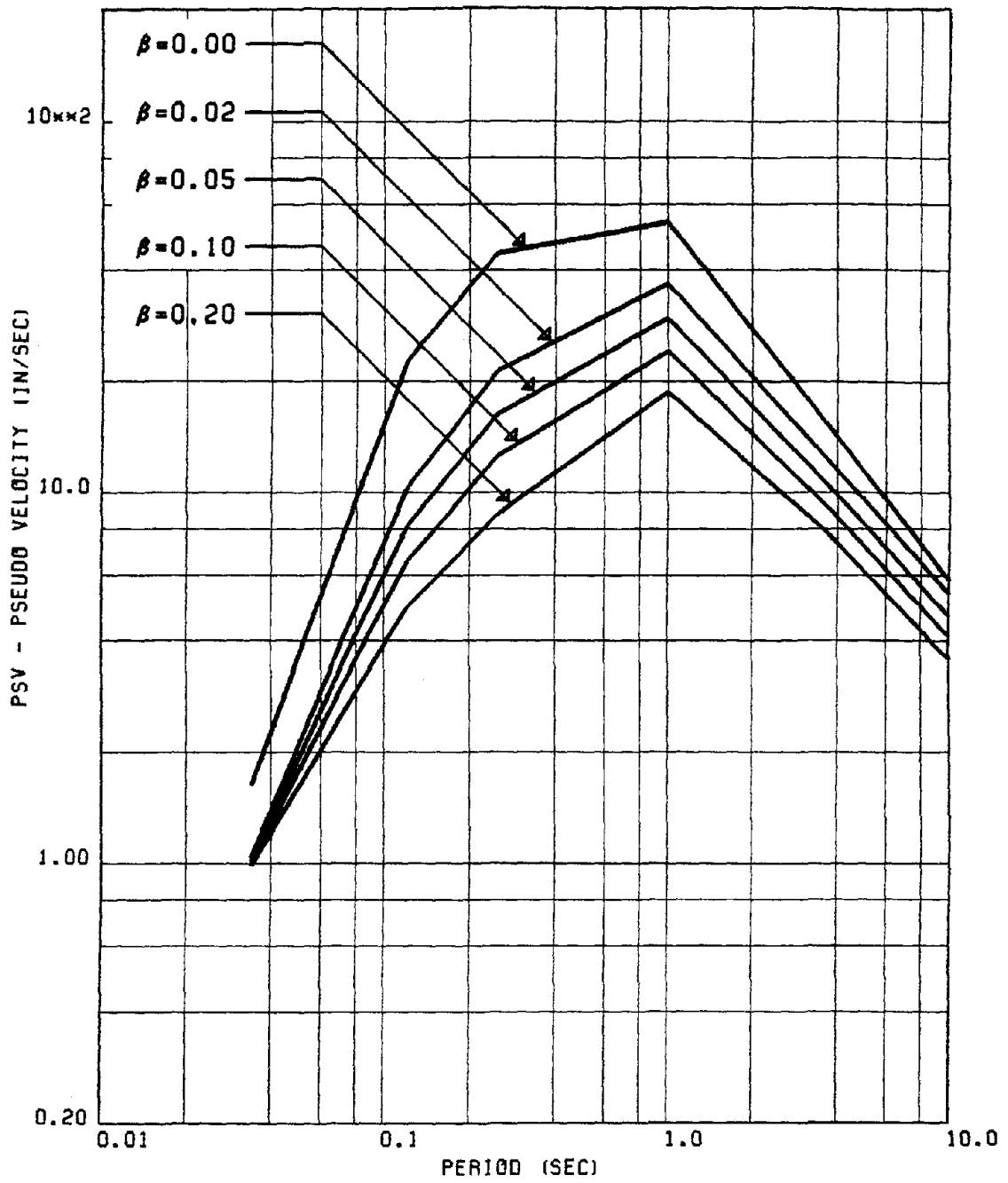
FIG. 173 PROPOSED SPECTRA FOR MEAN PSV FOR HORIZONTAL RECORDS OF GROUP #5
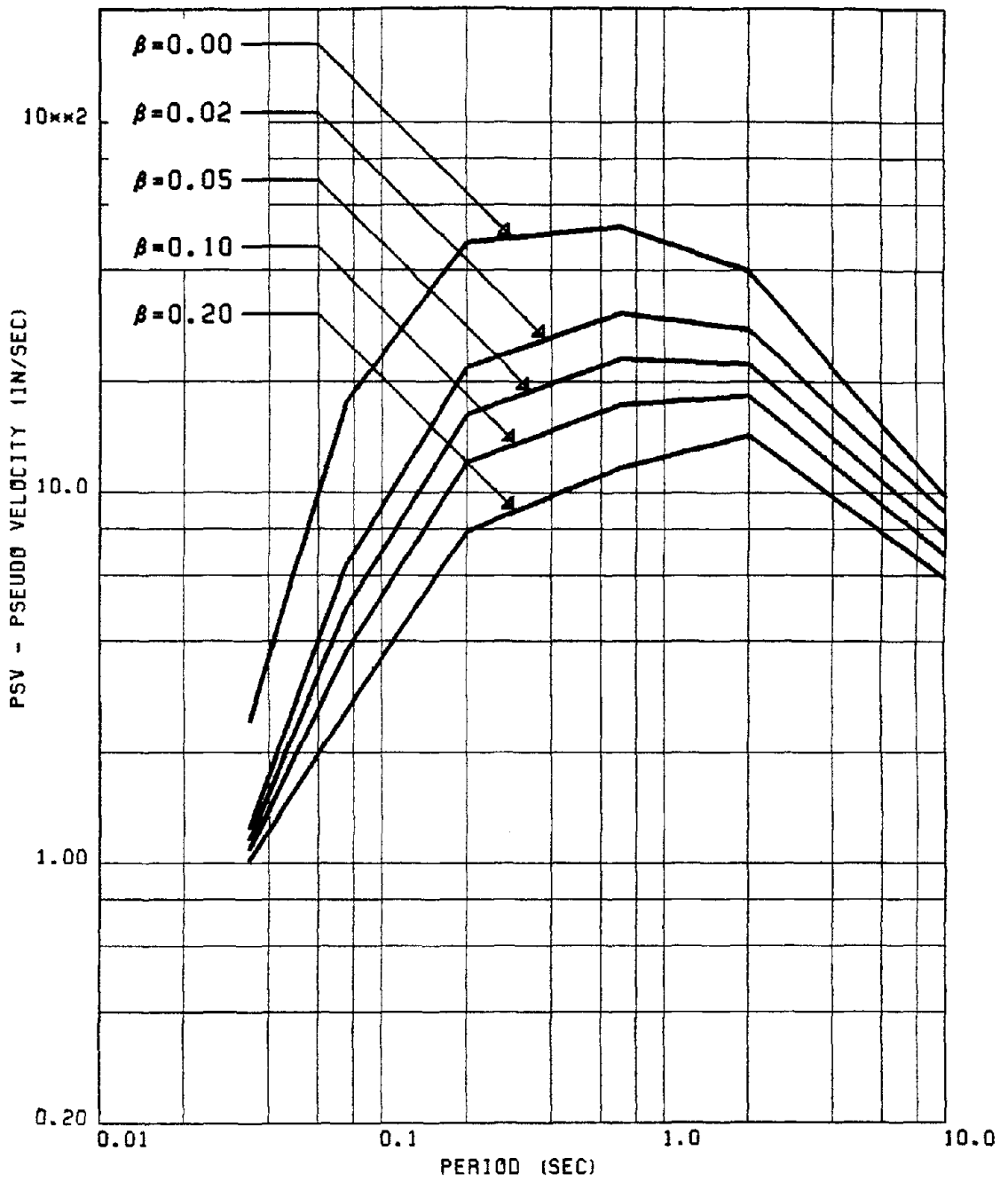
FIG. 174 PROPOSED SPECTRA FOR MEAN PSV FOR VERTICAL RECORDS OF GROUP #5

252
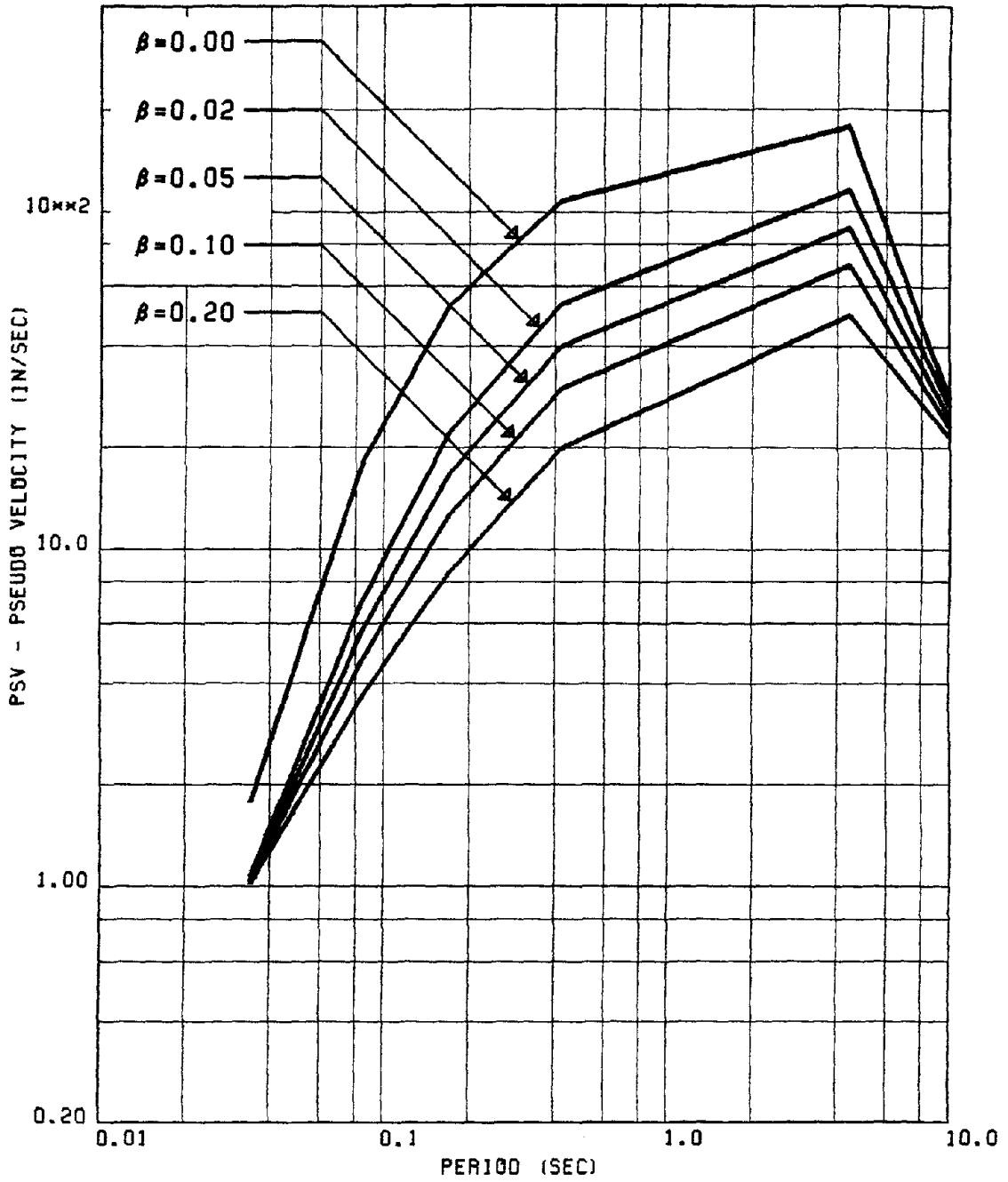
FIG. 175 PROPOSED (MEAN+SD) PSV SPECTRA FOR HORIZONTAL RECORDS OF GROUP #1
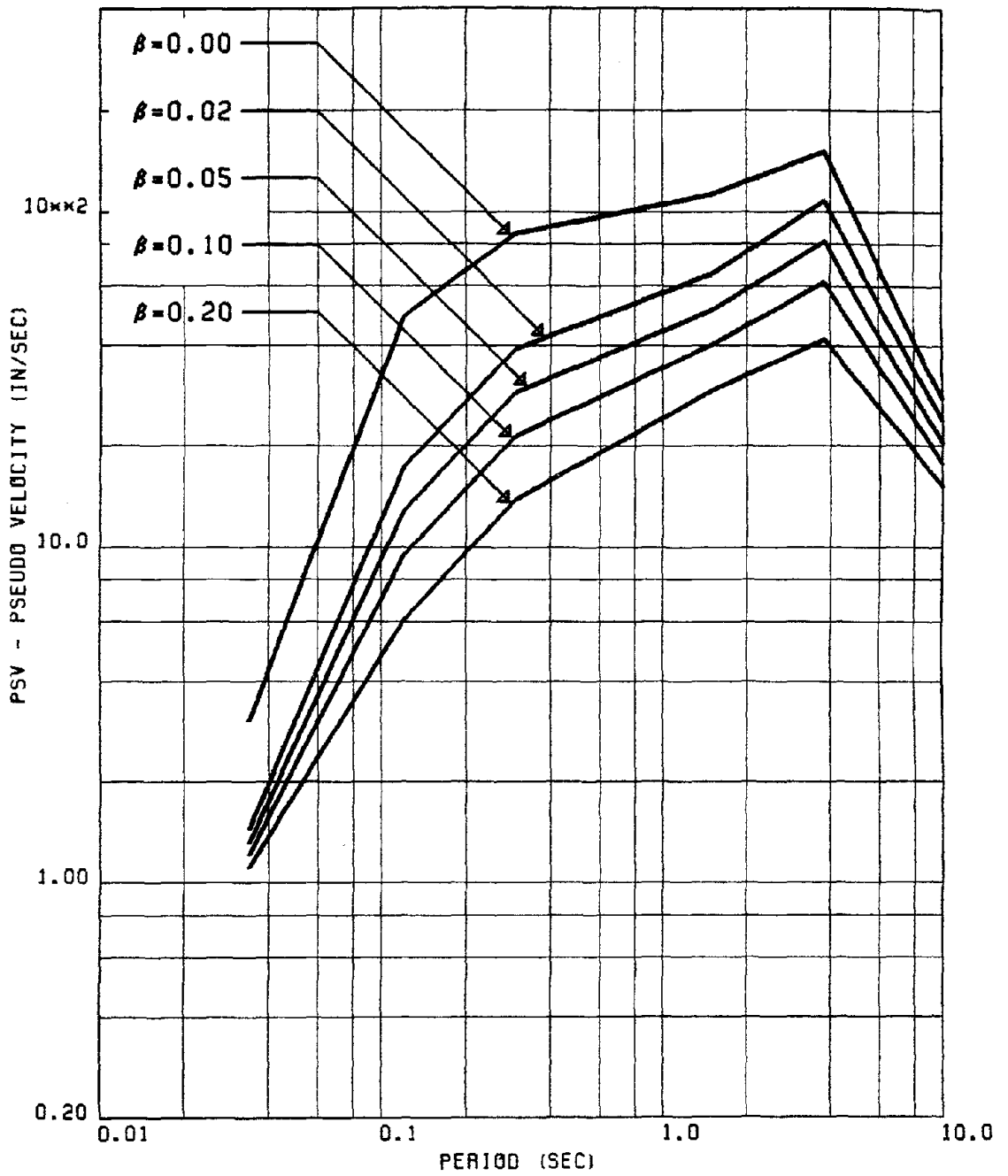
FIG. 176 PROPOSED (MEAN+SD) PSV SPECTRA FOR VERTICAL RECORDS OF GROUP #1

254
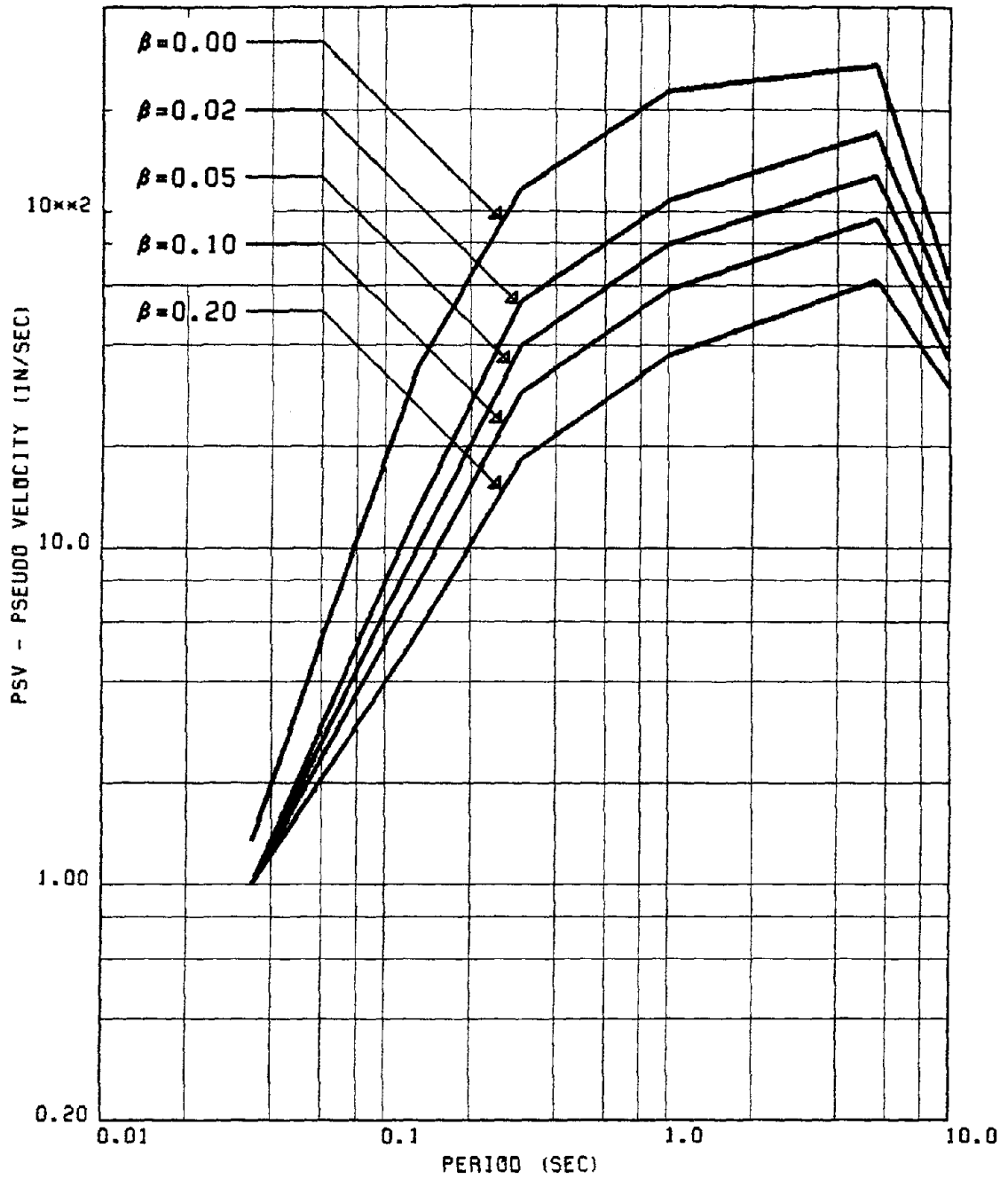
FIG. 177 PROPOSED (MEAN+SD) PSV SPECTRA FOR HORIZONTAL RECORDS OF GROUP #2
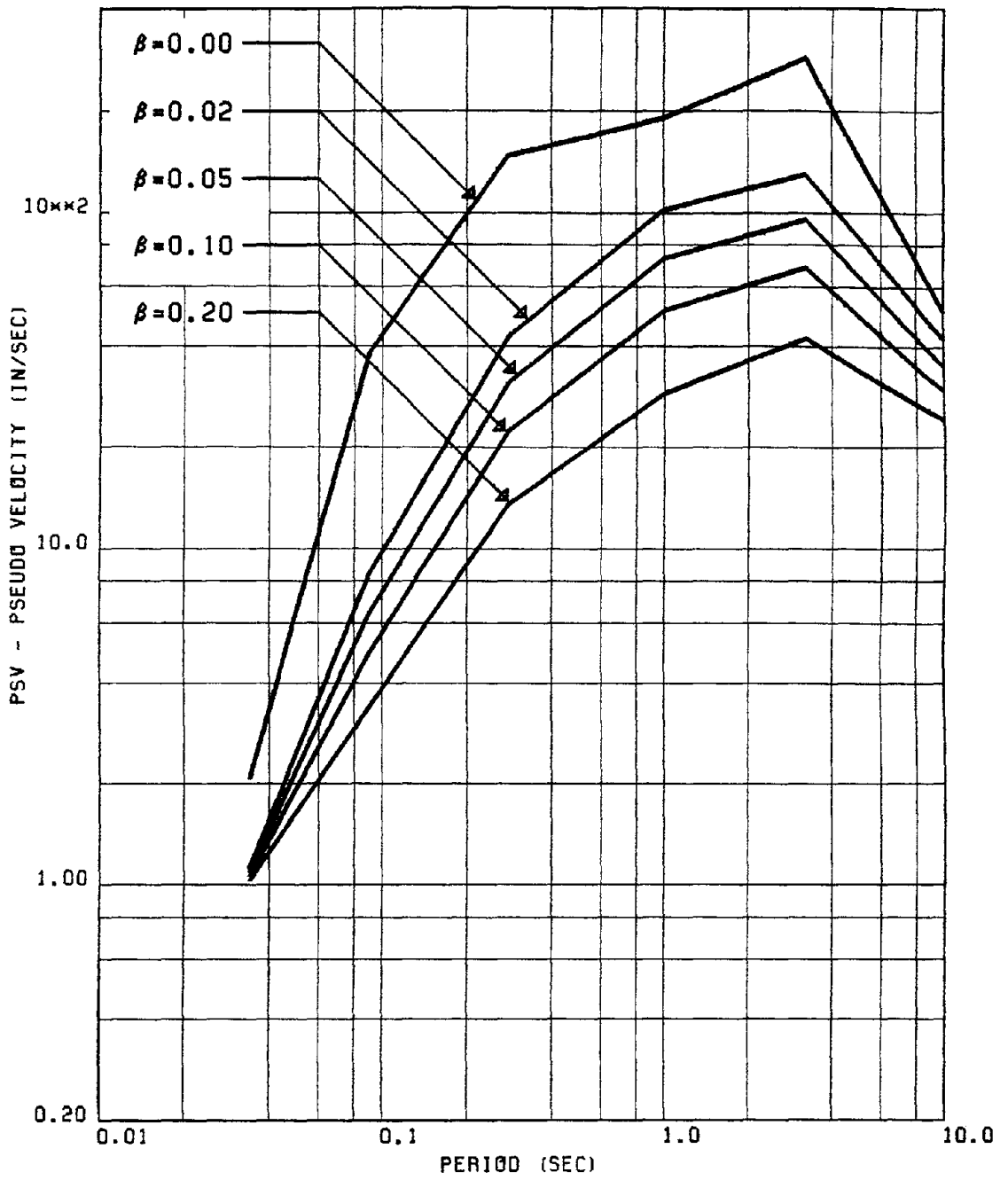
FIG. 178 PROPOSED (MEAN+SD) PSV SPECTRA FOR VERTICAL RECORDS OF GROUP #2

256
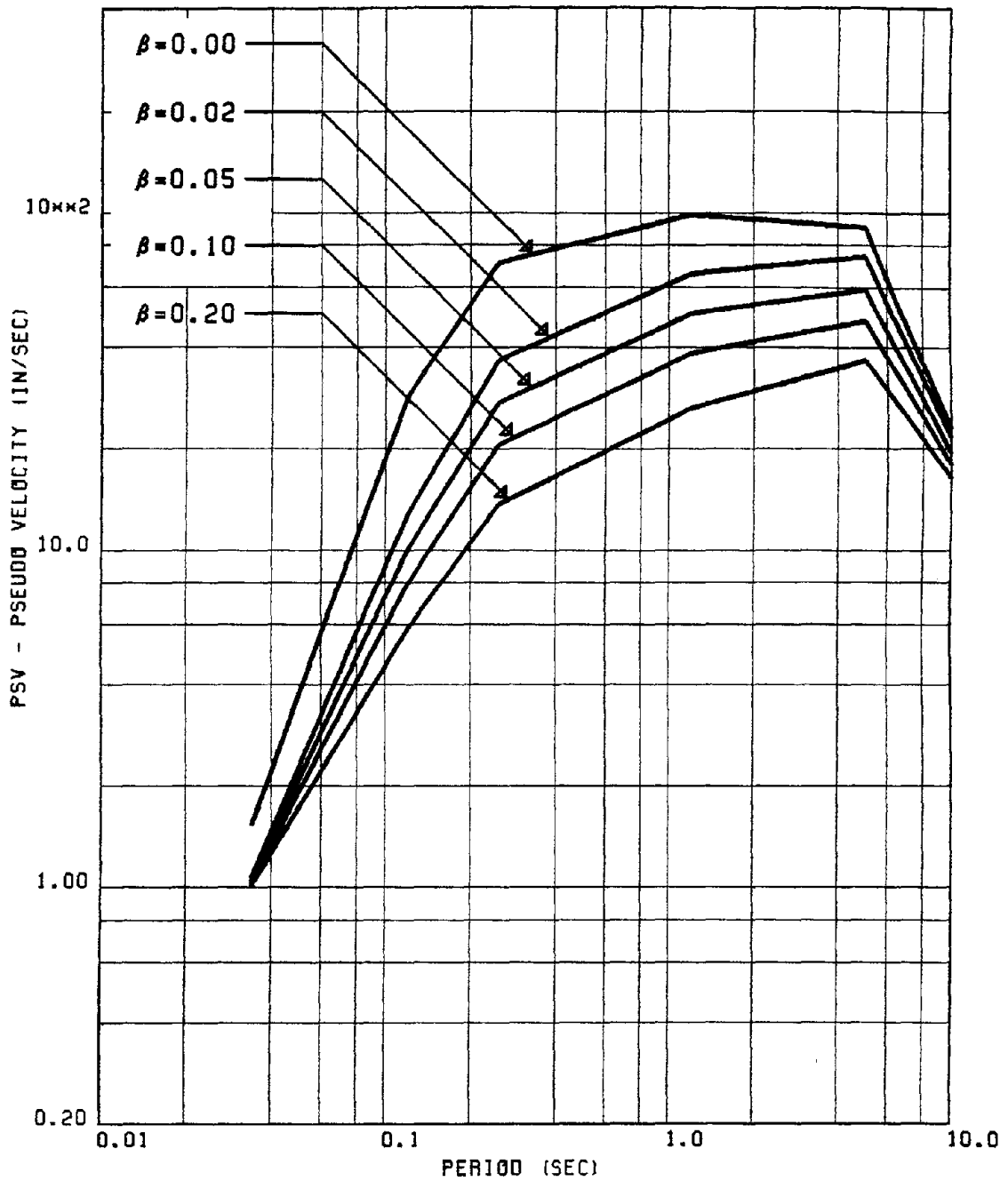
FIG. 179 PROPOSED (MEAN+SD) PSV SPECTRA FOR HORIZONTAL RECORDS OF GROUP #3
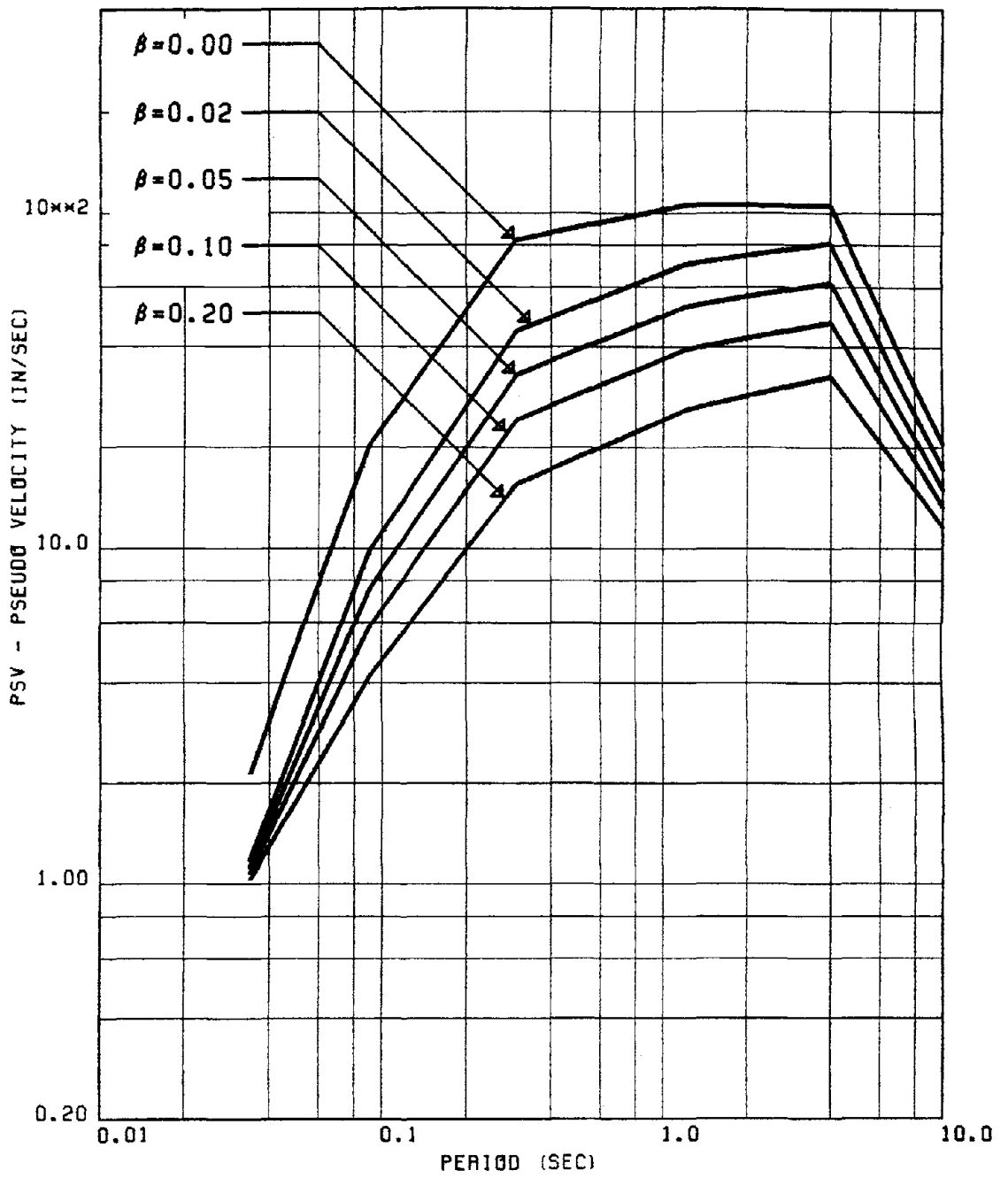
FIG. 180 PROPOSED (MEAN+SD) PSV SPECTRA FOR VERTICAL RECORDS OF GROUP #3
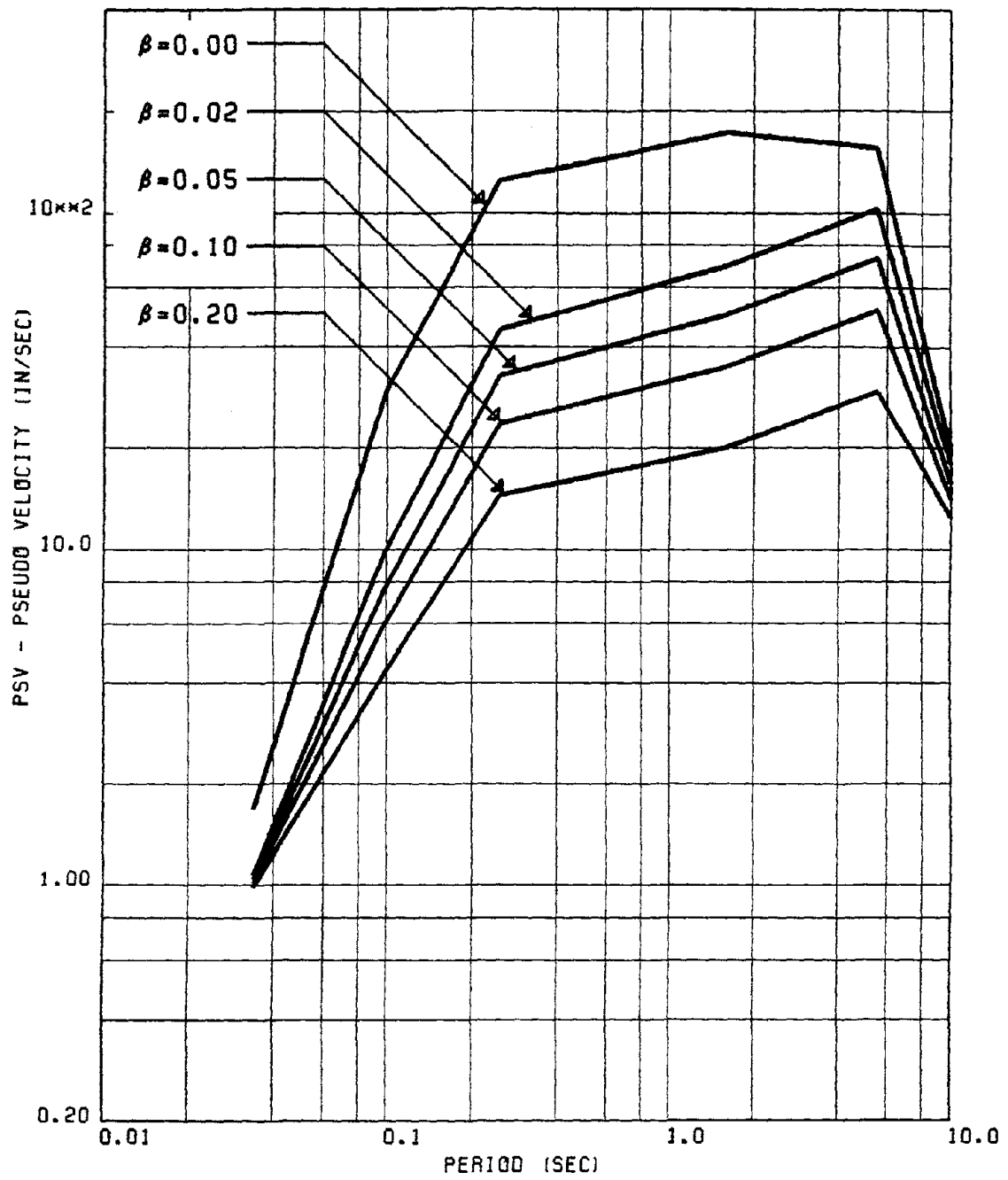
FIG. 181 PROPOSED (MEAN+SD) PSV SPECTRA FOR HORIZONTAL RECORDS OF GROUP #4
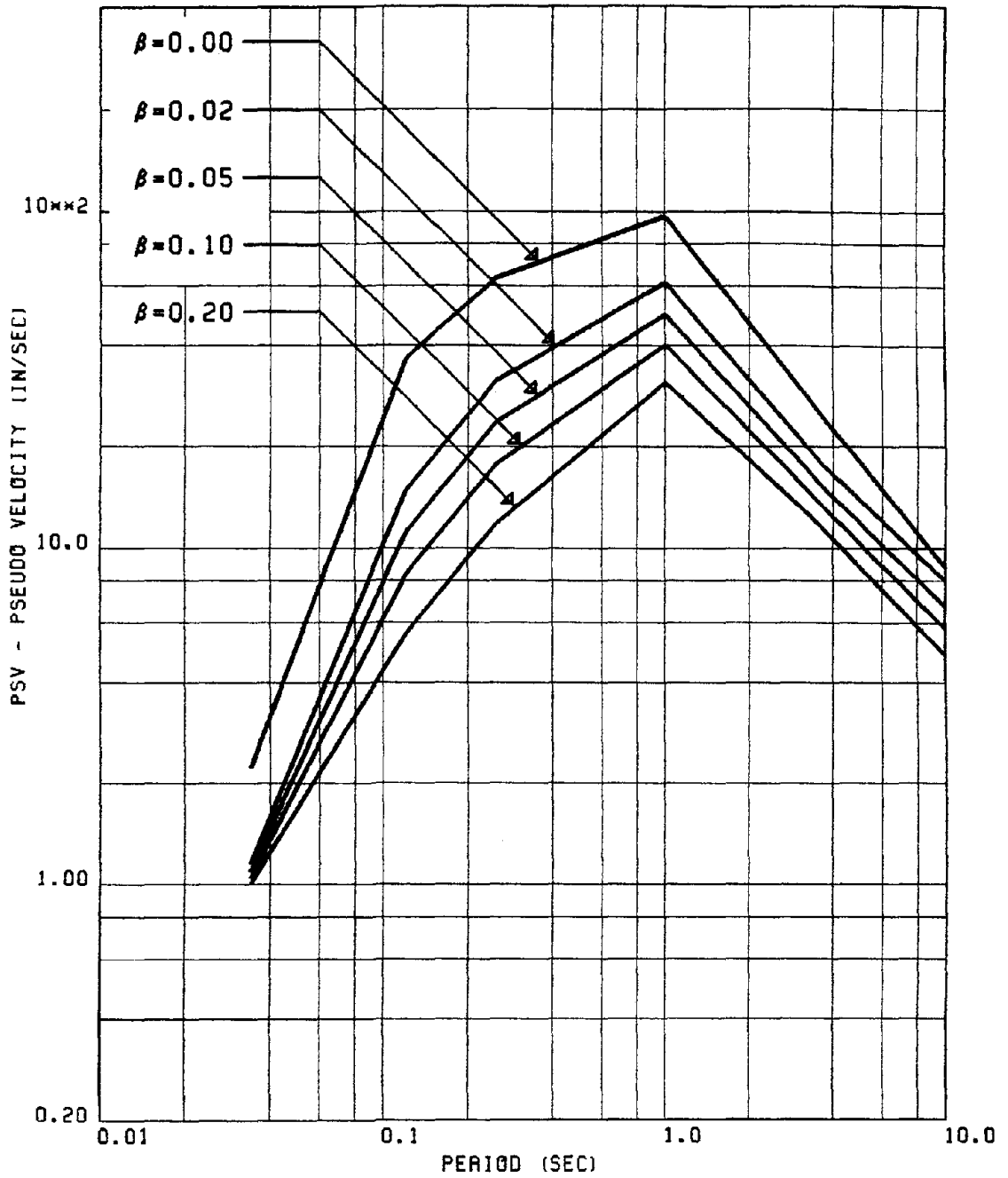
FIG. 182 PROPOSED (MEAN+SD) PSV SPECTRA FOR HORIZONTAL RECORDS OF GROUP #5
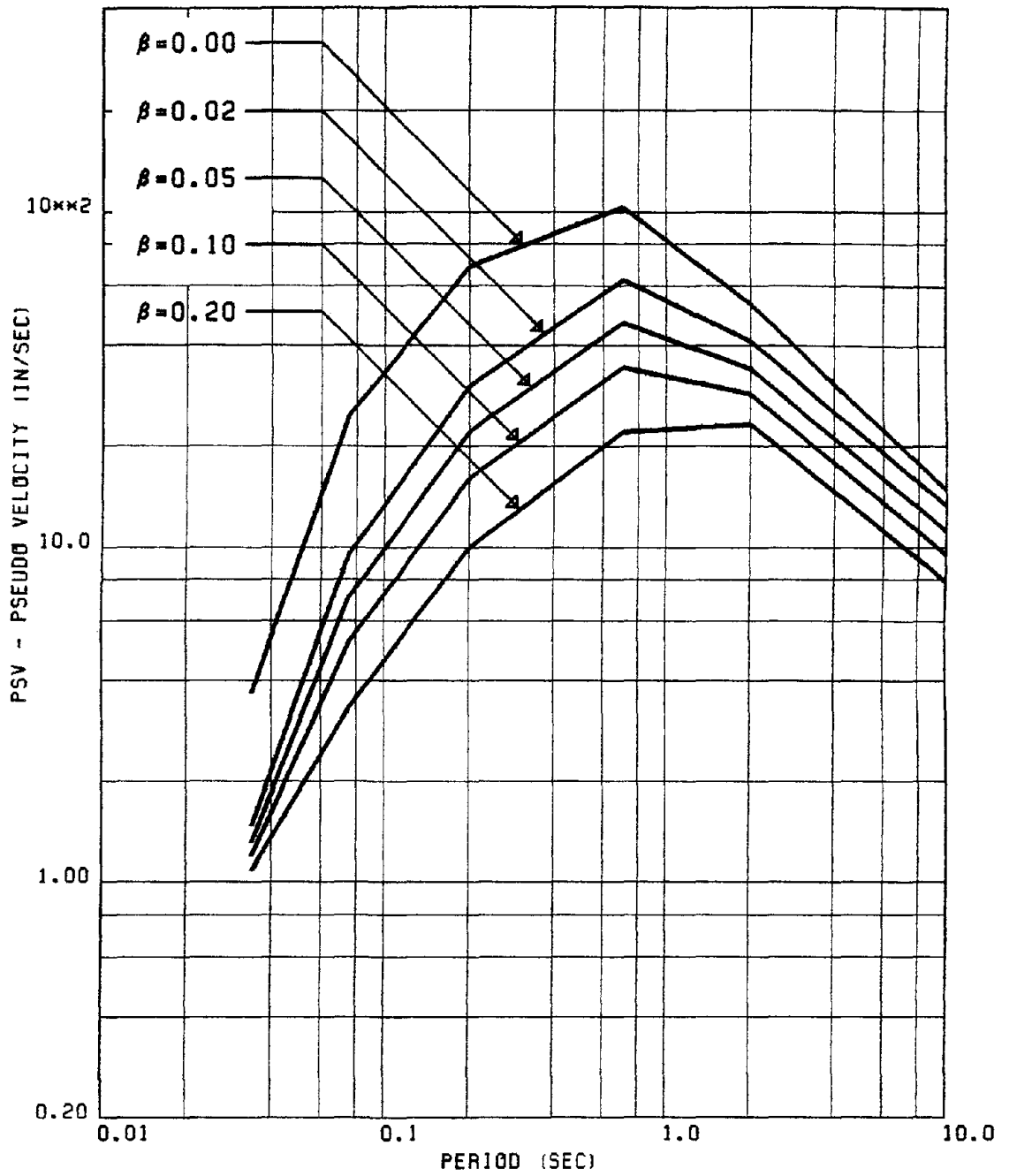
FIG. 183 PROPOSED (MEAN+SD) PSV SPECTRA FOR VERTICAL RECORDS OF GROUP #5
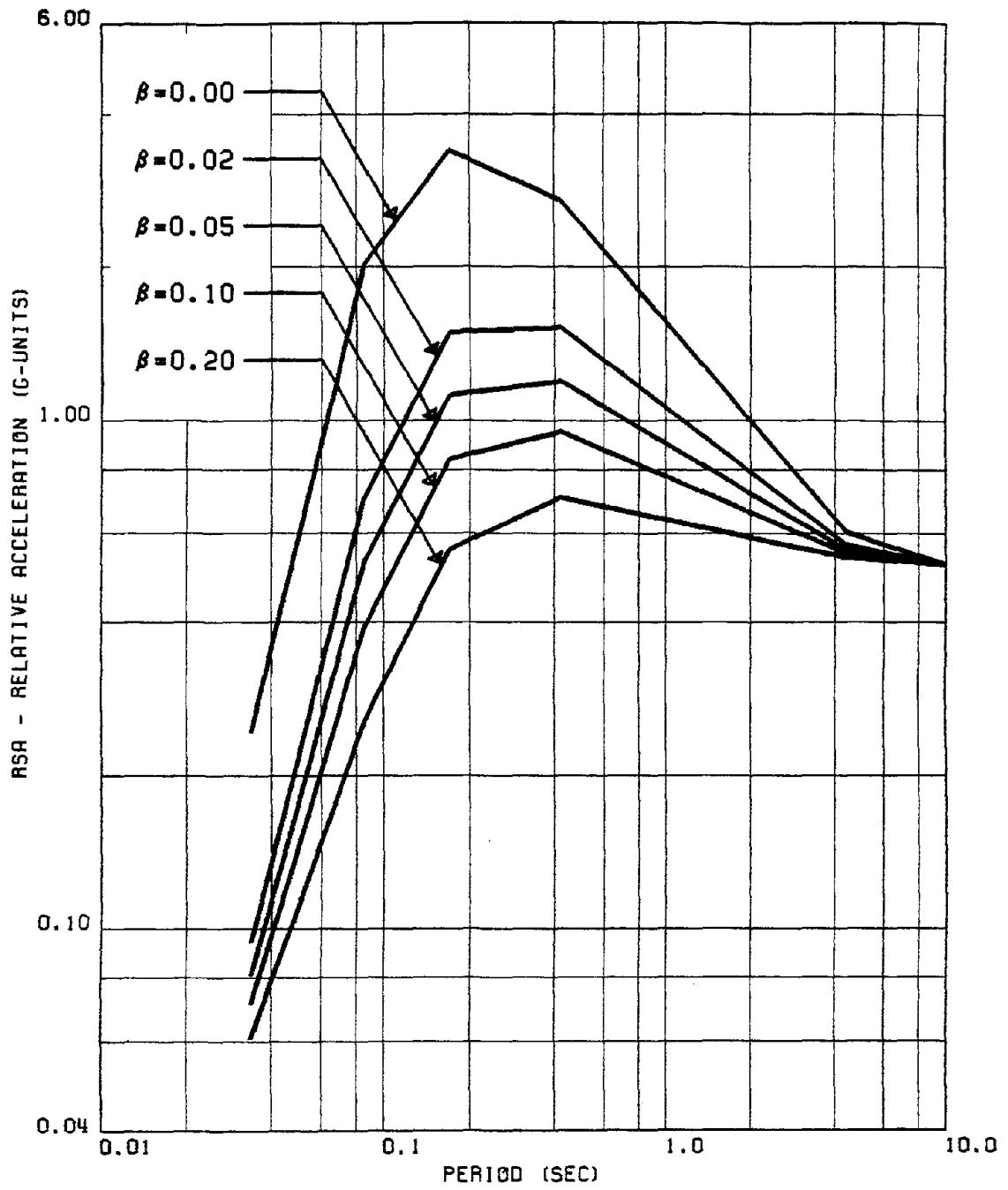
FIG. 184 PROPOSED SPECTRA FOR MEAN RSA FOR HORIZONTAL RECORDS OF GROUP #1
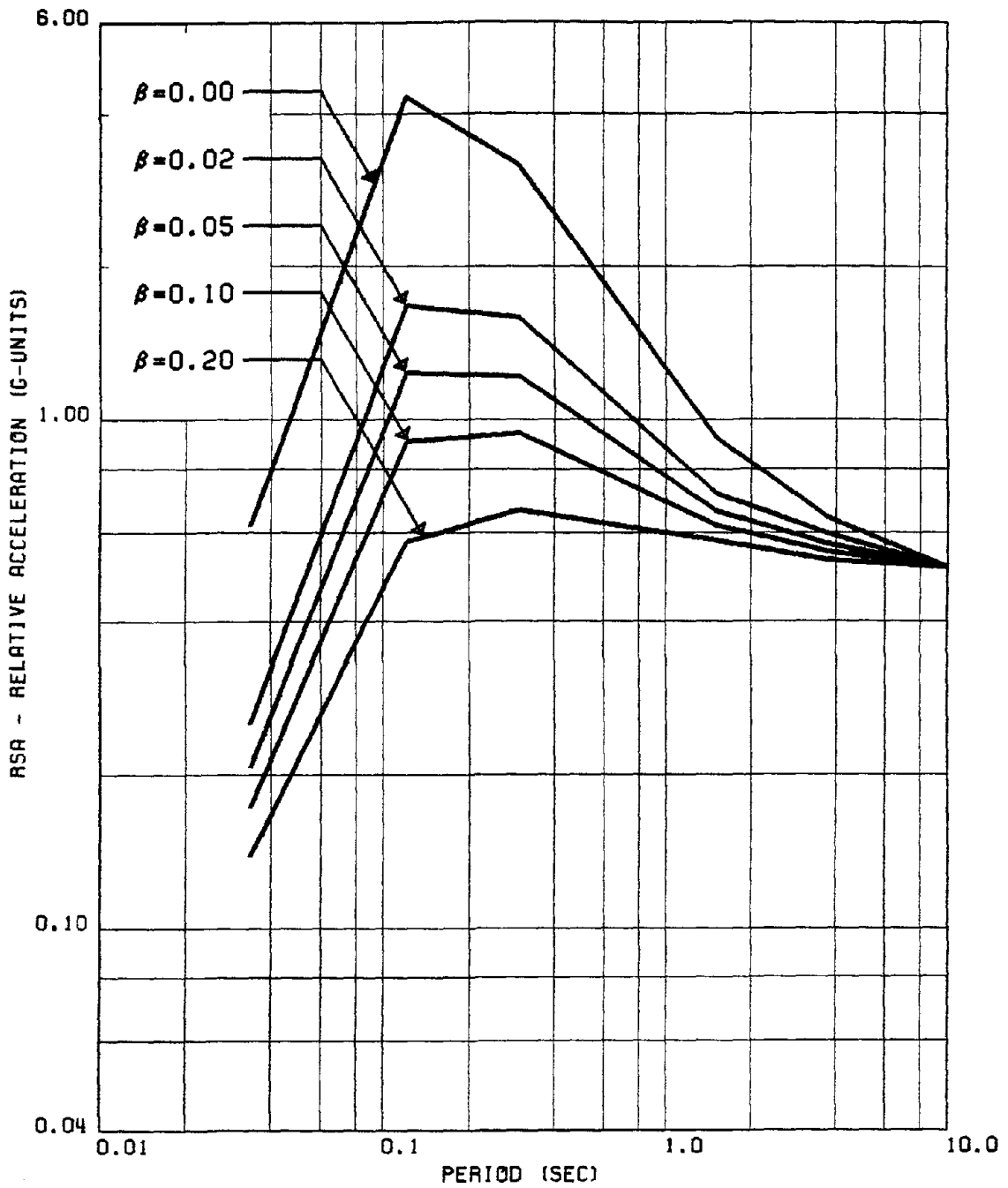
FIG. 185 PROPOSED SPECTRA FOR MEAN RSA FOR VERTICAL RECORDS OF GROUP #1

263
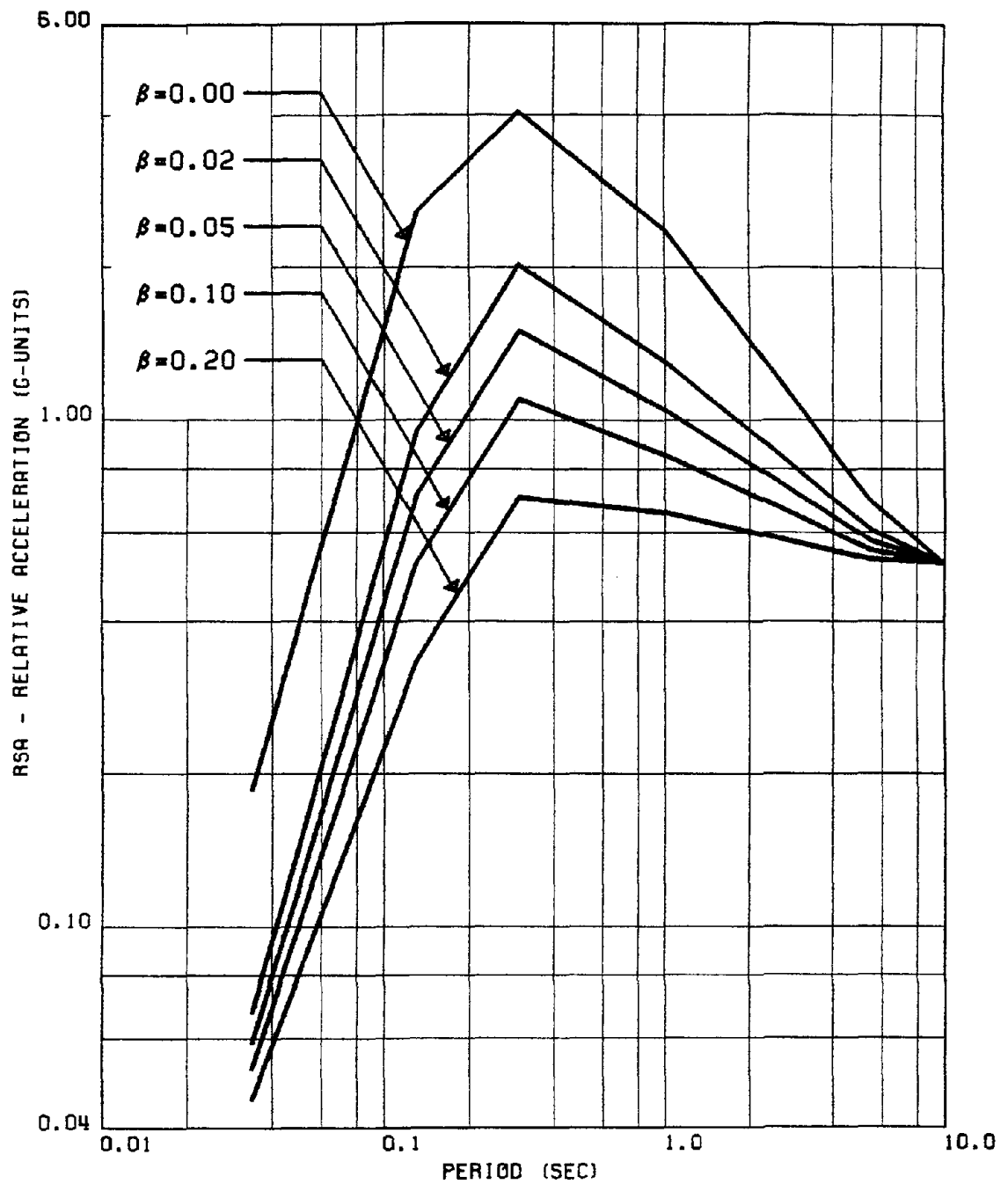
FIG. 186 PROPOSED SPECTRA FOR MEAN RSA FOR HORIZONTAL RECORDS OF GROUP #2
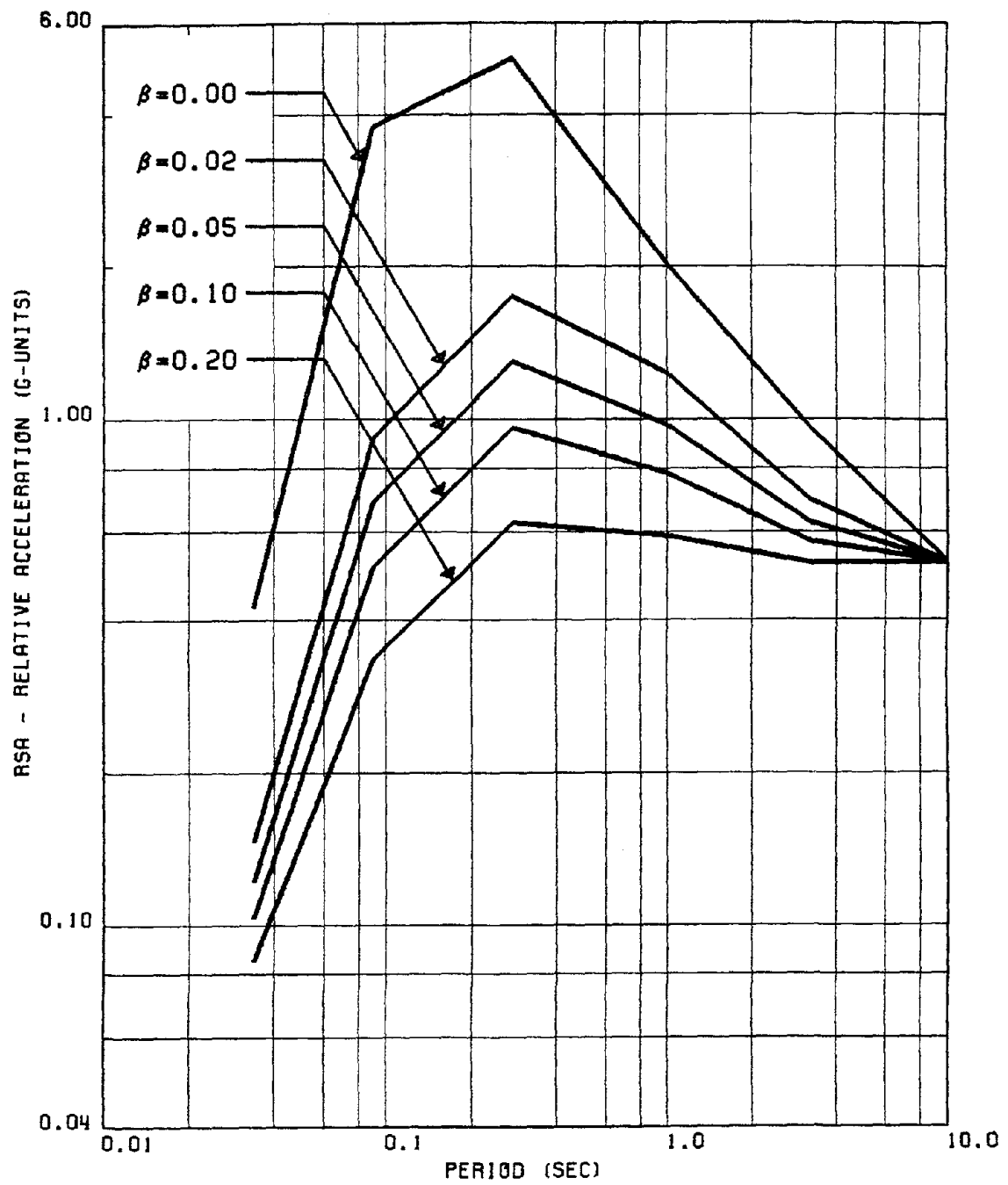
FIG. 187 PROPOSED SPECTRA FOR MEAN RSA FOR VERTICAL RECORDS OF GROUP #2
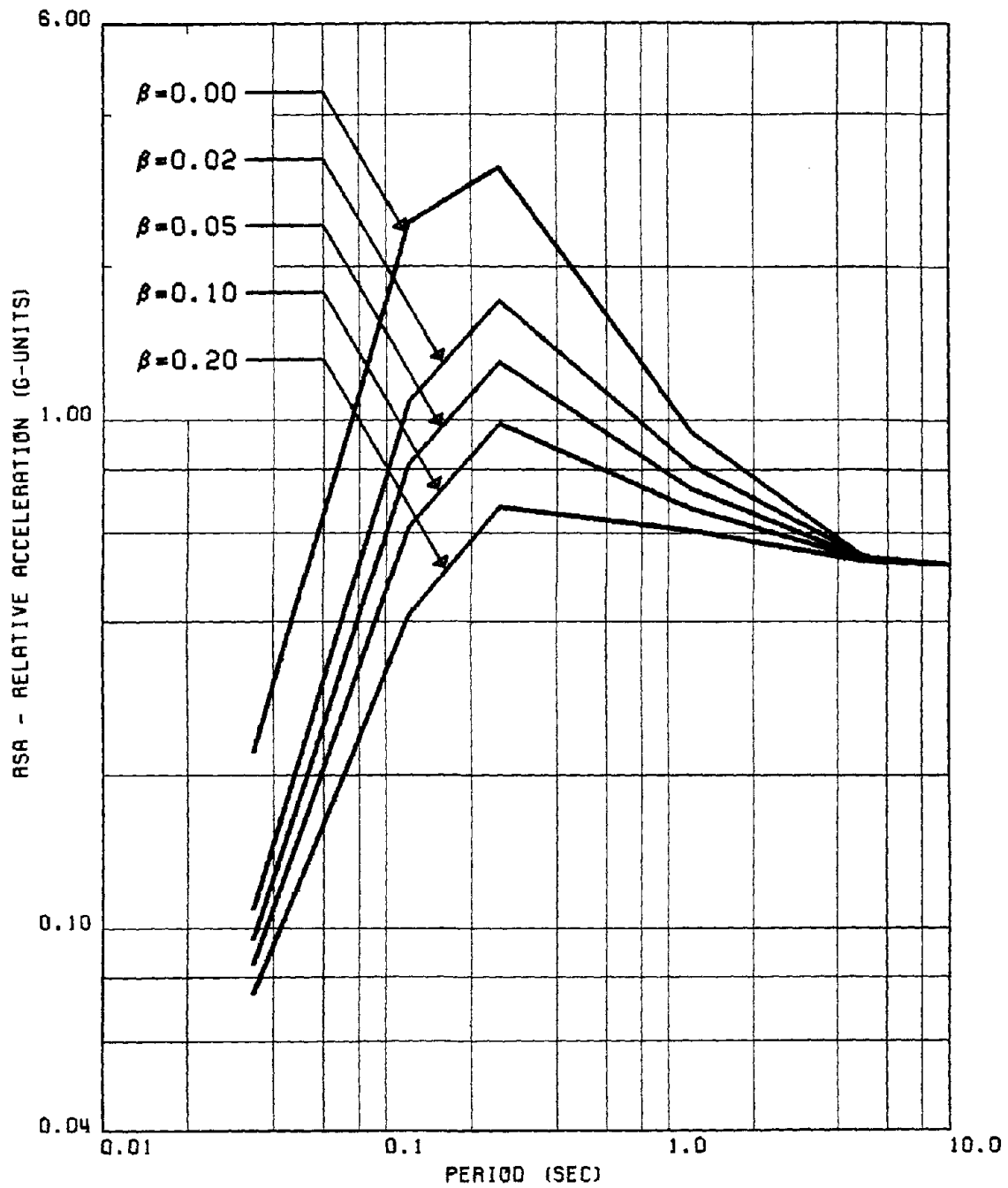
FIG. 188 PROPOSED SPECTRA FOR MEAN RSA FOR HORIZONTAL RECORDS OF GROUP #3
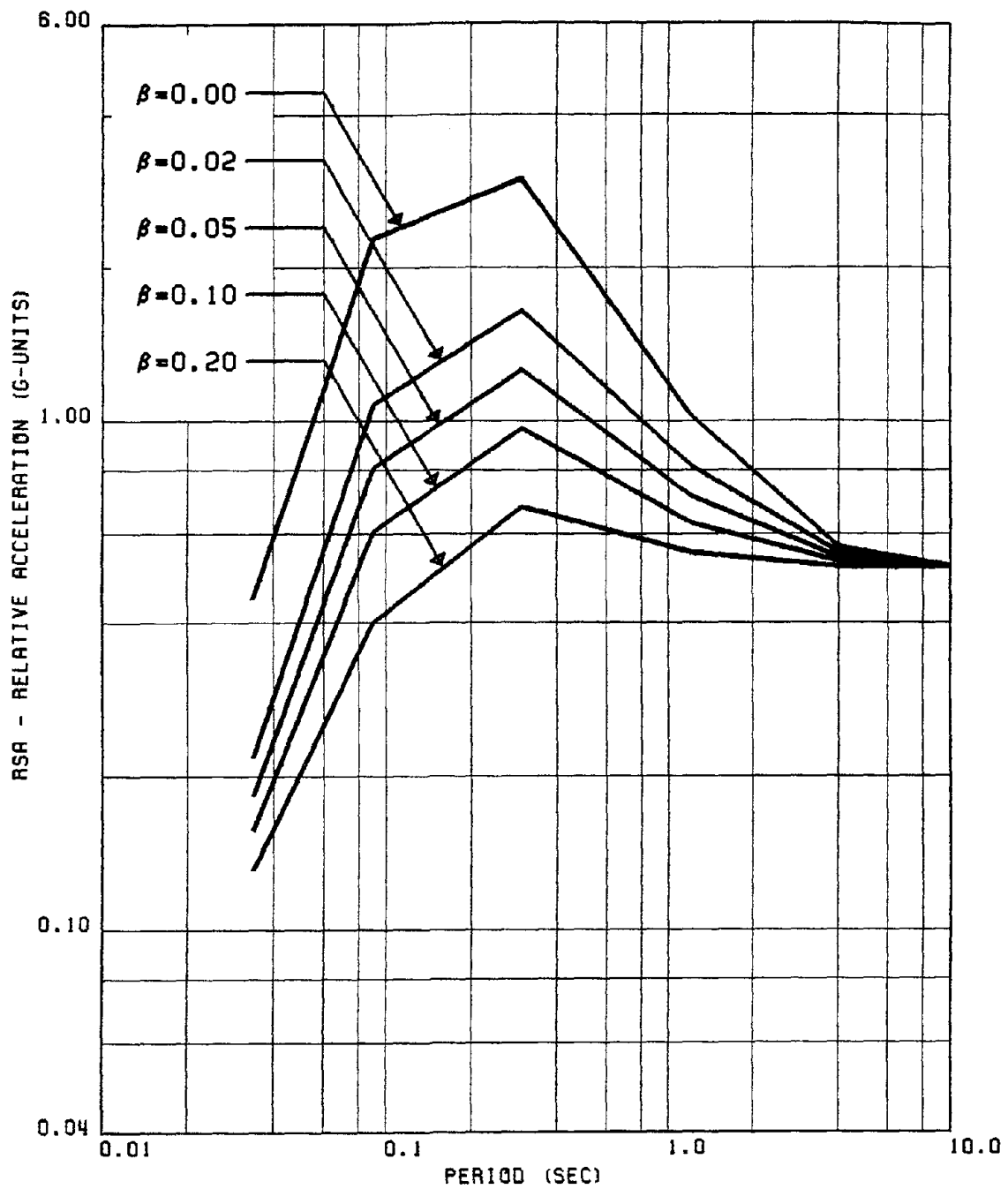
FIG. 189 PROPOSED SPECTRA FOR MEAN RSA FOR VERTICAL RECORDS OF GROUP #3

267
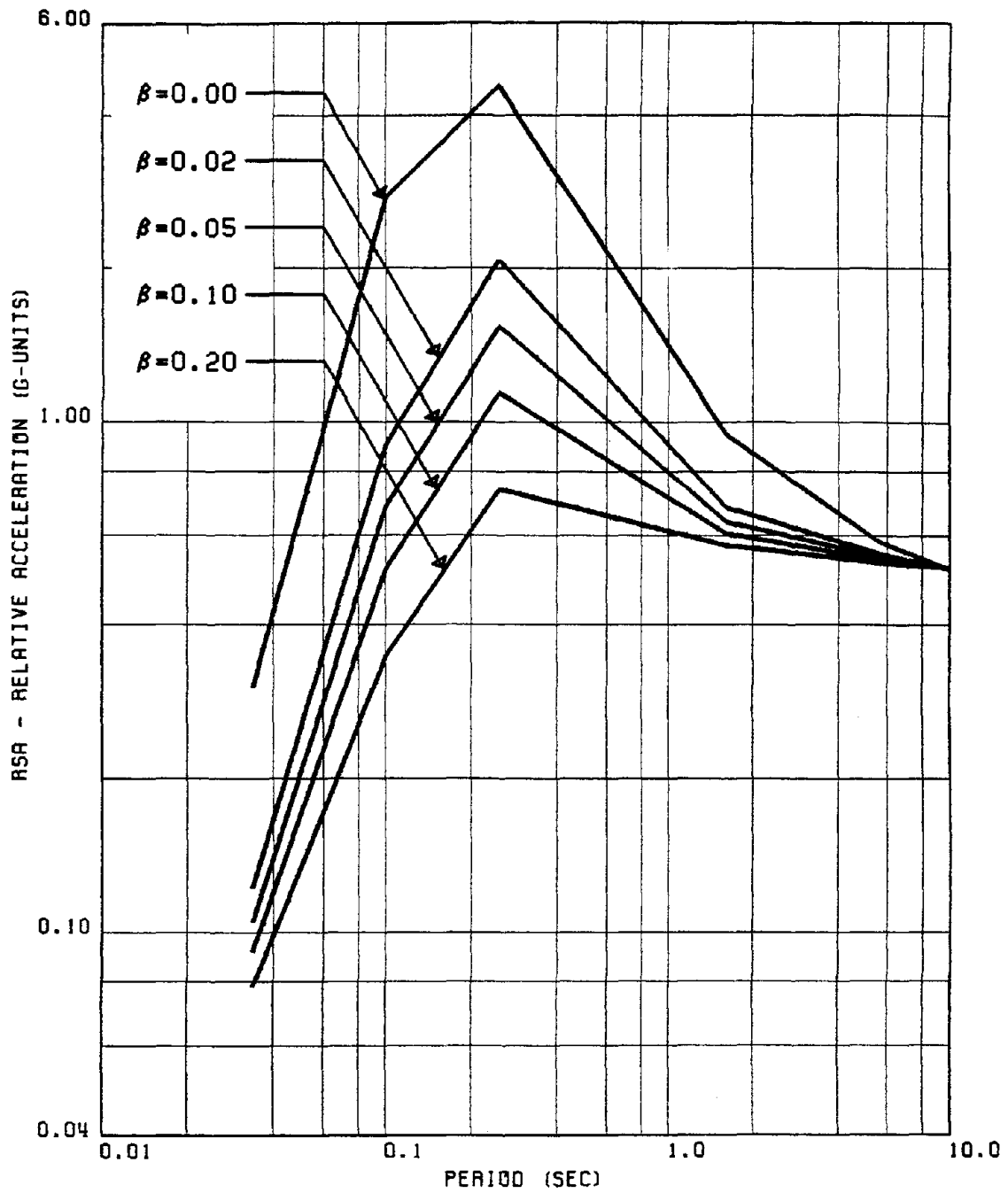
FIG. 190 PROPOSED SPECTRA FOR MEAN RSA FOR HORIZONTAL RECORDS OF GROUP #4
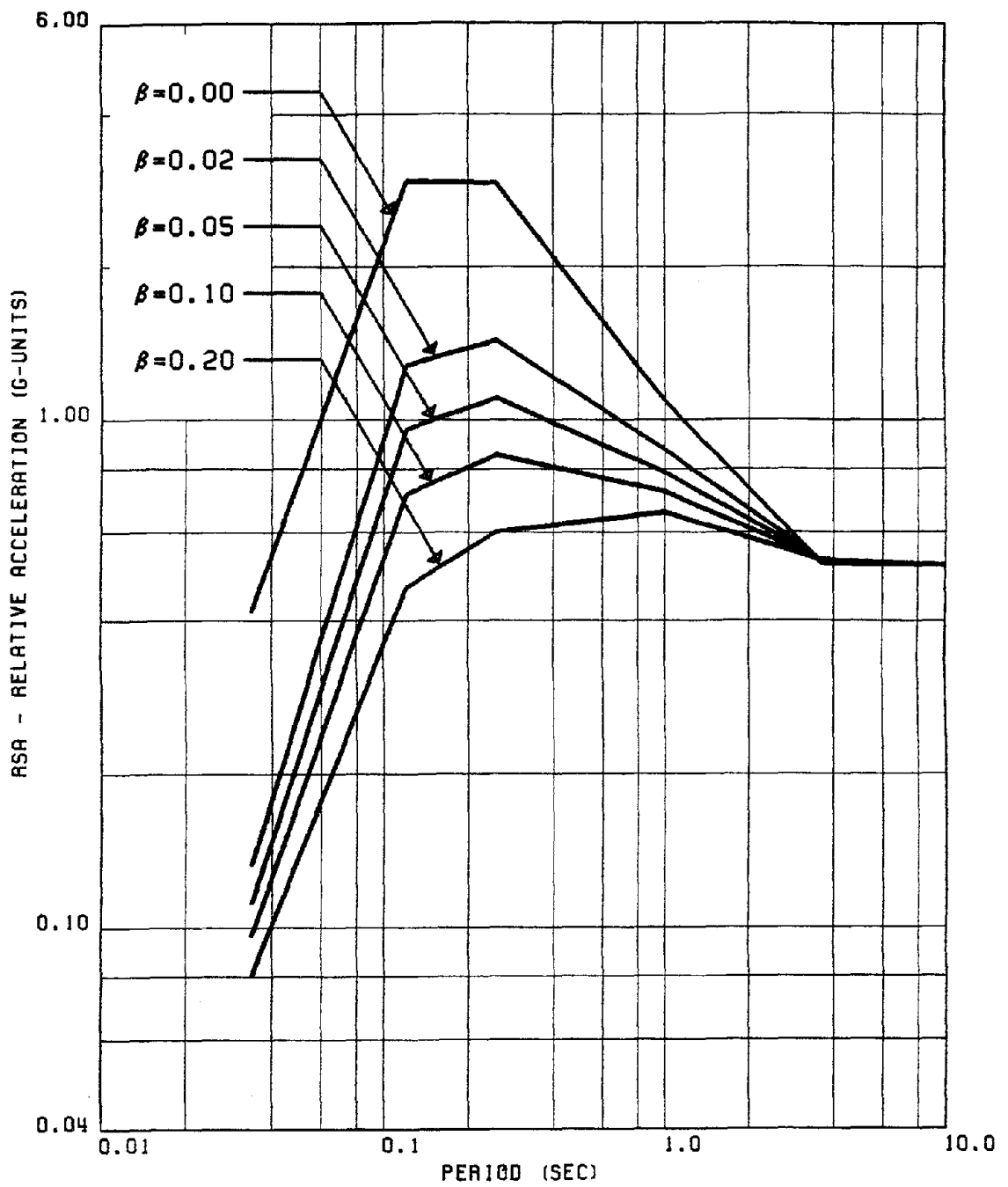
FIG. 191 PROPOSED SPECTRA FOR MEAN RSA FOR HORIZONTAL RECORDS OF GROUP #5

269
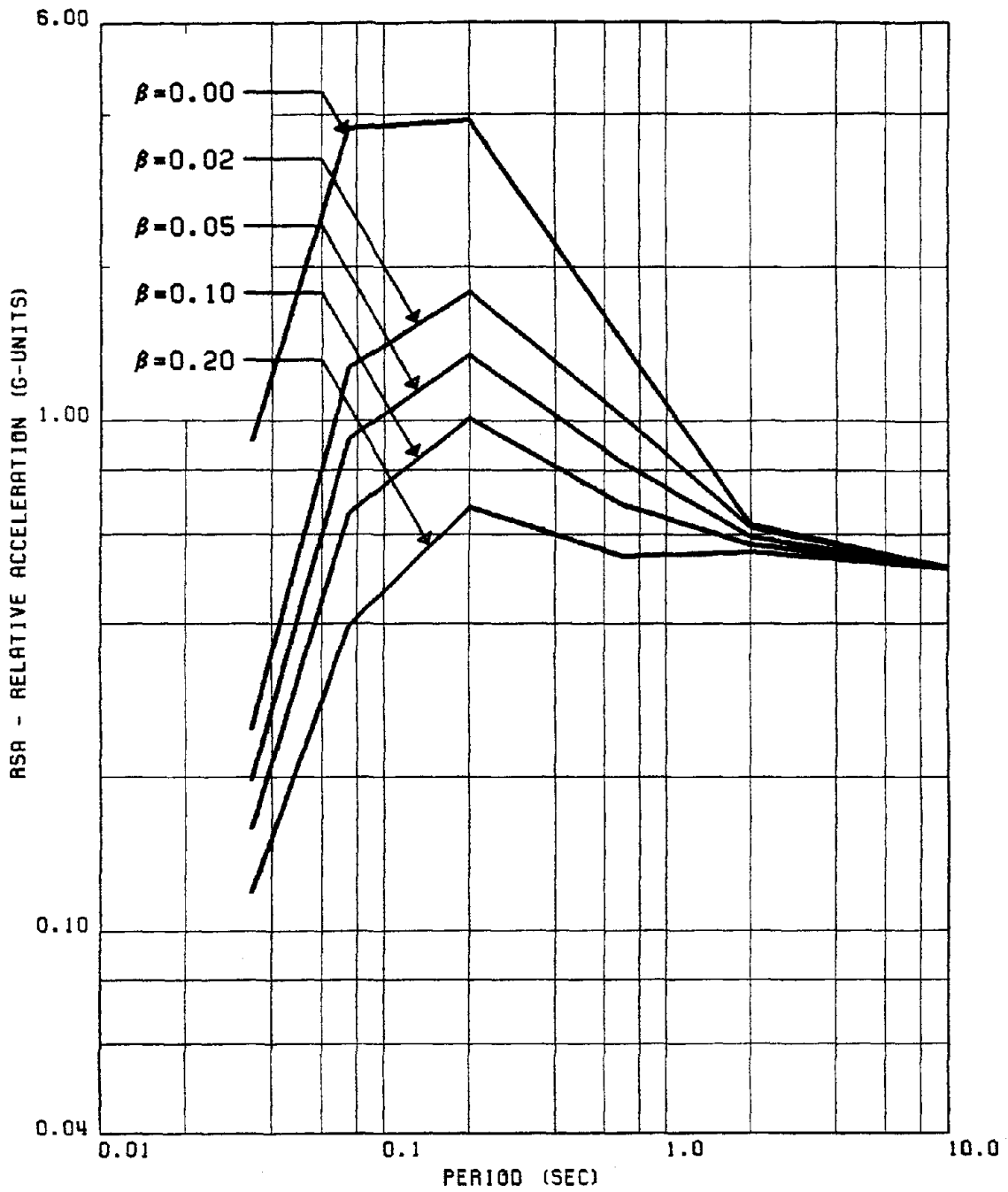
FIG. 192 PROPOSED SPECTRA FOR MEAN RSA FOR VERTICAL RECORDS OF GROUP #5
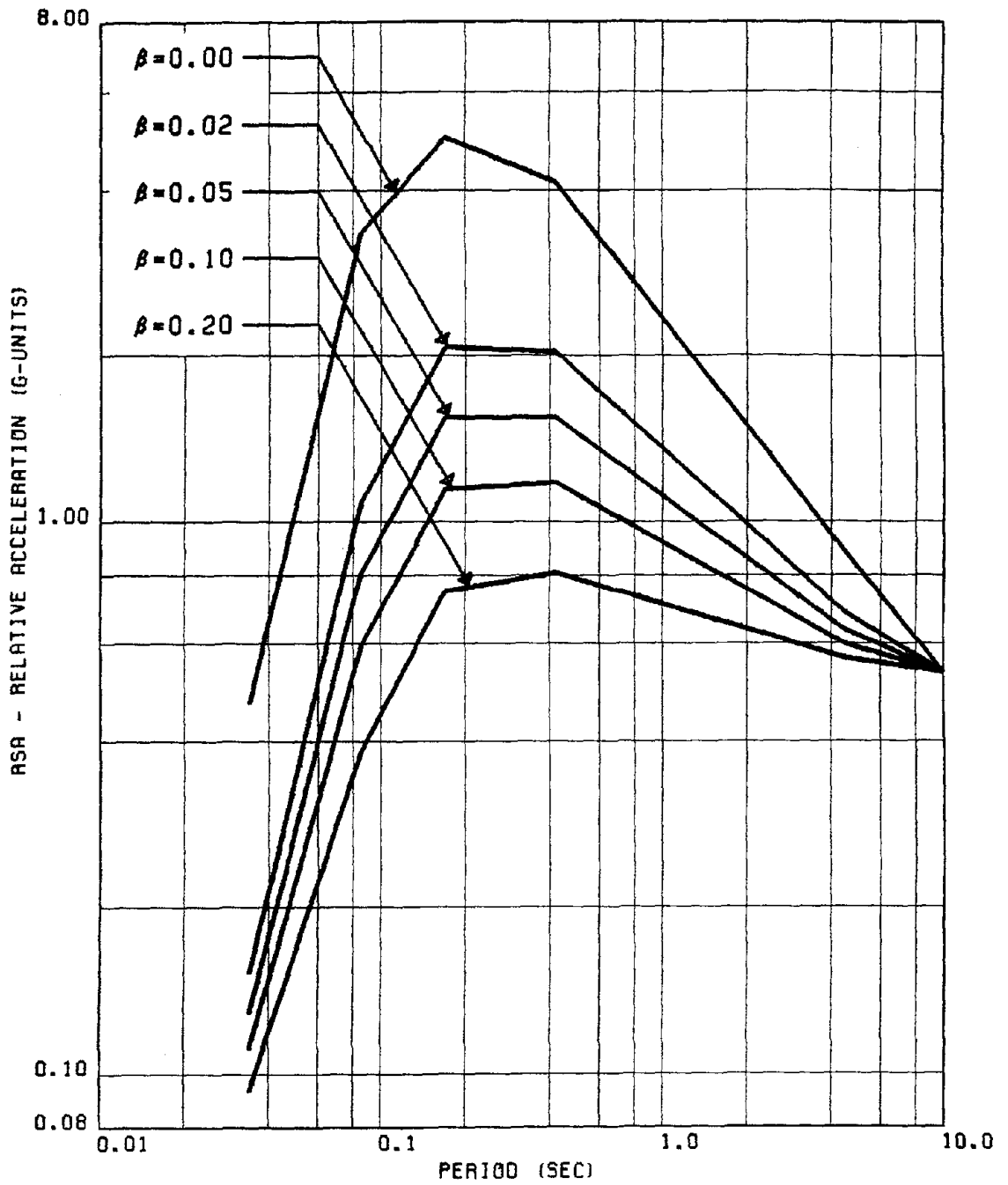
FIG. 193 PROPOSED (MEAN+SD) RSA SPECTRA FOR HORIZONTAL RECORDS OF GROUP #1

271
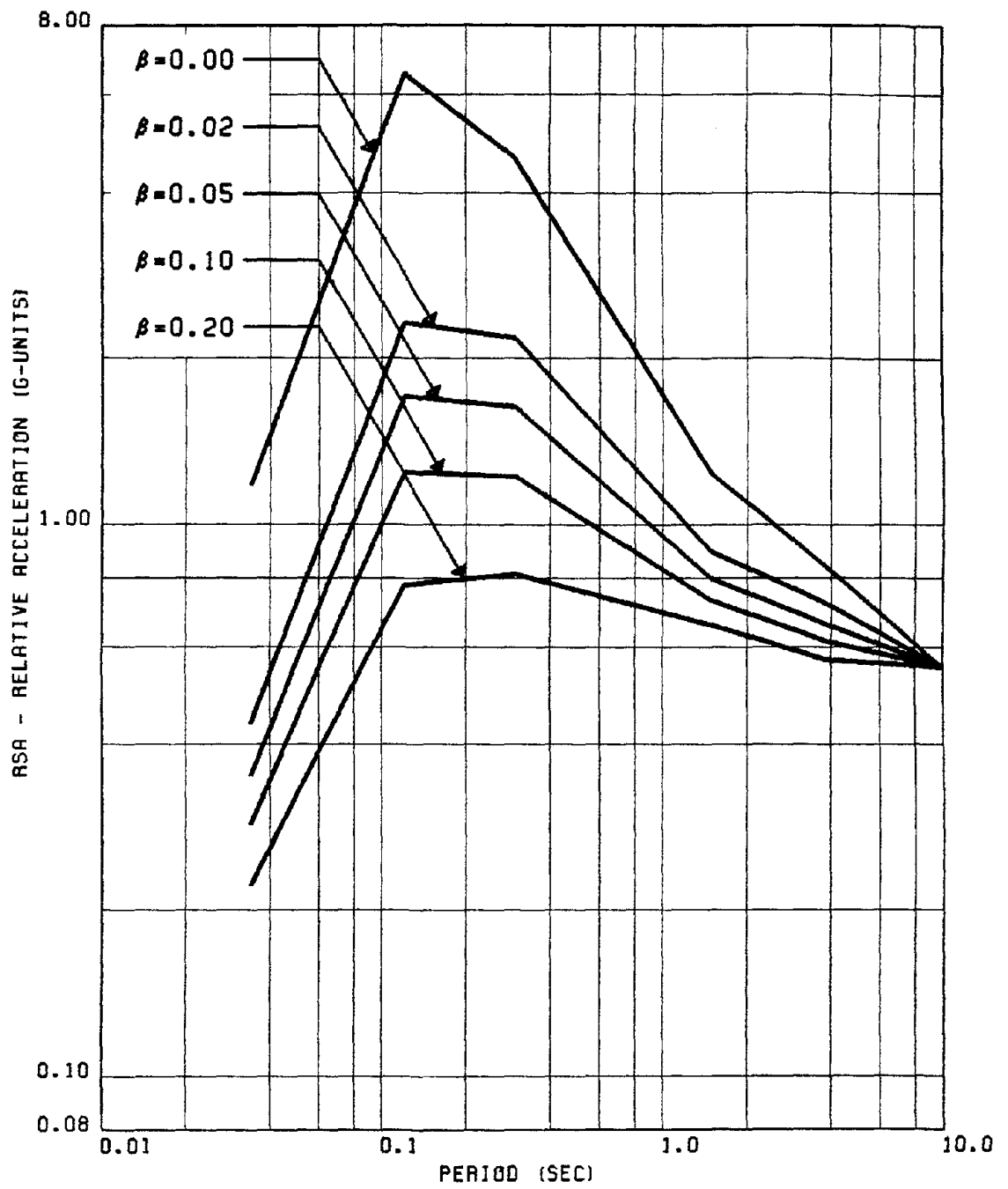
FIG. 194 PROPOSED (MEAN+SD) RSA SPECTRA FOR VERTICAL RECORDS OF GROUP #1
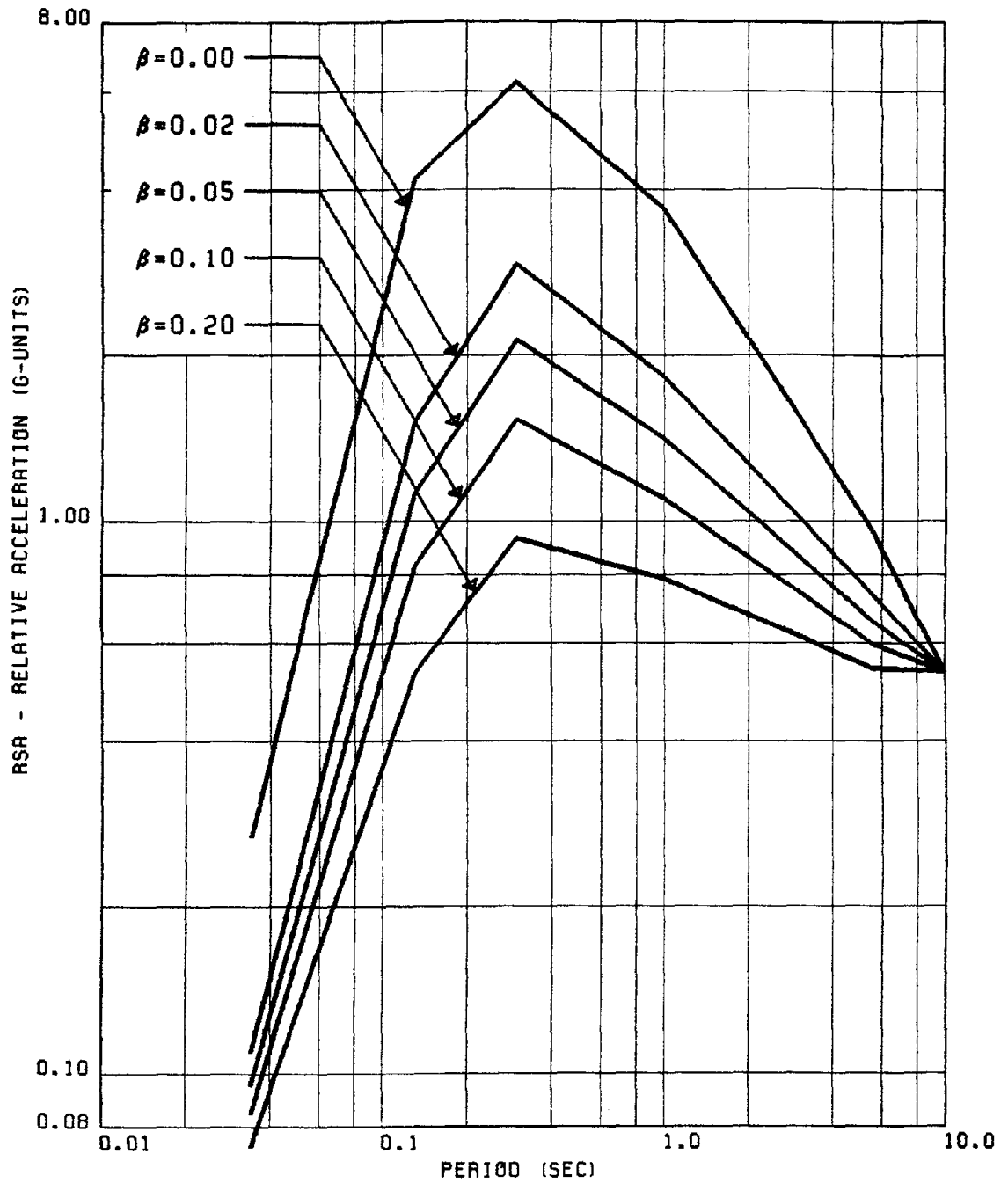
FIG. 195 PROPOSED (MEAN+SD) RSA SPECTRA FOR HORIZONTAL RECORDS OF GROUP #2
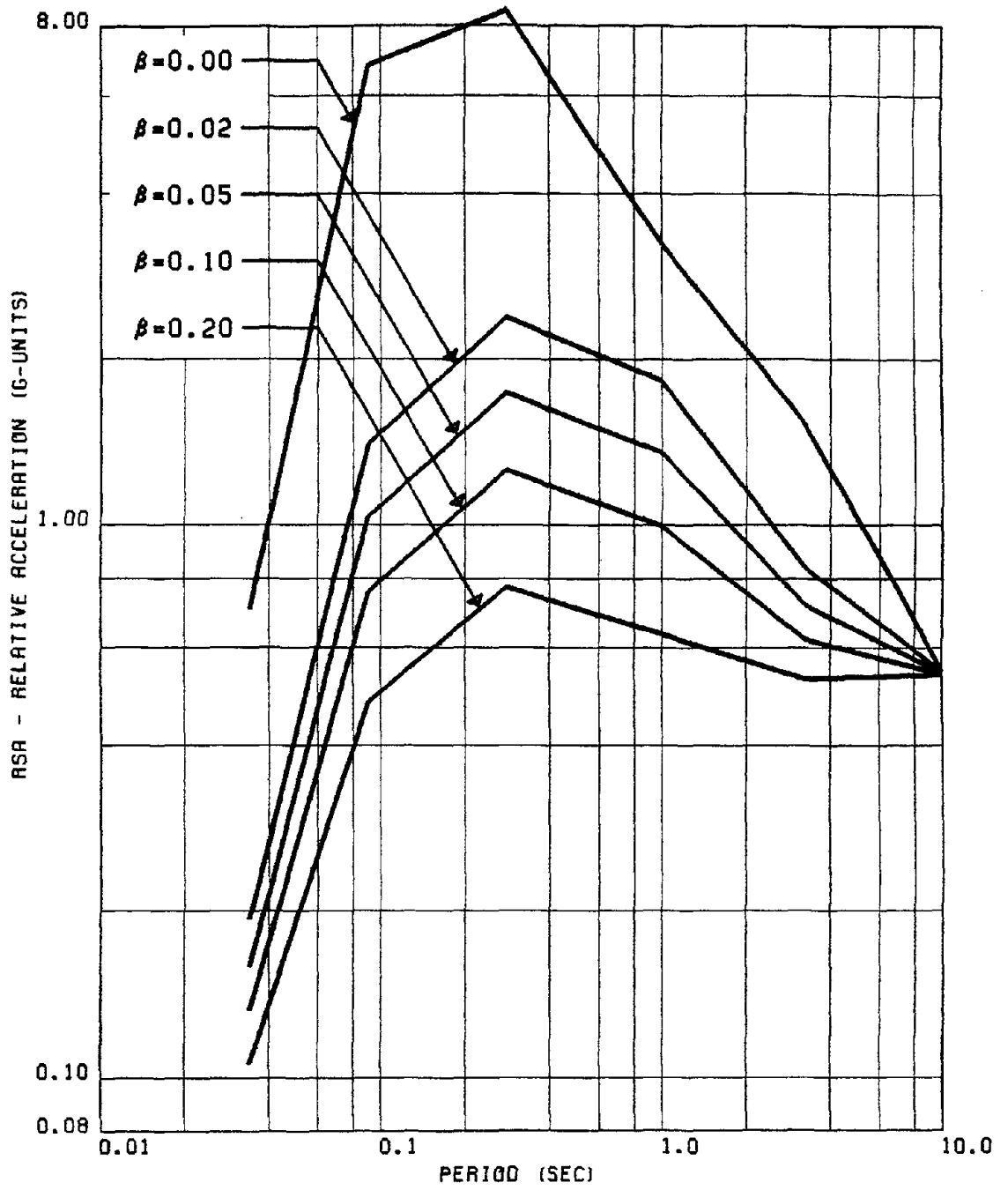
FIG. 196 PROPOSED (MEAN+SD) RSA SPECTRA FOR VERTICAL RECORDS OF GROUP *2

274
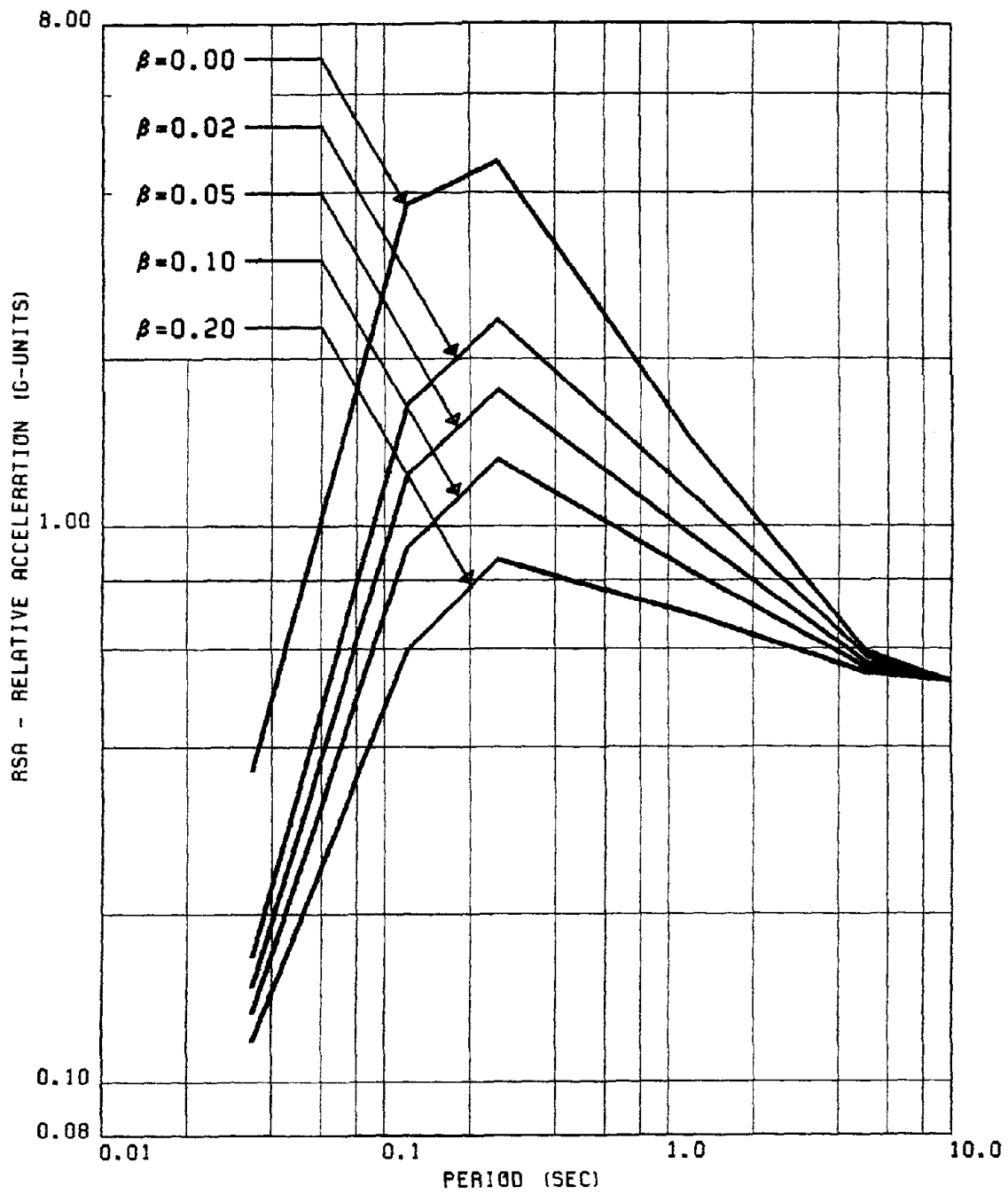
FIG. 197 PROPOSED (MEAN+SD) RSA SPECTRA FOR HORIZONTAL RECORDS OF GROUP #3
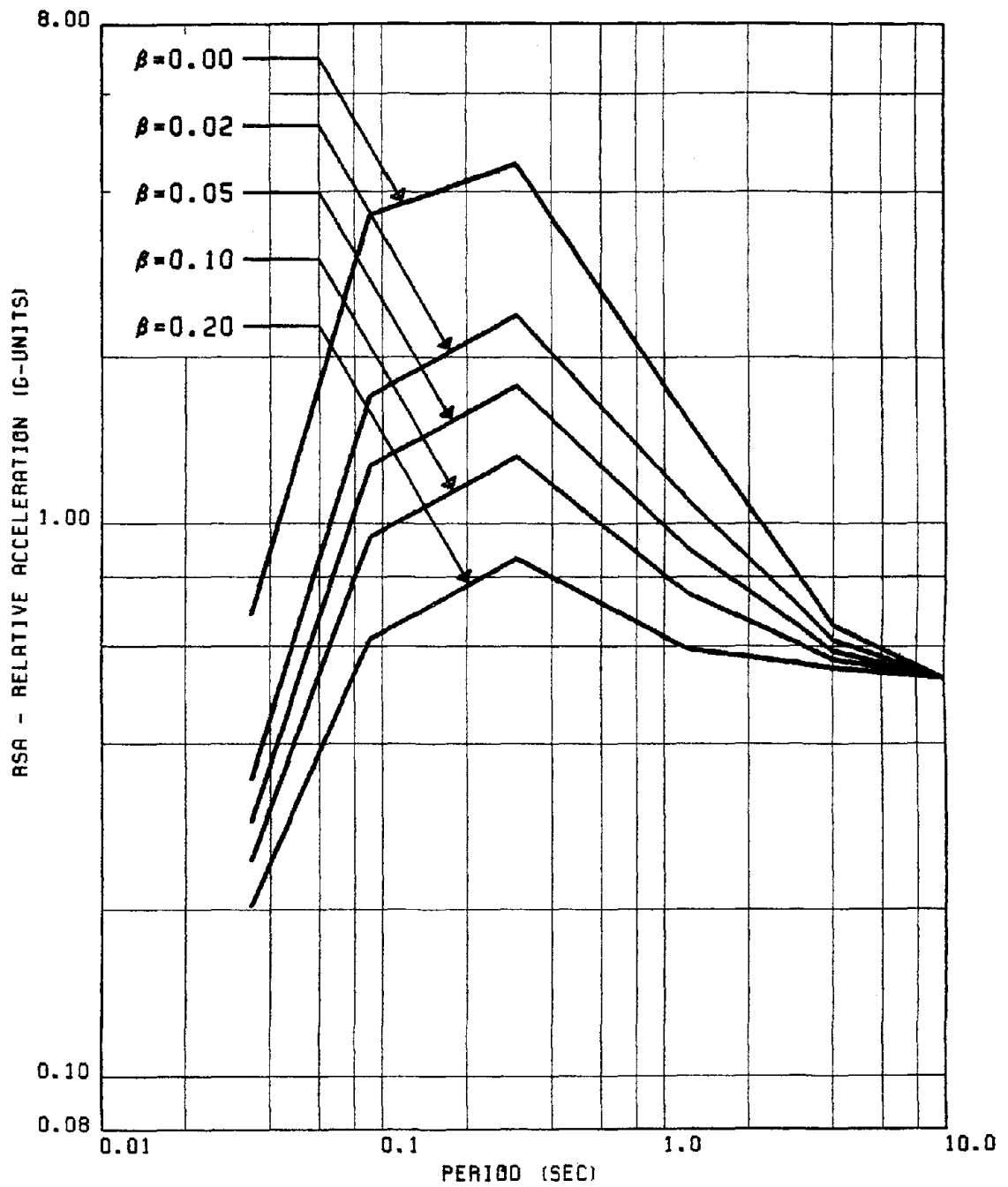
FIG. 198 PROPOSED (MEAN+SD) RSA SPECTRA FOR VERTICAL RECORDS OF GROUP #3
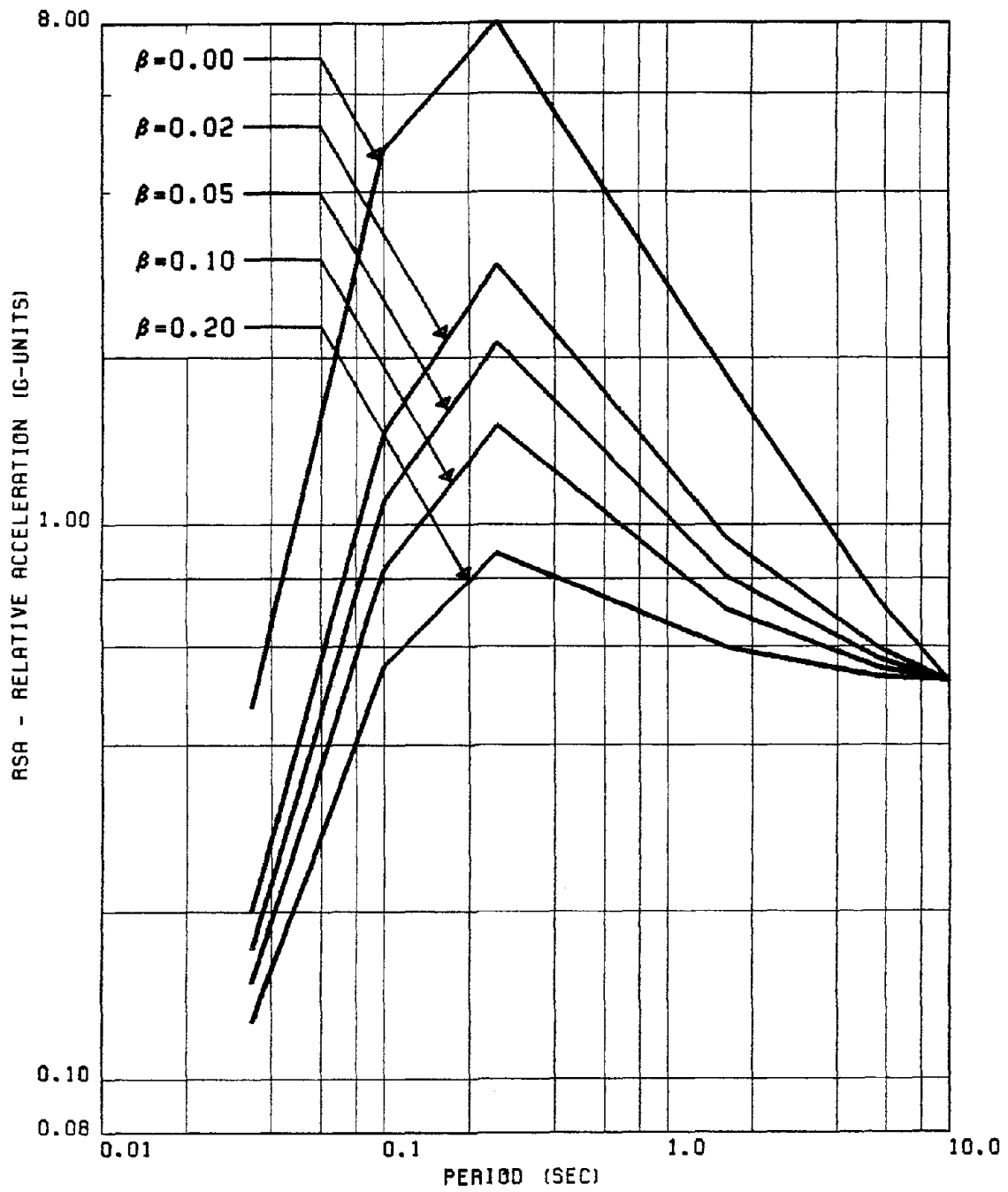
FIG. 199 PROPOSED (MEAN+SD) RSA SPECTRA FOR HORIZONTAL RECORDS OF GROUP #4
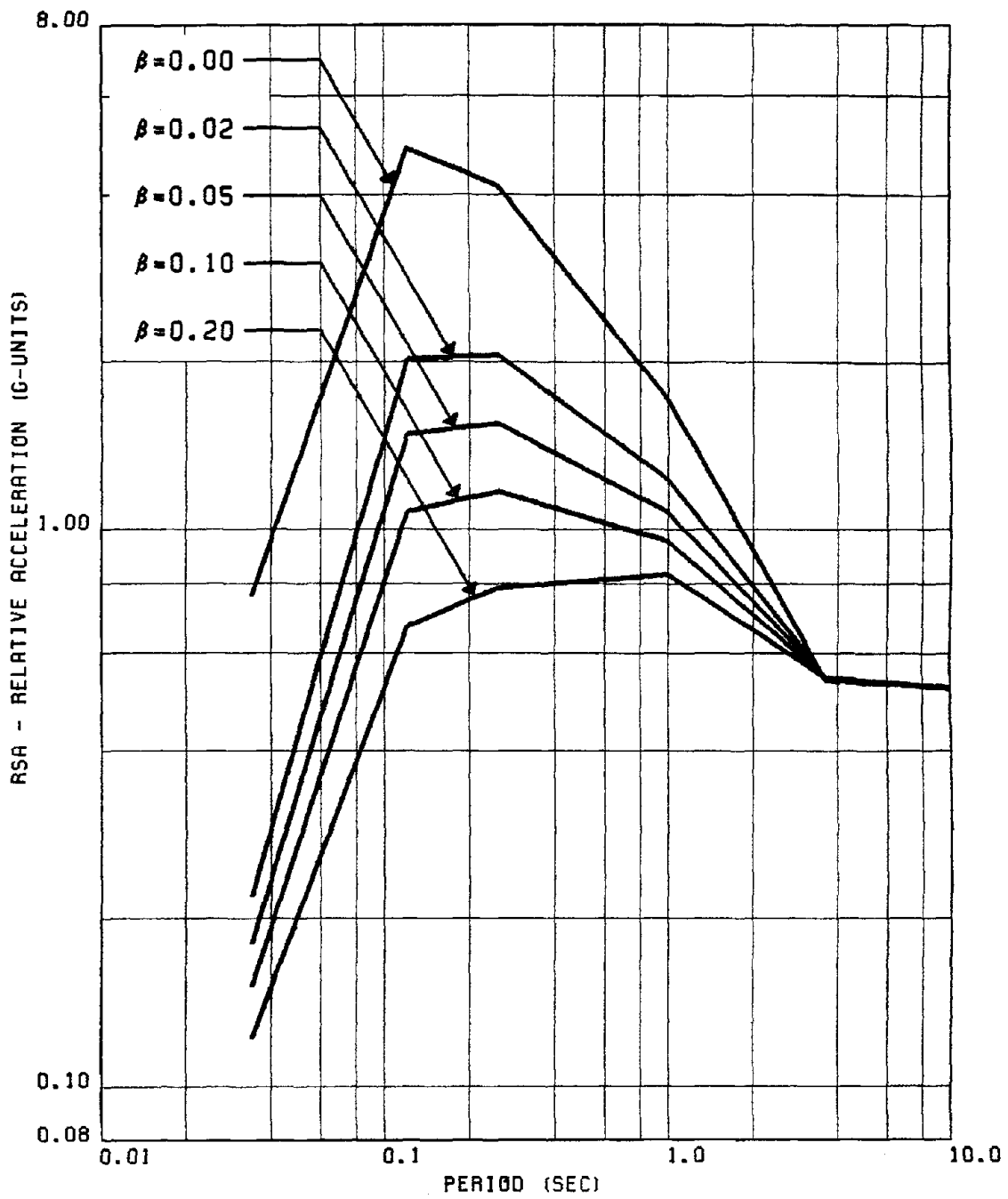
FIG. 200 PROPOSED (MEAN+SD) RSA SPECTRA FOR HORIZONTAL RECORDS OF GROUP *5
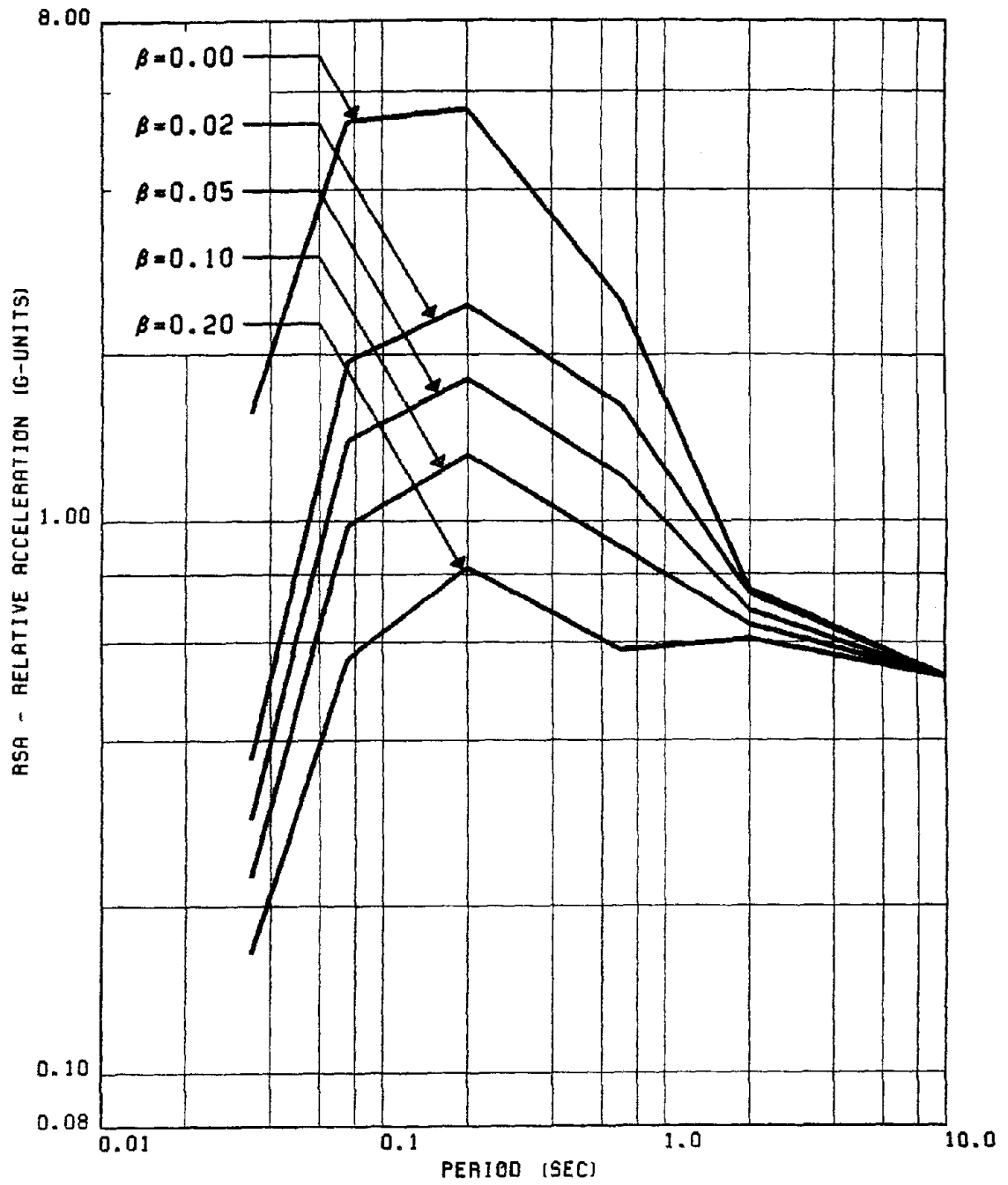
FIG. 201 PROPOSED (MEAN+SD) RSA SPECTRA FOR VERTICAL RECORDS OF GROUP #5
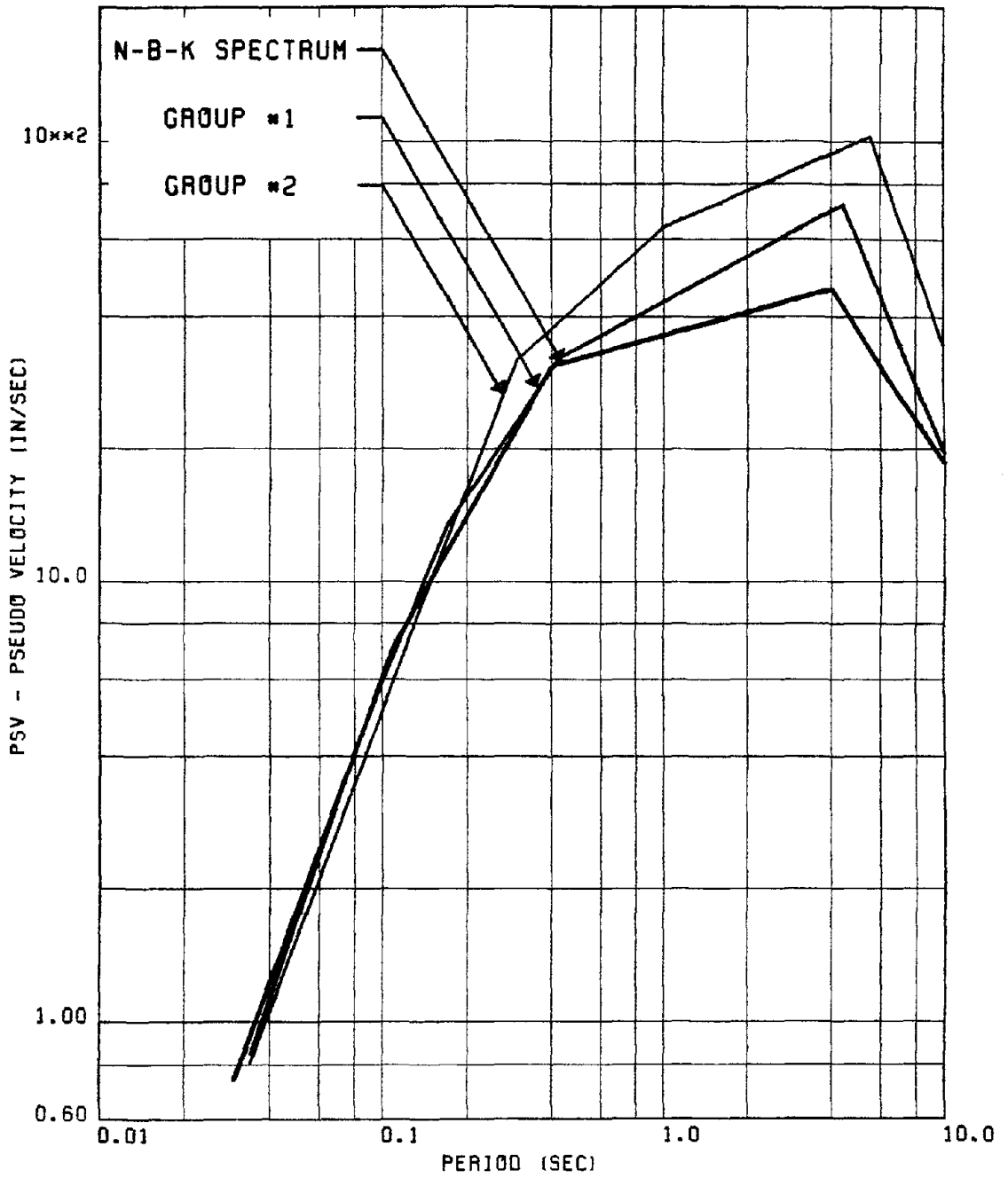
FIG. 202 COMPARISON OF THE PROPOSED & THE N-B-K 'HORIZONTAL' PSV SPECTRA
ALL THE SPECTRA ARE DRAWN FOR A PEAK ACCELERATION OF .40 G AND β= .05
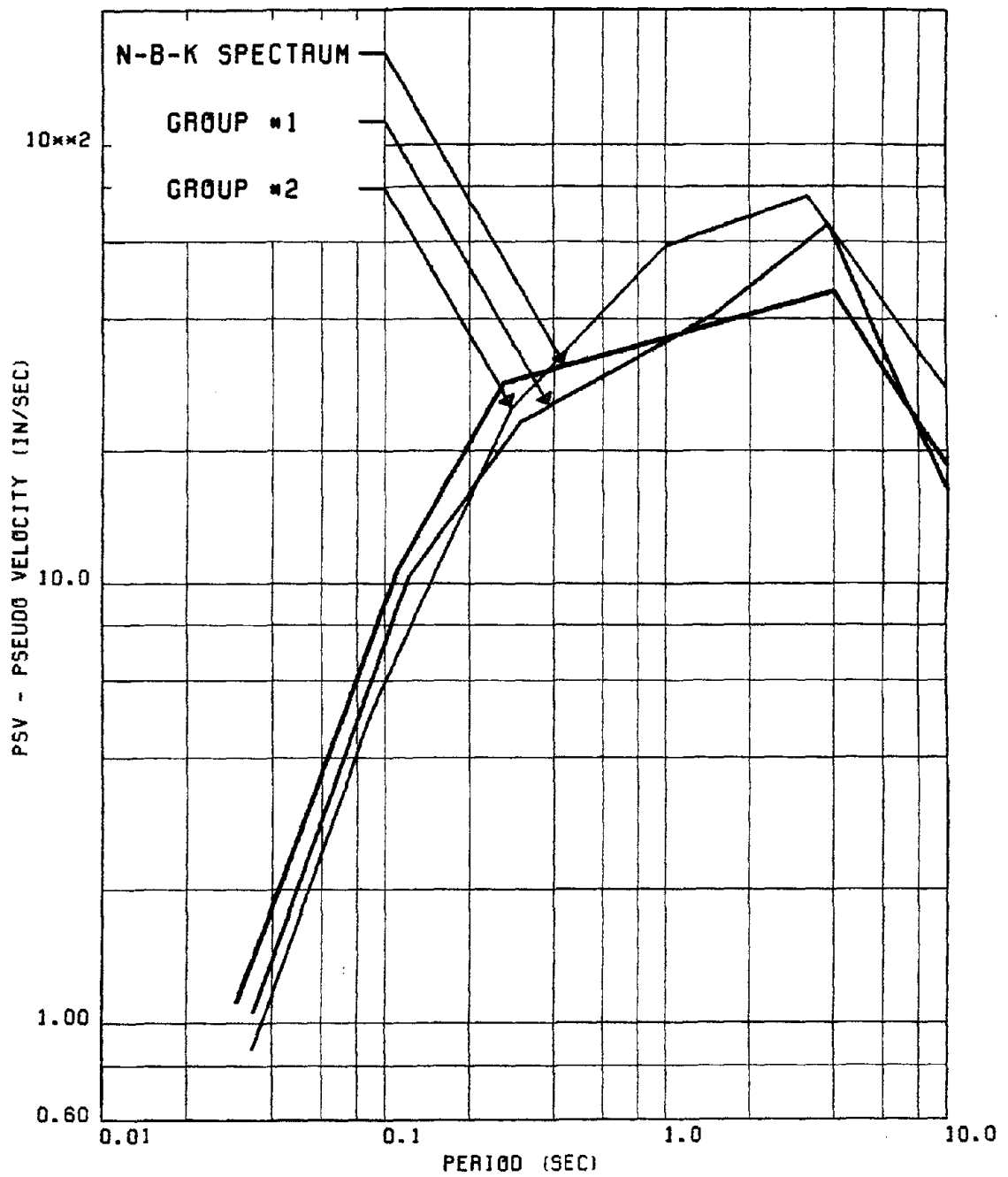
FIG. 203 COMPARISON OF THE PROPOSED & THE N-B-K 'VERTICAL' PSV SPECTRA
ALL THE SPECTRA ARE DRAWN FOR A PEAK ACCELERATION OF .40 G AND β= .05
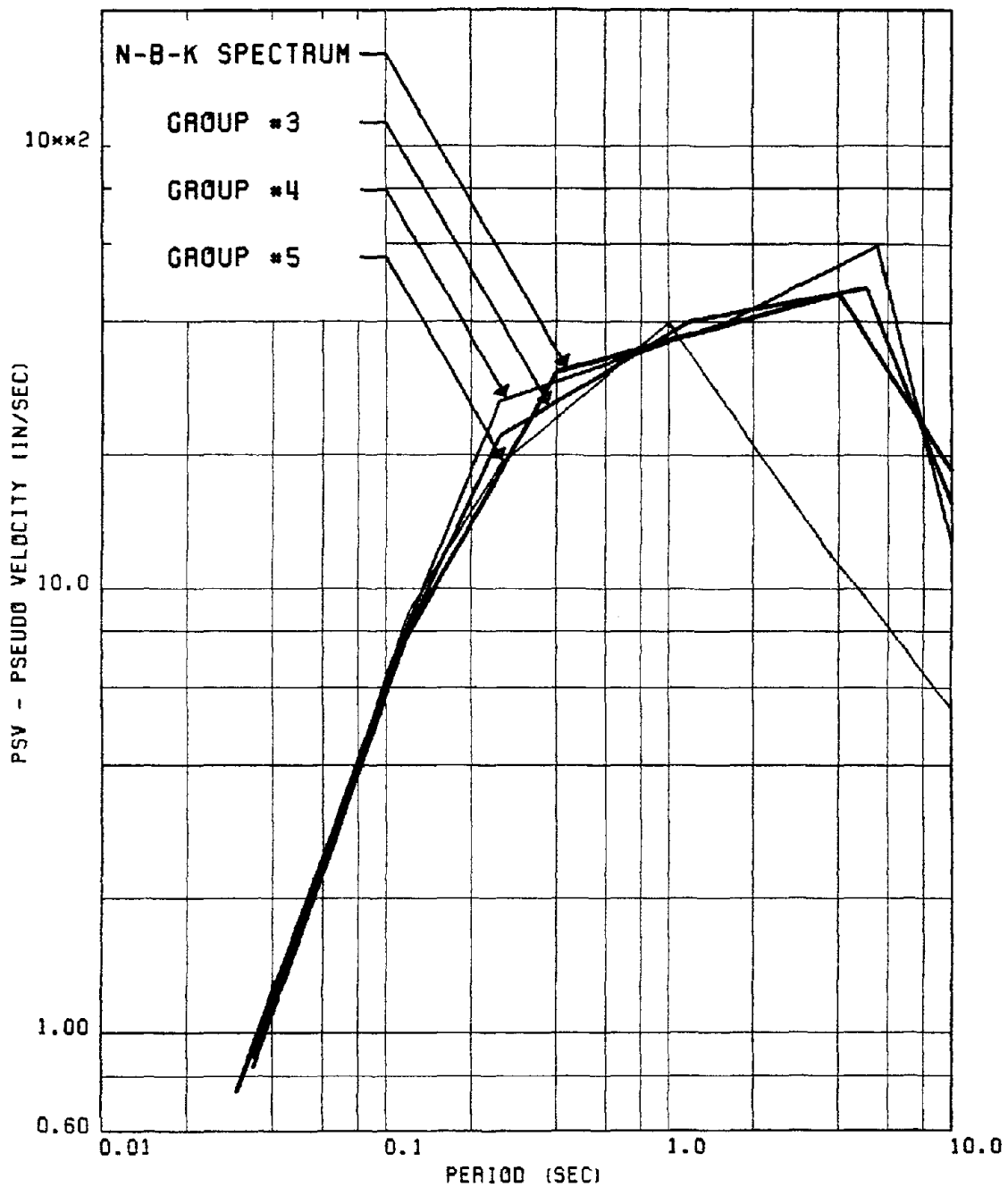
FIG. 204 COMPARISON OF THE PROPOSED & THE N-B-K 'HORIZONTAL' PSV SPECTRA
ALL THE SPECTRA ARE DRAWN FOR A PEAK ACCELERATION OF .40 G AND β = .05
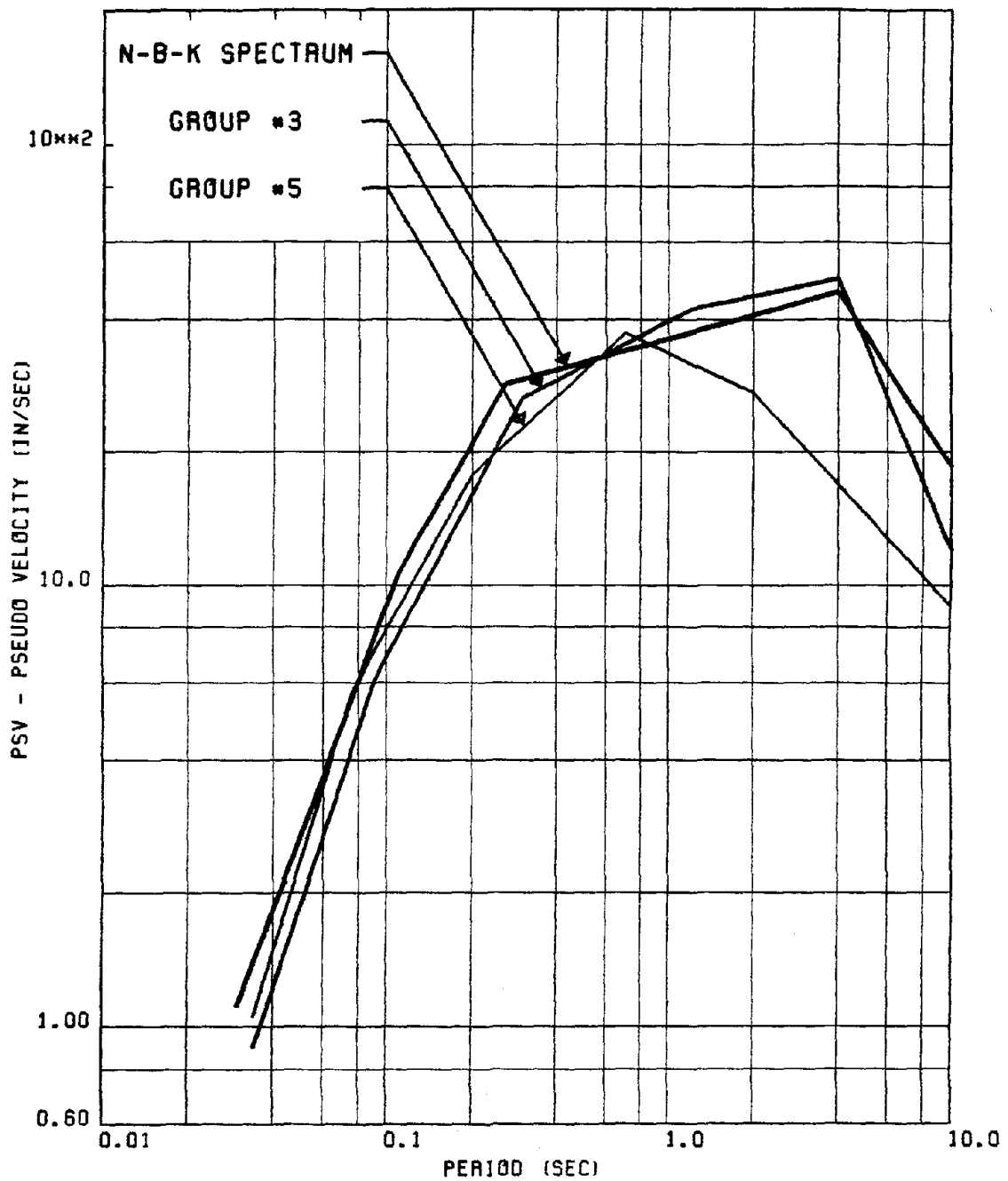
FIG. 205 COMPARISON OF THE PROPOSED & THE N-B-K 'VERTICAL' PSV SPECTRA
ALL THE SPECTRA ARE DRAWN FOR A PEAK ACCELERATION OF .40 G AND $\beta=$ .05
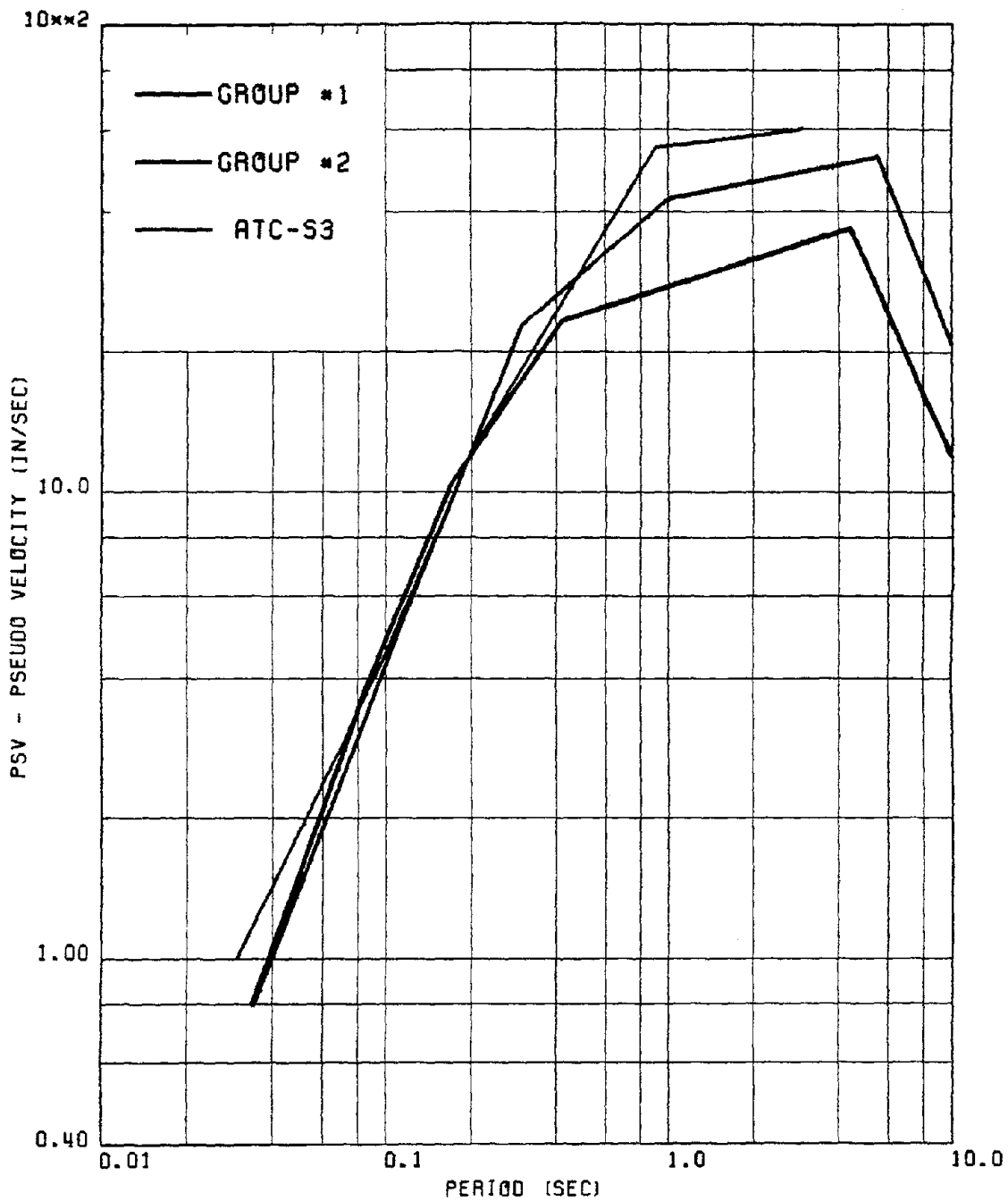
FIG. 206 COMPARISON OF THE ATC-S3 & THE PROPOSED 'HORIZONTAL' PSV SPECTRA
ALL THE SPECTRA ARE DRAWN FOR A PEAK ACCELERATION OF .40 G AND β= 0.05

FIG. 207 COMPARISON OF THE ATC-S3 & THE PROPOSED 'VERTICAL' PSV SPECTRA
ALL THE SPECTRA ARE DRAWN FOR A PEAK ACCELERATION OF .40 G AND $\beta=$ 0.05
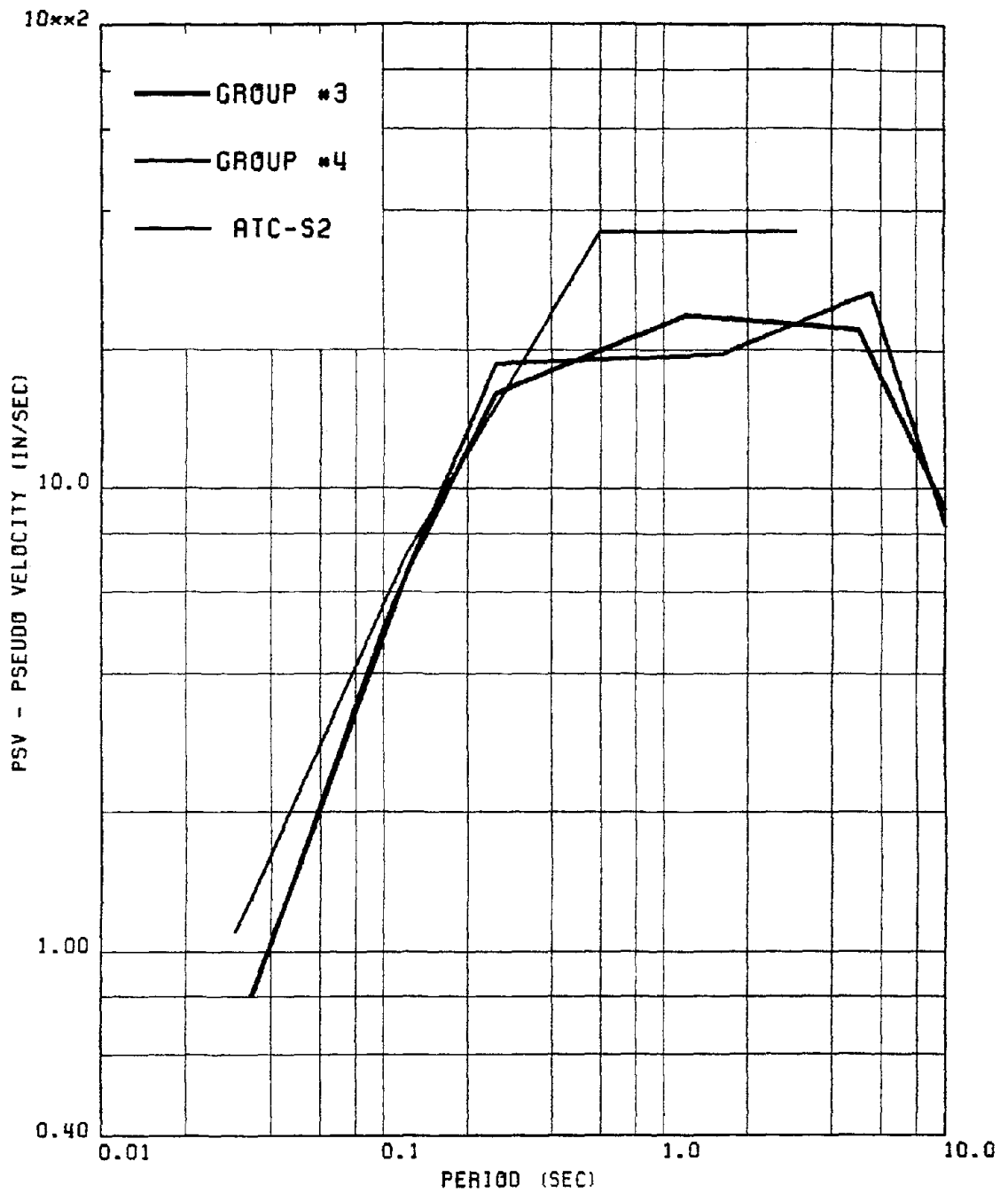
FIG. 208 COMPARISON OF THE ATC-S2 & THE PROPOSED 'HORIZONTAL' PSV SPECTRA
ALL THE SPECTRA ARE DRAWN FOR A PEAK ACCELERATION OF .40 G AND β= 0.05
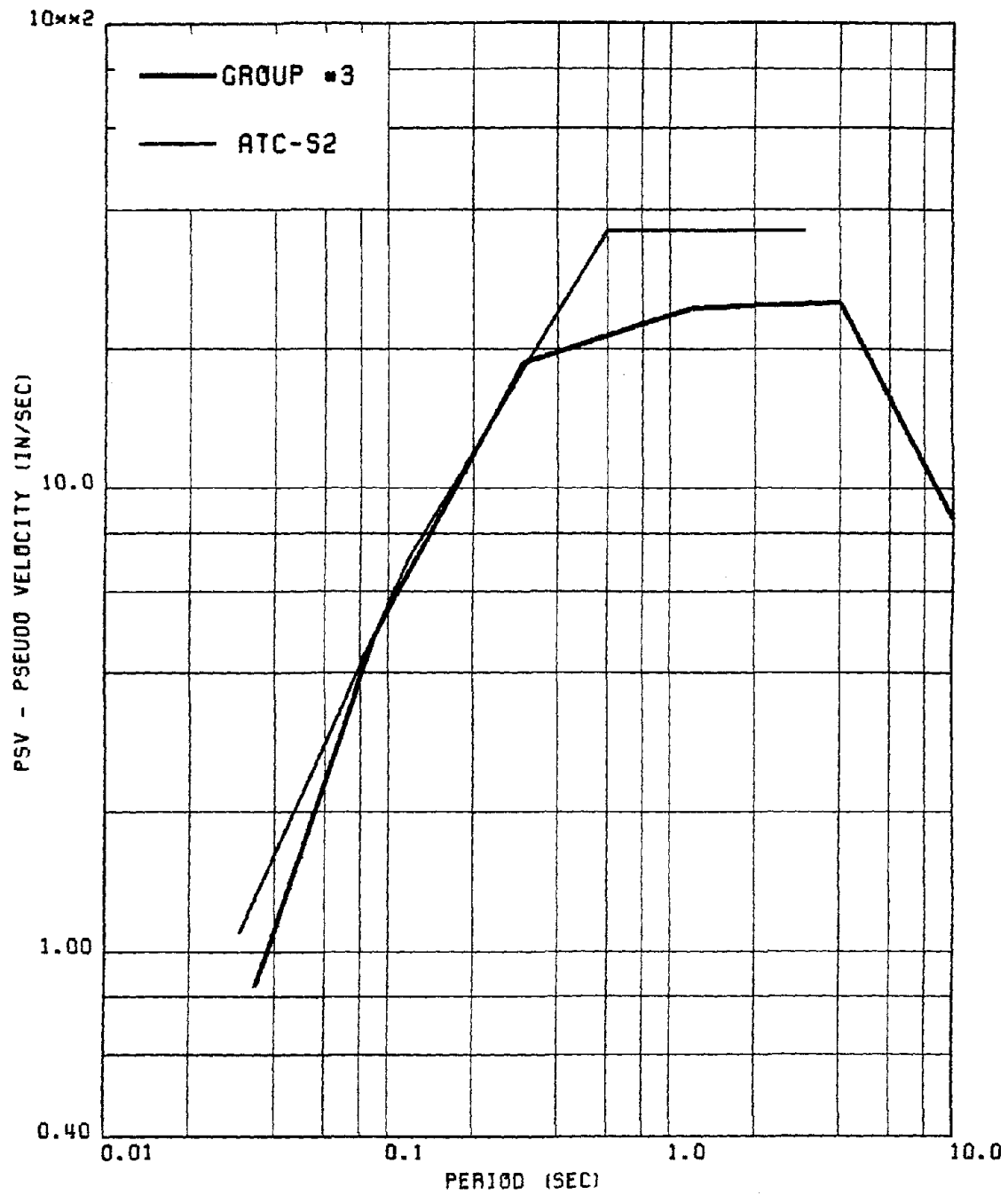
FIG. 209 COMPARISON OF THE ATC-S2 & THE PROPOSED 'VERTICAL' PSV SPECTRA
ALL THE SPECTRA ARE DRAWN FOR A PEAK ACCELERATION OF .40 G AND β= 0.05

287
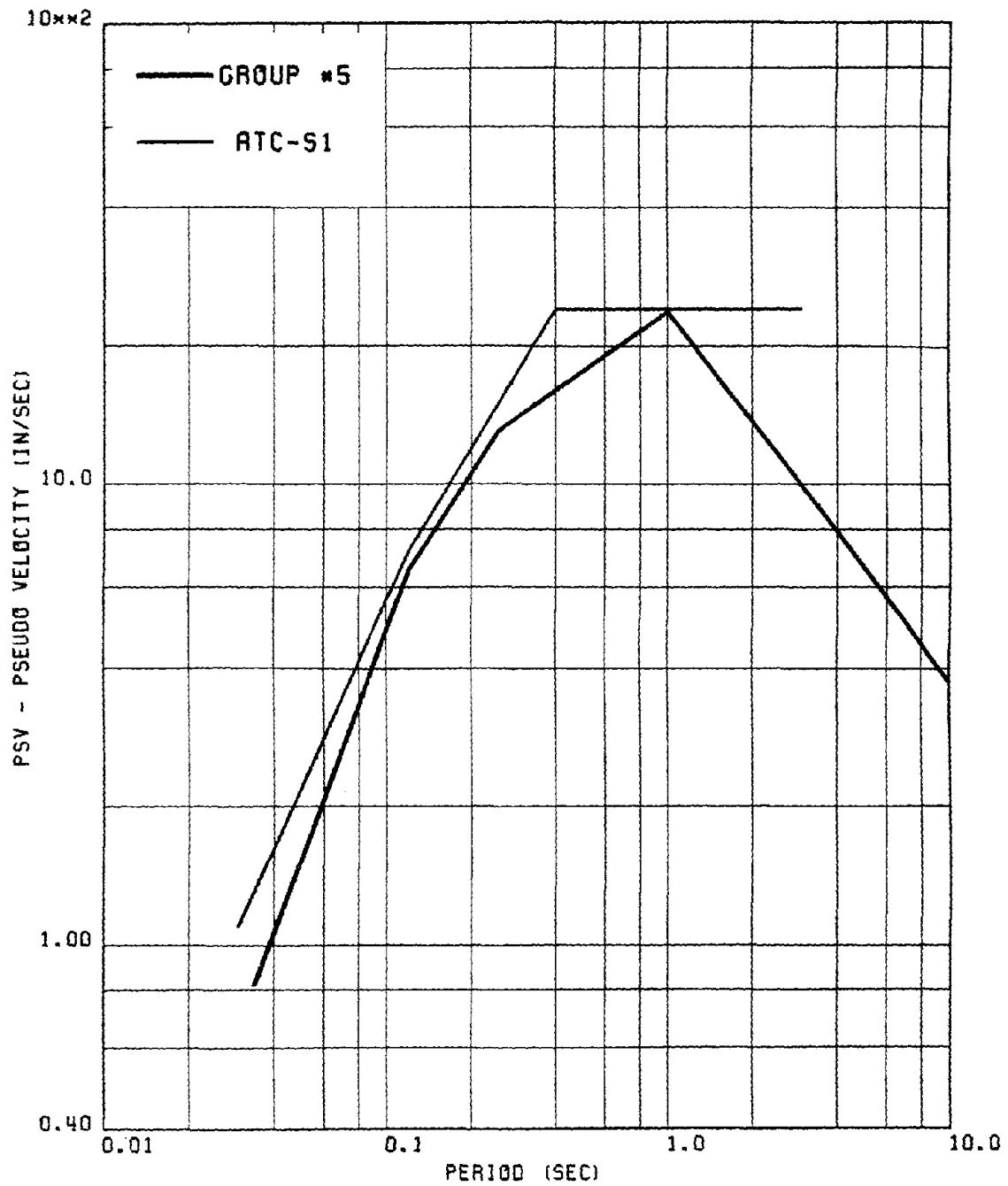
FIG. 210 COMPARISON OF THE ATC-S1 & THE PROPOSED 'HORIZONTAL' PSV SPECTRA
ALL THE SPECTRA ARE DRAWN FOR A PEAK ACCELERATION OF .40 G AND β= 0.05
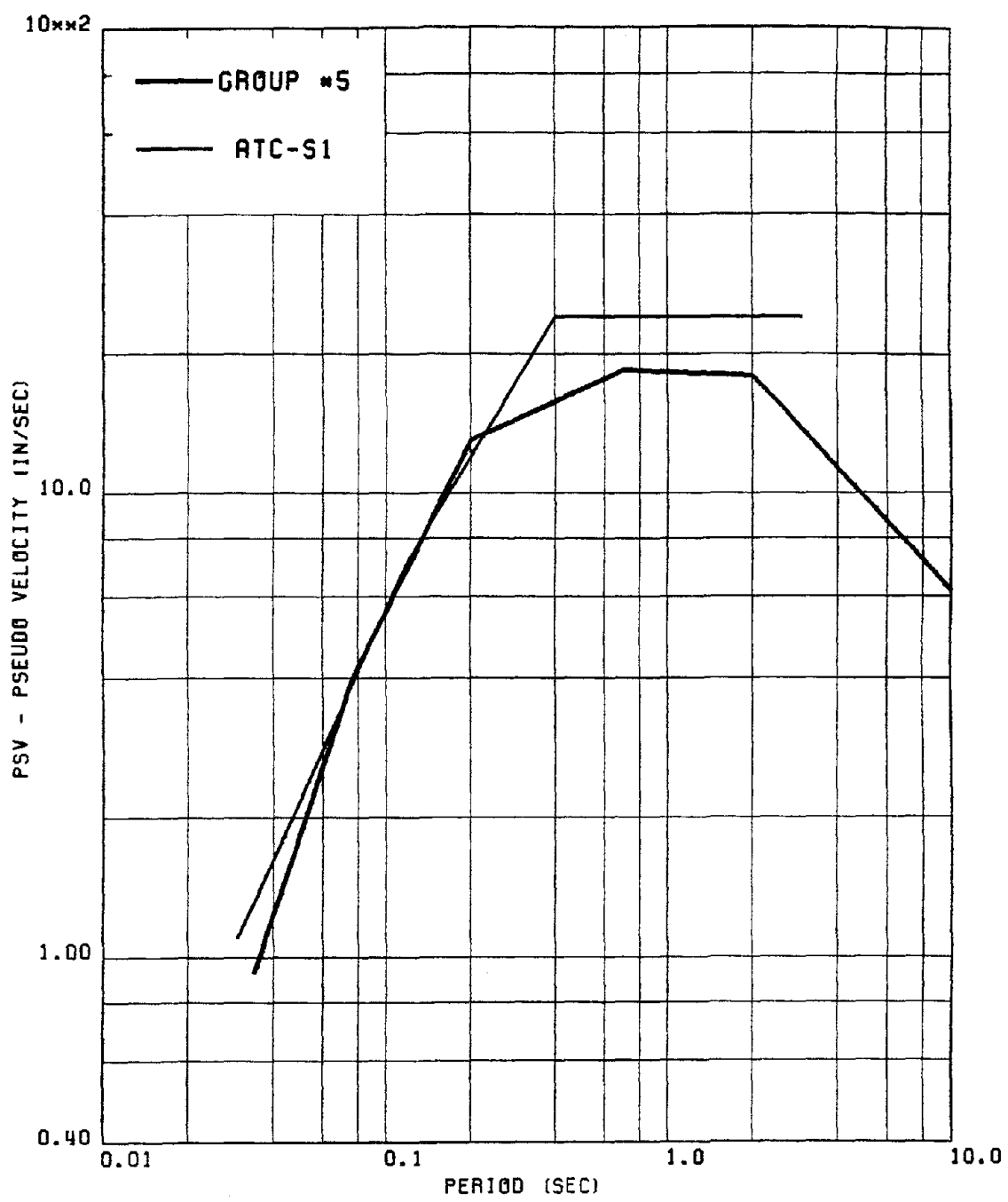
FIG. 211 COMPARISON OF THE ATC-S1 & THE PROPOSED 'VERTICAL' PSV SPECTRA
ALL THE SPECTRA ARE DRAWN FOR A PEAK ACCELERATION OF .40 G AND β= 0.05
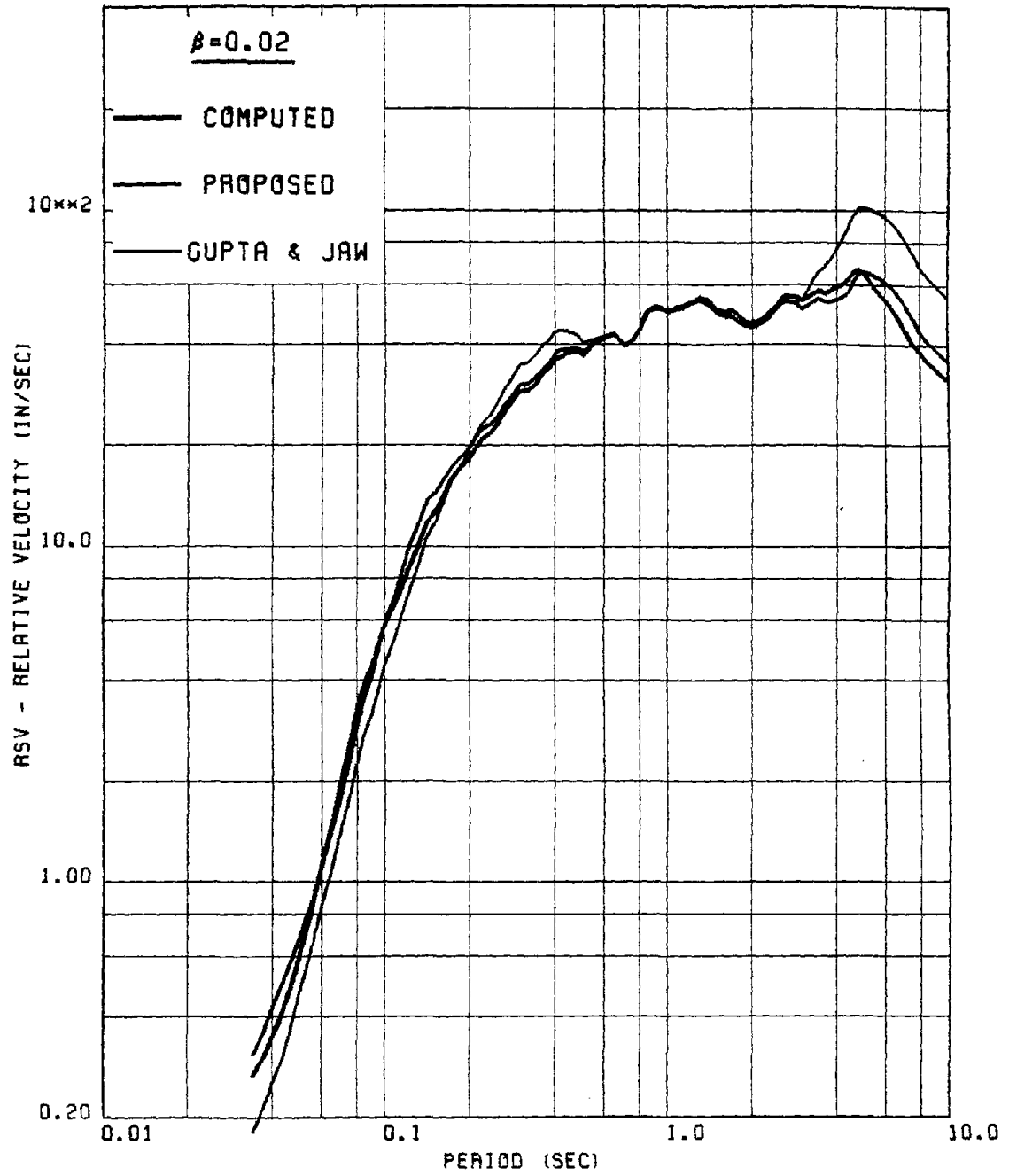
FIG. 212 COMPARISON OF PREDICTED AND COMPUTED RSV SPECTRA FOR GROUP #1H
NOTE : THE ACTUAL COMPUTED SPECTRUM IS REPRESENTED BY THE THICKER CURVE
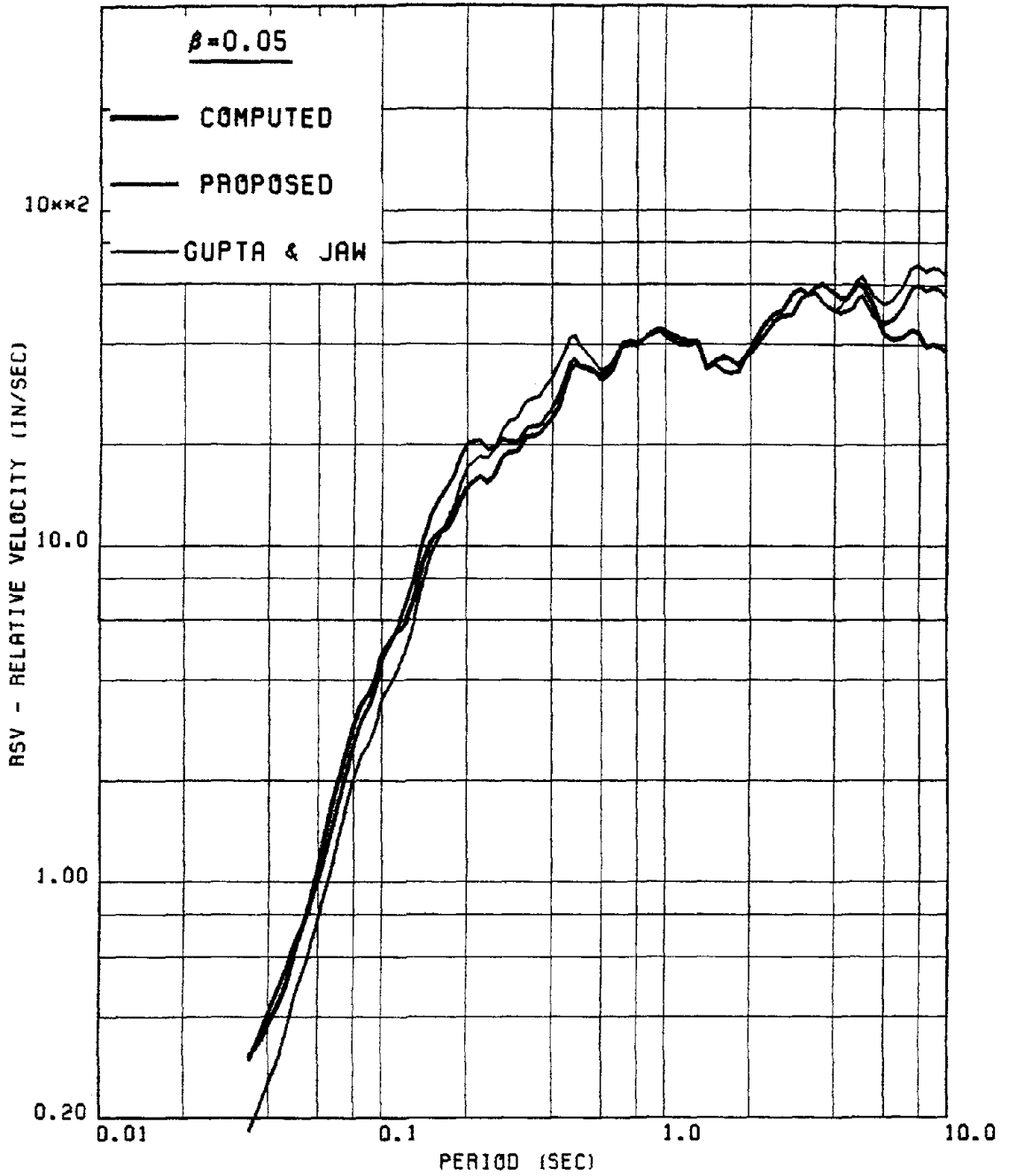
FIG. 213 COMPARISON OF PREDICTED AND COMPUTED RSV SPECTRA FOR GROUP #2V
NOTE : THE ACTUAL COMPUTED SPECTRUM IS REPRESENTED BY THE THICKER CURVE
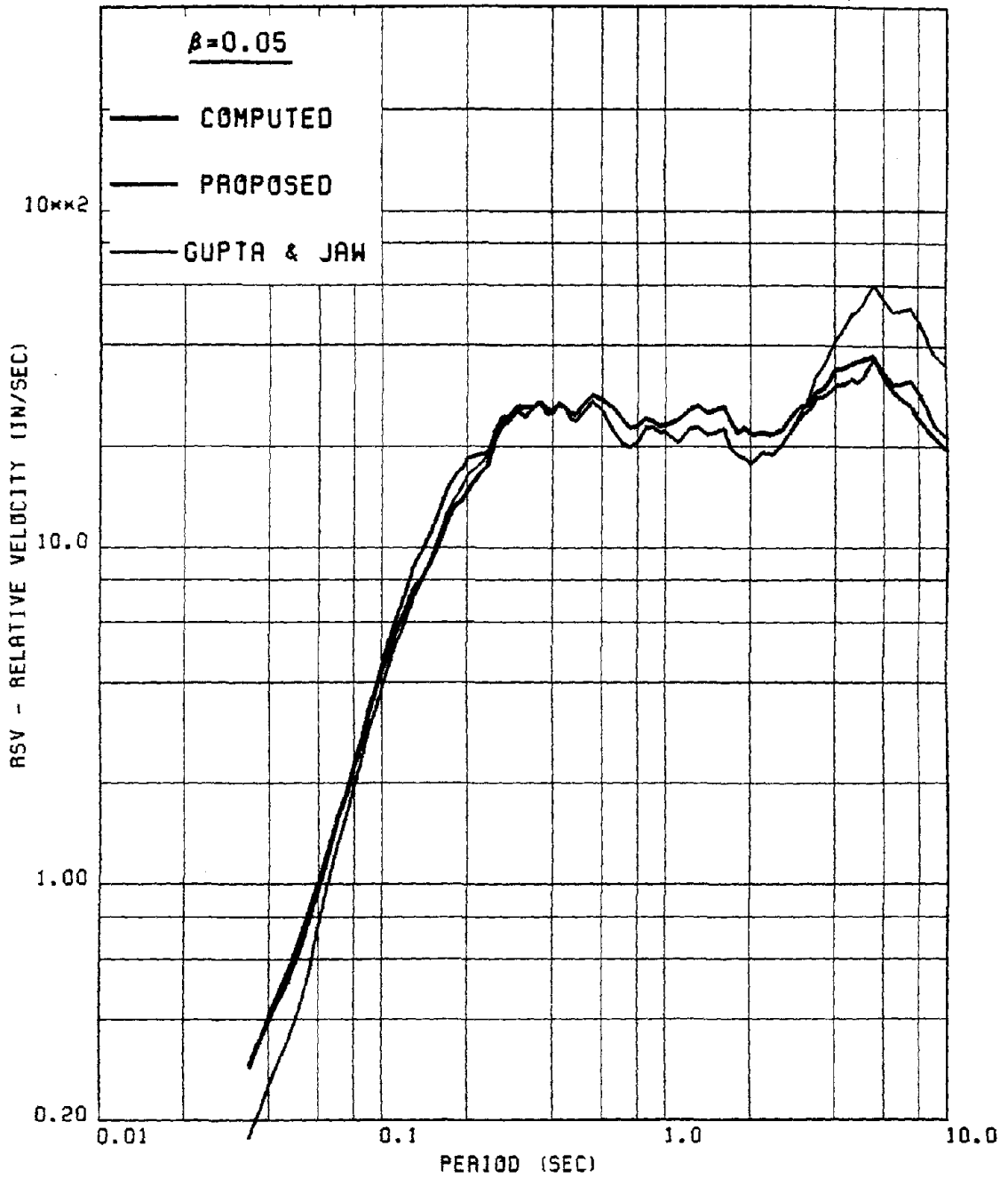
FIG. 214 COMPARISON OF PREDICTED AND COMPUTED RSV SPECTRA FOR GROUP #4H
NOTE : THE ACTUAL COMPUTED SPECTRUM IS REPRESENTED BY THE THICKER CURVE
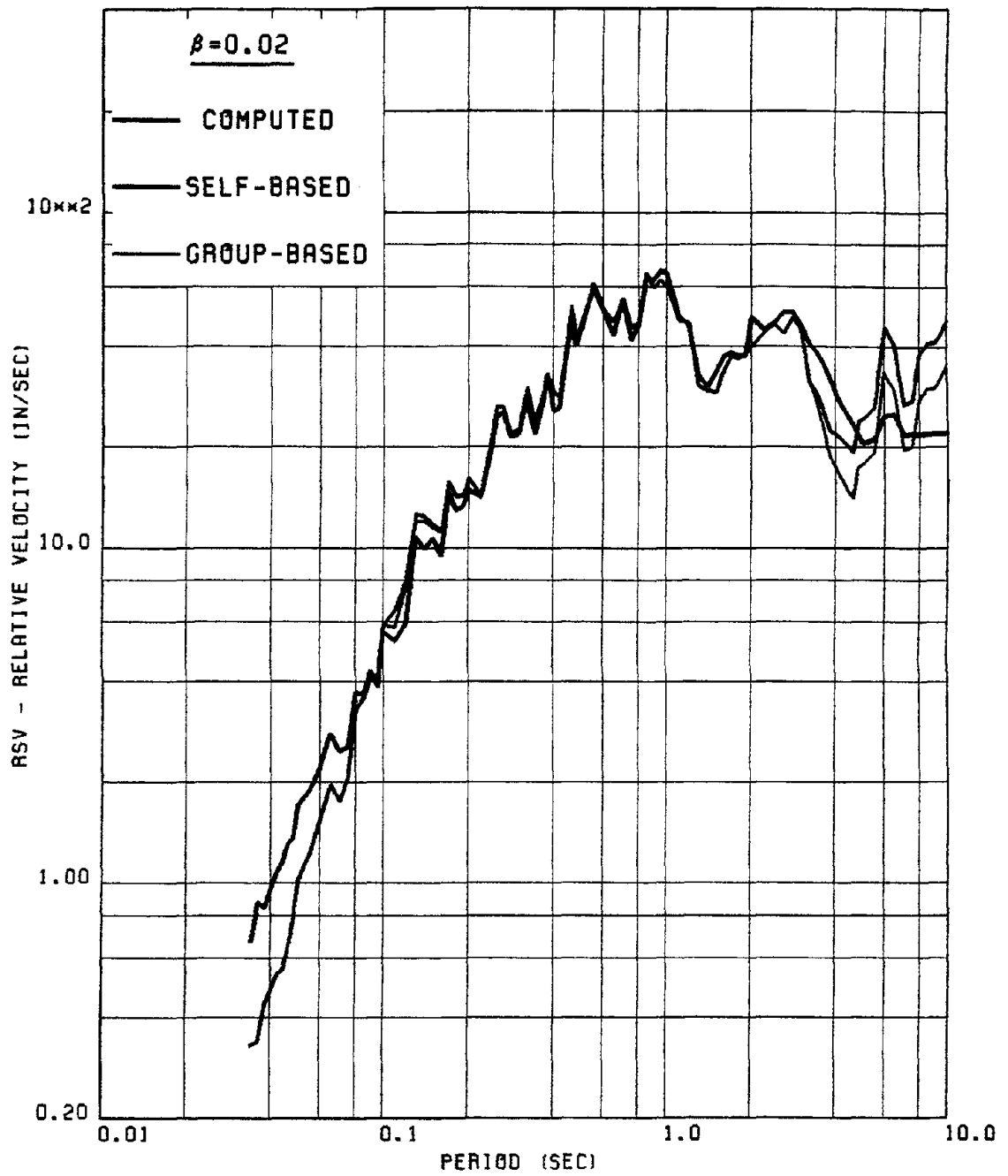
FIG. 215 RSV PREDICTION FOR EL-CENTRO SOOE RECORD USING THE PROPOSED METHOD
NOTE : 1) THE ACTUAL COMPUTED SPECTRUM IS REPRESENTED BY THE THICKER CURVE
      2) THE SPECTRA ARE NORMALIZED TO A PEAK ACCELERATION LEVEL OF .50 G
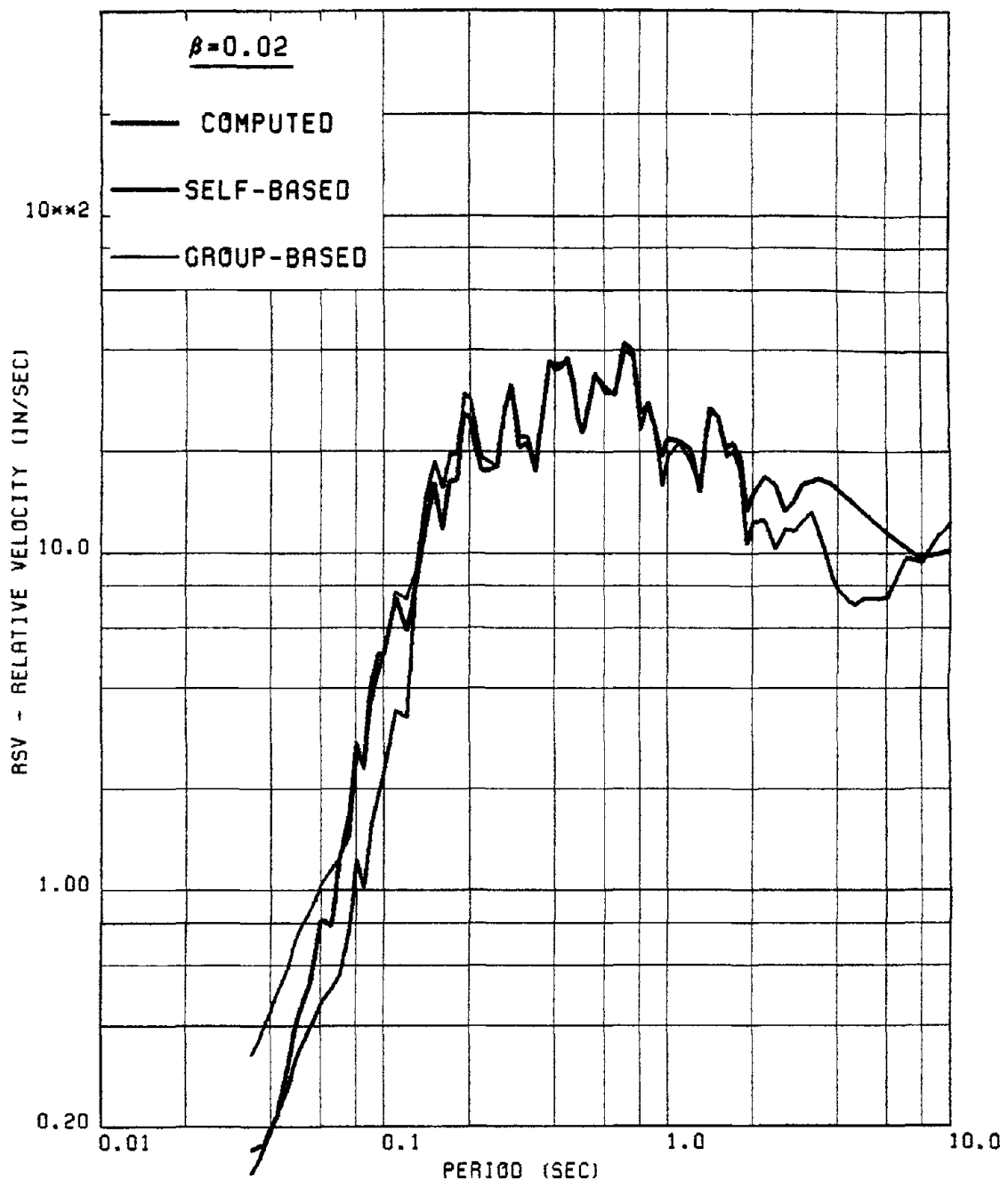
FIG. 216 RSV PREDICTION USING PROPOSED METHOD : 1951 FERNDALE S44W RECORD
NOTE : 1) THE ACTUAL COMPUTED SPECTRUM IS REPRESENTED BY THE THICKER CURVE
2) THE SPECTRA ARE NORMALIZED TO A PEAK ACCELERATION LEVEL OF .50 G
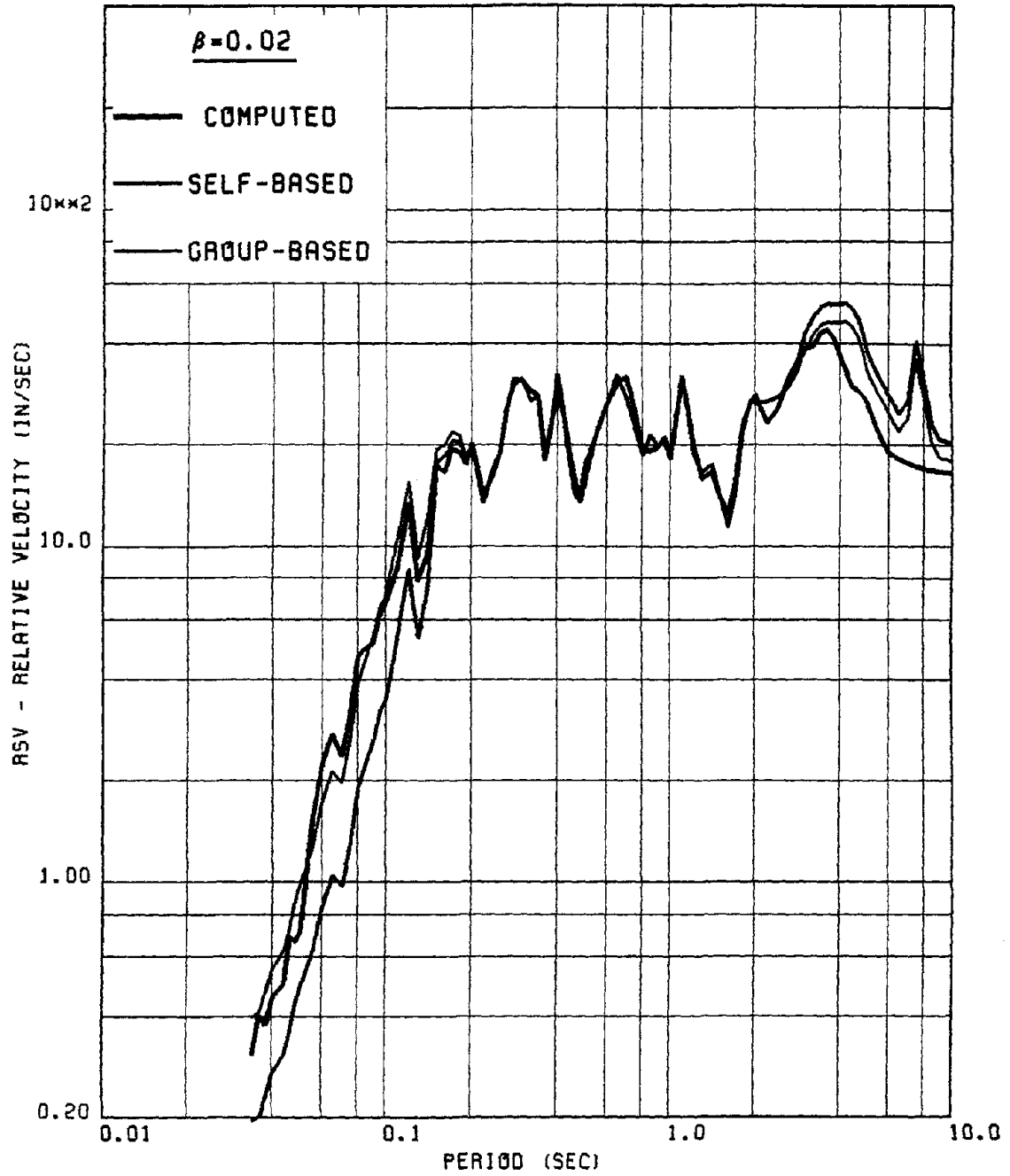
FIG. 217 ASV PREDICTION USING PROPOSED METHOD: CAL TECH LAB VERTICAL RECORD
NOTE : 1) THE ACTUAL COMPUTED SPECTRUM IS REPRESENTED BY THE THICKER CURVE
       2) THE SPECTRA ARE NORMALIZED TO A PEAK ACCELERATION LEVEL OF .50 G
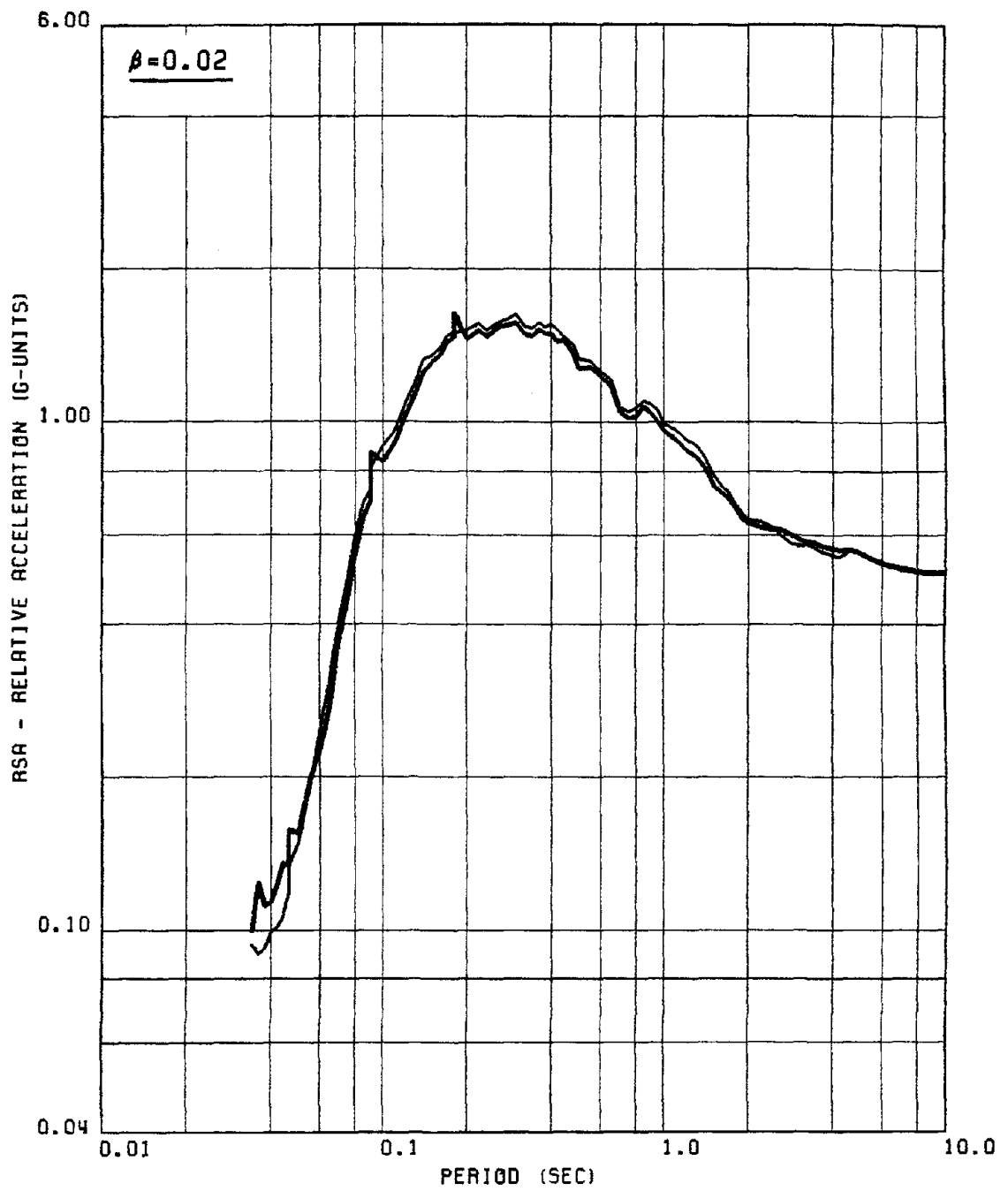
FIG. 218 COMPARISON OF PREDICTED AND COMPUTED RSA SPECTRA FOR GROUP *1H
NOTE : THE PREDICTED SPECTRUM IS REPRESENTED BY THE THICKER CURVE
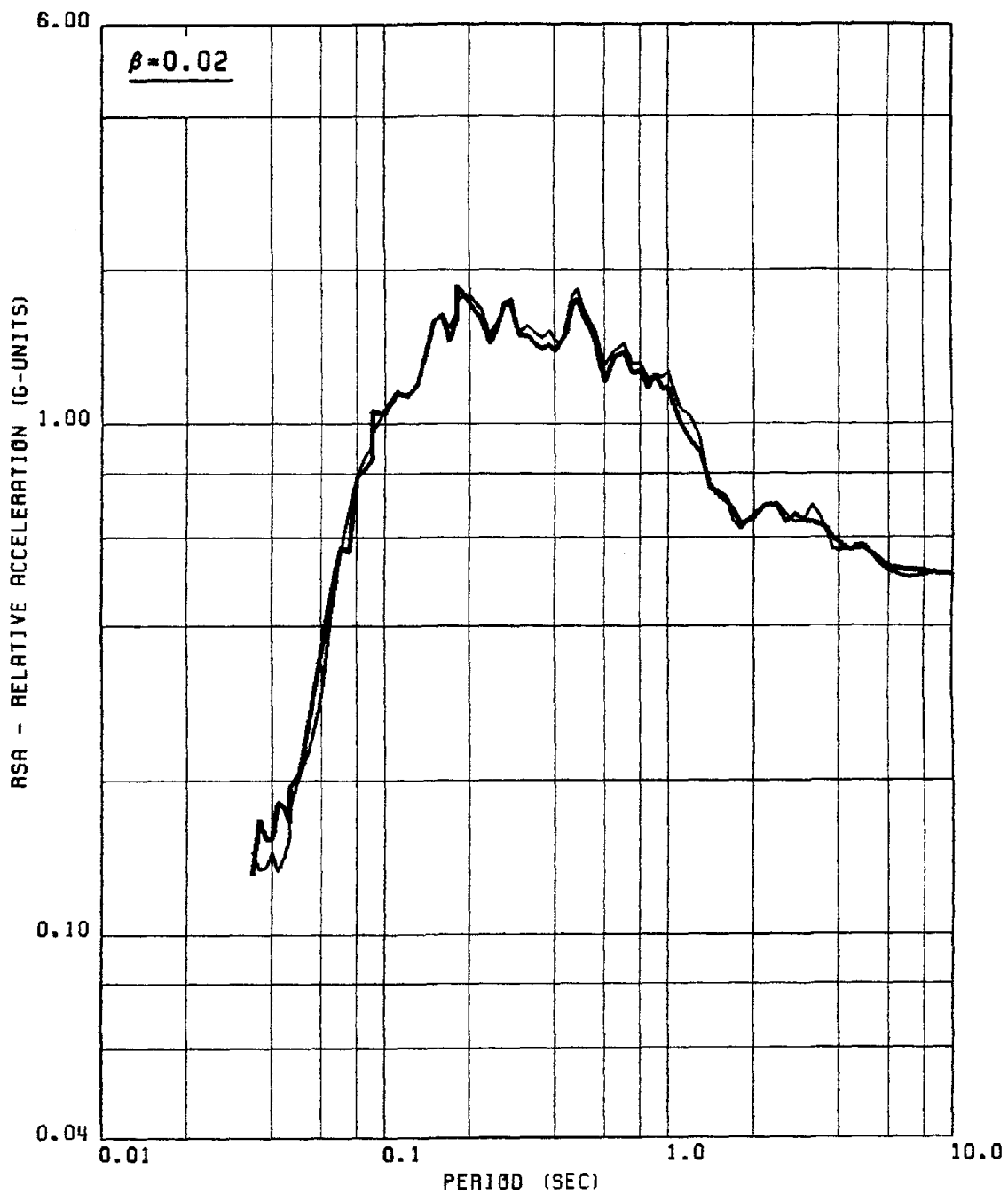
FIG. 219 COMPARISON OF PREDICTED AND COMPUTED RSA SPECTRA FOR GROUP #2V
NOTE : THE PREDICTED SPECTRUM IS REPRESENTED BY THE THICKER CURVE
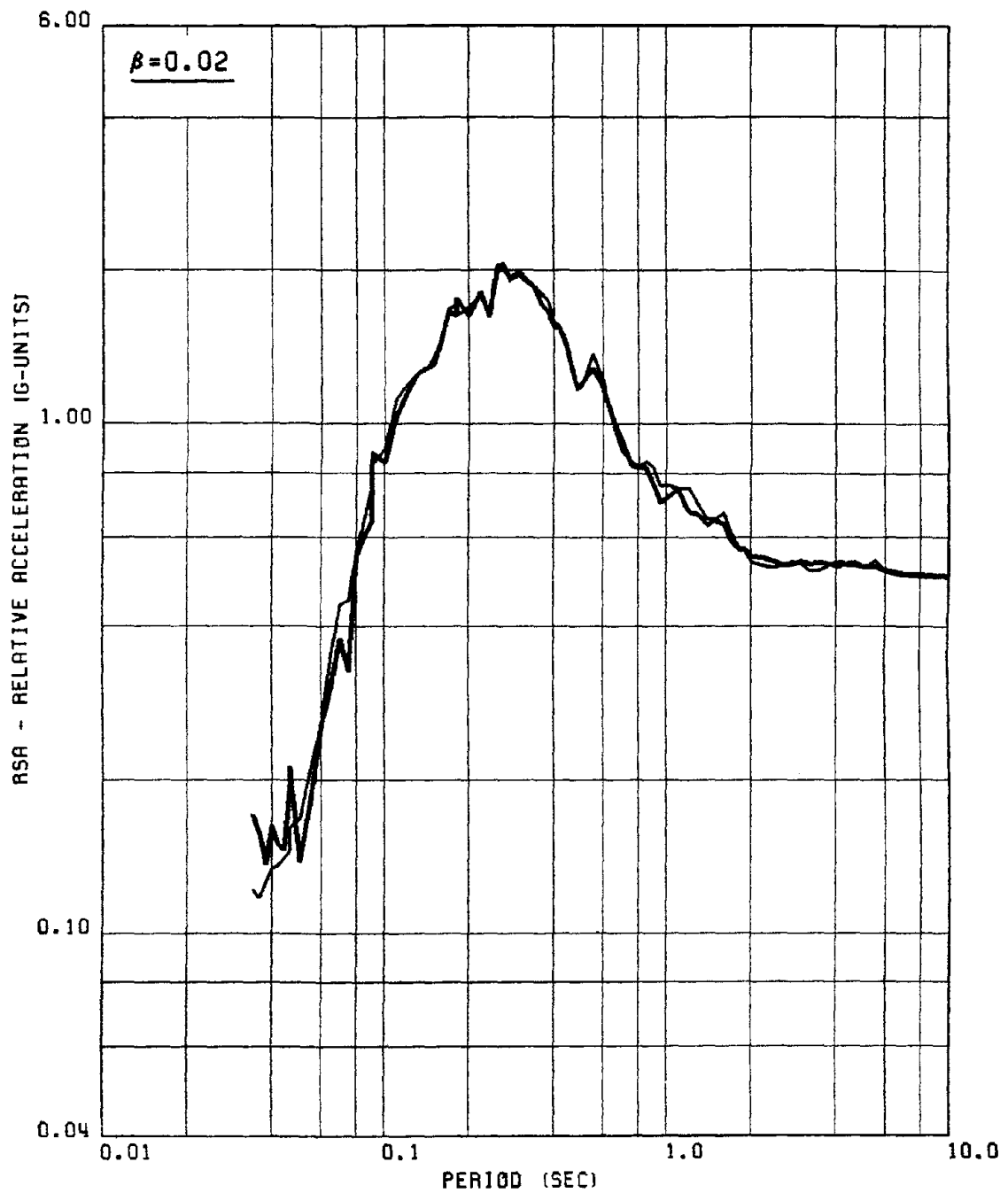
FIG. 220 COMPARISON OF PREDICTED AND COMPUTED RSA SPECTRA FOR GROUP #4H
NOTE : THE PREDICTED SPECTRUM IS REPRESENTED BY THE THICKER CURVE
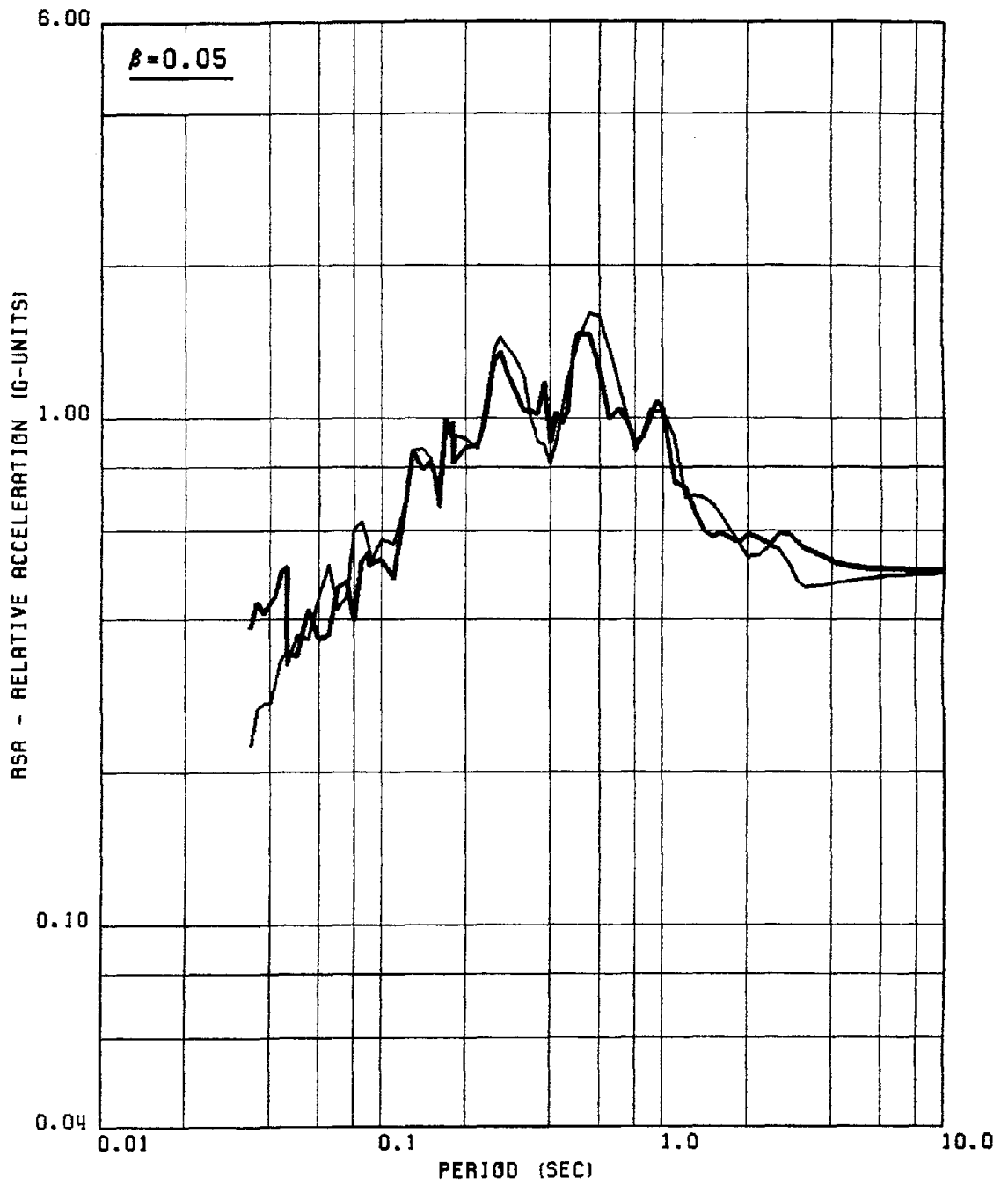
FIG. 221 COMPARISON OF PREDICTED AND COMPUTED RSA FOR EL-CENTRO S00E RECORD
NOTE : 1) THE THICKER CURVE INDICATES THE PREDICTED SPECTRUM FOR THE RECORD
2) THE SPECTRA SHOWN ARE NORMALIZED FOR A PEAK ACCELERATION OF .50 G
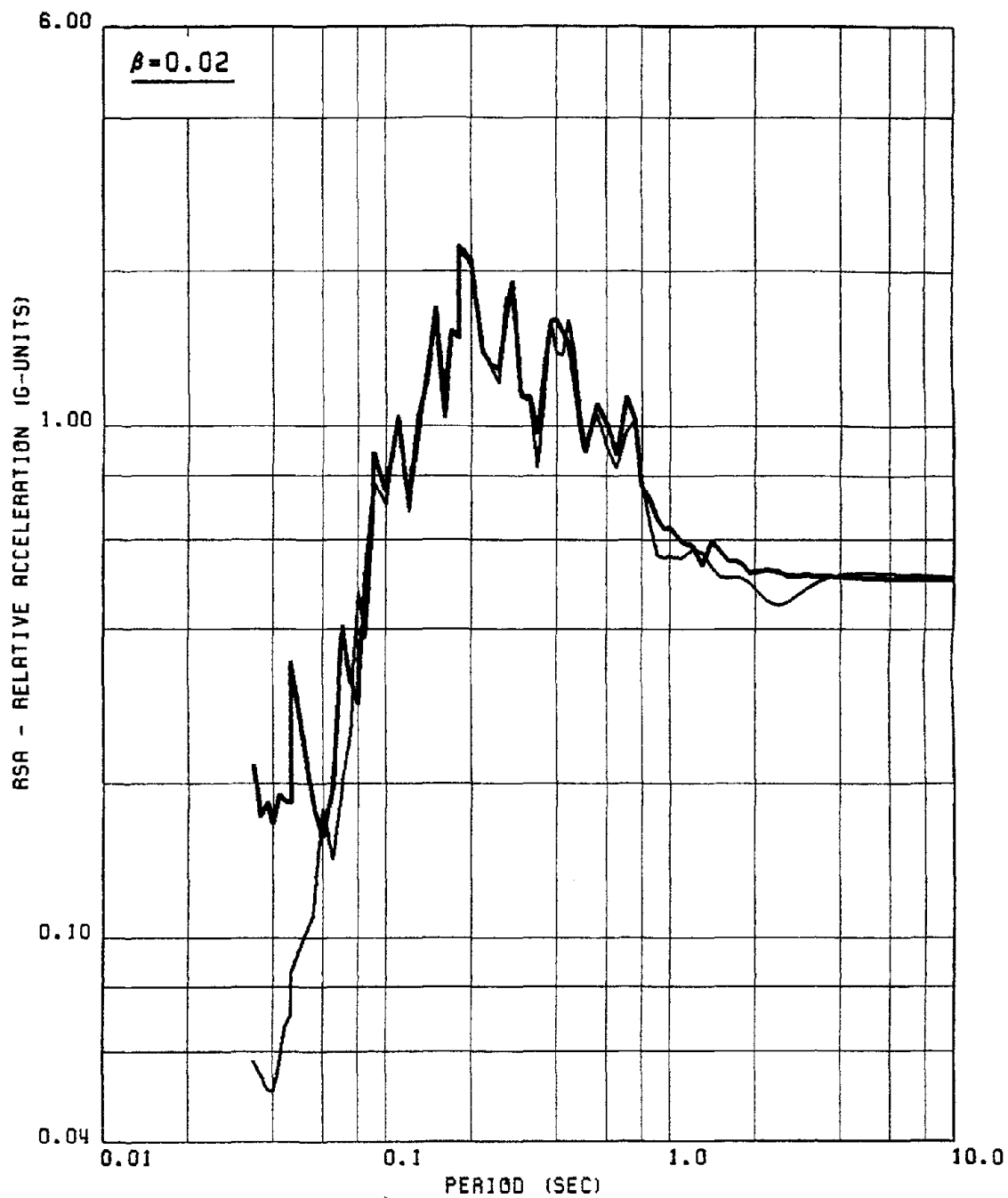
FIG. 222 COMPARISON OF PREDICTED & COMPUTED RSA. 1951 FERNDALE S44W RECORD
NOTE : 1) THE THICKER CURVE INDICATES THE PREDICTED SPECTRUM FOR THE RECORD
       2) THE SPECTRA SHOWN ARE NORMALIZED FOR A PEAK ACCELERATION OF .50 G
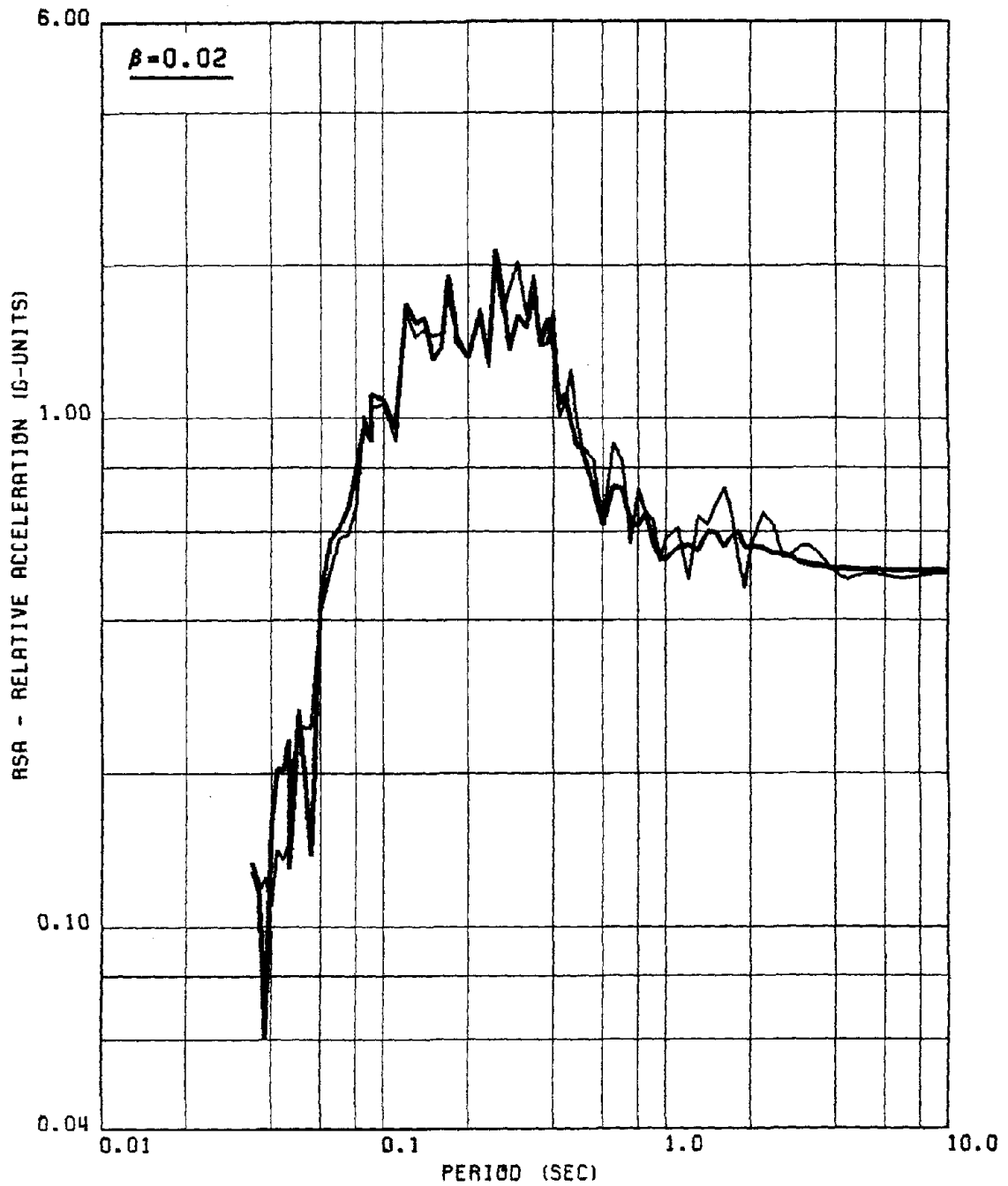
FIG. 223 COMPARISON OF PREDICTED & COMPUTED RSA-PACOIMA DAM VERTICAL RECORD
NOTE : 1) THE THICKER CURVE INDICATES THE PREDICTED SPECTRUM FOR THE RECORD
2) THE SPECTRA SHOWN ARE NORMALIZED FOR A PEAK ACCELERATION OF .50 G
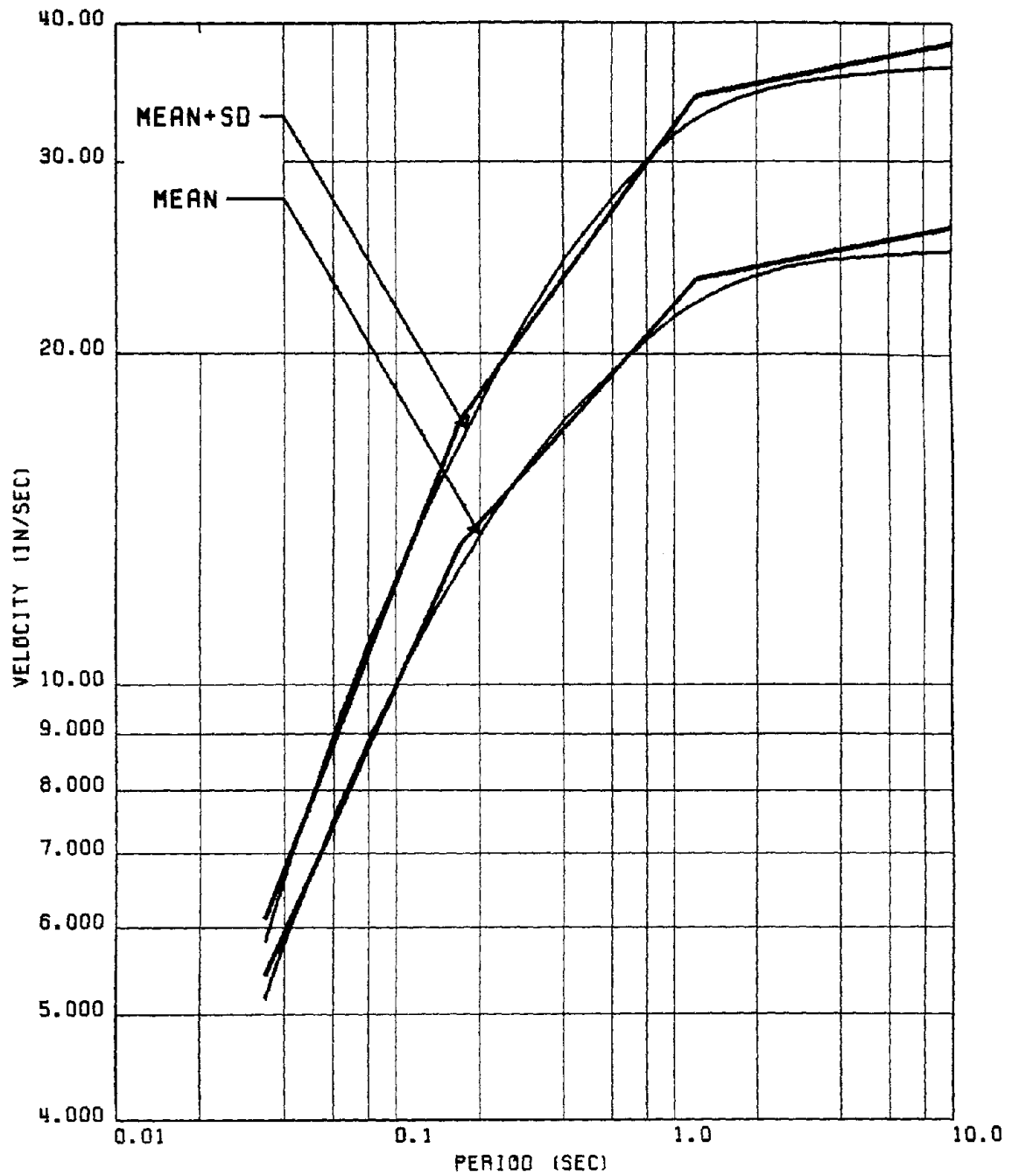
FIG. 224 PROPOSED & COMPUTED MEAN & (MEAN+SD) 'HORIZONTAL' RSV FOR GROUP #1
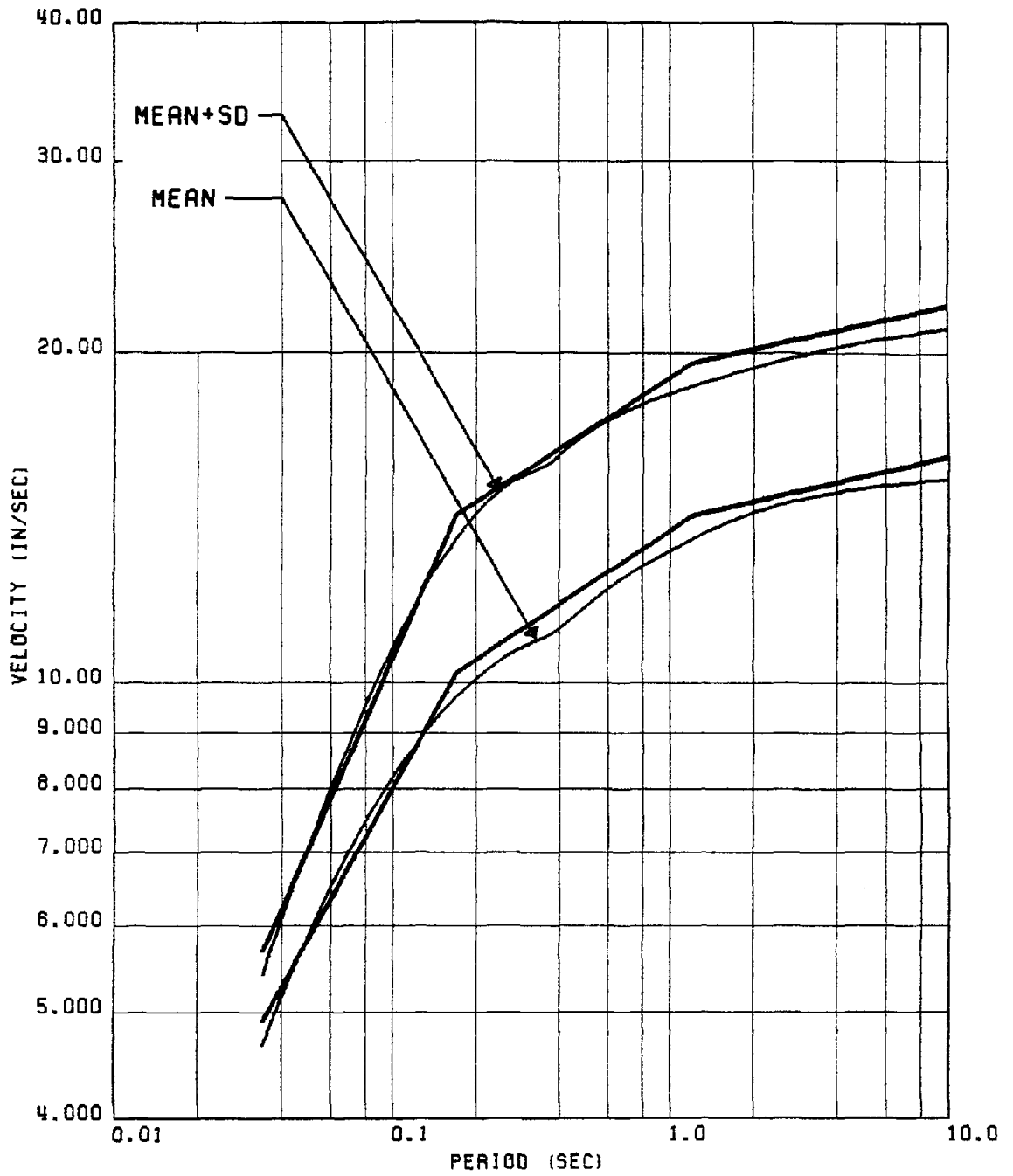NOTE : THE PROPOSED MASSLESS SPECTRA ARE INDICATED BY THE THICKER CURVES
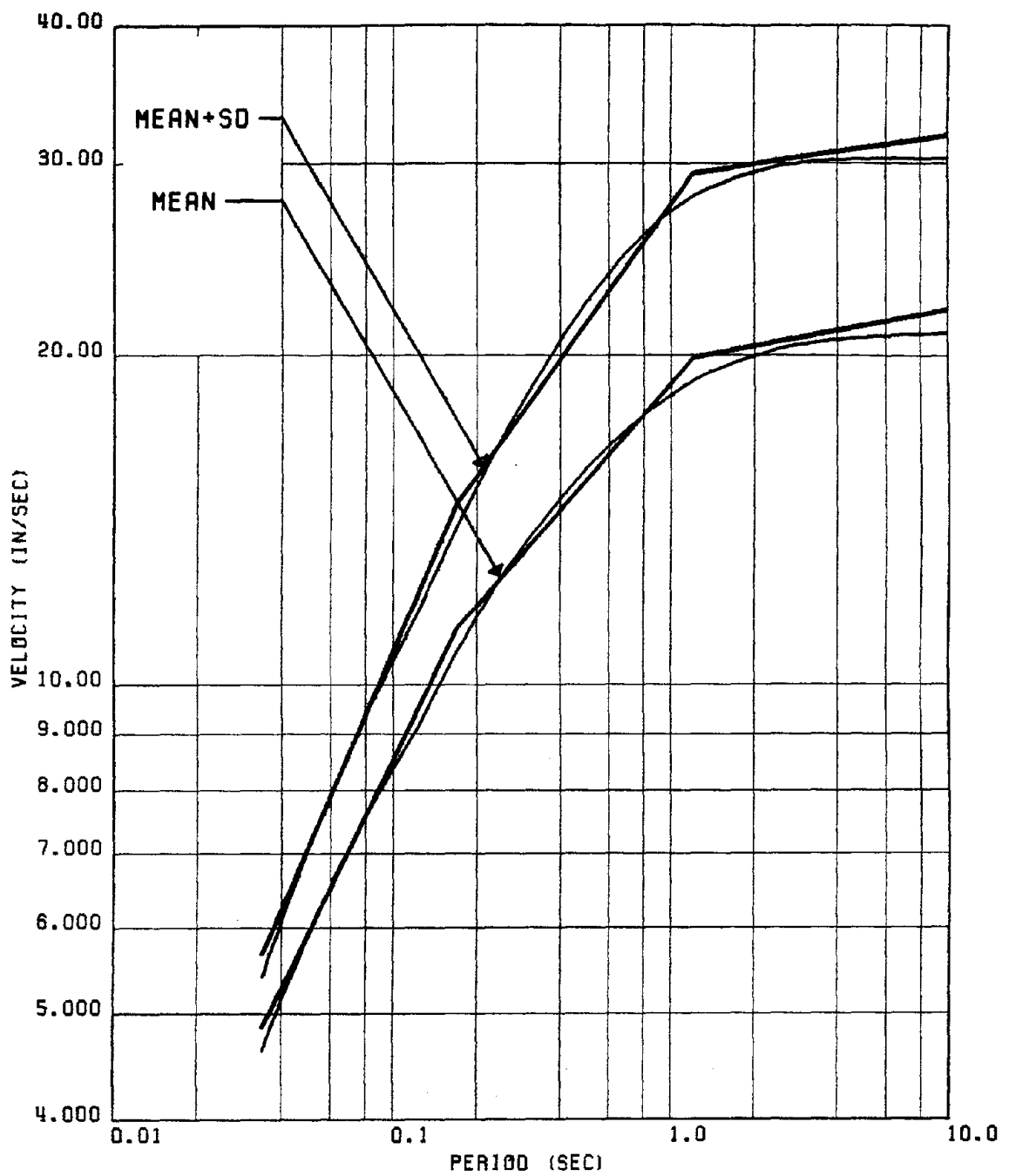
FIG. 225 PROPOSED & COMPUTED MEAN & (MEAN+SD) 'VERTICAL' RSV FOR GROUP #1
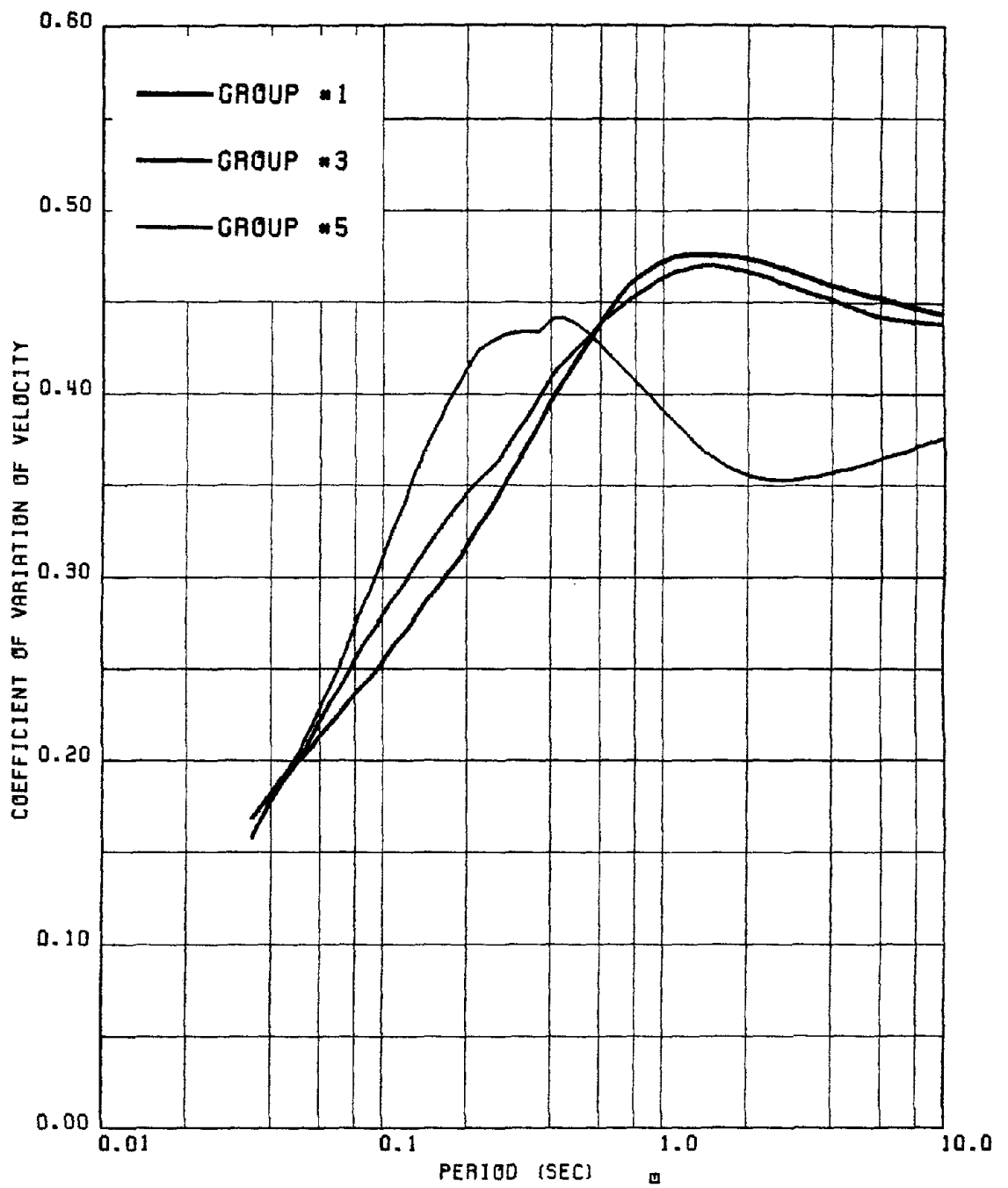NOTE : THE PROPOSED MASSLESS SPECTRA ARE INDICATED BY THE THICKER CURVES
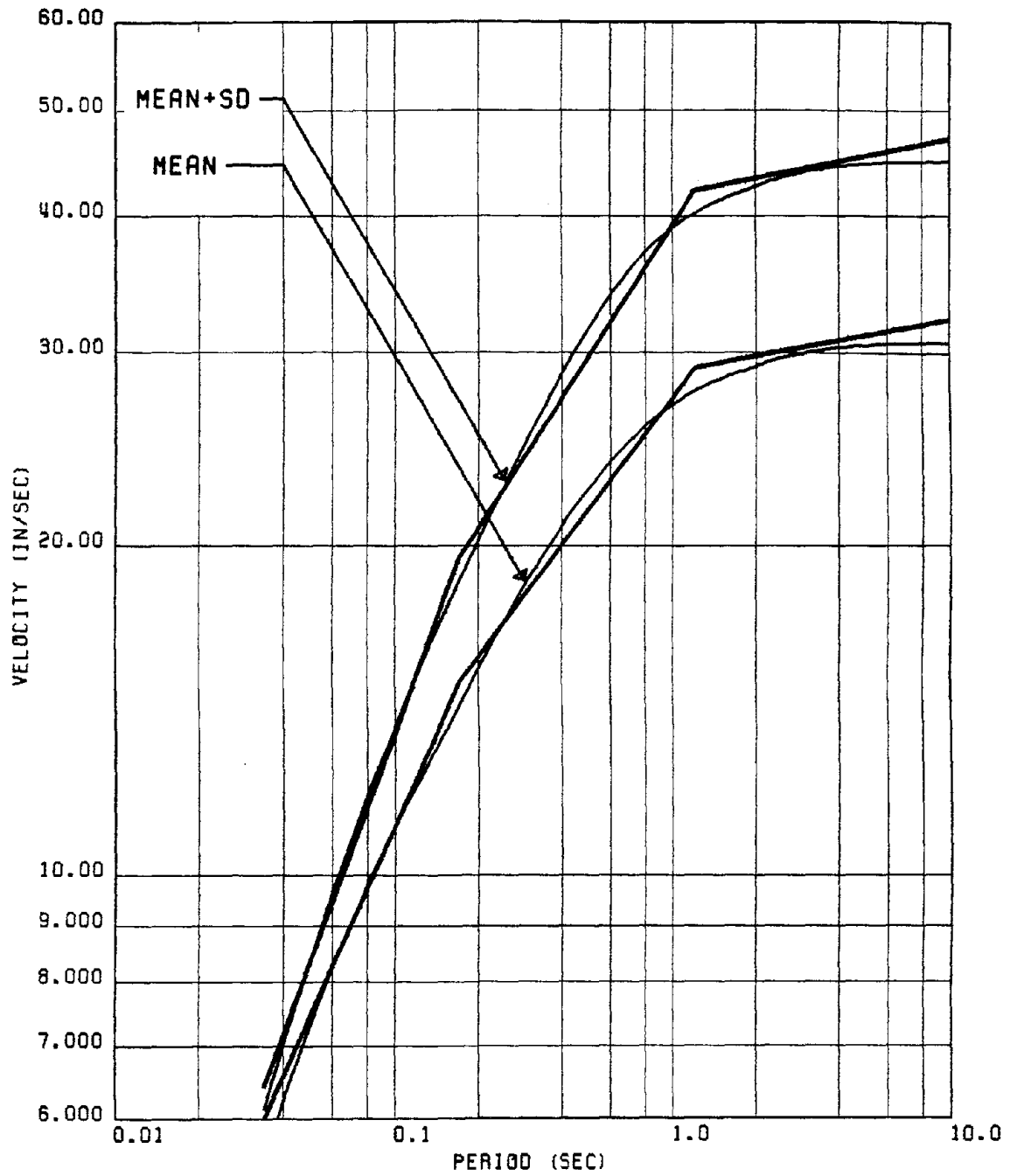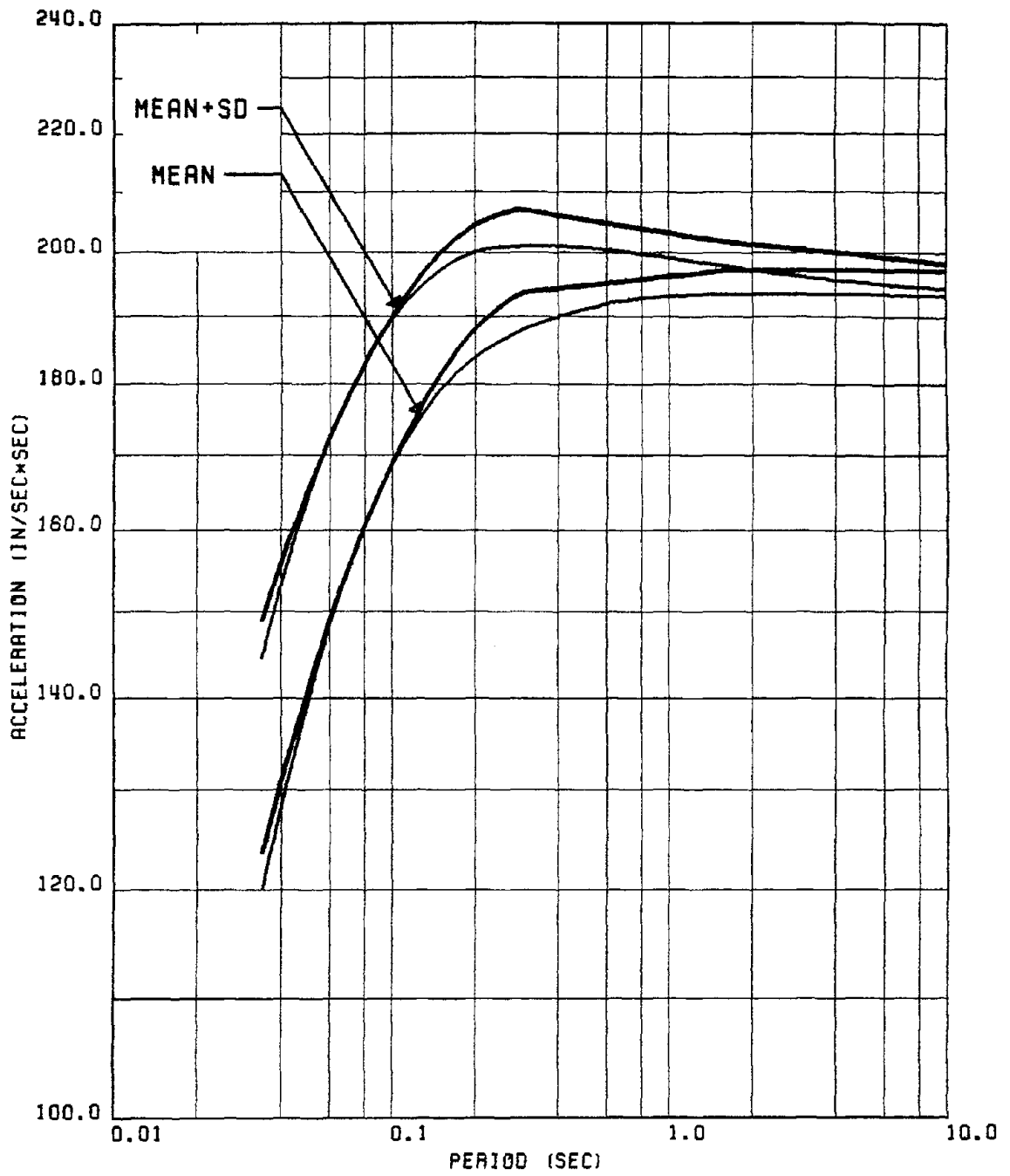
FIG. 226 PROPOSED & COMPUTED MEAN & (MEAN+SD) 'HORIZONTAL' RSV FOR GROUP #2
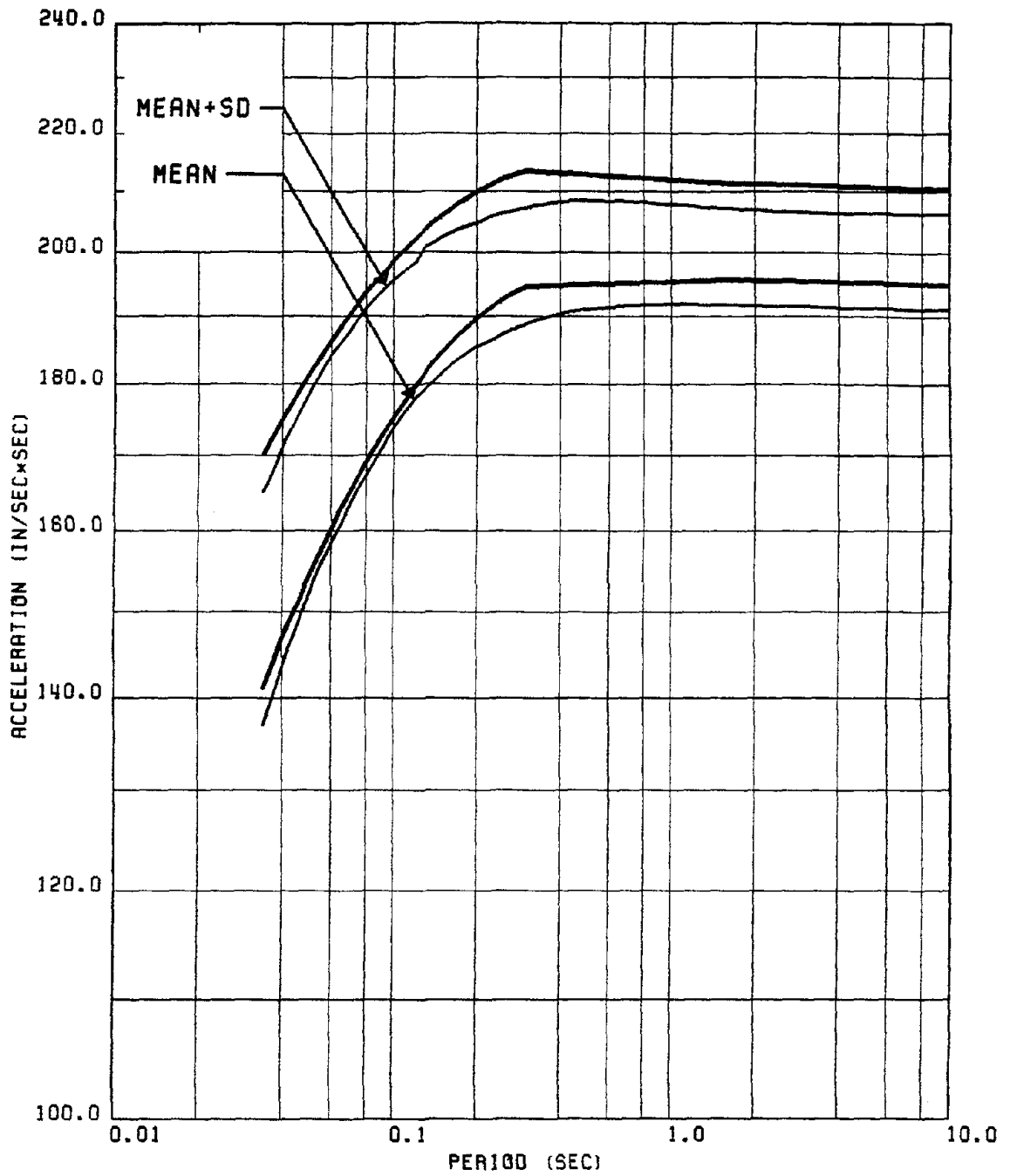NOTE : THE PROPOSED MASSLESS SPECTRA ARE INDICATED BY THE THICKER CURVES
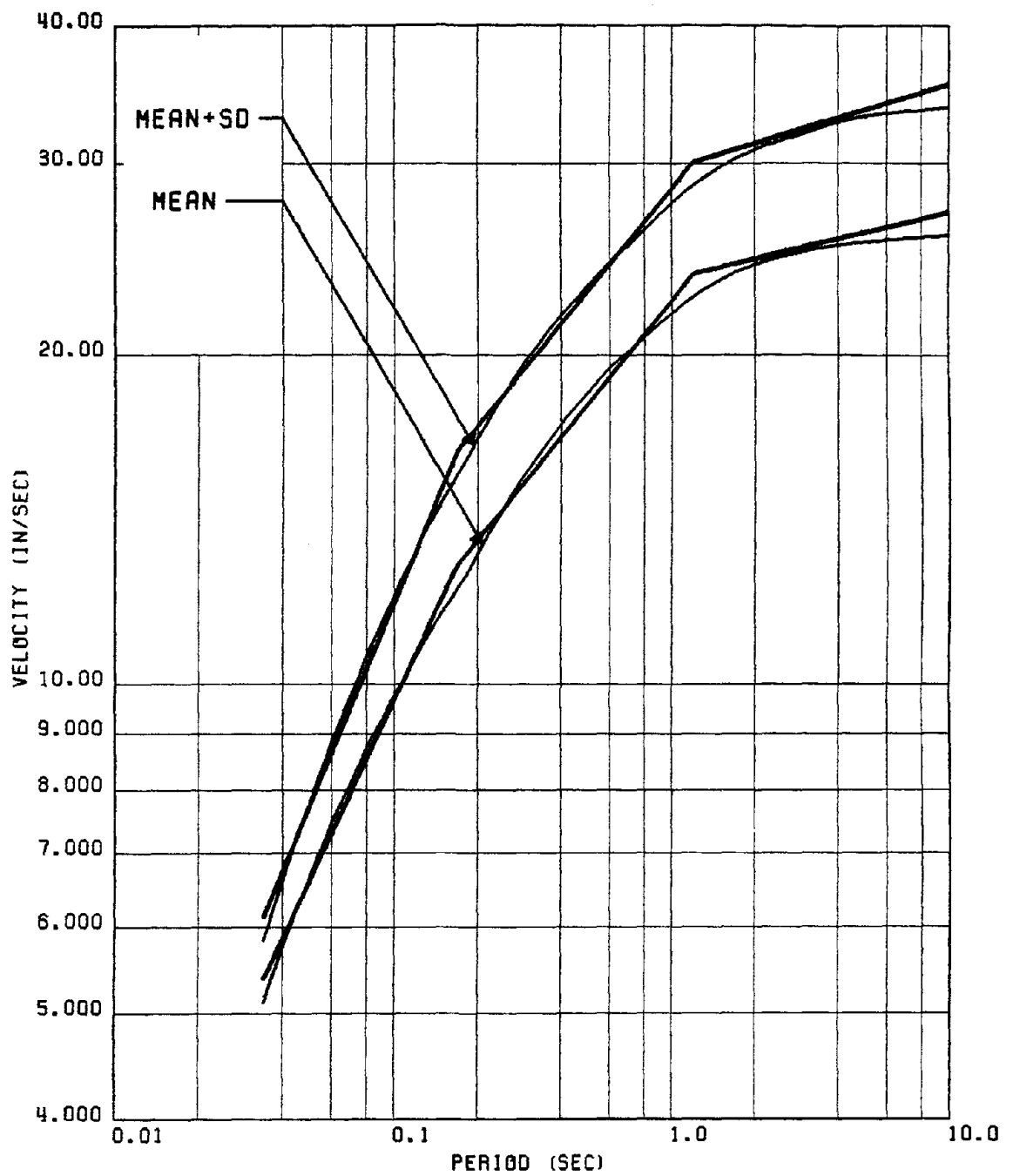
FIG. 227 PROPOSED & COMPUTED MEAN & (MEAN+SD) 'VERTICAL' RSV FOR GROUP #2
NOTE : THE PROPOSED MASSLESS SPECTRA ARE INDICATED BY THE THICKER CURVES
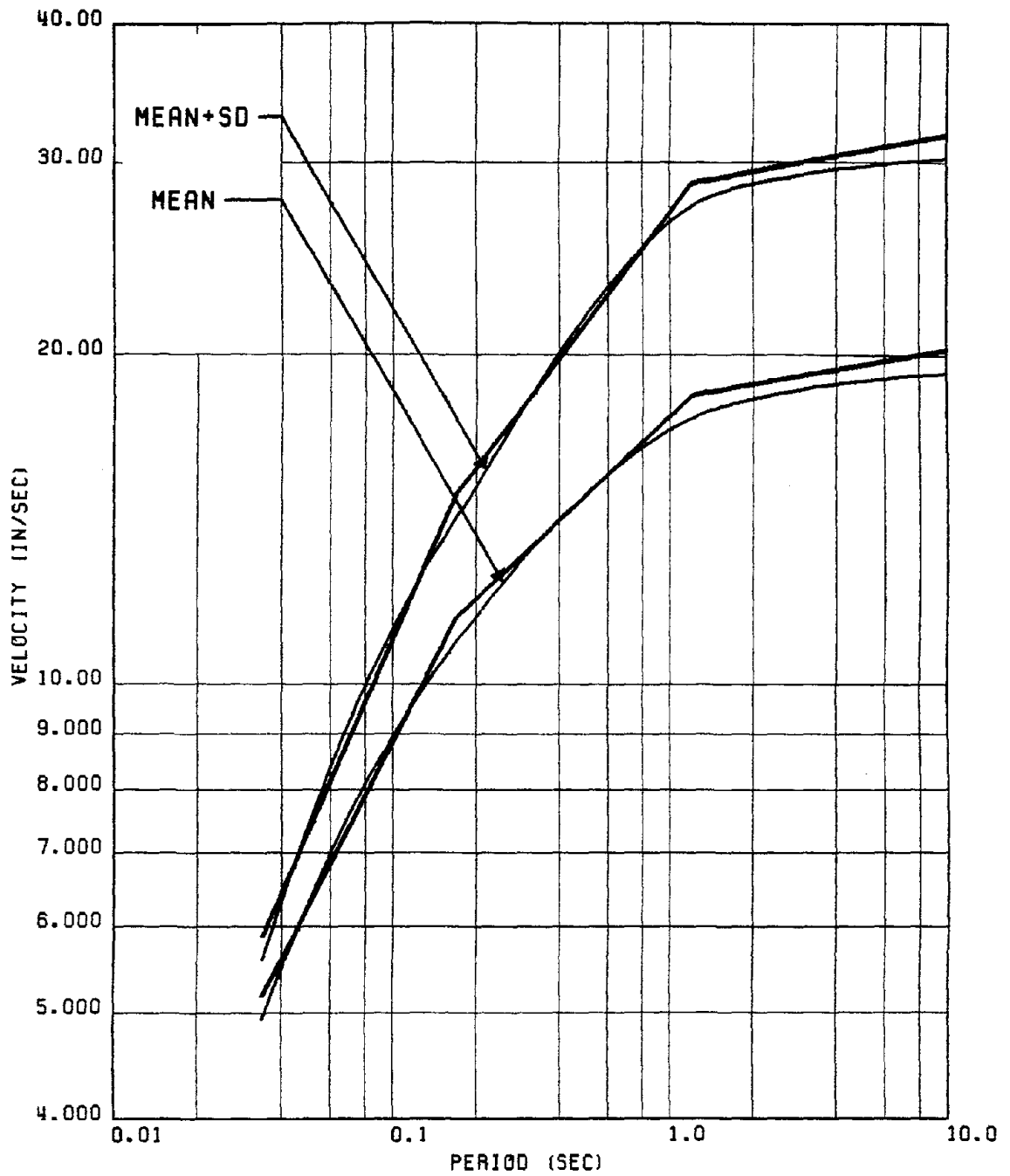
FIG. 228 PROPOSED & COMPUTED MEAN & (MEAN+SD) 'HORIZONTAL' RSV FOR GROUP #3
NOTE : THE PROPOSED MASSLESS SPECTRA ARE INDICATED BY THE THICKER CURVES
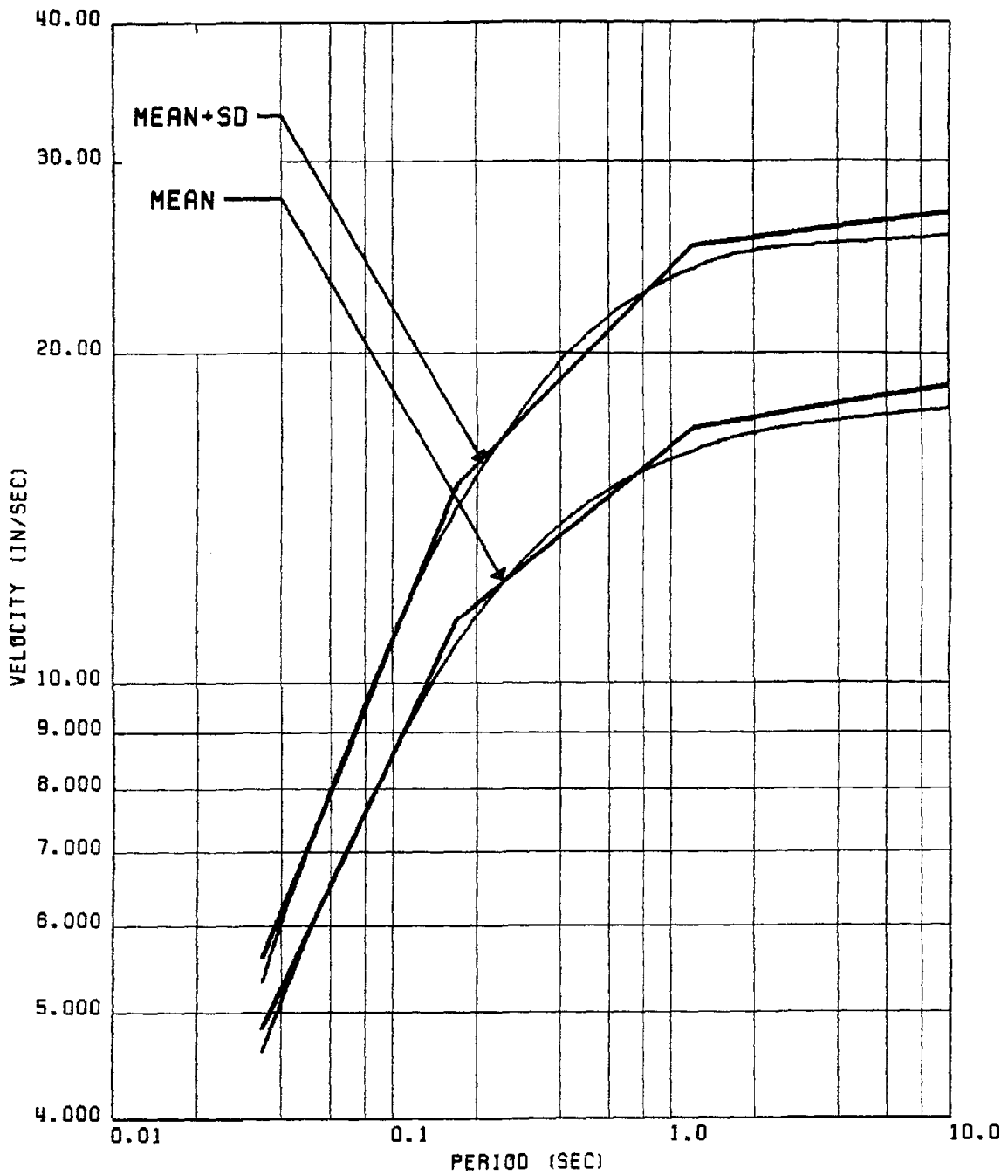
FIG. 229 PROPOSED & COMPUTED MEAN & (MEAN+SD) 'VERTICAL' RSV FOR GROUP #3
NOTE : THE PROPOSED MASSLESS SPECTRA ARE INDICATED BY THE THICKER CURVES
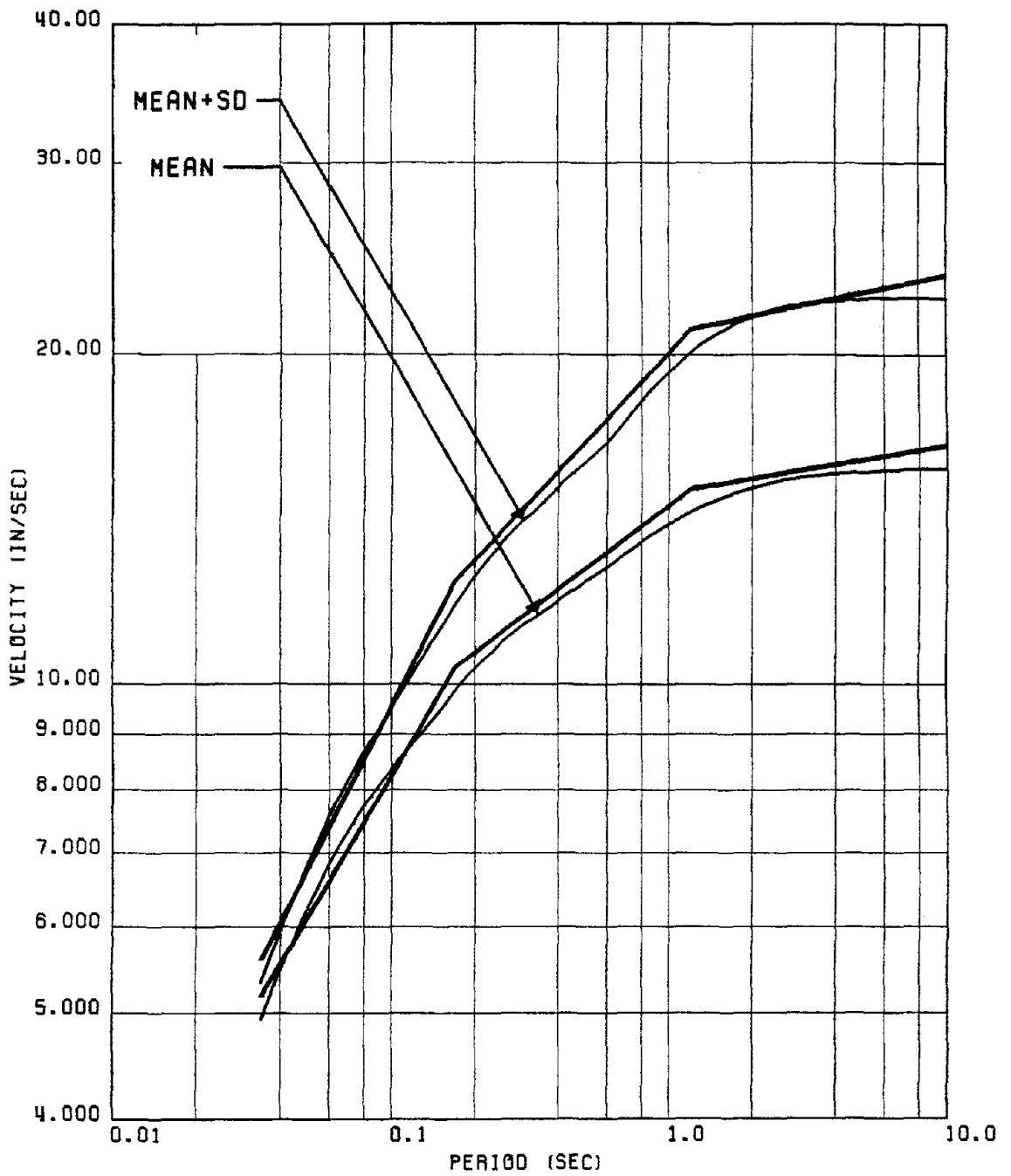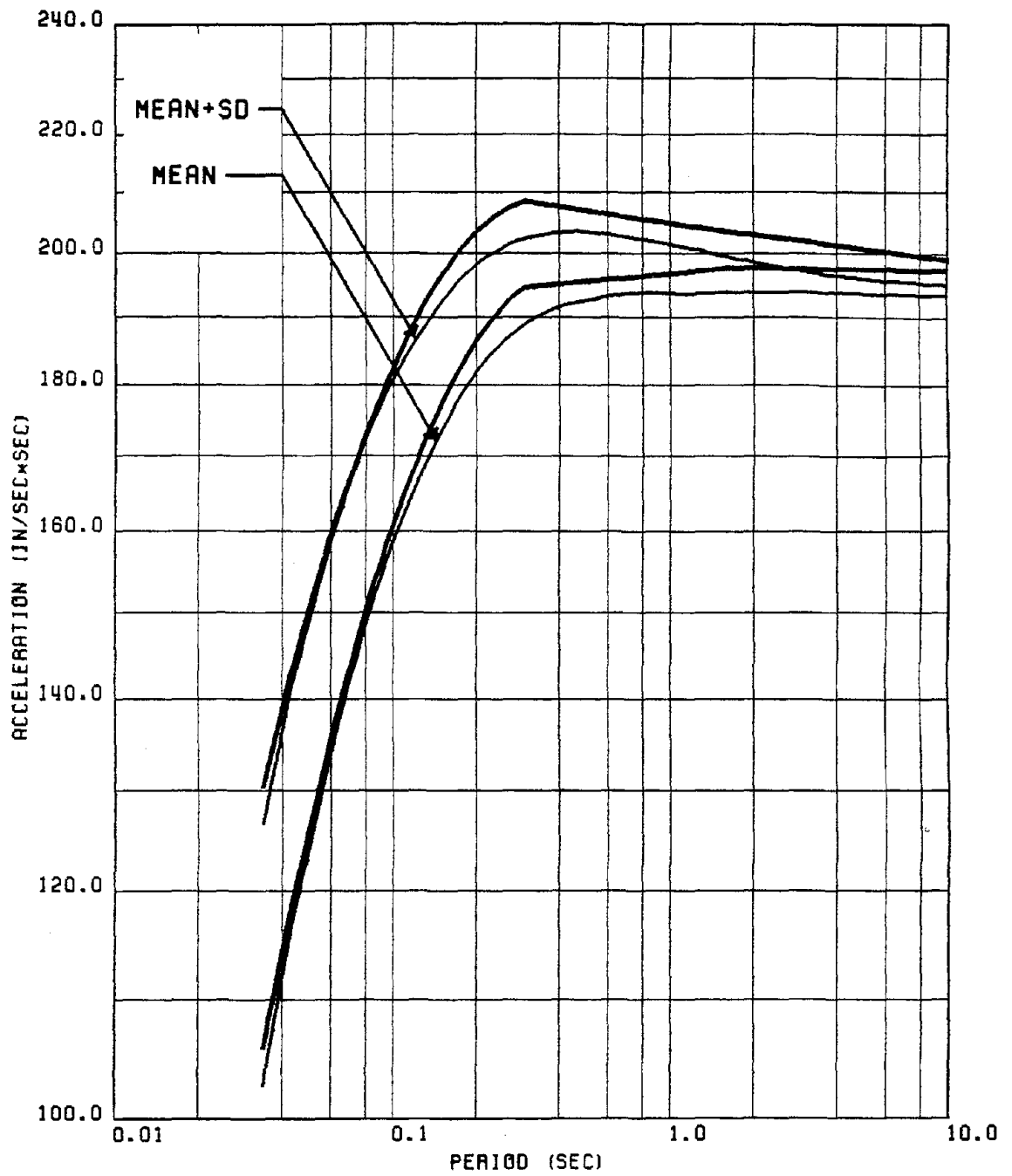
FIG. 230 PROPOSED & COMPUTED MEAN & (MEAN+SD) 'HORIZONTAL' RSV FOR GROUP #4
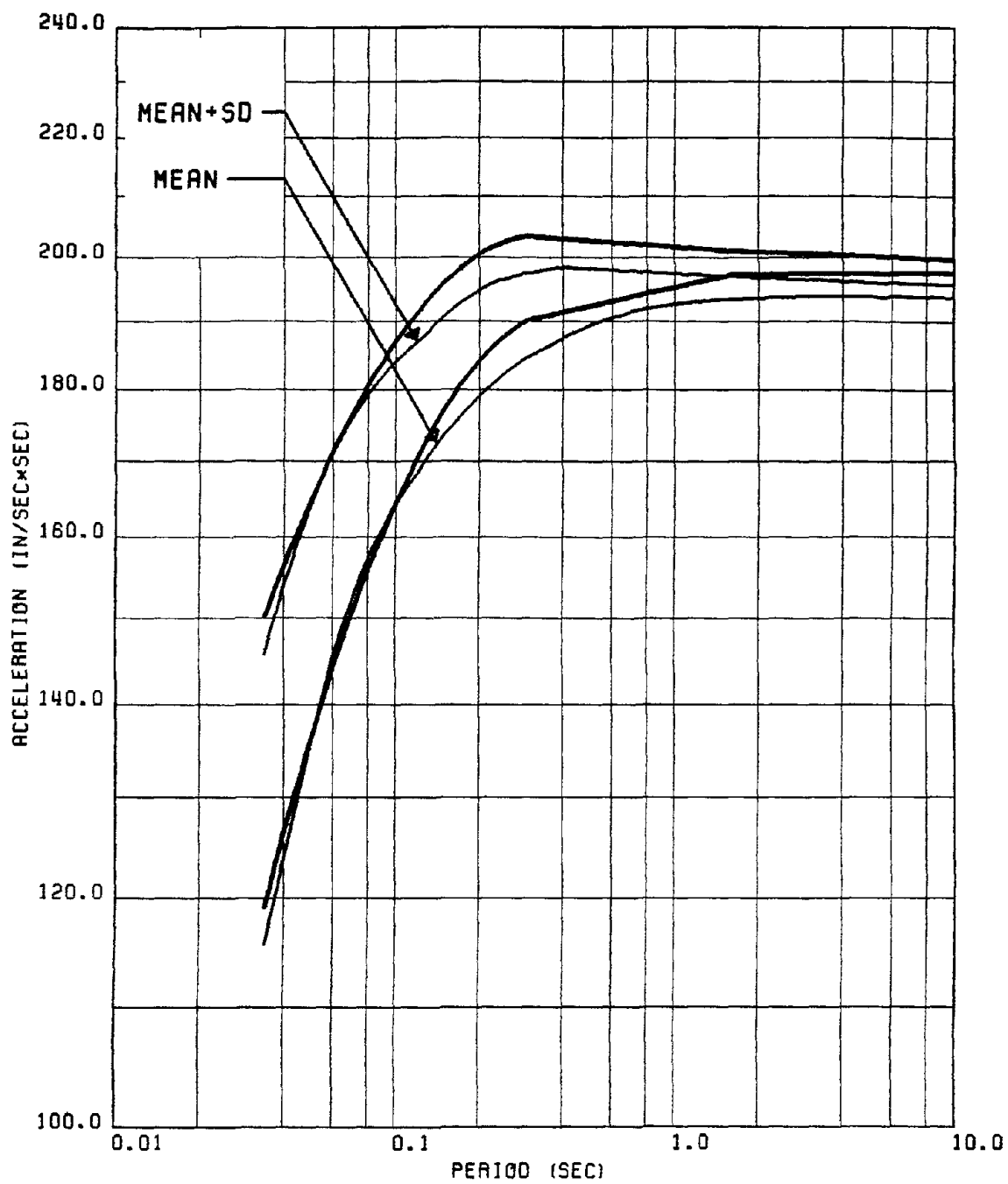NOTE : THE PROPOSED MASSLESS SPECTRA ARE INDICATED BY THE THICKER CURVES
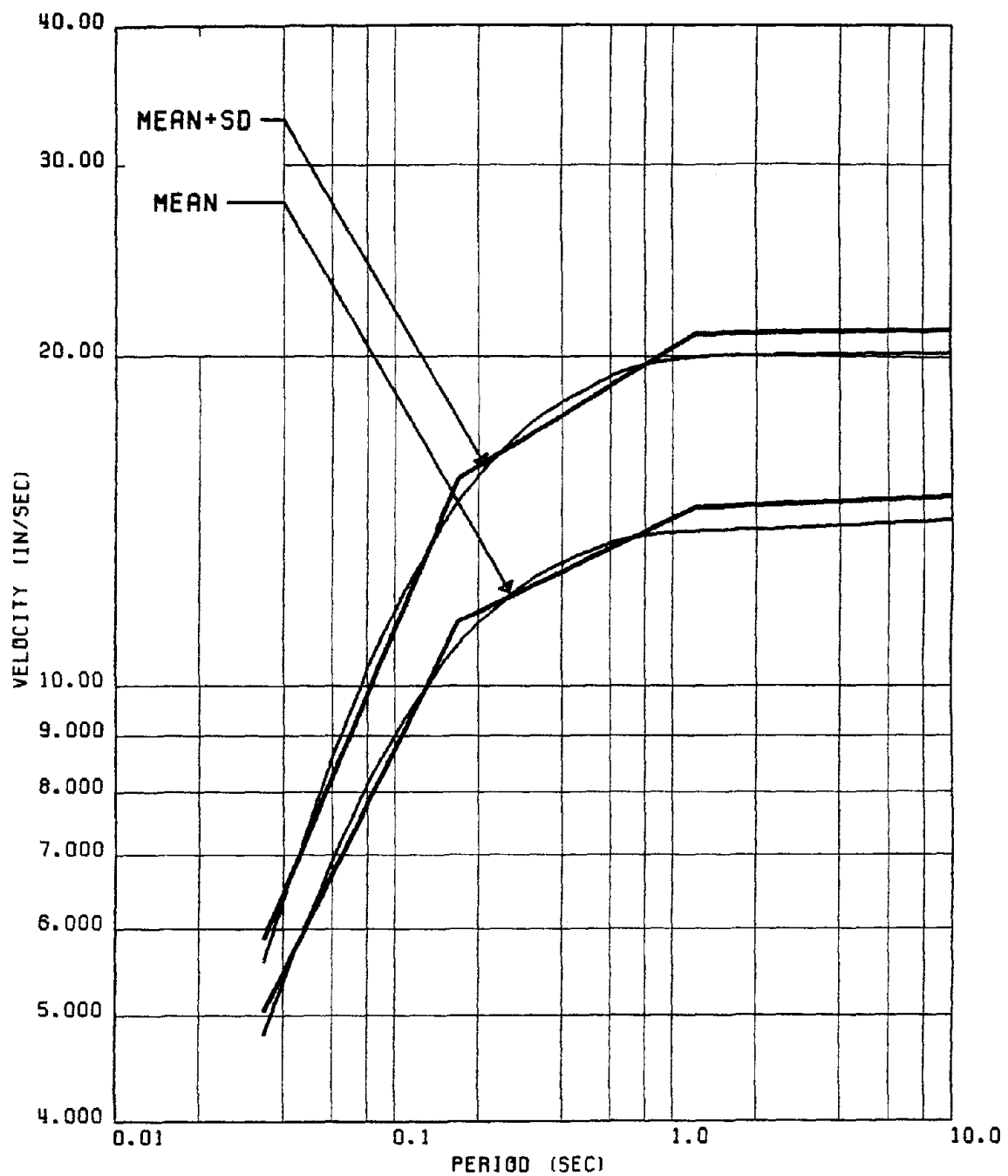
FIG. 231 PROPOSED & COMPUTED MEAN & (MEAN+SD) 'HORIZONTAL' RSV FOR GROUP #5
NOTE : THE PROPOSED MASSLESS SPECTRA ARE INDICATED BY THE THICKER CURVES

FIG. 232 PROPOSED & COMPUTED MEAN & (MEAN+SD) 'VERTICAL' RSV FOR GROUP *5
NOTE : THE PROPOSED MASSLESS SPECTRA ARE INDICATED BY THE THICKER CURVES

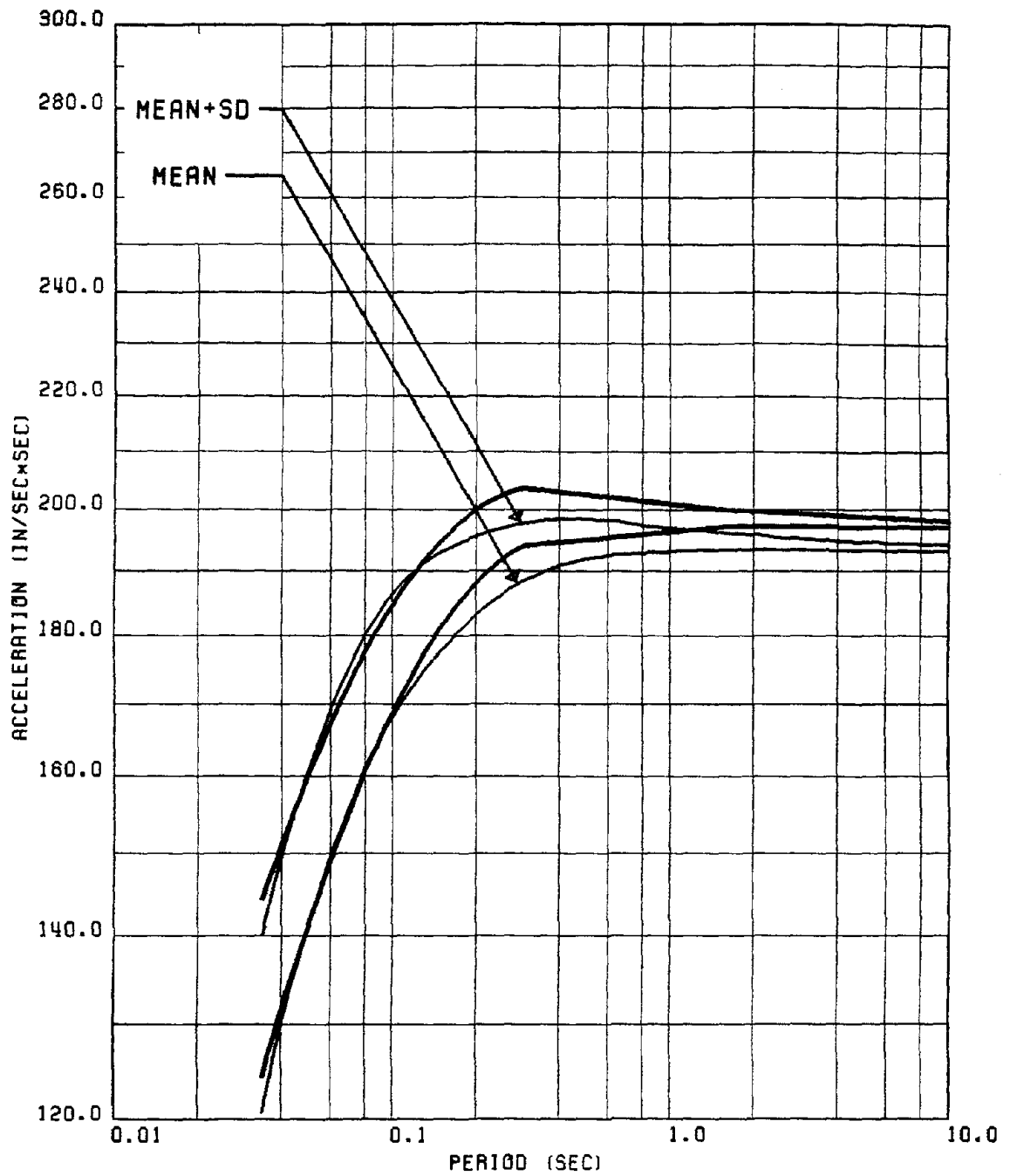FIG. 233 COEFFICIENT OF VARIATION OF 'VERTICAL' RSV FOR MASSLESS OSCILLATOR

FIG. 234 PROPOSED & COMPUTED MEAN & (MEAN+SD) 'HORIZONTAL' RSA FOR GROUP #1
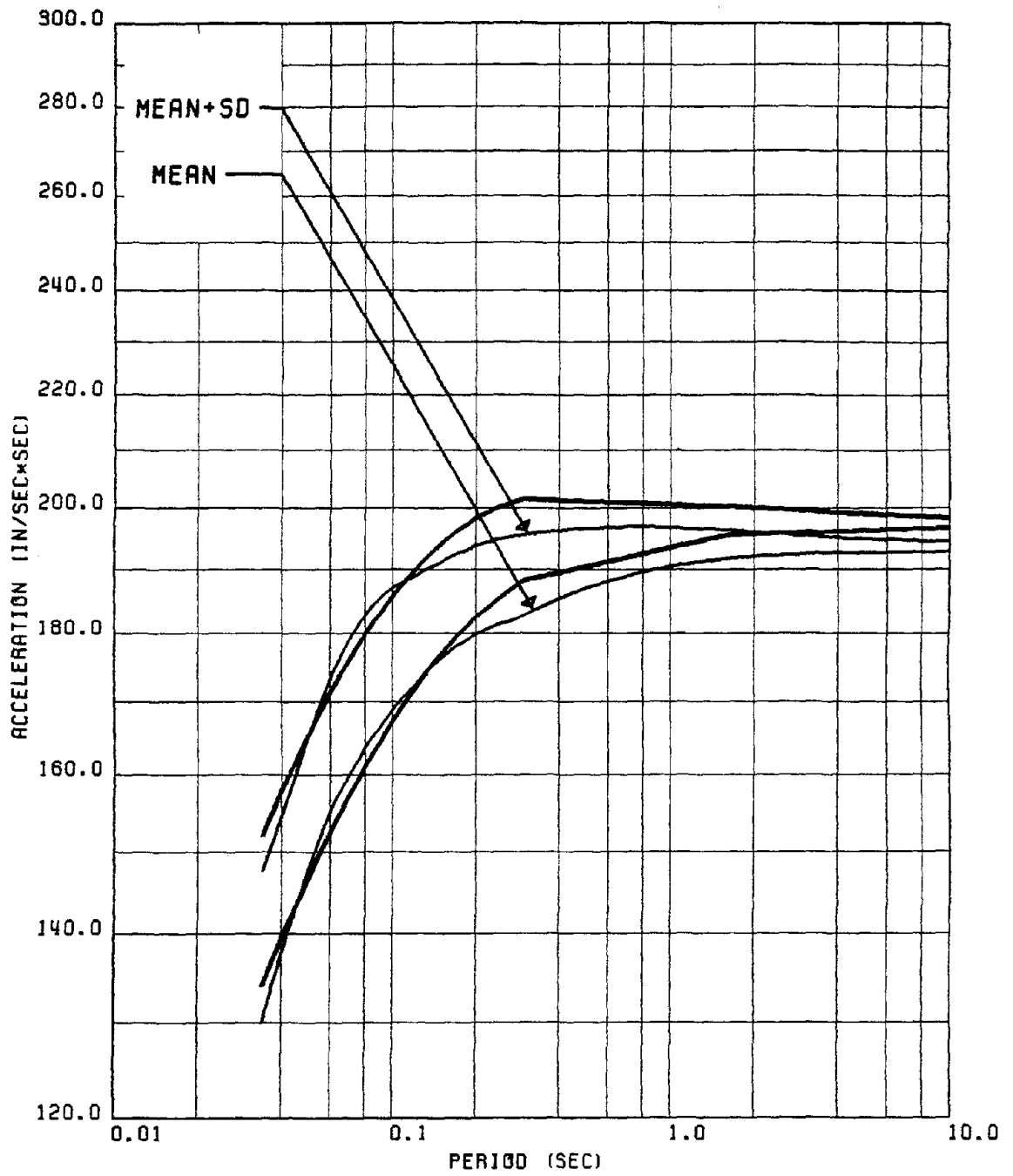NOTE : THE PROPOSED MASSLESS SPECTRA ARE INDICATED BY THE THICKER CURVES

FIG. 235 PROPOSED & COMPUTED MEAN & (MEAN+SD) 'VERTICAL' RSA FOR GROUP #1
NOTE : THE PROPOSED MASSLESS SPECTRA ARE INDICATED BY THE THICKER CURVES

FIG. 236 PROPOSED & COMPUTED MEAN & (MEAN+SD) 'HORIZONTAL' RSA FOR GROUP #2
NOTE : THE PROPOSED MASSLESS SPECTRA ARE INDICATED BY THE THICKER CURVES

FIG. 237 PROPOSED & COMPUTED MEAN & (MEAN+SD) 'VERTICAL' RSA FOR GROUP #2
NOTE : THE PROPOSED MASSLESS SPECTRA ARE INDICATED BY THE THICKER CURVES
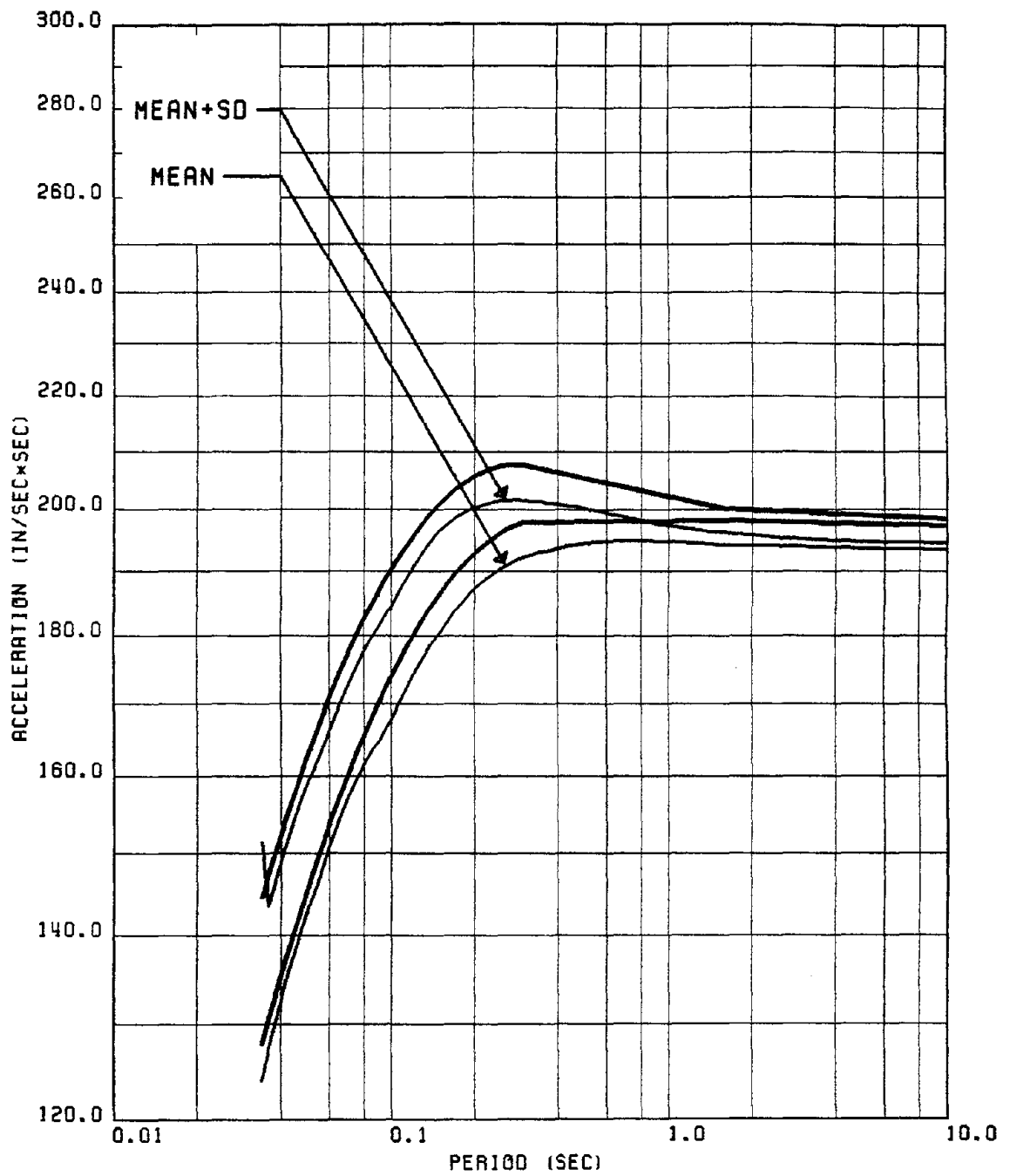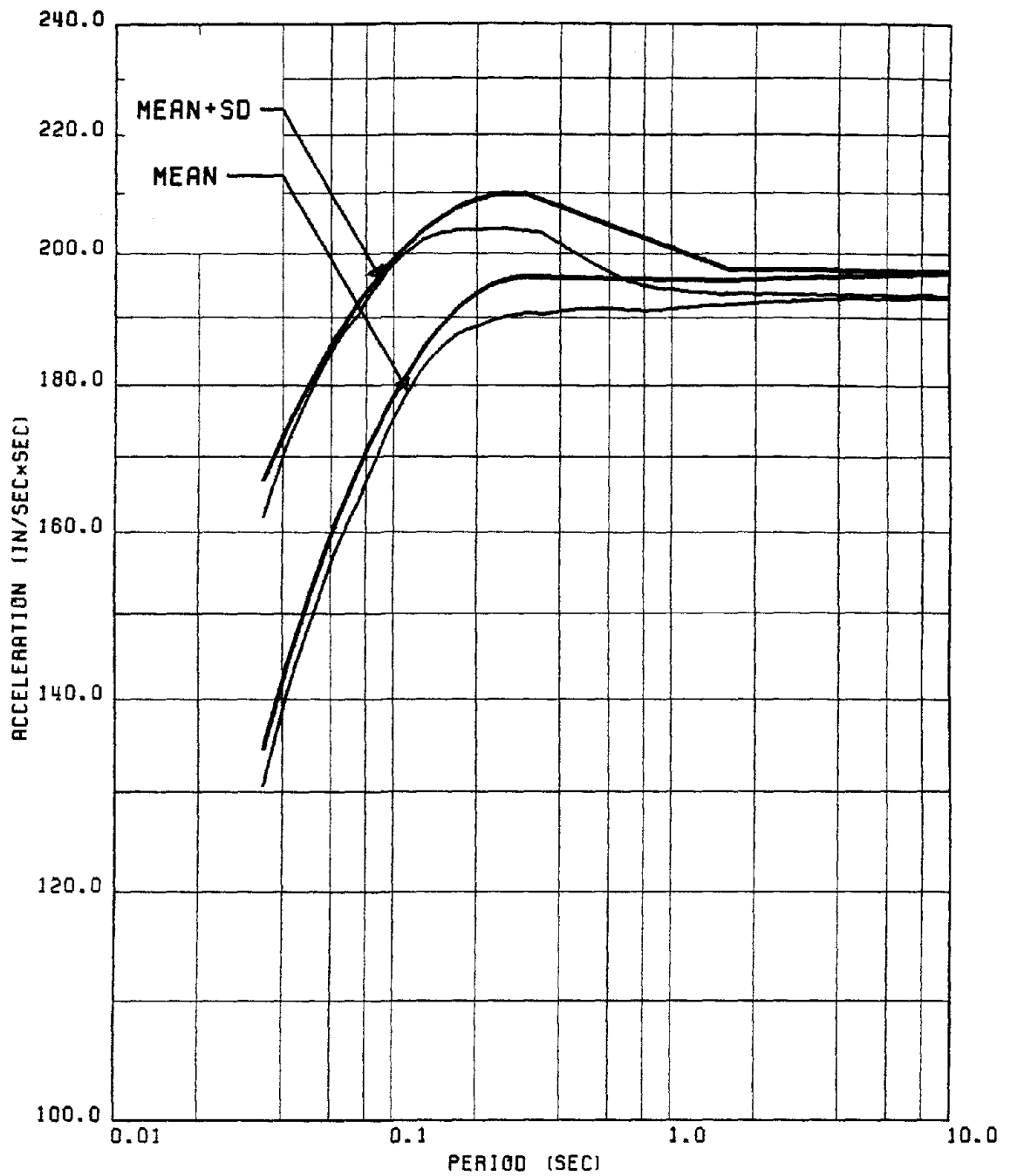
FIG. 23B PROPOSED & COMPUTED MEAN & (MEAN+SD) 'HORIZONTAL' RSA FOR GROUP #3
NOTE : THE PROPOSED MASSLESS SPECTRA ARE INDICATED BY THE THICKER CURVES

FIG. 239 PROPOSED & COMPUTED MEAN & (MEAN+SD) 'VERTICAL' RSA FOR GROUP #3
NOTE : THE PROPOSED MASSLESS SPECTRA ARE INDICATED BY THE THICKER CURVES

FIG. 240 PROPOSED & COMPUTED MEAN & (MEAN+SD) 'HORIZONTAL' RSA FOR GROUP #4
NOTE : THE PROPOSED MASSLESS SPECTRA ARE INDICATED BY THE THICKER CURVES

FIG. 241 PROPOSED & COMPUTED MEAN & (MEAN+SD) 'HORIZONTAL' RSA FOR GROUP #5
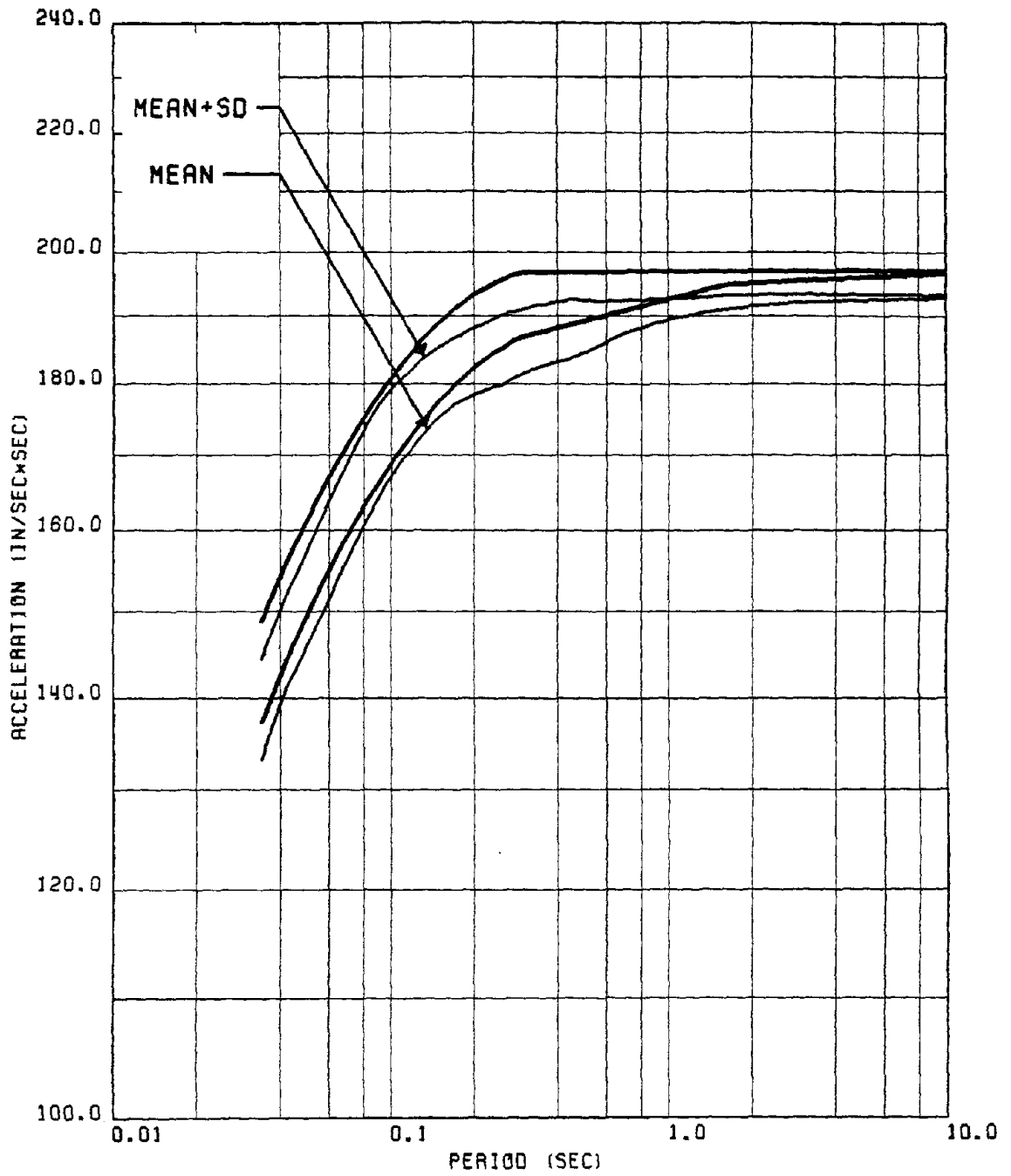NOTE : THE PROPOSED MASSLESS SPECTRA ARE INDICATED BY THE THICKER CURVES

FIG. 242 PROPOSED & COMPUTED MEAN & (MEAN+SD) 'VERTICAL' RSA FOR GROUP #5
NOTE : THE PROPOSED MASSLESS SPECTRA ARE INDICATED BY THE THICKER CURVES
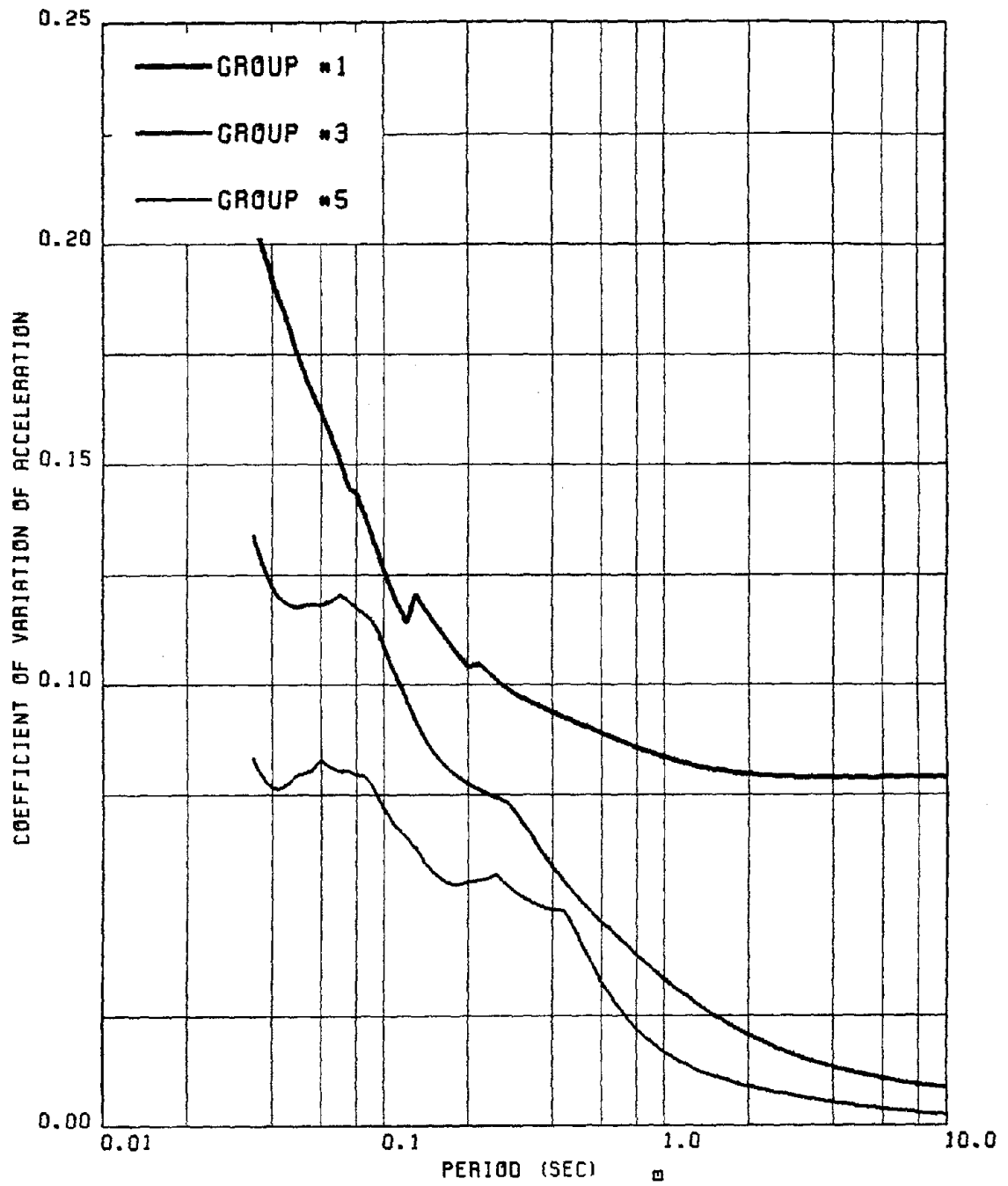
FIG. 243 COEFFICIENT OF VARIATION OF 'VERTICAL' RSA FOR MASSLESS OSCILLATOR